Fisheries and Oceans Canada | Pêches et Océans Canada
Ecosystems and Oceans Science | Sciences des écosystèmes et des océans

Canadian Science Advisory Secretariat (CSAS)

Research Document 2022/001

Pacific Region

Bocaccio (*Sebastes paucispinis*) stock assessment for British Columbia in 2019, including guidance for rebuilding plans

Paul J. Starr[1] and Rowan Haigh[2]
[1]Canadian Groundfish Research and Conservation Society
1406 Rose Ann Drive
Nanaimo, British Columbia V9T 4K8

[2]Pacific Biological Station
Science Branch
Fisheries and Oceans Canada
3190 Hammond Bay Road
Nanaimo, British Columbia V9T 6N7

May 2022

Canada

Foreword

This series documents the scientific basis for the evaluation of aquatic resources and ecosystems in Canada. As such, it addresses the issues of the day in the time frames required and the documents it contains are not intended as definitive statements on the subjects addressed but rather as progress reports on ongoing investigations.

Published by:

Fisheries and Oceans Canada
Canadian Science Advisory Secretariat
200 Kent Street
Ottawa ON K1A 0E6

http://www.dfo-mpo.gc.ca/csas-sccs/
csas-sccs@dfo-mpo.gc.ca

ISSN 1919-5044
ISBN 978-0-660-41097-5 Cat. No. Fs70-5/2022-001E-PDF

Correct citation for this publication:

Starr, P.J. and Haigh, R. 2022. Bocaccio (*Sebastes paucispinis*) stock assessment for British Columbia in 2019, including guidance for rebuilding plans. DFO Can. Sci. Advis. Sec. Res. Doc. 2022/001. vii + 292 p.

Aussi disponible en français :

*Starr, P. J. et Haigh, R. 2022. Évaluation du stock de bocaccios (*Sebastes paucispinis*) de la Colombie-Britannique en 2019 et lignes directrices relatives à l'élaboration de plans de rétablissement. Secr. can. des avis sci. du MPO. Doc. de rech. 2022/001. vii + 324 p.*

TABLE OF CONTENTS

LIST OF MAIN TABLES

LIST OF MAIN FIGURES

ABSTRACT

Bocaccio rockfish (*Sebastes paucispinis*, BOR) is ubiquitous along the British Columbia (BC) coast (at ~60-300 m depth), occurring in low densities along the west coast of Vancouver Island (WCVI), across Goose Island and Mitchell gullies in Queen Charlotte Sound and into the lower parts of Hecate Strait.

In 2002, the Committee on the Status of Endangered Wildlife in Canada (COSEWIC) assessed the status of the BC population of Bocaccio rockfish (BOR) as “Threatened”. In November 2013, BOR was reassessed by COSEWIC as “Endangered”. Under COSEWIC and SARA (the Species at Risk Act), an endangered species is defined as one that is facing imminent extirpation or extinction. BOR has been assessed twice by DFO Science (in 2009 and then in 2012) using a Bayesian surplus production model which evaluated this species to be in the DFO Critical Zone. This led to setting mortality caps at the minimum acceptable levels of harm while still allowing the multispecies trawl fishery, which takes BOR in conjunction with other trawl species, to continue operating while still rebuilding. Beginning in 2017, there has been mounting evidence of a strong BOR recruitment event in BC waters, leading to difficulty in 2018 and 2019 for commercial operators to stay within the existing low catch limits that were set to encourage rebuilding in the BC BOR population. The purpose of this stock assessment is to evaluate the current BOR stock status and to assess the potential impact of this new recruitment on the DFO Precautionary Approach (PA) status of BOR in the future.

This stock assessment evaluates a single BC coastwide population harvested by multiple fisheries. Analyses of biology and distribution did not support separate regional stocks for BOR. A single coastwide stock was also assumed for the two previous BOR stock assessments.

We use an annual catch-at-age model tuned to six fishery-independent trawl survey series, a truncated bottom trawl CPUE series, annual estimates of commercial catch since 1935, and age composition data from survey series (31 years of data from four surveys) and the commercial fishery (12 years of data). The model starts from an assumed equilibrium state in 1935, and the survey data cover the period 1967 to 2019 (although not all years are represented). Two fisheries are modelled: one a combined bottom and midwater trawl fishery and an ‘other’ fishery, which combines halibut longline, sablefish trap, salmon troll, rockfish hook and line, etc. The second fishery is a compromise that acknowledges other methods capturing this species while keeping the complexity to a minimum, given the lack of good information from these additional fisheries.

Three base runs using a two-sex model were implemented in a Bayesian framework (using the Markov Chain Monte Carlo procedure) under a scenario that fixed natural mortality to three levels (0.07, 0.08, 0.09) while estimating steepness of the stock-recruit function, catchability for the surveys and CPUE, and selectivity for four of the six surveys and the commercial trawl fleet. These three runs were combined into a composite base case which explored the major axis of parameter uncertainty in this stock assessment. Nine sensitivity analyses were performed to test the effect of alternative model assumptions.

The composite base case suggests that the BOR spawning population lies in the Critical Zone (with a probability >0.99), as do the three component runs. This is in spite of the stock being moderately productive and exploitation rates being uniformly low. For instance, the median exploitation by the trawl fishery, which accounts for 95% of the catch, in the final year is estimated to be 0.025 (0.012-0.044) even at the very low biomass levels. A strong cohort, estimated at 44 times the long term average recruitment (range: 30-58), was born in 2016 and is projected to bring this stock out of the Critical Zone by the beginning of 2023 and will have a better than 50% probability of being in the Healthy Zone in that same year.

These predictions are entirely dependent on the assessed size of the 2016 year class, which is highly uncertain. However, there is evidence, beginning in 2017, that this cohort is large and dominates the available data. Three of the synoptic surveys, particularly the Queen Charlotte Sound survey in 2019, show strong quantitative increases in abundance and in distribution. This cohort dominates the age and length frequencies in the commercial trawl, beginning in 2018. Similar strong recruitment (in 2010 and 2013) in the US BOR population, located south of Monterey, has lifted that stock out of an 'overfished' designation and was assessed in 2017 to be approaching $0.5B_0$. We suggest that the demonstrable capacity of the four active synoptic surveys plus the high quality monitoring of the trawl fishery catches and discards will verify the progress of this strong cohort as it recruits to the fishery.

1. INTRODUCTION

In 2002, the Committee on the Status of Endangered Wildlife in Canada (COSEWIC) assessed the status of the British Columbia (BC) population of Bocaccio rockfish (BOR, *Sebastes paucispinis*) as "Threatened". In November 2013, BOR was reassessed by COSEWIC as "Endangered". Under COSEWIC and SARA (Species at Risk Act), an endangered species is defined as one that is facing imminent extirpation or extinction. The rationale for this status from the COSEWIC Assessment and Status Report for Bocaccio (COSEWIC 2013) was that "*COSEWIC assessed Bocaccio as 'Endangered' because Bocaccio has been in continuous decline for 60 years and it has declined by 28% in the 10-year period since it was first assessed by COSEWIC. New surveys initiated since the last assessment indicate that these recent declines have occurred in areas of highest biomass off the west coast of Vancouver Island and in Queen Charlotte Sound*". Bocaccio was not listed under Schedule 1 of SARA, although DFO manages this species under the Fisheries Act, which allows Bocaccio to be integrated within the overall DFO management of the groundfish fleet, and can take steps to actively minimise the catch of this species.

Bocaccio has been the subject of two detailed scientific reviews in the early 2000s (Stanley et al. 2001, 2004), was formally assessed in 2008 (Stanley et al. 2009), and the 2008 stock assessment was updated in 2012 (Stanley et al. 2012). The 2012 stock assessment estimated the spawning biomass to be less than the Limit Reference Point (LRP), which placed the stock in DFO's Precautionary Approach (PA) 'Critical Zone', necessitating the development of a rebuilding plan. The latter typically involves simulations and rebuilding efforts over 1.5 to 2 generations (see DFO's guidance for rebuilding and Section 9.3). The immediate response was to set mortality caps at the minimum acceptable levels of harm while still allowing the multispecies trawl fishery, which takes BOR in conjunction with other trawl species, to continue operating while still rebuilding. Beginning in 2017, there has been mounting evidence of a strong BOR recruitment event in BC waters, leading to difficulty in 2018 and 2019 for commercial operators to stay within the existing low catch limits that were set to encourage rebuilding in the BC BOR population. Science support was requested to review the rebuilding plan objectives, and, if indicated by the review, adjust the rebuilding plan objectives so that they can be monitored and evaluated while remaining consistent with the Rebuilding Plan guidance document.

The model used for the 2008 and the 2012 BOR stock assessments was a Bayesian surplus production model, which relied on changes in the abundance indices to assess stock status, while assuming that recruitment is deterministic and relatively constant. Biological data in the form of ages or lengths cannot be used directly in a surplus production model, although such data can be used indirectly to construct an informed prior on the intrinsic growth rate parameter *r*, which determines the model productivity. However, a surplus production model cannot evaluate a strong recruitment event, given the limitations of the model structure: such an evaluation requires the use of an age-structured model.

A modified version of the Coleraine statistical catch-at-age software (Hilborn et al. 2003) called Awatea (APPENDIX D) was used to model the BOR population. The assessment model included:

- sex-specific parameters;
- abundance indices by year (y):
  four synoptic surveys – QCS = Queen Charlotte Sound (10y), WCVI = west coast Vancouver Island (9y), WCHG = west coast Haida Gwaii (7y), HS = Hecate Strait (8y);
  two historical surveys – NMFS Triennial = US National Marine Fisheries Service triennial off WCVI (7y), GIG = Goose Island Gully (8y); one bottom trawl CPUE series (17y, 1996-2012);

- proportions-at-age data (also called age frequencies or 'AF') by year (y): five sets – commercial trawl catch (12y) , QCS Synoptic (10y), WCVI Synoptic (8y), WCHG Synoptic (8y), and HS Synoptic (6y);
- maximum modelled age of 50 y, with older ages accumulated into the final age class;
- estimated selectivities for the commercial fishery and for the four sets of synoptic survey indices.

The input data were reweighted once based on the recommendations of Francis (2011) to balance abundance and composition data (APPENDIX D). The mean-age weightings used in the component runs of the base case and the sensitivity runs appear in Table E.5.

DFO Fisheries Management requested that DFO Science provide advice regarding the assessment of this stock relative to reference points that are consistent with the DFO fishery decision-making framework incorporating the Precautionary Approach (DFO 2009), including the implications of a range of harvest strategies on stock status. In the absence of updated science advice, there is uncertainty about the risks posed to the BC BOR stock as catch levels will likely increase in response to the apparent strong recruitment event. This stock assessment provides an update on the stock status of BOR and also serves to inform DFO rebuilding plans for this species.

1.1. ASSESSMENT BOUNDARIES

This assessment includes Pacific Marine Fisheries Commission (PMFC[1]) major areas (3CD and 5ABCDE) along the BC coast (Figure 1). This paper follows the 2008 and 2012 BOR stock assessments by assuming that there is a single BC stock of BOR. The available biological data were examined for evidence of stock separation (see Section D.3), and none was found, an unsurprising conclusion given the relatively small amount of available data. Area-specific stock differences (growth, size, and composition taken by gear type) were not discernible (APPENDIX D).

The PMFC areas are similar but not identical to the management areas used by the Groundfish Management Unit (GMU), which uses combinations of DFO Pacific Fishery Management Areas. We have not used GMU management areas because catch reporting from these areas has only been available since 1996. However, PMFC areas are sufficiently similar to the GMU areas such that managers can prorate any catch policy using historical catch ratios outlined in APPENDIX A.

1.2. RANGE AND DISTRIBUTION

BOR is ubiquitous along the BC coast (Figure 2), with most catches taken near the bottom in the depth range of 60-300 m (Figures C.1 and G.2). Catches appear to be greatest on the edge of the continental shelf where it slopes away, as well as along the edges of the main gullies in Queen Charlotte Sound and the more southern sections of Hecate Strait (Stanley et al. 2009). Stanley et al. (2009) noted that BOR is a schooling semi-pelagic species, leading to the observation that the adults likely do not occupy specific sites other than preferring high-relief boulder fields and rocks (Love et al. 2002). The species appears to be a relatively short-lived compared to other *Sebastes* species such as Pacific Ocean Perch (*S. alutus*) or Rougheye Rockfish (*S. aleutianus*), a characteristic shared with other semi-pelagic *Sebastes* species (e.g. Widow Rockfish, *S. entomelas*). The available age data indicate that this species reaches maximum ages around 50-55 years, with one male specimen reaching age 70, three specimens

[1] See APPENDIX A for historical background on the PMFC.

aged 60 or greater, and the 99th percentile of the age distribution at age 50 years (APPENDIX D).

Genetic studies have shown no strong evidence for stock differences between the west coast of Vancouver Island and central California, but suggest that a Hecate Strait sample might have differed from those to the south (Matala et al. 2004). American BOR stock assessments treat this species as having “two demographic clusters”, with one cluster located south of Monterey (southern/central California) and the other located off the BC coast (He and Field 2017). They note that BOR is relatively scarce in the region between Cape Mendocino (central California) and the mouth of the Columbia River; in particular, they comment on the lack of small fish in this region, implying that this portion of the population may not be self-sustaining. They also note that there are north/south differences in growth, maturity and longevity, although genetic evidence seems to indicate a single west coast population.

APPENDIX G provides maps of hotspots by fishing locality, where the top three mean CPUE hotspots occur in localities ‘Pine Island’, ‘W Cape Cook’, and ‘N Frederick-Langara (shallow)’ (Fig. G.5). Two of the hotspots for total catch (Fig. G.6) are geographically concentrated in ‘SE Goose’ and ‘SW Goose’, with the third top locality being ‘Nootka’ off the WCVI.

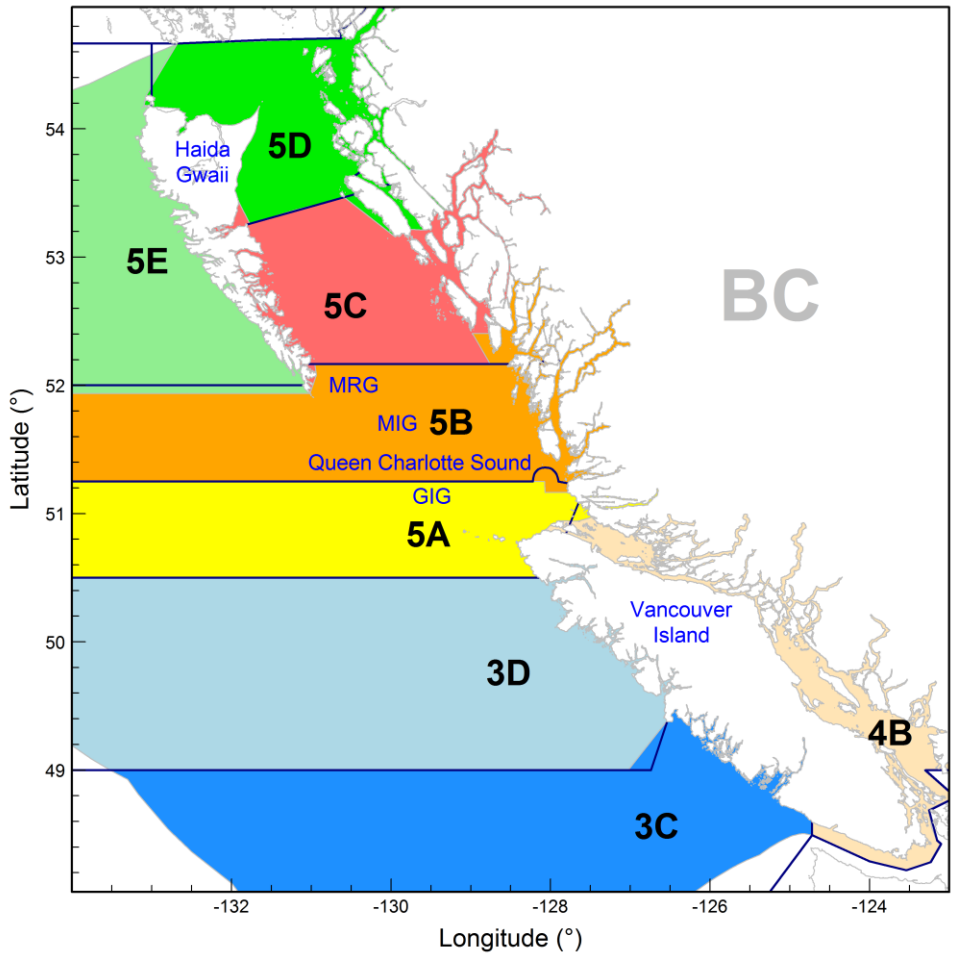

Figure 1. Pacific Marine Fisheries Commission (PMFC) major areas (outlined in dark blue) compared with Groundfish Management Unit areas for Bocaccio (shaded). For reference, the map indicates Moresby Gully (MRG), Mitchell’s Gully (MIG), and Goose Island Gully (GIG). This assessment covers one coastwide stock: PMFC 3CD + 5ABCDE.

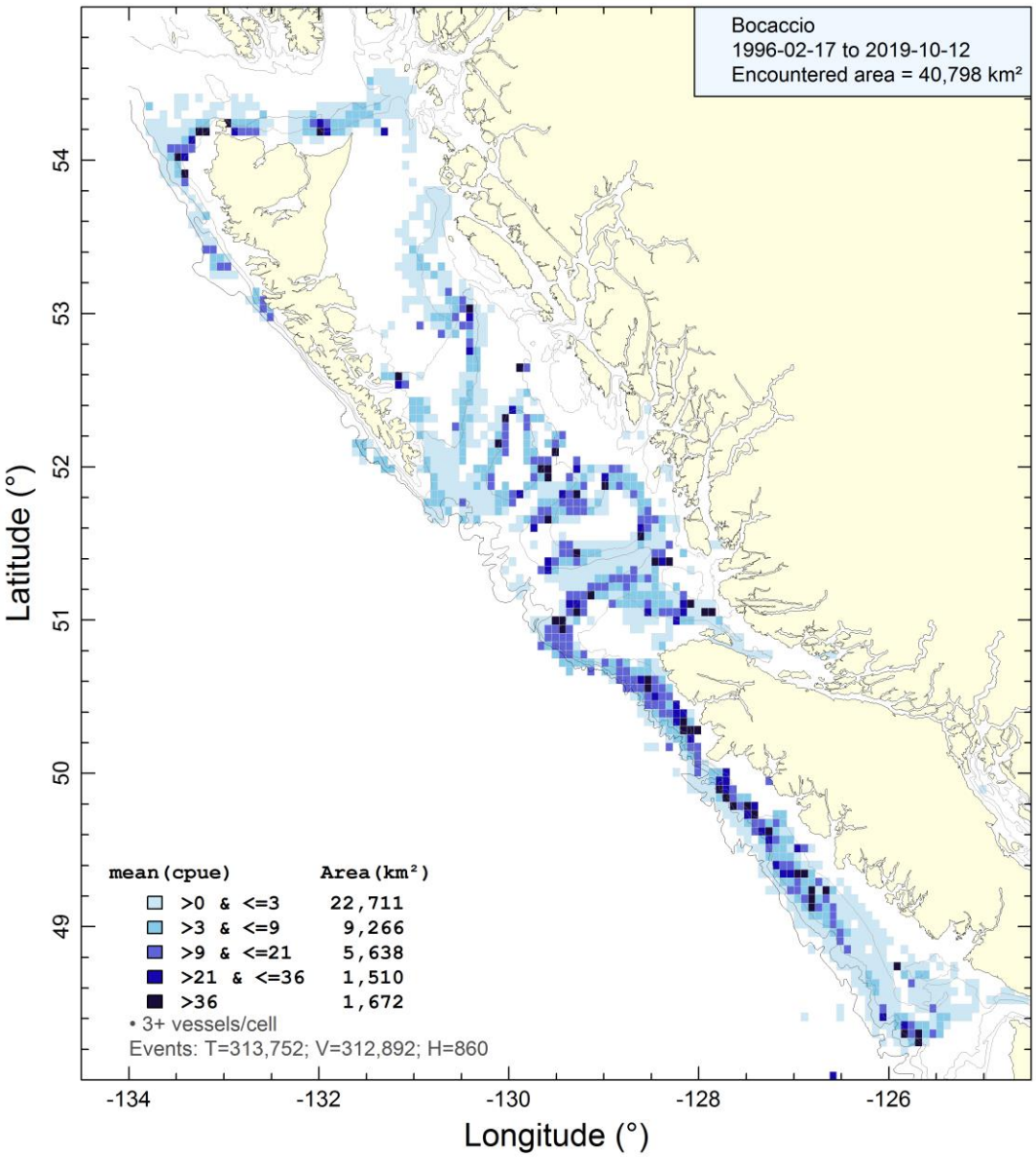

Figure 2. Aerial distribution of BOR mean trawl (bottom + midwater) catch per unit effort (kg/hour) from 1996 to 2019 in grid cells 0.075° longitude by 0.055° latitude (roughly 32 km² each). Isobaths show the 100, 200, 500, and 1000 m depth contours. Note that cells with <3 fishing vessels are not displayed.

2. CATCH DATA

This stock assessment recognises two commercial fisheries: (i) a combined bottom and midwater trawl fishery (with the bottom trawl predominating), and (ii) an 'other' capture methods fishery, which combines halibut longline, sablefish trap, salmon troll, rockfish hook and line, and lingcod troll. Recreational BOR catches were investigated but were not included because the available catch estimates did not indicate that this fishery captured much BOR. The catch-all fishery 'other' was needed in recognition of the significant catches of BOR by non-trawl methods, particularly in the historical period, but represent a compromise regarding model complexity and lack of information to properly characterise the 'other' fishery.

The 2008 and 2012 BOR stock assessments (Stanley et al. 2009, 2012) indirectly estimated catch in the halibut longline and salmon troll fisheries using historical effort data. That is, starting with modern (post-1996) estimates of the incidental catch of BOR per unit of effort in each of these fisheries, the authors multiplied this constant scalar by a historical estimate of the respective total annual effort as well as by the estimated total biomass in each year. There was no selectivity function applied because this was a surplus production model, which assumes that the entire biomass is vulnerable to fishing. Because the BOR biomass indices suggest that the BOR population has been in a monotonic declining trend, this procedure implies that catches were large at the beginning of the series, but declined as the biomass declined, especially if effort also tended to be high at the beginning of the series. This procedure is recursive; that is, biomass was used twice because it was first used to estimate the catch, then these estimates were summed to get the biomass. There is nothing to stop this procedure from repeating itself if the model gets a better fit to the data with an increasing biomass. Another problem with the procedure is that it assumes a constant catchability relationship between biomass and effort, which seems unlikely over such a long time span. The catches estimated in these fisheries using this procedure were enormous compared to modern catches: the 1935 catch of BOR in the halibut longline fishery was 1200 t and the salmon troll fishery was estimated to have caught nearly 400 t in the same year. The sum of these two catches exceeded by far the maximum annual catch of BOR that we were able to reconstruct over the entire catch history (see APPENDIX A) and there is no evidence that catches of this magnitude were actually taken before the Second World War. When this issue was reviewed by the BOR Technical Working Group (TWG), these catch levels were considered extremely unlikely and the approach was dropped.

The methods used to prepare a catch history for this BOR assessment, along with the full catch history, are presented in detail in APPENDIX A. Information about species caught concurrently with BOR commercial catches is presented in Appendix G. The average annual BOR catch for all capture methods over the most recent five years (2015-19) was 69 metric tonnes (t) coastwide.

3. FISHERIES MANAGEMENT

APPENDIX A summarises all management actions taken for BOR in BC since 1993. The Rebuilding Plans for Groundfish Species (including Bocaccio, Appendix 9 in DFO 2019) set out the mortality caps and initial quota allocations for BOR along the BC coast. In 2019/20 this included:

- a 61.9 t mortality cap managed via individual transferable quota for the groundfish trawl fishery;
- a 4.7 t mortality cap managed via trip limits of 45-272 kg/trip for hook and line groundfish fisheries; and
- a 7.1 t mortality cap managed via trip limits and retention prohibitions for salmon troll and recreational fisheries.

Mortality caps were also identified to account for First Nation Food, Social, and Ceremonial (FSC) and survey mortality.

4. SURVEY DESCRIPTIONS

Six sets of fishery independent survey indices have been used to track changes in the biomass of this population coastwide (APPENDIX B):

QCS Synoptic – a random-stratified synoptic (species comprehensive) trawl survey covering all of Queen Charlotte Sound (QCS) and targeting a wide range of finfish species. This survey has been repeated 10 times between 2003 to 2019, using three different commercial vessels but with a consistent design, including the same net.

WCVI Synoptic – a random-stratified synoptic trawl survey covering the west coast of Vancouver Island (WCVI). This survey was repeated seven times between 2004 to 2016 using the research vessel FV *Ricker* and was conducted in 2018 using a commercial vessel after the retirement of the *Ricker*. The survey employs a consistent design, including the same net, and targets a wide range of finfish species.

WCHG Synoptic – a random-stratified synoptic trawl survey covering the west coast (WC) of Graham Island in Haida Gwaii (HG) and the western part of Dixon Entrance. This survey has been repeated 7 times between 2006 to 2018 using three commercial vessels and a consistent design, including the same net and targeting a wide range of finfish species. The 2014 survey has been omitted from the series because less than ½ of the tows were completed. A WCHG survey operated in 1997 was not added to this series.

HS Synoptic – a random-stratified synoptic trawl survey covering all of Hecate Strait and extending into Dixon Entrance and across the top of Graham Island. This survey has been repeated 8 times between 2005 to 2019 using two vessels and a consistent design, including targeting a wide range of finfish species.

NMFS Triennial – the United States National Marine Fisheries Service (NMFS) Triennial survey series covered the lower half of the west coast of Vancouver Island for seven years from 1980 to 2001. Only the Canadian portion of the Vancouver INPFC (International North Pacific Fisheries Commission) area was used.

GIG Historical – an early composite series of 7 indices extending from 1967 to 1984 in Goose Island Gully (GIG). Most of these surveys were performed by the research vessel *G.B. Reed*, but two commercial vessels (*Eastward Ho* and *Ocean Selector*) were used in 1984 and 1994 respectively. Only tows located in Goose Island Gully (GIG) have been used to ensure continuity across all surveys.

The Hecate Strait multi-species assemblage bottom trawl survey and the WCVI shrimp and QCS shrimp trawl surveys have been omitted from this stock assessment (even though they were included in the 2008 and 2012 stock assessments) because the presence of BOR in these surveys has been either sporadic or the coverage, either spatial or by depth, has been incomplete, rendering these surveys poor candidates to provide abundance series for this species. Rockfish stock assessments, beginning with Yellowtail Rockfish (Starr et al. 2014[2]), have explicitly omitted using the two shrimp surveys because of the truncated depth coverage, which ends at 160 m for the WCVI shrimp survey, and the constrained spatial coverage of the QCS shrimp survey as well as its truncated depth coverage which ends at 231 m.

The relative biomass survey indices were used as data in the models along with the associated relative error for each index value. Process error, in the form of 0.25, was added to the survey relative errors (APPENDIX E).

[2] Starr, P.J., Kronlund, A.R., Olsen, N. and Rutherford, K. 2014. Yellowtail Rockfish (*Sebastes flavidus*) stock assessment for the coast of British Columbia, Canada (unpublished working paper). DFO Can. Sci. Advis. Sec. Res. Doc.

5. COMMERCIAL CPUE

Commercial catch per unit effort (CPUE) data were used to generate indices of abundance as input to the model fitting procedure. This series of indices, extending from 1996 to 2012, provided stability to the population model. The series was truncated at 2012 because, on the advice of the BOR Technical Working Group (TWG), it was felt that avoidance behaviour by the fleet would bias the indices after quotas were considerably reduced in 2013 in response to the COSEWIC 'Endangered' status.

The CPUE abundance index series was standardised for changes to vessel configuration, catch timing (seasonality), and location of catch (e.g., latitude and depth) to remove potential biases in CPUE that may result from changes in fishing practices and other non-abundance effects. This procedure was followed in two steps, with the model fitted to the positive catches assuming a lognormal distribution and to the presence/absence of BOR assuming a binomial distribution. These two models were then combined using a multiplicative "delta-lognormal" model (Eq. C.4: Fletcher et al. 2005). In these models, abundance was represented as a 'year effect' and the explanatory variables were selected sequentially by a General Linear Model, which accounted for variation in the available data. Other factors that might affect the behaviour of fishers, particularly economic factors, do not enter these models due to a lack of applicable data, thus resulting in indices that may not entirely reflect changes in the underlying stock abundance. APPENDIX C provides details on the CPUE analyses and APPENDIX E provides one sensitivity to the removing of the CPUE index series. Process error of 0.1514 was added to the CPUE observation errors (see Appendix E for derivation).

6. BIOLOGICAL INFORMATION

6.1. BIOLOGICAL SAMPLES

Age proportion samples from 2002 to 2018 were available from commercial trawl (combined bottom and midwater) catches of BOR, with a total of 12 years covered. Age frequency (AF) samples were also available from the four modern synoptic surveys. Only otoliths aged using the 'break and burn' (B&B) method were included in age samples used in this assessment because an earlier surface ageing method was known to be biased, especially with increasing age. During the 2018 Redstripe Rockfish review meeting, one participant mentioned that surface ageing is currently the preferred method for ageing very young rockfish (≤ 3y), which was later confirmed by the ageing lab. Commercial fishery age frequency data were summarised for each quarter, weighted by the BOR catch weight for the sampled trip. The total quarterly samples were scaled up to the entire year using the quarterly landed commercial catch weights of BOR. See APPENDIX D (Section D.2.1) for details.

Sampled AFs from bottom and midwater trawl were combined after comparing cumulative AFs for each gear type by sex and capture year (a few of the earlier years comprising mostly sorted samples but the majority of the samples are unsorted) and concluding that there were no consistent differences in the AFs between the two gear types for either sex (females: Figure D.11, males: Figure D.12). Consequently, the model was run assuming a joint selectivity for these two trawl methods by combining the AFs and the catch data into a single trawl fishery. There are no ageing data for the combined 'other' fishery, which primarily consisted of non-trawl fishery data. This lack of AF data required fixing the selectivity for 'other' using prior parameter values based on the maturity ogive.

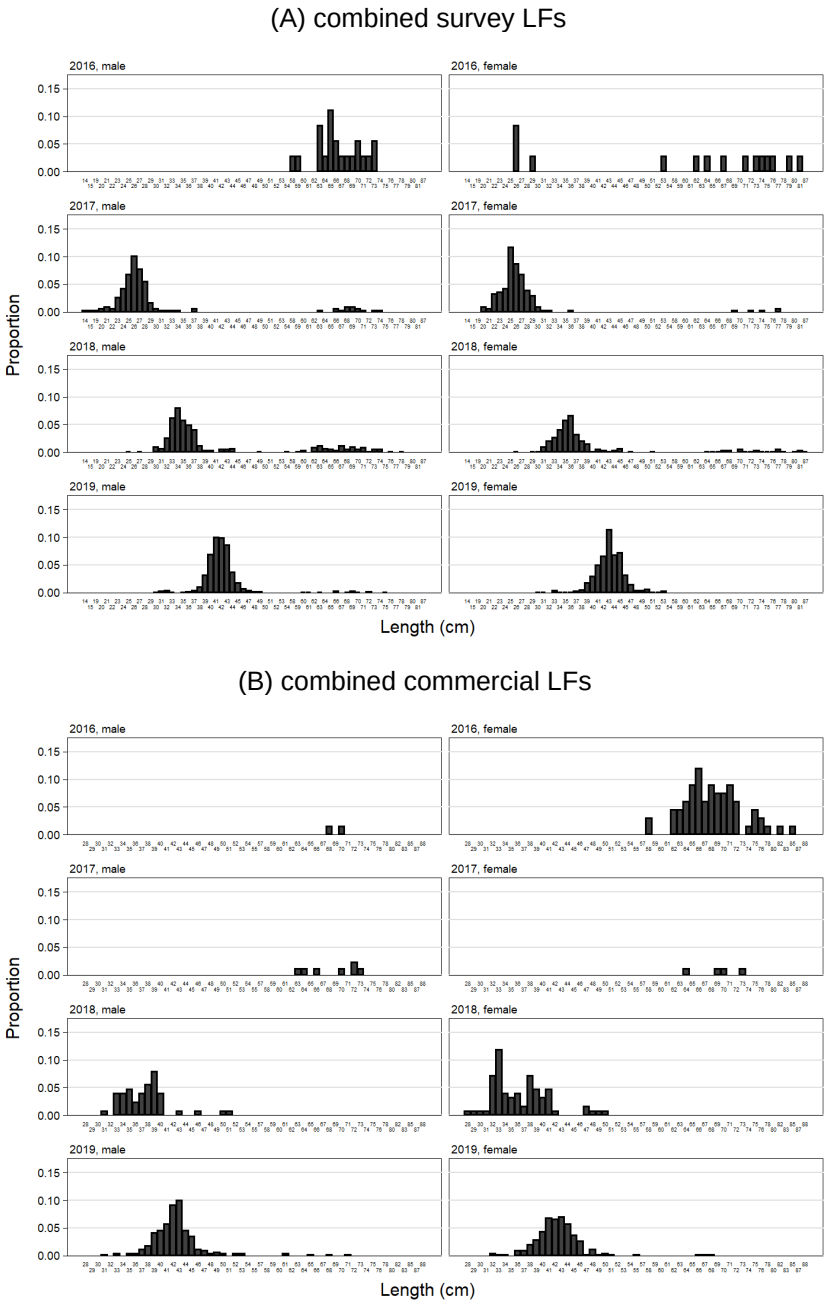

Figure 3. Unweighted BOR length frequencies by year, beginning in 2016. All available research survey data are combined in the top panel, while the commercial data are combined in the bottom panel. The number of length observations in each data source/year/sex cell can be found in Table D.14.

Considerable amounts of age frequency data were available for most survey years from the four synoptic survey series used in the model. This was because the surveys were instructed to sample every captured BOR, given the low stock status estimated for this species. However the number of fish sampled in most years was low because of the poor abundance levels for this species (see Table D.6 for the number of age observations by year and survey). There were no biological data available from the NMFS Triennial or the GIG Historical surveys, which required fixing the selectivities for these two using prior parameter values based on the maturity ogive.

The survey AFs were scaled to represent the total survey in a manner similar to that used for the commercial samples: within an area stratum, samples were weighted by the BOR catch density in the sampled tows; stratum samples were then weighted by the stratum areas (described in APPENDIX D Section D.2.2).

6.2. AGEING ERROR

Ageing error is a common issue in most age-structured stock assessments. Figure D.18 suggests that BOR ages estimated by the primary readers were often not reproduced consistently by secondary readers when performing spot-check analyses. The base population model for BOR, by necessity, used an ageing error matrix. In past assessments, a matrix based on uniform distributions between minimum and maximum ages by all readers for each age (Figure D.19) had been tried; however, for BOR such a matrix was not usable (model did not converge).

After many trials, one ageing error matrix was adopted that comprised: (i) narrow error for ages 1-4 from a normal distribution with quantiles 0.01 to 0.99 spanning three age classes along rows from the diagonal (Figure D.20, left), and (ii) wide error for ages 5-50 where the error was based on expanding CVs (increasing from 0.2 to 0.4 for ages 5 to 50) spanning seven age classes along rows from the diagonal (Figure D.20, right). The narrow error structure was adopted for the young ages (1-4y) because we had adjusted the age proportions to match a presumed 2016 year class. The narrow ageing error matrix (Figure D.20, left) was used in its entirety as a sensitivity run to explore the effect of this assumption on the stock assessment results.

6.3. TREATMENT OF THE 2016 COHORT

Figure D.18 shows that there was ageing error even in the youngest ages, with misclassification occurring because of lack of experience among the agers with otoliths from such young fish in this species (Stephen Wischniowski 2019, DFO Sclerochronology Laboratory, pers. comm.). This led to problems when fitting the model to the age frequency data, with some runs putting the strong cohort into the 2015 year class rather than into 2016. Misalignment in the birth year would result in misleading projections, with the biomass increasing too soon. This was not an acceptable result, given that one of the primary purposes of this stock assessment was to evaluate the impact of this large recruitment event.

The length frequency data associated with the large recruitment event were examined by year, sex and data source (research survey or commercial). The length frequencies clearly showed the recruitment of a single year class that dominated the available data, with a sharp increase in the number of observations (Table D.14) and with modal progression of lengths in each year (research: Figure 3, top; commercial: Figure 3, bottom). Median length by sex and year corroborated the growth progression of the new recruitment, with the 2016 cohort showing up in the survey data as age 1 in 2017, lying between 23 and 29 cm for both males and females (Figure D.21; Table D.15). The cohort grew to 31-39 cm as age 2s in both the commercial and research data and was between 39-47 cm by 2019 as age 3s (Figure D.21; Figure D.22). These lengths were consistent with the length-at-age predictions made by the two growth models used in this stock assessment (Table D.16).

Given this evidence that the observed strong recruitment of BOR could be assigned to a single cohort, we assumed that all juvenile BOR in the age composition data belonged to the 2016 cohort by combining the observed frequencies for ages 1 to 4 into a single proportion that was placed in the appropriate age class depending on the year. This was done for both the commercial and survey data.

6.4. GROWTH PARAMETERS

Growth and allometric length-weight parameters were estimated from BOR length and age data using biological samples collected from the recent synoptic surveys conducted between 2003 and 2019 (APPENDIX D). We were concerned that the ageing error discussed above (see Section 6.2) could potentially bias the estimation of the growth parameters. In order to compensate for this possible bias, we fitted the growth model in a Bayesian context while adjusting for ageing error using the Stan probabilistic programming language which fits the von-Bertalanffy model as a random effects non-linear model (Sean Anderson 2019, DFO Groundfish, pers. comm. and Bocaccio TWG). We implemented this model under two ageing error assumptions: (i) CV of age by age readers' determination of age, and (ii) empirical CV of lengths at age. The resulting models differed little among each other or with the maximum likelihood model fitted without ageing error (see Table D.5). We selected the model that used the empirical CV of lengths at age for use in the stock assessment because it showed the most contrast with the maximum likelihood model. We also ran a sensitivity model run using the maximum likelihood growth function.

Female BOR are notably larger on average than males and BOR are among the largest of all *Sebastes* species (L_∞: F=80.1 cm, M=67.9 cm).

6.5. MATURITY AND FECUNDITY

The proportions of females that mature at ages 1 through 40 were computed from biological samples. Stage of maturity was determined macroscopically, partitioning the samples into one of seven maturity stages (Stanley and Kronlund 2000; described in APPENDIX D). Fish assigned to stages 1 or 2 were considered immature while those assigned to stages 3-7 were considered mature. Data representing staged and aged females (using the B&B method) were pooled from research and commercial trips and the observed proportion mature at each age was calculated. All months were used in creating the maturity curve because these data provided cleaner fits than using a subset of months. A monotonic increasing maturity-at-age vector was constructed by fitting a half-Gaussian function (Equation D.3, equivalent to that in Equation E.7) to the observed maturity values (APPENDIX D, Section D.1.4). The ogive used in the model assigned proportions mature to zero for ages 1 to 4, then switched to the fitted monotonic function for ages 5 to 40, all forced to 1 (fully mature) after age 10. This strategy follows previous BC rockfish stock assessments where it was recognised that younger ages are not well sampled and those that are tend to be larger and more likely to be mature (e.g., Stanley et al. 2009) (Figure D.22). Females older than age 10 were assumed to be 100% mature and maturity was assumed to be constant over time. Fecundity was assumed to be proportional to the female body weight.

6.6. NATURAL MORTALITY

We were not successful in estimating BOR natural mortality (*M*) within the model because of difficulties in finding true minima, given the low abundance of mature fish and the considerable amount of ageing error assumed in the model. Models which appeared to minimise had very poor MCMC diagnostics, indicating a failure for the procedure to converge. The American BOR stock assessments either fix or estimate *M* at 0.15-0.18 (MacCall 2008; He and Field 2017). These values seemed too high for BC BOR, given that 1% of the age observations were >50 and that there were three observations at 60 or greater. Table D.9 gives estimates of *M* using three estimators (Hoenig 1983; Then et al. 2015; Gertseva 2018, pers. comm. citing Hamel 2015) across three trial maximum ages (50, 55, and 60). These *M* estimates vary from 0.077 to 0.136, although we discount the Then et al. (2015) estimates after a computational

issue was identified by Vladlena Gertseva (2018, Northwest Fisheries Science Center, NOAA, pers. comm.) in the Redstripe Rockfish assessment (Starr and Haigh 2020a). We tried fixed values of *M* from 0.06 to 0.10, with mixed results. These models often had difficulty in finding appropriate minima and were sensitive to the starting *M* values, with models that failed to minimise succeeding when the fixed *M* value was adjusted by a very small increment. We obtained usable MCMC diagnostics with *M*=0.07, M=0.08 and *M*=0.09 as well as for *M*=0.06 and *M*=0.095. The model with fixed *M*=0.06 tended to rebuild more quickly than the models with higher *M* and estimated very low stock sizes. We rejected these models because we believed that the ageing data were inconsistent with a low *M*. At the other extreme, the high fixed *M* models estimated very large stock sizes that we felt were inconsistent with stock sizes estimated for other rockfish species in recent stock assessments (e.g. Widow Rockfish: Starr and Haigh 2021b). Consequently, we chose to proceed with *M*=0.07, 0.08 and 0.09 as the basis of our major axis of uncertainty, given the prior estimates from the credible natural mortality estimators and consistency with other BC rockfish stock assessments where the age distributions were similar to that seen in BOR.

6.7. STEEPNESS

A Beverton-Holt (BH) stock-recruitment function was used to generate average recruitment estimates in each year based on the biomass of female spawners (Equation E.10). Recruitments were allowed to deviate from this average (Equations E.17 and E.24) in order to improve the fit of the model to the data. The BH function was parameterised using a 'steepness' parameter, *h,* which specified the proportion of the maximum recruitment that was available at 0.2 B_0, where B_0 is the unfished equilibrium spawning biomass (mature females). The parameter *h* was estimated, constrained by a prior developed for west coast rockfish by Forrest et al. (2010) after removing all information for QCS POP (Edwards et al. 2012b). This prior took the form of a beta distribution with equivalent of mean 0.674 and standard deviation 0.168.

7. AGE-STRUCTURED MODEL

A two-sex, age-structured, stochastic model was used to reconstruct the population trajectory of BOR from 1935 to the beginning of 2020. Ages were tracked from 1 to 50, where 50 acted as an accumulator age category. The population was assumed to be in equilibrium with average recruitment and with no fishing at the beginning of the reconstruction. Selectivities by sex for the four synoptic surveys (but not the WCVI Triennial and GIG Historical surveys) and the trawl commercial fishery were estimated using four parameters describing double half-Gaussian functions, although the right-hand limb was assumed to be fixed at the maximum selectivity to avoid the creation of a cryptic population (dome-shaped selectivity was not explored). A second fishery, consisting of amalgamated line and trap fisheries used a fixed selectivity based on the maturity ogive. The model and its equations are described more fully in Appendix E.

The model was fit to the available data by minimising a function which summed the negative log-likelihoods arising from each data set, the deviations from mean recruitment and the penalties stemming from the Bayesian priors.

A composite base case for Bocaccio Rockfish comprised three model runs, and the MCMC posterior samples from the three were pooled for scientific advice to managers. Decisions made during the stock assessment of BOR included:

- fixed natural mortality *M* to three levels: 0.07, 0.08, and 0.09 for a total of three reference models, using 50 as the pooled age *A*:
    - Run01 – fix *M*=0.07, *A*=50;

- Run02 – fix M=0.08, A=50;
- Run03 – fix M=0.09, A=50;

- used six survey abundance index series (WCVI Synoptic, QCS Synoptic, WCHG Synoptic, HS Synoptic, GIG Historical, WCVI Triennial), the first four with AF data;
- used one commercial fishery abundance index series (bottom trawl CPUE index);
- assumed two fisheries (1=commercial trawl; 2=non-trawl capture methods), each with pooled catches and AF data only for the trawl fishery;
- assumed two sexes (females, males);
- used fairly arbitrary selectivity priors based on the fitted maturity function; assumed an age shift of plus one year for males relative to females;
- applied abundance reweighting: added CV process error to index CVs, c_p=0.25 for surveys and c_p=0.1514 for commercial CPUE series (see Appendix F);
- applied composition reweighting: adjusted AF effective sample sizes using the mean-age method of Francis (2011);
- fixed standard deviation of recruitment residuals (σ_R) to 0.9;
- excluded the 1995 survey index from the GIG Historical series (design incompatible);
- excluded water hauls from the WCVI Triennial series;
- excluded the 2016 WCVI Synoptic survey age frequency (caused instability in the minimisations and MCMC simulations);
- used the 'wide' ageing error matrix described in APPENDIX D, Section D.2.3 and plotted in Figure D.20 (right panel).

All model runs were reweighted one time for (i) abundance, by adding process error $c_p \in$ { 0.25, 0.25, 0.25, 0.25, 0.25, 0.25, and 0.1514 } to the index CVs for the six surveys and the commercial trawl CPUE, respectively, and (ii) composition using the procedure of Francis (2011) for age frequencies (see Table E.5).

Nine sensitivity analyses were run (with full MCMC simulations) relative to the central run of the composite base case (Run02: M=0.08, A=50, 'wide' ageing error matrix) to test the sensitivity of the outputs to alternate model assumptions:

- S01 (Run05) – used constrained 'narrow' ageing error matrix (Figure D.20, left);
- S02 (Run07) – decreased σ_R from 0.9 to 0.6;
- S03 (Run08) – increased σ_R from 0.9 to 1.2;
- S04 (Run09) – dropped CPUE index series;
- S05 (Run10) – dropped GIG Historical and WCVI Triennial survey series;
- S06 (Run11) – reduced all commercial catch from 1965 to 1995 by 33%;
- S07 (Run12) – increased all commercial catch from 1965 to 1995 by 50%;
- S08 (Run13) – used MLE von Bertalanffy growth model estimated with no ageing error;
- S09 (Run14) – used full maturity ogive, allowing estimated maturities for ages 1 to 4.

The MPD (mode of the posterior distribution) 'best fit' was used as the starting point for a Bayesian search across the joint posterior distributions of the parameters using the Monte Carlo Markov Chain (MCMC) procedure. All models (base and sensitivity runs), except for S04 and S05, were judged to have converged after 6 million iterations, sampling every 5000th, to give 1200 draws (1000 samples after dropping the first 200 for burn in).

8. MODEL RESULTS

8.1. BASE CASE

8.1.1. Central Run

The model fits to the abundance indices were generally satisfactory (Figures F.1 to F.7), although there were some very large residuals, particularly for the lack of fit to the 2019 QCS Synoptic survey index (Figure F.2). In general, the survey indices were low (given the apparent low BOR biomass) and had little contrast, which meant that the model had little difficulty in fitting the data points. Two notable exceptions to this generalisation was the lack of fit to the very large 1980 Triennial survey index and the failure to match the large uptick in the 2019 QCS Synoptic index. The overall downward trend to the biomass also allowed for a reasonable fit to the CPUE series (Figure F.8).

Fits to the commercial age frequency data showed trends in the residuals, with long runs of negative residuals in the fits to the survey AF data. In particular, the model struggled to match the strong 2016 age frequencies which clearly dominated in the years when that cohort was present. Most of the Pearson residuals generally lay between –1 and +1 although there were some residuals around –2 associated with the 2016 cohort (e.g., Figures F.13, F.15). However, model estimates of mean age tended to match the observed mean ages in nearly every year and for all five age frequency data sets (commercial trawl and the four synoptic surveys; Figure F.20). We tended to accept model runs where the correspondence of the model mean age matched the observed mean age (as in Figure F.20) because we discovered that the models which failed to minimise tended to completely miss these observations, with the model mean age estimates consistently above or below the observations by a wide margin.

Unlike other recent rockfish stock assessments, recruitment estimates have been consistently low at all biomass levels. This is because all the ageing data were relatively recent (since 2003) and, because recent biomass levels have been low, model estimates of recruitment are also low regardless of the underlying level of biomass, resulting in an unusual stock-recruitment relationship (Figure F.21). This behaviour also caused significant auto-correlation in the recruitment deviations at every lag out to about age 10 (Figure F.22). The recruitment for these pre-2016 year classes will also be affected by the size of the 2016 cohort and the requirement imposed in the model for the entire recruitment series to have a mean of zero in log space.

The MPD estimates for the commercial selectivity function differed little from the prior and neatly overlaid the female maturity ogive (see Figure F.23). This was not the case for some of the survey selectivities, with the QCS survey having a broader left-hand variance term while showing little change in the age at maximum selectivity. On the other hand the WCVI survey showed a two-year leftward shift in the maximum selectivity age, but was balanced by little change in the left side variance parameter.

MCMC traces showed acceptable convergence properties (no trend with increasing sample number) for the estimated parameters (Figure F.25), as did diagnostic analyses that split the posterior samples into three equal consecutive segments (Figure F.26) and checked for parameter autocorrelation out to 60 lags (Figure F.27). Most of the parameters (e.g., R_0, h, μ_7)

did not move very much from the initial MPD estimate to a median value that differed from the MPD (Figure F.28).

8.1.2. Composite Base Case

The composite base case comprised three runs which explored the effect of a variable *M* for this stock assessment: (1) $M_{1,2}$ = 0:07, (2) $M_{1,2}$ = 0:08, and (3) $M_{1,2}$ = 0:09.

Uncertainty in *M* was thought to be the most important component of uncertainty in this stock assessment, particularly when it was not possible to estimate this parameter. We explored additional sources of uncertainty through sensitivity runs.

For each run, 1000 MCMC samples were generated then pooled to provide an average stock trajectory for population status and advice to managers. Estimating *M* was not possible given the uninformative nature of the data, showing difficulty with finding a true minimum in the data and with the MCMC runs that estimated *M* exhibiting unstable behaviour without converging.

The three component runs outlined above converged without serious pathologies in the MCMC diagnostics (similar diagnostic results to those outlined for the central run, see APPENDIX E). Figures F.29 to F.31 show diagnostics for the R_0 parameter in each of the three component runs, and Figure F.32 shows the distribution of all the estimated parameters. In most cases, the component runs had parameter estimates with very similar distributions. The R_0, *h*, and *q* parameters varied with *M*, with R_0 increasing and *h* and *q*'s decreasing with increasing *M*. The selectivity patterns differed little among the three *M* estimates (Figure F.32).

The composite base case, comprising three pooled MCMC runs, was used to calculate a set of parameter estimates (Table 1) and derived quantities at equilibrium and those associated with maximum sustainable yield (MSY) (Table 2). The composite base case population trajectory from 1935 to 2020 and projected biomass to 2080 (Figure 4), assuming a constant catch policy of 200 tonnes/year, indicates that the median stock biomass will rebuild to above DFO's Upper Stock Reference (USR = $0.8B_{MSY}$) in less than five years. A phase plot of the time-evolution of spawning biomass and exploitation rate in the two modelled fisheries in MSY space (Figure 5) suggests that the stock has been overfished since the 1990s, with a current position at B_{2020}/B_{MSY} = 0.096 (0.042-0.23) and $u_{2019(trawl)}/u_{MSY}$ = 0.29 (0.12-0.66); $u_{2019(other)}/u_{MSY}$ = 0.011 (0.0042-0.026).

Table 1. Quantiles of the posterior distribution based on 3000 MCMC samples for the main estimated model parameters for the composite base case BOR stock assessment. Except for R_0, subscripts refer to the data source, where 1=QCS Synoptic survey, 2=WCVI Synoptic survey, 3=WCHG Synoptic survey, 4=HS Synoptic survey, 5=WCVI Triennial survey, 6=GIG Historical survey and 7=commercial trawl fishery or CPUE index series. Selectivity parameters appear on the right side of the table.

Value	5%	50%	95%	Value	5%	50%	95%
R_0	703	1,713	4,633	μ_1	7.83	12.0	16.7
h	0.503	0.671	0.846	μ_2	7.60	10.0	13.1
q_1	0.0190	0.0355	0.0578	μ_3	8.74	12.5	16.3
q_2	0.0211	0.0394	0.0647	μ_4	9.69	13.8	17.9
q_3	0.00195	0.00356	0.00566	μ_7	9.24	11.1	13.4
q_4	0.00438	0.00826	0.0136	Δ_1	0.499	0.983	1.46
q_5	0.0340	0.0573	0.0910	Δ_2	0.393	0.863	1.35
q_6	0.0130	0.0221	0.0342	Δ_3	0.473	0.976	1.46
q_7	0.000196	0.000321	0.000445	Δ_4	0.509	0.979	1.45
	-	-	-	Δ_7	0.576	1.04	1.51
	-	-	-	$\log v_{1L}$	3.72	4.59	5.35
	-	-	-	$\log v_{2L}$	3.01	3.80	4.58
	-	-	-	$\log v_{3L}$	2.18	3.30	4.49
	-	-	-	$\log v_{4L}$	3.67	4.41	5.07
	-	-	-	$\log v_{7L}$	2.97	3.55	4.14

Table 2. Parameter and derived parameter quantiles from the 3000 samples of the MCMC posterior of the composite base case. Note that all vulnerable biomass definitions are provided using the respective fishery selectivity. Definitions: B_0 – unfished equilibrium spawning biomass (mature females), V_0 – unfished equilibrium vulnerable biomass (males and females), B_{2020} – spawning biomass at the start of 2020, V_{2020} – vulnerable biomass in the middle of 2019, u_{2019} – exploitation rate (ratio of total catch to vulnerable biomass) in the middle of 2019, u_{max} – maximum exploitation rate (calculated for each sample as the maximum exploitation rate from 1935-2019), B_{MSY} – equilibrium spawning biomass at MSY (maximum sustainable yield), u_{MSY} – equilibrium exploitation rate at MSY, V_{MSY} – equilibrium vulnerable biomass at MSY. All biomass values (including MSY) are in tonnes. The average catch over the last 5 years (2015-19) was 69 t.

From model output

Value	**5%**	**50%**	**95%**
B_0	16,460	32,289	71,710
V_0 (trawl)	27,930	55,089	123,319
V_0 (other)	27,286	53,564	119,116
B_{2019}	552	899	1,655
V_{2020} (trawl)	3,046	5,703	12,273
V_{2020} (other)	2,582	4,709	9,812
B_{2020} / B_0	0.0132	0.0278	0.0578
V_{2020} / V_0 (trawl)	0.0496	0.104	0.213
V_{2020} / V_0 (other)	0.0426	0.0875	0.175
u_{2019} (trawl)	0.0121	0.025	0.0441
u_{2019} (other)	0.000467	0.000930	0.00161
u_{max} (trawl)	0.0369	0.0588	0.0792
u_{max} (other)	0.00654	0.00968	0.0124

MSY-based quantities

Value	**5%**	**50%**	**95%**
MSY	703	1,461	3,623
B_{MSY}	4,134	9,462	22,469
$0.4B_{MSY}$	1,653	3,785	8,988
$0.8B_{MSY}$	3,307	7,570	17,976
B_{2020} / B_{MSY}	0.0417	0.0963	0.2340
B_{MSY} / B_0	0.225	0.291	0.353
V_{MSY}	7,858	17,554	41,876
V_{MSY} / V_0 (trawl)	0.252	0.319	0.378
V_{MSY} / V_0 (other)	0.253	0.328	0.396
u_{MSY}	0.054	0.085	0.133
u_{2019} / u_{MSY} (trawl)	0.116	0.291	0.664
u_{2019} / u_{MSY} (other)	0.00421	0.0109	0.0258

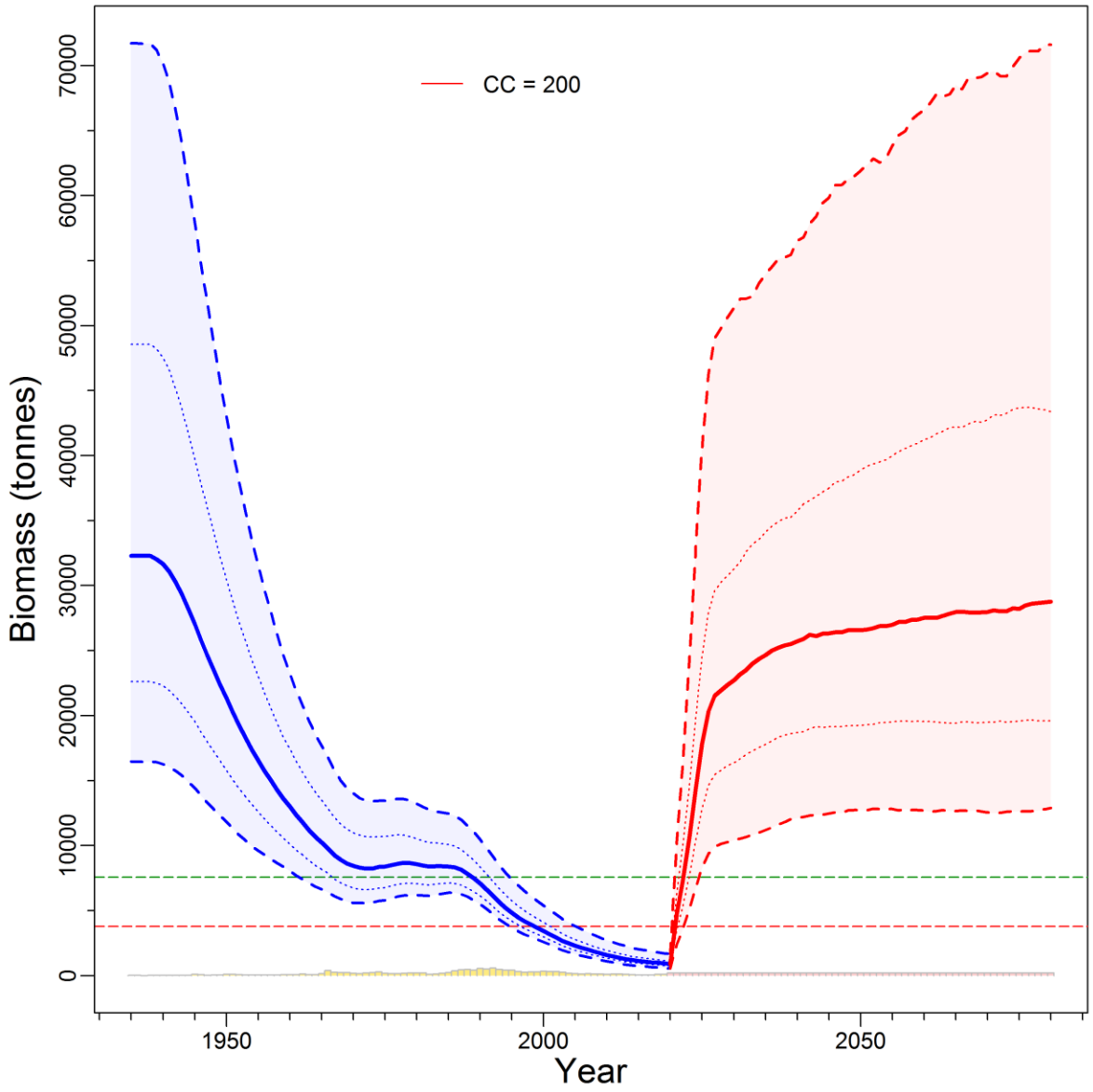

Figure 4. Estimates of spawning biomass B_t (tonnes) for the composite base case. The median biomass trajectory appears as a solid curve surrounded by a 90% credibility envelope (quantiles: 0.05-0.95) in light blue and delimited by dashed lines for years t=1935-2020; projected biomass appears in light red for years t=2021-2080. Also delimited is the 50% credibility interval (quantiles: 0.25-0.75) delimited by dotted lines. The horizontal dashed lines show the median LRP = $0.4B_{MSY}$ and USR = $0.8B_{MSY}$. Catch and assumed catch policy (200 tonnes/year) are represented as bars along the bottom axis.

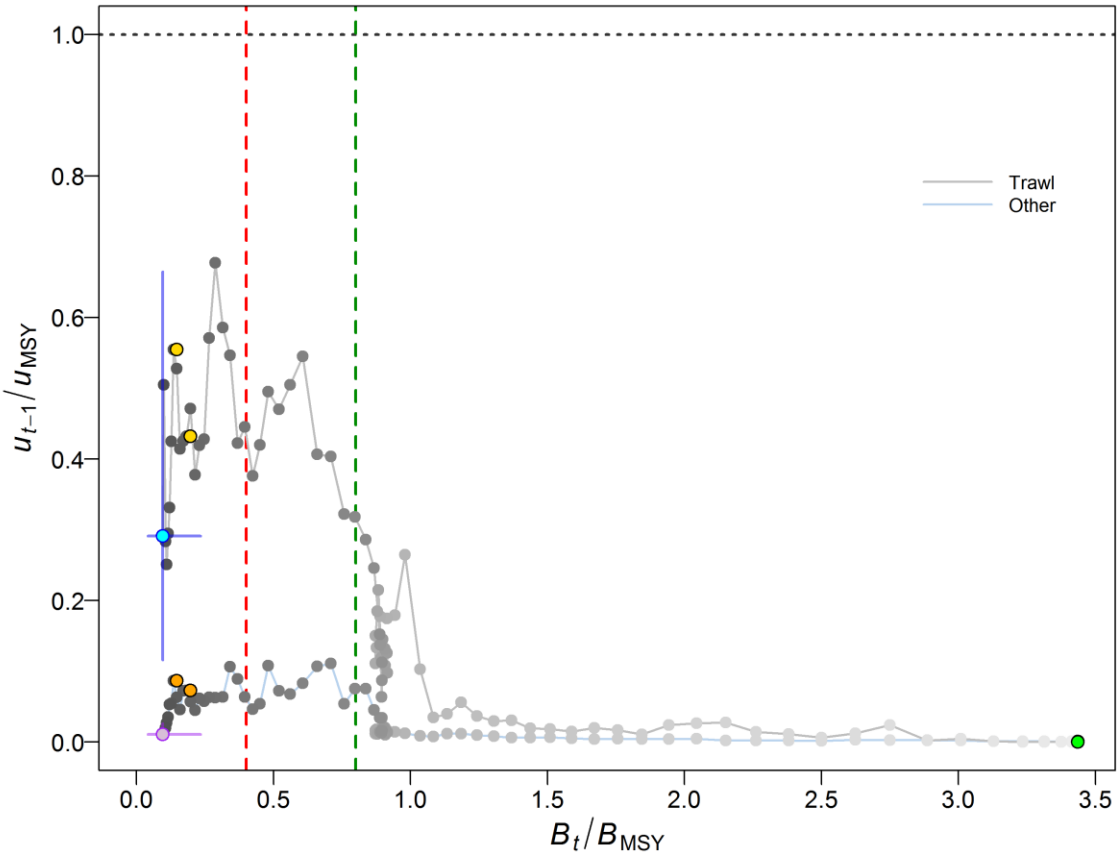

Figure 5. Phase plot through time of the medians of the ratios B_t/B_{MSY} (the spawning biomass at the start of year t relative to B_{MSY}) and two measures of fishing pressure: trawl ($u_{t-1(trawl)}/u_{MSY}$: cyan dot) and other ($u_{t-1(other)}/u_{MSY}$: purple dot) (both represent the exploitation rate in the middle of year t-1 relative to u_{MSY} for each fishery) for the composite base case. The filled green circle is the starting year (1935). Years then proceed from light grey through to dark grey with the final year (t=2020) as a filled cyan or purple circle, and the blue/purple lines represent the 0.05 and 0.95 quantiles of the posterior distributions for the final year. Previous assessment years (2008, 2012) are indicated by gold/orange circles. Red and green vertical dashed lines indicate the PA provisional LRP = $0.4B_{MSY}$ and USR = $0.8B_{MSY}$, and the horizontal grey dotted line indicates u_{MSY}.

8.2. SENSITIVITY ANALYSES

Nine sensitivity analyses were run (with full MCMC simulations) relative to the central run of the composite base case (see Section 7 for details) to test the sensitivity of the outputs to alternative model assumptions. Each sensitivity run was reweighted once (as were the component base runs) before MCMC simulation. The differences among the sensitivity runs (including the central run) are summarised in tables of median parameter estimates (Table F.61) and median MSY-based quantities (Table F.62).

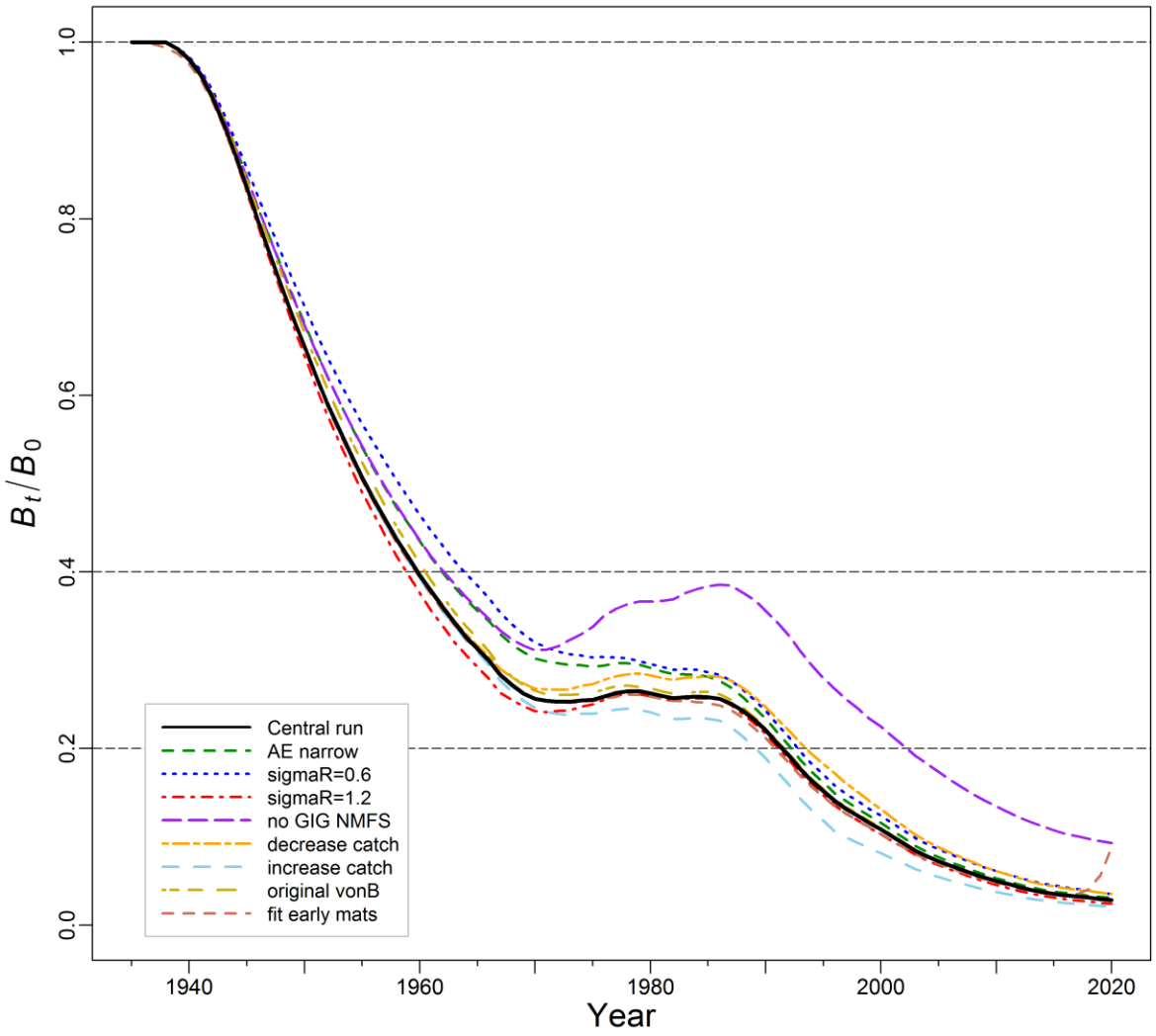

Figure 6. Model median trajectories of spawning biomass as a proportion of unfished equilibrium biomass (B_t/B_0) for the central run and eight sensitivity runs (see legend lower left). Horizontal dashed lines show alternative reference points used by other jurisdictions: $0.2B_0$ (~DFO's USR), $0.4B_0$ (often a target level above B_{MSY}), and B_0 (equilibrium spawning biomass).

The trajectories of the B_t medians relative to B_0 (Figure 6) indicate that dropping the GIG Historical and the WCVI Triennial surveys (S05) resulted in the most optimistic scenario, while the most pessimistic run S07 was the increased pre-1996 catches (foreign and pre-observer domestic). All of these sensitivity runs (apart from S05), tended to closely reflect the central run, particularly at the end of the reconstruction period where all models estimated similar low spawning biomass levels at the beginning of 2020. The overall conclusion is that, other than being sensitive to values of *M*, the model outcome is largely driven by the data because the only substantive changes in advice resulted when data series were omitted or changed. It is interesting to note that this model, unlike other recent rockfish models, needs the stabilising influence of the CPUE series and the early trawl survey data, because the runs which omitted these data were not credible. This may be due to the lack of contrast in the research survey biomass indices and the consequent poor recruitment which result in a monotonic declining trend, which is known to be hard to fit in this type of model.

The diagnostic plots (Figures F.40-F.42) suggest that six of the nine sensitivities exhibited good MCMC behaviour, one was marginal but provisionally acceptable, one had poor diagnostics and one was so poor it needed to be rejected:

- Good – no trend in traces, split-chains align, little or no autocorrelation
    - S02 (σ_R=0.6)
    - S03 (σ_R =1.2)
    - S06 (-33% pre-1996 commercial catch)
    - S07 (+50% pre-1996 commercial catch)
    - S08 (use MLE non-linear von Bertalanffy model)
    - S09 (use full maturation ogive, including maturity estimates for ages 1–4)
- Marginal – trace trends temporarily interrupted, split-chains somewhat frayed, some autocorrelation
    - S01 ('narrow' ageing error matrix)
- Poor – trace trends fluctuate or show a persistent increase/decrease, split-chains differ from each other, substantial autocorrelation
    - S05 (drop GIG Historical and WCVI Triennial surveys)
- Unacceptable – trace trends show a persistent increase that has not levelled, split-chains differ markedly from each other, substantial autocorrelation
    - S04 (drop CPUE series)

The run that dropped CPUE (S04) clearly did not converge, climbing in one long correlated trend (see Figure F.40). The model needs the stability introduced by this series, because the biomass trajectory is a 'one-way trip', a configuration that is notoriously difficult to estimate reliably (Hilborn and Walters 1992). Consequently, the results from this run have not been reported. Similarly, the run which dropped the two early surveys (S05) also showed convergence difficulties, although not as extreme as for sensitivity run S04. These results are reported, showing a model run which does not decline as rapidly as the central run and has a median estimate of B_{2020}/B_0 of 0.093, which is notably higher than for the remaining sensitivity runs (Figure 6).

The 'narrow' ageing error run was meant to show the sensitivity of the stock assessment to this ageing error assumption. Although the relative trajectory for this run departs from the central run between 1960 and 1980, the two runs converge after 1980 and end up in the same place (Figure 6), indicating that the model predictions are robust to the ageing error assumptions tested. Similarly, decreasing σ_R to 0.6 increased the model predictions for B_t/B_0 slightly relative to the central run (median B_{2020}/B_0 is estimated at 0.033 instead of 0.021) while there was virtually no difference compared to the central run when σ_R was increased to 1.2.

Changing the catch histories predictably affected the model predictions, with run S06 (decrease by 33%) slightly improving B_t/B_0 relative to the central run while the opposite occurred when the catch was increased by 50% (run S07). It is not known how accurate the reconstructed catch history is in the base runs and the other sensitivity runs, but what is presented is the best that can be done at present with the available information.

Sensitivity run S08 uses the MLE von-Bertalanffy growth model which makes virtually identical model predictions compared to the central run. This is a good result, indicating that this stock

assessment is not sensitive to the alternative growth model estimated in a more traditional manner. Finally, sensitivity run S09 shows that the assumption that young (<age 5) BOR make no contribution to the spawning population has an important effect on the current estimates of stock status, given that the 2016 cohort has only reached age 4 by the end of 2019 (beginning of 2020). While we are not prepared to alter this assumption (for reasons given in APPENDIX D, Section D.1.4), we note that the 2020 estimates of stock status for all runs except S09 represent the status of the BOR population prior to the recruitment of the 2016 cohort.

9. ADVICE FOR MANAGERS

9.1. REFERENCE POINTS

The Sustainable Fisheries Framework (SFF, DFO 2009) established provisional reference points, which incorporate the 'precautionary approach' (PA), to guide management and assess harvest in relation to sustainability. These reference points are the limit reference point (LRP) of $0.4B_{MSY}$ and the upper stock reference point (USR) of $0.8B_{MSY}$, which have been adopted by previous rockfish assessments (Edwards et al. 2012 a,b, 2014 a,b; Starr et al. 2014[2], 2016; Haigh et al. 2018; Starr and Haigh 2021a,b) and so are used here. Note that, to determine the suitability of these reference points for this stock (or any *Sebastes* stock) would require a separate investigation involving simulation testing using a range of operating models.

The zone below $0.4B_{MSY}$ is termed the 'Critical Zone' by the SFF, the zone lying between $0.4B_{MSY}$ and $0.8B_{MSY}$ is termed the 'Cautious Zone', and the region above the upper stock reference point ($0.8B_{MSY}$) is termed the 'Healthy Zone'. Generally, stock status is evaluated as the probability of the spawning female biomass in year t being above the reference points, i.e., $P(B_t > 0.4B_{MSY})$ and $P(B_t > 0.8B_{MSY})$. The SFF also stipulates that, when in the Healthy Zone, the fishing mortality must be at or below that associated with MSY under equilibrium conditions (u_{MSY}). Furthermore, fishing mortality is to be proportionately ramped down when the stock is deemed to be in the Cautious Zone, and set equal to zero when in the Critical Zone.

The term 'stock status' should be interpreted as 'perceived stock status at the time of the assessment for the year ending in 2019 (i.e., beginning of year 2020)' because the value is calculated as the ratio of two estimated biomass values (B_{2020}/B_{MSY}) by a specific model using the data available up to 2019. Further, the estimate of B_{MSY} depends on the model assessment of stock productivity as well as the catch split among fisheries (if there are more than one). Therefore, comparisons of stock status among various model scenarios can be misleading because the B_{MSY} space is not the same from one model to the next.

MSY-based reference points estimated within a stock assessment model can be highly sensitive to model assumptions about natural mortality, stock recruitment dynamics (Forrest et al. 2018), and the distribution of catch among the component fisheries. As a result, other jurisdictions use reference points that are expressed in terms of B_0 rather than B_{MSY} (e.g., N.Z. Ministry of Fisheries 2011), because B_{MSY} is often poorly estimated as it depends on estimated parameters and a consistent fishery distribution (although B_0 shares several of these same problems). Therefore, the reference points of $0.2B_0$ and $0.4B_0$ are also presented in APPENDIX E. These are default values used in New Zealand respectively as a 'soft limit', below which management action needs to be taken, and a 'target' biomass for low productivity stocks, a mean around which the biomass is expected to vary. The 'soft limit' is equivalent to the upper stock reference (USR, $0.8B_{MSY}$) in the provisional DFO Sustainable Fisheries Framework while a 'target' biomass is not specified by the provisional DFO SFF. Results are provided comparing projected biomass to B_{MSY} and to current spawning biomass B_{2020}, and comparing projected harvest rate

to current harvest rate u_{2019} (APPENDIX E). A full suite of results based on COSEWIC indicators is also presented in APPENDIX E (and see Section 9.3).

9.2. STOCK STATUS AND DECISION TABLES

Stock status for DFO managers is usually defined as the current spawning biomass relative to the estimated spawning biomass required for maximum sustainable yield (MSY). Plots that depict distributions of B_{2020}/B_{MSY} in three zones (Critical, Cautious, Healthy) delimited by $0.4B_{MSY}$ (LRP) and $0.8B_{MSY}$ (USR), show that the BOR composite base case lies in the Critical Zone with a probability >0.99, as do the three component runs (Figure 7).

Stock status plots for sensitivity runs based on the central run of the BOR composite base case (Figure 8) show that almost all of the sensitivity runs also lie with a high probability in the Critical Zone, with the exceptions of S05 (drop GIG and Triennial surveys) and S09 (use entire estimated maturity ogive), with both runs showing some probability of being in the Cautious Zone (46% for S05 and 28% for S09). Sensitivity run S05 shows poor MCMC convergence properties and should be interpreted as showing the importance of including the early surveys as opposed to providing a credible estimate of stock status. The results from sensitivity run S09 demonstrate the importance of the new recruitment from the 2016 year class and the sensitivity of the estimate of stock status to the assumption that BOR less than age 5 do not contribute to the spawning population.

Decision tables for the BOR composite base case provide advice to managers as probabilities that current and projected biomass B_t (t = 2020, ..., 2030) will exceed biomass-based reference points (or that projected exploitation rate u_t will fall below harvest-based reference points) under constant-catch policies (Table 3) or constant harvest rate policies (Table 4). These two tables present probabilities that projected B_t using the composite base case will exceed the LRP and the USR or will be less than the harvest rate at MSY (in Table 3 only). Alternative decision tables for the composite base case can be found in APPENDIX E (Tables F5-F52), including the number of years to reach the various targets (Tables F53-F.60).

Assuming that a catch of 200 t will be taken each year for the next 5 years, Table 3 indicates that a manager would be >99% certain that both B_{2025} and B_{2030} lie above the LRP of $0.4B_{MSY}$, 92% certain that B_{2025} and 97% certain that B_{2030} lie above the USR of $0.8B_{MSY}$, and 100% certain that u_{2025} and u_{2030} lie below u_{MSY} for the composite base case. Similarly, Table 4 indicates that under a harvest policy of 0.04/year, a manager would be >99% certain that both B_{2025} and B_{2030} lie above the LRP of $0.4B_{MSY}$, 91% certain that B_{2025} and 93% certain that B_{2030} lie above the USR of $0.8B_{MSY}$. Generally, it is up to managers to choose the preferred catch levels or harvest levels using their preferred risk levels. For example, it may be desirable to be 95% certain that B_{2025} exceeds an LRP whereas exceeding a USR might only require a 50% probability. Assuming this risk profile, all the catch policies in Table 3 and the harvest policies in Table 4 would satisfy the specified LRP and USR constraints. Assuming that u_{MSY} is a target exploitation rate, all the catch policies in Table 3 beginning in 2024 define harvest rates that would be less than u_{MSY} with a probability of at least 95%.

We caution that, although uncertainty is built into the assessment and its projections by taking a Bayesian approach for parameter estimation and by constructing a composite base case that spans ranges of inestimable parameter values, these results depend heavily on the assumed model structure, the informative priors, and data assumptions (particularly the average recruitment assumptions) used for the projections. This latter problem should not be a large problem over the next 5-10 years, if the 2016 year class is anywhere near as strong as this stock assessment suggests.

Table 3. Decision tables for the reference points $0.4B_{MSY}$, $0.8B_{MSY}$, and u_{MSY} for 1-10 year projections for a range of constant catch policies (in tonnes) using the composite base case. Values are the probability (proportion of 3000 MCMC samples) of the female spawning biomass at the start of year t being greater than the B_{MSY} reference points, or the exploitation rate of vulnerable biomass in the middle of year t being less than the u_{MSY} reference point. For reference, the average catch over the last 5 years (2015-2019) was 69 t.

$P(B_t > 0.4B_{MSY})$

Catch policy	2020	Projection year 2021	2022	2023	2024	2025	2026	2027	2028	2029	2030
0	<0.01	0.66	0.88	0.97	0.99	>0.99	>0.99	>0.99	>0.99	>0.99	>0.99
50	<0.01	0.66	0.88	0.97	0.99	>0.99	>0.99	>0.99	>0.99	>0.99	>0.99
100	<0.01	0.66	0.88	0.97	0.99	>0.99	>0.99	>0.99	>0.99	>0.99	>0.99
150	<0.01	0.66	0.88	0.97	0.99	>0.99	>0.99	>0.99	>0.99	>0.99	>0.99
200	<0.01	0.65	0.87	0.97	0.99	>0.99	>0.99	>0.99	>0.99	>0.99	>0.99
250	<0.01	0.65	0.87	0.97	0.99	>0.99	>0.99	>0.99	>0.99	>0.99	>0.99
300	<0.01	0.65	0.87	0.96	0.99	>0.99	>0.99	>0.99	>0.99	>0.99	>0.99
350	<0.01	0.65	0.86	0.96	0.99	>0.99	>0.99	>0.99	>0.99	>0.99	>0.99
400	<0.01	0.64	0.86	0.96	0.99	>0.99	>0.99	>0.99	>0.99	>0.99	>0.99
450	<0.01	0.64	0.86	0.96	0.99	0.99	>0.99	>0.99	>0.99	>0.99	>0.99
500	<0.01	0.64	0.86	0.96	0.99	0.99	>0.99	>0.99	>0.99	>0.99	>0.99
550	<0.01	0.64	0.85	0.96	0.98	0.99	>0.99	>0.99	>0.99	>0.99	>0.99
600	<0.01	0.64	0.85	0.95	0.98	0.99	0.99	>0.99	>0.99	0.99	0.99

$P(B_t > 0.8B_{MSY})$

Catch policy	2020	Projection year 2021	2022	2023	2024	2025	2026	2027	2028	2029	2030
0	0	0.21	0.49	0.73	0.87	0.94	0.96	0.97	0.97	0.97	0.98
50	0	0.20	0.49	0.73	0.87	0.93	0.96	0.97	0.97	0.97	0.97
100	0	0.20	0.49	0.73	0.86	0.93	0.96	0.97	0.97	0.97	0.97
150	0	0.20	0.48	0.72	0.85	0.93	0.96	0.96	0.96	0.97	0.97
200	0	0.20	0.48	0.72	0.85	0.92	0.95	0.96	0.96	0.96	0.97
250	0	0.20	0.48	0.72	0.85	0.92	0.95	0.96	0.96	0.96	0.96
300	0	0.20	0.48	0.71	0.85	0.92	0.94	0.95	0.96	0.96	0.96
350	0	0.20	0.47	0.71	0.84	0.91	0.94	0.95	0.95	0.96	0.96
400	0	0.19	0.47	0.70	0.84	0.91	0.94	0.95	0.95	0.95	0.95
450	0	0.19	0.46	0.70	0.83	0.90	0.93	0.94	0.94	0.95	0.95
500	0	0.19	0.46	0.70	0.83	0.90	0.93	0.94	0.94	0.94	0.94
550	0	0.19	0.46	0.69	0.82	0.89	0.93	0.93	0.93	0.93	0.94
600	0	0.19	0.45	0.68	0.82	0.89	0.92	0.93	0.93	0.93	0.93

$P(u_t < u_{MSY})$

Catch policy	2020	Projection year 2021	2022	2023	2024	2025	2026	2027	2028	2029	2030
0	1	1	1	1	1	1	1	1	1	1	1
50	1	1	1	1	1	1	1	1	1	1	1
100	>0.99	>0.99	1	1	1	1	1	1	1	1	1
150	0.98	>0.99	>0.99	1	1	1	1	1	1	1	1
200	0.95	0.99	>0.99	>0.99	>0.99	1	1	1	1	1	1
250	0.89	0.97	0.99	>0.99	>0.99	>0.99	1	1	1	1	1
300	0.81	0.94	0.99	0.99	>0.99	>0.99	>0.99	>0.99	>0.99	>0.99	>0.99
350	0.72	0.91	0.97	0.99	>0.99	>0.99	>0.99	>0.99	>0.99	>0.99	>0.99
400	0.63	0.86	0.96	0.99	0.99	>0.99	>0.99	>0.99	>0.99	>0.99	>0.99
450	0.56	0.82	0.93	0.97	0.99	0.99	0.99	>0.99	>0.99	0.99	0.99
500	0.49	0.76	0.91	0.96	0.98	0.99	0.99	0.99	0.99	0.99	0.99
550	0.42	0.71	0.88	0.95	0.97	0.98	0.99	0.99	0.99	0.99	0.99
600	0.36	0.65	0.85	0.93	0.96	0.98	0.98	0.98	0.98	0.98	0.98

Table 4. Decision tables for the reference points $0.4B_{MSY}$ and $0.8B_{MSY}$ for 1-10 year projections for a range of constant harvest rate policies (as proportion of vulnerable biomass) using the composite base case. Values are the probability (proportion of 3000 MCMC samples) of the female spawning biomass at the start of year t being greater than the B_{MSY} reference points. For reference, the average harvest rate over the last 5 years (2015-2019) was 0.026.

$P(B_t > 0.4B_{MSY})$

Harvest		Projection year									
policy	2020	2021	2022	2023	2024	2025	2026	2027	2028	2029	2030
0.00	<0.01	0.66	0.88	0.97	0.99	>0.99	>0.99	>0.99	>0.99	>0.99	>0.99
0.01	<0.01	0.66	0.88	0.97	0.99	>0.99	>0.99	>0.99	>0.99	>0.99	>0.99
0.02	<0.01	0.66	0.88	0.97	0.99	>0.99	>0.99	>0.99	>0.99	>0.99	>0.99
0.03	<0.01	0.66	0.87	0.97	0.99	>0.99	>0.99	>0.99	>0.99	>0.99	>0.99
0.04	<0.01	0.65	0.87	0.96	0.99	>0.99	>0.99	>0.99	>0.99	>0.99	>0.99
0.05	<0.01	0.65	0.87	0.96	0.99	>0.99	>0.99	>0.99	>0.99	>0.99	>0.99
0.06	<0.01	0.65	0.86	0.96	0.99	>0.99	>0.99	>0.99	>0.99	>0.99	0.99
0.07	<0.01	0.65	0.86	0.96	0.99	0.99	>0.99	>0.99	>0.99	0.99	0.99
0.08	<0.01	0.64	0.86	0.96	0.98	0.99	>0.99	>0.99	0.99	0.99	0.99
0.09	<0.01	0.64	0.85	0.95	0.98	0.99	0.99	0.99	0.99	0.99	0.98
0.10	<0.01	0.64	0.85	0.95	0.98	0.99	0.99	0.99	0.99	0.98	0.98
0.11	<0.01	0.64	0.85	0.95	0.98	0.99	0.99	0.99	0.98	0.97	0.97
0.12	<0.01	0.63	0.84	0.95	0.98	0.99	0.99	0.98	0.98	0.97	0.96

$P(B_t > 0.8B_{MSY})$

Harvest		Projection year									
policy	2020	2021	2022	2023	2024	2025	2026	2027	2028	2029	2030
0.00	0	0.21	0.49	0.73	0.87	0.94	0.96	0.97	0.97	0.97	0.98
0.01	0	0.2	0.49	0.73	0.86	0.93	0.96	0.96	0.96	0.97	0.97
0.02	0	0.2	0.49	0.72	0.85	0.92	0.95	0.96	0.96	0.96	0.96
0.03	0	0.2	0.48	0.72	0.85	0.92	0.94	0.95	0.95	0.95	0.95
0.04	0	0.2	0.48	0.71	0.84	0.91	0.93	0.94	0.94	0.94	0.93
0.05	0	0.2	0.47	0.7	0.83	0.9	0.92	0.93	0.92	0.92	0.92
0.06	0	0.19	0.47	0.7	0.83	0.89	0.92	0.92	0.91	0.9	0.89
0.07	0	0.19	0.46	0.69	0.82	0.88	0.91	0.91	0.89	0.88	0.87
0.08	0	0.19	0.46	0.68	0.81	0.87	0.89	0.89	0.87	0.85	0.85
0.09	0	0.19	0.45	0.67	0.8	0.86	0.88	0.87	0.85	0.83	0.81
0.10	0	0.19	0.45	0.66	0.79	0.85	0.86	0.85	0.83	0.8	0.78
0.11	0	0.18	0.44	0.65	0.78	0.83	0.85	0.83	0.8	0.77	0.75
0.12	0	0.18	0.43	0.65	0.77	0.82	0.84	0.81	0.77	0.74	0.71

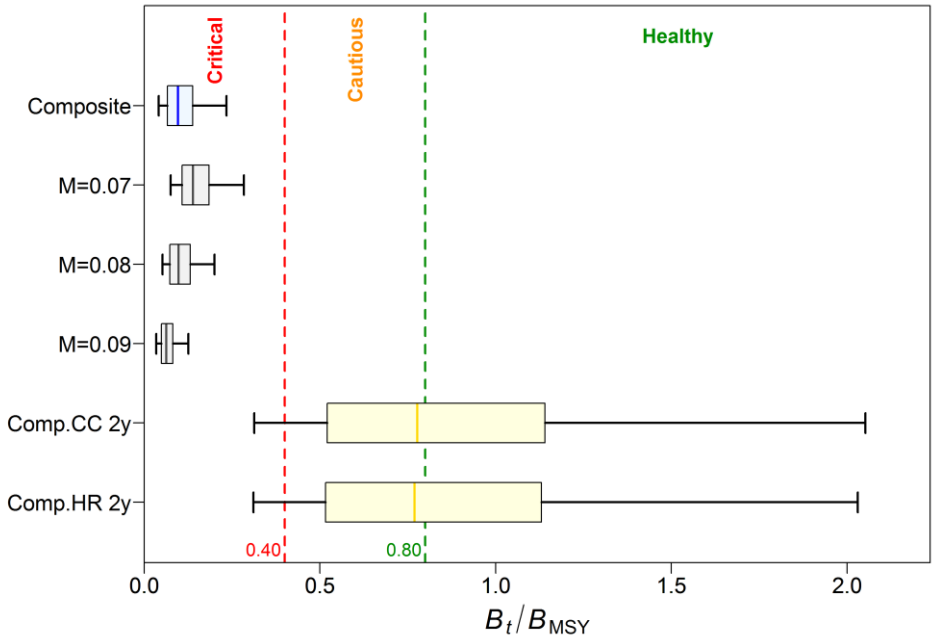

Figure 7. Status of the coastal BOR stock relative to the DFO PA provisional reference points of $0.4B_{MSY}$ and $0.8B_{MSY}$ for the t=2020 composite base case and the component base runs that are pooled to form the composite base case. Also shown are projected stock status for the composite base case at the beginning of 2022 after fishing at a constant catch=200 tonnes/year or a constant exploitation rate of 0.04/year. Model year 2022 is the second year that the 2016 cohort is assumed to contribute to the spawning population. Boxplots show the 0.05, 0.25, 0.5, 0.75 and 0.95 quantiles from the MCMC posterior.

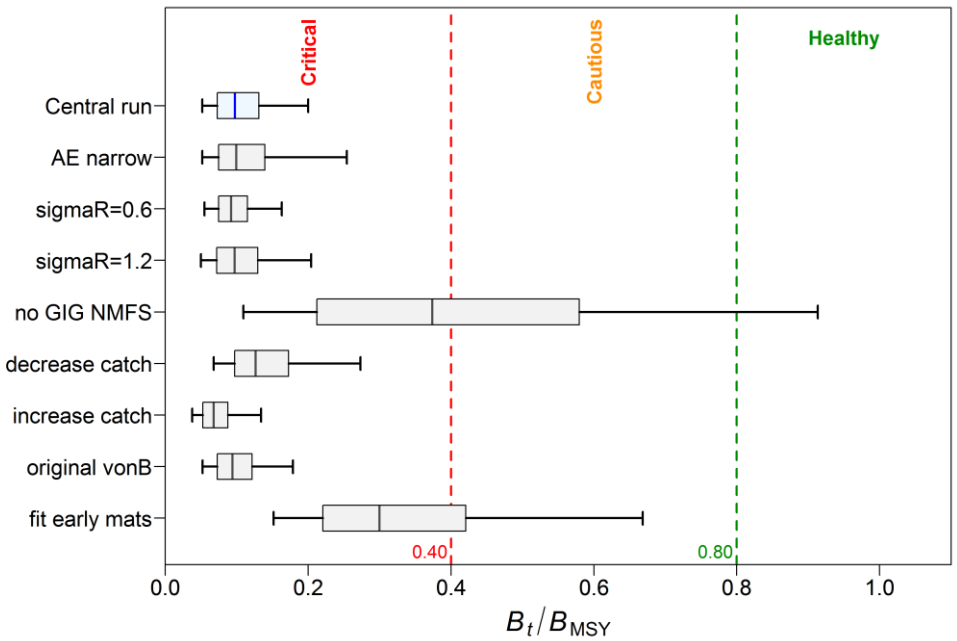

Figure 8. Stock status at beginning of 2020 of the BOR stock relative to the DFO PA provisional reference points of $0.4B_{MSY}$ and $0.8B_{MSY}$ for the central run of the composite base case and eight sensitivity runs (see y-axis notation and sensitivity descriptions in the main text). Boxplots show the 0.05, 0.25, 0.5, 0.75 and 0.95 quantiles from the MCMC posterior. APPENDIX E contains the details of these sensitivity runs.

9.3. STOCK REBUILDING

Bocaccio was assessed in 2012 and reference points were established. The biomass was estimated to be less than the Limit Reference Point (LRP), necessitating the development of a rebuilding plan, which was drafted based on the 2012 stock assessment. While the latter provided valuable short-term, tactical advice, it did not contain all of the information that should be considered in a rebuilding plan (e.g. simulations and evaluation of rebuilding efforts projected over 1.5 to 2 generations, as described in the rebuilding plan policy). The Department's guidance document for the development of Rebuilding Plans recommends that rebuilding plans undergo regular performance reviews (in addition to annual monitoring and evaluation).

According to DFO's (2009) SFF Precautionary Approach policy, a key component specifies that:

> *"when a stock has reached the Critical Zone, a rebuilding plan must be in place with the aim of having a high probability of the stock growing out of the Critical Zone within a reasonable timeframe"*

Further, GMU's IFMP document (Appendix 9) contains rebuilding objectives and milestones for various species, including Bocaccio:

> **Rebuilding objective** – *"Achieve rebuilding throughout the species' range and grow out of the critical zone within three generations, with a 65% probability of success."*
>
> **Milestones** – *"Achieve a positive stock trajectory trend in each 5 year interval, such that the biomass at the end of each 5 year period is greater than the biomass at the beginning of the same 5 year period. Between major assessments, progress towards this goal will be monitored by annually reviewing fishery dependent and fishery independent indices of stock trajectory."*

The median stock status, estimated by the composite base case to be $B_{2020}/B_0 = 0.028$, places this stock in DFO's Critical Zone; however, because the proportion mature in the model was forced to zero for ages 1-4, the spawning population in 2020 (end of 2019) does not include any fish from the 2016 cohort, which would be age 4 in 2020. Sensitivity run S09 explores the effect of allowing the fitted model estimates for the proportion mature for ages 1-4 to operate, which allows some of these young fish to enter the spawning population and raises the median stock status to $B_{2020}/B_0 = 0.088$ with a 0.46 probability of being in the Cautious Zone (Figure 8). While this result shows that even small proportions of the 2016 year class could have a positive effect on the estimated stock status, this outcome depends on the large estimated size of the 2016 year class and ignores the possibility that the proportion mature may be overestimated in the younger age classes.

Rebuilding for BOR can be tracked through the following decision tables in APPENDIX E:

- Tables F.5 and F.6 provide probabilities of 10-y projected spawning biomass exceeding the LRP, i.e., $P(B_{2021,\ldots2030} > 0.4B_{MSY})$ for constant catch and harvest rate policies, respectively;
- Tables F.21 and F.22 provide probabilities of projected spawning biomass for three generations (60 years, assuming generation time is 20 years) at 5-year intervals exceeding the LRP for constant catch and harvest rate policies, respectively;
- Tables F.53 to F.60 provide the time in years it would take to achieve various targets, including the LRP, for constant catch and harvest rate policies, respectively, with probabilities of 50%, 65%, 80%, and 95%.

The Bocaccio stock is unusual in that the large 2016 recruitment event will raise the spawning stock above the LRP with 95% probability by 2023 under all constant catch (Table F.5) and

harvest rate (Table F.6) scenarios presented, thus meeting the first GMU objective. Further, it will remain above the LRP for the next three generations under constant catch polices with a high probability (Table F.21), thus meeting the second GMU objective. Only under harvest rate scenarios greater than 0.08/year does the spawning stock biomass begin to decline such that the probability of remaining above the LRP falls below 95% (Table F.22). Parallel tables F.53 and F.54 show time to exceed the LRP with 95% probability to be 3 years. If managers are less stringent in their certainty, e.g., a 65% probability of success stated in the first rebuilding objective above, then Tables F55 and F.56 indicate that exceeding the LRP will occur in 1 year.

A major uncertainty in these projections is the absolute size of the 2016 cohort, with the composite base model estimating this cohort to be 44 times the long-term average recruitment (range: 30-58). In an attempt to better understand the sensitivity of the projection results to this large cohort size, the projections were repeated using the MCMC samples taken from the lowest 5% of the posterior distribution of the estimated 2016 cohort (Figure 9). The biomass trajectories represented by these 150 sample draws were then projected across the same range of fixed catch and fixed harvest rate scenarios presented in Table 3 and Table 4. Figure 10 is analogous to Figure 4, showing the biomass trajectory using only the 150 lowest (5%) samples projected at a fixed catch level of 200 tonnes/year. This figure and the associated decision tables (Tables F.63 and F.64) indicate that the overall delay in rebuilding predicted from this truncated scenario is only 2-3 additional years relative to the equivalent prediction based on the full 2016 cohort posterior. The main reason for this continued optimism is that the predicted cohort strength from this truncated scenario is still 31 times (range 20-37) greater than the long-term average (which includes the 2016 cohort) and that this truncated sub-sample will contain many runs with lower overall productivity, which will result in overall lower levels of B_0, B_{MSY} and MSY-based reference points.

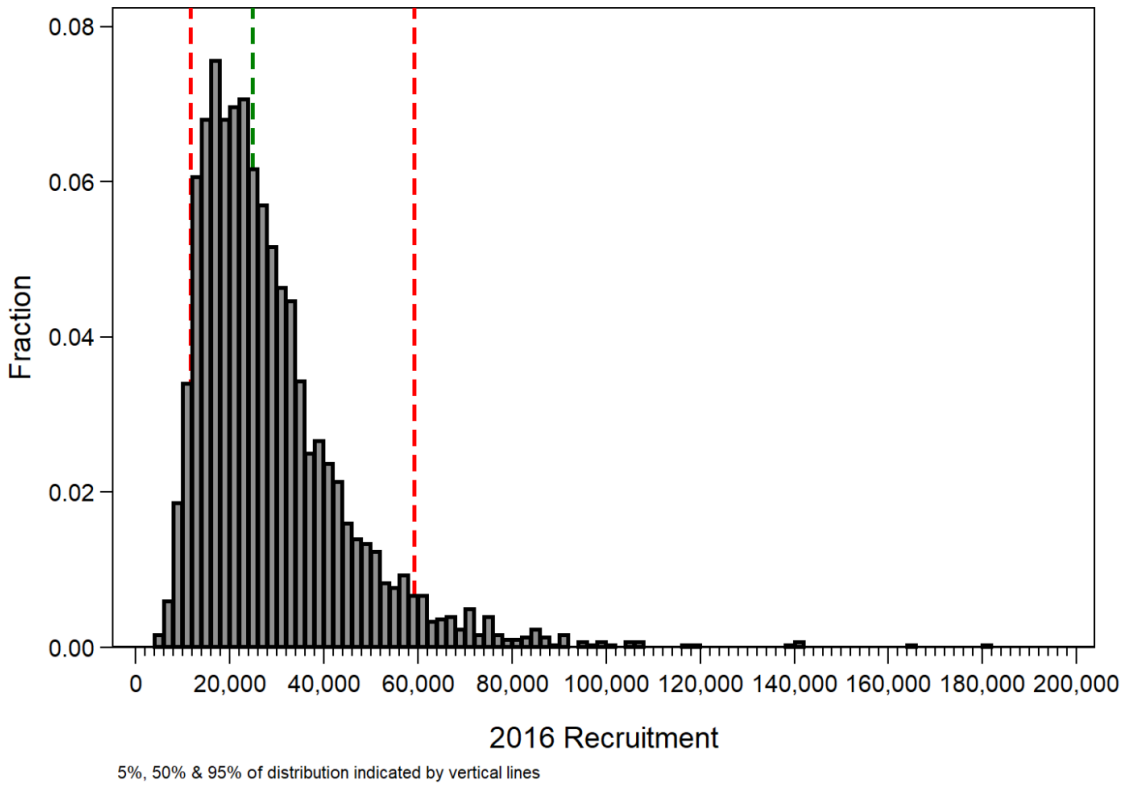

Figure 9. Posterior distribution of the 2016 recruitment cohort for the coastwide BOR stock. The 5%, 50% and 95% percentiles of the distribution are marked with dashed vertical lines.

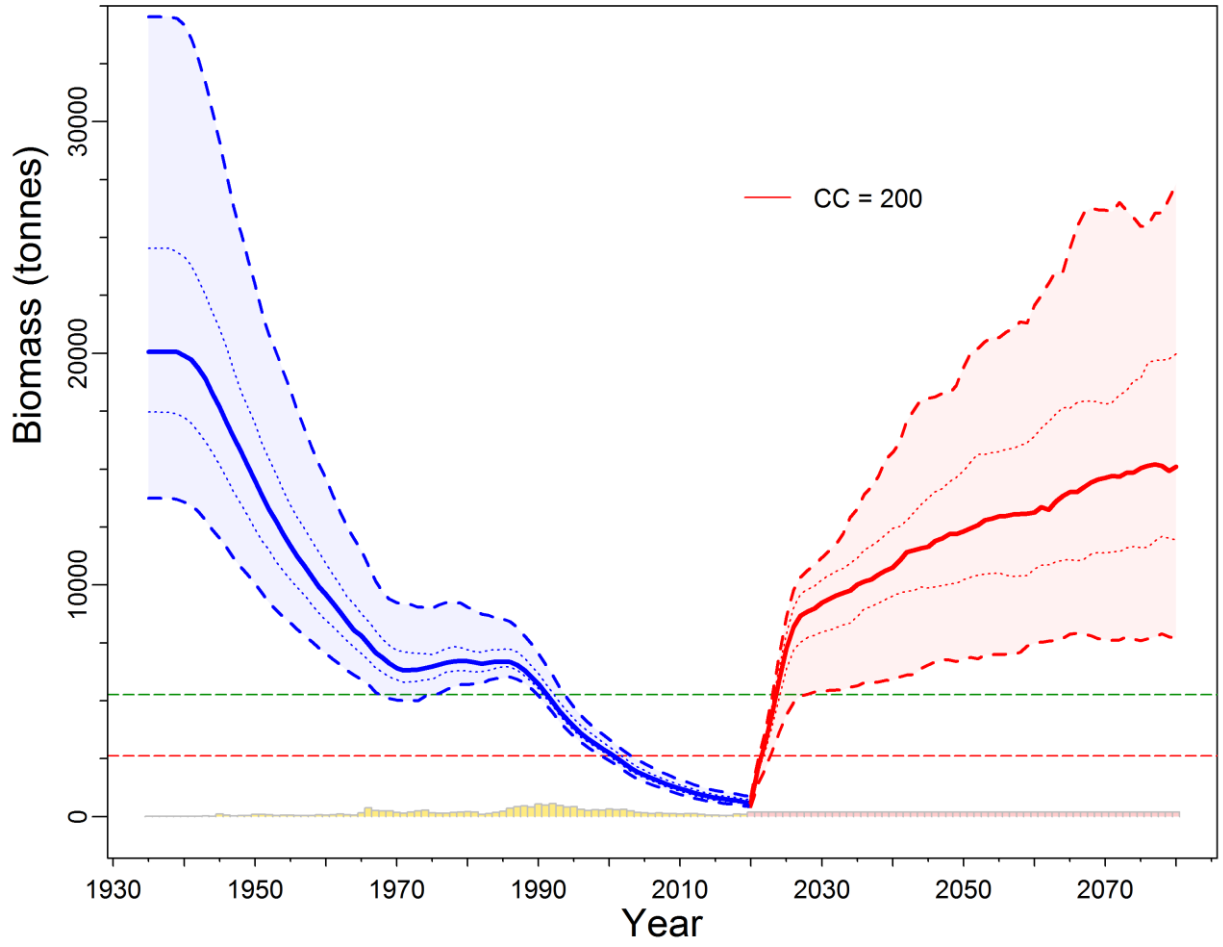

Figure 10. Estimates of spawning biomass B_t (tonnes) for the MCMC draws with the lowest (bottom 0.05 quantile) estimates for the 2016 cohort size from the composite base case. The median biomass trajectory appears as a solid curve surrounded by a 90% credibility envelope (quantiles: 0.05-0.95) in light blue and delimited by dashed lines for years t=1935-2020; projected biomass appears in light red for years t=2021-2080. Also delimited is the 50% credibility interval (quantiles: 0.25-0.75) delimited by dotted lines. The horizontal dashed lines show the median LRP and USR. Catch and assumed catch policy (200 tonnes/year) are represented as bars along the bottom axis.

The COSEWIC assessment criteria are based on a decline in the total number of mature individuals over the most recent 10 years or 3 generations, whichever is longer. Given our modelling framework, we calculated decline in terms of female spawning biomass rather than mature individuals, because we have no estimates of mature males and vulnerable biomass can be a mixture of mature and immature fish. Because the generation time for Bocaccio is estimated to be 20 years, three generations (60 years) was used as the period over which to calculate the decline.

COSEWIC indicator A1 is reserved for those species where the causes of the reduction are clearly reversible, understood, and ceased. Indicator A2 is used when the population reduction may not be reversible, may not be understood, or may not have ceased. Similar to Yellowmouth Rockfish in a recovery potential analysis (Edwards et al 2012a), Bocaccio would like likely fall into category A2b (where the 'b' indicates that the designation was based on 'an index of abundance appropriate to the taxon'). Under A2, a species is considered Endangered or Threatened if the decline has been ≥50% or ≥30%, respectively. Using these guidelines, the recovery reference criteria become $0.5B_{t\text{-}3G}$ (a 50% decline) and $0.7B_{t\text{-}3G}$ (a 30% decline), where

$B_{t\text{-}3G}$ is the biomass three generations (60 years) previous to the biomass in year t, e.g., P($B_{2021,...,2080} > 0.5|0.7\ B_{1961,...B2020}$). This criterion would indicate recovery of BOR in 4 years for $0.5B_{t\text{-}3G}$ (Tables F.37, F.38) and 5 years for $0.7B_{t\text{-}3G}$ (Tables F.39, F.40). Using the stricter targets of $0.5B_0$ and $0.7B_0$ would require longer times to achieve with 65% certainty (Tables F.55, F.56).

9.4. ASSESSMENT SCHEDULE

Advice was also requested concerning the appropriate time interval between future stock assessments and, for the interim years between stock updates, potential values of indicators that could trigger a full assessment earlier than usual (as per DFO 2016). The response to this issue depends completely on the strength of the recruiting 2016 year class. If it continues to show a strength consistent with the evaluation in this stock assessment, coastal BOR should rebuild to levels above USR in 4-5 years. The existing synoptic trawl surveys, particularly the QCS and WCVI surveys, should provide adequate signals of continuing stock strength. The next full stock assessment should be scheduled after 2025, such that there will be at least two new indices from both the QCS and WCVI Synoptic surveys. If BOR continues to show strength in these surveys, a new stock assessment could be delayed even longer. Regardless of when a new stock assessment is to be initiated, at least 6-12 months lead time is required before the new stock assessment is initiated to allow for the reading of new ageing structures that will be needed for the interpretation of the population trajectory. Advice for interim years is explicitly included in the decision tables and managers can select another line on the table if stock abundance appears to have changed or if greater certainty of staying above the reference point is desired. Another possible intermediate option would be to repeat model fits without modification to the three component runs comprising the combined base run in late 2021 or early 2022 by adding in the index values and associated biological data from the four synoptic surveys. All four surveys will have added one additional index year by that time. This will allow for a relatively straightforward evaluation of the progress of the 2016 cohort without requiring a full re-analysis of the available data.

10. GENERAL COMMENTS

In common with other BC rockfish stock assessments, this stock assessment depicts a slow-growing, low productivity stock. However what is unusual about this stock assessment is that coastal BOR appears to be even less productive than would be expected, given the apparent rate of natural mortality suggested by the available ageing information. This is borne out by the low exploitation rates estimated by the model, which reach their highest point at around 0.06/year, a level much lower than that seen in other recent rockfish stock assessments. For instance, the recently completed Widow Rockfish stock assessment (Starr and Haigh, 2020b) estimated a maximum median exploitation rate near 0.16/year for a stock which was evaluated to be in the Healthy Zone and which has shown a number of good recruitment events. On the other hand, BOR has steadily declined over the period 1935-2020, in spite of the low exploitation rates and the successful management that has reduced recent average removals to less than 100 tonnes per year.

Although the high relative errors associated with the various BOR survey indices (APPENDIX B) indicate that this methodology is not ideal for monitoring this schooling semi-pelagic species (Stanley et al. 2009), the available survey series either show a declining trend, or more recently, no trend. This is consistent with the ageing data which show few, if any, notable recruitment events and with the CPUE series, which also depicts a declining trend from 1996 to 2012. These are the signals that combined give a pessimistic stock assessment that is largely consistent with the 2009 and 2012 Bayesian surplus production stock assessments.

However, what distinguishes this stock assessment from the previous two BOR stock assessments is the signal of new recruitment in the form of the strong 2016 year class. The median estimate by the composite base model is that this cohort is 44 times the long-term average recruitment (95% credible range: 30-58). There have been many anecdotal reports of juvenile BOR from amateur fishers as well as the commercial fishing fleet, who have complained that this new BOR recruitment is making it difficult to stay within the allotted catch caps while fishing for other species. Additionally, independent young-of-year surveys along the central BC coast (Alejandro Frid 2019, Central Coast Indigenous Resource Alliance, pers. comm.) and along the California coast (John Field 2019, Southwest Fisheries Science Center, NOAA, pers. comm.) have also detected a substantial number of juvenile BOR in 2016 and in following years. The data presented in this paper corroborate the existence of this new recruitment. For instance, compare over time the distribution of BOR densities in the QCS survey, with the 2015 survey devoid of BOR (Figure B.29, right), followed by the 2017 survey where BOR is much more frequent, but with low densities because they are 25-cm age-1 fish (Figure B.30, right). By the time the 2019 survey was conducted, BOR were found throughout the survey area, in good densities (Figure B.31, right) and the model was unable to match the increase in the observed biomass in spite of the wide error bars (Figure F.2), which implies that this index was very large relative to the previous indices. The length frequency data presented in Figure 3 show a single cohort dominating the frequencies by number, which progresses annually in accordance with the growth model in both the amalgamated survey data and in the commercial fishery data. Another measure of the increased abundance of BOR in the surveys is the number of biological samples collected, because the standing instructions were to sample every BOR encountered. For instance, both the QCS and WCVI surveys show large increases in the number sampled in 2018 and 2019 compared to previous surveys (Table D.6). While these are independent data sources that can attest to an observed increase in the abundance of BOR, the difficulty for the stock assessment is to estimate the absolute size of this recruitment and its consequent impact on rebuilding this depleted population.

The US population of BOR south of Monterey was "*formally designated as overfished in March of 1999*" (He et al. 2015). However, that designation has now been lifted after two large recruitment events in 2010 and 2013. The stock was reassessed in 2017, confirming the existence and size of the 2013 year class (He and Field 2017), with He and Field (2017) reporting an increase in stock status from $0.37B_0$ in 2015 to $0.49B_0$ in 2017, a substantial increase over a short period largely attributed to the improved recruitment. These results confirm that the relative size of the biomass increase shown in Figure 4 has also been seen previously in the California BOR population.

Foreign fleet effort in 1965-76 along the BC coast targeted POP, and BOR catch for these years was estimated as an assumed bycatch; therefore, the magnitude of the foreign fleet removals of BOR is uncertain. Another source of uncertainty in the catch series comes from domestic landings from the mid-1980s to 1995 (pre-observer coverage) which may have misreported lesser rockfish species to bypass quota restrictions on more desirable species like POP. However, the sensitivity runs on catch (S06: -33%; S07: +50%) show that catch uncertainty did not have a major effect on the model's biomass trajectory or on the estimates of the relative stock size in 2020 (Figure 6, Figure 8).

The use of commercial CPUE as an index of abundance is generally avoided in BC rockfish stock assessments (primarily due to uncertainty in vessel behaviour in response to regulations). However, we have successfully used CPUE based on the bycatch of the evaluated species in the BC bottom trawl fishery in three recent stock assessments (Widow Rockfish: Starr and Haigh 2021b; Redstripe Rockfish: Starr and Haigh, 2021a; Shortspine Thornyhead: Starr and Haigh 2017). The presumption in these instances was that these species are taken passively by

the fishery in conjunction with a range of other finfish species. As long as the CPUE estimation model included the incidence of zero tows as well as the tows which captured the species, the resulting series would potentially track abundance. Because of the high level of observer coverage in the BC bottom trawl fishery, there is confidence that zero tows are being recorded reasonably accurately. In the case of this BOR stock assessment, the presence of the CPUE series in the model stabilised the estimation procedure, particularly in the MCMC simulations. This has been demonstrated by Sensitivity run S04, which shows that the stock assessment would fail without the use of these data. In addition, the fit of the estimated model trajectory to the CPUE indices for the central run indicates that there is consistency between the CPUE series and survey biomass series, with minimal pattern in the residuals (see Figure F.8). We dropped this series after 2012 because of reports that the fleet was actively avoiding this species which could result in a biased series.

A major source of uncertainty for this stock assessment is the inability of the model to estimate *M*, given the available data. As discussed in Section 6.6, this assessment attempted to bracket plausible values of natural mortality based on the observed frequency of older ages in the data. Given the prior estimates provided by credible natural mortality estimators, we proceeded with *M*=0.07, 0.08 and 0.09 as the basis of this axis of uncertainty, having determined that *M* values outside this range had lower credibility given model behaviour and the observed range of available ages, especially for values where $M \geq 0.10$. The high natural morality rates estimated in California BOR populations are inconsistent with the BC age distributions because our maximum ages are twice those seen in California. Furthermore, runs using higher *M* values estimated very large unfished equilibrium biomass that were greater than those estimated in other recent BC *Sebastes* stock assessments for species with similar life history characteristics. Lower fixed values for *M* resulted in faster rebuilding periods coupled with low stock size/productivity estimates. These observations, along with the fact that there were few ages older than age = 50, indicated that model estimates using $M<0.07$ seemed unlikely. However, Figure 7 indicates that the choice of *M* had little impact on the stock status of BOR, with all the component runs comprising the composite base case sitting well within the DFO Critical Zone, even though estimates of stock status (B_{2020}/B_{MSY}, B_{2020}/B_0) changed consistently with *M*.

All this points to the size of the 2016 year class as being the most important uncertainty in this stock assessment. The considerable amount of observational evidence for the existence of this large cohort was discussed above, so there is little uncertainty about this aspect of the recruitment. The US BOR population off the southern California coast has undergone two recent large recruitment events in 2010 and 2013 that has allowed the stock to recover from a depleted state, so it is reasonable to expect that this more northern population could be similarly affected with a lag. The episodic nature of *Sebastes* recruitment is well known and it appears that the BC population has had a very long interval between episodes of good recruitment. Therefore, it seems reasonable to accept the conclusion by this stock assessment that the size of the 2016 year class is considerably larger than the long term mean recruitment and that it is likely to be large enough to rapidly move this stock out of the Critical Zone and into the Healthy Zone.

A projection sensitivity was run using only the lowest 5% of the posterior distribution of the 2016 cohort (Figure 9). The predicted rebuilding times using this truncated sub-sample were only 2-3 years longer than for the times predicted by the full 2016 posterior (see Tables F.63 and F.64), indicating that even the least optimistic portion of the 2016 year class posterior distribution is expected to result in fast rebuilding. The reason for this prediction is that the cohort strength from this truncated scenario is still 31 times (range 20-37) greater than the long-term average (which includes the 2016 cohort). We note that these large ratios for the 2017 recruitment are a function of the very low recruitments estimated by this stock assessment. While the size of the

2016 cohort is very large, cohorts of similar magnitude have been estimated in other *Sebastes* stock assessments (e.g., Widow Rockfish: Starr and Haigh in 2021b).

In addition to the uncertainties noted above in catch history accuracy, CPUE index confounding, data scarcity and projection uncertainty, there are other issues that lead to uncertainty in the results. There are no biomass indices before the mid-1960s and the surveys from that period did not use strong statistical designs. The available age composition data are all recent (only beginning in 2003) and do not seem to be as informative as in other recent rockfish stock assessments, probably because of the considerable amount of ageing error.

Model estimates for the survey catchability coefficients (q) are uniformly low. This is because survey biomass indices (I_{tg}), which contribute the primary source of quantitative information for BOR in BC waters, were all very low before the recruitment of the 2016 cohort. Both tow encounters and tow catch of BOR by all surveys in these years were very low (see density plots provided in Appendix B). However, the QCS Synoptic and WCVI Synoptic surveys detected the increased incidence of BOR after the recruitment of the 2016 cohort. This can be seen in the sequential comparison of density plots for the QCS Synoptic survey, which show an increase in BOR observations from 2015 (Figure B.29) when BOR were virtually invisible, to 2017 (Figure B.30) when many observations of low BOR density appeared, to 2019 (Figure B.31) when many BOR observations had considerable weight (because the 2016 cohort had reached age three in the survey area). A similar comparison can be made for the WCVI Synoptic survey, with the 2016 density plot (Figure B.41) showing very low density of BOR, followed by 2018 (Figure B.42) when there were multiple BOR high-density observations of 2-year old fish. The appearance of these elevated index values late in the time series were not fit well by the model, and the estimated q-values remained low in this assessment. Assuming that future indices remain high, q should increase because the model will estimate that the surveys are catching a greater proportion of the available fish along the BC coast.

The decision tables provide guidance to the selection of short-term catch recommendations and describe the range of possible future outcomes over the projection period at fixed levels of annual catch. The accuracy of the projections is predicated on the model being correct. Uncertainty in the parameters is explicitly addressed using a Bayesian approach but reflects only the specified model and weights assigned to the various data components. These tables indicate that there is little short-term differences among the projected policies.

Another uncertainty flagged in the peer review meeting was the capacity of trawl survey gear to monitor BOR, given the semi-pelagic nature of this species. Habitat preference shifts from pelagic to benthic as members of this species get older. Usually, juveniles and sub adults disperse from kelp canopies to deeper high-relief reef habitats (Love 2011). However, Field et al. (2010) noted that, after a large recruitment event in California, young BOR appeared in suboptimal habitats (low-relief substrata such as sandy bottoms), perhaps due to density-dependent competition for space. This recruitment effect could potentially bias abundance indices from trawl surveys, which can only be deployed over low-relief bottoms, by over-representing year classes when they are large. While young adults often migrate off bottom to chase food, older BOR tend to remain stationary in crevices and caves typical of high-relief habitat (Love 2011), which would make BOR relatively less vulnerable to trawl gear as they age. The peer review participants also noted that survey gear suitability among the various hook and line methods can vary because BOR is primarily attracted to mobile bait (by trolling, jigging, etc.) and tends to shun stationary bait such as that on longline gear (Brian Mose 2019, Groundfish Technical Advisory Committee, pers. comm.). Such behaviour means that the primary survey gears used in BC (bottom trawl and longline) are not optimal for monitoring BOR.

Despite these limitations, the QCS and WCVI Synoptic surveys appear to be capable of monitoring this species reasonably well (at least when abundance is elevated), and should be the best indicator of the continued strength of the 2016 year class. This will allow close monitoring of the situation as the coastal BOR population increases along with an inevitable increase in the bycatch of this species while fishing for the more abundant species. The other two surveys (HS and WCHG Synoptic) appear to be less effective for BOR in terms of catching power, but model runs which dropped these surveys failed to minimise, so they also provide relevant stock information (or model stability). We note that, because catches in the commercial groundfish fisheries are well-monitored, the bycatch of BOR will be well known. Therefore, between having good estimates of BOR catch along with the monitoring power of the four synoptic surveys, the situation for this species will be closely observed, allowing for corrective action to be taken if required.

11. FUTURE RESEARCH AND DATA REQUIREMENTS

The following issues should be considered when planning future stock assessments and management evaluations for Bocaccio rockfish:

1. Continue the suite of fishery-independent trawl surveys that have been established across the BC coast. This includes obtaining age and length composition samples, which will allow the estimation of survey-specific selectivity ogives.
2. Explore how single populations, such as BOR, are part of a complex system consisting of biological and economic components (Walker and Salt 2006). Such systems can have multiple stable states, which may have implications in our understanding of BOR population dynamics and resilience.
3. Explore the effects of climate change on BOR populations and identify how shifts in the ecosystem affect our perception of equilibrium conditions under different climate regimes. This could include exploring the use of environmental covariates as predictors of recruitment, as well as investigating the role of episodic recruitment in the evolutionary strategy used by BOR.
4. The Regional Peer Review meeting held in December 2019 identified the following modelling components that could be investigated the next time that BOR is fully re-assessed:
    a. Investigate using length frequency data in the model to identify cohorts. This could include recovering early length data from surveys such as the NMFS Triennial survey.
    b. Drop commercial age data after 2012 because there may be a selectivity shift due to the management changes invoked for truncating the CPUE series. Alternatively remove these data to test the sensitivity of the model to these data.
    c. There appear to be fewer older females than males in the population, particularly in the survey data. This observation could be modelled as a differential natural mortality in females or as dome-shaped selectivity for females, given the possibility that older BOR are thought to migrate to untrawlable areas. It is also possible that the early age selectivity for the large cohorts may be different than for the smaller cohorts because of differential habitat occupation.
    d. There is some evidence among rockfish species that fecundity and spawning success improves as fish get older and larger. Fecundity is thought to increase more rapidly (Dick et al. 2017) than the cubic assumption that was made in the current stock assessment and this process could be incorporated into future stock assessments.

e. It was suggested that trawl survey biomass indices for semi-pelagic rockfish could be better estimated using a model-based approach (such as presented for CPUE in Appendix C rather than the design-based approach used in Appendix B).

f. Cohort size estimates made by age-structured models often become smaller as the cohort progresses in age once more data are gathered for the cohort. This effect can be investigated through retrospective analyses which discard annual data as the model moves backward in time.

g. It was noted that selectivity curves for longline surveys/fisheries in California are shifted to the right of selectivity curves for trawl surveys/fisheries. The existence of this shift should be considered if line surveys are used in the future to monitor BOR in BC.

12. ACKNOWLEDGEMENTS

Allan Hicks (International Pacific Halibut Commission) has previously supported the Awatea version of the Coleraine age-structured stock assessment model used in many of DFO's offshore rockfish stock assessments, and for Bocaccio specifically, provided advice on subsetting the recruitment data to attenuate the large 2016 year class. The staff in the Sclerochronology Laboratory at the Pacific Biological Station (PBS) were, as always, quick to process BOR otolith requests, expediting the ageing of the QCS Synoptic survey samples within a month of collection. Members of the BOR technical working group – Sean Anderson, Bruce Turris, Brian Mose, Rob Tadey, and Chris Grandin – were very helpful during a meeting to review data inputs and model assumptions. Written peer reviews by Jaclyn Cleary (PBS, DFO) and Kelly Andrews (Northwest Fisheries Science Center [NWFSC], NOAA) provided helpful guidance and discussion during the regional peer review (RPR) meeting. Greg Workman facilitated the RPR meeting as Chair and Jill Campbell acted as rapporteur. Additional feedback by other RPR participants, particularly John Field (Southwest Fisheries Science Center, NOAA) and Chantel Wetzel (NWFSC, NOAA), contributed greatly to the process.

13. REFERENCES CITED

COSEWIC. 2013. COSEWIC assessment and status report on the Bocaccio *Sebastes paucispinis* in Canada. Committee on the Status of Endangered Wildlife in Canada. Ottawa. x + 49 pp.

DFO. 2009. A fishery decision-making framework incorporating the Precautionary Approach.

DFO. 2016. Guidelines for providing interim-year updates and science advice for multi-year assessments. DFO Can. Sci. Advis. Sec. Sci. Advis. Rep. 2016/020.

DFO. 2019. Pacific Region Integrated Fisheries Management Plan – Groundfish: Effective February 21, 2019 (Version 1.1).

Dick, E.J., Beyer, S., Mangel, M. and Ralston, S. 2017. A meta-analysis of fecundity in rockfishes (genus *Sebastes*). Fisheries Research 187: 73-85.

Edwards, A.M., Haigh, R. and Starr, P.J. 2012a. Stock assessment and recovery potential assessment for Yellowmouth Rockfish (*Sebastes reedi*) along the Pacific coast of Canada. DFO Can. Sci. Advis. Sec. Res. Doc. 2012/095. iv + 188 p.

Edwards, A.M., Haigh, R. and Starr, P.J. 2014a. Pacific Ocean Perch (*Sebastes alutus*) stock assessment for the north and west coasts of Haida Gwaii, British Columbia. DFO Can. Sci. Advis. Sec. Res. Doc. 2013/092. vi + 126 p.

Edwards, A.M., Haigh, R. and Starr, P.J. 2014b. Pacific Ocean Perch (*Sebastes alutus*) stock assessment for the west coast of Vancouver Island, British Columbia. DFO Can. Sci. Advis. Sec. Res. Doc. 2013/093. vi + 135 p.

Edwards, A.M., Starr, P.J. and Haigh, R. 2012b. Stock assessment for Pacific ocean perch (*Sebastes alutus*) in Queen Charlotte Sound, British Columbia. DFO Can. Sci. Advis. Sec. Res. Doc. 2011/111. viii + 172 p.

Field, J.C., Dick, E.J., Pearson, D. and MacCall, A.D. 2010. Status of bocaccio, *Sebastes paucispinis*, in the Conception, Monterey and Eureka INPFC areas for 2009. Stock status report, Southwest Fisheries Science Center, NOAA.

Fletcher, D., Mackenzie, D. and Villouta, E. 2005. Modelling skewed data with many zeros: A simple approach combining ordinary and logistic regression. Environmental and Ecological Statistics12, 45–54.

Forrest, R.E., McAllister, M.K., Dorn, M.W., Martell, S.J.D. and Stanley, R.D. 2010. Hierarchical Bayesian estimation of recruitment parameters and reference points for Pacific rockfishes (*Sebastes* spp.) under alternative assumptions about the stock-recruit function. Can. J. Fish. Aquat. Sci. 67: 1611–1634.

Forrest, R.E., Holt, K.R. and Kronlund, A.R. 2018. Performance of alternative harvest control rules for two Pacific groundfish stocks with uncertain natural mortality: bias, robustness and trade-offs. Fish. Res. 206: 259-286.

Francis, R.I.C.C. 2011. Data weighting in statistical fisheries stock assessment models. Can. J. Fish. Aquat. Sci. 68(6): 1124–1138.

Haigh, R., Starr, P.J., Edwards, A.M., King, J.R. and Lecomte, J.B. 2018. Stock assessment for Pacific Ocean Perch (*Sebastes alutus*) in Queen Charlotte Sound, British Columbia in 2017. DFO Can. Sci. Advis. Sec. Res. Doc. 2018/038. v + 227 p.

Hamel, O.S. 2015. A method for calculating a meta-analytical prior for the natural mortality rate using multiple life history correlates. ICES J. Mar. Sci. 72(1): 62-69.

He, X. and Field, J.C. 2017. Stock assessment update: Status of Bocaccio, *Sebastes paucispinis*, in the Conception, Monterey and Eureka INPFC areas for 2017. Stock status update, Pacific Fishery Management Council, Portland, Oregon.

He, X., Field, J.C., Pearson, D.E., Lefebvre, L. and Lindley, S. 2015. Status of Bocaccio, *Sebastes paucispinis*, in the Conception, Monterey and Eureka INPFC areas for 2015. Stock status report, Pacific Fishery Management Council, Portland, Oregon.

Hilborn, R. and Walters, C.J. 1992. Quantitative Fisheries Stock Assessment: Choice, Dynamics and Uncertainty. Chapman and Hall, New York NY.

Hilborn, R., Maunder, M., Parma, A., Ernst, B., Payne, J. and Starr, P. 2003. Coleraine: A generalized age-structured stock assessment model. User's manual version 2.0. University of Washington Report SAFS-UW-0116. Tech. rep., University of Washington.

Hoenig, J.M. 1983. Empirical use of longevity data to estimate mortality rates. Fish. Bull. 82(1): 898-903.

Love, M.S. 2011. Certainly More Than You Want to Know About The Fishes of The Pacific Coast: A Postmodern Experience. Really Big Press, Santa Barbara CA.

Love, M.S., Yoklavich, M. and Thorsteinson, L. 2002. The Rockfishes of the Northeast Pacific. University of California Press, Berkeley and Los Angeles, California.

MacCall, A.D. 2008. Status of Bocaccio off California in 2007. In Status of the Pacific coast groundfish fishery through 2007, stock assessments and rebuilding analyses. Portland OR, Pacific Fishery Management Council.

Matala, A.P., Gray, A.K. and Gharrett, A.J. 2004. Microsatellite variation indicates population structure of Bocaccio. N. Amer. J. Fish. Manage. 24: 1189-1202.

New Zealand Ministry of Fisheries. 2011. Operational Guidelines for New Zealand's Harvest Strategy Standard. Ministry of Fisheries, New Zealand.

Stanley, R.D., McAllister, M. and Starr, P. 2012. Updated stock assessment for Bocaccio (*Sebastes paucispinis*) in British Columbia waters for 2012. DFO Can. Sci. Advis. Sec. Res. Doc. 2012/109. ix + 73 p.

Stanley, R.D., McAllister, M., Starr, P. and Olsen, N. 2009. Stock assessment for bocaccio (*Sebastes paucispinis*) in British Columbia waters. DFO Can. Sci. Advis. Sec. Res. Doc. 2009/055. xiv + 200 p.

Stanley, R.D., Rutherford, K. and Olsen, N. 2001. Preliminary status report on bocaccio (*Sebastes paucispinis*). DFO Can. Stock Assess. Sec. Res. Doc. 2001/148. 55 p.

Stanley, R.D., Starr, P. and Olsen, N. 2004. Bocaccio update. DFO Can. Sci. Advis. Sec. Res. Doc. 2004/027. vii + 64 p.

Stanley, R.D. and Kronlund, A.R. 2000. Silvergray rockfish (*Sebastes brevispinis*) assessment for 2000 and recommended yield options for 2001/2002. DFO Can. Sci. Advis. Sec. Res. Doc. 2000/173. 116 p.

Starr, P.J. and Haigh, R. 2017. Stock assessment of the coastwide population of Shortspine Thornyhead (*Sebastolobus alascanus*) in 2015 off the British Columbia coast. DFO Can. Sci. Advis. Sec. Res. Doc. 2017/015. ix + 174 p.

Starr, P.J. and Haigh, R. 2021a. Redstripe Rockfish (*Sebastes proriger*) stock assessment for British Columbia in 2018. DFO Can. Sci. Advis. Sec. Res. Doc. 2021/014. vii + 340 p.

Starr, P.J. and Haigh, R. 2021b. Widow Rockfish (*Sebastes entomelas*) stock assessment for British Columbia in 2019. DFO Can. Sci. Advis. Sec. Res. Doc. 2021/039. viii + 238 p.

Starr, P.J., Haigh, R. and Grandin, C. 2016. Stock assessment for Silvergray Rockfish (*Sebastes brevispinis*) along the Pacific coast of Canada. DFO Can. Sci. Advis. Sec. Res. Doc. 2016/042. vi + 170 p.

Then, A.Y., Hoenig, J.M., Hall, N.G. and Hewitt, D.A. 2015. Evaluating the predictive performance of empirical estimators of natural mortality rate using information on over 200 fish species. ICES J. Mar. Sci. 72(1): 82-92.

Walker, B. and Salt, D. 2006. Resilience Thinking: Sustaining Ecosystems and People in a Changing World. Island Press. Washington DC. 192 p.

APPENDIX A. CATCH DATA

A.1. BRIEF HISTORY OF THE FISHERY

Forrester (1969) provides a brief history of the Pacific Marine Fisheries Commission (PMFC), which is reproduced (with some modification) below. Currently, the PMFC is called the Pacific States Marine Fisheries Commission; however, this document retains the acronym 'PMFC' for historical context.

> *The Pacific Marine Fisheries Commission (PMFC) was created in 1947 when the states of Washington, Oregon, and California jointly formed an interstate agreement (called a 'compact') with the consent of the 80th Congress of the USA. In 1956, informal agreement was reached among various research agencies along the Pacific coast to establish a uniform description of fishing areas as a means of coordinating the collection and compilation of otter trawl catch statistics. This work was undertaken by the PMFC with the informal cooperation of the Fisheries Research Board of Canada. Areas 1A, 1B, and 1C encompass waters off the California coast, while Areas 2A-2D involve waters adjacent to Oregon and a small part of southern Washington. The remainder of the Washington coast and the waters off the west coast of Vancouver Island comprise Areas 3A-3D, while United States and Canadian inshore waters (Juan de Fuca Strait, Strait of Georgia, and Puget Sound) are represented by Areas 4A and 4B, respectively. Fishing grounds between the northern end of Vancouver Island and the British Columbia-Alaska boundary are represented by Areas 5A-5E. The entire Alaskan coast is designated as Area 6, but except for a small amount of fishing in inshore channels, this area has not been trawled intensively by North American nationals.*

The early history of the British Columbia (BC) trawl fleet was covered by Forrester and Smith (1972). A trawl fishery for slope rockfish has existed in BC since the 1940s. Aside from Canadian trawlers, foreign fleets targeted Pacific Ocean Perch (POP, *Sebastes alutus*) in BC waters for approximately two decades. These fleets were primarily from the USA (1959–1976), the USSR (1965–1968), and Japan (1966–1976). Consequently, the foreign vessels removed large amounts of rockfish biomass, including species other than POP, in Queen Charlotte Sound (QCS, Ketchen 1976, 1980b), off the west coast of Haida Gwaii (WCHG, Ketchen 1980a,b), and off the west coast of Vancouver Island (WCVI, Ketchen 1976, 1980a,b). All foreign fleets were excluded from Canadian waters inside of 200 nm with the declaration of the EEZ in 1977. Canadian effort escalated in 1985, and for the next decade, landings by species were often misreported to avoid species-specific trip limits.

Before 1977, no quotas were in effect for any slope rockfish species. Since then, the groundfish management unit (GMU) at the Department of Fisheries and Oceans (DFO) imposed a combination of species/area quotas, area/time closures, and trip limits on major finfish species. Quotas in the form of mortality caps were first introduced for Bocaccio (BOR, *Sebastes paucispinis*) in 2013 for the BC coast (Table A.1, and see Table A.2 for additional management actions).

Bocaccio was the subject of two detailed data reviews (Stanley et al. 2001; Stanley et al. 2004) and was formally assessed by Fisheries and Oceans Canada (DFO) in 2008 (Stanley et al. 2009). This assessment was updated in 2012 (Stanley et al. 2012). Bocaccio was assessed by the Committee on the Status of Endangered Wildlife in Canada (COSEWIC) as Threatened in 2002 and re-assessed as Endangered in 2013. In 2011, a decision was made to **not** list Bocaccio under Schedule 1 of the *Species At Risk Act* (SARA). While DFO continues to

manage this species under the *Fisheries Act*, actions to address conservation concerns were outlined in the order not to list (SI/2011-56 July 6, 2011).

Bocaccio is ubiquitous along the British Columbia (BC) coast and most catches are taken close to the bottom over depths of 60-350 m along the WCVI and in Queen Charlotte Sound (Figure A.1, left). After COSEWIC's assessment of BOR as Threatened in 2002, voluntary catch restrictions were adopted by all fleets beginning in 2004 (Table A.2). Subsequent assessments by Stanley et al. (2009, 2012) placed BOR in DFO's Critical Zone, which led to official mortality caps in 2013 (150 t/y coastwide) that were subsequently reduced to 80 t/y by 2016 (Table A.1). The effect of this reduced effort is clearly evident in Figure A.1 (right panel).

In 2013, a rebuilding plan for Bocaccio was formulated (see Appendix 9 in DFO 2019) which set out the mortality caps and initial quota allocations for BOR along the BC coast. In 2019/20 this included: (i) a 61.9 t mortality cap managed via individual transferable quota for the groundfish trawl fishery; (ii) a 4.7 t mortality cap managed via trip limits of 45-272 kg/trip for hook and line groundfish fisheries; and (iii) a 7.1 t mortality cap managed via trip limits and retention prohibitions for salmon troll and recreational fisheries. Mortality caps were also identified to account for FSC and survey mortality.

In 2012, measures were introduced to reduce and manage the bycatch of corals and sponges by the BC groundfish bottom trawl fishery. These measures were developed jointly by industry and environmental non-governmental organisations (Wallace et al. 2015), and included: limiting the footprint of groundfish bottom trawl activities (Figure A.2), establishing a combined bycatch conservation limit for corals and sponges, and establishing an encounter protocol for individual trawl tows when the combined coral and sponge catch exceeded 20 kg. These measures have been incorporated into DFO's Pacific Region Groundfish Integrated Fisheries Management Plan (Feb 21, 2019, version 1.1) and apply to all vessels using trawl gear in BC.

Table A.1. Annual Mortality Caps (MCs) for BOR caught in BC waters: year can either be calendar year (1993-1996) or fishing year (1997 on). MCs are generally based on a 0.93:0.07 split between trawl (T) and ZN Rockfish. All fleets agreed to avoid BOR and the non-trawl fleets were given trip limits from 100 to 600 lbs of BOR per landings of their respective target species (see Table A.2 for management action details, indicated by note letter).

Year	Start	End	MC (t/y)	Trip Limit (kg/trip)	Notes
1993	1/1/1993	12/31/1993	-	-	-
1994	1/15/1994	12/31/1994	-	-	a
1995	1/1/1995	12/31/1995	-	-	b
1996	2/6/1996	3/31/1997	-	-	c,d
1997	4/1/1997	3/31/1998	-	-	e,f
1998	4/1/1998	3/31/1999	-	-	-
1999	4/1/1999	3/31/2000	-	-	-
2000	4/1/2000	3/31/2001	-	-	g
2001	4/1/2001	3/31/2002	-	-	h
2002	4/1/2002	3/31/2003	-	-	i,j
2003	4/1/2003	3/31/2004	-	-	k
2004	4/1/2004	3/31/2005	-	-	l
2005	4/1/2005	3/31/2006	-	-	m,n,o
2006	4/1/2006	3/31/2007	-	-	p,q,r
2007	3/10/2007	3/31/2008	-	-	s
2008	3/8/2008	2/20/2009	-	-	-
2009	2/21/2009	2/20/2010	-	-	-
2010	2/21/2010	2/20/2011	-	-	-
2011	2/21/2011	2/20/2013	-	-	-
2012	2/21/2011	2/20/2013	-	-	t
2013	2/21/2013	2/20/2014	T:150, ZN:11	-	u,v,w,x,y
2014	2/21/2014	2/20/2015	T:150, ZN:11	-	-
2015	2/21/2015	2/20/2016	T:110, ZN:8	-	z,a
2016	2/21/2016	2/20/2017	T:80, ZN:6	-	B
2017	2/21/2017	2/20/2018	T:80	-	-
2018	2/21/2018	2/20/2019	T:80	45 to 272	-
2019	2/21/2019	2/20/2020	T:80	45 to 272	c

Table A.2. Codes to notes on management actions and quota adjustments that appear in Table A.1. Abbreviations that appear under 'Management Actions': DFO = Department of Fisheries & Oceans, DMP = dockside monitoring program, GTAC =Groundfish Trawl Advisory Committee, H&L = hook and line, IFMP = Integrated Fisheries Management Plan, IVQ = individual vessel quota, MC =Mortality Cap, TAC =Total Allowable Catch. See Archived Integrated Fisheries Management Plans - Pacific Region for further details.

	Year	Management Actions
a	1994	TWL: Started a dockside monitoring program (DMP) for the Trawl fleet.
b	1995	H&L: Implemented catch limits (monthly) on rockfish aggregates for H&L.
c	1996	TWL: Started 100% onboard observer program for offshore Trawl fleet.
d	1996	H&L: Started DMP for H&L fleet.
e	1997	TWL: Started IVQ system for Trawl *Total Allowable Catch* (TAC) species (April 1, 1997)
f	1997	TWL: Implemented catch limits (15,000 lbs per trip) on combined non-TAC rockfish for the Trawl fleet.
g	2000	ALL: Formal discussions between the hook and line rockfish (ZN), halibut and trawl sectors were initiated in 2000 to establish individual rockfish species allocations between the sectors to replace the 92/8 split. Allocation arrangements were agreed to for rockfish species that are not currently under TAC. Splits agreed upon for these rockfish will be implemented in the future when or if TACs are set for those species.

	Year	Management Actions
h	2001	BOR: PSARC (now CSAP) concerned that the decline of abundance indices for Bocaccio from the West Coast Vancouver Island (WCVI) Shrimp survey data and, in particular, the U.S. Triennial survey data reflected a serious decline. A detailed review of all survey indices was recommended to assess trends in Bocaccio abundance.
i	2002	TWL: Closed areas to preserve four hexactinellid (glassy) sponge reefs.
j	2002	BOR: Status of Bocaccio was designated as `Threatened' by the Committee on the Status of Endangered Wildlife in Canada (COSEWIC) in November 2002. The designation was based on a new status report that indicated a combination of low recruitment and high fishing mortality had resulted in severe declines and low spawning abundance of this species. As the Species at Risk Act (SARA) was not yet in place, there was no legal designation for Bocaccio. Protection under SARA would only come in the event that this species was listed, by regulation, under the Act.
k	2003	ALL: Species at Risk Act (SARA) came into force in 2003.
l	2004	BOR: DFO reviewed management measures in the groundfish fisheries to assess the impacts on listed species under SARA. Voluntary program for the trawl fleet was developed and implemented in 2004 in which groundfish trawl vessels directed the proceeds of all landed Bocaccio Rockfish for research and management purposes. Ongoing to 2019.
m	2005	BOR: DFO consulted with First Nations, stakeholders, and the Canadian public on Bocaccio COSEWIC designation for 1.5 years and planned recommendations for further action to be presented to the Minister of Environment and Governor in Council (Cabinet) in spring 2005. A final listing decision by Governor in Council was expected in October 2005.
n	2005	BOR: As a proactive measure, industry reduced the harvest of Bocaccio, beginning in 2004, and resulted in a reduction of the Bocaccio catch by over 50% percent. Subsequently, measures to avoid Bocaccio were taken in the fishing years 2005/06 through 2019/20.
o	2005	BOR: The Government of Canada announced in November 2005 that Bocaccio be sent back to COSEWIC for further information or consideration.
p	2006	ALL: Introduced an *Integrated Fisheries Management Plan* (IFMP) for all directed groundfish fisheries.
q	2006	H&L: Implemented 100% at-sea electronic monitoring and 100% dockside monitoring for all groundfish H&L fisheries.
r	2006	H&L: Implemented mandatory retention of rockfish for H&L.
s	2007	BOR: COSEWIC reconfirmed Bocaccio's Threatened designation, and the species re-entered the SARA listing process in 2007.
t	2012	TWL: Froze the footprint of where groundfish bottom trawl activities can occur (all vessels under the authority of a valid Category T commercial groundfish trawl license selecting Option A as identified in the IFMP).
u	2013	TWL: To support groundfish research, the groundfish trawl industry agreed to the trawl TAC offsets to account for unavoidable mortality incurred during the joint DFO-Industry groundfish multi-species surveys in 2013.
v	2013	BOR: COSEWIC had previously designated Bocaccio as Threatened in November 2002. Its status was re-examined and designated Endangered in November 2013.
w	2013	BOR: DFO formulated a plan for stepped reductions from current Bocaccio catch levels of approximately 137 tonnes (inclusive of trawl, groundfish hook and line, salmon troll, and recreational sectors) to a target level of 75 tonnes over 3 years (2013/14 to 2015/16). This plan accounted for First Nations' priority access for food, social, and ceremonial purposes. DFO worked with fishing interests to develop measures that would reduce Bocaccio catch and enable stock rebuilding over the long term.
x	2013	BOR: Annual Trawl *Mortality Cap* (MC) for Bocaccio was initially set at 150 tonnes. The IVQ carryover/underage limit was set to 15% of each vessels' Bocaccio holdings (in effect until 2019/20 fishery year).
y	2013	BOR: All H&L groundfish fisheries subject to Bocaccio trip limits based on landings of directed species. For example, Halibut directed trips could land up to 200 pounds of Bocaccio when 15,000 pounds or less of Halibut was landed, 300 pounds of Bocaccio when 30,000 pounds of Halibut was landed and 400 pounds of Bocaccio when greater than 30,000 pounds of Halibut was landed. The Dogfish, Lingcod, ZN Rockfish, and Sablefish fisheries were subject to similar trip limits for Bocaccio. These trip limits remained in effect until 2015/16.
z	2015	ALL: Research allocations were specified starting in 2015 to account for the mortalities associated with survey catches to be covered by TACs.
A	2015	BOR: DFO Groundfish Management Unit refined the generalised primary objective for Bocaccio to specify that the aim was to also: *Achieve rebuilding throughout the species' range and grow out of the critical zone ($B>0.4B_{MSY}$) within three generations, with a 65% probability of success.* To support and monitor progress towards the objective, milestones were also established: *Achieve a positive stock trajectory trend in each 5-year interval, such that the biomass at the end of each 5-year period is greater than the biomass at the beginning of the same 5-year period. Between major assessments, progress towards this goal will be monitored by annually reviewing fishery-dependent and fishery-independent indices of stock trajectory*.
B	2015	BOR: To reduce Bocaccio mortality in the groundfish H&L fisheries new trip limits were introduced. For example, Halibut directed trips could land 100 pounds plus 1% of the amount of Halibut landed in excess of 10,000 pounds to a maximum of 600 pounds of Bocaccio. The Dogfish, Lingcod, ZN Rockfish, and Sablefish directed fisheries were subject to the same trip limits. These trip limits remained in effect during the 2019/20 fishing year.
C	2015	BOR: Bocaccio trawl MC reduced to 110~t coastwide.
D	2016	BOR: Bocaccio trawl MC reduced to 80~t coastwide. Bocaccio remains a quota species in the trawl fishery, but not in the hook and line fisheries.

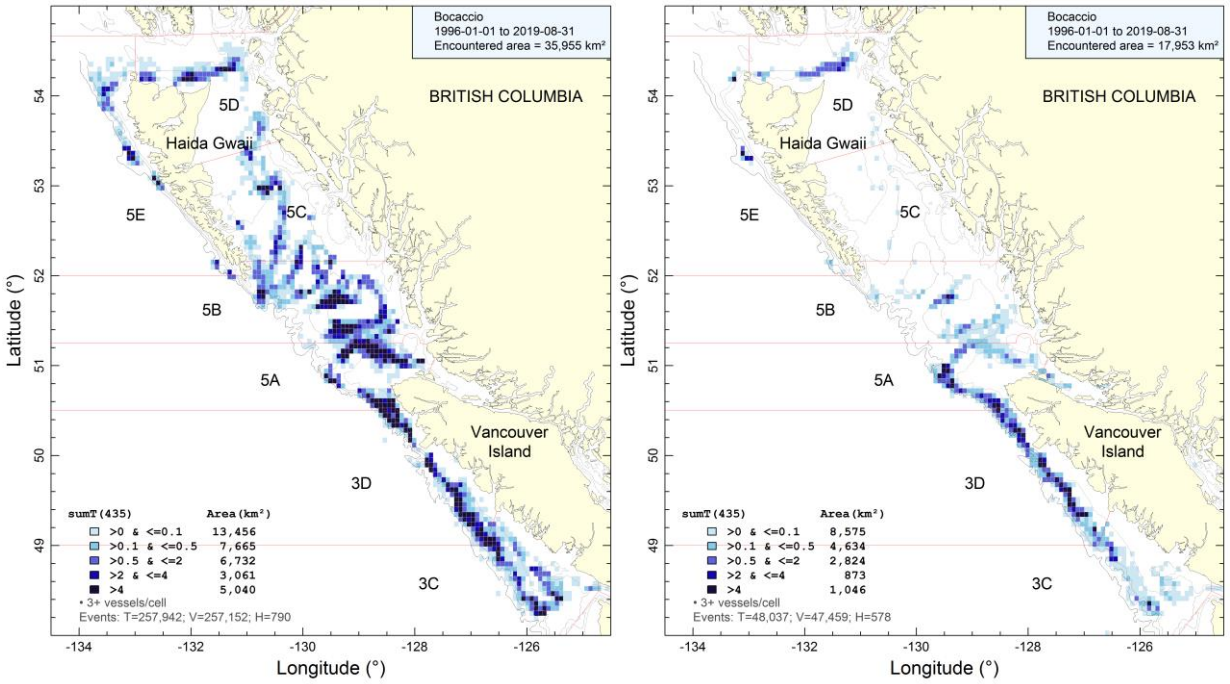

Figure A.1. Aerial distribution of accumulated BOR catch (tonnes) by bottom trawl (left) and midwater trawl (right) from 1996 to 2019 in grid cells 0.075° longitude by 0.055° latitude (roughly 32 km²). Isobaths show the 100, 200, 500, and 1200 m depth contours. Note that cells with <3 fishing vessels are not displayed.

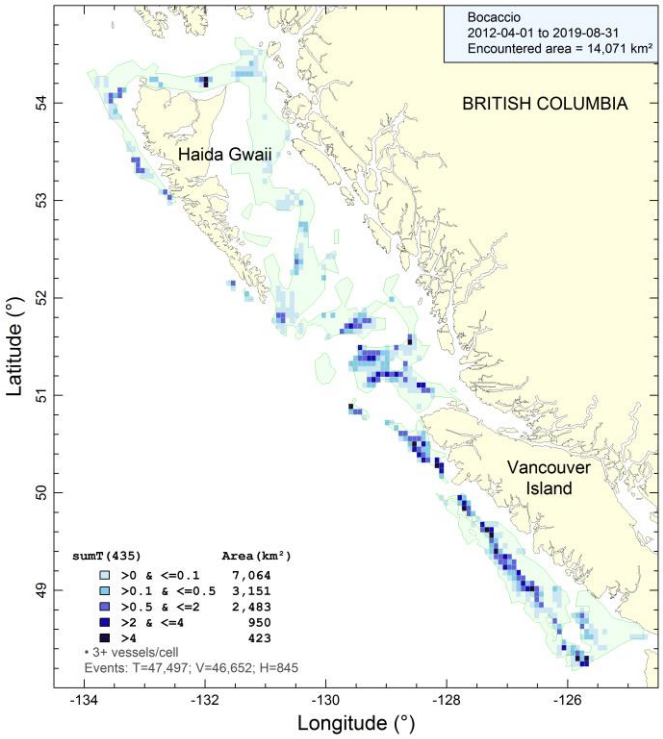

Figure A.2. Aerial distribution of accumulated BOR bottom trawl catch (tonnes) after the introduction of the trawl footprint in April 2012, limiting areas in which trawl vessels can operate. Note that cells with <3 fishing vessels are not displayed.

A.2. CATCH RECONSTRUCTION

This assessment reconstructs BOR catch back to 1918 but considers the start of the fishery to be 1935 (Figure A.3) before the fishery started to increase during World War II. Prior to this, trawl catches were negligible and halibut fleet catches were estimated to be roughly 4 tonnes per year. During the period 1950–1975, US vessels routinely caught more rockfish than did Canadian vessels. Additionally, from the mid-1960s to the mid-1970s, foreign fleets (Russian and Japanese) removed large amounts of rockfish, primarily POP. These large catches were first reported by various authors (Westrheim et al. 1972; Gunderson et al. 1977; Leaman and Stanley 1993); however, Ketchen (1980a,b) re-examined the foreign fleet catch, primarily because statistics from the USSR called all rockfish 'perches' while the Japanese used the term 'Pacific ocean perch' indiscriminately. In the catch reconstruction, all historical foreign catches (annual rockfish landings) were tracked separately from Canadian BOR landings, converted to BOR (Section A.2.2), and added to the latter during the reconstruction process.

A.2.1. Data sources

Starting in 2015, all official Canadian catch tables from the databases below (except PacHarv3) have been merged into one table called 'GF_MERGED_CATCH', which is available in DFO's GFFOS database. All groundfish DFO databases are now housed on the DFBCV9TWVASP001 server. Bocaccio catch by fishery sector ultimately comes from the following seven DFO databases:

- PacHarv3 sales slips (1982-1995) – hook and line only;
- GFCatch (1954-1995) – trawl and trap;
- PacHarvHL merged data table (1986-2006) – halibut, Dogfish+Lingcod, H&L rockfish;
- PacHarvSable fisherlogs (1995-2005) – Sablefish;
- PacHarvest observer trawl (1996-2007) – trawl;
- GFFOS groundfish subset from Fishery Operation System (2006-2019) – all fisheries and modern surveys; and
- GFBioSQL joint-venture hake and research survey catches (1947-2019) – multiple gear types. GFBioSQL is an SQL Server database that mirrors the GFBio Oracle database.

All data sources other than PacHarv3 were superseded by GFFOS from 2007 on because this latter repository was designed to record all Canadian landings and discards from commercial fisheries and research activities.

Prior to the modern catch databases, historical landings of aggregate rockfish – either total rockfish (TRF) or rockfish other than POP (ORF) – are reported by eight different sources (see Haigh and Yamanaka 2011). The earliest historical source of rockfish landings comes from Canada Dominion Bureau of Statistics (1918-1950).

The purpose of this procedure is to estimate the catch of any rockfish species (generically designated as RRF) from ratios of RRF/ORF or RRF/TRF, add the estimated discards from the ratio RRF/TAR (where TAR is the target species landed by fishery), to reconstruct the total catch of species RRF.

A.2.2. Reconstruction details

A.2.2.1. Definition of terms

A brief synopsis of the catch reconstruction (CR) follows, with a reminder of the definition of terms:

Fisheries: there are five fisheries in the reconstruction (even though trawl dominates the BOR fishery):

- T = groundfish trawl (bottom + midwater),
- H = Halibut longline,
- S = Sablefish trap/longline,
- DL = Schedule II (mostly Dogfish and Lingcod troll/longline),
- ZN = hook and line rockfish (called 'ZN' from 1986 on).

TRF: acronym for "total rockfish" (all species of *Sebastes* + *Sebastolobus*).

ORF: acronym for "other rockfish" (= TRF minus POP), landed catch aggregated by year, fishery, and PMFC (Pacific Marine Fisheries Commission) major area.

POP: Pacific Ocean Perch.

RRF: Reconstructed rockfish species – in this case, Bocaccio (BOR).

TAR: Target species landed catch.

L & D: L = landed catch, D =releases (formerly called "discards")

gamma: mean of annual ratios, $\sum_i \mathrm{RRF}_i^L / \mathrm{ORF}_i^L$, grouped by major PMFC area and fishery using default reference years i = 1997-2005. For BOR, the reference years were set to 1996-2000 for the trawl fishery and 2007-2011 for the non-trawl fisheries.

delta: mean of annual ratios, $\sum_i \mathrm{RRF}_i^D / \mathrm{TAR}_i$, grouped by major PMFC area and fishery using reference years i = 1997-2006 for the trawl fishery and 2000-2004 for all other fisheries. Observer records were used to gather data on releases. For BOR, dockside monitoring program (DMP) data from 2007 to 2012 were examined but these lack the area-specific detail of the observer logs, which occur at the fishing event level.

The stock assessment population model uses calendar year, requiring calendar year catch estimates. The reconstruction defaults to using 'official' (reported) catch numbers by fishery starting in years 1996 (T), 2000 (H), 2007 (S,DL), and 1986 (ZN), which are the years when these fisheries implemented reliable observer coverage. These defaults were not used for BOR. Instead, landings were reconstructed before 1996 for the trawl fishery and before 2006 for the non-trawl fisheries. Although reported data existed in earlier time periods, the BOR TWG considered that BOR catches reported from 1985 (start of restrictive trip limits) to 1994 (start of the DMP) were likely inflated, given the incentives for operators to misreport their catch during this period.

The reconstruction of Canadian BOR landings involved the estimation of landings for the years before the years of reported catch using `gamma` ratios (Table A.3). These ratios were also used to convert foreign landings of ORF to BOR. The ratios were calculated from a relatively modern period (1996-2000 for trawl, 2007-2011 for non-trawl); therefore, an obvious caveat to this procedure is that ratios derived from a modern fishery may not reflect catch ratios during the historical foreign fleet activity or regulatory regimes not using IVQs (individual vessel quotas).

Consequently, we use an early set of years to estimate these ratios in an attempt to minimise this potential issue.

After BOR landings were estimated, non-retained catch (releases or discards) were estimated and added during years identified by fishery: T = 1954-1995, H = 2018-2005, and S/DL/ZN = 1986-2005. The non-retained catch is estimated using the `delta` ratios of BOR discarded by a fishery to fishery-specific landed targets (TAR): T = BOR, H = Pacific Halibut, S = Sablefish, DL = lingcod + Spiny Dogfish, ZN = BOR (Table A.3).

The current annual BOR catches by trawl fishery and those from the non-trawl fisheries appear in Table A.4 and Figure A.3. The combined fleet catches were used in the population models.

A.2.2.2. Reconstruction results

Table A.3. Estimated 'gamma' (BOR/ORF) and 'delta' (discard) ratios for each fishery and PMFC area used in the catch reconstruction of Bocaccio.

gamma (proportion BOR/ORF)

PMFC	Trawl	Halibut	Sablefish	Dogfish/ Lingcod	H&L Rockfish
3C	0.00193	0.00113	-	0.00031	0.00012
3D	0.01197	0.00463	0.00055	0.01906	0.00081
5A	0.01523	0.02245	0.00330	0.22907	0.00890
5B	0.01800	0.01514	0.00034	0.30409	0.00944
5C	0.02281	0.00857	0.00010	0.29631	0.00149
5D	0.01999	0.00849	-	0.17682	0.00051
5E	0.04567	0.00663	-	0.19369	0.00008

delta (discard rate)

PMFC	Trawl	Halibut	Sablefish	Dogfish/ Lingcod	H&L Rockfish
3C	2.48357	-	-	0.00004	-
3D	0.02340	-	-	0.00011	-
5A	0.01419	0.00152	0.00011	0.00132	-
5B	0.00730	0.00020	-	0.02039	0.01821
5C	0.00949	0.00022	-	0.00968	-
5D	0.00920	0.00022	-	0.00187	-
5E	0.01138	0.00013	-	0.00122	-

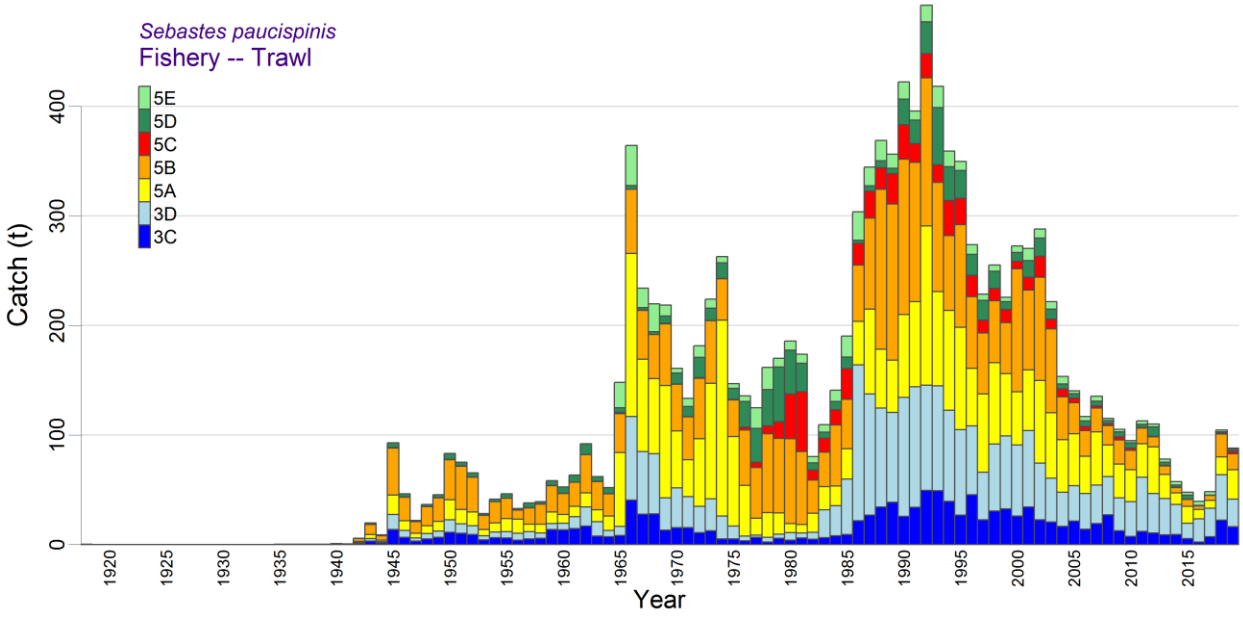

Figure A.3. Reconstructed total (landed + released) catch (t) for BOR from the trawl fishery in PMFC major areas 3C to 5E.

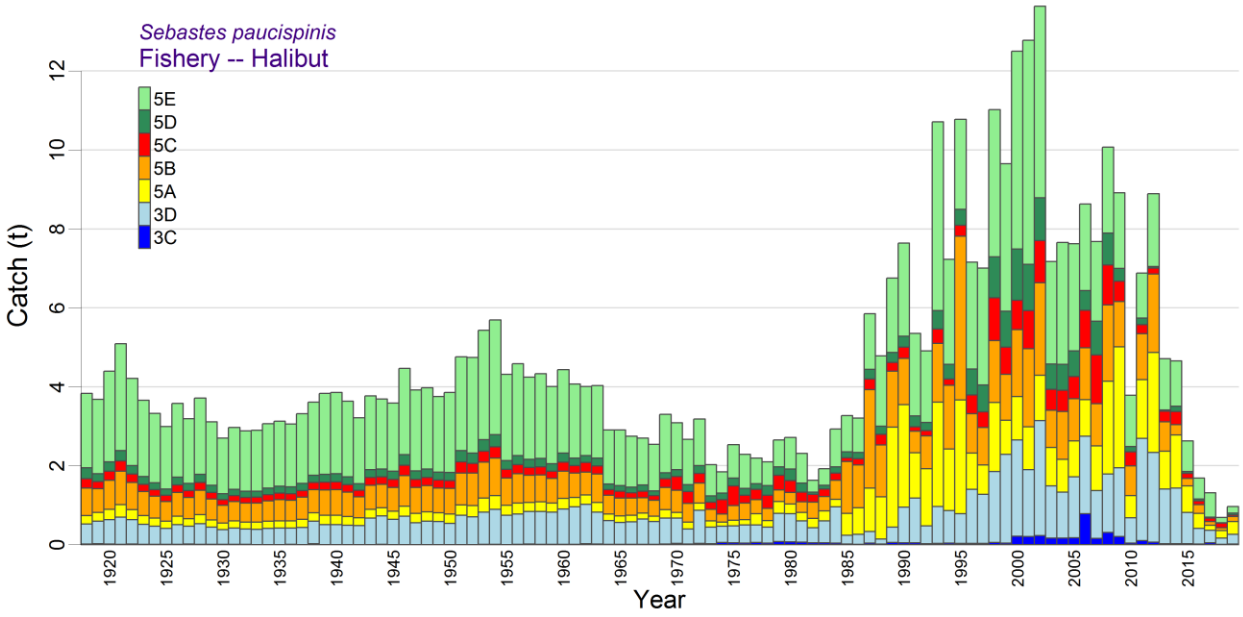

Figure A.4. Reconstructed total (landed + released) catch (t) for BOR from the halibut fishery in PMFC major areas 3C to 5E.

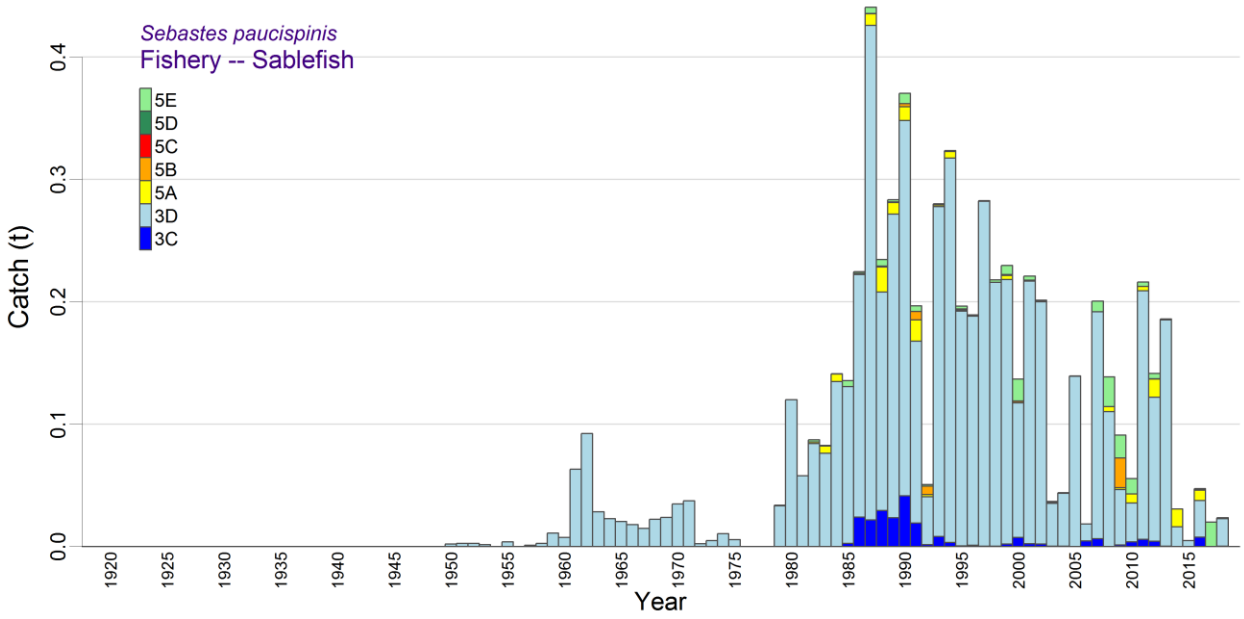

Figure A.5. Reconstructed total (landed + released) catch (t) for BOR from the sablefish fishery in PMFC major areas 3C to 5E.

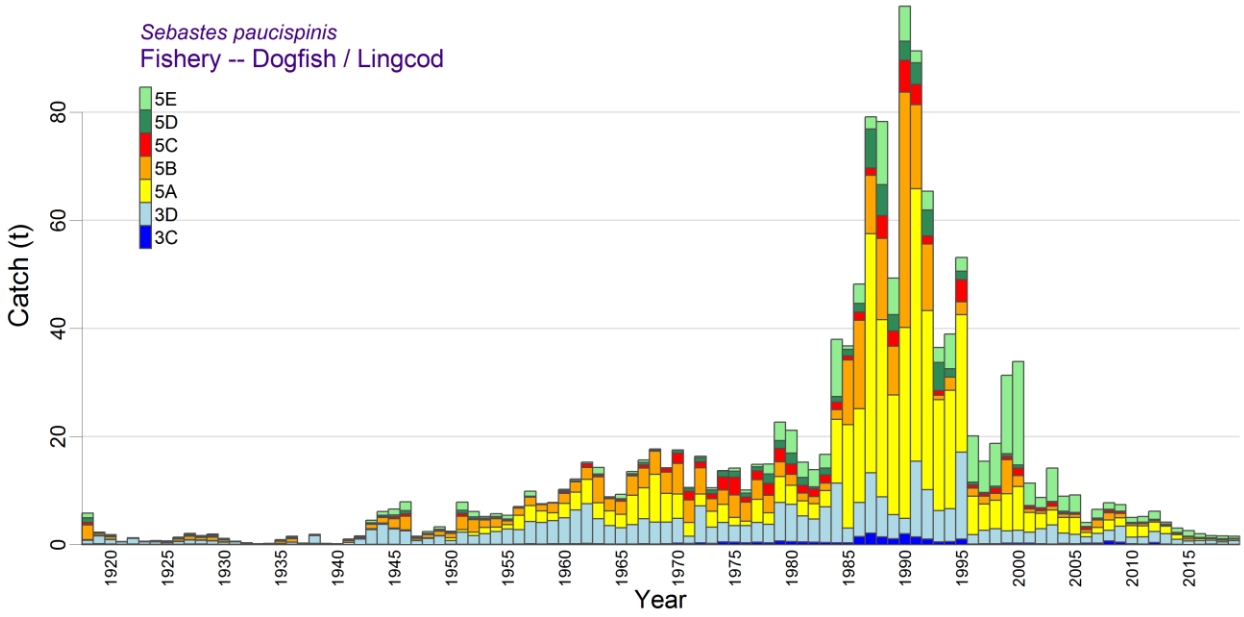

Figure A.6. Reconstructed total (landed + released) catch (t) for BOR from the dogfish/lingcod fishery in PMFC major areas 3C to 5E.

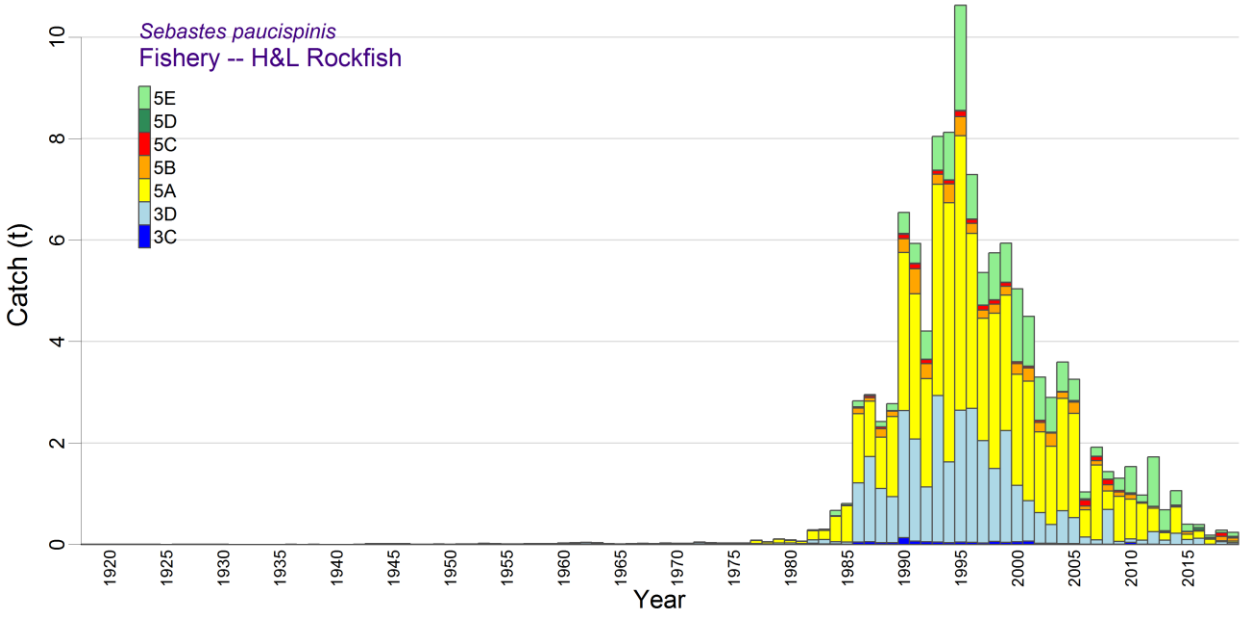

Figure A.7. Reconstructed total (landed + released) catch (t) for BOR from the hook and line rockfish fishery in PMFC major areas 3C to 5E.

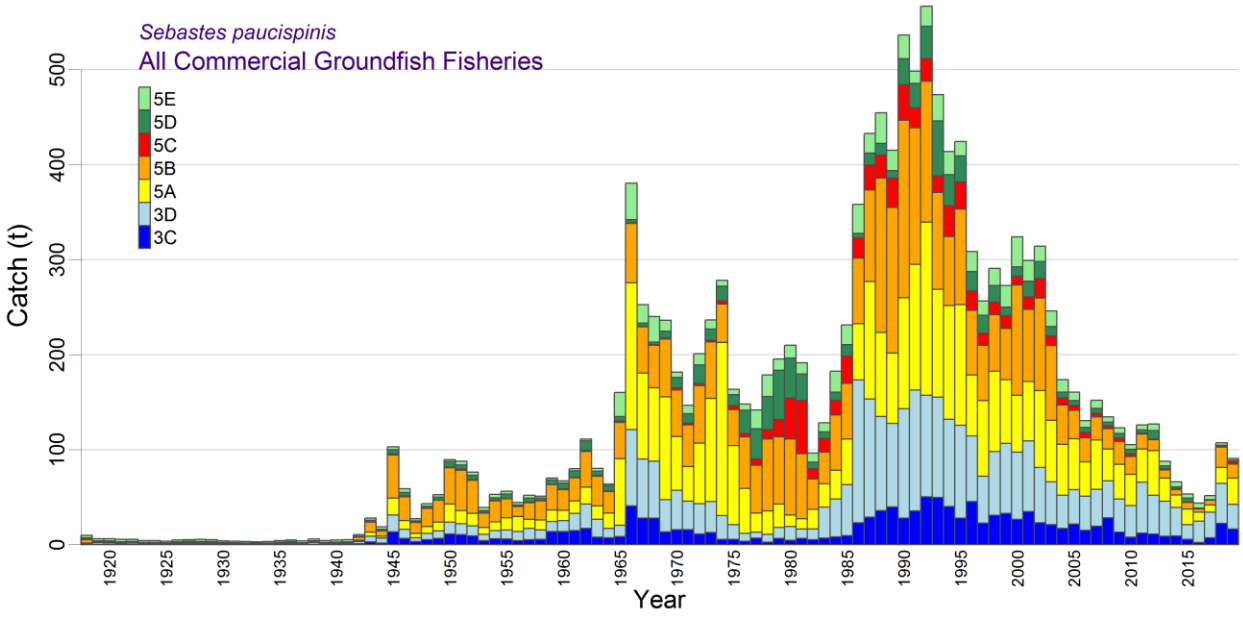

Figure A.8. Reconstructed total (landed + released) catch (t) for BOR from all commercial groundfish fisheries in PMFC major areas 3C to 5E.

Table A.4. Reconstructed catches (in tonnes, landings + releases) of BOR in coastwide PMFC areas (3C to 5E combined) from each fishery and for coastwide BC. Shaded columns indicate catches used in the stock assessment model, where 'Other' sums the catch by Halibut, Sablefish, Dogfish/Lingcod, and H&L Rockfish fisheries.

Year	Trawl	Halibut	Sablefish	Dogfish +Lingcod	H&L Rockfish	Other	BC Coast
1918	0.206	3.8	0	5.9	0.007	9.7	9.9
1919	0.064	3.7	0	2.3	0.008	6.0	6.1
1920	0.055	4.4	0	1.8	0.005	6.2	6.3
1921	0.015	5.1	0	0.598	0.003	5.7	5.7
1922	0.031	4.2	0	1.3	0.006	5.5	5.5
1923	0.017	3.7	0	0.642	0.003	4.3	4.4
1924	0.021	3.3	0	0.755	0.003	4.1	4.1
1925	0.021	3.0	0	0.673	0.002	3.7	3.7
1926	0.043	3.6	0	1.4	0.003	5.0	5.0
1927	0.065	3.2	0	2.1	0.005	5.3	5.4
1928	0.051	3.7	0	1.7	0.004	5.4	5.5
1929	0.064	3.1	0	2.0	0.004	5.1	5.2
1930	0.036	2.7	0	1.2	0.003	3.9	3.9
1931	0.016	3.0	0	0.619	0.002	3.6	3.6
1932	0.011	2.9	0	0.325	0.001	3.2	3.2
1933	0.005	2.9	0	0.185	0.001	3.1	3.1
1934	0.026	3.1	0	0.242	0.001	3.3	3.4
1935	0.191	3.1	0	0.933	0.001	4.0	4.2
1936	0.26	3.1	0	1.6	0.003	4.7	5.0
1937	0.194	3.3	0	0.304	0.001	3.6	3.8
1938	0.324	3.6	0	1.9	0.008	5.5	5.8
1939	0.339	3.8	0	0.231	0.001	4.0	4.4
1940	0.718	3.9	0	0.19	0.001	4.1	4.8
1941	0.533	3.6	0	1.0	0.002	4.6	5.1
1942	5.8	3.2	0	1.6	0.005	4.8	11
1943	20	3.8	0	4.5	0.015	8.3	28
1944	8.7	3.7	0	6.1	0.020	9.8	19
1945	93	3.6	0	6.6	0.017	10	103
1946	46	4.5	0	7.9	0.016	12	58
1947	22	3.9	0	1.6	0.004	5.5	28
1948	37	4.0	0	2.4	0.007	6.4	43
1949	45	3.7	0	3.3	0.009	7.0	52
1950	83	3.9	0.002	2.5	0.004	6.4	89
1951	75	4.8	0.003	7.9	0.013	13	88
1952	65	4.7	0.003	6.1	0.011	11	76
1953	28	5.4	0.002	5.2	0.022	11	39
1954	41	5.7	0	5.7	0.017	11	52
1955	46	4.3	0.004	5.4	0.014	9.7	56
1956	33	4.6	0	7.0	0.014	12	45
1957	38	4.2	0.001	9.9	0.018	14	52
1958	39	4.3	0.003	7.5	0.016	12	51
1959	58	4.0	0.011	7.8	0.019	12	70
1960	53	4.4	0.007	10	0.031	14	67
1961	63	4.1	0.063	12	0.034	16	79
1962	92	4.0	0.092	15	0.041	19	111
1963	62	4.0	0.028	14	0.036	18	80
1964	52	2.9	0.023	8.8	0.017	12	64
1965	148	2.9	0.021	9.3	0.014	12	160
1966	364	2.7	0.018	14	0.021	17	381

Year	Trawl	Halibut	Sablefish	Dogfish +Lingcod	H&L Rockfish	Other	BC Coast
1967	234	2.7	0.015	16	0.023	19	253
1968	220	2.5	0.022	18	0.016	21	241
1969	218	3.3	0.024	14	0.030	17	235
1970	161	3.1	0.035	18	0.026	21	182
1971	133	2.7	0.037	11	0.021	14	147
1972	181	3.2	0.002	16	0.046	19	200
1973	224	2.0	0.005	11	0.034	13	237
1974	263	1.8	0.011	14	0.032	16	279
1975	147	2.5	0.006	14	0.030	17	164
1976	136	2.3	0	10	0.028	12	148
1977	125	2.2	0	15	0.085	17	142
1978	162	2.1	0	15	0.052	17	179
1979	170	2.7	0.034	23	0.110	26	196
1980	186	2.7	0.120	21	0.090	24	210
1981	174	2.3	0.058	15	0.068	17	191
1982	80	1.6	0.087	14	0.290	16	96
1983	109	1.9	0.082	17	0.300	19	128
1984	141	2.9	0.141	38	0.670	42	183
1985	190	3.3	0.136	37	0.805	41	231
1986	304	3.2	0.225	48	2.8	54	358
1987	345	5.9	0.441	79	3.0	88	433
1988	369	4.8	0.235	78	2.4	85	454
1989	356	6.8	0.283	49	2.8	59	415
1990	422	7.6	0.370	100	6.5	114	536
1991	396	5.4	0.197	91	5.9	102	498
1992	492	4.9	0.051	65	4.2	74	566
1993	418	11	0.280	36	8.0	55	473
1994	359	7.2	0.324	39	8.1	55	414
1995	350	11	0.197	53	11	75	425
1996	274	7.2	0.189	20	7.3	35	309
1997	229	7.0	0.283	15	5.4	28	257
1998	255	11	0.218	19	5.7	36	291
1999	226	9.7	0.230	31	5.9	47	273
2000	273	13	0.137	34	5.0	52	325
2001	270	13	0.221	11	4.5	29	299
2002	288	14	0.201	8.7	3.3	26	314
2003	222	7.2	0.037	14	2.9	24	246
2004	153	7.7	0.044	8.9	3.6	20	173
2005	140	7.6	0.139	9.2	3.3	20	160
2006	117	8.6	0.018	4.1	1.0	14	131
2007	136	7.7	0.200	6.5	1.9	16	152
2008	115	10	0.139	7.7	1.4	19	134
2009	105	8.9	0.091	7.4	1.3	18	123
2010	95	3.8	0.055	5.0	1.5	10	105
2011	113	6.9	0.216	5.2	0.974	13	126
2012	110	8.9	0.142	6.2	1.7	17	127
2013	78	4.7	0.186	4.2	0.684	9.8	88
2014	57	4.7	0.031	3.1	1.1	8.9	66
2015	48	2.6	0.005	2.6	0.399	5.6	54
2016	39	1.7	0.047	2.0	0.394	4.1	43
2017	48	1.3	0.020	1.7	0.186	3.2	51
2018	105	0.686	0.024	1.6	0.281	2.6	108
2019	88	0.962	0	1.6	0.243	2.8	91

A.2.3. Changes to the reconstruction algorithm since 2011

A.2.3.1. 2012 – Pacific Ocean Perch

In two previous stock assessments for POP in areas 3CD and 5DE (Edwards et al. 2014a,b), the authors documented two departures from the catch reconstruction algorithm introduced by Haigh and Yamanaka (2011). The first dropped the use of trawl and trap data from the sales slip database `PacHarv3` because catches were sometimes reported by large statistical areas that cannot be clearly mapped to PMFC areas. In theory, `PacHarv3` should report the same catch as that in the `GFCatch` database (Rutherford 1999), but area inconsistencies cause catch inflation when certain large statistical areas cover multiple PMFC areas. Therefore, only the `GFCatch` database for the trawl and trap records from 1954 to 1995 were used, rather than trying to mesh `GFCatch` and `PacHarv3`. The point is somewhat moot as assessments since 2015 by the Offshore Rockfish Program use the merged-catch data table (Section A.2.1). Data for the H&L fisheries from `PacHarv3` are still used as these do not appear in other databases.

The second departure was the inclusion of an additional data source for BC rockfish catch by the Japanese fleet reported in Ketchen (1980a).

A.2.3.2. 2014 – Yellowtail Rockfish

The Yellowtail Rockfish assessment (Starr et al. 2014) selected offshore areas that reflected the activity of the foreign fleets' impact on this species to calculate `gamma` (RRF/ORF) and `delta` ratios (RRF/TAR). This option was not used in the BOR reconstruction.

A.2.3.3. 2015 – Shortspine Thornyhead

The Shortspine Thornyhead assessment (Starr and Haigh 2017) was the first to use the merged catch table (`GF_MERGED_CATCH` in `GFFOS`). Previous assessments required the meshing together of caches from six separate databases: `GFBioSQL` (research, midwater joint-venture Hake, midwater foreign), `GFCatch` (trawl and trap), `GFFOS` (all fisheries), `PacHarvest` (trawl), `PacHarvHL` (hook and line), and `PacHarvSable` (trap and longline). See Section A.2.1 for further details.

A.2.3.4. 2015 – Yelloweye Rockfish

The Yelloweye Rockfish (YYR) assessment (Yamanaka et al. 2018) introduced the concept of depth-stratified `gamma` and `delta` ratios; however, this functionality has not been used for offshore rockfish to date.

Also in the YYR assessment, rockfish catch from seamounts was removed (implemented in all subsequent reconstructions, including the BOR one), as well as an option to exclude rockfish catch from the foreign fleet and the experimental Langara Spit POP fishery (neither were excluded from the BOR reconstruction). The latter option is more likely appropriate for inshore rockfish species because they did not experience historical offshore foreign fleet activity or offshore experiments.

A.2.3.5. 2018 – Redstripe Rockfish

The Redstripe Rockfish assessment (Starr and Haigh, 2021a), introduced the use of summarising annual `gamma` and `delta` ratios from reference years (Section A.2.2) by calculating the geometric mean across years instead of using the arithmetic mean. This choice reduces the influence of single anomalously large annual ratios. The geometric mean was used in the BOR reconstruction.

Also new in 2018 was the ability to estimate RRF (using gamma) for landings later than 1996, should the user have reason to replace observed landings with estimated ones. For BOR, observed landings by fishery were used starting in 1996 for the trawl fishery and 2006 for the non-trawl fisheries; prior to these years, landings were estimated using gamma.

Another feature introduced in 2018 was the ability to specify years by fishery for discard regimes, that is, when discard ratios were to be applied. Previously, these had been fixed to 1954-1995 for the trawl fishery and 1986-2005 for the non-trawl fisheries. For BOR, discard regimes by fishery were set to T = 1954-1995, H = 2018-2005, and S/DL/ZN = 1986-2005. As previously, years before the discard period assume no discarding, and years after the discard period assume that discards have been reported in the databases.

A.2.3.6. 2019 – Widow Rockfish

The Widow Rockfish (WWR) assessment (Starr and Haigh, 2021) found a substantial amount of WWR reported as foreign catch in the database GFBioSQL that came from midwater gear off WCVI. Subsequently, the catch reconstruction algorithm was changed to assign GFBio foreign catch to four of the five fisheries based on gear type:

- bottom and midwater trawl gear assigned to the T fishery,
- longline gear assigned to the H fishery,
- trap and line-trap mix gear assigned to the S fishery, and
- h&l gear assigned to the ZN fishery.

The assignment only happens if the user chooses to use foreign catch in the reconstruction (see Section A.2.3.3). These foreign catches occurred well after the foreign fleet activity between 1965 and the implementation of an exclusive economic zone in 1977. BOR foreign catches in GFBio occurred primarily in 1987-1991 (17.9 t).

A.2.3.7. 2019 – Bocaccio

During the Bocaccio assessment, the technical working group identified specific reference years for the calculation of gamma: 1990-2000 for trawl (to capture the years before decreasing mortality caps for BOR were placed on the trawl fleet) and 2007-2011 for non-trawl (to capture years after some form of observer program like electronic monitoring was applied to the hook and line fleets). The catch reconstruction algorithm was previously coded to only allow one set of reference years to be applied across all fisheries. The algorithm was changed so that a user can now specify separate reference years for each fishery.

Once the merged catch table (GF_MERGED_CATCH in GFFOS) was introduced (Section A.2.3.3), catch from all databases other than PacHarv3 have been reconciled so that caches are not double counted. In this assessment, the remaining two catch data sources (GFM and PH3, for brevity) were re-assessed by comparing ORF data, and the CR algorithm was changed in how the data sources were merged for the categories RRF landed, RRF discarded, ORF landed, POP landed, and TRF landed:

- GFM catch is the only source needed for FID 1 (Trawl fishery), as was previously assumed;
- GFM and PH3 catches appear to supplement each other for FIDs 2 (Halibut fishery), 3 (Sablefish fishery), and 4 (Dogfish/Lingcod fishery), and the catches were added in any given year up to 2005 (electronic monitoring started in 2006 and so the GFFOS database was reporting all catch for these fisheries by then);

- GFM and PH3 catches appear to be redundant for FID 5 (H&L Rockfish fishery), and so the maximum catch was used in any given year.

Also new in the BOR assessment was the introduction of historical Sablefish (SBF) and Lingcod (LIN) trawl landings from 1950 to 1975 (Ketchen 1976) for use in calculating historical discards for FIDs 3 and 4 during this period. These landings could not be used directly because they were taken by the trawl fleet; therefore, an estimation of SBF and LIN landed catch by FIDs 3 and 4, respectively, relative to SBF and LIN landed catch by FID 1 (trawl) was calculated from GFM. Annual ratios of SBF_3/SBF_1 and LIN_4/LIN_1 from 1996-2011 were chosen to calculate a geometric mean; the ratios from 2012 on started to diverge from those in the chosen period. The procedure yielded average ratios: $SBF_3/SBF_1 = 10.235$ and $LIN_4/LIN_1 = 0.351$, which were used to scale the 1950-75 trawl landings of SBF and LIN, respectively. From these estimated landings, discards of BOR were calculated by applying `delta` (see Section A.2.2.1).

Another departure was the re-allocation of PH3 records to the various catch reconstruction fisheries based on data from 1952-95. The distribution of effort (events) and catch by species for each gear type (Table A.5) led to the code revision in Table A.6.

Table A.5. PacHarv3 (PH3) number of events reportedly catching each species and catch (t) of species from 1952-95 by gear type and species code, where SCO = Scorpionfishes, POP = Pacific Ocean Perch, YTR = Yellowtail Rockfish, YMR =Yellowmouth Rockfish, YYR = Yelloweye Rockfish, SST = Shortspine Thornyhead, PAH = Pacific Halibut, SBF = Sablefish, DOG = Spiny Dogfish, and LIN = Lingcod.

EVENTS

Code	PH3 Gear Description	SCO	POP	YTR	YMR	YYR	SST	PAH	SBF	DOG	LIN
10	GILL NET, SALMON	55	-	-	-	17	-	-	-	-	164
11	NET, SET	-	-	-	-	-	-	-	-	1	-
20	SEINE, PURSE, SALMON	4	-	-	-	2	-	-	-	-	14
30	TROLL, SALMON	4281	49	69	1	2587	11	613	40	77	5201
31	TROLL, FREEZER, SALMON	614	1	14	2	294	2	91	8	31	1752
36	JIG, HAND, NON-SALMON	1126	25	241	13	914	4	1	1	152	845
40	LONGLINE	2893	109	355	100	2738	327	4484	603	1248	2377
50	TRAWL, OTTER, BOTTOM	3910	2419	2335	1521	557	1435	-	2469	748	3098
51	TRAWL, MIDWATER	770	155	770	175	21	26	-	51	210	173
57	SHRIMP TRAWL	173	10	2	-	21	-	-	2	12	82
70	SEINE, BEACH	4	-	-	-	-	-	-	-	-	2
90	TRAP	74	-	1	1	14	18	-	753	3	34

CATCH

Code	PH3 Gear Description	SCO	POP	YTR	YMR	YYR	SST	PAH	SBF	DOG	LIN
10	GILL NET, SALMON	3.6	-	-	-	1.0	-	-	-	-	16
11	NET, SET	-	-	-	-		-	-	-	2.5	-
20	SEINE, PURSE, SALMON	0.2	-	-	-	0.7	-	-	-	-	4.3
30	TROLL, SALMON	3060	1.3	5.6	0.0	925	2.0	538	20	70	5757
31	TROLL, FREEZER, SALMON	73	0.0	2.2	0.4	31	4.0	52	0.1	99	695
36	JIG, HAND, NON-SALMON	2133	5.2	40	4.6	745	0.1	0.3	1.1	175	1883
40	LONGLINE	6921	11	29	35	7922	91	48384	10785	21799	6119
50	TRAWL, OTTER, BOTTOM	117534	79327	28758	17609	1818	3468	-	6090	12637	45811
51	TRAWL, MIDWATER	17737	469	14867	735	3.3	7.7	-	7.9	1400	103
57	SHRIMP TRAWL	23	0.6	2.1	-	0.3	-	-	0.0	18	34
70	SEINE, BEACH	0.1	-	-	-	-	-	-	-	-	0.6
90	TRAP	76	-	0.0	0.6	3.6	6.4	-	50886	34	4.4

Table A.6. Code extract from Oracle SQL query 'ph3_fcatORF.sql' that defines catch reconstruction FIDs (1=Trawl, 2=Halibut, 3=Sablefish, 4=Dogfish/Lingcod, 5=H&L Rockfish) from gear types and dominant species caught (by weight) per event in PH3 table 'CATCH_SUMMARY'.

FID definition in SQL query 'ph3_fcatORF.sql'

```
(CASE -- in order of priority
  -- originally TRAWL (otter bottom, midwater, shrimp, herring)
  WHEN TAR.GR_GEAR_CDE IN (50,51,57,59) THEN 1
  -- Partition LONGLINE
  WHEN TAR.GR_GEAR_CDE IN (40) AND TAR.Target IN ('614') THEN 2
  WHEN TAR.GR_GEAR_CDE IN (40) AND TAR.Target IN ('455') THEN 3
  WHEN TAR.GR_GEAR_CDE IN (40) AND TAR.Target IN ('044','467') THEN 4
  WHEN TAR.GR_GEAR_CDE IN (40) AND TAR.Target NOT IN ('614','455','044','467')) THEN 5
  -- Partition TROLL (salmon, freezer salmon)
  WHEN TAR.GR_GEAR_CDE IN (30,31) AND TAR.Target IN ('614') THEN 2
  WHEN TAR.GR_GEAR_CDE IN (30,31) AND TAR.Target IN ('455') THEN 3
  WHEN TAR.GR_GEAR_CDE IN (30,31) AND TAR.Target IN ('044','467') THEN 4
  WHEN TAR.GR_GEAR_CDE IN (30,31) AND TAR.Target NOT IN ('614','455','044','467')) THEN 5
  -- Partition JIG (hand non-salmon)
  WHEN TAR.GR_GEAR_CDE IN (36) AND TAR.Target IN ('614') THEN 2
  WHEN TAR.GR_GEAR_CDE IN (36) AND TAR.Target IN ('455') THEN 3
  WHEN TAR.GR_GEAR_CDE IN (36) AND TAR.Target IN ('044','467') THEN 4
  WHEN TAR.GR_GEAR_CDE IN (36) AND TAR.Target NOT IN ('614','455','044','467')) THEN 5
  -- originally TRAP (experimental, salmon, longline, shrimp & prawn, crab)
  WHEN TAR.GR_GEAR_CDE IN (86,90,91,92,97,98) THEN 3
  -- Unassigned Trawl, Halibut, Sablefish, Dogfish-Lingcod, H&L Rockfish
  WHEN TAR.Target IN ('394','396','405','418','440','451') THEN 1
  WHEN TAR.Target IN ('614') THEN 2
  WHEN TAR.Target IN ('455') THEN 3
  WHEN TAR.Target IN ('044','467') THEN 4
  WHEN TAR.Target IN ('388','401','407','424','431','433','442') THEN 5
  ELSE 0 END) AS \"fid\",
```

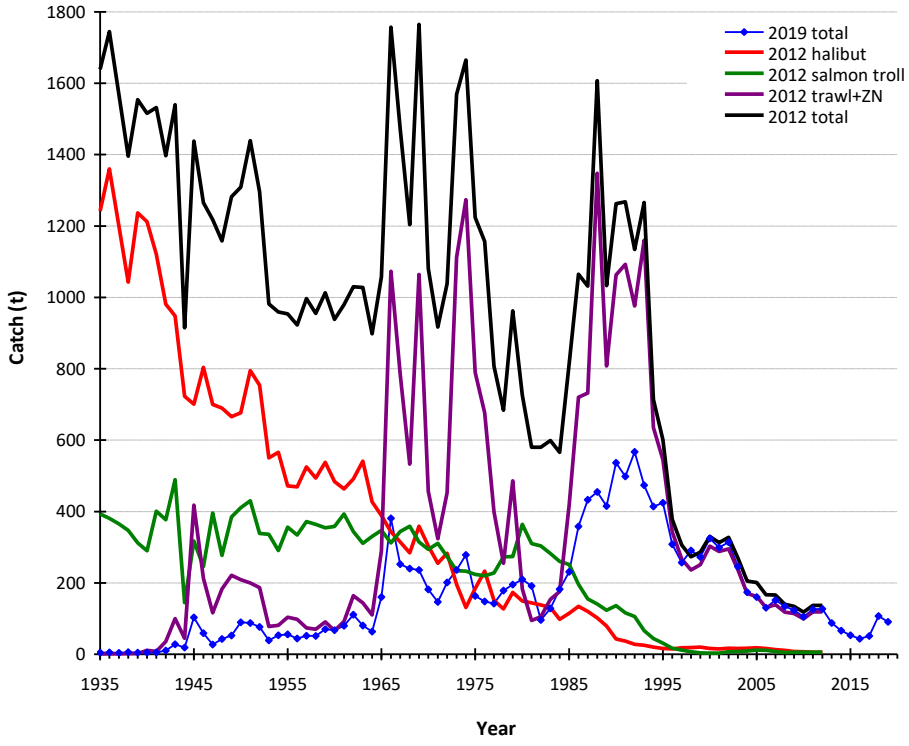

Figure A.9. Comparison of the median catches used in the 2012 BOR stock assessment by major sector compared to the total catches used in this stock assessment (final column, Table A.4).

A.2.4. Departures from previous BOR assessments

The 2008 and 2012 BOR stock assessments (Stanley et al. 2009; Stanley et al. 2012) indirectly estimated catch in the halibut longline and salmon troll fisheries using historical effort data. That is, starting with modern (post-1996) estimates of the incidental catch of BOR per unit of effort in each of these fisheries, they multiplied this constant scalar by a historical estimate of the respective annual effort and by the estimated total biomass in each year. There was no selectivity function applied because this was a surplus production model, which assumes that the entire biomass is vulnerable to fishing. Because the BOR biomass indices suggest that the BOR population has been in a monotonic declining trend, this procedure implies that catches were large at the beginning of the series, but declined as the biomass declined, especially if effort also tended to be high at the beginning of the series. The procedure is recursive; that is, biomass was used twice because it was first used to estimate the catch, then these estimates were summed to get the biomass. There is nothing to stop this procedure from repeating itself if the model gets a better fit to the data with an increasing biomass. Another problem with the procedure is that it assumes a constant catchability relationship between biomass and effort in these bycatch fisheries, which seems unlikely over such a long time span.

The catches estimated using this procedure in these fisheries were enormous compared to modern catches: the 1935 catch of BOR in the halibut longline fishery was 1200 t and the salmon troll fishery was estimated to have caught nearly 400 t in the same year (Figure A.9). The sum of these two catches exceeded by far the maximum annual catch of BOR that we were able to reconstruct over the entire catch history (Figure A.9) and there is no evidence that catches of this magnitude were actually taken before the Second World War. When this issue was reviewed by the BOR TWG, these catch levels were considered extremely unlikely and the approach was dropped.

Another departure between this stock assessment and the previous two BOR stock assessments are the very large catches assigned to the trawl fleet during the 1960s and 1970s and then again during the late 1980s and early 1990s (Figure A.9). These stem from the 2009 stock assessment (Stanley et al. 2009) where an early version of the procedure described in Section A.2.2 was applied. Since then, the procedure has been refined (see Section A.2.3), particularly in the interpretation of the late-1980s and early-1990s catches, which are now largely recognised as being inflated to cover for the actual catch of desirable species such as POP (Brian Mose, CGRCS, pers. comm.).

A.2.5. Caveats

The available catch data before 1996 (first year of onboard observer program) present difficulties for use in a stock assessment model without some form of interpretation, both in terms of misreporting (i.e., reporting catches of one species as another) or misidentifying species and the possible existence of at-sea discarding due to catches exceeding what was permitted for retention. Although there were reports that fishermen misreported the location of catches, this issue is not a large problem for an assessment of a coastwide stock. Additionally, there was a significant foreign fishery for rockfish in BC waters, primarily by the United States, the Soviet Union and Japan. These countries tended to report their catches in aggregate form, usually lumping rockfish into a single category. These fisheries ceased after the declaration of the 200 nm exclusive economic zone by Canada in 1977.

Table A.7. Trawl catch (tonnes) by gear type for the coastwide BC BOR stock from years when trawl fleet activity was monitored by onboard observers.

Year	Bottom Trawl	Midwater Trawl	Hook & Line
1996	221	43.3	19.3
1997	199	28.3	9.9
1998	228	24.9	5.6
1999	172	51.3	9.9
2000	236	34.2	16.5
2001	229	39.4	21.9
2002	241	44.1	19.1
2003	187	33.3	14.5
2004	131	19.1	15.8
2005	114	22.4	17.2
2006	91.6	21.3	13.0
2007	99.4	31.1	15.9
2008	75.4	33.7	18.9
2009	81.0	18.9	17.4
2010	67.2	23.8	10.1
2011	63.2	43.9	13.1
2012	65.7	40.8	16.6
2013	41.7	28.1	9.7
2014	40.7	12.3	8.6
2015	30.9	14.1	5.5
2016	23.6	13.7	4.0
2017	31.2	14.1	3.1
2018	61.1	30.8	2.4
2019	37.9	21.1	2.3

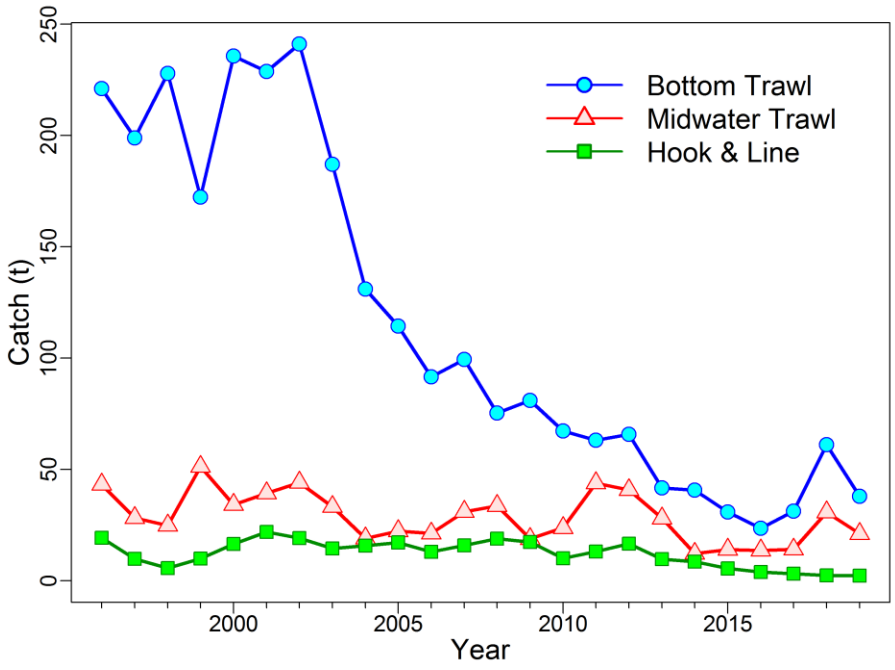

Figure A.10. Reported catch (landings + released) by gear of BOR since the implementation of the trawl's onboard-observer program in 1996.

The accuracy and precision of reconstructed catch series inherently reflect the problems associated with the development of a commercial fishery:

- trips offloading catch with no area information,
- unreported discarding,
- recording catch of one species as another to avoid quota violations,
- developing expertise in monitoring systems,
- shifting regulations,
- changing data storage technologies, etc.

Many of these problems have been eliminated through the introduction of observer programs (onboard observers starting in 1996 for the offshore trawl fleet, electronic monitoring starting in 2006 for the H&L fleets), dockside [observer] monitoring, and tradable individual vessel quotas (starting in 1997) that confer ownership of the resource to the fishing sector.

The catch reconstruction procedure does not rebuild catch by gear type (e.g., bottom trawl vs. midwater trawl, trap vs. longline). While adding this dimension is possible, it would mean splitting catches back in time using ratios observed in the modern fishery, which likely would not accurately represent historical activity by gear type (see Section A.2.2 for similar caveats regarding the use of modern catch ratios to reconstruct the catch of one species from a total rockfish catch). In this assessment, we combined the catches of BOR by bottom and midwater trawl because the biological data (Appendix D) by gear did not support two fleets in the population model and it was inconclusive whether there was a demonstrable difference in selectivity. Table A.7 and Figure A.10 show the reported coastwide catch (landings plus non-retained) by gear type. Note the effect of voluntary catch reductions starting in 2004 followed by regulatory mortality caps.

A.3. SCALING CATCH POLICY TO GMU AREA TACS

The area definitions used by DFO Groundfish Science (PMFC areas) differ somewhat from those used by the DFO Groundfish Management, which uses Pacific Fishery Management Areas (PFMA). The reasons for these discrepancies vary depending on the species, but they occur to address different requirements by Science and Management. For Science, there is a need to reference historical catch using areas that are consistently reported across all years in the databases and catch records. The PMFC and GMU areas, while similar but not identical (Figure 1), address current management requirements.

As this assessment covers the coastwide (PMFC areas 3CD + 5ABCDE) stock of BOR, and GMU only issues a coastwide TAC (or mortality cap), there is no need to scale the catch policies presented in the decision tables (Appendix F). Should managers wish to assign TACs to individual regions,

Table A.8 offers some guidance on the distribution of catches over the five years before voluntary/regulatory catch reductions in 2004 in each of the PMFC areas. For instance, 29% of the coastwide BOR catch occurred in PMFC area 5B, 23% occurred in 5A, and 22% occurred in 3D.

Table A.8. Catch of BOR from the combined fishery in PMFC areas from 5 years prior to voluntary/regulatory catch reductions in 2004. Annual proportions of catch by area are shown in rows marked by year. Area-specific 5-year geometric means of annual proportions (normalised) are shown in the final row.

Catch(t)

Year	3C	3D	5A	5B	5C	5D	5E	BC
1999	32.838	73.683	67.090	54.199	13.399	8.746	22.883	272.838
2000	26.643	70.747	60.026	116.116	9.264	9.792	31.531	324.120
2001	34.812	74.450	62.491	75.906	13.250	16.386	21.910	299.205
2002	23.032	58.136	80.917	97.448	20.823	17.723	15.990	314.069
2003	20.948	45.026	65.093	78.576	10.203	9.848	16.300	245.993

Proportion

Year	3C	3D	5A	5B	5C	5D	5E	BC
1999	0.1204	0.2701	0.2459	0.1986	0.0491	0.0321	0.0839	1
2000	0.0822	0.2183	0.1852	0.3583	0.0286	0.0302	0.0973	1
2001	0.1163	0.2488	0.2089	0.2537	0.0443	0.0548	0.0732	1
2002	0.0733	0.1851	0.2576	0.3103	0.0663	0.0564	0.0509	1
2003	0.0852	0.1830	0.2646	0.3194	0.0415	0.0400	0.0663	1
GeoMean	0.0936	0.2184	0.2303	0.2822	0.0443	0.0413	0.0726	0.9827
Normalise	0.0953	0.2222	0.2344	0.2871	0.0451	0.0420	0.0739	1

A.4. REFERENCES – CATCH

Canada Dominion Bureau of Statistics. 1918-1950. Fisheries Statistics of Canada (British Columbia). Tech. rep., Canada Dominion Bureau of Statistics, Ottawa, ON.

Edwards, A.M., Haigh, R. and Starr, P.J. 2014a. Pacific Ocean Perch (*Sebastes alutus*) stock assessment for the north and west coasts of Haida Gwaii, British Columbia. DFO Can. Sci. Advis. Sec. Res. Doc. 2013/092. vi + 126 p.

Edwards, A.M., Haigh, R. and Starr, P.J. 2014b. Pacific Ocean Perch (*Sebastes alutus*) stock assessment for the west coast of Vancouver Island, British Columbia. DFO Can. Sci. Advis. Sec. Res. Doc. 2013/093. vi + 135 p.

Forrester, C.R. and Smith, J.E. 1972. The British Columbia groundfish fishery in 1971, some aspects of its investigation and related fisheries. Fish. Res. Board Can. Tech. Rep. 338: 67 p.

Gunderson, D.R., Westrheim, S.J., Demory, R.L. and Fraidenburg, M.E. 1977. The status of Pacific Ocean Perch (*Sebastes alutus*) stocks off British Columbia, Washington, and Oregon in 1974. Fish. Mar. Serv. Tech. Rep. 690: iv + 63 p.

Haigh, R. and Yamanaka, K.L. 2011. Catch history reconstruction for rockfish (*Sebastes* spp.) caught in British Columbia coastal waters. Can. Tech. Rep. Fish. Aquat. Sci. 2943: viii + 124 p.

Ketchen, K.S. 1976. Catch and effort statistics of the Canadian and United States trawl fisheries in waters adjacent to the British Columbia coast 1950-1975. Fisheries and Marine Service, Nanaimo, BC, Data Record 6.

Ketchen, K.S. 1980a. Assessment of groundfish stocks off the west coast of Canada (1979). Can. Data Rep. Fish. Aquat. Sci. 185: xvii + 213 p.

Ketchen, K.S. 1980b. Reconstruction of Pacific Ocean Perch (*Sebastes alutus*) stock history in Queen Charlotte sound. Part I. Estimation of foreign catches, 1965–1976. Can. Manuscr. Rep. Fish. Aquat. Sci. 1570: iv + 46 p.

Leaman, B.M. and Stanley, R.D. 1993. Experimental management programs for two rockfish stocks off British Columbia, Canada. In S. J. Smith, J. J. Hunt and D. Rivard, eds., Risk evaluation and biological reference points for fisheries management, p. 403-418. Canadian Special Publication of Fisheries and Aquatic Sciences 120.

Rutherford, K.L. 1999. A brief history of GFCatch (1954-1995), the groundfish catch and effort database at the Pacific Biological Station. Can. Tech. Rep. Fish. Aquat. Sci. 2299: v + 66 p.

Starr, P.J. and Haigh, R. 2017. Stock assessment of the coastwide population of Shortspine Thornyhead (*Sebastolobus alascanus*) in 2015 off the British Columbia coast. DFO Can. Sci. Advis. Sec. Res. Doc. 2017/015. ix + 174 p

Starr, P.J. and Haigh, R. 2021a. Redstripe Rockfish (*Sebastes proriger*) stock assessment for British Columbia in 2018. DFO Can. Sci. Advis. Sec. Res. Doc. 2021/014. vii + 340 p.

Starr, P.J. and Haigh, R. 2021b. Widow Rockfish (*Sebastes entomelas*) stock assessment for British Columbia in 2019. DFO Can. Sci. Advis. Sec. Res. Doc. 2021/039. viii + 238 p.

Wallace, S., Turris, B., Driscoll, J., Bodtker, K., Mose, B. and Munro, G. 2015. Canada's Pacific groundfish trawl habitat agreement: A global first in an ecosystem approach to bottom trawl impacts. Mar. Pol. 60: 240-248.

Westrheim, S.J., Gunderson, D.R. and Meehan, J.M. 1972. On the status of Pacific Ocean Perch (*Sebastes alutus*) stocks off British Columbia, Washington, and Oregon in 1970. Fish. Res. Board Can. Tech. Rep. 326: 48 p.

Yamanaka, K.L., McAllister, M.M., Etienne, M.P., Edwards, A.M. and Haigh, R. 2018. Assessment for the outside population of Yelloweye Rockfish (*Sebastes ruberrimus*) for British Columbia, Canada in 2014. DFO Can. Sci. Advis. Sec. Res. Doc. 2018/001. ix + 150 p.

APPENDIX B. TRAWL SURVEYS

B.1. INTRODUCTION

This appendix summarises the derivation of relative Bocaccio Rockfish (BOR) abundance indices from the following bottom trawl surveys:

- a set of historical surveys operated in the Goose Island Gully of Queen Charlotte Sound (Section B.3);
- National Marine Fisheries Service (NMFS) Triennial survey operated off the lower half of Vancouver Island (Section B.4);
- Queen Charlotte Sound (QCS) synoptic survey (Section B.5);
- West Coast Vancouver Island (WCVI) synoptic survey (Section B.6);
- West Coast Haida Gwaii (WCHG) synoptic survey (Section B.7);
- Hecate Strait (HS) synoptic survey (Section B.8);

Only surveys which were used in the BOR stock assessment are presented. The Hecate Strait multi-species survey, the WCVI shrimp and Queen Charlotte Sound shrimp surveys have been omitted because the presence of BOR in these surveys has been either sporadic or the coverage, either spatial or by depth, has been incomplete, rendering these surveys poor candidates to provide abundance series for this species. Rockfish stock assessments, beginning with Yellowtail Rockfish (Starr et al. 2014), have explicitly omitted using the two shrimp surveys because of the truncated depth coverage, which ends at 160 m for the WCVI shrimp survey, and the constrained spatial coverage of the QC Sound shrimp survey as well as its truncated depth coverage, which ends at 231 m.

B.2. ANALYTICAL METHODS

Catch and effort data for strata i in year y yield catch per unit effort (CPUE) values U_{yi}. Given a set of data $\{C_{yij}, E_{yij}\}$ for tows $j = 1,\ldots,n_{yi}$,

Eq. B.1 $$U_{yi} = \frac{1}{n_{yi}} \sum_{j=1}^{n_{yi}} \frac{C_{yij}}{E_{yij}},$$

where C_{yij} = catch (kg) in tow j, stratum i, year y;
E_{yij} = effort (h) in tow j, stratum i, year y;
n_{yi} = number of tows in stratum i, year y.

CPUE values U_{yi} convert to CPUE densities δ_{yi} (kg/km^2) using:

Eq. B.2 $$\delta_{yi} = \frac{1}{vw} U_{yi},$$

where v = average vessel speed (km/h);
w = average net width (km).

Alternatively, if vessel information exists for every tow, CPUE density can be expressed

Eq. B.3 $$\delta_{yi} = \frac{1}{n_{yi}} \sum_{j=1}^{n_{yi}} \frac{C_{yij}}{D_{yij} w_{yij}},$$

where C_{yij} = catch weight (kg) for tow j, stratum i, year y;

D_{yij} = distance travelled (km) for tow j, stratum i, year y;

w_{yij} = net opening (km) for tow j, stratum i, year y;

n_{yi} = number of tows in stratum i, year y.

The annual biomass estimate is then the sum of the product of CPUE densities and bottom areas across m strata:

Eq. B.4 $$B_y = \sum_{i=1}^{m} \delta_{yi} A_i = \sum_{i=1}^{m} B_{yi},$$

where δ_{yi} = mean CPUE density (kg/km^2) for stratum i, year y;

A_i = area (km^2) of stratum i;

B_{yi} = biomass (kg) for stratum i, year y;

m = number of strata.

The variance of the survey biomass estimate V_y (kg^2) follows:

Eq. B.5 $$V_y = \sum_{i=1}^{m} \frac{\sigma_{yi}^2 A_i^2}{n_{yi}} = \sum_{i=1}^{m} V_{yi},$$

where σ_{yi}^2 = variance of CPUE density (kg^2/km^4) for stratum i, year y;

V_{yi} = variance of the biomass estimate (kg^2) for stratum i, year y.

The coefficient of variation (CV) of the annual biomass estimate for year y is

Eq. B.6 $$CV_y = \frac{\sqrt{V_y}}{B_y}.$$

B.3. EARLY SURVEYS IN QUEEN CHARLOTTE SOUND GOOSE ISLAND GULLY

B.3.1. Data selection

Tow-by-tow data from a series of historical trawl surveys were available for 12 years spanning the period from 1965 to 1995. The first two surveys, in 1965 and 1966, were wide-ranging, with the 1965 survey extending from near San Francisco to halfway up the Alaskan Panhandle (Westrheim 1966a, 1967b). The 1966 survey was only slightly less ambitious, ranging from the southern US-Canada border in Juan de Fuca Strait into the Alaskan Panhandle (Westrheim 1966b, 1967b). It was apparent that the design of these two early surveys was exploratory and that these surveys would not be comparable to the subsequent Queen Charlotte Sound (QCS) surveys which were much narrower in terms of area covered and which had a much higher density of tows in the Goose Island Gully (GIG). This can be seen in the small number of tows used by the first two surveys in GIG (Table B.1). As a consequence, these surveys are not included in this series.

The 1967 ([left panel]: Figure B.1) and 1969 ([left panel]: Figure B.2) surveys (Westrheim 1967a, 1969; Westrheim et al. 1968) also performed tows on the west coast of Vancouver Island, the west coast of Haida Gwaii and SE Alaska, but both of these surveys had a reasonable number of tows in the GIG grounds (Table B.1). The 1971 survey ([left panel]: Figure B.3) was entirely confined to GIG (Harling et al. 1971) while the 1973 ([left panel]: Figure B.4), 1976 ([left panel]: Figure B.5) and 1977 ([left panel]: Figure B.6) surveys covered both Goose Island and Mitchell Gullies in QCS (Harling et al. 1973; Westrheim et al. 1976; Harling and Davenport 1977).

A 1979 survey (Nagtegaal and Farlinger 1980) was conducted by a commercial fishing vessel (*Southward Ho*, Table B.1), with the distribution of tows being very different from the preceding and succeeding surveys (plot not provided; see Figure C5 in Edwards et al. 2012). As well, the distribution of tows by depth was also different from the other surveys (Table B.2). These observations imply a substantially different survey design and consequently this survey was not included in the time series.

The 1984 survey was conducted by two vessels: the *G.B. Reed* and the *Eastward Ho* (Nagtegaal et al. 1986). Part of the design of this survey was to compare the catch rates of the two vessels (one was a commercial fishing vessel and the other a government research vessel – Greg Workman, DFO, pers. comm.), thus they both followed similar design specifications, including the configuration of the net. Unfortunately, the tows were not distributed similarly in all areas, with the *G.B. Reed* fishing mainly in the shallower portions of the GIG, while the *Eastward Ho* fished more in the deeper and seaward parts of the GIG ([left panel]: Figure B.7) although the two vessels fished more contiguously in Mitchell Gully (immediately to the north). When the depth-stratified catch rates for Pacific Ocean Perch (the main design species of the surveys) of the two vessels were compared within the GIG only (using a simple ANOVA), the *Eastward Ho* catch rates were significantly higher ($p=0.049$) than those observed for the *G.B. Reed*. However, the difference in catch rates was no longer significant when tows from Mitchell's Gully were added to the analysis ($p=0.12$). Given the lack of significance when the full suite of available tows were compared, along with the uneven spatial distribution of tows among vessels within the GIG (although the ANOVA was depth-stratified, it is possible that the depth categories were too coarse), the most parsimonious conclusion was that there was no detectable difference between the two vessels. Consequently, all the GIG tows from both vessels were pooled for this survey year.

The 1994 survey, also conducted by a commercial vessel (the *Ocean Selector*, Table B.2), was modified by the removal of 19 tows which were part of an acoustic experiment and therefore were not considered appropriate for biomass estimation (they were tows used to estimate species composition for ensonified schools). Although this survey was designed to emulate as closely as possible the previous *G.B. Reed* surveys in terms of tow location selection (same fixed tow locations, G. Workman, DFO, pers. comm.), the timing of this survey was about two to three months earlier than the previous surveys (starting in mid-June rather than August or September, Table B.3).

The 1995 survey, conducted by two commercial fishing vessels: the *Ocean Selector* and the *Frosti* (Table B.2), used a random stratified design with each vessel duplicating every tow (G. Workman, DFO, pers. comm.). This type of design was entirely different from the fixed station (based on Loran coordinates) used in the previous surveys. As well, the focus of this survey was on Pacific Ocean Perch (POP), with tows optimised to capture this species. Given the difference in design (random stations rather than fixed locations), this survey was not used in the stock assessment.

Given that the only area that was consistently monitored by these surveys was the GIG grounds, tows lying between 50.9°N & 51.6°N latitude from the eight acceptable survey years, covering the period from 1967 to 1994, were used to index the BOR population (Table B.1).

Table B.1. Number of tows in GIG and in other areas (Other) by survey year and vessel conducting the survey for the 12 historical (1965 to 1995) surveys. Survey years in grey were not used in the assessment

Survey	GB Reed		Southward Ho		Eastward Ho		Ocean Selector		Frosti	
Year	Other	GIG	Other	GIG	Other	GIG	Other	GIG	Other	GIG
1965	76	8	-	-	-	-	-	-	-	-
1966	49	15	-	-	-	-	-	-	-	-
1967	17	33	-	-	-	-	-	-	-	-
1969	3	32	-	-	-	-	-	-	-	-
1971	3	36	-	-	-	-	-	-	-	-
1973	13	33	-	-	-	-	-	-	-	-
1976	23	33	-	-	-	-	-	-	-	-
1977	15	47	-	-	-	-	-	-	-	-
1979			20	59	-	-	-	-	-	-
1984	19	42			15	27	-	-	-	-
1994	-	-	-	-	-	-	2	69	-	-
1995	-	-	-	-	-	-	2	55	1	57

Table B.2. Total number of tows by 20 fathom depth interval (in metres) in GIG and in other areas (Other) by survey year for the 12 historical (1965 to 1995) surveys. Survey years in grey were not used in the assessment. Some of the tows in the GIG portion of the table have usability codes other than 0,1,2, or 6.

Areas other than GIG

Survey	20 fathom depth interval (m)									Total
year	66-146	147-183	184-219	220-256	257-292	293-329	330-366	367-402	440-549	Tows
1965	3	15	26	17	6	6	1	1	1	76
1966	3	11	18	8	2	1	3	2	1	49
1967	1	-	6	1	2	1	1	4		16
1969	-	1	-	1	-	1	-	-	-	3
1971	-	-	-	-	-	-	-	-	-	-
1973	-	-	4	3	2	2	2	-	-	13
1976	-	-	4	4	4	4	4	-	-	20
1977	-	-	3	2	2	3	2	-	-	12
1979	11	2	1	5	1			-	-	20
1984	-	-	4	10	7	7	6	-	-	34
1994	-	-	-	-	-	-	-	-	-	-
1995	-	-	-	-	-	-	-	-	-	-

GIG

Survey	20 fathom depth interval (m)									Total
year	66-146	147-183	184-219	220-256	257-292	293-329	330-366	367-402	440-549	Tows
1965		2	4	1	1	-	-	-	-	8
1966	3	2	3	5	2	-	-	-	-	15
1967	1	6	11	6	10	-	-	-	-	34
1969	-	9	11	6	6	-	-	-	-	32
1971	-	5	15	9	10	-	-	-	-	39
1973	-	7	11	7	8	-	-	-	-	33
1976	-	7	15	8	6	-	-	-	-	36
1977	1	12	14	14	9	-	-	-	-	50
1979	23	12	18	6		-	-	-	-	59
1984	-	13	25	17	13	1	-	-	-	69
1994	-	15	18	20	18		-	-	-	71
1995	2	23	47	22	15	6	-	-	-	115

The original depth stratification of these surveys was in 20 fathom (36.1 m) intervals, ranging from 36 fathoms (66 m) to 300 fathoms (549 m). These depth strata were combined for analysis into three ranges which encompassed most rockfish: 120–183 m, 184–218 m and 219–300 m, for a total of 332 tows from the eight accepted survey years (Table B.3).

Table B.3. Number of tows available by survey year and depth stratum for the analysis of the historical GIG trawl survey series. Survey year in grey was not used in the BOR stock assessment.

Survey Year	Depth stratum 120-183 m (70–100 fm)	184-218 m (100–120 fm)	219-300 m (120–160 fm)	Total	Start Date	End Date
1967	7	11	15	33	07-Sep-67	03-Oct-67
1969	8	11	12	31	14-Sep-69	24-Sep-69
1971	4	15	17	36	14-Oct-71	28-Oct-71
1973	7	11	15	33	07-Sep-73	24-Sep-73
1976	7	13	13	33	09-Sep-76	26-Sep-76
1977	13	14	20	47	24-Aug-77	07-Sep-77
1984	13	23	33	69	05-Aug-84	08-Sep-84
1994	10	16	24	50	21-Jun-94	06-Jul-94
1995	22	45	45	112	11-Sep-95	22-Sep-95

A doorspread density (Eq. B.3) was calculated for each tow based on the catch of BOR, using a fixed doorspread value of 61.6 m (Yamanaka et al. 1996) for every tow and the recorded distance travelled. Unfortunately, the speed, effort and distance travelled fields were not well populated for these surveys. Therefore, missing values for these fields were filled in with the mean values for the survey year. This resulted in the majority of the tows having distances towed near 3 km, which was the expected result given the design specification of ½ hour tows at an approximate speed of 6 km/h (about 3.2 knots).

B.3.2. Results

Maps showing the locations where BOR were caught in the Goose Island Gully (GIG) indicate that this species is found throughout the gully, although in small amounts, in every year as well as extending into the south-eastern branch of the gully (see Figure B.1 to Figure B.8). BOR was taken relatively frequently, but in small amounts, with 193 of the 444 (including 1995; 43%) valid tows capturing BOR with a median catch weight of 9.5 kg. The largest valid BOR tow in terms of catch weight was 1,587 kg in 1976. BOR were mainly taken at depths from 161 to 241 m (5% and 95% quantiles of the starting depth empirical distribution), with the minimum and maximum observed BOR catch weights at starting tow depths of 146 and 287 m respectively (Figure B.9).

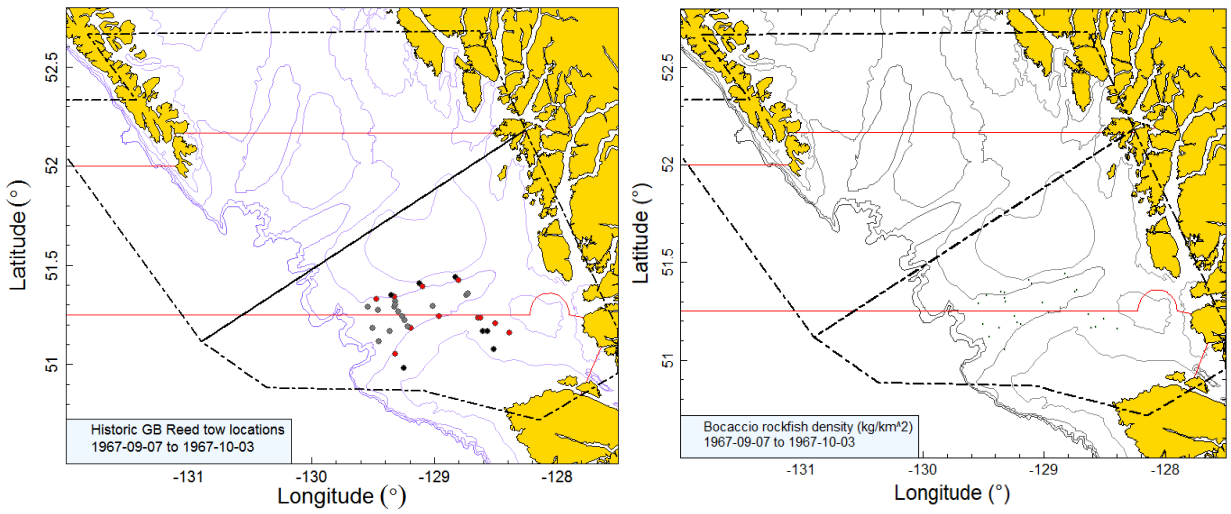

Figure B.1. Valid tow locations and density plots for the historic 1967 Goose Island Gully (GIG) survey. Tow locations are colour-coded by depth range: black=120–183m; red=184-218m; grey=219-300m. Circle sizes in the right-hand density plot scaled across all years (1967, 1969, 1971, 1973, 1976, 1977, 1984, and 1994), with the largest circle = 8,919 kg/km^2 in 1976. Black boundary lines show the extent of the modern Queen Charlotte Sound synoptic survey and the red solid lines indicate the boundaries between PMFC areas 5A, 5B and 5C.

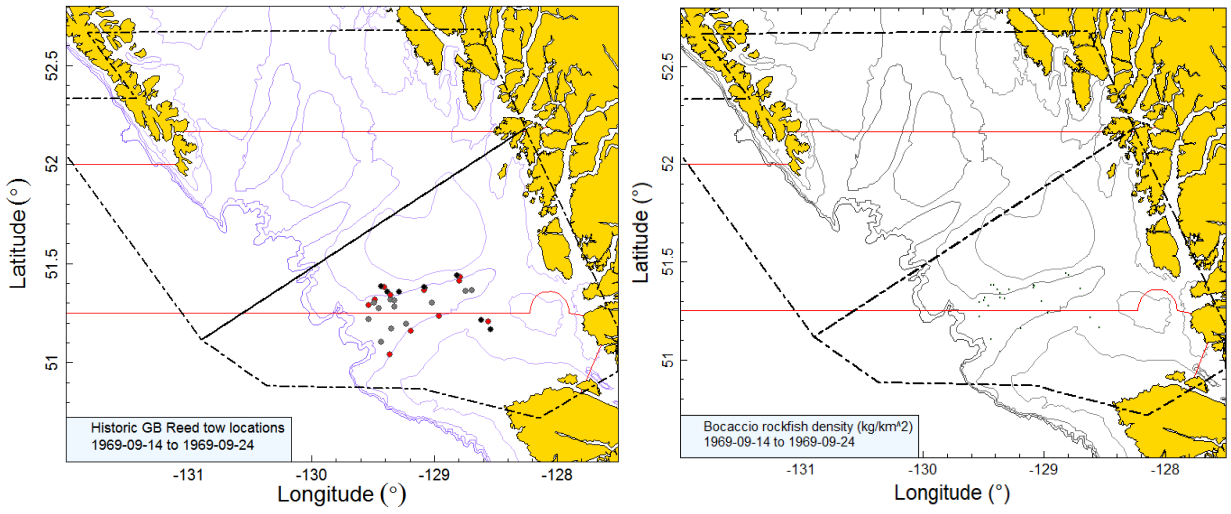

Figure B.2. Tow locations and density plots for the historic 1969 Goose Island Gully (GIG) survey (see Figure B.1 caption).

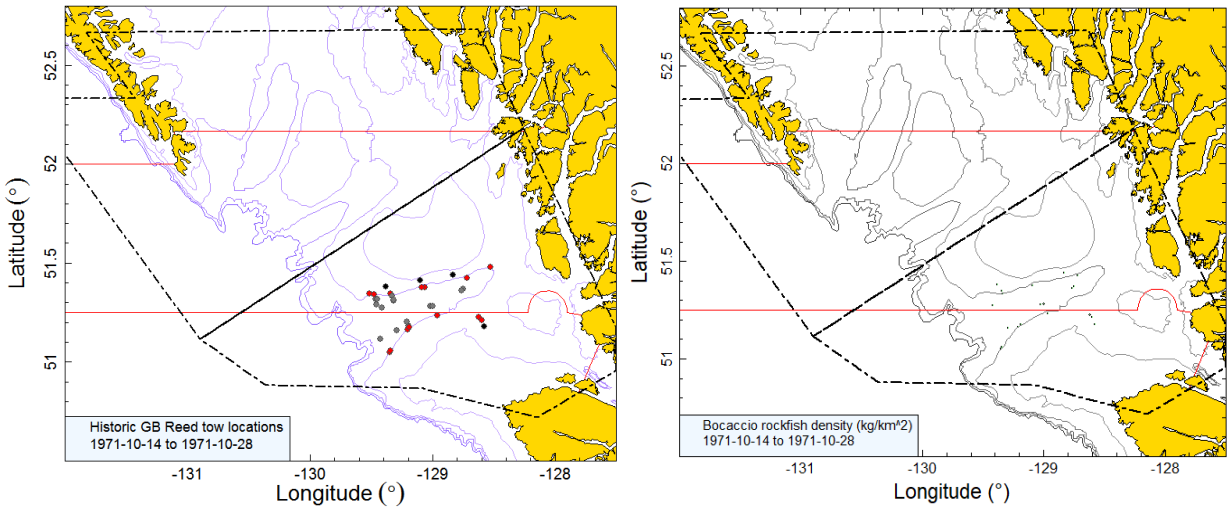

Figure B.3. Tow locations and density plots for the historic 1971 Goose Island Gully (GIG) survey (see Figure B.1 caption).

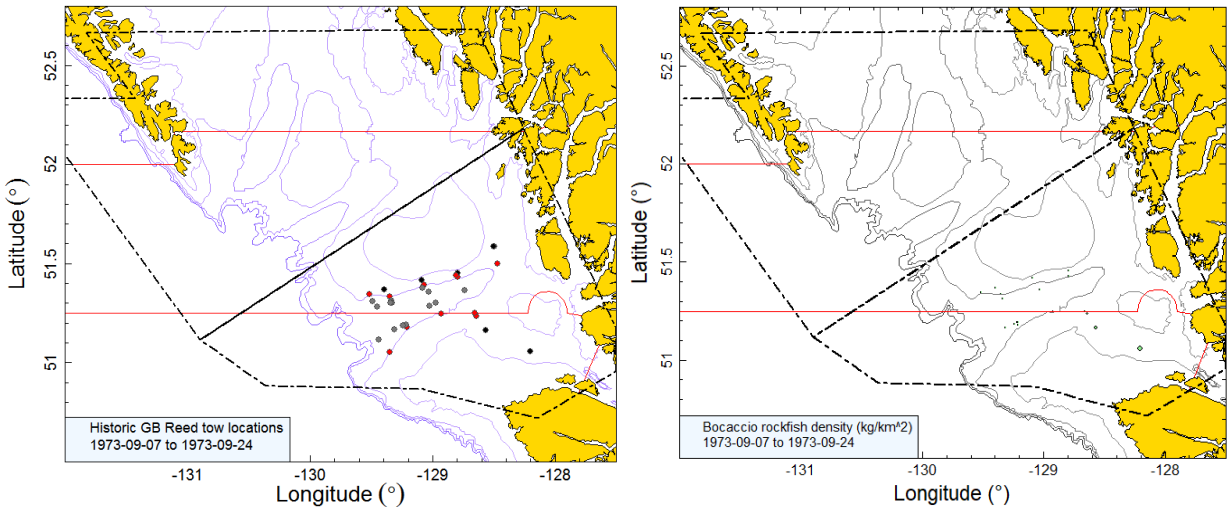

Figure B.4. Tow locations and density plots for the historic 1973 Goose Island Gully (GIG) survey (see Figure B.1 caption).

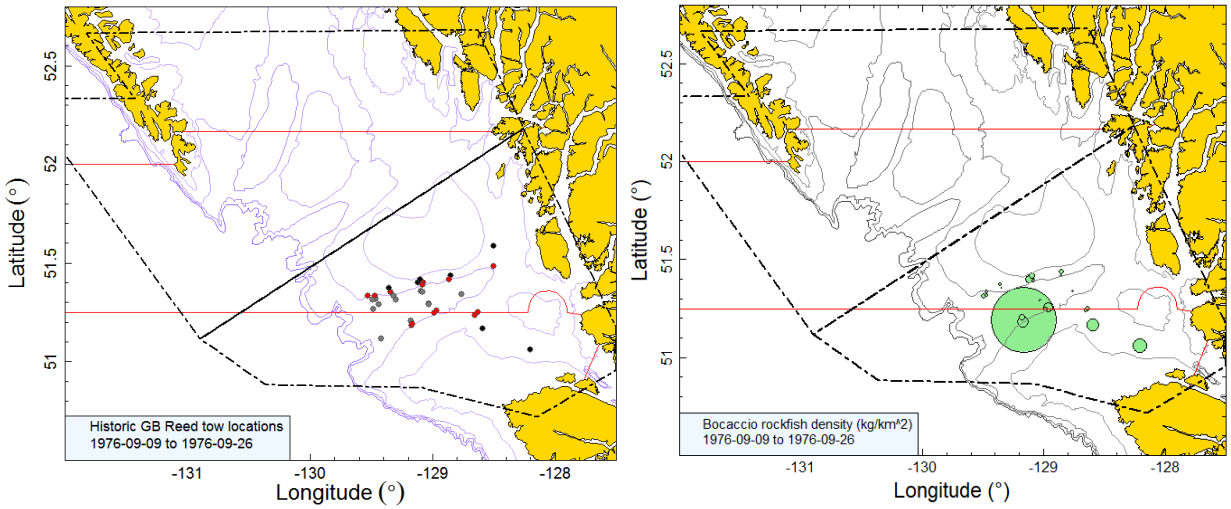

Figure B.5. Tow locations and density plots for the historic 1976 Goose Island Gully (GIG) survey (see Figure B.1 caption).

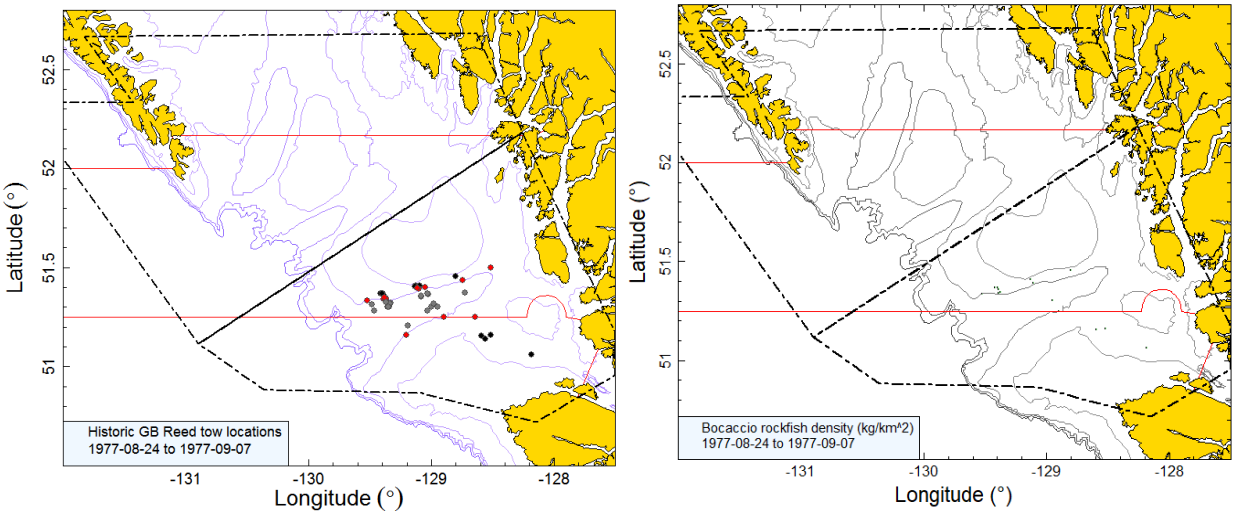

Figure B.6. Tow locations and density plots for the historic 1977 Goose Island Gully (GIG) survey (see Figure B.1 caption).

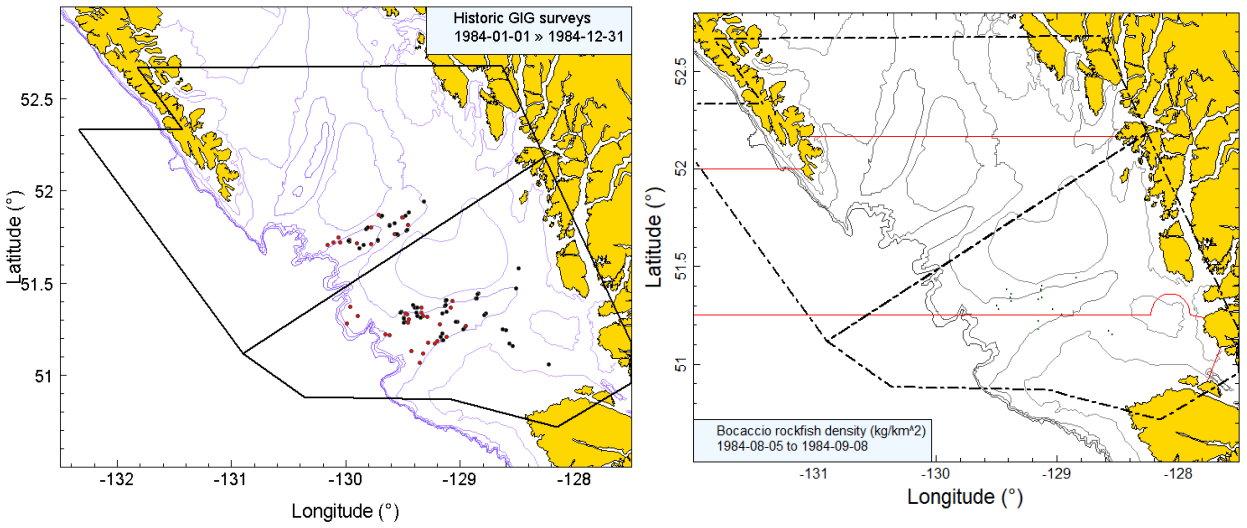

Figure B.7. [left panel]: Tow location colours indicate the vessel fishing rather than depth: black=G.B. Reed; red=Eastward Ho. Additional locations fished by vessel in Mitchell Gully are also shown; [right panel]: density plot for the historic 1984 Goose Island Gully (GIG) survey (see Figure B.1 caption).

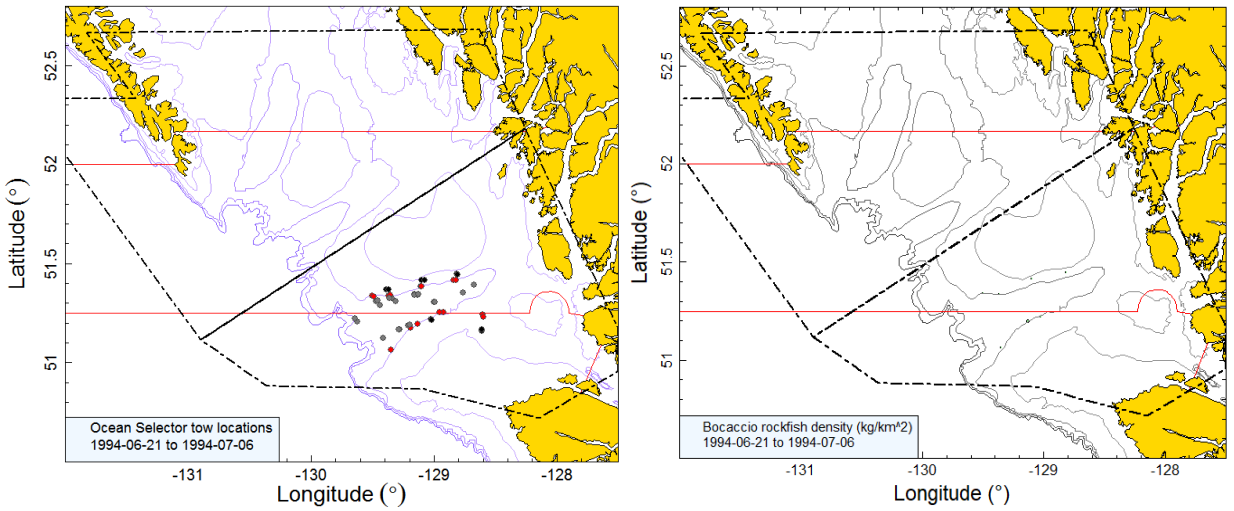

Figure B.8. Tow locations and density plots for the Ocean Selector 1994 Goose Island Gully (GIG) survey (see Figure B.1 caption).

Estimated biomass levels in the GIG for BOR from the historical GIG trawl surveys were variable, with the maximum biomass recorded in 1976 (at 1,237 t) and the minimum biomass in 1994 (at 68 t) (Figure B.10; Table B.4). Survey relative errors were very variable for this species, ranging from a low of 0.16 in 1967 to 0.63 in 1976 (Table B.4). The proportion of tows which caught BOR was generally high and variable between years, ranging between 14% in

1967 and 81% in 1976 (Figure B.11). Overall, 193 tows from a total 444 valid tows (including 1995: 43%) contained BOR.

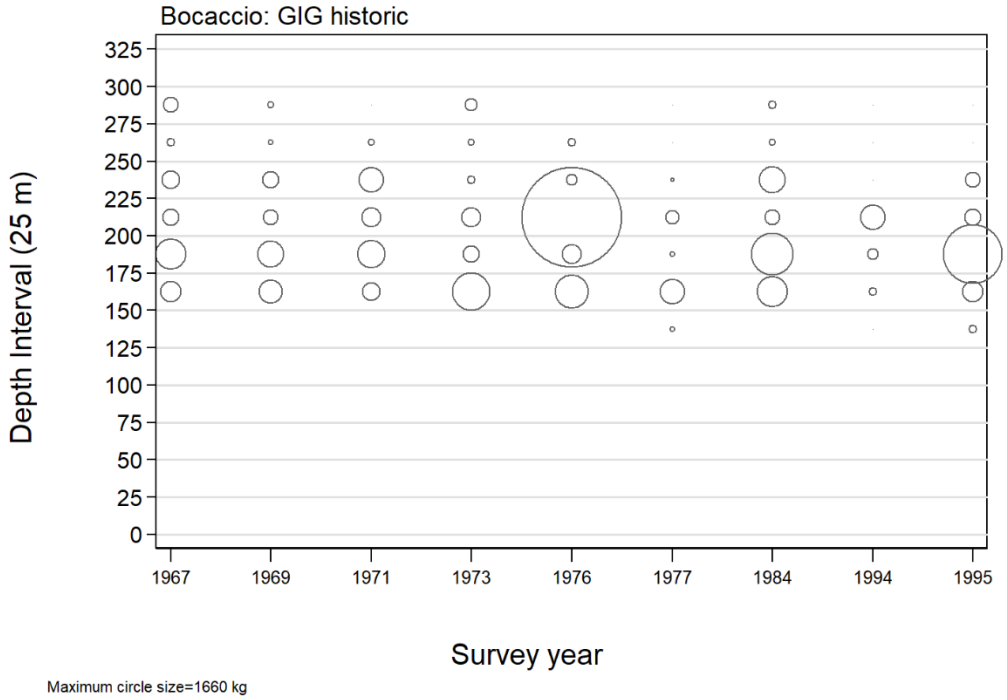

Figure B.9. Distribution of observed catch weights of BOR for the historic Goose Island Gully (GIG) surveys (Table B.3) by survey year and 25 m depth zone. Depth zones are indicated by the mid point of the depth interval and circles in the panel are scaled to the maximum value (1660 kg) in the 200–225 m interval in 1976. The 1% and 99% quantiles for the BOR empirical start of tow depth distribution= 154 m and 280 m respectively.

Table B.4. Biomass estimates for BOR from the historical Goose Island Gully trawl surveys for the years 1967 to 1994. Biomass estimates are based on three depth strata (Table B.3), assuming that the survey tows were randomly selected within these areas. Bootstrap bias corrected confidence intervals and CVs are based on 500 random draws with replacement.

Survey Year	**Biomass (t)** (Eq. B.4)	**Mean bootstrap biomass (t)**	**Lower bound biomass (t)**	**Upper bound biomass (t)**	**Bootstrap CV**	**Analytic CV** (Eq. B.6)
1967	342	337	238	459	0.163	0.170
1969	316	317	191	448	0.206	0.209
1971	289	283	129	576	0.394	0.366
1973	504	493	189	1,035	0.442	0.440
1976	1,237	1,176	295	3,245	0.629	0.669
1977	114	115	55	211	0.323	0.318
1984	281	283	149	461	0.284	0.289
1994	68	67	17	174	0.556	0.550

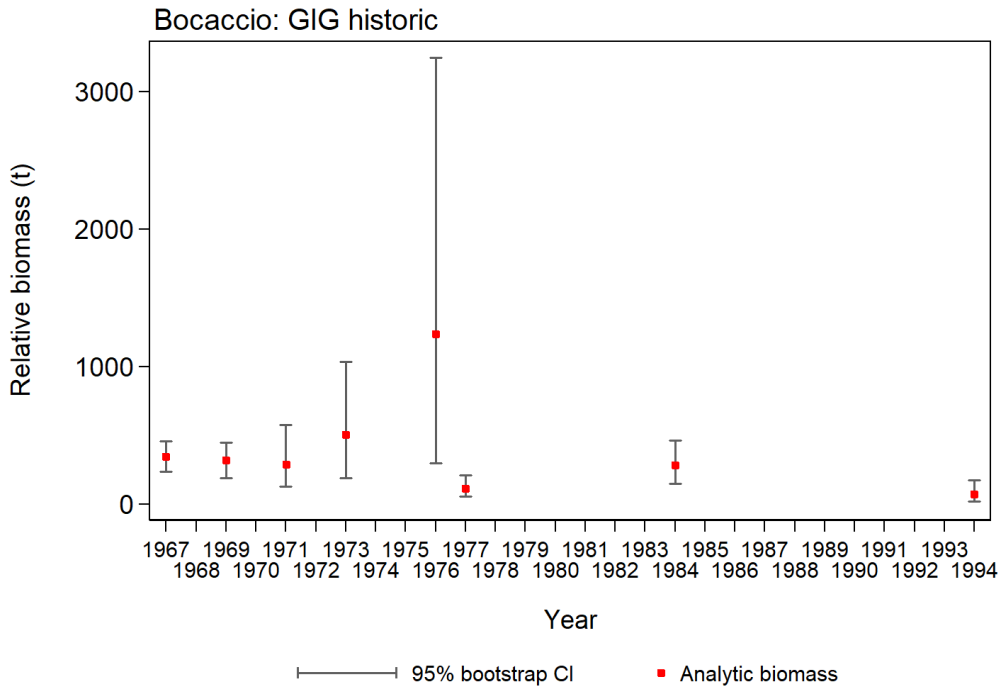

Figure B.10. Plot of biomass estimates for the BOR historic Goose Island Gully (GIG) surveys: 1967 to 1994 (values provided in Table B.4). Bias corrected 95% confidence intervals from 500 bootstrap replicates are plotted.

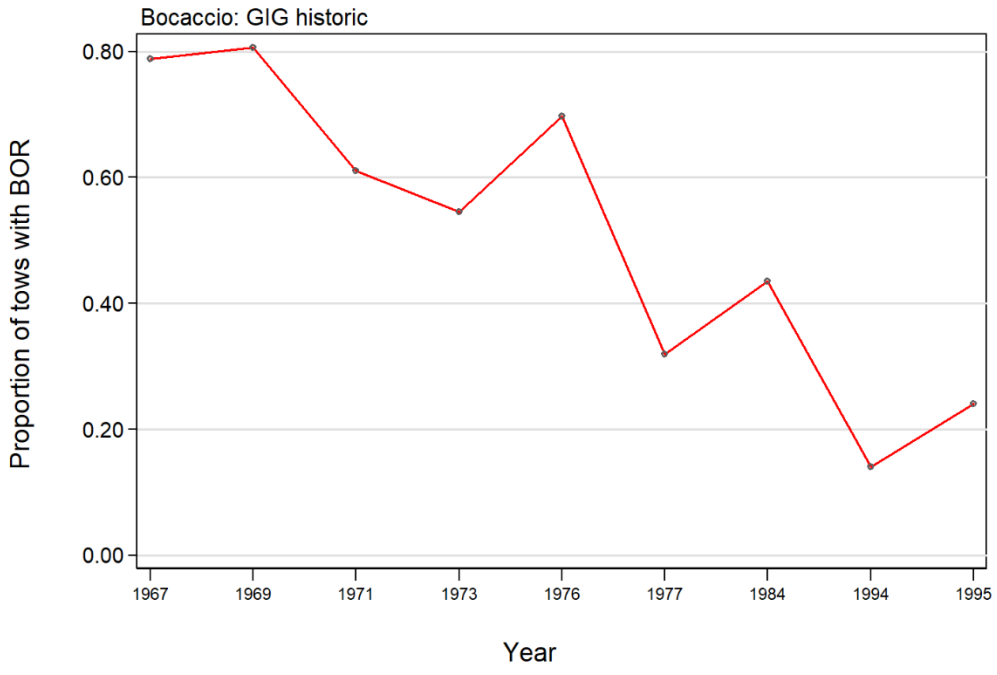

Figure B.11. Proportion of tows by year which contain BOR from the historic Goose Island Gully (GIG) surveys: 1967 to 1995.

B.4. NMFS TRIENNIAL TRAWL SURVEY

B.4.1. Data selection

Tow-by-tow data from the US National Marine Fisheries Service (NMFS) triennial survey covering the Vancouver INPFC (International North Pacific Fisheries Commission) region were provided by Mark Wilkins (NMFS, pers. comm.) for the seven years that the survey operated in BC waters (Table B.5; 1980: Figure B.12; 1983: Figure B.13; 1989: Figure B.14; 1992: Figure B.15; 1995: Figure B.16; 1998: Figure B.17; 2001: Figure B.18). These tows were assigned to strata by the NMFS, but the size and definition of these strata have changed over the life of the survey (Table B.6). The NMFS survey database also identified in which country the tow was located. This information was plotted and checked against the accepted Canada/USA marine boundary: all tows appeared to be appropriately located with respect to country, based on the tow start position (Figure B.12 to Figure B.18). The NMFS designations were accepted for tows located near the marine border.

Table B.5. Number of tows by stratum and by survey year for the NFMS triennial survey. Strata coloured grey have been excluded from the analysis due to incomplete coverage across the seven survey years or were from locations outside the Vancouver INPFC area (Table B.6).

Stratum	1980		1983		1989		1992		1995		1998		2001	
No.	CDN	US	CDN	US	CDN	US	CDN	US	CDN	US	CDN	US	CDN	US
10	-	17	-	7	-	-	-	-	-	-	-	-	-	-
11	48	-	-	39	-	-	-	-	-	-	-	-	-	-
12	-	-	38	-	-	-	-	-	-	-	-	-	-	-
17N	-	-	-	-	-	8	-	9	-	8	-	8	-	8
17S	-	-	-	-	-	27	-	27	-	25	-	26	-	25
18N	-	-	-	-	1	-	1	-	-	-	-	-	-	-
18S	-	-	-	-	-	32	-	23	-	12	-	20	-	14
19N	-	-	-	-	58	-	53	-	55	-	48	-	33	-
19S	-	-	-	-	-	4	-	6	-	3	-	3	-	3
27N	-	-	-	-	-	2	-	1	-	2	-	2	-	2
27S	-	-	-	-	-	5	-	2	-	3	-	4	-	5
28N	-	-	-	-	1	-	1	-	2	-	1	-	-	-
28S	-	-	-	-	-	6	-	9	-	7	-	6	-	7
29N	-	-	-	-	7	-	6	-	7	-	6	-	3	-
29S	-	-	-	-	-	3	-	2	-	3	-	3	-	3
30	-	4	-	2	-	-	-	-	-	-	-	-	-	-
31	7	-	-	11	-	-	-	-	-	-	-	-	-	-
32	-	-	5	-	-	-	-	-	-	-	-	-	-	-
37N	-	-	-	-	-	-	-	-	-	1	-	1	-	1
37S	-	-	-	-	-	-	-	-	-	2	-	1	-	1
38N	-	-	-	-	-	-	-	-	1	-	-		-	-
38S	-	-	-	-	-	-	-	-	-	2	-	-	-	3
39	-	-	-	-	-	-	-	-	6	-	4	-	2	-
50	-	5	-	1	-	-	-	-	-	-	-	-	-	-
51	4	-	-	10	-	-	-	-	-	-	-	-	-	-
52	-	-	4	-	-	-	-	-	-	-	-	-	-	-
Total	59	26	47	70	67	87	61	79	71	68	59	74	38	72

All usable tows had an associated median net width (with 1-99% quantiles) of 13.4 (11.3-15.7) m and median distance travelled of 2.8 (1.4-3.5) km, allowing for the calculation of the area swept by each tow. Biomass indices and the associated analytical CVs for BOR were calculated for the total Vancouver INPFC region and for each of the Canadian- and US-Vancouver sub-regions, using appropriate area estimates for each stratum and year (Table B.6). Strata that were not surveyed consistently in all seven years of the survey were

dropped from the analysis (Table B.5; Table B.6), allowing the remaining data to provide a comparable set for each year (Table B.7).

The stratum definitions used in the 1980 and 1983 surveys were different than those used in subsequent surveys, particularly in Canadian waters (Table B.7). Therefore, the 1980 and 1983 Canadian indices were scaled by the ratio (9166 km^2 / 7399 km^2 = 1.24) of the total stratum areas relative to the 1989 and later surveys so that the coverage from the first two surveys would be comparable to the surveys conducted from 1989 onwards. Correspondingly, the 1980 and 1983 US indices were scaled down slightly (4699 km^2 /4738 km^2 = 0.99) in the same manner. The tow density was much higher in US waters although the overall number of tows was approximately the same for each country (Table B.7). This occurred because the size of the total area fished in the INPFC Vancouver area was about twice as large in Canadian waters than in US waters (Table B.7). Note that the northern extension of the survey varied from year to year (see Figure B.12 to Figure B.18), but this difference has been compensated for by using a constant survey area for all years and assuming that catch rates in the unsampled areas were the same as in the sampled area.

Table B.6. Stratum definitions by year used in the NMFS triennial survey to separate the survey results by country and by INPFC area. Stratum definitions in grey are those strata which have been excluded from the final analysis due to incomplete coverage across the seven survey years or because the locations were outside the Vancouver INPFC area.

Year	Stratum No.	Area (km^2)	Start	End	Country	INPFC area	Depth range
1980	10	3537	47°30	US-Can Border	US	Vancouver	55-183 m
1980	11	6572	US-Can Border	49°15	CDN	Vancouver	55-183 m
1980	30	443	47°30	US-Can Border	US	Vancouver	184-219 m
1980	31	325	US-Can Border	49°15	CDN	Vancouver	184-219 m
1980	50	758	47°30	US-Can Border	US	Vancouver	220-366 m
1980	51	503	US-Can Border	49°15	CDN	Vancouver	220-366 m
1983	10	1307	47°30	47°55	US	Vancouver	55-183 m
1983	11	2230	47°55	US-Can Border	US	Vancouver	55-183 m
1983	12	6572	US-Can Border	49°15	CDN	Vancouver	55-183 m
1983	30	66	47°30	47°55	US	Vancouver	184-219 m
1983	31	377	47°55	US-Can Border	US	Vancouver	184-219 m
1983	32	325	US-Can Border	49°15	CDN	Vancouver	184-219 m
1983	50	127	47°30	47°55	US	Vancouver	220-366 m
1983	51	631	47°55	US-Can Border	US	Vancouver	220-366 m
1983	52	503	US-Can Border	49 °15	CDN	Vancouver	220-366 m
1989&after	17N	1033	47°30	47°50	US	Vancouver	55-183 m
1989&after	17S	3378	46°30	47°30	US	Columbia	55-183 m
1989&after	18N	159	47°50	48°20	CDN	Vancouver	55-183 m
1989&after	18S	2123	47°50	48°20	US	Vancouver	55-183 m
1989&after	19N	8224	48°20	49°40	CDN	Vancouver	55-183 m
1989&after	19S	363	48°20	49°40	US	Vancouver	55-183 m
1989&after	27N	125	47°30	47°50	US	Vancouver	184-366 m
1989&after	27S	412	46°30	47°30	US	Columbia	184-366 m
1989&after	28N	88	47°50	48°20	CDN	Vancouver	184-366 m
1989&after	28S	787	47°50	48°20	US	Vancouver	184-366 m
1989&after	29N	942	48°20	49°40	CDN	Vancouver	184-366 m
1989&after	29S	270	48°20	49°40	US	Vancouver	184-366 m
1995&after	37N	102	47°30	47°50	US	Vancouver	367-500 m
1995&after	37S	218	46°30	47°30	US	Columbia	367-500 m
1995&after	38N	66	47°50	48°20	CDN	Vancouver	367-500 m
1995&after	38S	175	47°50	48°20	US	Vancouver	367-500 m

Table B.7. Number of usable tows performed and area surveyed in the INPFC Vancouver region separated by the international border between Canada and the United States. Strata 18N, 28N, 37, 38 and 39 (Table B.6) were dropped from this analysis as they were not consistently conducted over the survey period. All strata occurring in the Columbia INPFC region (17S and 27S; Table B.6) were also dropped. Thirty-two "water hauls" are separately listed in this table.

	Tows: Canada waters			Tows: US waters			All Tows			Coverage (km^2)		
Year	Usable tows	Water hauls	Total	Usable tows	Water hauls	Total	Usable tows	Water hauls	Total	Canada waters	US waters	Total
1980	48	11	59	23	3	26	71	14	85	7,399	4,738	12,137
1983	39	8	47	65	5	70	104	13	117	7,399	4,738	12,137
1989	63	2	65	55		55	117	3	120	9,166	4,699	13,865
1992	59	-	59	47	3	50	106	3	109	9,166	4,699	13,865
1995	62	-	62	35	-	35	97	-	97	9,166	4,699	13,865
1998	54	-	54	42	-	42	96	-	96	9,166	4,699	13,865
2001	36	-	36	37	-	37	73	-	73	9,166	4,699	13,865
Total	361	21	382	304	11	315	664	33	697	–	–	–

Six hundred and ninety-seven tows across seven survey years remained in the data set after the inconsistently surveyed strata identified in Table B.6 were removed (Table B.7). A further 32 tows were identified as "water hauls" (Table B.7) after a reviewer from NOAA for the 2014 Yellowtail Rockfish stock assessment (DFO 2015) pointed out that a number of the early Triennial survey tows had been so designated because they caught no fish or invertebrates and recommended that they should be discarded from the estimation procedure.

B.4.2. Methods

The data were analysed using the equations in Section B.1. When calculating the variance for this survey, it was assumed that the variance and CPUE within any stratum were equal, even for strata that were split by the Canada/USA border. The total biomass $\left(B_{y_i}\right)$ within a stratum that straddled the border was split between the two countries $\left(B_{y_{i_c}}\right)$ by the ratio of the relative area within each country:

Eq. B.7 $$B_{y_{i_c}} = B_{y_i} \frac{A_{y_{i_c}}}{A_{y_i}},$$

where $A_{y_{i_c}}$ = area (km^2) within country *c* in year *y* and stratum *i*.

The variance $V_{y_{i_c}}$ for that part of stratum *i* within country *c* was calculated as being in proportion to the ratio of the square of the area within each country *c* relative to the total area of stratum *i*. This assumption resulted in the CVs within each country stratum being the same as the CV in the entire stratum:

Eq. B.8 $$V_{y_{i_c}} = V_{y_i} \frac{A^2_{y_{i_c}}}{A^2_{y_i}}.$$

The partial variance $V_{y_{i_c}}$ for country *c* was used in Eq. B.5 instead of the total variance in the stratum V_{y_i} when calculating the variance for the total biomass in Canadian or American waters. CVs were calculated as in Eq. B.6.

The biomass estimates Eq. B.4 and the associated standard errors were adjusted to a constant area covered using the ratios of area surveyed provided in Table B.7. This was required to adjust the Canadian biomass estimates for 1980 and 1983 to account for the smaller area surveyed in those years compared to the succeeding surveys. The 1980 and 1983 biomass estimates from Canadian waters were consequently multiplied by the ratio 1.24 (= 9166 km^2 / 7399 km^2) to make them equivalent to the coverage of the surveys from 1989 onwards.

Biomass estimates were bootstrapped using 500 random draws with replacement to obtain bias-corrected (Efron 1982) 95% confidence intervals for each year and for the two regions (Canadian-Vancouver and US-Vancouver) based on the distribution of biomass estimates and using the above equations.

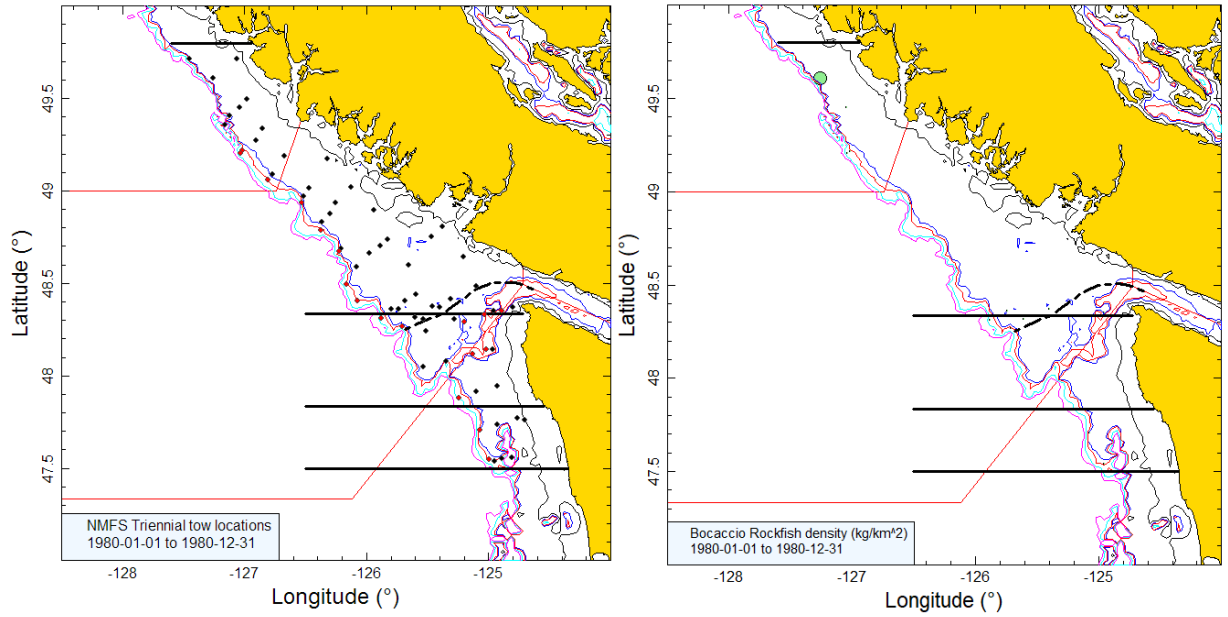

Figure B.12. [left panel]: plot of tow locations in the Vancouver INPFC region for the 1980 NMFS triennial survey in US and Canadian waters. Tow locations are colour-coded by depth range: black=55–183m; red=184-366m. Dashed line shows approximate position of the Canada/USA marine boundary. Horizontal lines are the stratum boundaries: 47°30', 47°50', 48°20' and 49°50'. Tows south of the 47°30' line were not included in the analysis. [left panel]:water hauls (Table B.7) have been excluded; [right panel]: circle sizes in the density plot are scaled across all years (1980, 1983, 1989, 1992, 1995, 1998, and 2001), with the largest circle = 220,761 kg/km^2 in 1989 (US waters). The red solid lines indicate the boundaries between PMFC areas 3B, 3C and 3D.

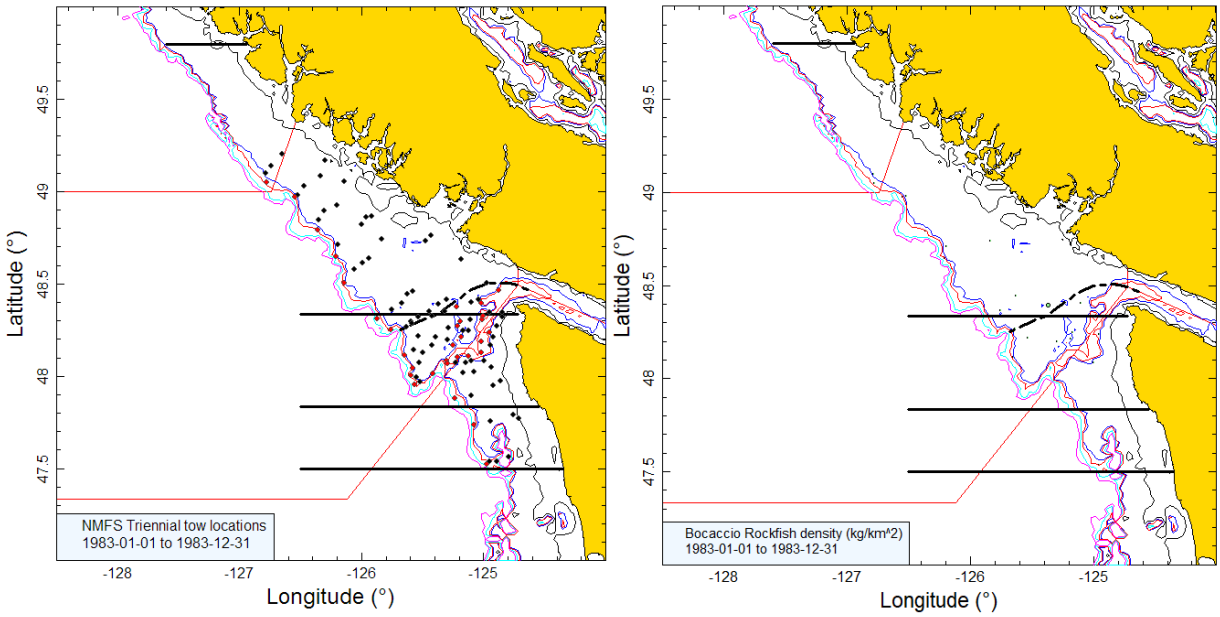

Figure B.13. Tow locations and density plots for the 1983 NMFS triennial survey in US and Canadian waters (see Figure B.12 caption).

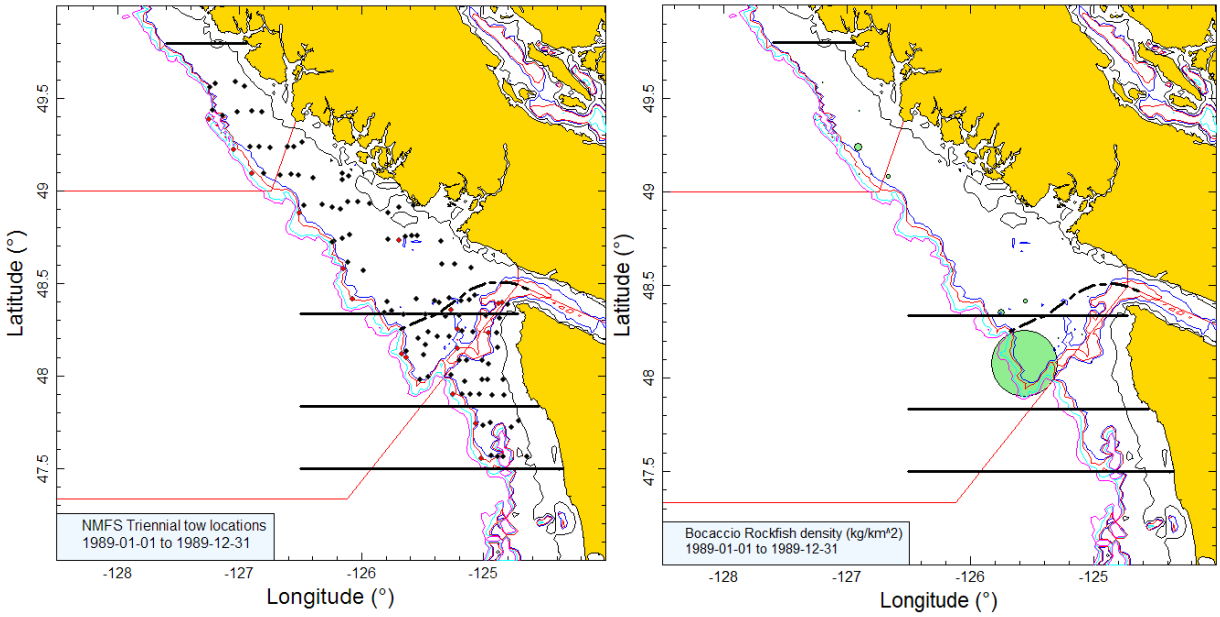

Figure B.14. Tow locations and density plots for the 1989 NMFS triennial survey in US and Canadian waters (see Figure B.12 caption).

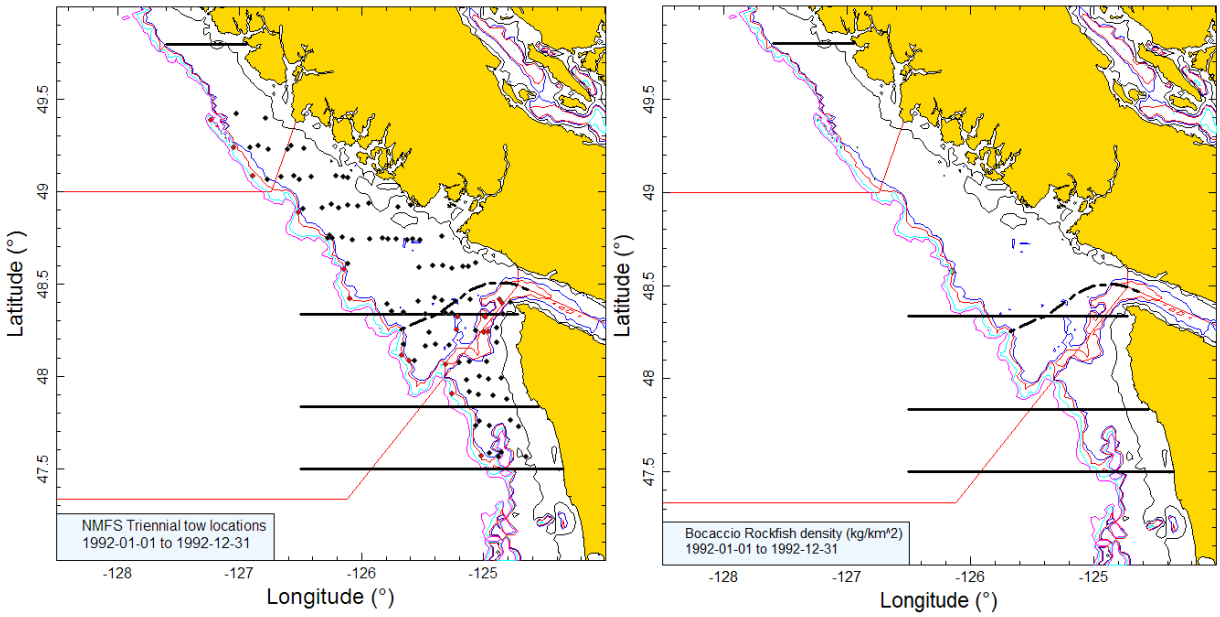

Figure B.15. Tow locations and density plots for the 1992 NMFS triennial survey in US and Canadian waters (see Figure B.12 caption).

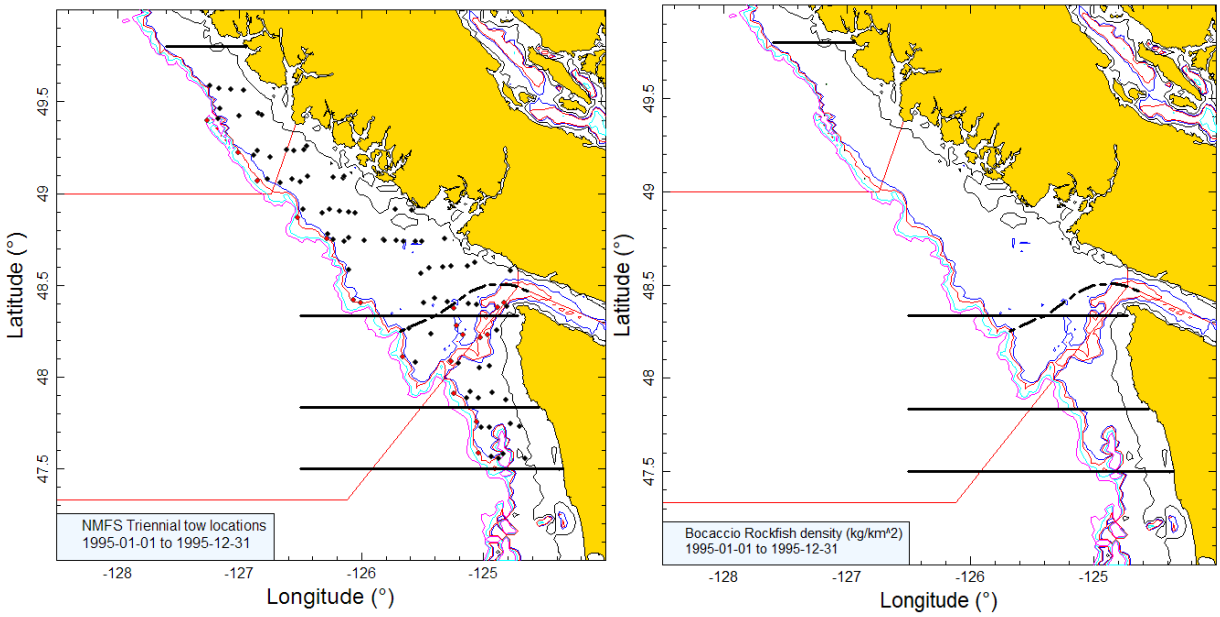

Figure B.16. Tow locations and density plots for the 1995 NMFS triennial survey in US and Canadian waters (see Figure B.12 caption).

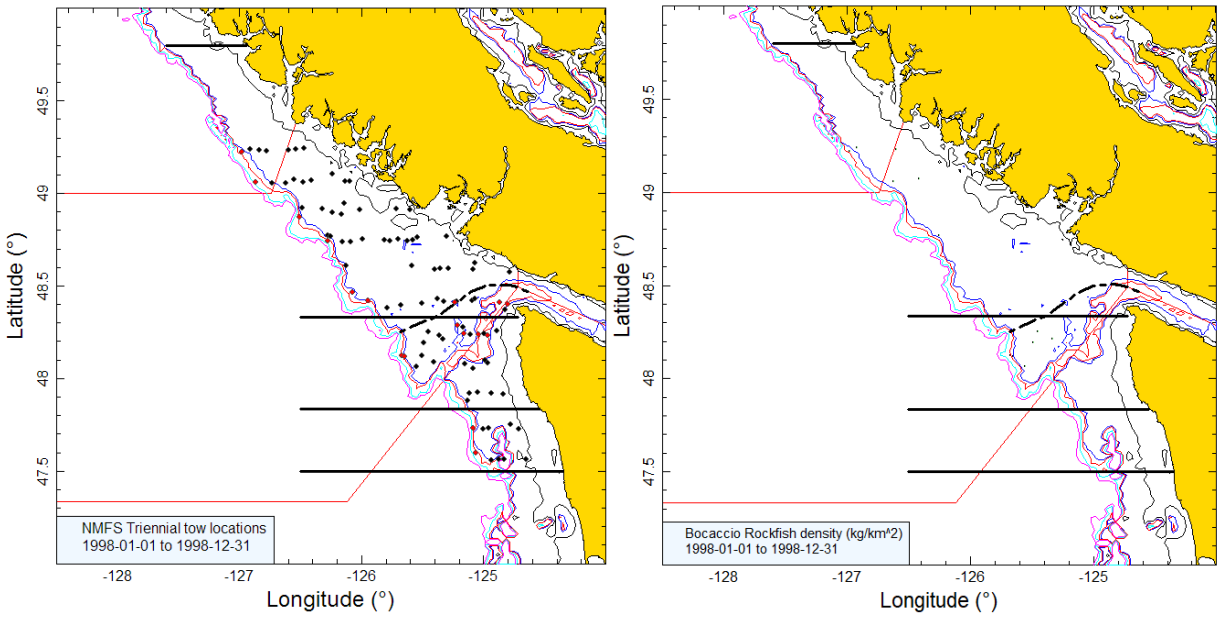

Figure B.17. Tow locations and density plots for the 1998 NMFS triennial survey in US and Canadian waters (see Figure B.12 caption).

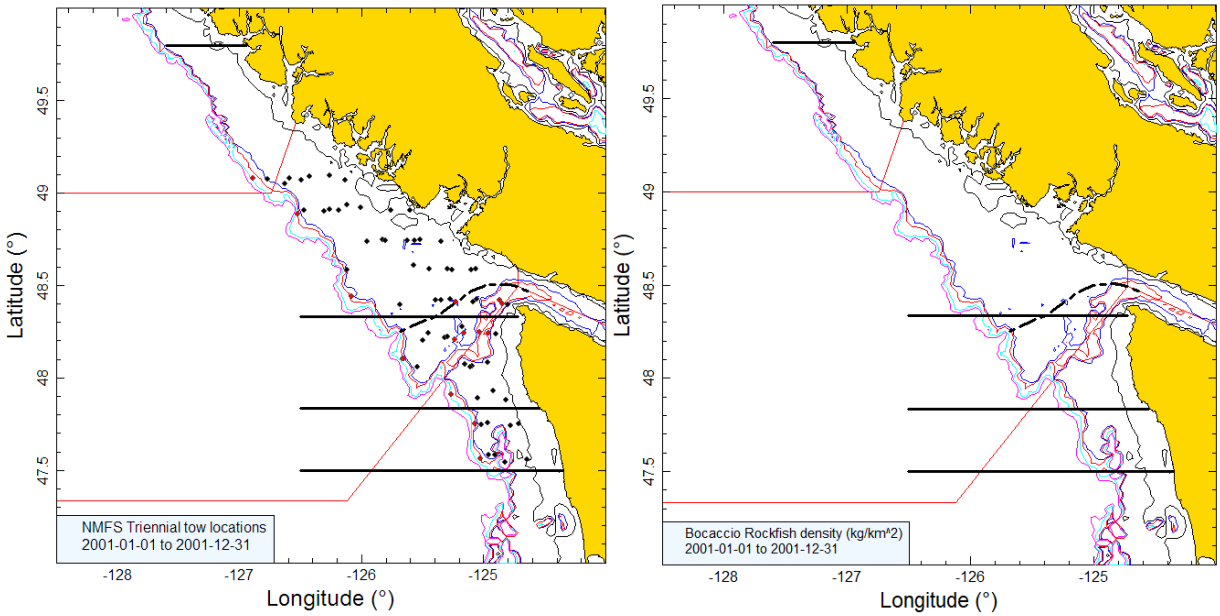

Figure B.18. Tow locations and density plots for the 2001 NMFS triennial survey in US and Canadian waters (see Figure B.12 caption).

B.4.3. Results

The occurrence of BOR in this survey was highly variable, with the median catch weight for the tows catching BOR at 6.4 kg while there were only six tows (of 91 tows) which caught more than 100 kg of BOR. There were two extremely large catches of BOR over the seven years of the survey, one taking over 1,500 kg in 1980 off Nootka Sound at the edge of the shelf ([right panel] Figure B.12) and the other catching just under 9,000 kg in 1989 in Juan de Fuca canyon (US waters: [right panel] Figure B.14). Catches were generally sparse and relatively infrequent,

occurring along the shelf edge and in the deep gully entering Juan de Fuca Strait (e.g., Figure B.12 and Figure B.14). Figure B.19 shows that this species was mainly found between 117 and 229 m (5 and 95% quantiles of [bottom_depth]), with only four observations deeper than 229 m and the deepest at 302 m, indicating that this survey encompassed the full depth range for this species.

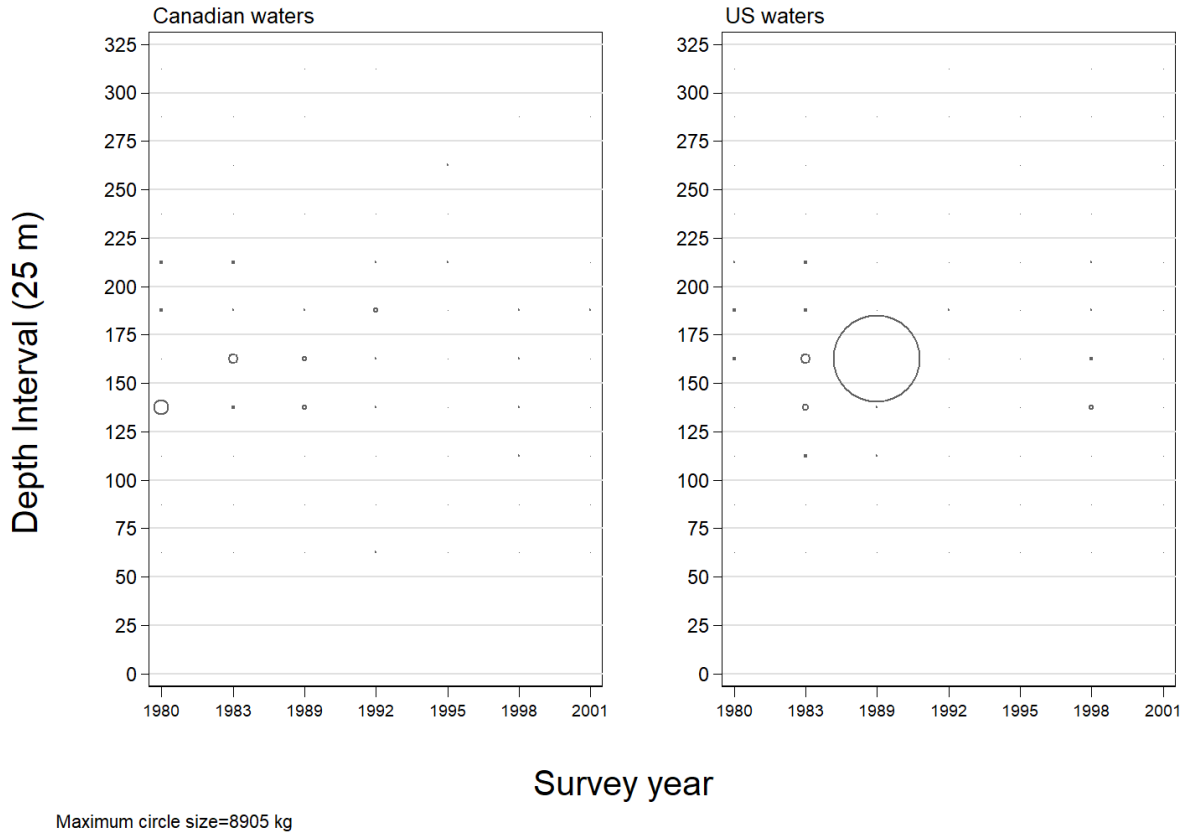

Figure B.19. Distribution of BOR catch weights for each survey year summarised into 25 m depth intervals for all tows (Table B.7) in Canadian and US waters of the Vancouver INPFC area. Catches are plotted at the mid-point of the interval.

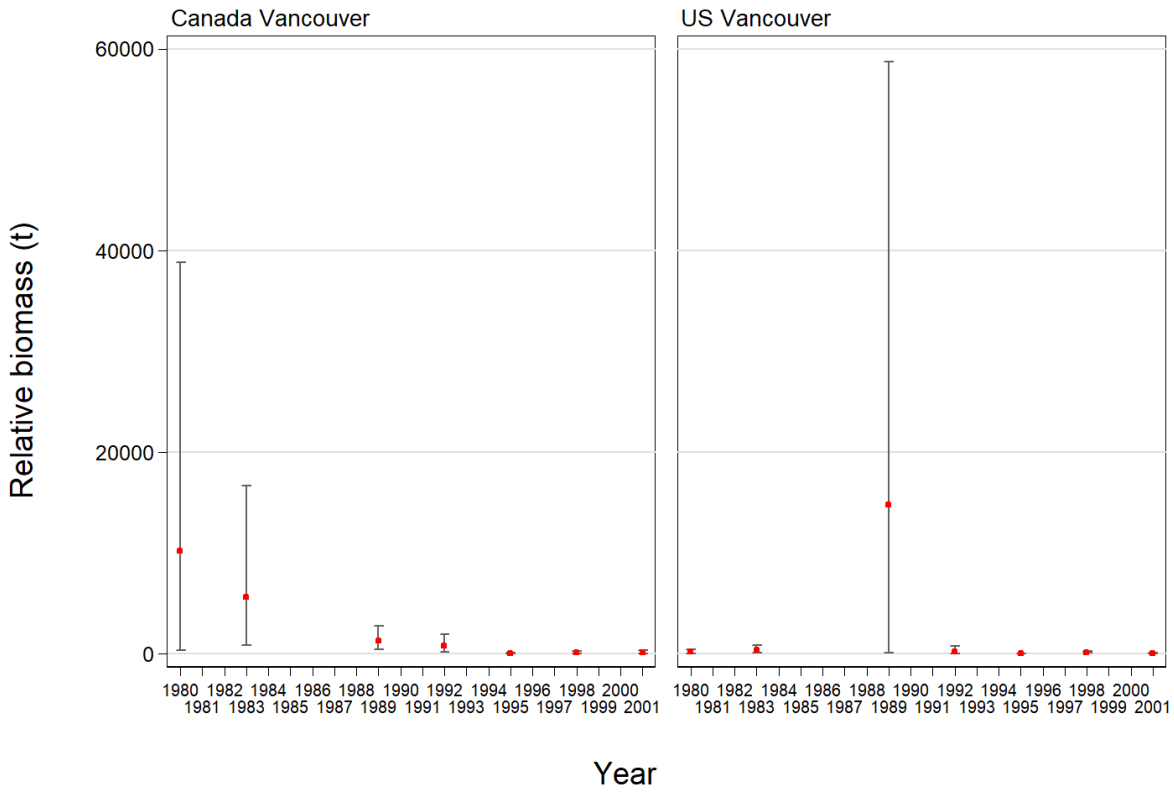

Figure B.20. Biomass estimates for BOR in the INPFC Vancouver region (Canadian waters only, US waters only) with 95% error bars estimated from 500 bootstrap random draws with replacement.

Table B.8. Two set of biomass estimates for BOR in the Vancouver INPFC region (Canadian waters; US waters) with 95% confidence bounds based on the bootstrap distribution of biomass. Bootstrap estimates are based on 500 random draws with replacement.

Estimate series	Year	Biomass (Eq. B.4)	Mean bootstrap biomass	Lower bound biomass	Upper bound biomass	CV bootstrap	CV Analytic (Eq. B.6)
Canada Vancouver	1980	10,179	9,645	347	38,784	0.950	0.942
	1983	5,592	5,433	875	16,632	0.699	0.689
	1989	1,320	1,280	395	2,754	0.456	0.456
	1992	794	803	151	1,918	0.618	0.652
	1995	65	65	13	128	0.455	0.467
	1998	143	139	43	262	0.410	0.403
	2001	120	115	0	360	0.789	0.798
US Vancouver	1980	174	173	0	438	0.588	0.610
	1983	372	363	117	808	0.476	0.459
	1989	14,774	15,930	87	58,732	0.912	0.991
	1992	224	153	28	747	0.879	0.670
	1995	11	11	1	30	0.662	0.629
	1998	140	124	70	255	0.370	0.365
	2001	27	25	0	94	0.973	0.955

The two very large tows resulted in large biomass estimates for the respective years and region coupled with very large relative errors (Figure B.20; Table B.8). Because the large Canadian tow occurred in the first year of the survey, there is an apparent declining trend in the Canadian series when coupled with a relatively strong showing in the 1983 survey. The large US tow swamps all the other biomass estimates on both sides of the border, particularly given the large

error bars. Note that the bootstrap estimates of relative error do not include any uncertainty with respect to the ratio expansion required to make the 1980 and 1983 survey estimates comparable to the 1989 and later surveys. Therefore, it is likely that the true uncertainty for this series is even greater than estimated.

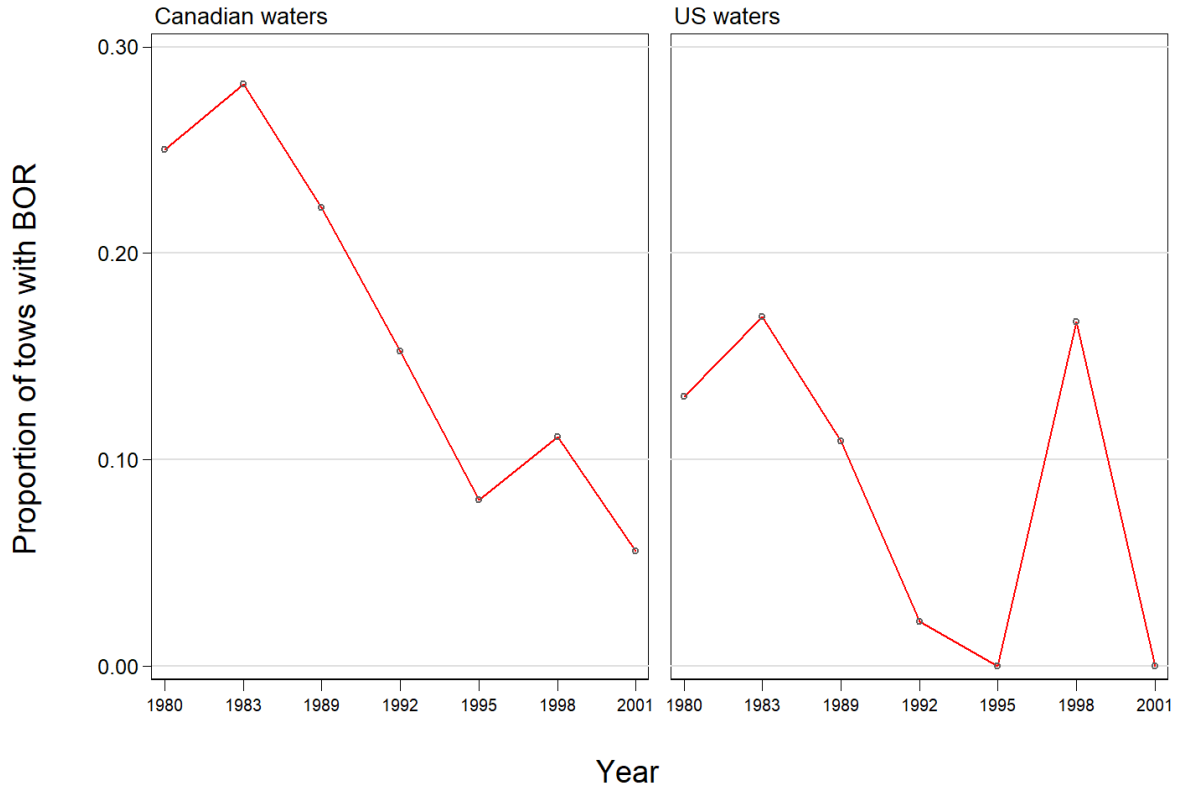

Figure B.21. Proportion of tows with BOR by year for the Vancouver INPFC region (Canadian and US waters).

Only 87 tows of the 665 valid tows captured BOR (13%), with half of the tows that captured BOR having less than 6.4 kg. The proportion of tows which contained BOR was lower in US waters than in Canadian waters, with the US proportions by year ranging from 0 to 17% (mean=8.5%) while the equivalent Canadian values were 6–28% with a mean value of 16% (Figure B.21). The incidence of BOR in Canadian waters for this survey is similar to the synoptic survey operating in the 2000s off the west coast of Vancouver Island, with the latter survey having a mean incidence of 15% (range: 5-29%) of the tows containing BOR.

The seven Triennial survey indices from the Canada Vancouver region, spanning the period 1980 to 2001, were used as abundance indices in the stock assessment model (described in Appendix F).

B.5. QUEEN CHARLOTTE SOUND SYNOPTIC TRAWL SURVEY

B.5.1. Data selection

This survey has been conducted ten times over the period 2003 to 2019 in the Queen Charlotte Sound (QCS), which lies between the top of Vancouver Island and the southern portion of Moresby Island and extends into the lower part of Hecate Strait between Moresby Island and the mainland. The design divided the survey into two large areal strata which roughly

correspond to the PMFC regions 5A and 5B while also incorporating part of 5C (all valid tow starting positions are shown by survey year in Figure B.22 to Figure B.29). Each of these two areal strata was divided into four depth strata: 50–125 m; 125–200 m; 200–330 m; and 330–500 m (Table B.9).

Table B.9. Number of usable tows for biomass estimation by year and depth stratum for the Queen Charlotte Sound synoptic survey over the period 2003 to 2019. Also shown is the area of each stratum for the 2019 survey and the vessel conducting the survey by survey year.

		South depth strata				North depth strata				Total
Year	Vessel	50-125	125-200	200-330	330-500	50-125	125-200	200-330	330-500	tows[1]
2003	*Viking Storm*	29	56	29	6	5	39	50	19	233
2004	*Viking Storm*	42	48	31	8	20	38	37	6	230
2005	*Viking Storm*	29	60	29	8	8	45	37	8	224
2007	*Viking Storm*	33	61	24	7	19	56	48	7	255
2009	*Viking Storm*	34	60	28	8	10	44	43	6	233
2011	*Nordic Pearl*	38	67	24	8	10	51	45	8	251
2013	*Nordic Pearl*	32	65	29	10	9	46	44	5	240
2015	*Frosti*	30	65	26	4	12	49	44	8	238
2017	*Nordic Pearl*	36	57	29	8	12	51	40	7	240
2019	*Nordic Pearl*	35	62	26	9	15	52	35	8	242
Area (km^2)[2]		5,012	5,300	2,640	528	1,740	3,928	3,664	1,236	24,048[2]

[1] GFBio usability codes=0,1,2,6 [2] Total area (km^2) for 2019 synoptic survey

Table B.10. Number of missing doorspread values by year for the Queen Charlotte Sound synoptic survey over the period 2003 to 2019 as well as showing the number of available doorspread observations and the mean doorspread value for each survey year.

Year	Number tows with missing doorspread [1]	Number tows with doorspread observations [2]	Mean doorspread (m) used for tows with missing values [2]
2003	13	236	72.1
2004	8	267	72.8
2005	1	258	74.5
2007	5	262	71.8
2009	2	248	71.3
2011	30	242	67.0
2013	42	226	69.5
2015	0	249	70.5
2017	1	264	64.7
2019	8	264	62.9
Total	110	2,516	69.7

[1] valid biomass estimation tows only [2] includes tows not used for biomass estimation

A doorspread density value (Eq. B.3) was generated for each tow based on the catch of BOR from the mean doorspread for the tow and the distance travelled. [`distance travelled`] is a database field which is calculated directly from the tow track. This field is used preferentially for the variable D_{yij} in Eq. B.3. A calculated value ([`vessel speed`] X [`tow duration`]) is used for this variable if [`distance travelled`] is missing, but there were only two instances of this occurring in the ten trawl surveys. Missing values for the [`doorspread`] field were filled in with the mean doorspread for the survey year (110 values over all years, Table B.10).

B.5.2. Results

Up to the 2017 survey, BOR seemed to be widely but sporadically distributed in QCS, with catches observed throughout the survey footprint, but at very low levels (Figure B.22 to Figure B.29). Beginning in 2017, the spatial distribution of BOR catches broadened considerably compared to previous years (Figure B.30). Examination of the length frequencies from this catch (see Section 2.4, Appendix D) showed that a new one year old cohort (given the modal length)

was recruiting. This new cohort had no apparent impact on the 2017 biomass estimate but, by the following biennial survey in 2019, the presence of this 2016 cohort was apparent as a wide distribution of strong catch rates throughout the survey coverage (Figure B.31). BOR were mainly taken in a tight depth range (127 to 210 m: 5–95% quantiles for all positive weight observations), with only one observation below 300 m in depth (Figure B.32).

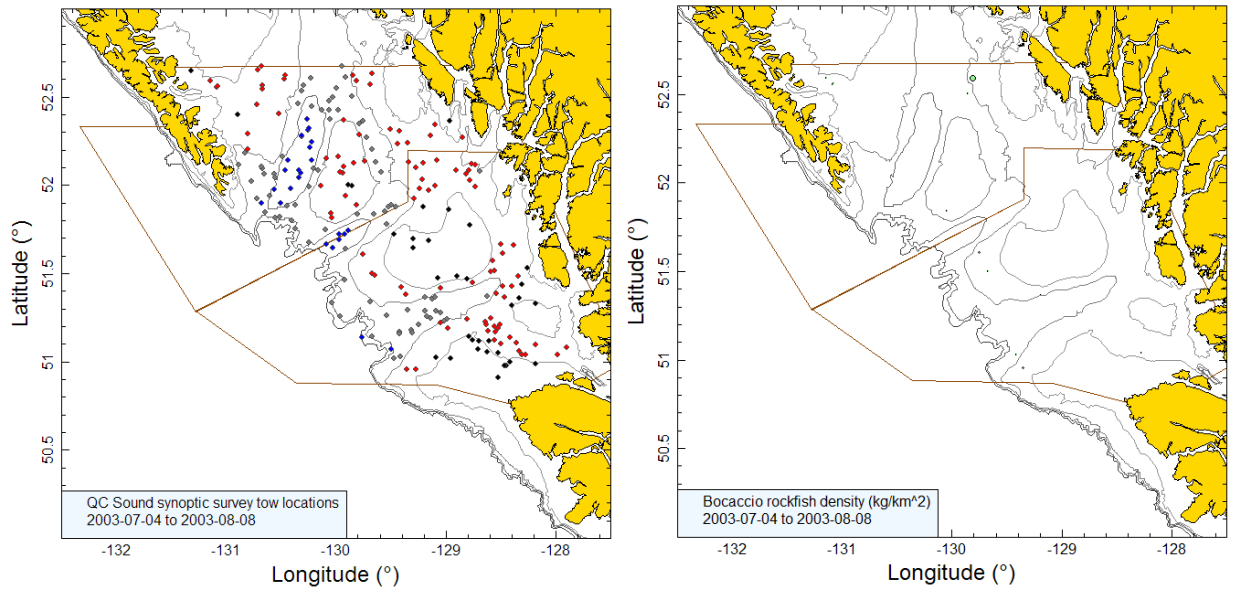

Figure B.22. Valid tow locations (50-125m stratum: black; 126-200m stratum: red; 201-330m stratum: grey; 331-500m stratum: blue) and density plots for the 2003 QC Sound synoptic survey. Circle sizes in the right-hand density plot scaled across all years (2003–2005, 2007, 2009, 2011, 2013, 2015, 2017, 2019), with the largest circle = 6,128 kg/km^2 in 2019. Boundaries delineate the North and South areal strata.

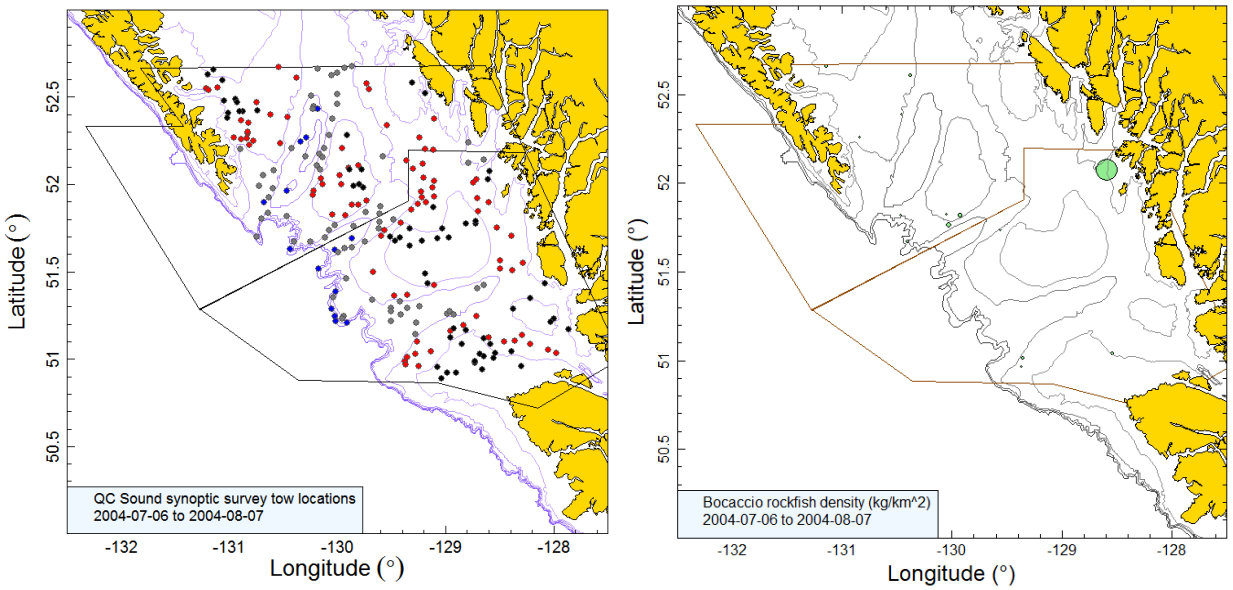

Figure B.23. Tow locations and density plots for the 2004 Queen Charlotte Sound synoptic survey (see Figure B.22 caption).

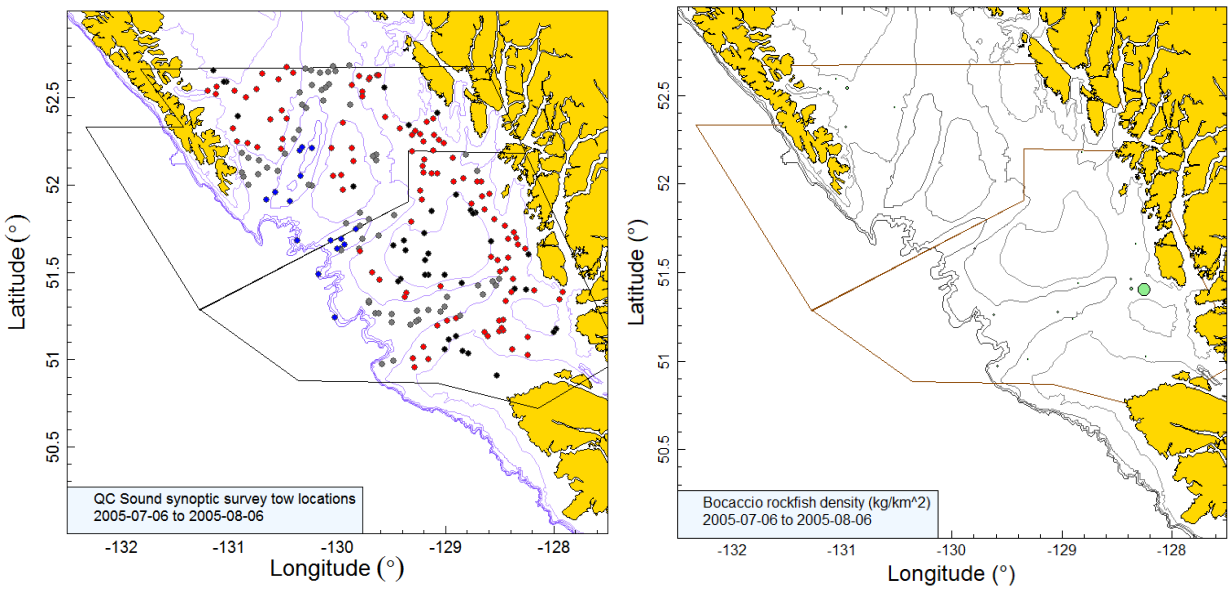

Figure B.24. Tow locations and density plots for the 2005 Queen Charlotte Sound synoptic survey (see Figure B.22 caption).

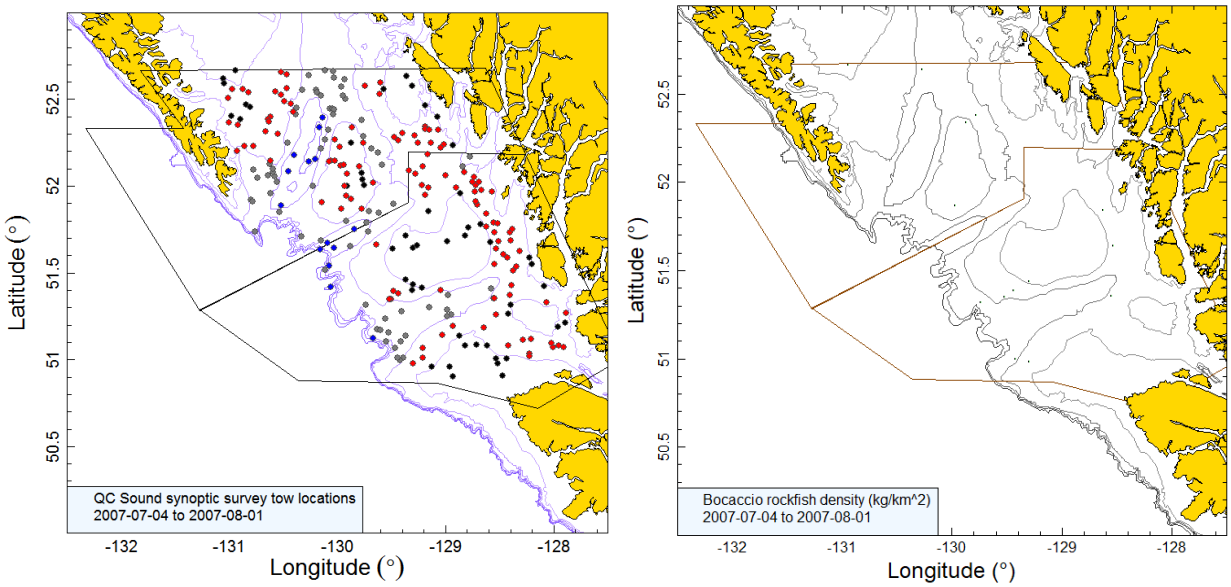

Figure B.25. Tow locations and density plots for the 2007 Queen Charlotte Sound synoptic survey (see Figure B.22 caption).

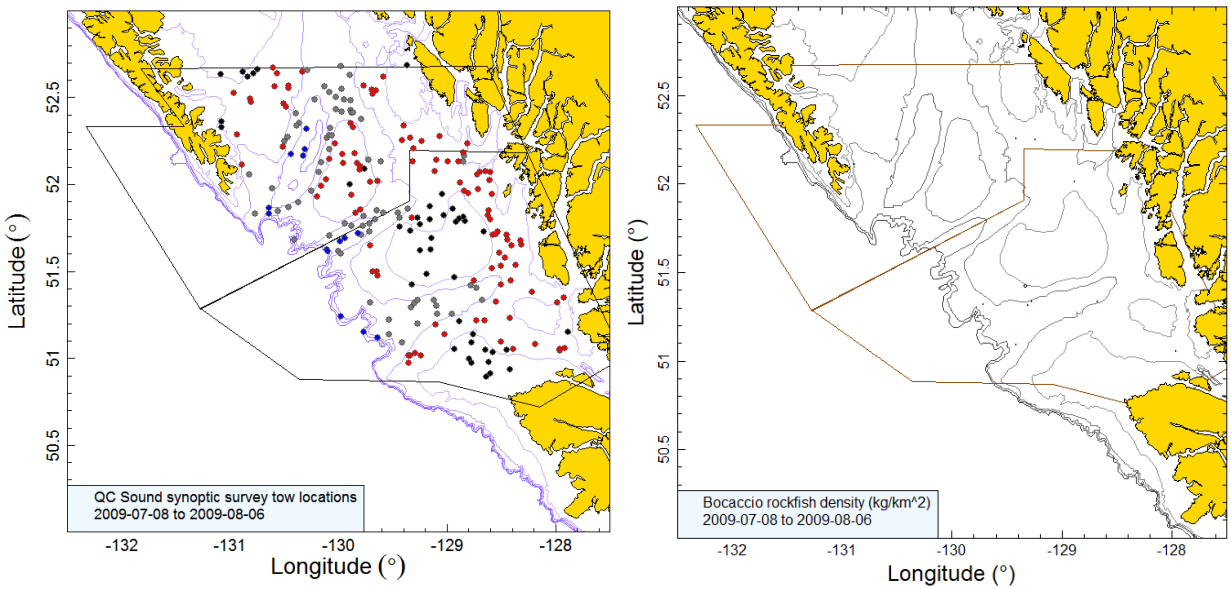

Figure B.26. Tow locations and density plots for the 2009 Queen Charlotte Sound synoptic survey (see Figure B.22 caption).

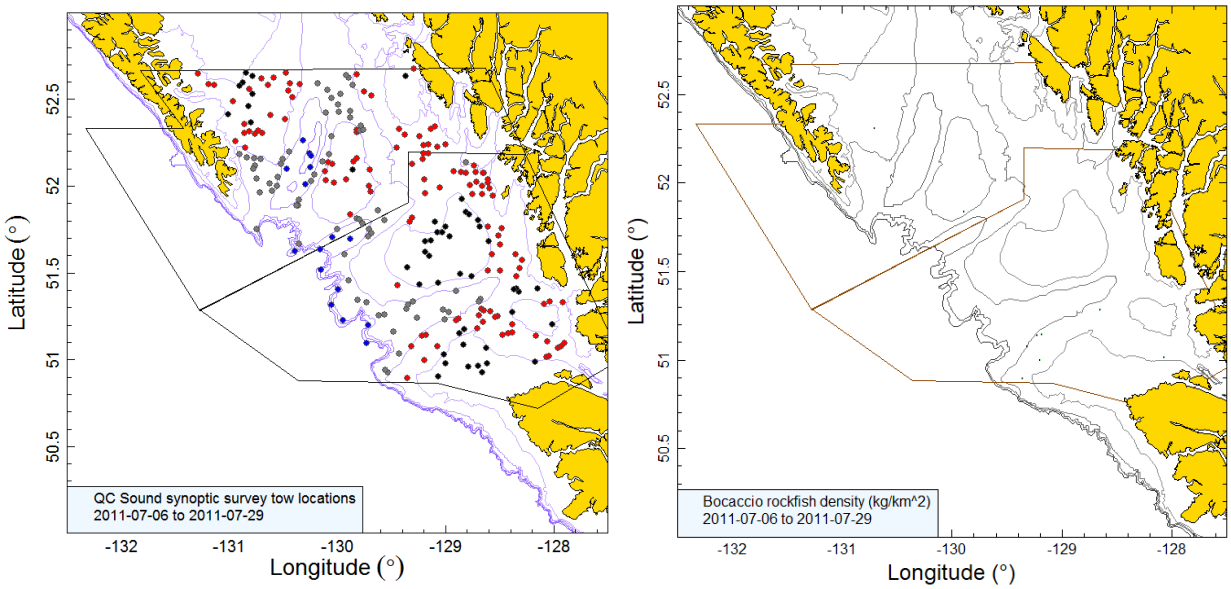

Figure B.27. Tow locations and density plots for the 2011 Queen Charlotte Sound synoptic survey (see Figure B.22 caption).

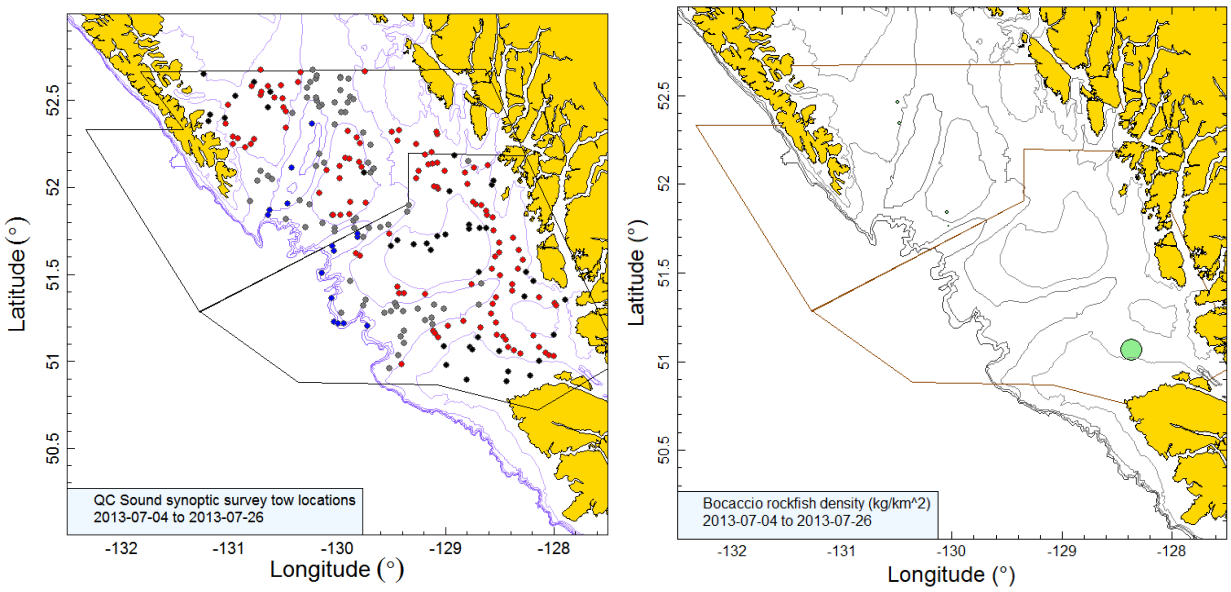

Figure B.28. Tow locations and density plots for the 2013 Queen Charlotte Sound synoptic survey (see Figure B.22 caption).

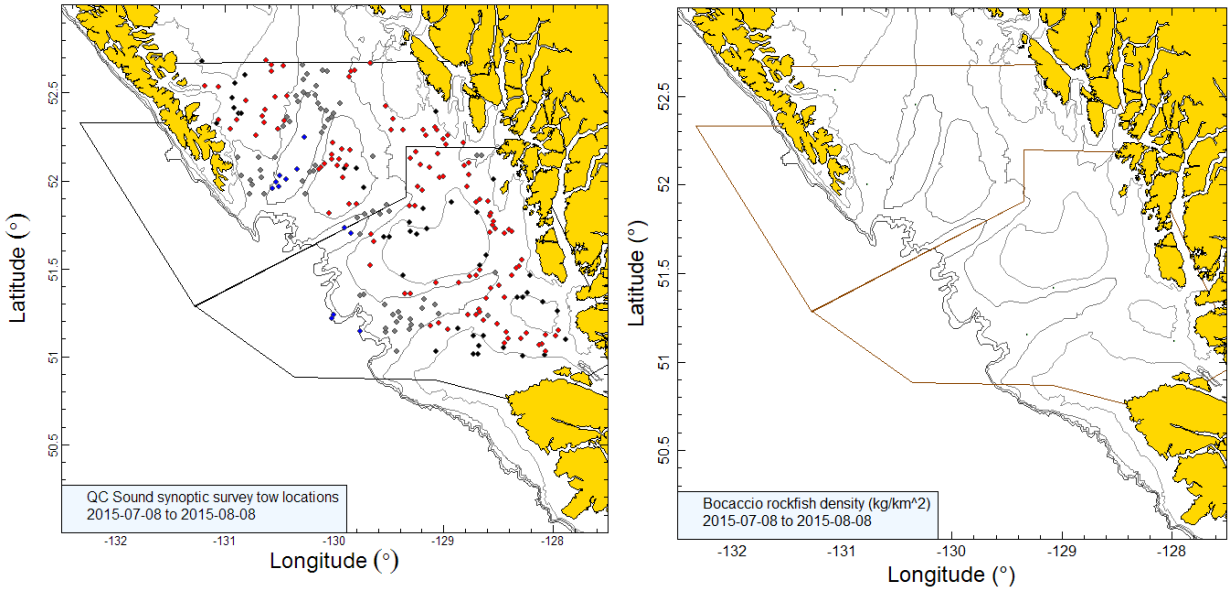

Figure B.29. Tow locations and density plots for the 2015 Queen Charlotte Sound synoptic survey (see Figure B.22 caption).

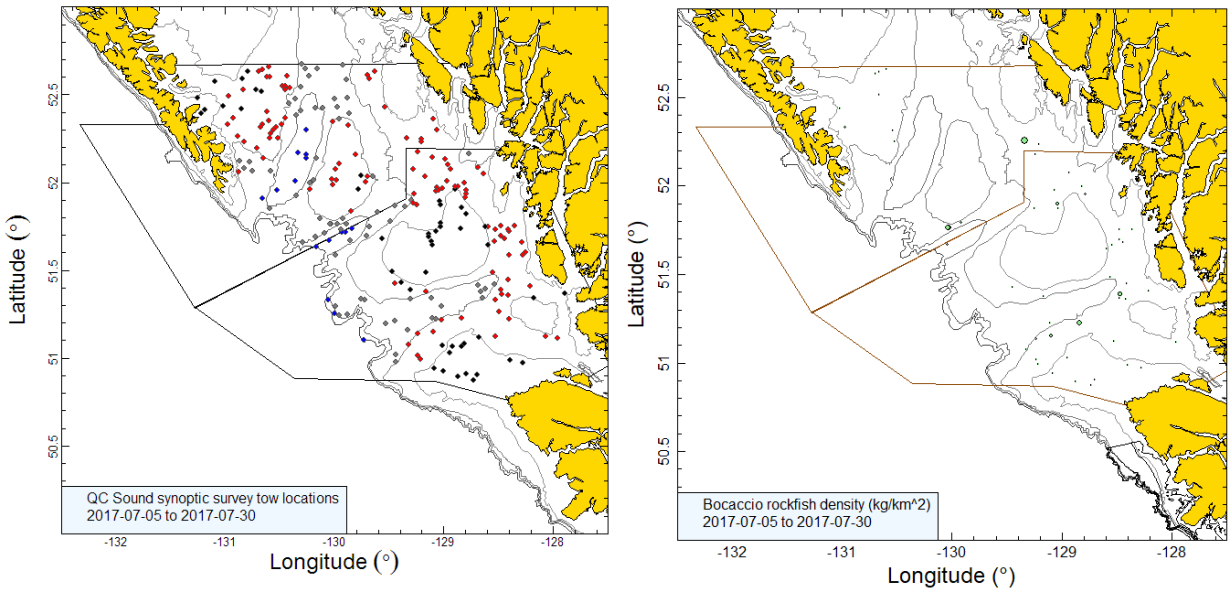

Figure B.30. Tow locations and density plots for the 2017 Queen Charlotte Sound synoptic survey (see Figure B.22 caption).

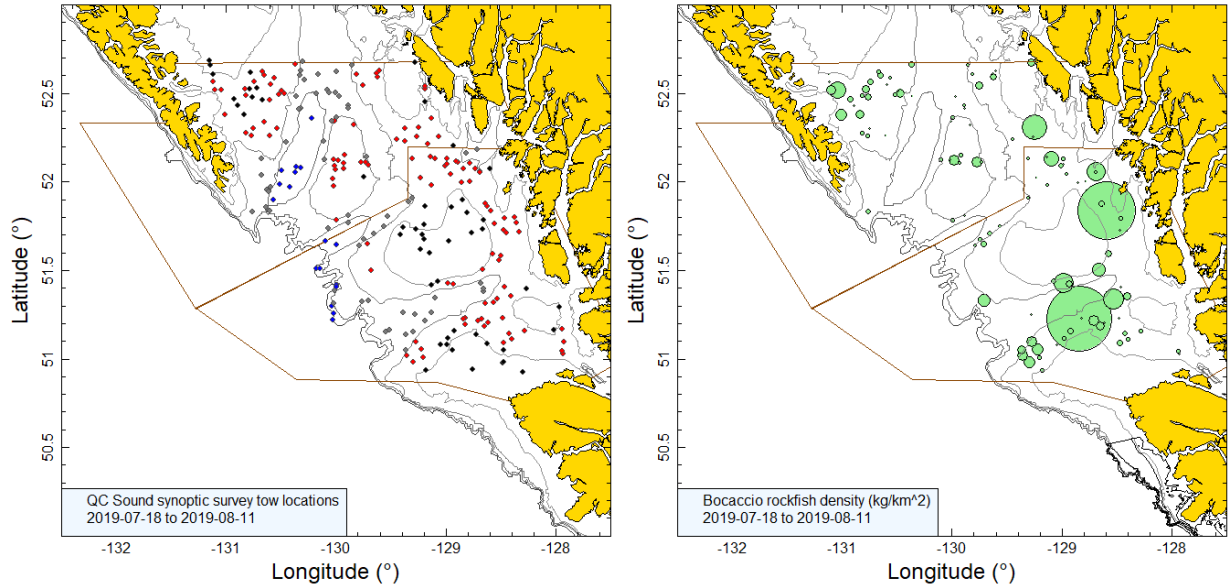

Figure B.31. Tow locations and density plots for the 2019 Queen Charlotte Sound synoptic survey (see Figure B.22 caption).

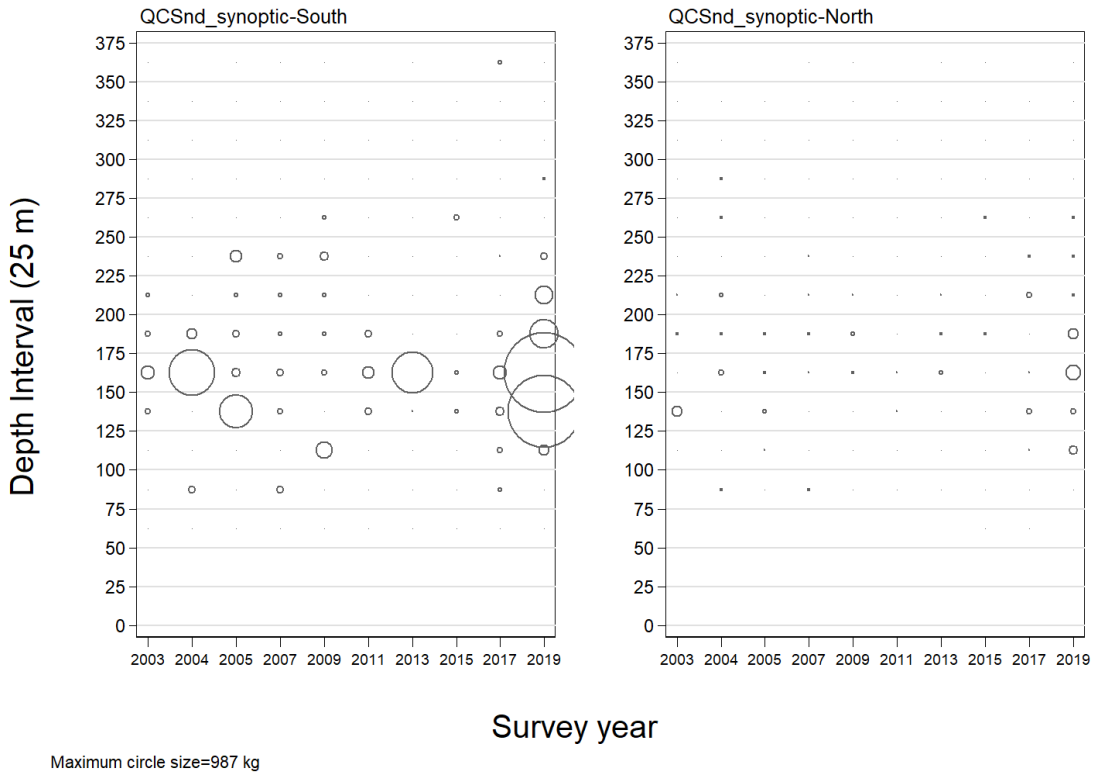

Figure B.32. Distribution of observed catch weights for tows used in biomass estimation for BOR in the two main Queen Charlotte Sound synoptic survey areal strata (Table B.9) by survey year and 25 m depth zone. Catches are plotted at the mid-point of the interval and circles in the panel are scaled to the maximum value (987 kg) in the 150–175 m interval in the 2019 southern stratum. The 1% and 99% quantiles for the BOR empirical start of tow depth distribution= 106 m and 259 m respectively.

Table B.11. Biomass estimates for BOR from the Queen Charlotte Sound synoptic trawl survey for the survey years 2003 to 2019. Bootstrap bias corrected confidence intervals and CVs are based on 500 random draws with replacement.

Survey Year	**Biomass (t)** (Eq. B.4)	**Mean bootstrap biomass (t)**	**Lower bound biomass (t)**	**Upper bound biomass (t)**	**Bootstrap CV**	**Analytic CV** (Eq. B.6)
2003	108	105	30	282	0.594	0.605
2004	313	302	45	884	0.763	0.781
2005	298	275	64	818	0.721	0.711
2007	47	47	22	86	0.345	0.353
2009	89	88	20	221	0.609	0.623
2011	36	35	15	78	0.429	0.436
2013	183	194	8	621	0.872	0.896
2015	21	21	6	42	0.435	0.457
2017	82	80	45	133	0.286	0.278
2019	1,671	1,688	640	3,084	0.383	0.400

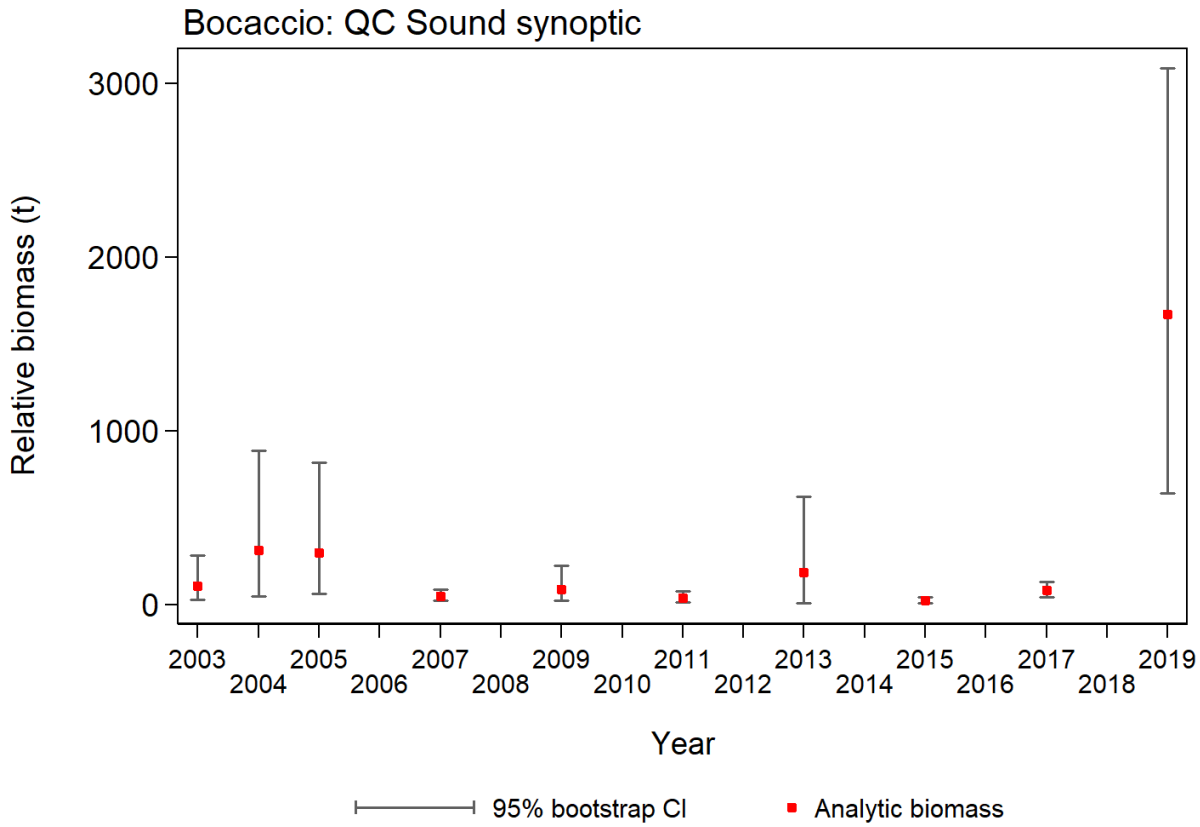

Figure B.33. Plot of biomass estimates for BOR (values provided in Table B.11) from the Queen Charlotte Sound synoptic survey over the period 2003 to 2019. Bias corrected 95% confidence intervals from 500 bootstrap replicates are plotted.

Estimated BOR doorspread biomass levels were very low over the first nine survey years, followed by an extremely large increase in 2019 that can be attributed to the very strong 2016 cohort (see Section 2.4, Appendix D; Table B.11; Figure B.33). The estimated relative errors are generally large, ranging from 0.29 to 0.87, although the recent increase in biomass has, at 0.38, one of the lower error terms in the series (Table B.11). Between 2 and 42% of the South stratum tows and 2 to 46% of the North stratum tows captured BOR, with the high proportional catch coming with the recruitment of the large 2016 cohort (Figure B.34). Overall, 251 of the 2,286 valid survey tows (10.5%) contained BOR, with both the North and South strata having average proportion non-zero tows between 9–11%. The median catch weight for positive tows was 4.0 kg/tow across the ten surveys, and the maximum catch weight in a tow was 832 kg in the 2019 survey.

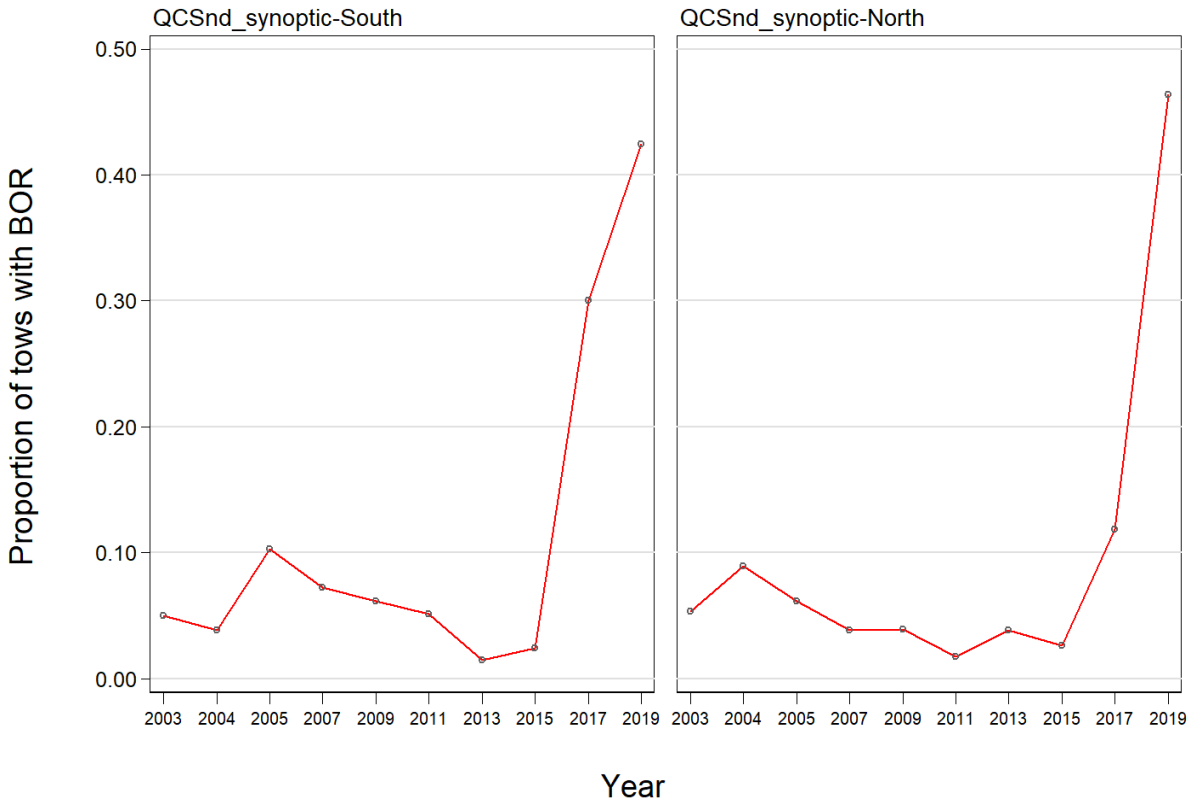

Figure B.34. Proportion of tows by stratum and year which contain BOR from the Queen Charlotte Sound synoptic survey over the period 2003 to 2019.

B.6. WEST COAST VANCOUVER ISLAND SYNOPTIC TRAWL SURVEY

B.6.1. Data selection

This survey has been conducted seven times in the period 2004 to 2016 off the west coast of Vancouver Island by RV *W.E. Ricker*. An eighth survey was conducted in 2018 by the RV *Nordic Pearl* due to the decommissioning of the *W.E. Ricker*. It comprises a single areal stratum, separated into four depth strata: 50-125 m; 125-200 m; 200-330 m; and 330-500 m (Table B.12). Approximately 150 to 200 2-km^2 blocks are selected randomly among the four depth strata when conducting each survey (Olsen et. al. 2008).

A “doorspread density” value was generated for each tow based on the catch of BOR, the mean doorspread for the tow and the distance travelled (Eq. B.3). The distance travelled was provided as a data field, determined directly from vessel track information collected during the tow. There were only two missing values in this field (in 2004 and 2010) which were filled in by multiplying the vessel speed by the time that the net was towed. There were a large number of missing values for the doorspread field, which were filled in using the mean doorspread for the survey year or a default value of 64.6 m for the three years with no doorspread data (Table B.13). The default value is based on the mean of the observed doorspread from the net mensuration equipment, averaged across the years with doorspread estimates.

Table B.12. Stratum designations, number of usable and unusable tows, for each year of the west coast Vancouver Island synoptic survey. Also shown is the area of each depth stratum in 2018 and the start and end dates for each survey.

Survey year	Stratum depth zone				Total Tows[1]	Unusable tows	Start date	End date
	50-125 m	125-200 m	200-330 m	330-500 m				
2004	34	34	13	8	89	17	26-May-04	09-Jun-04
2006	61	62	28	13	164	12	24-May-06	18-Jun-06
2008	54	50	32	23	159	19	27-May-08	21-Jun-08
2010	58	47	22	9	136	8	08-Jun-10	28-Jun-10
2012	60	46	25	20	151	6	23-May-12	15-Jun-12
2014	55	49	29	13	146	7	29-May-14	20-Jun-14
2016	54	41	26	19	140	7	25-May-16	15-Jun-16
2018	69	64	36	21	190	12	19-May-18	12-Jun-18
Area (km^2)	5,716	3,768	708	572	10,764[2]	–	–	–

[1] GFBio usability codes=0,1,2,6
[2] Total area (km^2) for 2018 synoptic survey

Table B.13. Number of tows with and without doorspread measurements by survey year for the WCVI synoptic survey. Mean doorspread values for those tows with measurements are provided.

Survey Year	Number tows		Mean doorspread (m)
	Without doorspread	With doorspread	
2004	89	0	–
2006	96	69	64.3
2008	58	107	64.5
2010	136	0	–
2012	153	0	–
2014	14	139	64.3
2016	0	147	65.5
2018	0	202	64.3
All surveys	546	664	64.6

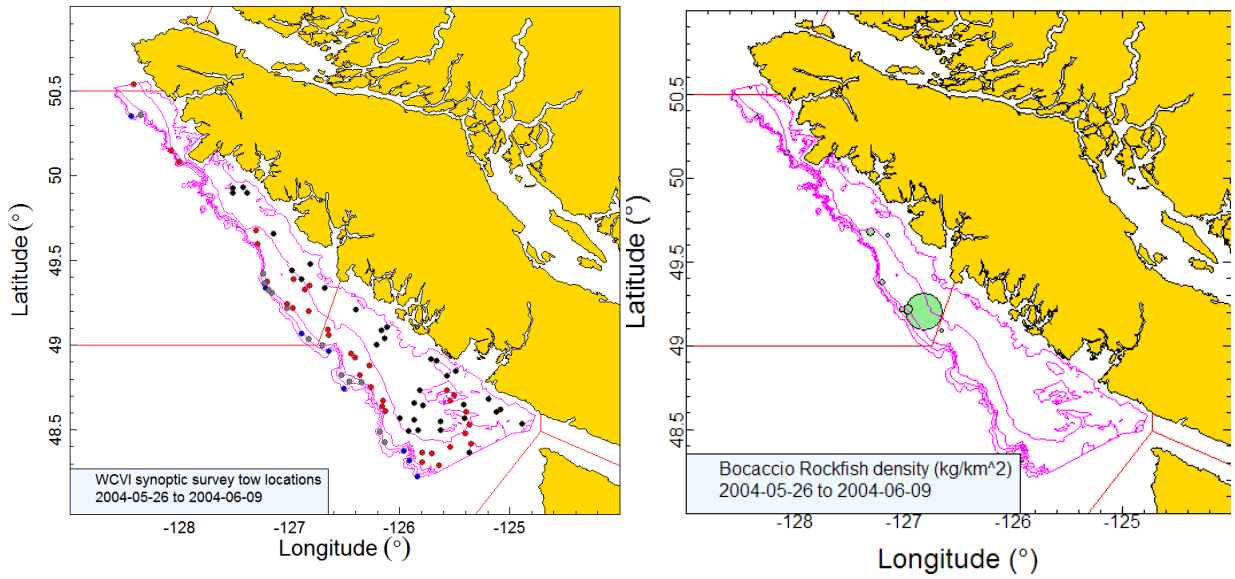

Figure B.35. Valid tow locations (50-125m stratum: black; 126-200m stratum: red; 201-330m stratum: grey; 331-500m stratum: blue) and density plots for the 2004 west coast Vancouver Island synoptic survey. Circle sizes in the right-hand density plot scaled across all years (2004, 2006, 2008, 2010, 2012, 2014, 2016, 2018), with the largest circle = 4,317 kg/km^2 in 2018. The red solid lines indicate the boundaries for PMFC areas 3C, 3D and 5A.

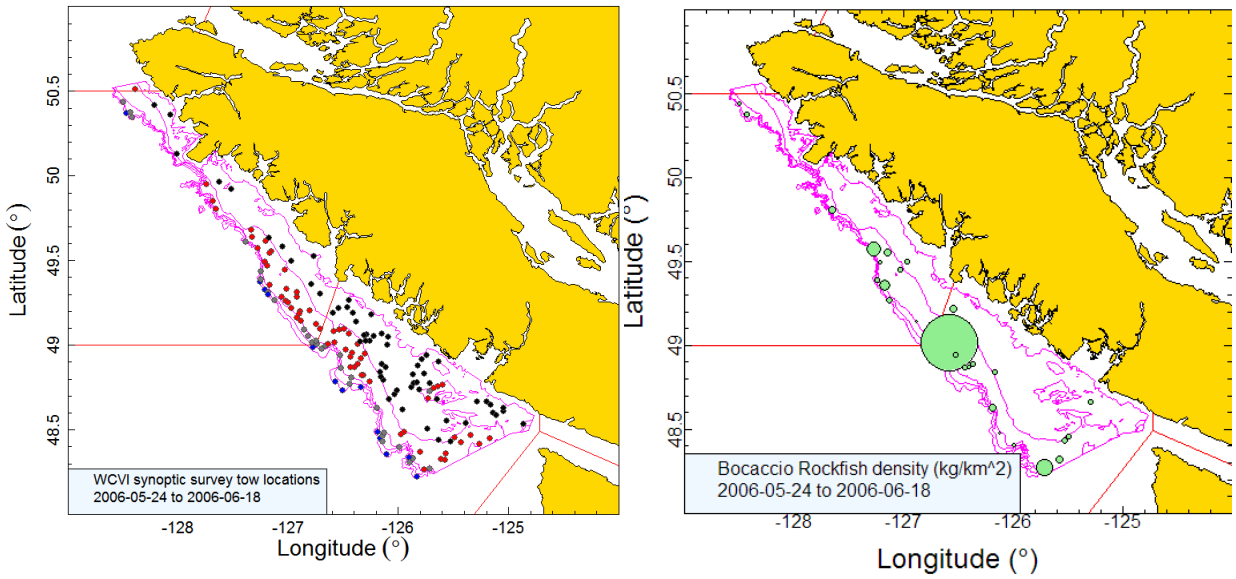

Figure B.36. Tow locations and density plots for the 2006 west coast Vancouver Island synoptic survey (see Figure B.35 caption).

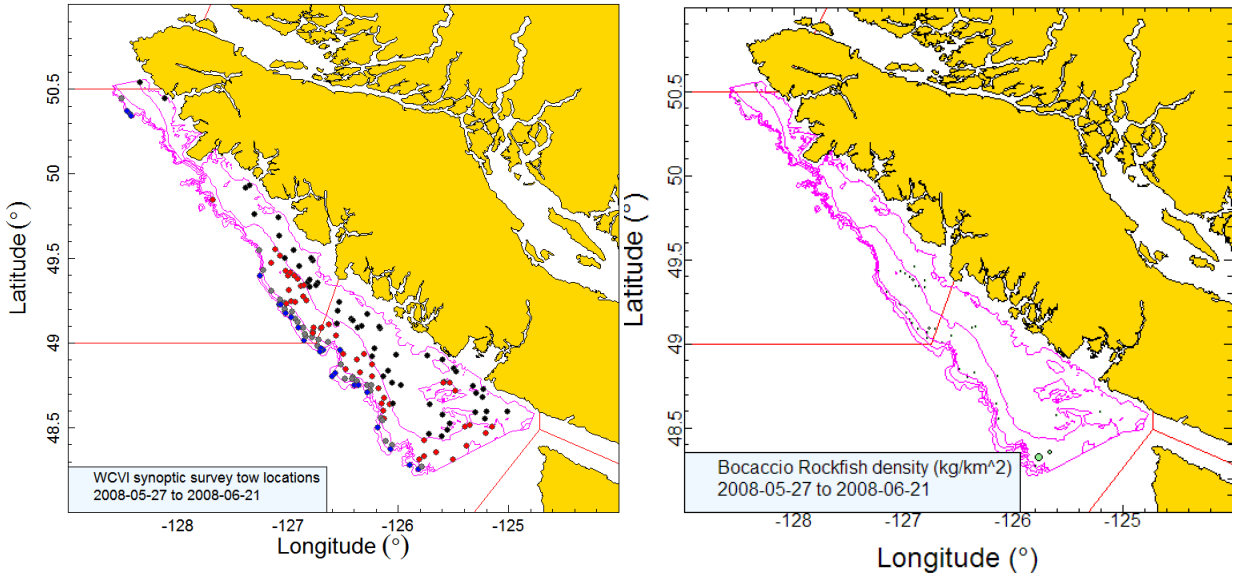

Figure B.37. Tow locations and density plots for the 2008 west coast Vancouver Island synoptic survey (see Figure B.35 caption).

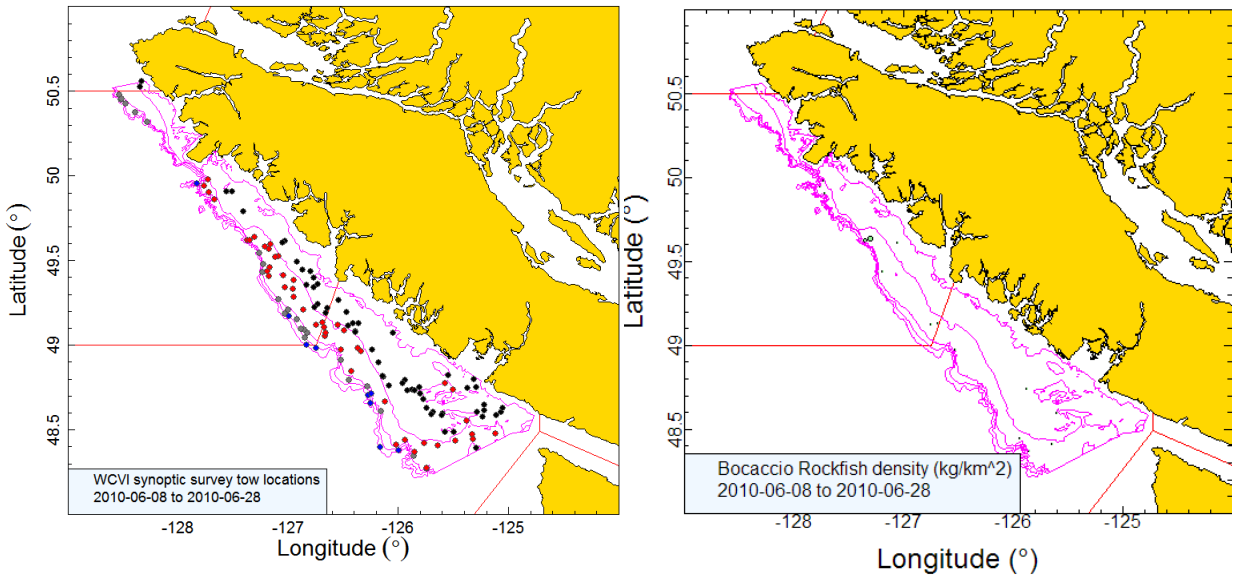

Figure B.38. Tow locations and density plots for the 2010 west coast Vancouver Island synoptic survey (see Figure B.35 caption).

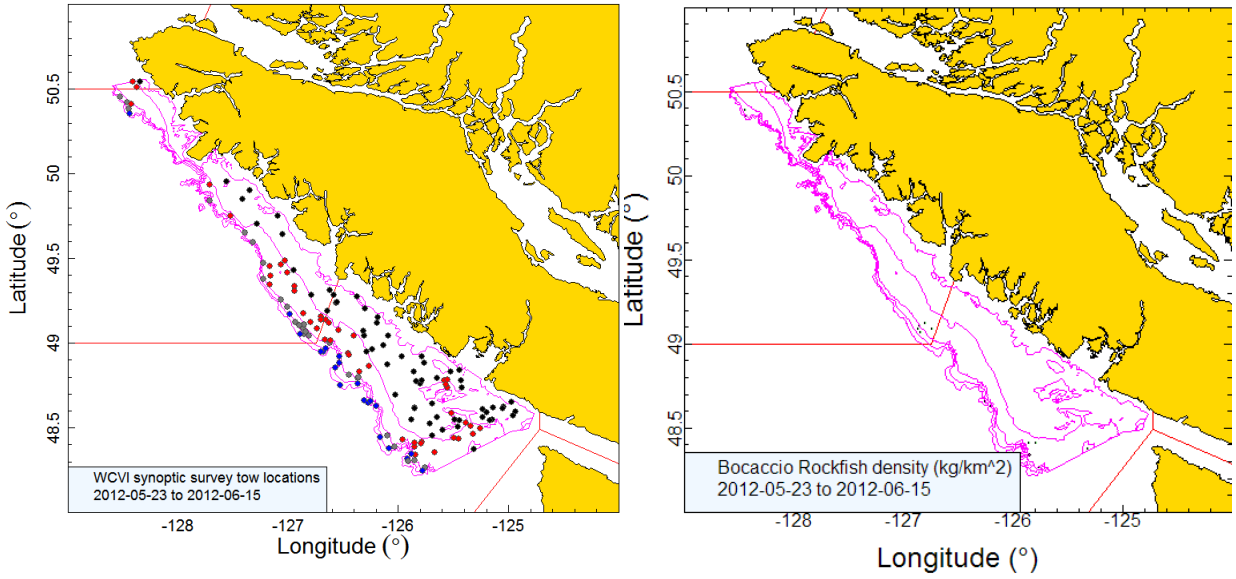

Figure B.39. Tow locations and density plots for the 2012 west coast Vancouver Island synoptic survey (see Figure B.35 caption).

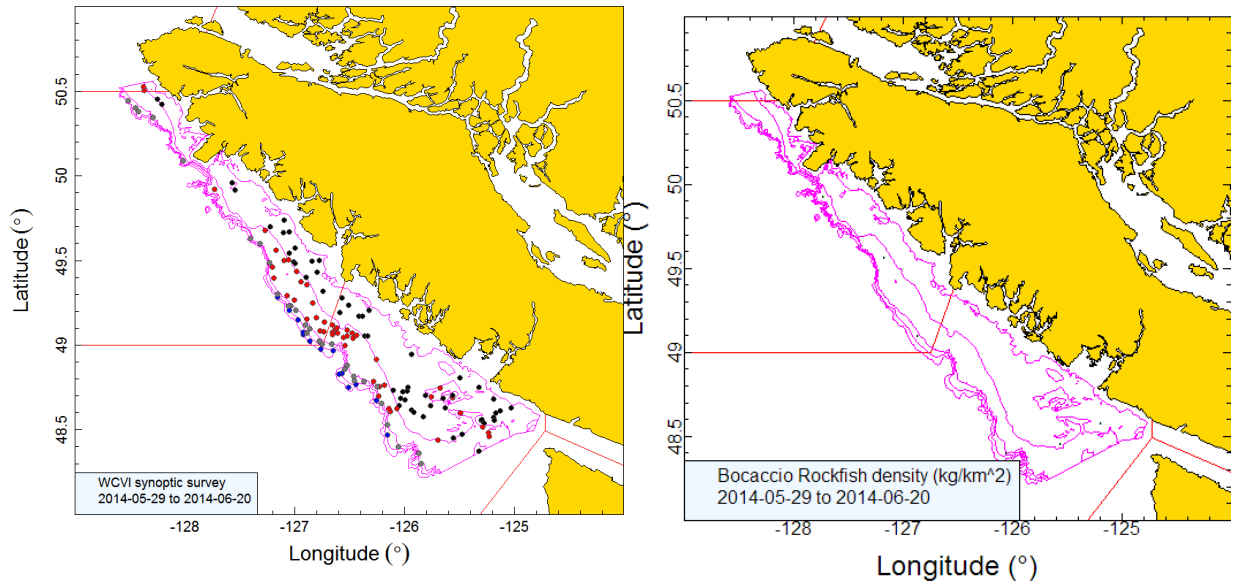

Figure B.40. Tow locations and density plots for the 2014 west coast Vancouver Island synoptic survey (see Figure B.35 caption).

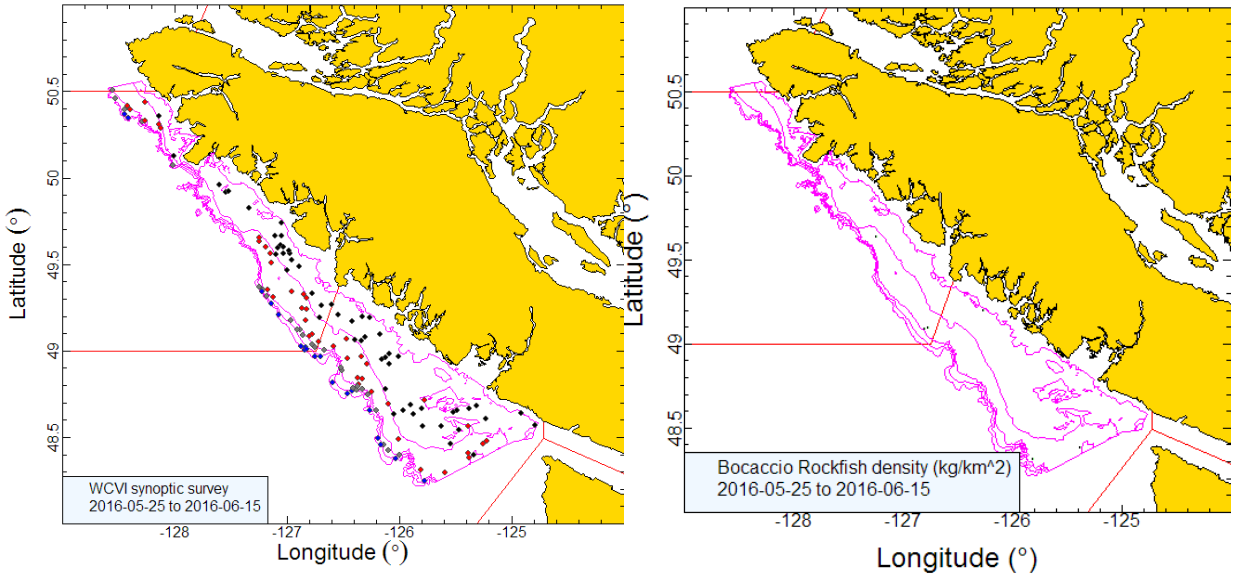

Figure B.41. Tow locations and density plots for the 2016 west coast Vancouver Island synoptic survey (see Figure B.35 caption).

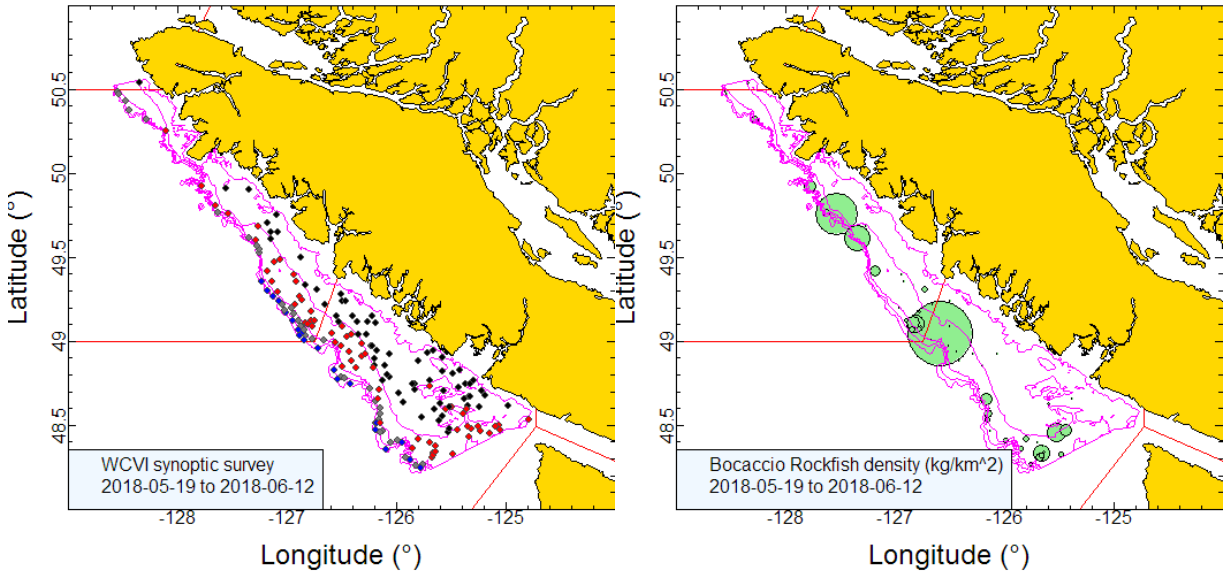

Figure B.42. Tow locations and density plots for the 2018 west coast Vancouver Island synoptic survey (see Figure B.35 caption).

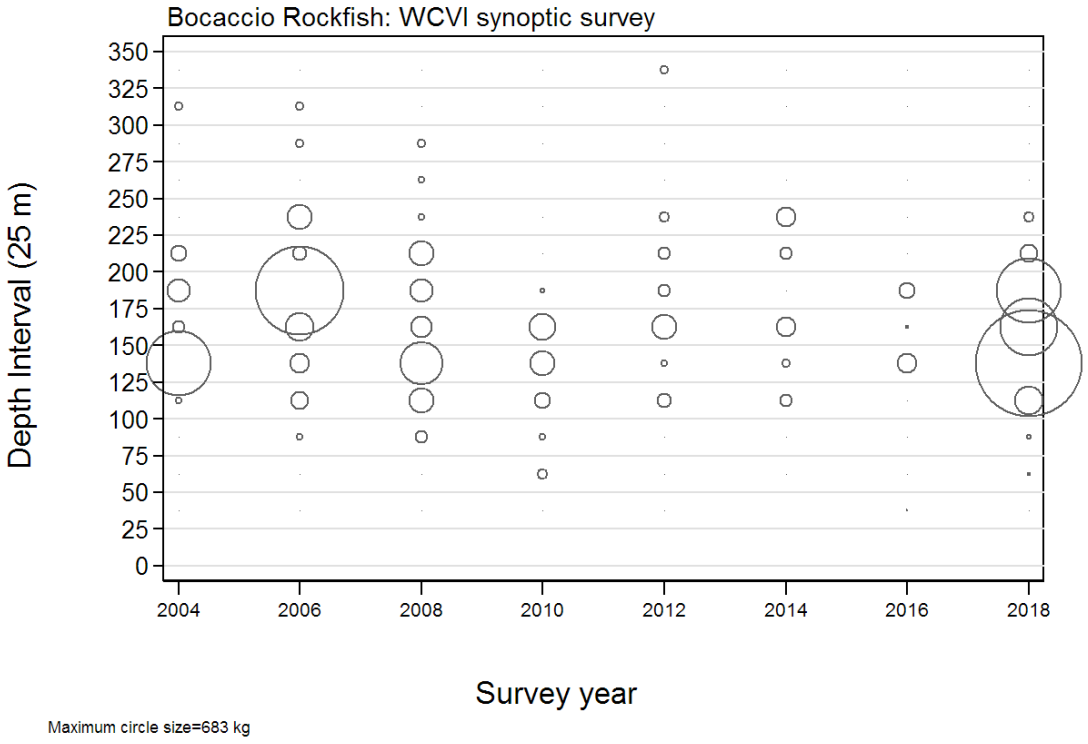

Figure B.43. Distribution of observed weights of BOR by survey year and 25 m depth zone. Catches are plotted at the mid-point of the interval and circles in the panel are scaled to the maximum value (683 kg) in the 125-150 m interval in 2018. The 1 and 99 percentiles for the BOR empirical start of tow depth distribution= 101 m and 300 m respectively.

B.6.2. Results

BOR are taken sporadically along the shelf edge from near the US border to at least the Brooks Peninsula below the top of Vancouver Island (Figure B.35 to Figure B.42). There does not seem to be any region that predominates in the spatial distribution, but the distribution appears to be more towards the south of Vancouver Island. Very few Bocaccio were taken in 2010, 2012, 2014 and 2016. BOR were mainly taken at depths from 113 to 219 m (5–95 percentiles). This species is rarely found at depths greater than 300 m, which is the 99th percentile of observed weights (Figure B.43). Estimated biomass levels for BOR from this trawl survey show higher biomass levels in 2004, 2006 and 2018 with low biomass levels in the intervening years. Relative errors are high, ranging from 28 to 76% across the eight surveys (Figure B.44; Table B.14).

The proportion of tows capturing BOR ranged between 5 and 29% for the eight surveys, with a mean value of 15% (Figure B.45). One hundred ninety-one of the 1175 usable tows from this survey contained BOR, with a median catch weight for positive tows of 3.8 kg/tow and maximum catch weight across all eight surveys of 592 kg (in 2018).

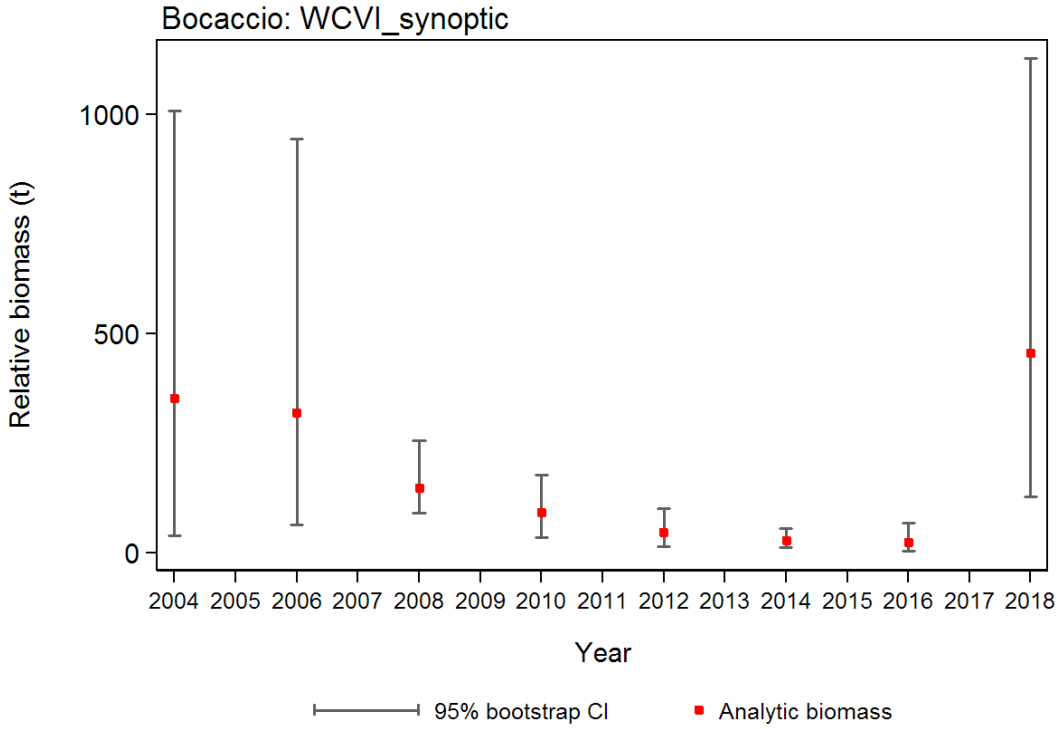

Figure B.44. Plot of biomass estimates for BOR from the 2004 to 2018 west coast Vancouver Island synoptic trawl surveys (Table B.14). Bias-corrected 95% confidence intervals from 1000 bootstrap replicates are plotted.

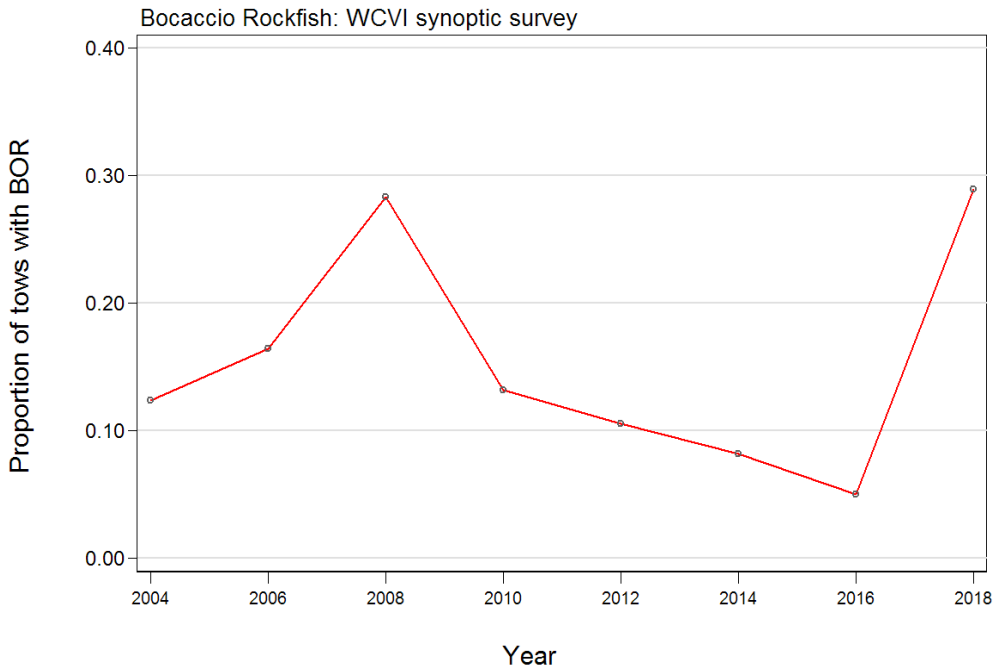

Figure B.45. Proportion of tows by stratum and year capturing BOR in the WCVI synoptic trawl surveys, 2004–2018.

Table B.14. Biomass estimates for BOR from the WCVI synoptic trawl survey for the survey years 2004 to 2018. Bootstrap bias-corrected confidence intervals and CVs are based on 1000 random draws with replacement.

Survey Year	Biomass (t) (Eq. B.4)	Mean bootstrap biomass (t)	Lower bound biomass (t)	Upper bound biomass (t)	Bootstrap CV	Analytic CV (Eq. B.6)
2004	353.3	357.4	40.1	1008.4	0.760	0.785
2006	319.4	305.7	65.6	943.1	0.704	0.721
2008	149.3	148.8	90.7	257.2	0.281	0.280
2010	93.5	93.7	35.4	178.4	0.383	0.387
2012	46.8	47.4	14.4	101.9	0.480	0.482
2014	29.5	29.4	12.2	57.0	0.367	0.364
2016	25.2	24.9	5.5	68.4	0.595	0.586
2018	456.4	454.0	128.3	1127.6	0.557	0.569

B.7. WEST COAST HAIDA GWAII SYNOPTIC TRAWL SURVEY

B.7.1. Data selection

The west coast Haida Gwaii (WCHG) survey has been conducted eight times in the period 2006 to 2018 off the west coast of Haida Gwaii. This includes a survey conducted in 2014 which did not complete a sufficient number of tows for it to be considered comparable to previous surveys and which is consequently omitted from Table B.15. This survey comprises a single areal stratum extending from 53°N to the BC-Alaska border and east to 133°W (e.g., Olsen et al. 2008). The 2006 survey (depth stratification: 150–200 m, 200–330 m, 330–500 m, 500–800 m, and 800–1300 m; Workman et al. 2007) has been re-stratified into the four depth strata used from 2007 onwards: 180–330 m; 330–500 m; 500–800 m; and 800–1300 m, based on the mean of the beginning and end depths of each tow (Table B.15). Tows S of 53°N from the 2006 survey have been dropped from biomass estimation. Plots of the locations of all valid tows by year and stratum are presented in Figure B.46 (2006), Figure B.47 (2007), Figure B.48 (2008),

Figure B.49 (2010), Figure B.50 (2012), Figure B.51 (2016) and Figure B.52 (2018). Note that the depth stratum boundaries for this survey differ from those used for the Queen Charlotte Sound (Edwards et al. 2012) and west coast Vancouver Island (Edwards et al. 2014) synoptic surveys due to the considerable difference in the seabed topography of the area being surveyed. The deepest stratum (800–1300 m) has been omitted from this analysis because of lack of coverage in 2007.

Table B.15. Stratum designations, vessel name, number of usable and unusable tows, for each completed year of the west coast Haida Gwaii synoptic survey. Also shown are the dates of the first and last survey tow in each year.

		Depth stratum							
Survey year	Vessel	180-330m	330-500m	500-800m	800-1300m	Total tows[1]	Unusable tows	Minimum date	Maximum date
2006	*Viking Storm*	55	26	16	13	97	13[2]	30-Aug-06	22-Sep-06
2007	*Nemesis*	68	34	9	0	111	5	14-Sep-07	12-Oct-07
2008	*Frosti*	71	31	8	8	110	9	28-Aug-08	18-Sep-08
2010	*Viking Storm*	82	29	12	6	123	2	28-Aug-10	16-Sep-10
2012	*Nordic Pearl*	75	29	10	16	114	11	27-Aug-12	16-Sep-12
2016	*Frosti*	69	28	5	10	101	8	28-Aug-16	24-Sep-16
2018	*Nordic Pearl*	67	31	10	11	108	11	05-Sep-18	20-Sep-18
Area (km^2)		1104	1024	956	2248	5,332[3]	–	–	–

[1] GFBio usability codes=0,1,2,6 and omitting the 800-1300 m stratum; [2] excludes 2 tows S of 53°N; [3] Total area in 2018 (km^2)

A doorspread density (Eq. B.3) was generated for each tow based on the catch of BOR from the mean doorspread for the tow and the distance travelled. [`distance travelled`] is a database field which is calculated directly from the tow track. This field is used preferentially for the variable D_{yij} in Eq. B.3. A calculated value ([`vessel speed`] X [`tow duration`]) is used for this variable if [`distance travelled`] is missing, but there were no instances of this occurring in the eight trawl surveys. Missing values for the [`doorspread`] field were filled in with the mean doorspread for the survey year (103 values over all years, Table B.16).

Table B.16. Number of valid tows with doorspread measurements, the mean doorspread values (in m) from these tows for each survey year and the number of valid tows without doorspread measurements.

Year	Tows with doorspread	Tows missing doorspread	Mean doorspread (m)
2006	93	30	77.7
2007	113	3	68.5
2008	123	4	80.7
2010	129	2	79.1
2012	92	49	73.8
2016	105	15	74.1
2018	130	0	67.0
Total/Average	995	103	73.1[1]

[1] average 2006–2018: all observations

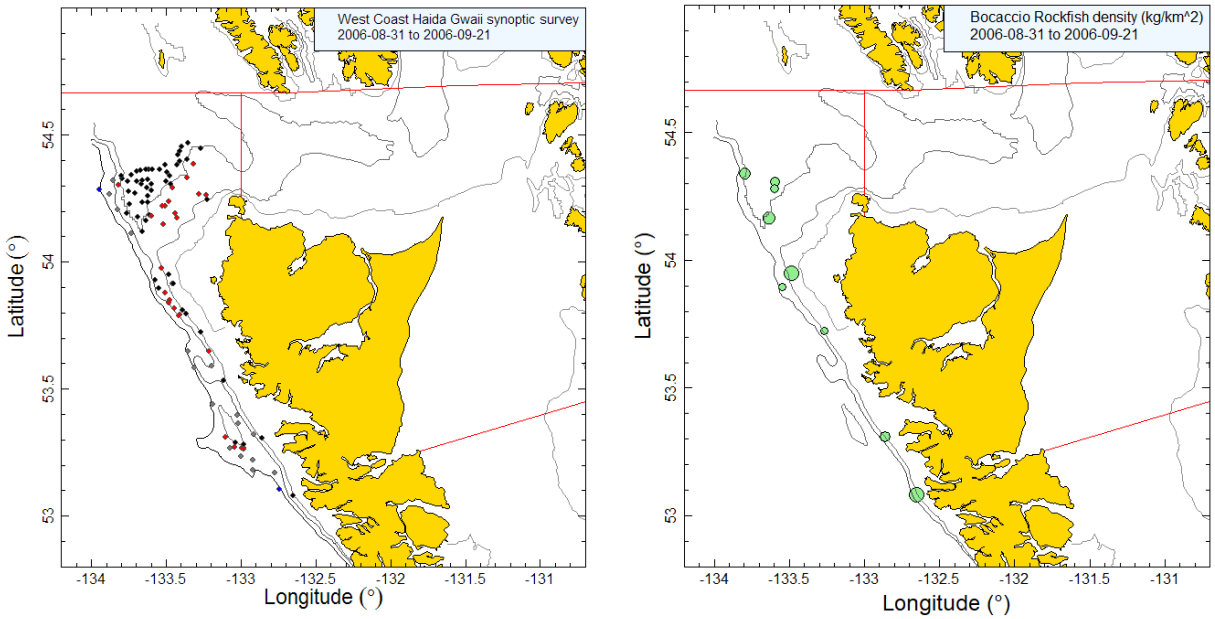

Figure B.46. Valid tow locations by stratum (180-330m: black; 330-500m: red; 500-800m: grey; 800-1300m: blue) and density plots for the 2006 Viking Storm synoptic survey. Circle sizes in the right-hand density plot scaled across all years (2006–2018), with the largest circle =336 kg/km^2 in 2018. The red lines show the Pacific Marine Fisheries Commission 5E and 5D major area boundaries.

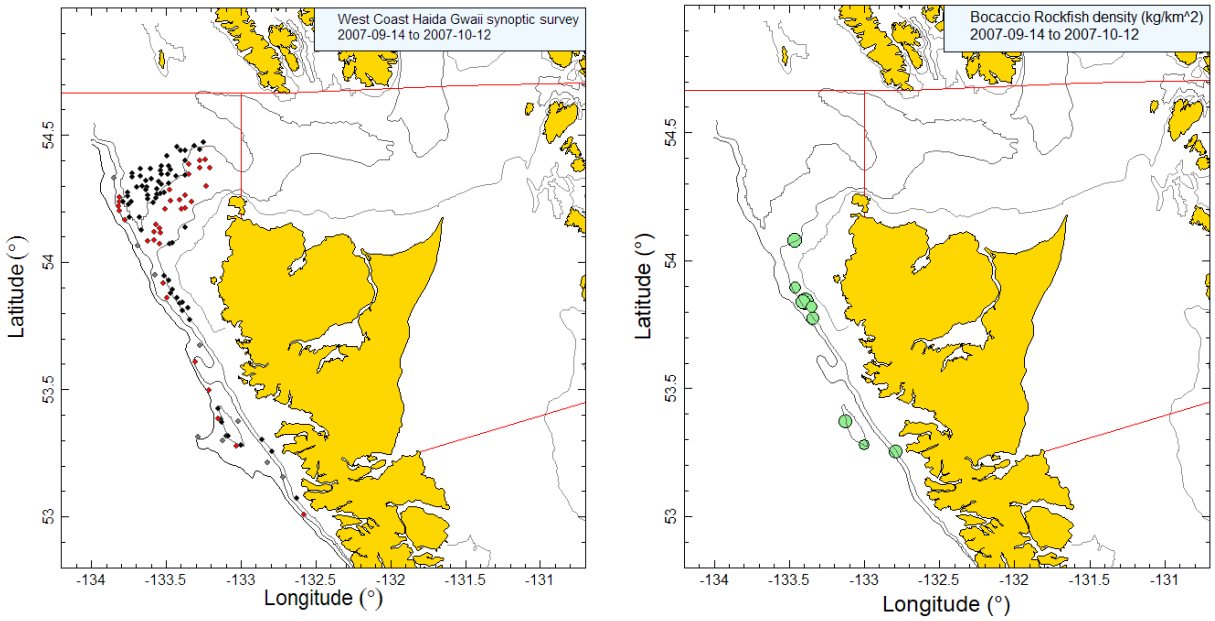

Figure B.47. Tow locations and density plots for the 2007 Nemesis synoptic survey (see Figure B.46 caption).

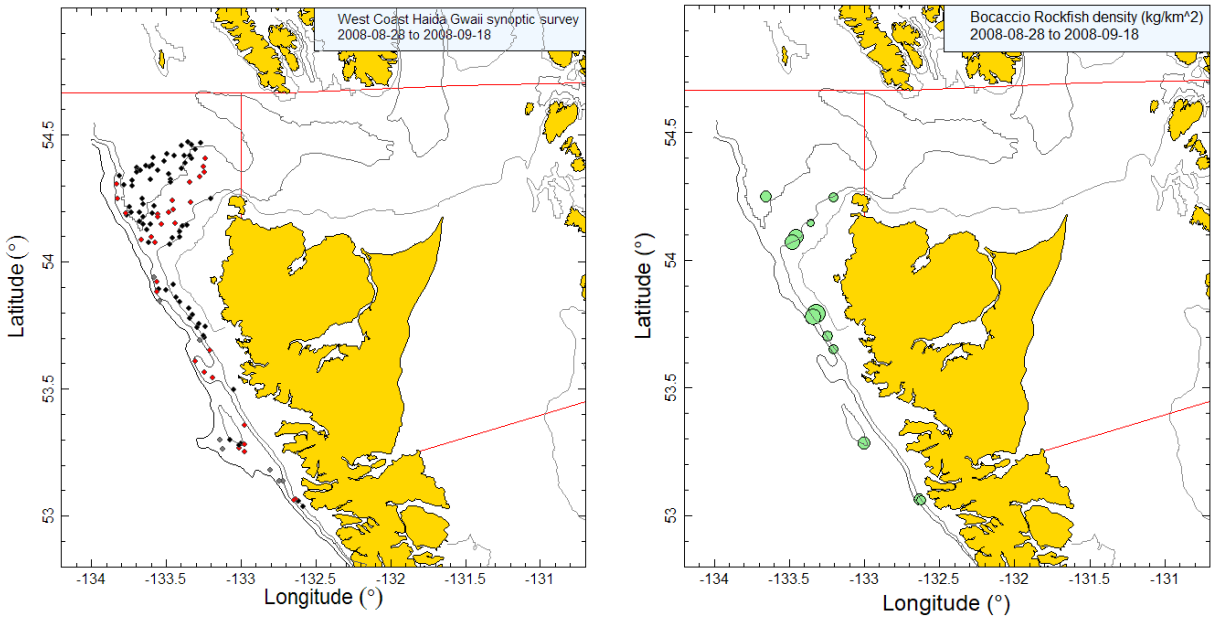

Figure B.48. Tow locations and density plots for the 2008 Frosti synoptic survey (see Figure B.46 caption).

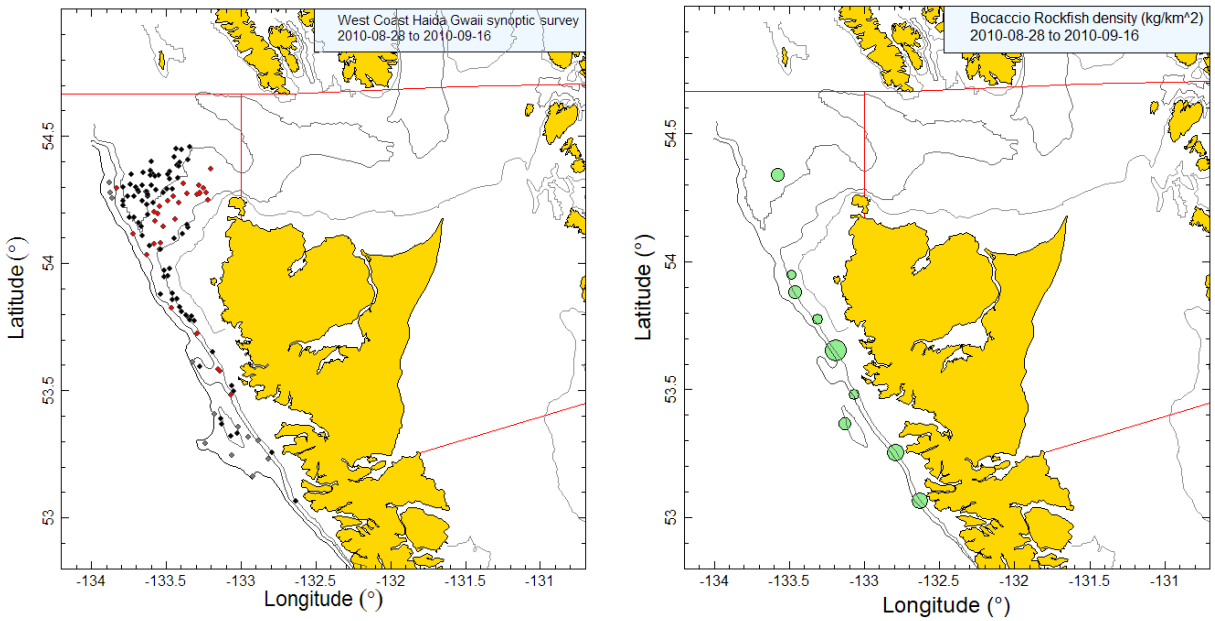

Figure B.49. Tow locations and density plots for the 2010 Viking Storm synoptic survey (see Figure B.46 caption).

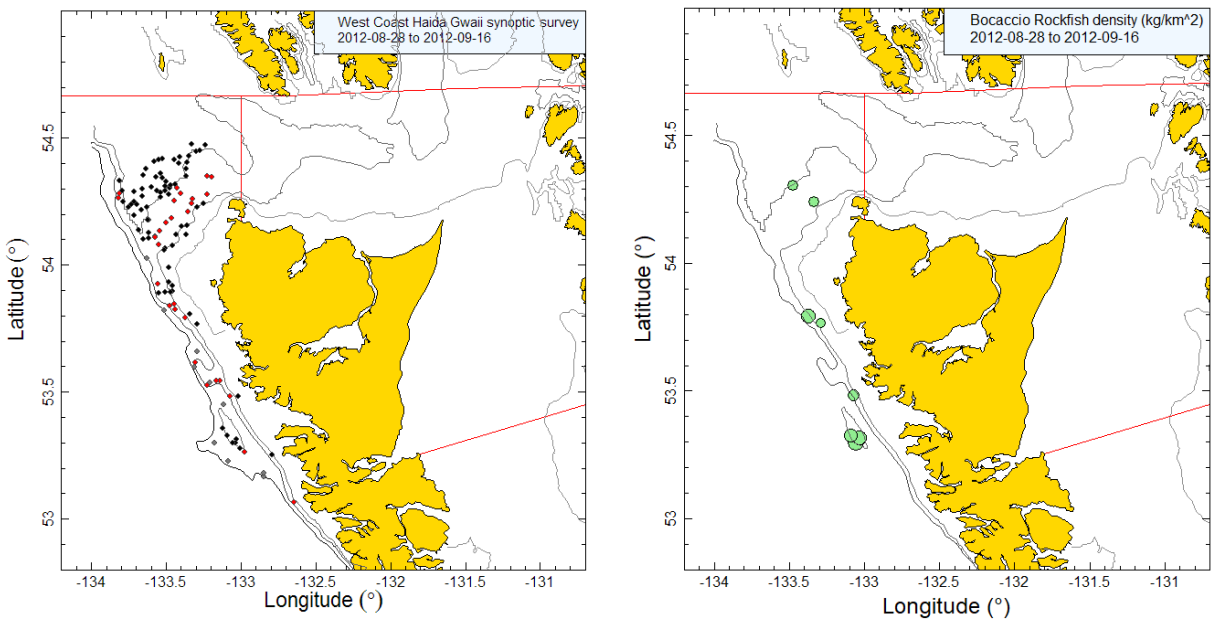

Figure B.50. Tow locations and density plots for the 2012 Nordic Pearl synoptic survey (see Figure B.46 caption).

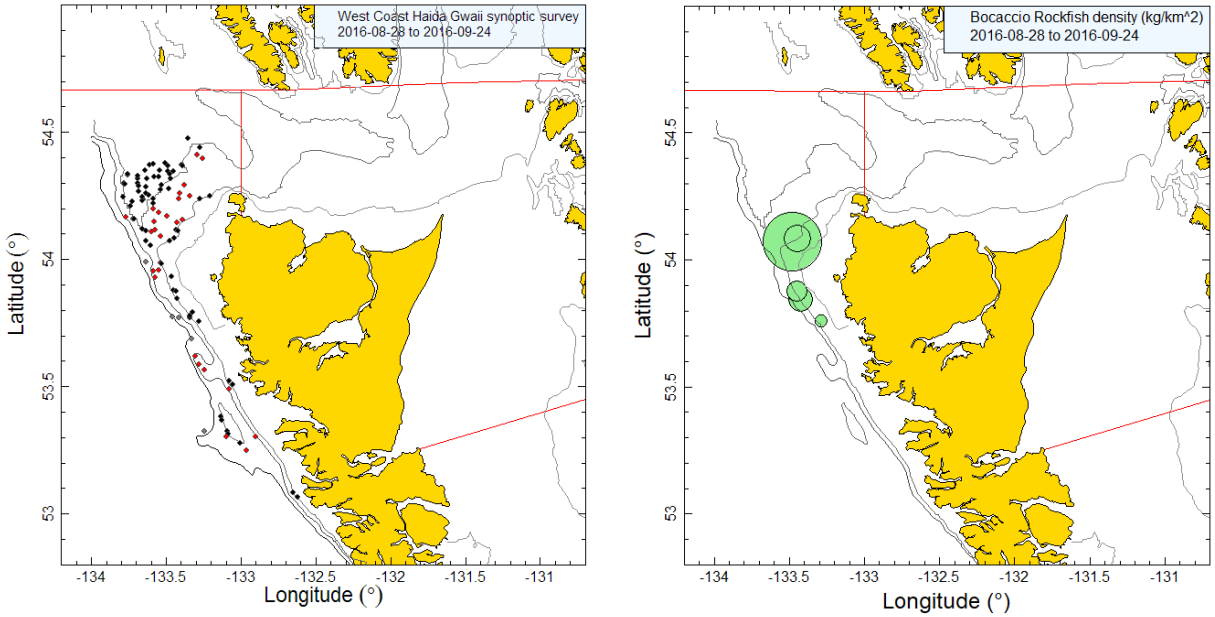

Figure B.51. Tow locations and density plots for the 2016 Frosti synoptic survey (see Figure B.46 caption).

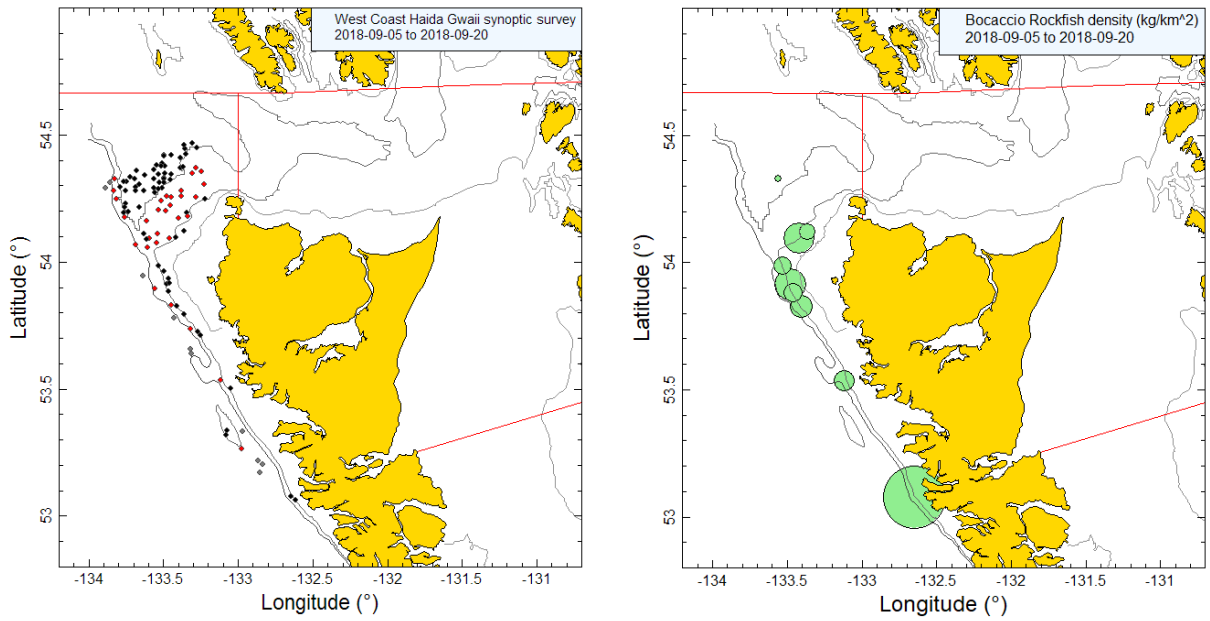

Figure B.52. Tow locations and density plots for the 2018 Nordic Pearl synoptic survey (see Figure B.46 caption).

B.7.2. Results

All seven usable surveys have taken BOR in the western part of Dixon Entrance and off the west coast of Graham Island and down to 53°N, the southernmost extent of this survey (Figure B.46 to Figure B.52). BOR were mainly taken at depths from 210 m to 316 m (5 to 95% quantiles of the starting tow depth), with the 50% of the observations lying between 223 m and 271 m depth (25–75% quantiles, Figure B.53). There were only three observations deeper than 316 m: 329 m, 341 m and 451 m,

Table B.17. Biomass estimates for BOR from the seven west coast Haida Gwaii synoptic surveys used in the stock assessment. Bootstrap bias-corrected confidence intervals and coefficients of variation (CVs) are based on 1000 random draws with replacement.

Survey Year	Biomass (t) (Eq. B.4)	Mean bootstrap biomass (t)	Lower bound biomass (t)	Upper bound biomass (t)	Bootstrap CV	Analytic CV (Eq. B.6)
2006	8.4	8.4	3.7	14.9	0.340	0.345
2007	8.0	7.8	3.3	13.5	0.334	0.329
2008	10.2	10.1	5.3	17.0	0.290	0.302
2010	6.7	6.7	2.5	12.0	0.360	0.360
2012	8.1	8.3	2.4	14.6	0.381	0.370
2016	7.8	8.0	1.1	22.2	0.659	0.666
2018	11.6	11.5	3.6	29.2	0.506	0.508

Estimated biomass levels for BOR from these trawl surveys are low and show no trend (ranging from 8 t in 2007 to 12 t in 2018) (Figure B.54; Table B.17). The estimated relative errors (RE) for these surveys are variable and generally large, ranging from 0.29 to 0.66 (Table B.17).

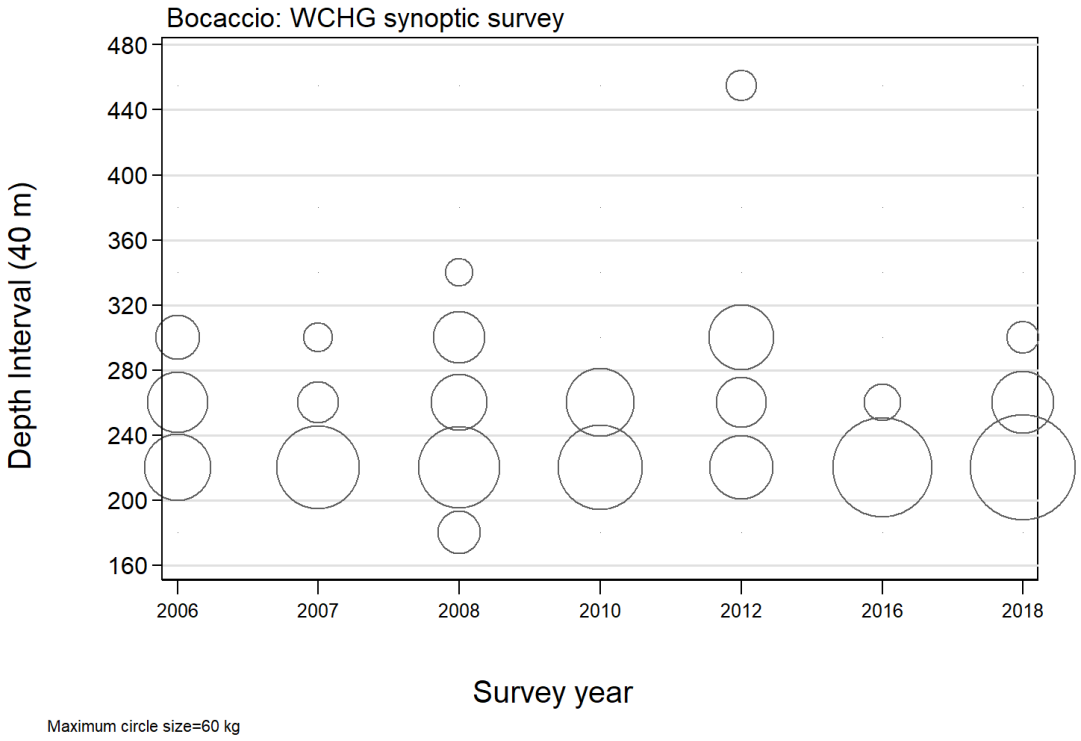

Figure B.53. Distribution of observed weights of BOR by survey year and 40 m depth zone intervals. Catches are plotted at the mid-point of the interval and circles in the each panel are scaled to the maximum value (60 kg – 200-240 m interval in 2018). Minimum and maximum depths observed for BOR: 195 m and 451 m, respectively.

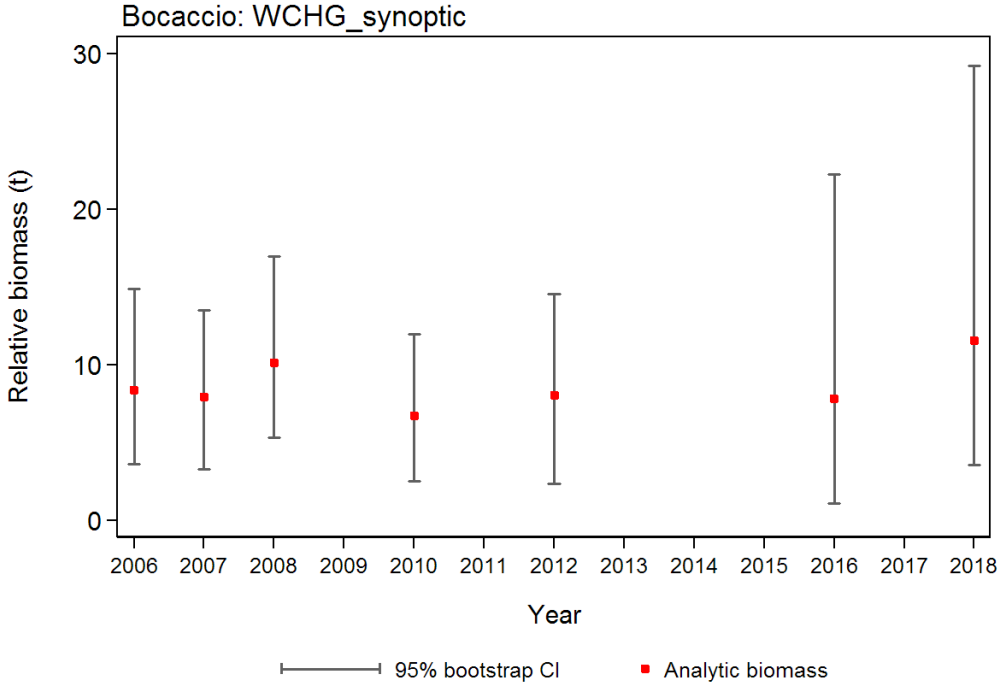

Figure B.54. Biomass estimates for BOR from the 2006 to 2018 west coast Haida Gwaii synoptic surveys (Table B.17). Bias-corrected 95% confidence intervals from 1000 bootstrap replicates are plotted.

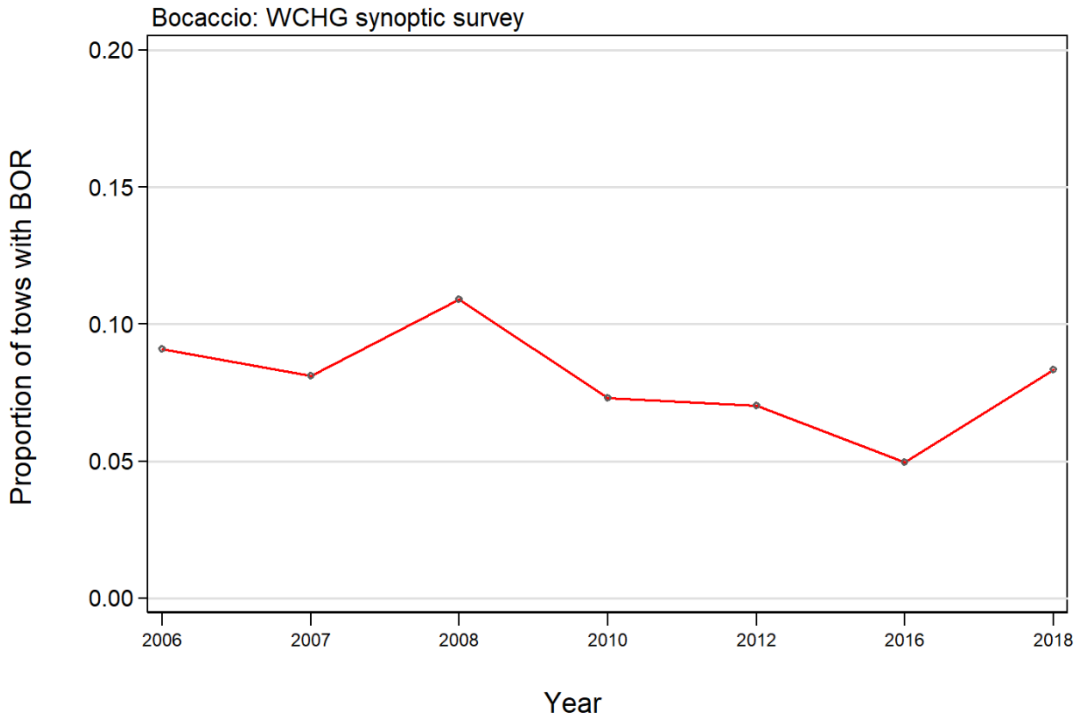

Figure B.55. Proportion of tows by year that contain BOR for the seven west coast Haida Gwaii synoptic surveys.

The proportion of tows that captured BOR was low, ranging from 5 to 11% of tows over the seven survey years, with an overall mean of 8% (Figure B.55). The median BOR catch weight for positive tows was 5.5 kg/tow and the maximum catch weight across the seven surveys was 44 kg in 2018.

B.8. HECATE STRAIT SYNOPTIC SURVEY

B.8.1. Data selection

This survey has been conducted in eight alternating years over the period 2005 to 2019 in Hecate Strait (HS) between Moresby and Graham Islands and the mainland and in Dixon Entrance at the top of Graham Island (all valid tow starting positions by survey year are shown in Figure B.56 to Figure B.63). This survey treats the full spatial coverage as a single areal stratum divided into four depth strata: 10–70 m; 70–130 m; 130–220 m; and 220–500 m (Table B.18).

Table B.18. Number of usable tows for biomass estimation by year and depth stratum for the Hecate Strait synoptic survey over the period 2005 to 2019. Also shown is the area of each depth stratum and the vessel conducting the survey by survey year.

Year	Vessel	Depth stratum				Total tows[1]
		10-70	70-130	130-220	220-500	
2005	Frosti	77	86	26	9	198
2007	W.E. Ricker	47	42	36	7	132
2009	W.E. Ricker	53	43	47	12	155
2011	W.E. Ricker	70	51	49	14	184
2013	W.E. Ricker	74	42	43	16	175
2015	W.E. Ricker	47	46	40	15	148
2017	Nordic Pearl	47	44	38	9	138
2019	Nordic Pearl	41	44	37	14	136
Area (km^2)		5,958	3,011	2,432	1,858	13,259[2]

[1] GFBio usability codes=0,1,2,6
[2] Total area (km^2) for 2019 synoptic survey

Table B.19. Number of missing doorspread values by year for the Hecate Strait synoptic survey over the period 2005 to 2019 as well as showing the number of available doorspread observations and the mean doorspread value for the survey year.

Year	Number tows with missing doorspread [1]	Number tows with doorspread observations [2]	Mean doorspread (m) used for tows with missing values [2]
2005	7	217	64.4
2007	97	37	59.0
2009	93	70	54.0
2011	13	186	54.8
2013	6	176	51.7
2015	0	151	59.4
2017	2	150	64.2
2019	6	140	59.2
Total	224	1,127	58.7

[1] valid biomass estimation tows only
[2] includes tows not used for biomass estimation

A doorspread density value (Eq. B.3) was generated for each tow based on the catch of BOR from the mean doorspread for the tow and the distance travelled. [`distance travelled`] is a database field which is calculated directly from the tow track. This field is used preferentially for the variable D_{yij} in Eq. B.3. A calculated value ([`vessel speed`] X [`tow duration`]) is used for this variable if [`distance travelled`] is missing, but there were no instances of this occurring among the valid tows in the eight trawl surveys. Missing values for the [`doorspread`] field were filled in with the mean doorspread for the survey year (224 values over all years: Table B.19).

B.8.2. Results

Catches of BOR have been taken sporadically throughout the area covered by the survey (Figure B.56 to Figure B.63). Furthermore, there seems to be little pattern in the observed spatial distribution of this species, with intermittent small amounts of catch. No tows exceeded 45 kg of BOR, where were mainly taken at depths from 79 to 200 m (5–95% quantiles), but there were sporadic observations at depths down to 50 m and one observation at 225 m (Figure B.64).

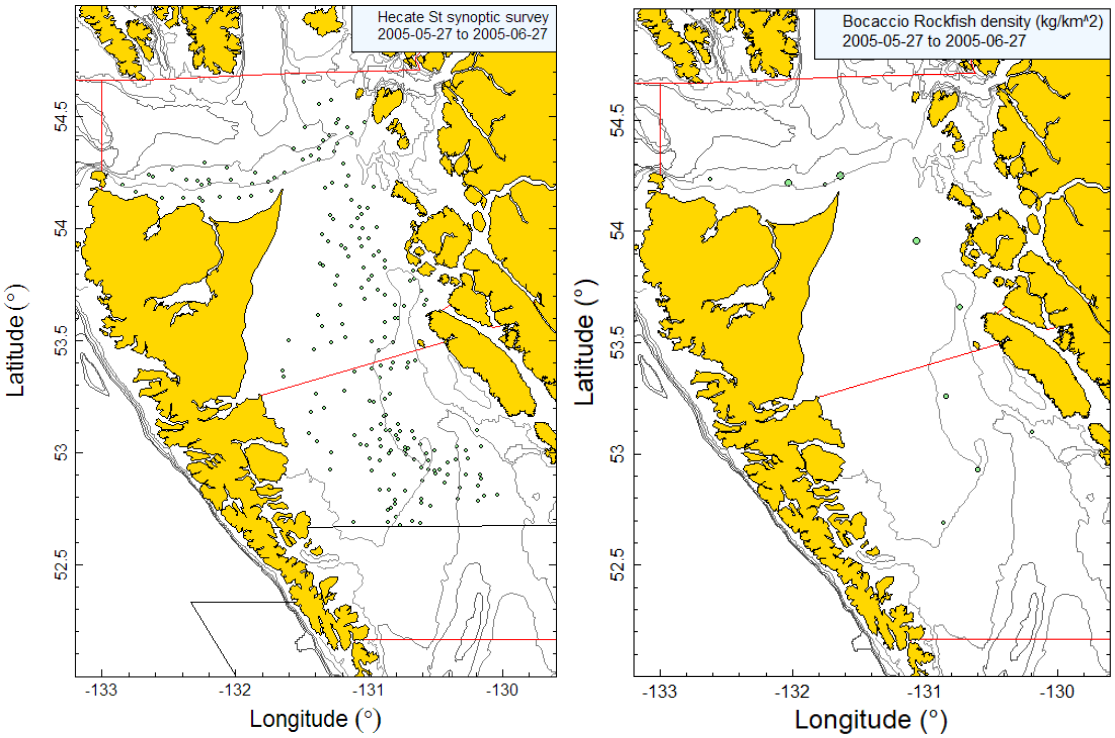

Figure B.56. Valid tow locations and density plots for the 2005 Hecate Strait synoptic survey. Circle sizes in the right-hand density plot scaled across all years (2005, 2007, 2009, 2011, 2013, 2015, 2017, 2019), with the largest circle = 522 kg/km^2 in 2011. Red lines indicate boundaries for PMFC major statistical areas 5C, 5D and 5E.

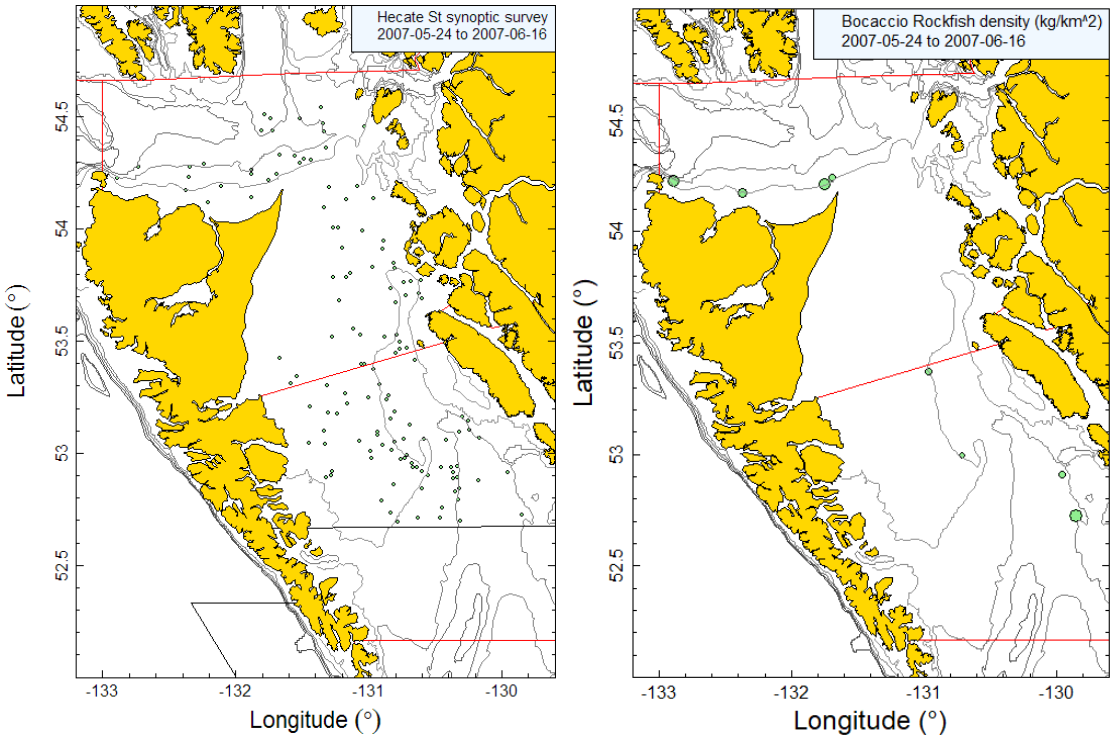

Figure B.57. Tow locations and density plots for the 2007 Hecate Strait synoptic survey (see Figure B.56 caption).

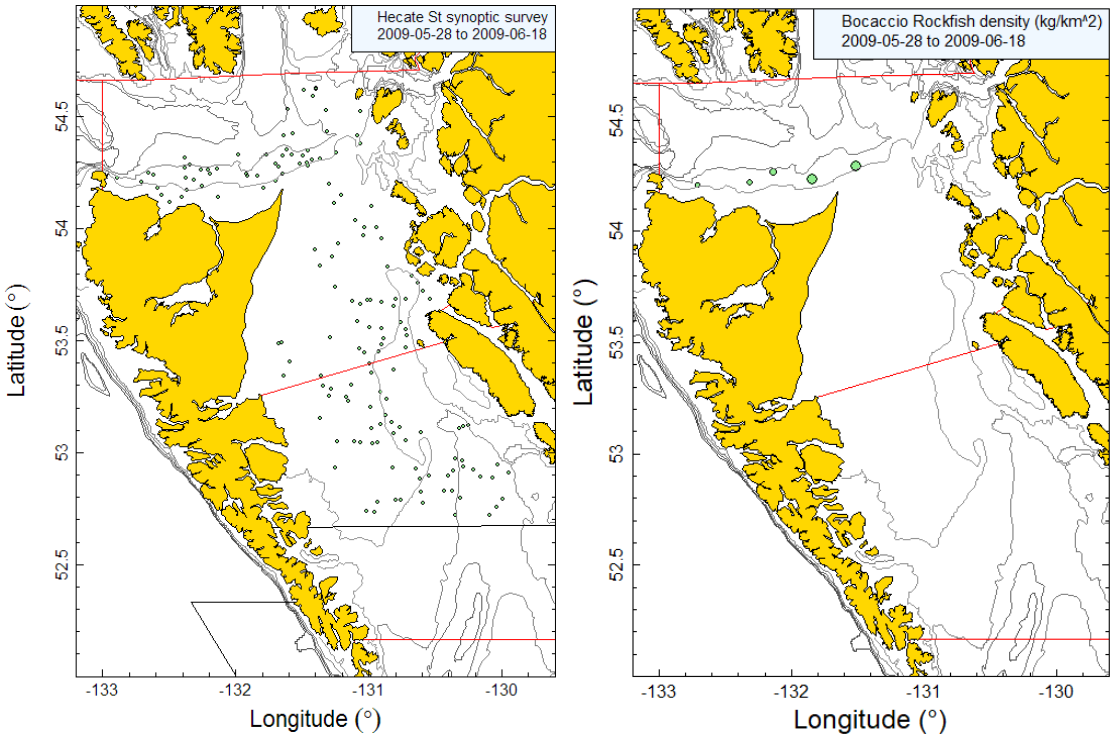

Figure B.58. Tow locations and density plots for the 2009 Hecate Strait synoptic survey (see Figure B.56 caption).

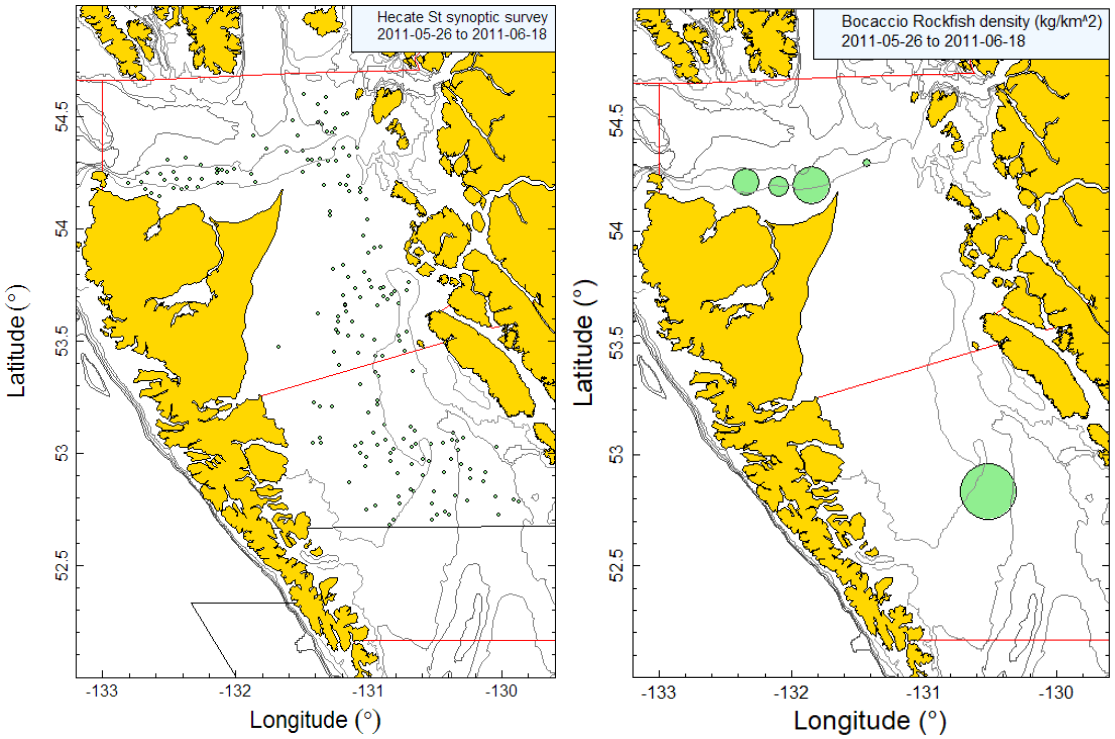

Figure B.59. Tow locations and density plots for the 2011 Hecate Strait synoptic survey (see Figure B.56 caption).

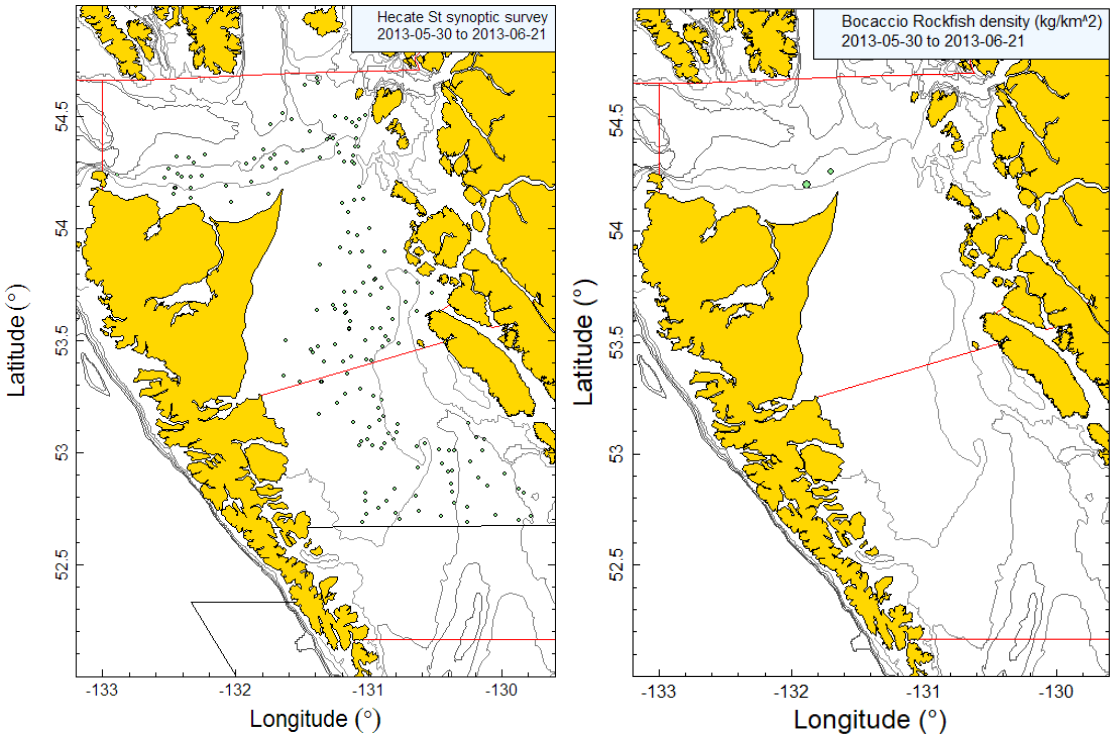

Figure B.60. Tow locations and density plots for the 2013 Hecate Strait synoptic survey (see Figure B.56 caption).

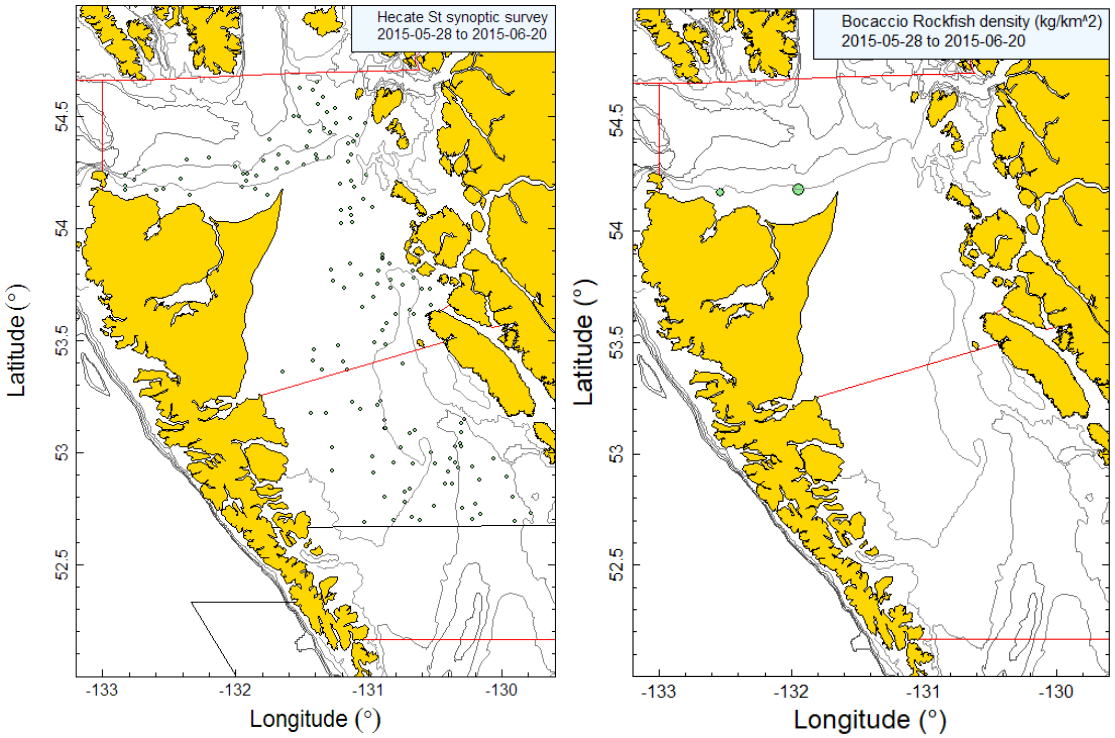

Figure B.61. Tow locations and density plots for the 2015 Hecate Strait synoptic survey (see Figure B.56 caption).

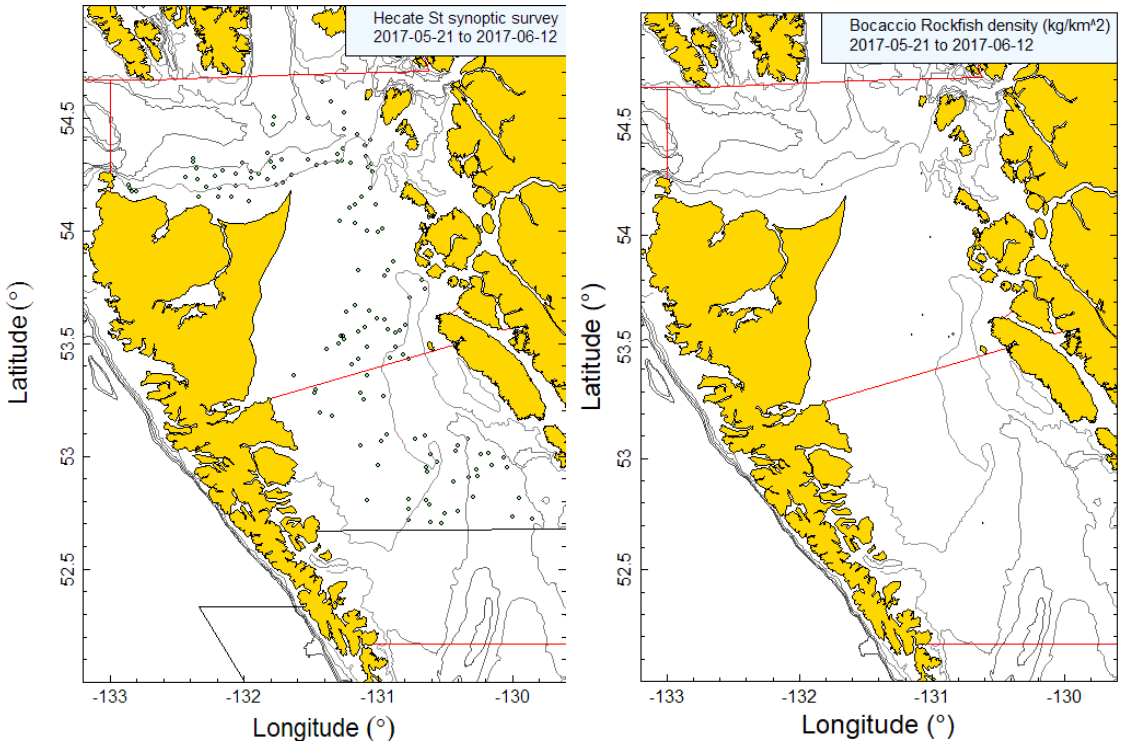

Figure B.62. Tow locations and density plots for the 2017 Hecate Strait synoptic survey (see Figure B.56 caption).

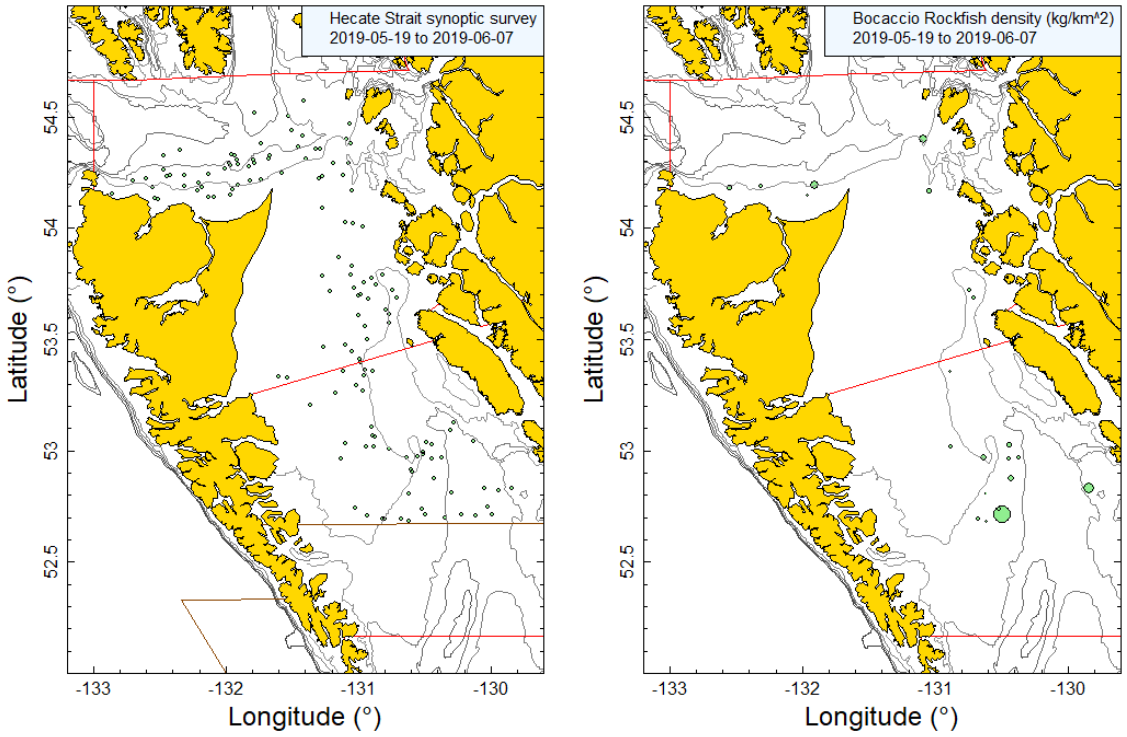

Figure B.63. Tow locations and density plots for the 2019 Hecate Strait synoptic survey (see Figure B.56 caption).

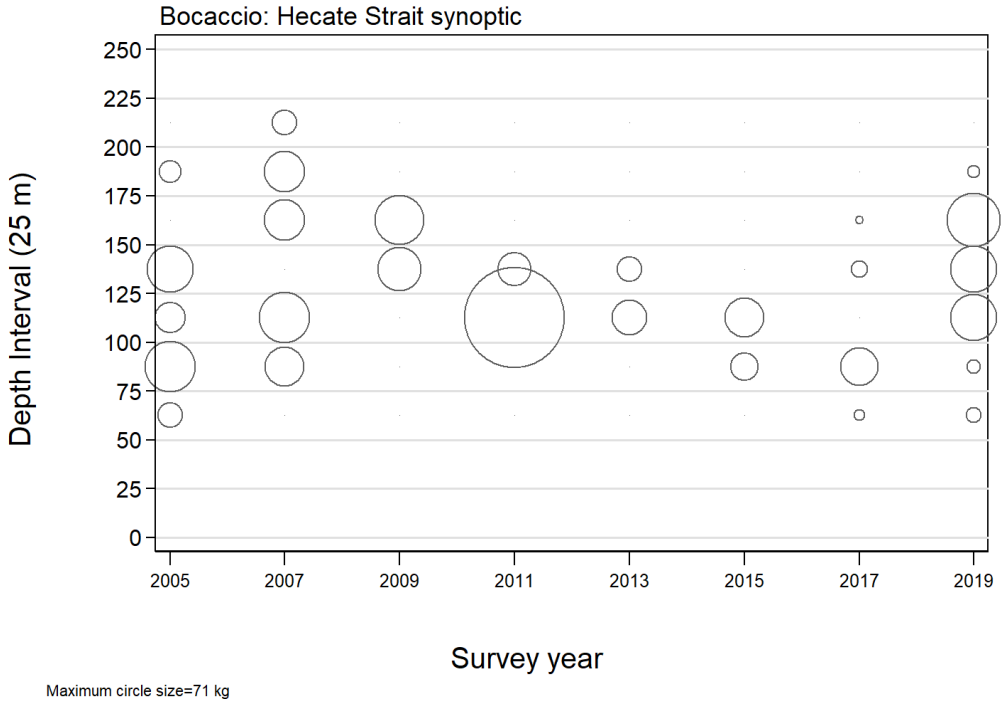

Figure B.64. Distribution of observed catch weights of BOR for the Hecate Strait synoptic survey (Table B.18) by survey year and 25 m depth zone. Catches are plotted at the mid-point of the interval and circles in the panel are scaled to the maximum value (71 kg) in the 100-125 m interval in 2011. The 1% and 99% quantiles for the BOR empirical start of tow depth distribution= 69 m and 225 m respectively.

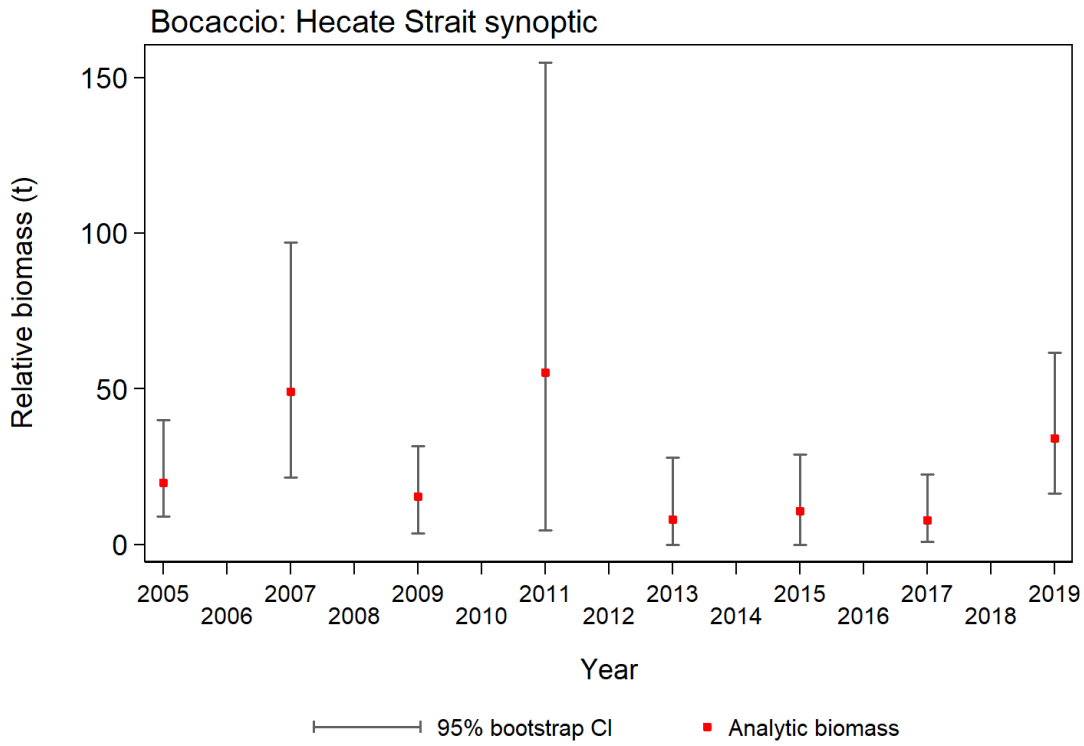

Figure B.65. Plot of biomass estimates for BOR values provided in Table B.20 from the Hecate Strait synoptic survey over the period 2005 to 2019. Bias corrected 95% confidence intervals from 500 bootstrap replicates are plotted.

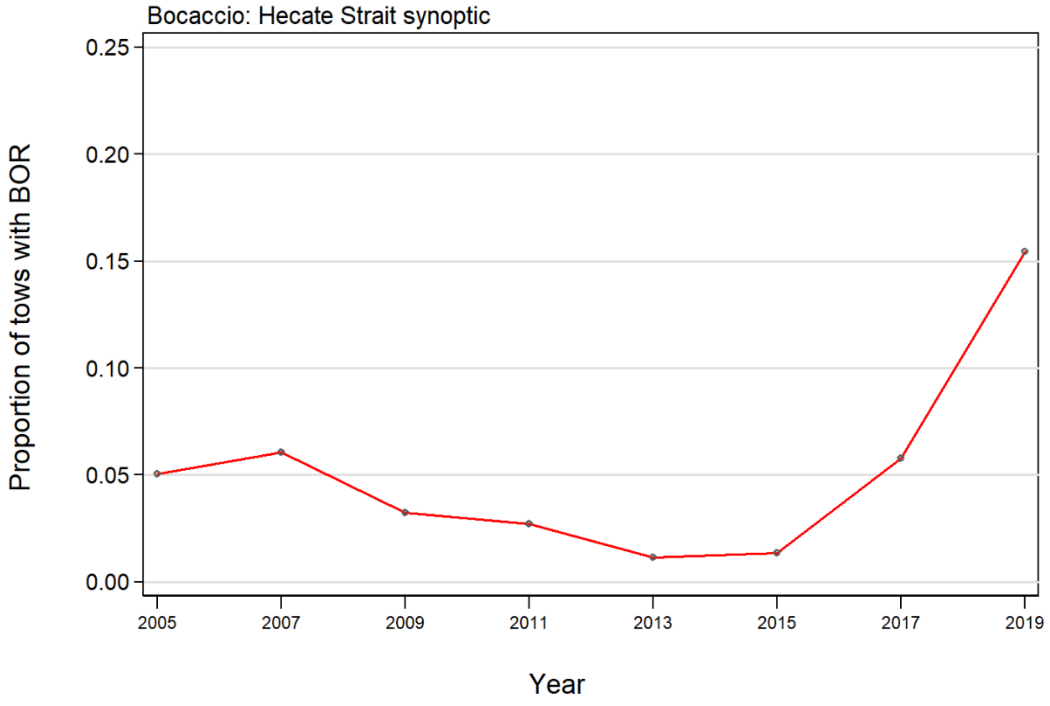

Figure B.66. Proportion of tows by year which contain BOR from the Hecate Strait synoptic survey over the period 2005 to 2019.

Table B.20. Biomass estimates for BOR from the Hecate Strait synoptic trawl survey for the survey years 2005 to 2019. Bootstrap bias corrected confidence intervals and CVs are based on 500 random draws with replacement.

Survey Year	Biomass (t) (Eq. B.4)	Mean bootstrap biomass (t)	Lower bound biomass (t)	Upper bound biomass (t)	Bootstrap CV	Analytic CV (Eq. B.6)
2005	19.7	19.4	8.9	40.0	0.384	0.367
2007	49.1	47.5	21.6	97.1	0.378	0.388
2009	15.5	15.1	3.6	31.6	0.473	0.485
2011	55.2	55.9	4.7	154.7	0.647	0.620
2013	8.1	7.5	0.0	27.8	0.799	0.785
2015	10.7	11.1	0.0	28.9	0.692	0.749
2017	7.7	8.1	0.9	22.5	0.665	0.699
2019	34.0	34.1	16.4	61.6	0.350	0.357

Estimated BOR doorspread biomass indices from this trawl survey showed no overall trend over the period 2005 to 2019, with the highest estimates recorded in 2007, 2011, 2019 and the lowest estimates in 2013, 2017 (Table B.20; Figure B.65). The estimated relative errors were high, ranging from 0.35 to 0.80 (Table B.20). The incidence of BOR in this survey is very low, with less than 10% of the tows capturing this species in all years except 2019 when 15% of the tows caught BOR (survey average: 5%) (Figure B.66). Overall, only 61 of the 1,266 usable survey tows contained BOR with a median catch weight for positive tows of 9.8 kg/tow and a maximum catch weight across all eight surveys of 71 kg in 2011.

B.9. REFERENCES – SURVEYS

DFO. 2015. Proceedings of the Pacific regional peer review on Stock assessment for Yellowtail Rockfish (*Sebastes flavidus*) in British Columbia; November 18-19, 2014. DFO Can. Sci. Advis. Sec. Proceed. Ser. 2015/020.

Edwards, A.M., Haigh, R. and Starr, P.J. 2014. Pacific Ocean Perch (*Sebastes alutus*) stock assessment for the west coast of Vancouver Island, British Columbia. DFO Can. Sci. Advis. Sec. Res. Doc. 2013/093. vi + 135 pp.

Edwards, A.M., Starr, P.J. and Haigh, R. 2012. Stock assessment for Pacific ocean perch (*Sebastes alutus*) in Queen Charlotte Sound, British Columbia. DFO Can. Sci. Advis. Sec. Res. Doc. 2011/111. viii + 172 pp.

Harling, W.R. and Davenport, D. 1977. *G.B. Reed* Groundfish Cruise No. 77-3 August 22 to September 8, 1977. Fish. Mar. Serv. Data Rep. 42: iii + 46 pp.

Harling, W.R., Davenport, D., Smith, H.S., Wowchuk, R.H. and Westrheim, S.J. 1971. *G.B. Reed* Groundfish Cruise No. 71-3, October 1-29, 1971. Fish. Res. Board Can. Tech. Rep. 290: 35 pp.

Harling, W.R., Davenport, D., Smith, M.S., Phillips, A.C. and Westrheim, S.J. 1973. *G.B. Reed* Groundfish Cruise No. 73-2, September 5-25, 1973. Fish. Res. Board Can. Tech. Rep. 424: 37 pp.

Nagtegaal, D.A. and Farlinger, S.P. 1980. Catches and trawl locations of the M/V *Southward Ho* during a rockfish exploration and assessment cruise to Queen Charlotte Sound, September 7-27, 1979. Can. Data Rep. Fish. Aquat. Sci. 216: iii + 95 pp.

Nagtegaal, D.A., Leaman, B.M. and Stanley, R.D. 1986. Catches and trawl locations of R/V *G.B. Reed* and M/V *Eastward Ho* during the Pacific Ocean Perch assessment cruise to Queen Charlotte Sound, August-September, 1984. Can. Data Rep. Fish. Aquat. Sci. 611: iii + 109 pp.

Olsen, N., Rutherford, K.L. and Stanley, R.D. 2008. West Coast Queen Charlotte Islands groundfish bottom trawl survey, August 25th to September 21st , 2008. Can. Manuscr. Rep. Fish. Aquat. Sci. 2858: vii + 50 pp.

Westrheim, S.J. 1966a. Report on the trawling operations of the Canadian Research Vessel *G.B. Reed* from Queen Charlotte Sound, British Columbia to Cape Spencer, Alaska, August 23 to September 7, 1965. Fish. Res. Board Can. Manuscr. Rep. 890: 27 pp.

Westrheim, S.J. 1966b. Report on the trawling operations of the Canadian Research Vessel *G.B. Reed* from Queen Charlotte Sound, British Columbia to Sitka Sound, Alaska, August 24 to September 15, 1966. Fish. Res. Board Can. Manuscr. Rep. 891: 27 pp.

Westrheim, S.J. 1967a. Report on the trawling operations of the Canadian Research Vessel *G.B. Reed* off British Columbia and Southeastern Alaska, September 6 - October 4, 1967. Fish. Res. Board Can. Manuscr. Rep. 934: 8 pp.

Westrheim, S.J. 1967b. *G.B. Reed* groundfish cruise reports, 1963-66. Fish. Res. Board Can. Tech. Rep. 30: ii + 286 pp.

Westrheim, S.J. 1969. Report of the trawling operations of the Canadian Research Vessel *G.B. Reed* off British Columbia, September 1969. Fish. Res. Board Can. Manuscr. Rep. 1063: 6 pp.

Westrheim, S.J., Harling, W.R. and Davenport, D. 1968. *G.B. Reed* Groundfish Cruise No. 67-2, September 6 to October 4, 1967. Fish. Res. Board Can. Tech. Rep. 46: 45 pp.

Westrheim, S.J., Leaman, B.M., Harling, W.R., Davenport, D., Smith, M.S. and Wowchuk, R.M. 1976. *G.B. Reed* Groundfish Cruise No. 76-3, September 8-27, 1976. Fish. Mar. Serv. Data Rec. 21: 47 pp.

Workman, G.D., Olsen, N. and Rutherford, K.L. 2007. West Coast Queen Charlotte Islands groundfish bottom trawl survey, August 28th to September 25th , 2006. Can. Manuscr. Rep. Fish. Aquat. Sci. 2804: vii + 44 pp.

Yamanaka, K.L., Richards, L.J. and Workman, G.D. 1996. Bottom trawl survey for rockfish in Queen Charlotte Sound, September 11 to 22, 1995. Can. Manuscr. Rep. Fish. Aquat. Sci. 2362: iv + 116 pp.

APPENDIX C. COMMERCIAL TRAWL CPUE

C.1. INTRODUCTION

Commercial catch and effort data have been used to generate indices of abundance in several ways. The simplest indices are derived from the arithmetic mean or geometric mean of catch divided by an appropriate measure of effort (Catch Per Unit Effort or CPUE) but such indices make no adjustments for changes in fishing practices or other non-abundance factors which may affect catch rates. Consequently, methods to standardise for changes to vessel configuration, the timing or location of catch and other possible effects have been developed to remove potential biases to CPUE that may result from such changes. In these models, abundance is represented as a "year effect" and the dependent variable is either an explicitly calculated CPUE represented as catch divided by effort, or an implicit CPUE represented as catch per tow or catch per record. In the latter case, additional effort terms can be offered as explanatory variables, allowing the model to select the effort term with the greatest explanatory power. It is always preferable to standardise for as many factors as possible when using CPUE as a proxy for abundance. Unfortunately, it is often not possible to adjust for factors that might affect the behaviour of fishers, particularly economic factors, resulting in indices that may not entirely reflect the underlying stock abundance.

This Appendix documents a standardised CPUE analysis for coastwide Bocaccio Rockfish (BOR) which was subsequently used in a coastwide BOR stock assessment.

C.2. METHODS

C.2.1. Arithmetic and Unstandardised CPUE

Arithmetic and unstandardised CPUE indices provide potential measures of relative abundance, but are generally considered unreliable because they fail to take into account changes in the fishery, including spatial and temporal changes as well as behavioural and gear changes. They are frequently calculated because they provide a measure of the overall effect of the standardisation procedure.

Arithmetic CPUE (Eq. C.1) in year y was calculated as the total catch for the year divided by the total effort in the year using Eq. C.1:

Eq. C.1 $$A_y = \sum_{i=1}^{n_y} C_{i,y} \Big/ \sum_{i=1}^{n_y} E_{i,y}$$

where $C_{i,y}$ is the `[catch]`, $E_{i,y}$ (`[tows]`) or $E_{i,y}$ (`[hours_fished]`) for record i in year y, and n_y is the number of records in year y.

Unstandardised (geometric) CPUE assumes a log-normal error distribution. An unstandardised index of CPUE (Eq. C.2) in year y was calculated as the geometric mean of the ratio of catch to effort for each i in year y, using Eq. C.2:

Eq. C.2 $$G_y = \exp\left[\frac{1}{n_y}\sum_{i=1}^{n_y} \ln\left(\frac{C_{i,y}}{E_{i,y}}\right)\right]$$

where $C_{i,y}$, $E_{i,y}$ and n_y are as defined for Eq. C.1

C.2.2. Standardised CPUE

These models are preferred over the unstandardised models described above because they can account for changes in fishing behaviour and other factors which may affect the estimated abundance trend, as long as the models are provided with adequate data. In the models described below, catch per record is used as the dependent variable and the associated effort is treated as an explanatory variable.

C.2.2.1. Lognormal Model

Standardised CPUE often assumes a lognormal error distribution, with explanatory variables to used represent changes in the fishery. A standardised CPUE index (Eq. C.3) is calculated from a generalised linear model (GLM) (Quinn and Deriso 1999) using a range of explanatory variables including `[year]`, `[month]`, `[depth]`, `[vessel]` and other available factors:

Eq. C.3 $$\ln(I_i) = B + Y_{y_i} + \alpha_{a_i} + \beta_{b_i} + ... + f(\chi_i) + f(\delta_i) + ... + \varepsilon_i$$

where I_i = C_i or catch;

B = the intercept;

Y_{y_i} = year coefficient for the year corresponding to record i;

α_{a_i} and β_{b_i} = coefficients for factorial variables a and b corresponding to record i;

$f(\chi_i)$ and $f(\delta_i)$ are polynomial functions (to the 3rd order) of the continuous variables χ_i and δ_i corresponding to record i;

ε_i = an error term.

The actual number of factorial and continuous explanatory variables in each model depends on the model selection criteria and the nature of the data. Because each record represents a single tow, $C_{i,y}$ has an implicit associated effort of one tow. Hours fished for the tow is represented on the right-hand side of the equation as a continuous (polynomial) variable.

Note that calculating standardised CPUE with Eq. C.3, while assuming a lognormal distribution and without additional explanatory variables, is equivalent to using Eq. C.2 as long as the same definition for $E_{i,y}$ is used.

Canonical coefficients and standard errors were calculated for each categorical variable (Francis 1999[3]). Standardised analyses typically set one of the coefficients to 1.0 without an error term and estimate the remaining coefficients and the associated error relative to the fixed coefficient. This is required because of parameter confounding. The Francis (1999) procedure rescales all coefficients so that the geometric mean of the coefficients is equal to 1.0 and calculates a standard error for each coefficient, including the fixed coefficient.

Coefficient-distribution-influence (CDI) plots are visual tools to facilitate understanding of patterns which may exist in the combination of coefficient values, distributional changes, and annual influence (Bentley et al. 2012). CDI plots were used to illustrate each explanatory variable added to the model.

[3] Francis, R.I.C.C. 1999. The impact of correlations on standardised CPUE indices. N.Z. Fish. Ass. Res. Doc. 99/42: 30 pp. (Unpublished report held in NIWA library, Wellington, NZ)

C.2.2.2. Binomial Logit Model

The procedure described by Eq. C.3 is necessarily confined to the positive catch observations in the data set because the logarithm of zero is undefined. Observations with zero catch were modelled by fitting a logit regression model based on a binomial distribution and using the presence/absence of BOR as the dependent variable (where 1 is substituted for $\ln(I_i)$ in Eq. C.3 if it is a successful catch record and 0 if it is not successful) and using the same data set. Explanatory factors were estimated in the model in the same manner as described in Eq. C.3. Such a model provides an alternative series of standardised coefficients of relative annual changes that is analogous to the series estimated from the lognormal regression.

C.2.2.3. Combined Model

A combined model (sometimes termed a "hurdle" model), integrating the two sets of relative annual changes estimated by the lognormal and binomial models, can be estimated using the delta distribution, which allows zero and positive observations (Fletcher et al. 2005). Such a model provides a single index of abundance which integrates the signals from the positive (lognormal) and binomial series.

This approach uses the following equation to calculate an index based on the two contributing indices, after standardising each series to a geometric mean=1.0:

Eq. C.4 $$ {}^{C}Y_y = {}^{L}Y_y \, {}^{B}Y_y $$

where ${}^{C}Y_y$ = combined index for year y,

${}^{L}Y_y$ = lognormal index for year y,

${}^{B}Y_y$ = binomial index for year y

Francis (2001) suggests that a bootstrap procedure is the appropriate way to estimate the variability of the combined index. Therefore, confidence bounds for the combined model were estimated using a bootstrap procedure based on 100 replicates, drawn with replacement.

The index series plots below present normalised values, i.e., each series is divided by its geometric mean so that the series is centred on 1. This facilitates comparison among series.

C.3. PRELIMINARY INSPECTION OF THE DATA

The analyses reported in this Appendix are based on tow-by-tow total catch (landings + discards) data collected over the period 1996–2018 for which detailed positional data for every tow are available. Each tow will have an estimate of retained and discarded catch because of the presence of an observer on board the vessel. These data are held in the DFO PacHarvTrawl (PacHarvest) and GFFOS databases (Fisheries and Oceans Canada, Pacific Region, Groundfish Data Unit).

Tow-by-tow catch and effort data for BOR from the BC trawl fishery operating from Juan de Fuca Strait to the Dixon Entrance from 1996 to 2018 were selected using the following criteria:

- Tow start date between 1 January 1996 and 31 December 2018;
- Bottom trawl type (includes 'unknown' trawl gear);
- Fished in PMFC regions: 3C, 3D, 5A, 5B, 5C, 5D or 5E;
- Fishing success code <=1 (code 0= unknown; code 1= useable);
- Catch of at least one fish or invertebrate species (no water hauls or inanimate object tows);

- Valid depth field;
- Valid latitude and longitude co-ordinates;
- Valid estimate of time towed that was > 0 hours and <= 6 hours.

Each record represents a single tow, which results in equivalency between the number of records and number of tows. Catch per record can therefore be used to represent CPUE because each record (tow) has an implicit effort component.

The catch and effort data for BOR were treated as a single area (totBC) representing all catch outside of the Strait of Georgia, upper Johnstone Strait and Juan de Fuca Strait, based on the declared distribution of trawl catches (see Appendix A). Only bottom trawl data were used as this is by far the most prevalent capture method for this species. Figure C.1 plots the distribution of depth for all successful BOR bottom trawl tows in the designated region. A depth range for this analysis was selected from this plot and is summarised in Table C.1.

Table C.1. Depth bins used in CPUE analyses of stock by gear.

Analysis	Trawl Gear	First year	Depth range (m)	Upper bound effort (h)	Minimum bin + records	N depth bins	N latitude bins	N locality bins
totBC (3CD5ABCDE)	Bottom trawl	1996	50–350	6	400	12	38	28

Vessel qualification criteria for the bottom trawl fisheries were based on number of trips per year and number of years fishing to avoid including vessels which only occasionally captured BOR. The vessel qualification criteria used in this analysis appear in Table C.2 and the distribution of tows by vessel and year is presented in Figure C.2. Once a vessel was selected, all data for the qualifying vessel were included, regardless of the number of trips in a year. Table C.2 shows the number of vessels used in this analysis and the fraction (87%) of the total catch represented in the core fleet. There was good vessel overlap across years (Figure C.2) in the fishery, where 17 of the 45 core vessels have participated in the fishery over the full 23 years of the analysis and a further 9 vessels were in the fishery for 20–22 years.

Table C.2. Vessel qualification criteria used in CPUE analyses of stock by gear.

		Vessel selection criteria			Data set characteristics				
Analysis	Trawl Gear	N years	N trips	Minimum positive Records	N vessels	% total catch[1]	catch (t)	Total records	Positive records
totBC (3CD5ABCDE)	Bottom	7	7	100	45	87	2,288	190,563	46,798

[1] total catch calculated with all filters applied except for the vessel and depth restrictions

Table C.3 reports the explanatory variables offered to the model, based on the tow-by-tow information in each record, with the number of available categories varying as indicated in Table C.1, Table C.2 and Table C.3. Table C.4 summarises the core vessel data used in the analysis by calendar year, including the number of records, the total hours fished and the associated BOR catch. This table also tracks the proportion of tows which did not report BOR.

Table C.3. Explanatory variables offered to the CPUE model, based on the tow-by-tow information.

Variable	Data type
Year	23 categories (calendar years)
Hours fished	continuous: 3rd order polynomial
Month	12 categories
DFO locality	Fishing locality areas identified by Rutherford (1995) (includes a final aggregated category) (Table C.1)
Latitude	Latitude aggregated by 0.1° bands starting at 48°N (includes a final aggregated category) (Table C.1)
Vessel	See Table C.2 for number of categories by analysis (no final aggregated category) (Table C.2)
Depth	See Table C.1 for number of categories by analysis (no final aggregated category) (Table C.1)
PFMC major area	7 categories: PMFC areas 3C, 3D, 5A, 5B, 5C, 5D, 5E

Table C.4. Summary data for the BOR bottom trawl fishery in totBC (3CD5ABCDE) by year for the core data set (after applying all data filters and selection of core vessels).

Year	Number vessels[1]	Number trips[1]	Number tows[1]	Number records[1]	Number records[2]	% zero records[2]	Total catch (t)[1]	Total hours[1]	CPUE (kg/h) (Eq. C.1)
1996	106	789	3,594	3,594	18,928	81.0	216.1	7,457	29.0
1997	82	670	3,468	3,468	14,822	76.6	193.3	7,342	26.3
1998	64	668	3,531	3,531	14,911	76.3	214.3	7,620	28.1
1999	56	654	3,328	3,328	14,521	77.1	162.9	7,177	22.7
2000	55	672	3,641	3,641	15,452	76.4	225.8	7,353	30.7
2001	57	713	3,653	3,653	13,810	73.5	220.5	7,040	31.3
2002	50	701	3,672	3,672	14,722	75.1	234.1	7,501	31.2
2003	48	695	3,362	3,362	13,346	74.8	178.9	6,708	26.7
2004	48	632	2,602	2,602	13,024	80.0	127.8	4,913	26.0
2005	48	729	3,083	3,083	13,419	77.0	111.5	6,106	18.3
2006	42	590	2,292	2,292	11,218	79.6	87.4	4,688	18.6
2007	43	491	2,258	2,258	10,348	78.2	99.6	4,620	21.6
2008	39	460	2,013	2,013	8,794	77.1	74.0	3,897	19.0
2009	40	498	2,356	2,356	10,035	76.5	80.5	4,526	17.8
2010	39	435	1,919	1,919	9,283	79.3	67.5	3,873	17.4
2011	36	380	1,564	1,564	9,325	83.2	61.8	3,190	19.4
2012	34	353	1,520	1,520	8,218	81.5	63.5	3,024	21.0
2013	32	315	1,025	1,025	8,095	87.3	40.8	1,937	21.1
2014	32	311	1,061	1,061	7,318	85.5	39.1	2,065	19.0
2015	31	307	988	988	7,511	86.8	29.6	1,906	15.5
2016	27	272	941	941	6,653	85.9	22.5	1,902	11.9
2017	29	289	938	938	6,739	86.1	29.9	1,917	15.6
2018	25	236	1,082	1,082	5,423	80.0	49.4	2,092	23.6

[1] calculated for tows with BOR catch >0; [2] calculated for all tows

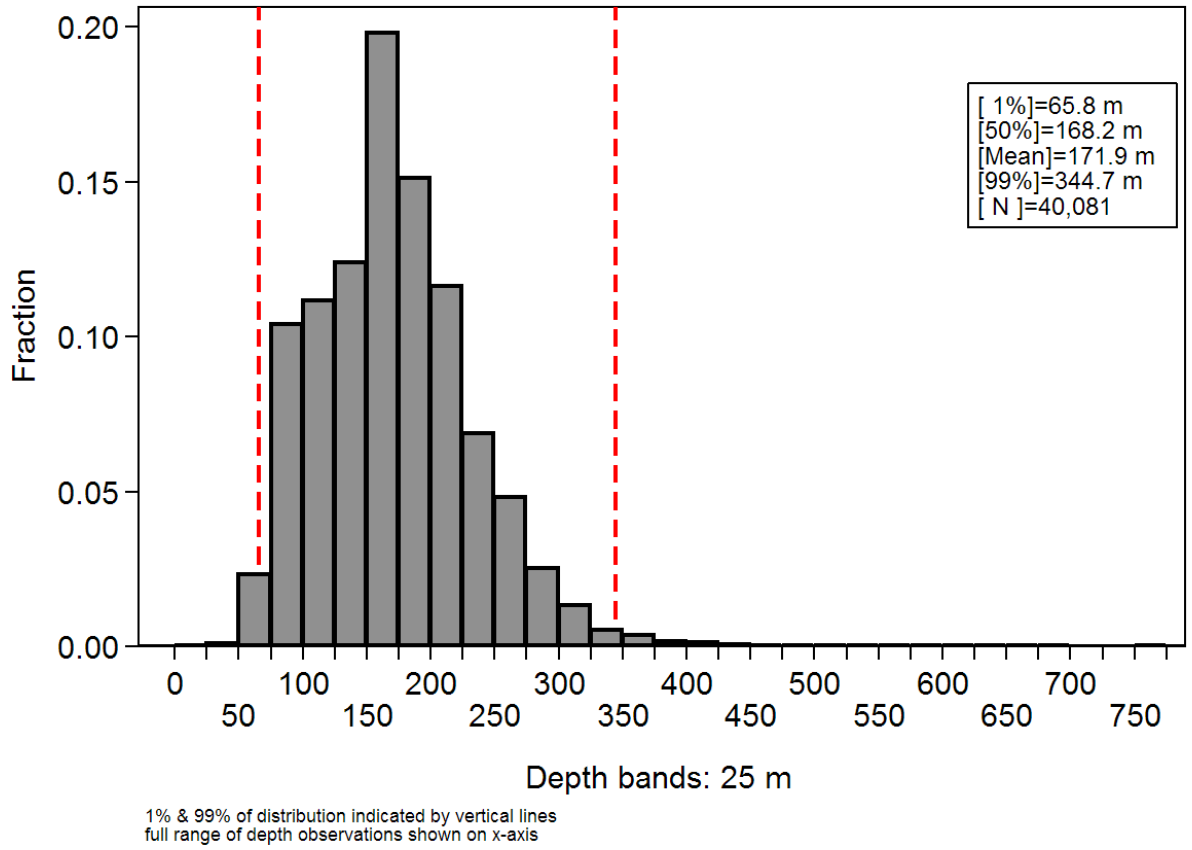

Figure C.1. Depth distribution of tows capturing BOR for the totBC (3CD5ABCDE) bottom trawl (BT) GLM analyses from 1996 to 2018 using 25 m intervals (each bin is labelled with the upper bound of the interval). Vertical lines indicate the 1% and 99% percentiles.

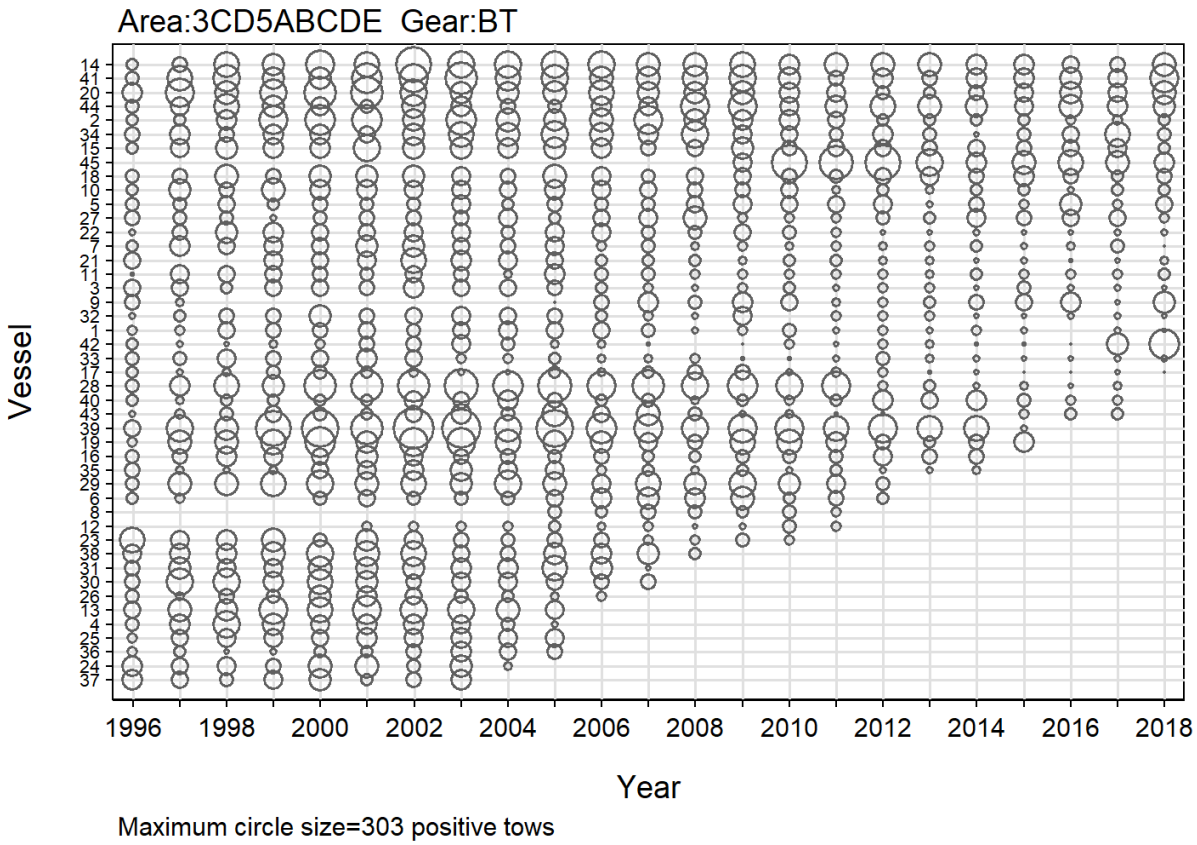

Figure C.2. Bubble plot showing vessel participation (number positive tows) by the core fleet in the totBC (3CD5ABCDE) BT GLM analyses. Vessels are coded in ascending order total effort by year.

C.4. RESULTS

C.4.1. totBC (3CD5ABCDE)

C.4.1.1. Bottom trawl fishery: positive lognormal model

A standardised lognormal General Linear Model (GLM) analysis was performed on positive catch records from the bottom trawl tow-by-tow data set generated as described in Section C.3. Eight explanatory variables (described in Section C.3 above) were offered to the model and ln(catch) was used as the dependent variable, where catch is the total by weight of landed plus discarded BOR in each record (tow) (Eq. C.3). The resulting CPUE index series is presented in Figure C.3.

The `[Year]` categorical variable was forced as the first variable in the model without regard to its effect on the model deviance. The remaining seven variables were offered sequentially, with a stepwise acceptance of the remaining variables with the best AIC. This process was continued until the improvement in the model R^2 was less than 1% (Table C.5). This model selected four of the seven remaining explanatory variables, including `[Vessel]`, `[DFO locality]`, `[0.1°Latitude_bands]` and `[Month]` in addition to `[Year]`. The final lognormal model accounted for 14% of the total model deviance (Table C.5), with the year variable explaining about 4% of the model deviance.

Model residuals showed a satisfactory fit to the underlying lognormal distributional assumption, with some skewness in the body of the distribution and deviations in the tails outside of +/- 2 standard errors (Figure C.4).

A stepwise plot showing the effect on the year indices as each explanatory variable was introduced into the model shows that the standardisation procedure made some relatively small upward adjustments to the unstandardised series at the beginning of the series and corresponding downward adjustments after 2009, resulting in a relatively smooth annual trend (Figure C.5).

*Table C.5. Order of acceptance of variables into the lognormal model of positive total mortalities (verified landings plus discards) of BOR totBC (3CD5ABCDE) bottom trawl fishery with the amount of explained deviance (R^2) for each variable. Variables accepted into the model are identified in bold with an *. Year was forced as the first variable.*

Variable	1	2	3	4	5	6
Year*	**0.0414**	-	-	-	-	-
Vessel*	0.0351	**0.0816**	-	-	-	-
DFO locality*	0.0279	0.0767	**0.1107**	-	-	-
0.1° Latitude bands*	0.0342	0.0790	0.1111	**0.1249**	-	-
Month*	0.0187	0.0580	0.0940	0.1229	**0.1376**	-
Hours fished	0.0155	0.0586	0.0970	0.1198	0.1335	0.1460
Depth bands*	0.0038	0.0445	0.0827	0.1114	0.1254	0.1382
PFMC major area	0.0151	0.0627	0.0960	0.1184	0.1308	0.1445
Improvement in deviance	0	0.0403	0.0290	0.0142	0.0127	0.0084

CDI plots of the four explanatory variables introduced to the model in addition to `[Year]` show relatively minor standardisation effects in the series. Most of the adjustment to the unstandardised series shown in Figure C.5 occurred with the addition of the variable `[Vessel]`. This is because there is a trend in this variable, with vessels having the lowest catching power leaving the fishery (Figure C.6) which results in the slight steepening of the series described above. The remaining three explanatory variables (`[DFO_locality]` (Figure C.7), `[0.1°Latitude_bands]` (Figure C.8) and `[Month]` (Figure C.9)) had little impact on the overall series.

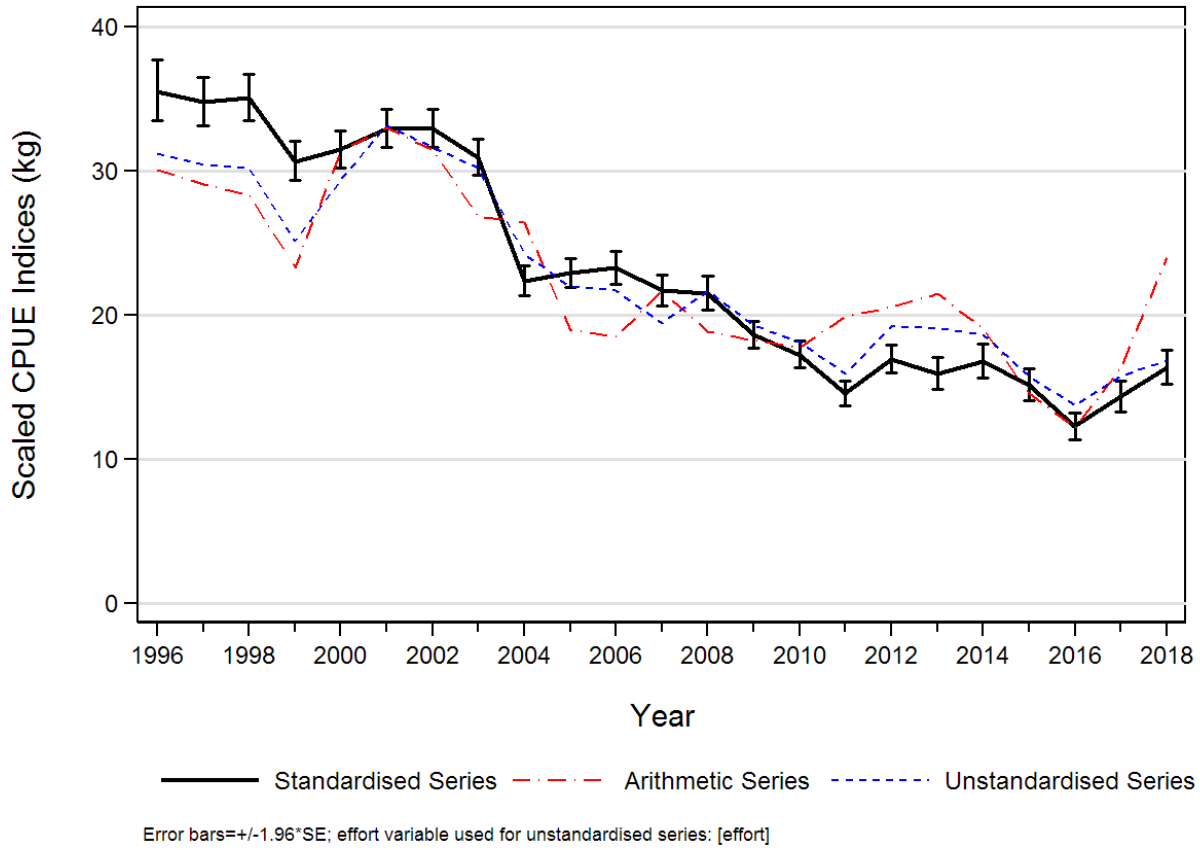

Figure C.3. Three positive catch CPUE series for BOR from 1996 to 2018 in the totBC (3CD5ABCDE) bottom trawl fishery. The solid line is the standardised CPUE series from the lognormal model (Eq. C.3). The arithmetic series (Eq. C.1) and the unstandardised series (Eq. C.2) are also presented. All three series have been scaled to same geometric mean.

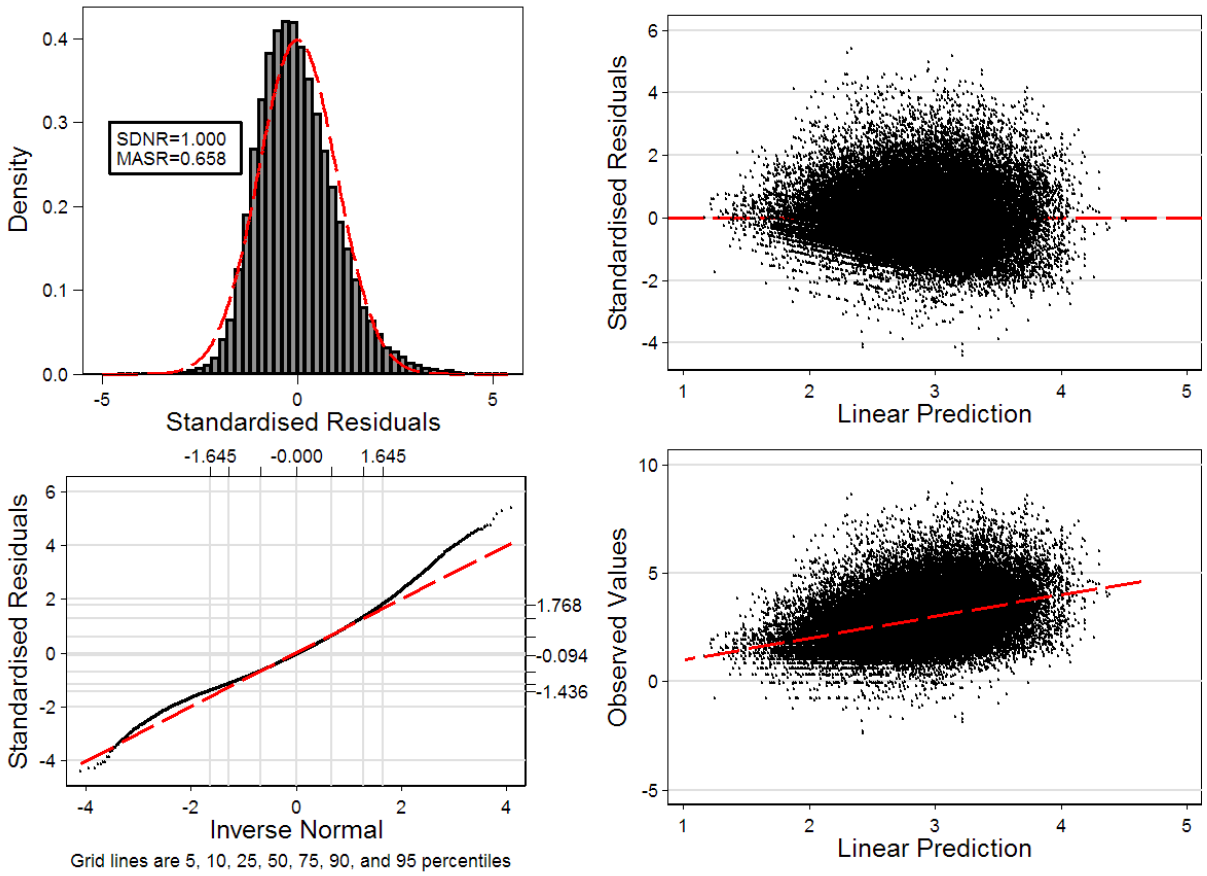

Figure C.4. Residual diagnostic plots for the GLM lognormal analysis for BOR in totBC (3CD5ABCDE) bottom trawl fishery. Upper left: histogram of the standardised residuals with overlaid lognormal distribution (SDNR = standard deviation of normalised residuals. MASR = median of absolute standardised residuals). Lower left: Q-Q plot of the standardised residuals with the outside horizontal and vertical lines representing the 5th and 95th percentiles of the theoretical and observed distributions. Upper right: standardised residuals plotted against the predicted CPUE. Lower right: observed CPUE plotted against the predicted CPUE.

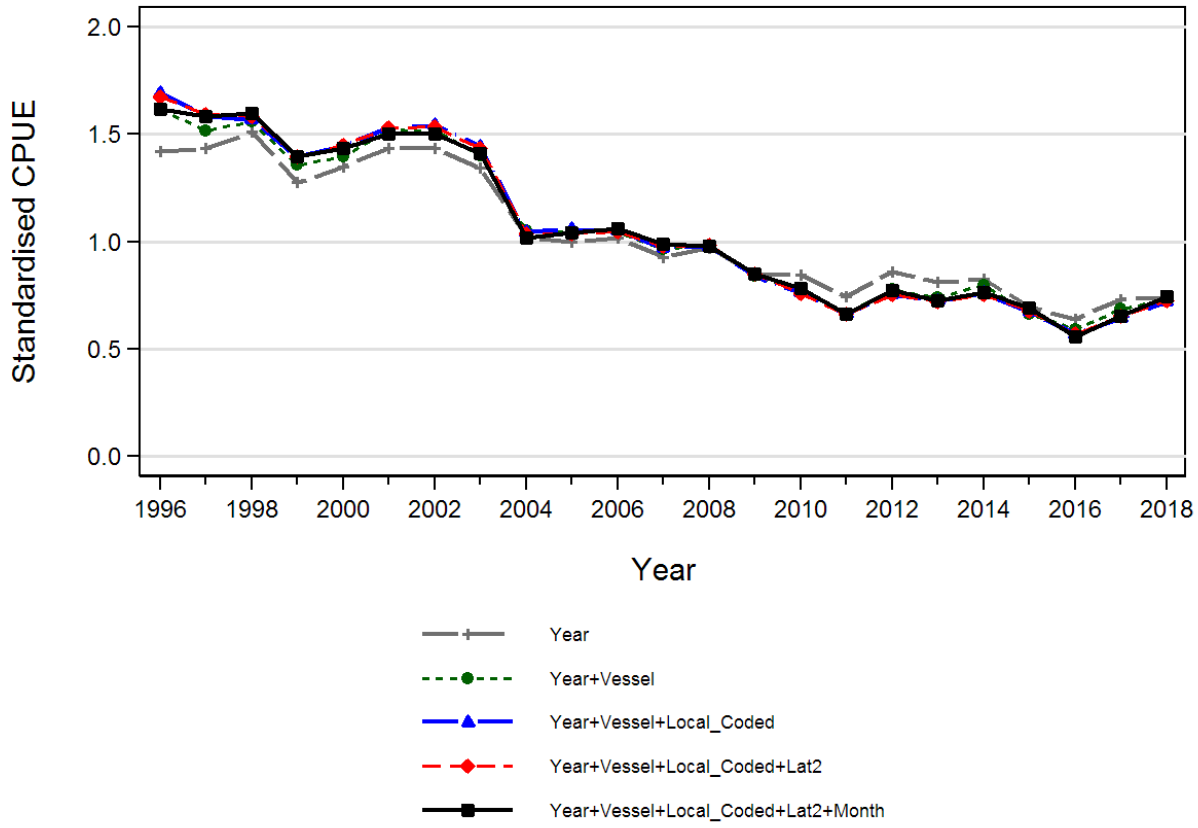

Figure C.5. Plot showing the year coefficients after adding each successive term of the standardised lognormal regression analysis for BOR in the totBC (3CD5ABCDE) bottom trawl fishery. The final model is shown with a thick solid black line. Each line has been scaled so that the geometric mean equals 1.0.

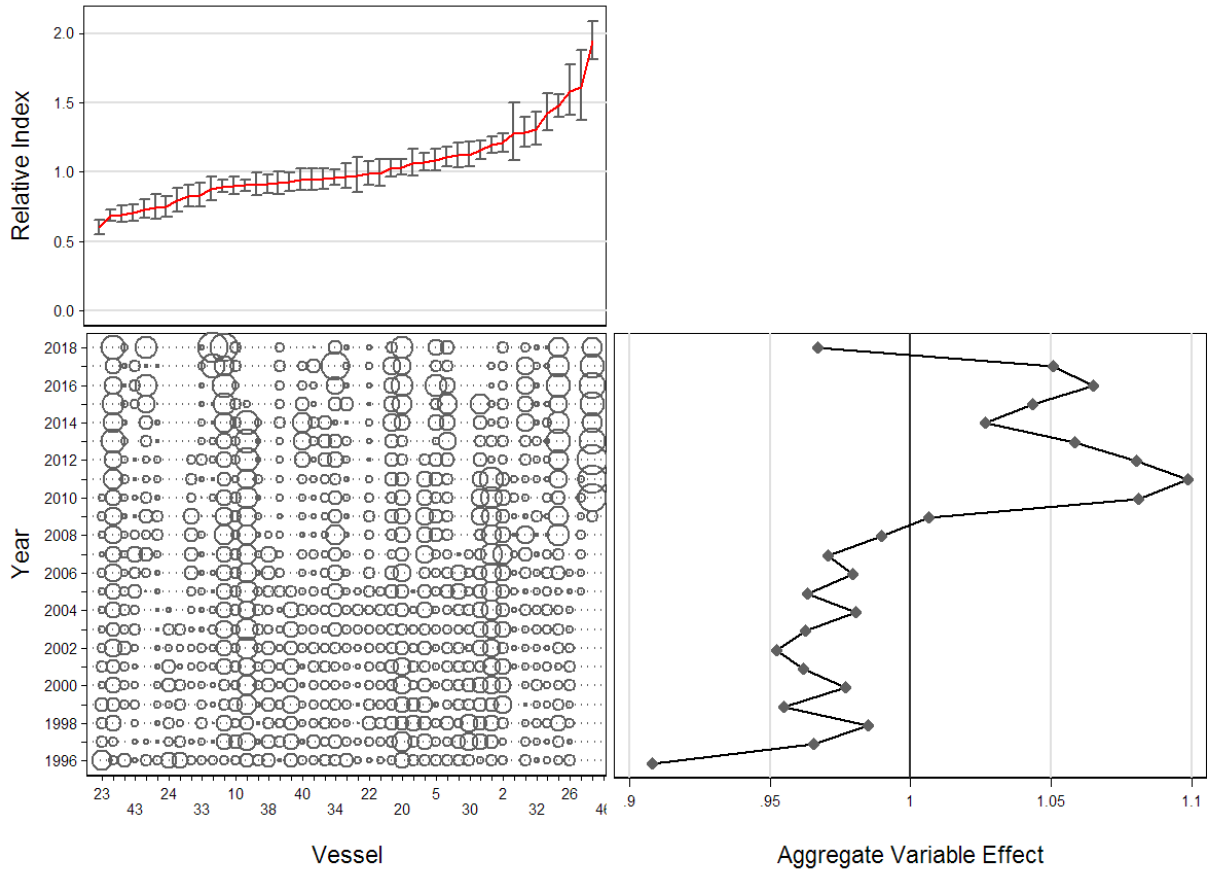

Figure C.6. CDI plot showing the effect of introducing the categorical variable [`Vessel`] to the lognormal regression model for BOR in the totBC (3CD5ABCDE) bottom trawl fishery. Each plot consists of subplots showing the effect by level of variable (top left), the relative distribution by year of variable records (bottom left), and the cumulative effect of variable by year (bottom right).

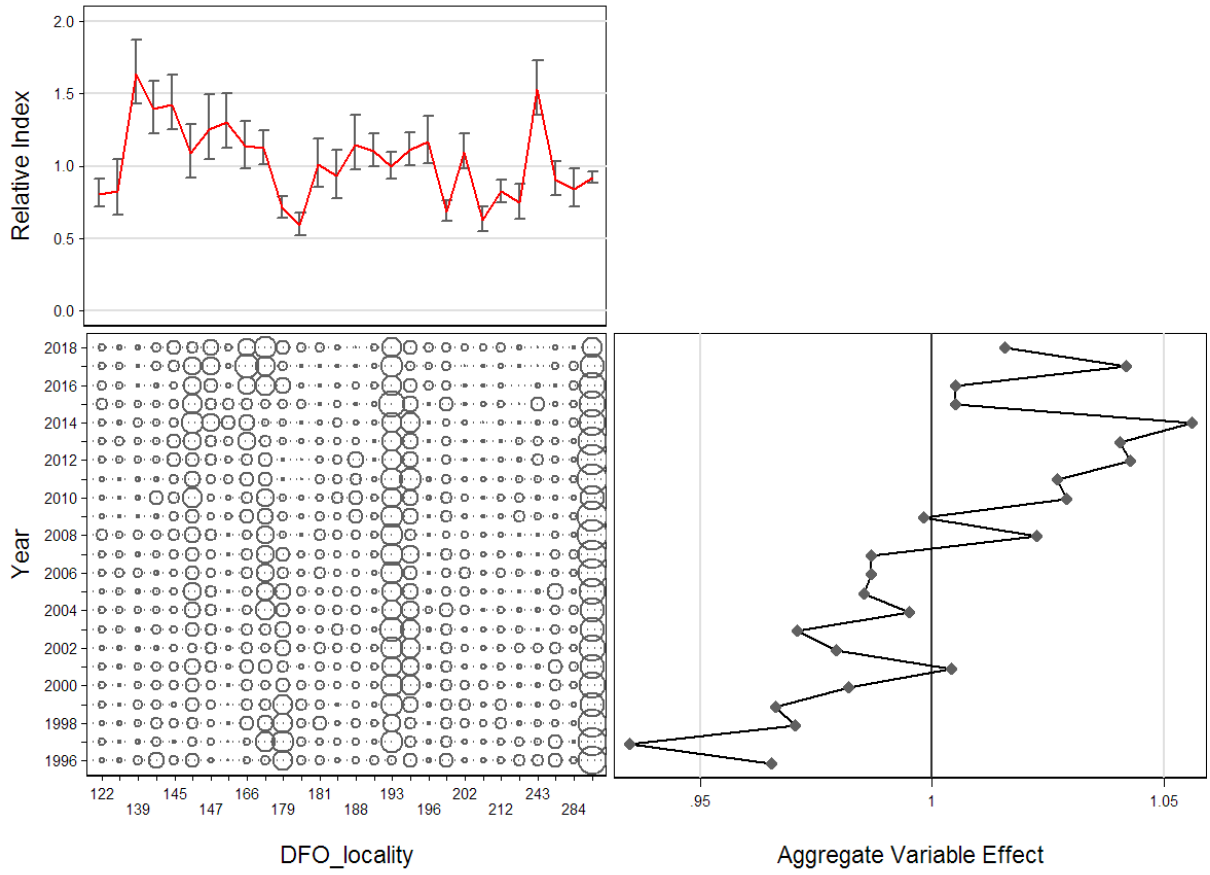

Figure C.7. CDI plot showing the effect of introducing the categorical variable [`DFO locality`] to the lognormal regression model for BOR in the totBC (3CD5ABCDE) bottom trawl fishery. Table C.6 provides the definitions for the coded values used for each locality in the above plot. Each plot consists of subplots showing the effect by level of variable (top left), the relative distribution by year of variable records (bottom left), and the cumulative effect of variable by year (bottom right).

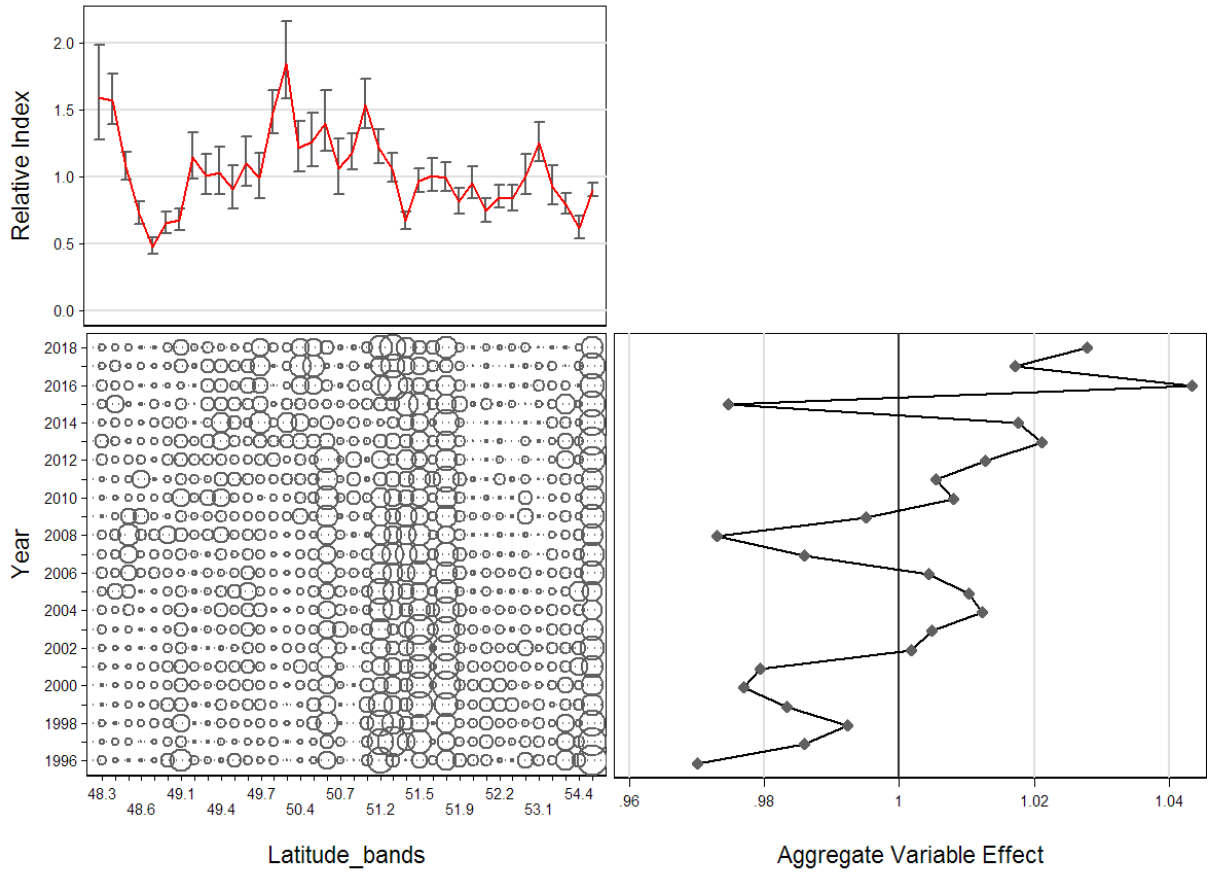

Figure C.8. CDI plot showing the effect of introducing the categorical variable [`Latitude bands`] to the lognormal regression model for BOR in the totBC (3CD5ABCDE) bottom trawl fishery. Each plot consists of subplots showing the effect by level of variable (top left), the relative distribution by year of variable records (bottom left), and the cumulative effect of variable by year (bottom right).

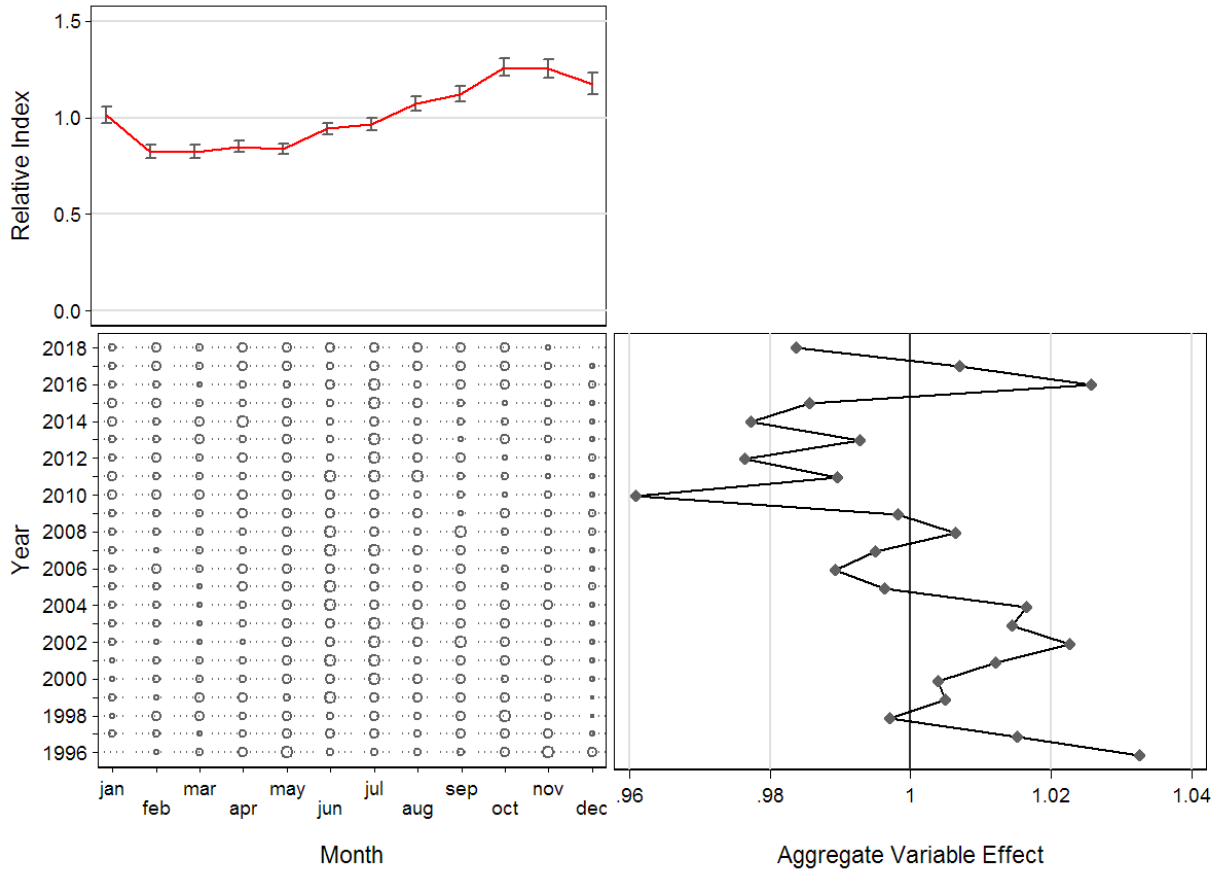

Figure C.9. CDI plot showing the effect of introducing the categorical variable [`Month`] to the lognormal regression model for BOR in the totBC (3CD5ABCDE) bottom trawl fishery. Each plot consists of subplots showing the effect by level of variable (top left), the relative distribution by year of variable records (bottom left), and the cumulative effect of variable by year (bottom right).

The lognormal year indices show a declining trend from the beginning of the series to 2016, with a possible upturn in the final two years of the series (Figure C.3). This model has reasonable diagnostics and shows only small changes from the unstandardised series.

*Table **C**.6. Definition of locality codes used in Figure C.7.*

Code	PFMC Major	DFO Minor	Minor Name	Locality Name	Lognormal Index
122	3C	23	Big Bank	Deep Big Bank/Barkley Canyon	0.806
125	3C	23	Big Bank	Nitinat Canyon	0.830
139	3C	24	Clayoquot Sd.	Clayoquot Canyon	1.636
140	3C	24	Clayoquot Sd.	South Estevan	1.394
145	3D	25	Estevan-Esperanza Inlet	North Estevan	1.427
146	3D	25	Estevan-Esperanza Inlet	Nootka	1.091
147	3D	25	Estevan-Esperanza Inlet	Esperanza East	1.251
165	3D	27	Quatsino Sd.	West Cape Cook	1.301
166	3D	27	Quatsino Sd.	Quatsino Sound	1.136
178	5A	11	Cape Scott-Triangle	Triangle	1.123
179	5A	11	Cape Scott-Triangle	Cape Scott Spit	0.709
180	5A	11	Cape Scott-Triangle	Mexicana	0.594
181	5A	11	Cape Scott-Triangle	Topknot	1.008
183	5A	11	Cape Scott-Triangle	South Scott Islands	0.931

Code	PFMC Major	DFO Minor	Minor Name	Locality Name	Lognormal Index
188	5A	11	Cape Scott-Triangle	Pisces Canyon	1.149
192	5B	8	Goose Island Bank	NE Goose	1.105
193	5B	8	Goose Island Bank	SE Goose	0.999
195	5B	8	Goose Island Bank	SW Goose	1.112
196	5B	8	Goose Island Bank	Mitchell's Gully	1.171
197	5B	8	Goose Island Bank	SE Cape St. James	0.685
202	5B	8	Goose Island Bank	SW Middle Bank	1.097
203	5B	8	Goose Island Bank	Outside Cape St. James	0.627
212	5C	2	2B-East	South Morseby	0.825
229	5C	6	5-Lower-SE Hecate Strait	East Horseshoe	0.745
243	5D	3	1 East-Dixon Entrance	McIntyre Bay	1.531
251	5D	4	4-Two Peaks-Dundas Is.	Two Peaks	0.907
284	5E	31	2A West - Rennell Sound	South Hogback	0.842

C.4.1.2. Bottom trawl fishery: binomial logit model

The same explanatory variables used in the lognormal model were offered sequentially to this model, beginning with the year categorical variable, until the improvement in the model R^2 was less than 1% (Table C.7). A binary variable which equalled 1 for positive catch tows and 0 for zero catch tows was used as the dependent variable. The final binomial model accounted for 13.5% of the total model deviance, with the year variable explaining about 1% of the model deviance.

*Table C.7. Order of acceptance of variables into the binomial model of presence/absence of verified landings plus discards of BOR in totBC (3CD5ABCDE) bottom trawl fishery with the amount of explained deviance (R^2) for each variable. Variables accepted into the model are marked in bold with an *. Year was forced as the first variable.*

Variable	1	2	3	4	5
Year*	**0.0105**	-	-	-	-
0.1° Latitude bands*	0.0711	**0.0818**	-	-	-
Depth bands*	0.0657	0.0771	**0.1233**	-	-
Vessel*	0.0383	0.0495	0.0930	**0.1348**	-
DFO locality	0.0627	0.0752	0.0969	0.1330	0.1443
Hours fished	0.0009	0.0114	0.0820	0.1243	0.1352
Month	0.0039	0.0143	0.0863	0.1271	0.1378
PFMC major area	0.0606	0.0722	0.0891	0.1330	0.1431
Improvement in deviance	0.0000	0.0713	0.0415	0.0115	0.0095

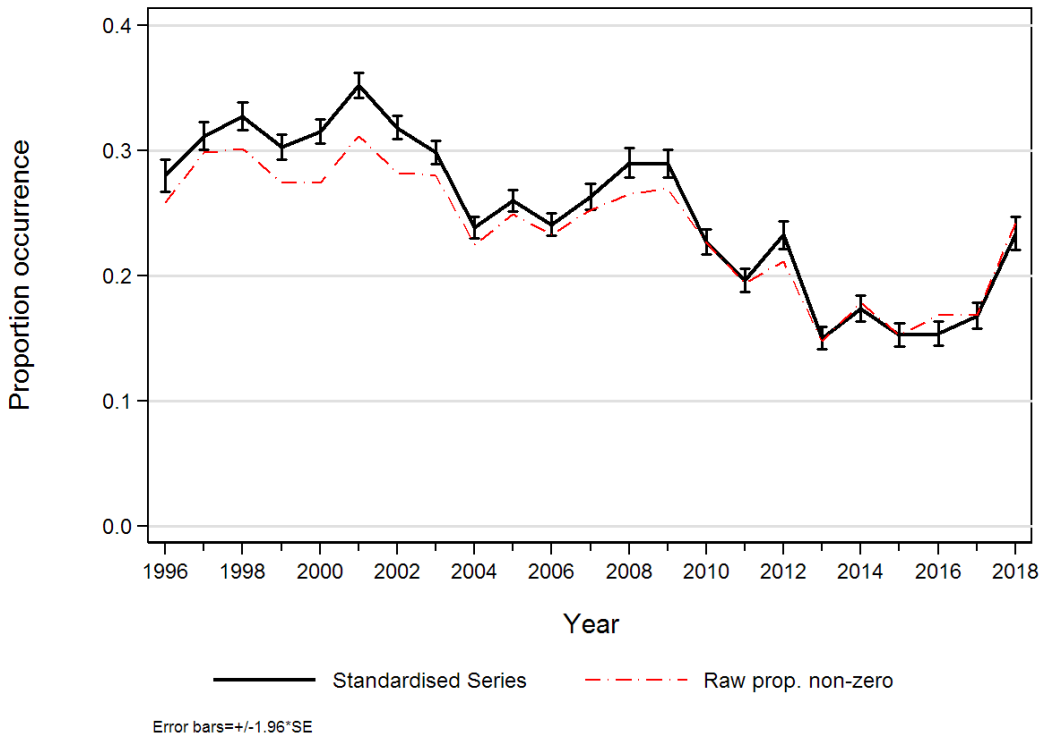

Figure C.10. Binomial index series for the totBC (3CD5ABCDE) bottom trawl fishery also showing the trend in proportion of zero tows from the same data set.

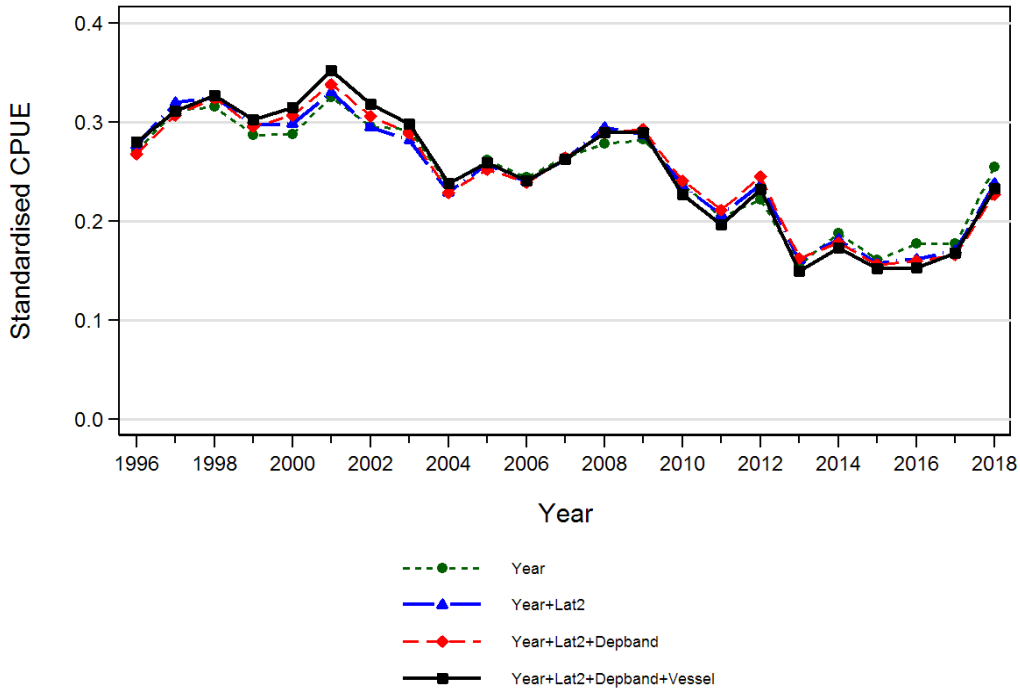

Figure C.11. Plot showing the year coefficients after adding each successive term of the standardised binomial regression analysis for BOR in the totBC (3CD5ABCDE) bottom trawl fishery. The final model is shown with a thick solid black line. Each line has been scaled so that the geometric mean equals 1.0.

The selected explanatory variables included [0.1°Latitude_bands], [Depth_bands] and [Vessel], in addition to [Year]. This model shows a trend similar to the lognormal model, generally declining towards the mid-2010s and then increasing in the final year (Figure C.10). there are regions of relatively little change at the beginning of the series and in the mid-2010s. A stepwise plot (Figure C.11) showing the effect of adding each successive explanatory variable indicates that there were only minor changes effected by the binomial standardisation, with the unstandardised "occurrence" function appearing similar to the standardised binomial series (Figure C.10).

The effect of the standardisation is to steepen the series. The addition of the [0.1°Latitude_bands] (Figure C.12), [Depth_bands] (Figure C.13) and the [Vessel] (Figure C.14) variables is to successively lift the early portion of the series and to drop the remaining portion. None of the three variables show trends in the data over time.

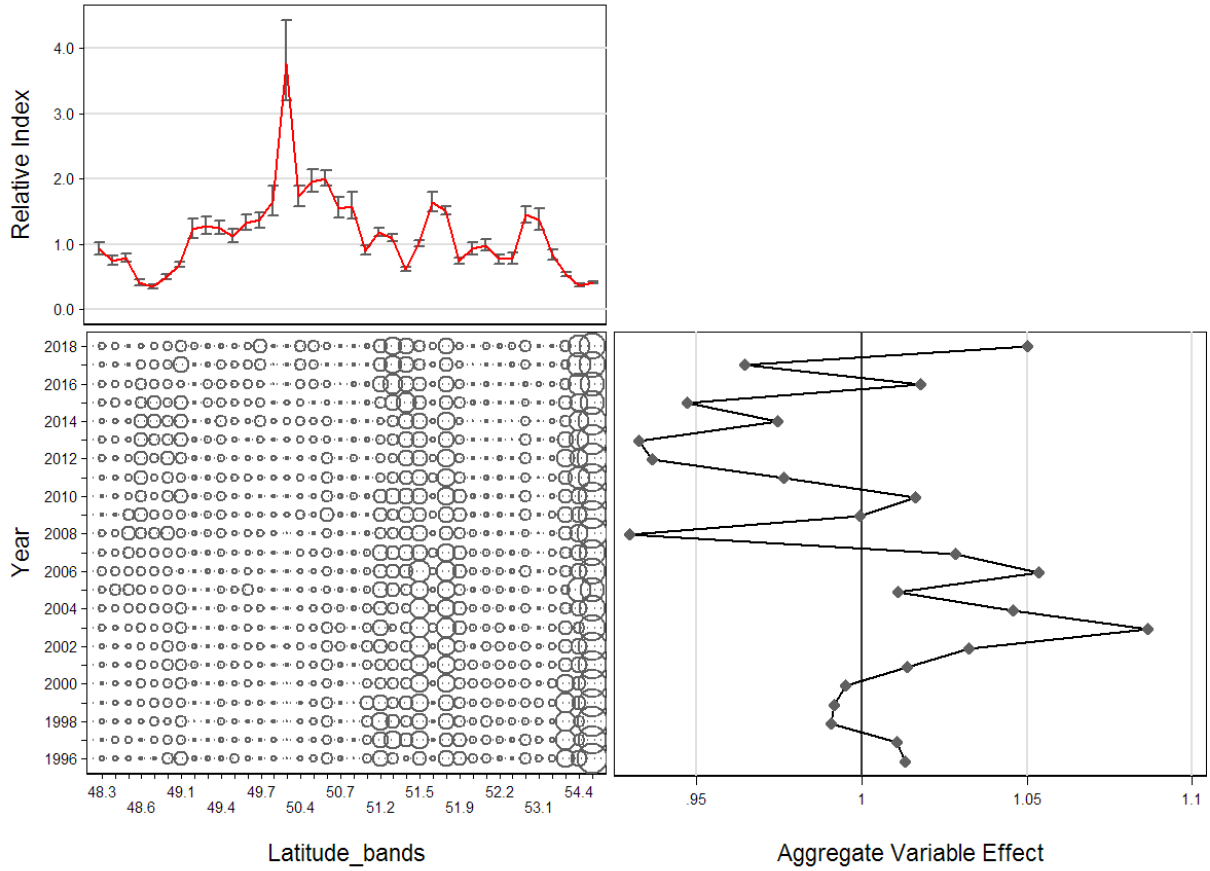

Figure C.12. CDI plot showing the effect of introducing the categorical variable [Latitude bands] to the binomial regression model for BOR in the totBC (3CD5ABCDE) bottom trawl fishery. Each plot consists of subplots showing the effect by level of variable (top left), the relative distribution by year of variable records (bottom left), and the cumulative effect of variable by year (bottom right).

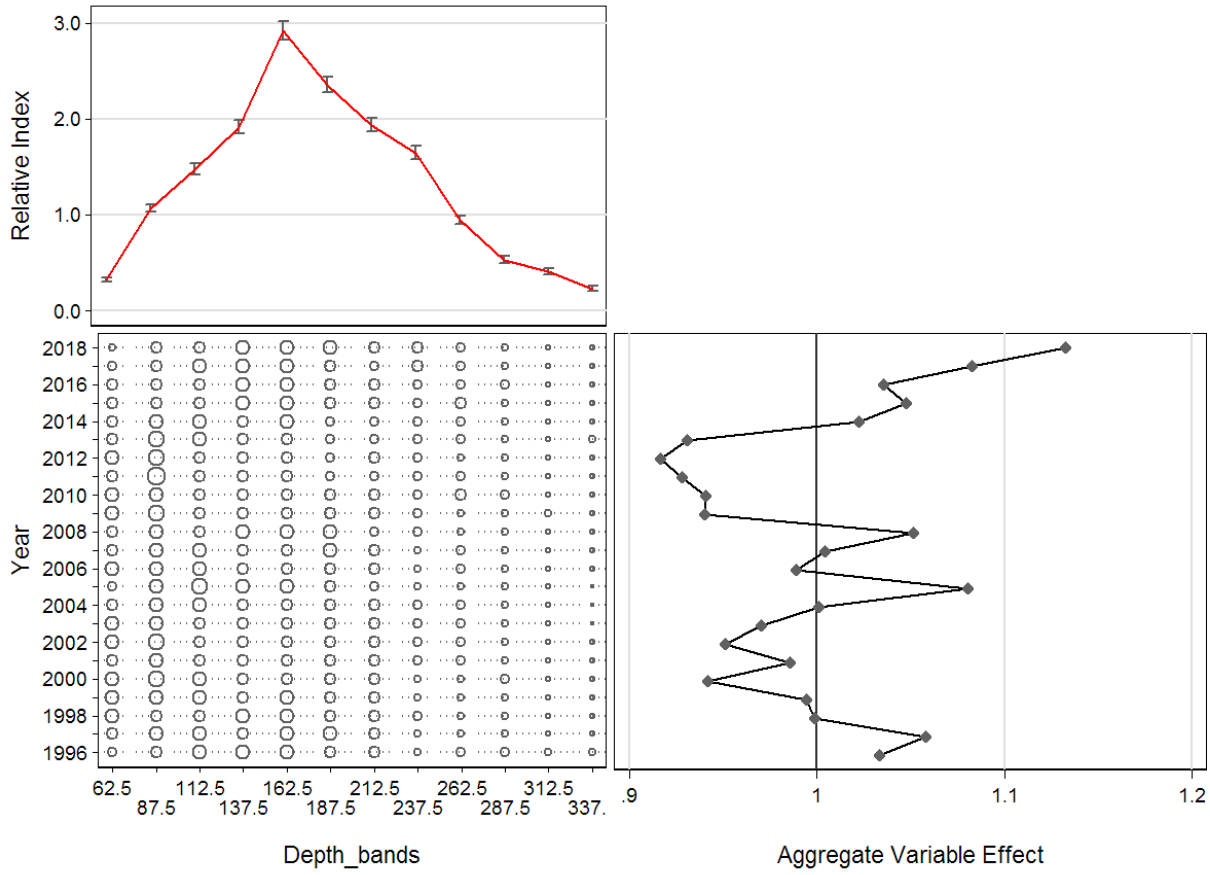

Figure C.13. CDI plot showing the effect of introducing the categorical variable [`Depth bands`] to the binomial regression model for BOR in the totBC (3CD5ABCDE) bottom trawl fishery. Each plot consists of subplots showing the effect by level of variable (top left), the relative distribution by year of variable records (bottom left), and the cumulative effect of variable by year (bottom right).

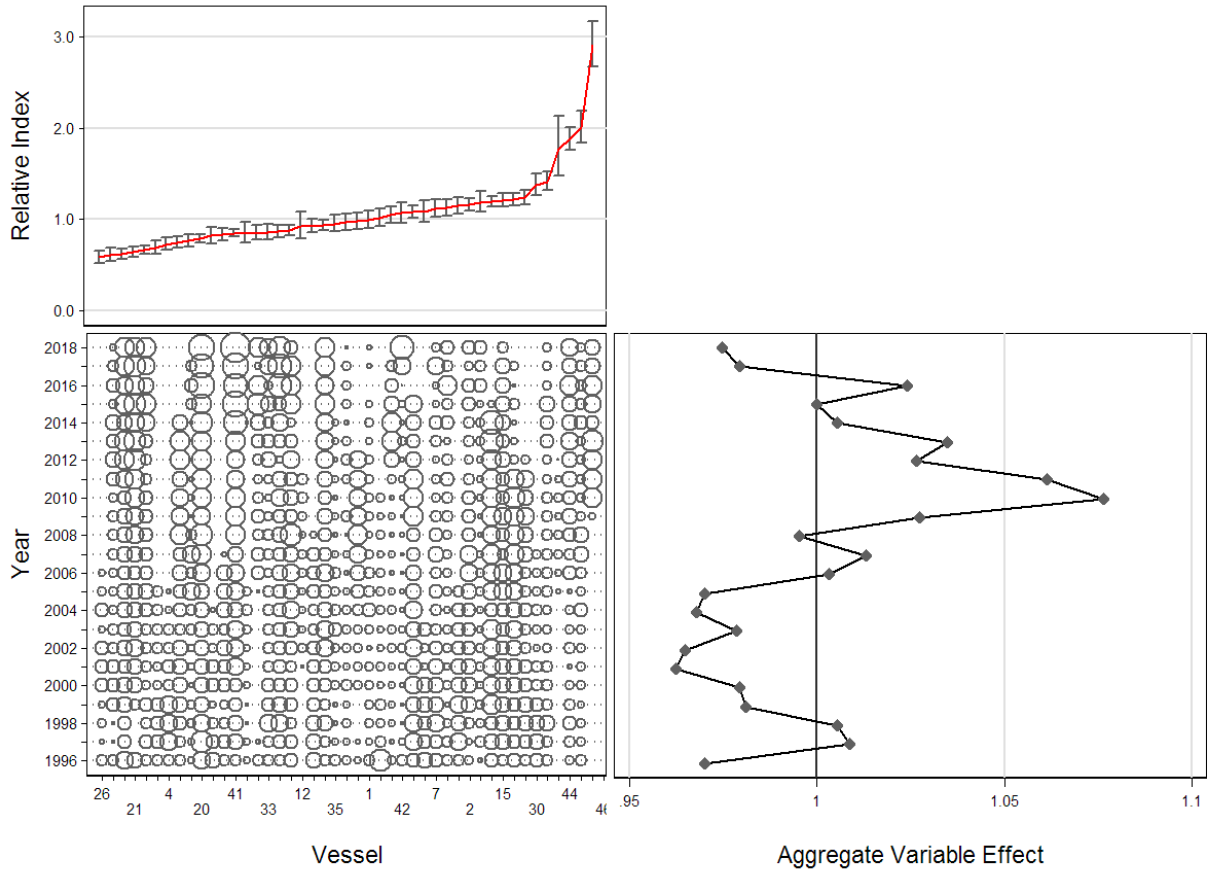

Figure C.14. CDI plot showing the effect of introducing the categorical variable [`Vessel`] to the binomial regression model for BOR in the totBC (3CD5ABCDE) bottom trawl fishery. Each plot consists of subplots showing the effect by level of variable (top left), the relative distribution of variable records by year (bottom left), and the cumulative effect of variable by year (bottom right).

C.4.1.3. Bottom trawl fishery: combined model

While the lognormal and binomial models show similar overall declining trends over the majority of the period, the multiplicative nature of the combined model equation (Eq. C.4) results in a stronger declining trend over the entire series to 2016, followed by a small increase in the final two years of the series (Figure C.15).

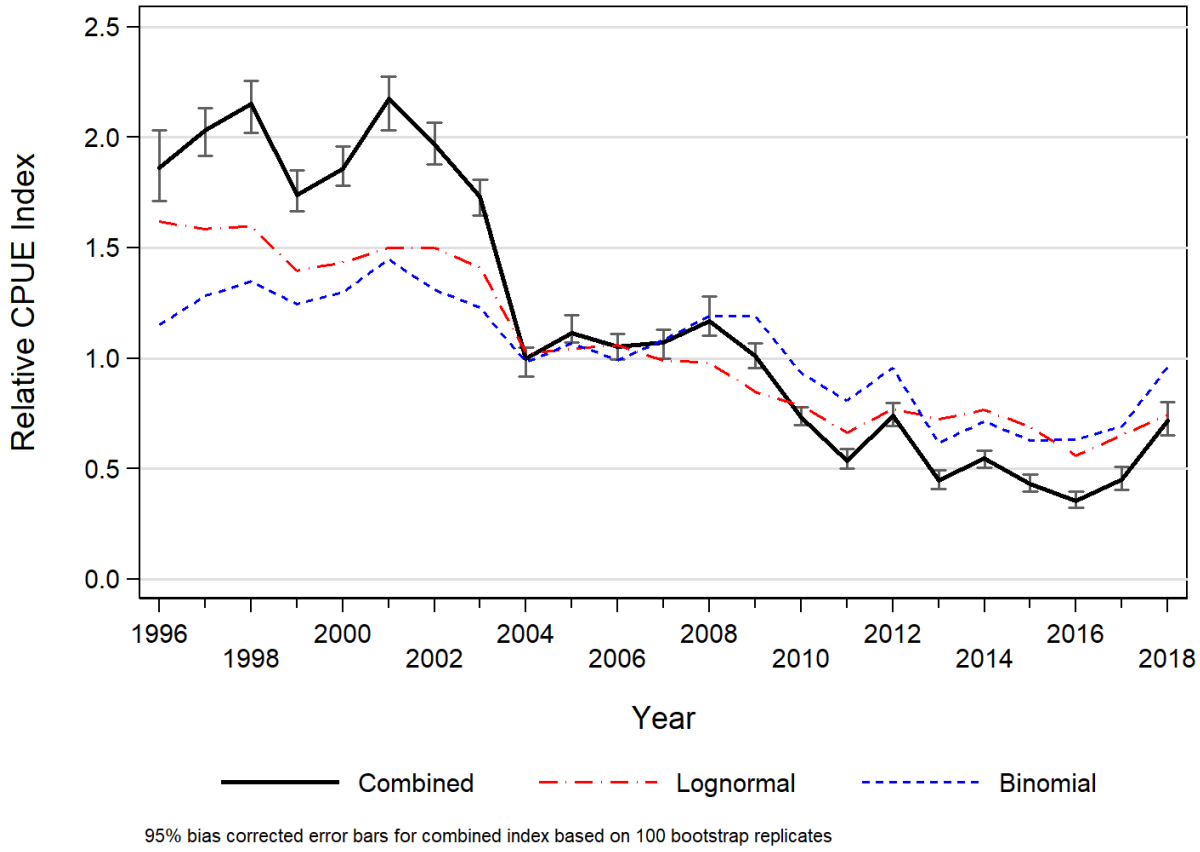

Figure C.15. Combined index series (Eq. C.4) for the totBC (3CD5ABCDE) bottom trawl fishery also showing the contributing lognormal and binomial index series. Confidence bounds based on 100 bootstrap replicates.

C.5. RELATIVE INDICES OF ABUNDANCE

Table C.8 summarises the suite of relative abundance indices and associated standard errors derived from this BOR CPUE analysis. The CPUE indices used in the age-structured stock assessment model appear as the delta-lognormal (combined) indices from the bottom trawl data (Figure C.15, Table C.8). The associated bootstrap standard errors (SE) were used as the initial CVs when fitting the stock assessment model. Only the indices up to 2012 were used in the stock assessment model because the indices were deemed by the BOR Technical Working Group to have become unreliable beginning in 2013 with the strong management measures introduced to reduce the catch of BOR, resulting in likely avoidance behaviour by fishers.

Table C.8. Relative indices of annual CPUE from the arithmetic, unstandardised, lognormal models of non-zero bottom trawl catches of BOR in totBC (3CD5ABCDE). Also shown are the indices from the binomial model of presence/absence in this fishery and the combined delta-lognormal model (Eq. C.4). All indices are scaled so that their geometric means equal 1.0. Upper and lower 95% analytic confidence bounds and associated standard error (SE) are presented for the lognormal model, while bootstrapped (100 replicates) upper and lower 95% confidence bounds and the associated SE are presented for the combined model.

	Arithmetic	Geometric	Lognormal (Eq. C.3)				Binomial	Combined (Eq. C.4)			
Year	Index (Eq. C.1)	Index (Eq. C.2)	Index	Lower bound	Upper bound	SE	Index (Eq. C.3)	Index	Lower bound	Upper bound	SE
1996	1.369	1.420	1.619	1.525	1.718	0.0304	1.151	1.864	1.712	2.033	0.0883
1997	1.324	1.387	1.585	1.510	1.663	0.0247	1.282	2.032	1.916	2.132	0.0607
1998	1.292	1.377	1.598	1.527	1.671	0.0230	1.348	2.153	2.022	2.256	0.0606
1999	1.062	1.145	1.397	1.337	1.460	0.0225	1.246	1.740	1.664	1.851	0.0483
2000	1.428	1.339	1.434	1.377	1.493	0.0208	1.297	1.860	1.782	1.959	0.0456
2001	1.503	1.511	1.500	1.440	1.563	0.0209	1.449	2.174	2.032	2.276	0.0616
2002	1.433	1.441	1.501	1.443	1.561	0.0202	1.310	1.965	1.879	2.068	0.0514
2003	1.223	1.376	1.410	1.354	1.469	0.0208	1.229	1.733	1.647	1.808	0.0419
2004	1.203	1.105	1.019	0.973	1.067	0.0235	0.981	1.000	0.918	1.047	0.0305
2005	0.863	1.001	1.043	0.999	1.089	0.0221	1.069	1.115	1.070	1.196	0.0281
2006	0.841	0.988	1.059	1.010	1.112	0.0246	0.992	1.051	0.994	1.112	0.0290
2007	0.987	0.884	0.988	0.940	1.038	0.0254	1.083	1.070	0.999	1.130	0.0331
2008	0.859	0.987	0.979	0.928	1.033	0.0273	1.193	1.168	1.101	1.279	0.0409
2009	0.831	0.879	0.848	0.807	0.891	0.0255	1.191	1.010	0.957	1.068	0.0311
2010	0.807	0.826	0.785	0.743	0.829	0.0278	0.933	0.732	0.699	0.776	0.0208
2011	0.908	0.726	0.663	0.625	0.703	0.0300	0.807	0.535	0.502	0.589	0.0201
2012	0.936	0.875	0.771	0.727	0.818	0.0301	0.957	0.738	0.692	0.798	0.0280
2013	0.978	0.868	0.725	0.676	0.778	0.0360	0.616	0.447	0.407	0.493	0.0224
2014	0.868	0.850	0.765	0.713	0.820	0.0356	0.714	0.546	0.503	0.580	0.0219
2015	0.665	0.718	0.689	0.640	0.742	0.0378	0.627	0.432	0.395	0.472	0.0198
2016	0.554	0.625	0.557	0.517	0.600	0.0380	0.632	0.352	0.325	0.396	0.0157
2017	0.743	0.718	0.652	0.605	0.704	0.0385	0.690	0.451	0.402	0.506	0.0231
2018	1.093	0.767	0.744	0.693	0.800	0.0365	0.961	0.715	0.651	0.802	0.0383

C.6. REFERENCES – CPUE

Bentley, N., Kendrick, T.H., Starr, P.J., and Breen, P.A. 2012. Influence plots and metrics: tools for better understanding fisheries catch-per-unit-effort standardizations. ICES J. Mar. Sci. 69(1): 84-88.

Fletcher, D., Mackenzie, D. and Villouta, E. 2005. Modelling skewed data with many zeros: A simple approach combining ordinary and logistic regression. Environmental and Ecological Statistics12, 45–54.

Francis, R.I.C.C. 2001. Orange roughy CPUE on the South and East Chatham Rise. N.Z. Fish. Ass. Rep. 2001/26: 30 pp.

Quinn, T.R. and R.B. Deriso. 1999. Quantitative Fish Dynamics. Oxford University Press. 542 pp.

APPENDIX D. BIOLOGICAL DATA

This appendix describes analyses of Bocaccio (BOR) biological data from the British Columbia (BC) coast for the purposes of the derivation of the length-weight relationship, von Bertalanffy growth models, maturity schedule, and natural mortality for use in the BOR catch-at-age stock assessment model (see Sections D.1 and D.1.6). As well, these data were investigated for functional differences among areas as potential indicators of stock separation (Section D.3). All biological analyses are based on BOR data extracted from the Fisheries and Oceans Canada (DFO) Groundfish database GFBioSQL on 3 Oct 2019 (10,442 records). General data selection criteria for most analyses are summarised in Table D.1, although data selection can vary between analyses.

Table D.1. Data selection criteria for analyses of BOR biological data for allometric and growth analyses.

Field	Criterion	Notes
Trip type	`[trip_type] == c(2,3)`	Definition of research observations.
	`[trip_type] == c(1,4,5)`	Definition of commercial observations
Sample type	`[sample_type] == c(1,2,6,7,8)`	Only random or total samples.
Ageing method	`[agemeth] == c(3, 17) or ==(0 & [year]>=1980) or == 1 for ages 1:3`	Break & burn|bake method unknown from 1980 on (assumed B&B) surface readings for young fish
Species category code	`[SPECIES_CATEGORY_CODE]==1 (or 3)`	1 = Unsorted samples 3 = Sorted (keeper) samples
Sex code	`[sex] == c(1,2)`	Clearly identified sex (1=male or 2=female).
Area code	`[stock]z` select valid stock area (BC coast)	PMFC major area codes 3:9

Note that GFBioSQL data codes for `sex` (1=male, 2=female) are reversed in the catch-at-age model codes (1=female, 2=male).

D.1. LIFE HISTORY

D.1.1. Length-Weight

A log-linear relationship with additive errors was fit to females, males, and combined to all valid weight and length data pairs i, $\{W_{is}, L_{is}\}$:

Eq. D.1 $$\ln(W_{is}) = \alpha_s + \beta_s \ln(L_{is}) + \varepsilon_{is}, \quad \varepsilon \sim N(0, \sigma^2)$$

where α_s and β_s are the intercept and slope parameters, respectively, for each sex s (2 for females, 1 for males).

Commercial and research survey samples, regardless of gear type, were used independently to derive length-weight parameters for consideration in the model (Table D.2); however, only research/survey data coastwide were adopted for use (Figure D.1). In addition, fits to data from regional groups by PMFC area are reported, with only minor differences between areas evident. Commercial fishery data were not as abundant as those from research surveys (Figure D.2).

*Table D.2. Length-weight parameter estimates, standard errors (SE) and number of observations (n) for Bocaccio Rockfish (females, males and combined) for all commercial and survey samples, regardless of gear type from 1989 to 2018. W = specimen weight (kg), W_{pred} = predicted weight from fitted data set. (**S**): survey data; (**C**): commercial data,*

Area	Sex	*n*	ln(*a*)	SE ln(*a*)	*b*	SE *b*	mean W_i	SD W_i	min W_i	max W_i	mean W_{pred}
Coast (**S**)	F	1,226	-12.060	0.030	3.183	0.008	1.945	2.080	0.070	8.940	2.439
	M	1,841	-12.003	0.024	3.168	0.006	2.287	1.653	0.038	7.530	2.509
	F+M	3,075	-12.031	0.019	3.176	0.005	2.152	1.846	0.038	8.990	2.482
Coast (**C**)	F	164	-11.167	0.258	2.971	0.061	4.377	1.503	0.998	8.190	3.663
	M	264	-11.190	0.268	2.977	0.064	3.704	0.836	1.601	7.098	3.275
	F+M	428	-11.163	0.176	2.971	0.042	3.962	1.183	0.998	8.190	3.420
3CD (**S**)	F	491	-12.139	0.045	3.208	0.012	2.190	2.317	0.070	8.940	2.806
	M	798	-12.057	0.036	3.183	0.009	2.280	1.570	0.078	5.248	2.564
	F+M	1,293	-12.090	0.029	3.193	0.007	2.246	1.889	0.070	8.940	2.654
3CD (**C**)	F	17	-12.008	0.583	3.159	0.136	4.792	1.153	2.365	6.425	3.130
	M	32	-11.671	0.658	3.078	0.157	3.381	0.575	1.870	4.465	2.832
	F+M	49	-11.941	0.358	3.142	0.085	3.870	1.057	1.870	6.425	2.950
5ABC (**S**)	F	646	-11.988	0.048	3.161	0.013	1.558	1.627	0.090	8.530	1.823
	M	892	-11.951	0.036	3.154	0.009	2.092	1.620	0.038	7.530	2.179
	F+M	1,540	-11.975	0.029	3.159	0.007	1.867	1.643	0.038	8.530	2.029
5ABC (**C**)	F	96	-11.557	0.317	3.074	0.075	4.336	1.543	0.998	8.018	4.007
	M	181	-11.961	0.290	3.167	0.069	3.623	0.812	1.601	6.404	3.479
	F+M	276	-11.724	0.200	3.111	0.048	3.857	1.149	0.998	8.018	3.658
5DE (**S**)	F	87	-11.863	0.076	3.136	0.019	3.342	2.708	0.082	8.914	3.722
	M	150	-11.920	0.086	3.148	0.021	3.495	1.768	0.076	6.805	3.615
	F+M	237	-11.885	0.056	3.140	0.014	3.439	2.156	0.076	8.914	3.652
5DE (**C**)	F	51	-11.498	0.376	3.035	0.088	4.383	1.599	1.482	8.190	3.963
	M	51	-10.640	0.753	2.839	0.177	4.196	0.873	1.995	7.098	3.377
	F+M	102	-11.255	0.355	2.981	0.083	4.290	1.285	1.482	8.190	3.579

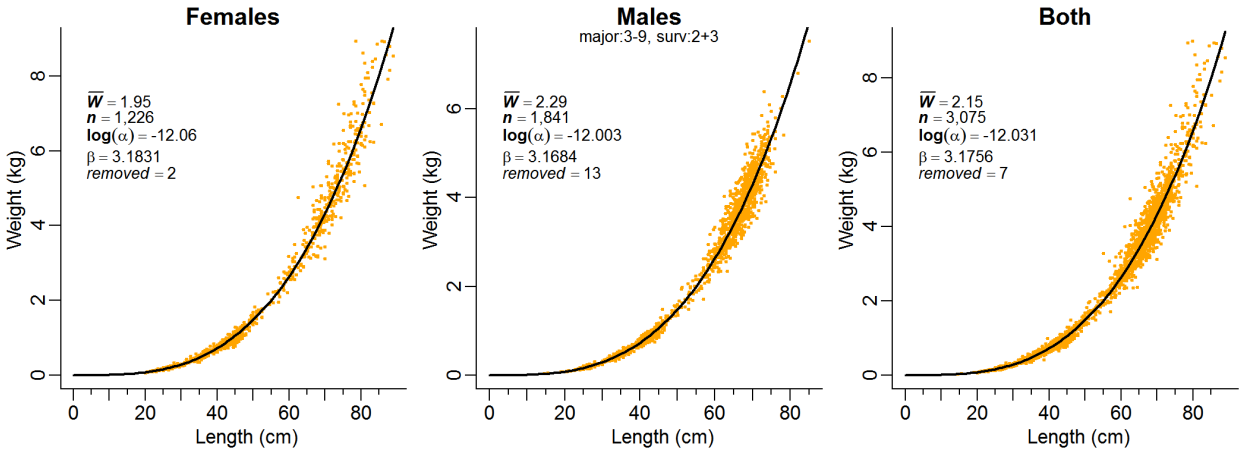

Figure D.1. Length-weight relationship for the coastwide stock of BOR derived from research survey samples. Records with absolute value of standardised residuals >3 (starting with a preliminary fit) were dropped, removing 2 observations before the final fit for females and 13 for males.

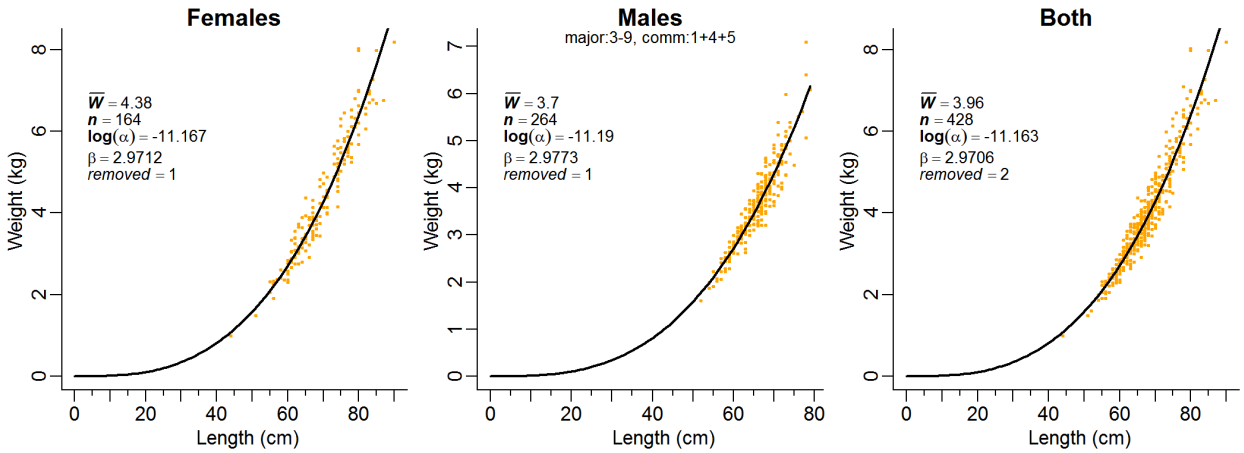

Figure D.2. Length-weight relationship for the coastwide stock of BOR derived from commercial fishing events, regardless of gear type. Records with absolute value of standardised residuals >3 (starting with a preliminary fit) were dropped, removing 1 observation before the final fit for females and males.

D.1.2. von Bertalanffy Growth

Otolith age data were equally split between surveys and commercial fishing; therefore, data from the survey were used in determining growth for the model, but both sources are presented here for comparison. Paired observations i of length and age by sex, $\{L_{is}, a_{is}\}$, for $s = 2,1$ (females, males) were selected from 4,024 specimens, 50 with surface-read otoliths and 3,970 using the break and burn (B&B) method (MacLellan 1997). Table D.3 summarises the availability of BOR otoliths.

Table D.3. Number of BOR specimen otoliths aged by break-and-burn and surface reading in GFBioSQL database (accessed 2019-10-03). Number of samples appear in parentheses and are not additive between the sexes (i.e., otoliths by sex usually come from the same sample). The 'Charter' samples are from research surveys conducted on a commercial vessel. These otoliths were collected over the period 2001 to 2019.

Trip Type	Activity	Age method	Female	Male	Unknown
Research	survey	surface read	23 (5)	27 (6)	---
Research	survey	break & burn	164 (66)	368 (147)	1 (1)
Charter	survey	unknown	2 (2)	2 (2)	---
Charter	survey	break & burn	562 (154)	809 (206)	1 (1)
Obs domestic	commercial	break & burn	687 (42)	1347 (42)	31 (1)

Growth was formulated as a von Bertalanffy model where lengths by sex, L_{is}, for fish $i = 1,\ldots,n_s$ are given by:

Eq. D.2 $$L_{is} = L_{\infty s}\left[1 - e^{-\kappa_s(a_{is} - t_{0s})}\right] + \varepsilon_{is}, \quad \varepsilon \sim N\left(0, \sigma^2\right)$$

where for each sex s,

$L_{\infty s}$ = the average length at maximum age of an individual,

κ_s = growth rate coefficient, and

t_{0s} = age at which the average size is zero.

The negative log likelihood for each sex s, used for minimisation is:

$$\ell\left(L_\infty, \kappa, t_0, \sigma\right) = n\ln\left(\sigma\right) + \frac{\sum_i^n \left(L_i - L_i\right)^2}{2\sigma^2}, \quad i = 1,\ldots,n$$

Fits to growth (Table D.4, Figure D.3) show that BOR females are larger than BOR males. Area-specific parameter estimates differ little between areas. Only the sex-specific coastwide parameters (L_∞, K, t_0) in Table D.4 were used in the population model. Regional growth fits are reported for comparison only.

Table D.4. Age-length parameter estimates for BOR (females, males, both combined) from von Bertalanffy growth model fits for survey and commercial samples, regardless of gear type, coastwide and regionally. The growth model used in sensitivity run S08 is defined in the first two lines of the table.

Area	Sex	*n*	L_∞(cm)	*K*	t_0 (cm)	σ
Coast: survey	Females	725	82.4	0.1134	-3.1	7.04
	Males	1,172	69.2	0.1536	-2.6	5.02
	Both	1,899	70.8	0.1601	-2.4	6.35
Coast: comm	Females	642	76.9	0.1817	-0.6	5.89
	Males	1,272	69.3	0.1849	-1.9	3.45
	Both	1,920	70.5	0.2258	-0.4	5.08
3CD: survey	Females	295	81.8	0.1233	-1.7	4.44
	Males	542	67.7	0.1908	-1.0	3.17
	Both	836	69.3	0.1916	-0.8	4.36
3CD: comm	Females	311	75.6	0.1588	-2.4	6.14
	Males	569	68.9	0.1425	-5.0	2.75
	Both	893	70.3	0.1726	-3.2	5.14
5ABC: survey	Females	358	77.7	0.1651	-2.2	7.31
	Males	522	68.8	0.1836	-2.3	5.55
	Both	880	69.6	0.2152	-1.7	6.57
5ABC: comm	Females	315	80.7	0.1578	-0.7	5.20
	Males	607	69.5	0.2108	-0.9	3.62
	Both	923	71.0	0.2271	-0.2	5.05
5DE: survey	Females	68	81.7	0.1704	-1.1	3.19
	Males	104	72.0	0.1991	-1.1	3.69
	Both	173	73.5	0.2380	-0.7	4.59
5DE: comm	Females	15	81.7	0.1183	-5.0	2.46
	Males	91	72.1	0.1165	-4.8	2.77
	Both	106	72.1	0.1696	-4.3	3.53

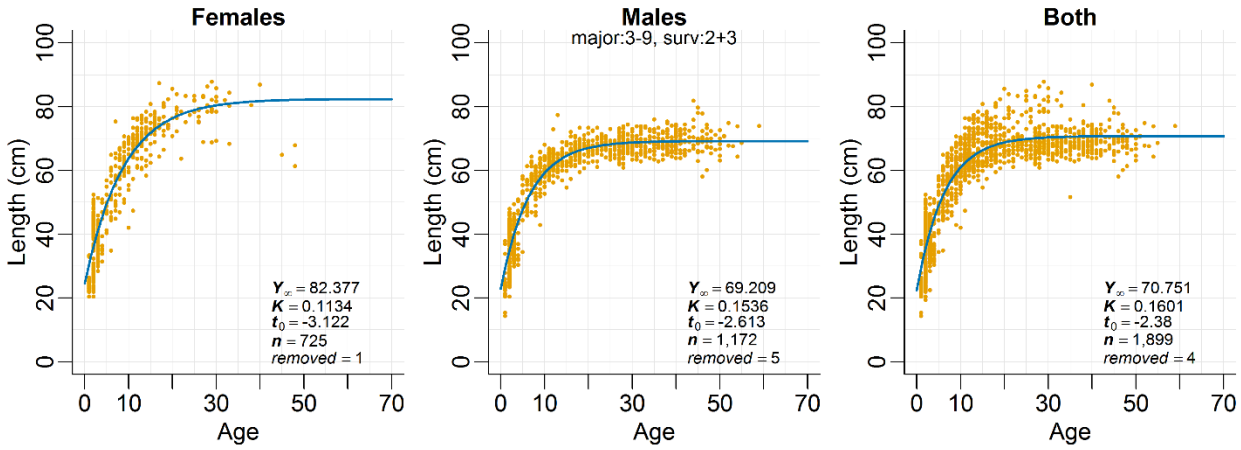

Figure D.3. Growth specified by age-length relationship: von Bertalanffy fits to BOR ages from research surveys determined by break-and-burn otoliths and surface-read otoliths from ages 1 to 3. Records with absolute value of standardised residuals >3 (starting with a preliminary fit) were dropped.

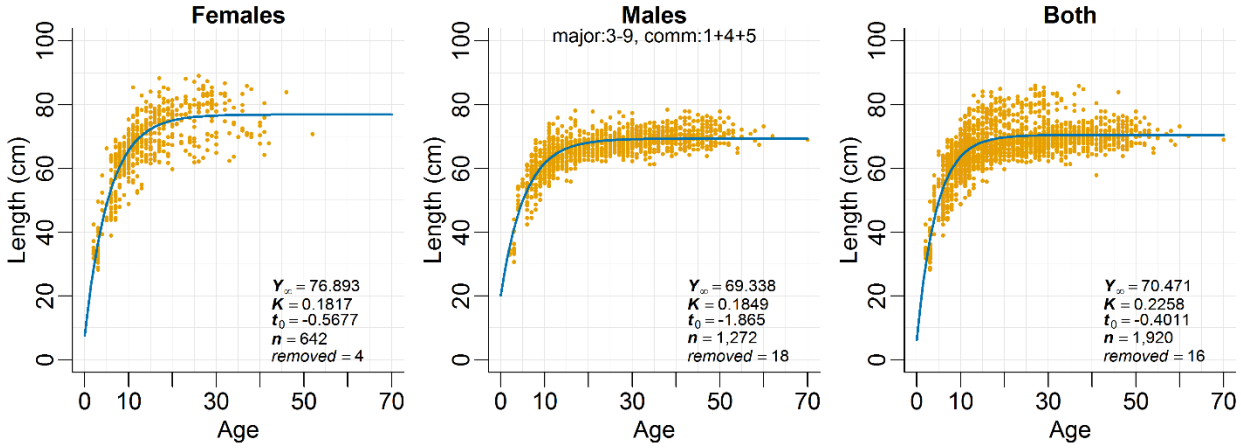

Figure D.4. Growth specified by age-length relationship: von Bertalanffy fits to BOR ages from the commercial fisheries determined by break-and-burn otoliths and surface-read otoliths from ages 1 to 3. Records with absolute value of standardised residuals >3 (starting with a preliminary fit) were dropped.

D.1.2.1. Growth adjusted for ageing error

Bocaccio ages are difficult to determine, with ageing error being higher than for other rockfish species (see Section D.2.3). A method for fitting growth curves while adjusting for ageing error in Stan probabilistic programming language was provided by Sean Anderson (2019, DFO Groundfish, pers. comm.) and implemented in R using the package `rstan` (Stan Development Team 2018). We computed two measurements of ageing error: (i) CV of age by age readers' determination of age, and (ii) CV of lengths at age (Figure D.5). Each were used in a Bayesian fit to von Bertalanffy parameters using the random-effects Stan model on data that had been fit via non-linear estimation to remove observations > 3 standard deviations from the fit. The median parameter estimates from Stan were compared to a non-linear fit of the same data (outliers removed), and the parameter estimates from the model using CVs from length-at-age were used in the Awatea population model.

Table D.5. Estimated von Bertalanffy parameters from the non-linear model (NLM) and median parameter estimates from 4000 MCMC samples. Note, the Stan model with no CV uses the same random-effects model but sets CV=0.005. Model highlighted in green was used in the base run of the stock assessment.

	Females			Males		
Model	Linf	K	t0	Linf	K	t0
NLM[1] fit	82.38	0.1134	-3.122	69.21	0.1536	-2.613
MCMC no CV	83.52	0.1056	-3.421	69.43	0.1461	-2.860
MCMC Len CV	80.13	0.1307	-2.422	67.89	0.2351	-0.628
MCMC Age CV	82.66	0.1106	-3.181	68.06	0.2130	-1.117

[1] fitted without ageing error (see Table D.4)

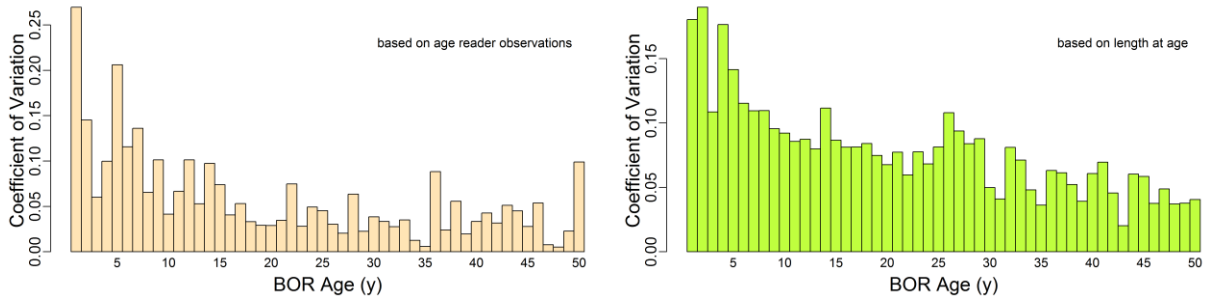

Figure D.5. Estimated CVs by age using age readers' age for each final (agreed-upon or true) age (left), and estimated CVs from lengths at true age (right).

D.1.3. Age Distribution

The median age of BOR by sex appeared to be consistent across the PMFC areas unless sampling was sparse, e.g., 5CDE commercially caught males (Figure D.6). Similarly, there is consistency across sex and major PMFC region by year if the sample sizes are sufficiently large. Unfortunately, the number of BOR sampled over the last two decades has tended to be low, largely because of the low abundance of this species. For instance, personnel were instructed to sample every Bocaccio captured in one of the four synoptic surveys, which resulted in fewer than 50 sampled in any one survey, at least until the recent strong recruitment event (Table D.6). Consequently the power of these observations is low given the small sample sizes available.

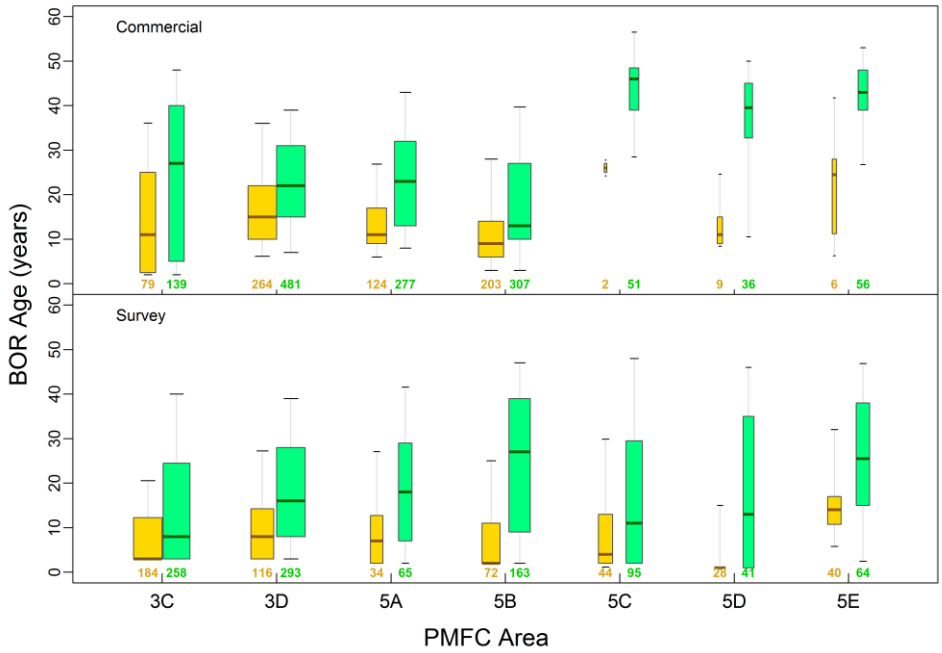

Figure D.6. Quantile plots of BOR age by sex and PMFC area for commercial trips (top) and surveys (bottom) from 1995 to 2019 (left boxes in gold = females, right boxes in green = males). Each quantile box includes all years with number of ages reported beneath.

Table D.6. Number of BOR age observations by year, sex and data source, beginning with the first year of the synoptic surveys.

	Commercial			QC Sound			WCVI			Hecate St			WCHG		
Year	M	F	Total	M	F	Total	M	F	Total	M	F	Total	M	F	Total
2003	-	-	-	28	10	38	-	-	-	-	-	-	-	-	-
2004	263	141	404	38	13	51	-	-	-	68	20	88	-	-	-
2005	59	42	101	56	12	68	10	4	14	-	-	-	-	-	-
2006	94	63	157	-	-	-	-	-	-	93	62	155	9	6	15
2007	142	43	185	31	12	43	9	3	12	-	-	-	5	5	10
2008	208	56	264	-	-	-	-	-	-	80	31	111	13	5	18
2009	93	26	119	21	4	25	7	1	8	-	-	-	-	-	-
2010	72	28	100	-	-	-	-	-	-	30	17	47	9	5	14
2011	61	19	80	11	3	14	16	6	22	-	-	-	-	-	-
2012	-	-	-	-	-	-	-	-	-	21	9	30	7	5	12
2013	41	7	48	22	12	34	3	-	3	-	-	-	-	-	-
2014	54	28	82	-	-	-	-	-	-	17	5	22	3	3	6
2015	96	55	151	4	2	6	3		3	-	-	-	-	-	-
2016	2	64	66	-	-	-	-	-	-	11	6	17	5	3	8
2017	-	-	-	90	73	163	19	29	48	-	-	-	-	-	-
2018	51	75	126	-	-	-	-	-	-	231	186	417	13	7	20
2019	-	-	-	406	423	829	32	26	58	-	-	-	-	-	-

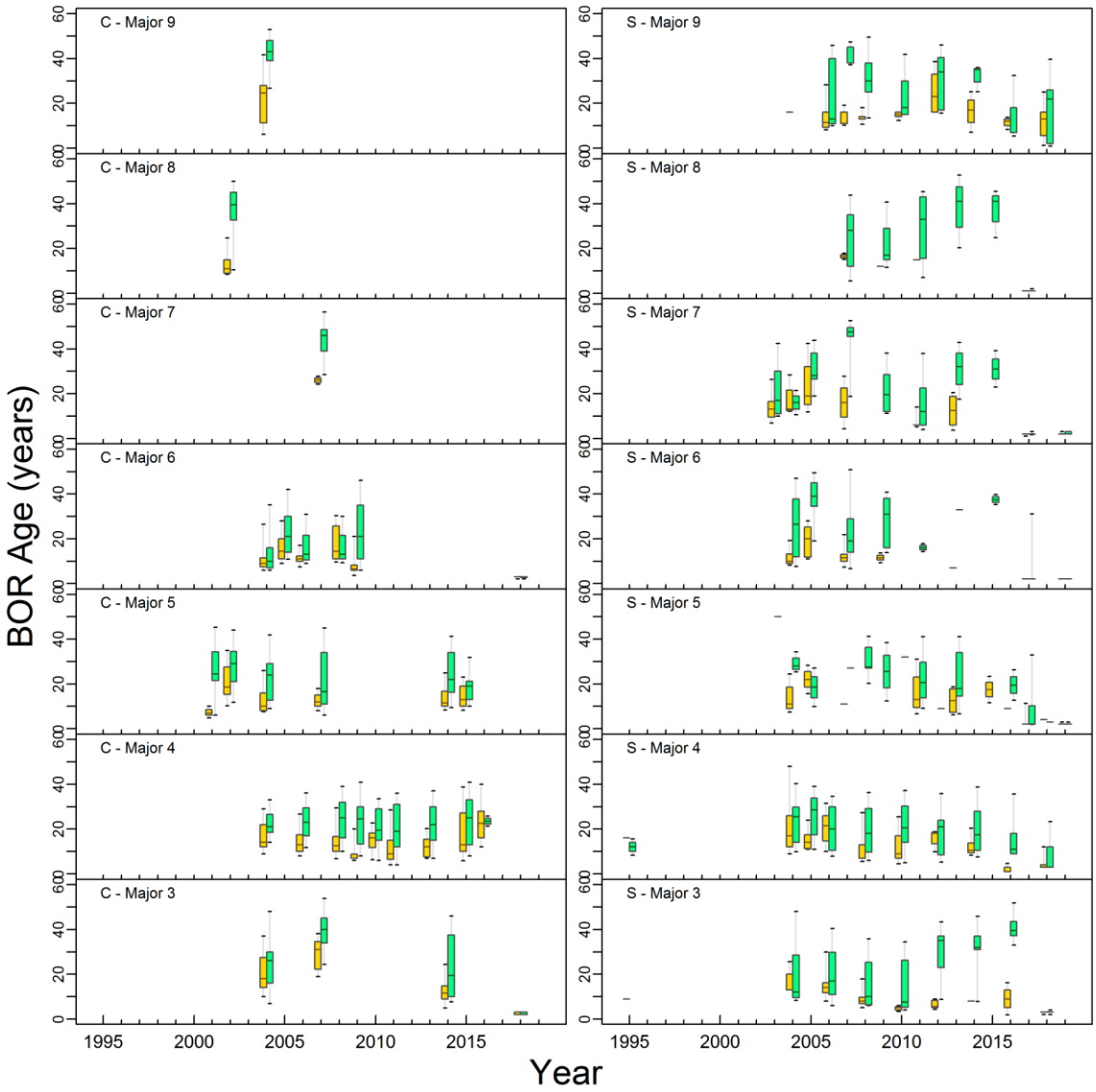

Figure D.7. Quantile plots of annual BOR age by sex and PMFC area for commercial trips (C) and surveys (S); PMFC major codes: 3=3C, 4=3D, 5=5A, 6=5B, 7=5C, 8=5D, 9=5E. Females = left boxes in gold; males = right boxes in green.

D.1.4. Maturity

This analysis was based on all “staged” (examined for maturity status) females in the DFO GFBioSQL database. Maturity codes for BOR in the database (Table D.7) come from `MATURITY_CONVENTION_CODE = 1`, which describes 7 maturity conditions for Rockfish (1977+).

Table D.7. GFBio maturity codes for rockfish, including BC BOR.

Code	Female	Male
1	Immature - translucent, small	Immature - translucent, string-like
2	Maturing - small yellow eggs, translucent or opaque	Maturing - swelling, brown-white
3	Mature - large yellow eggs, opaque	
4	Fertilized - large, orange-yellow eggs, translucent	Mature - large white, easily broken

Code	Female	Male
5	Embryos or larvae - includes eyed eggs	Ripe - running sperm
6	Spent - large flaccid red ovaries; maybe a few larvae	Spent - flaccid, red
7	Resting - moderate size, firm, red-grey ovaries	Resting - ribbon-like, small brown

Bubble plots of frequency data (maturity vs. month) derived from various sources appear in Figure D.8. Ideally, lengths- and ages-at-maturity are calculated at times of peak development stages (males: insemination season, females: parturition season; Westrheim 1975). However, all months were used in creating the maturity curve because these data provided cleaner fits than using a subset of months.

For the maturity analysis, all stages 3 and higher were assumed to be mature, and a maturity ogive was fit to the filtered data using a double-normal model:

Eq. D.3
$$m_{as} = \begin{cases} e^{-(a-\nu_s)^2/\rho_{sL}}, & a \le \nu_s \\ 1, & a > \nu_s \end{cases}$$

where, m_{as} = maturity at age a for sex s (combined),

ν_s = age of full maturity for sex s,

ρ_{sL} = variance for the left limb of the maturity curve for sex s.

To estimate a maturity ogive, the biological data were qualified as follows:

• stocks – coastwide	major=3:9	10,420 records
• ageing method (see note below)	ameth = c(0,1,3,17)	3,938 records
• sample type – total catch/random	stype = c(1,2,6,7)	3,839 records
• species category (unsorted)	scat = 1	3,839 records
• sex – females only	sex = 2	1,372 records
• maturity codes for rockfish	mats = c(1:7)	913 records
• ogive age limits	age = c(0,40)	907 records
• trip type – survey	ttype = c(2:3)	723 records
or – commercial	ttype = c(1,4,5)	184 records
• month – all months	month = c(1:12)	723|184 records

Generally, rockfish biological analyses use ages from otoliths processed and read using the 'break and burn' procedure (`ameth=3`) or coded as 'unknown' (`ameth=0`) but processed in 1980 or later. There is also a method termed 'break and bake' (`ameth=17`); however, no BOR were processed using this technique. Additionally, rockfish otoliths aged 1-3 y are sometimes processed using surface readings (`ameth=1`) because the ageing lab finds this technique more reliable than B&B for very young fish; see Table D.3 for BOR otoliths processed.

The above qualification yielded 723 female specimens from research surveys (and 184 records from the commercial fishery) with maturity readings and valid ages. Mature specimens comprised those coded 3 to 7 for rockfish (Table D.7). The empirical proportion of mature females at each age was calculated (Table D.8). A double-normal function (Eq. D.3) was fit to the observed proportions mature at ages 1 to 40 to smooth the observations and determine an increasing monotonic function for use in the stock assessment model (Figure D.9). Additionally, a logistic function used by Vivian Haist (VH) for length models in New Zealand rock lobster assessments (Haist et al. 2009) was used to compare with the double normal model.

Following a procedure adopted by Stanley et al. (2009) for Canary Rockfish (*S. pinniger*), the proportions mature for young ages fitted by Eq. D.3 were not used because the fitted line may overestimate the proportion of mature females (Figure D.9). Therefore, the maturity ogive used in the stock assessment model (last column in Table D.8) set proportion mature to zero for ages 1 to 4, then switched to the fitted monotonic function for ages 5 to 40, all forced to 1 (fully mature) after age 10 for survey data (after age 14 for fishery data). This strategy follows previous BC rockfish stock assessments where it was recognised that younger ages are not well sampled and those that are tend to be larger and more likely to be mature. The function of this ogive in the stock assessment model is to calculate the spawning biomass used in the Beverton-Holt stock recruitment function, and is treated as a constant known without error. The ages at 50% and full maturity are estimated from the double-normal fit at 6.5 y and 11 y, respectively, for survey samples and 6.6 y and 14.7 y, respectively, for fishery samples. Empirically, the age at full selectivity occurs at age 12 in the surveys and age 14 in the commercial fishery (Figure D.9).

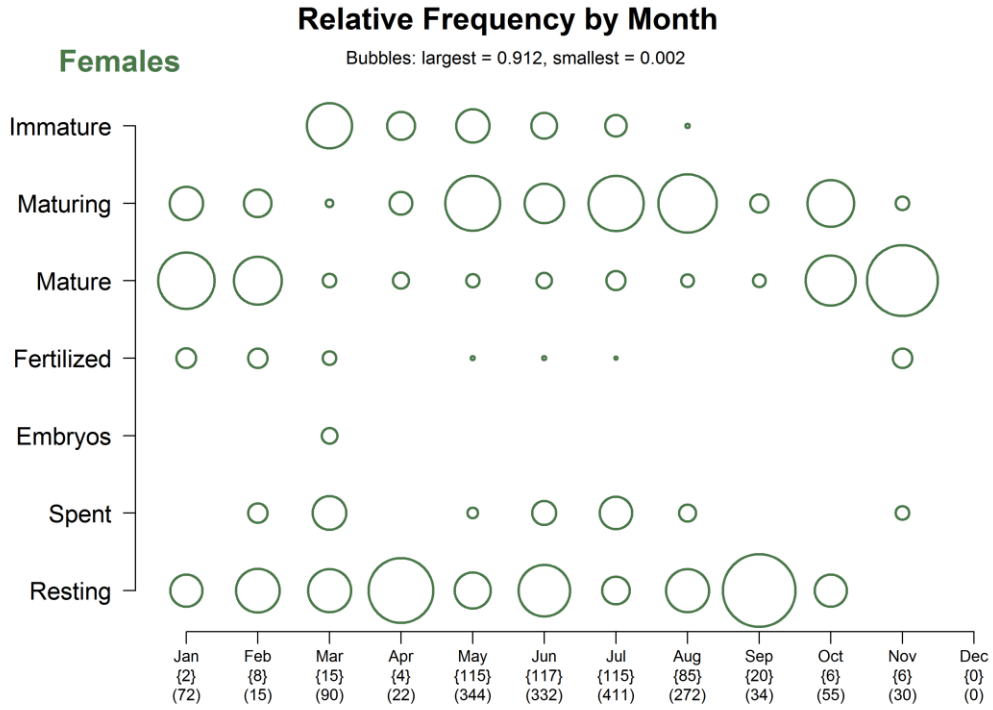

Figure D.8. Relative frequency of maturity codes by month for BOR females. Data include maturities from commercial and research specimens. Frequencies are calculated among each maturity category for every month.

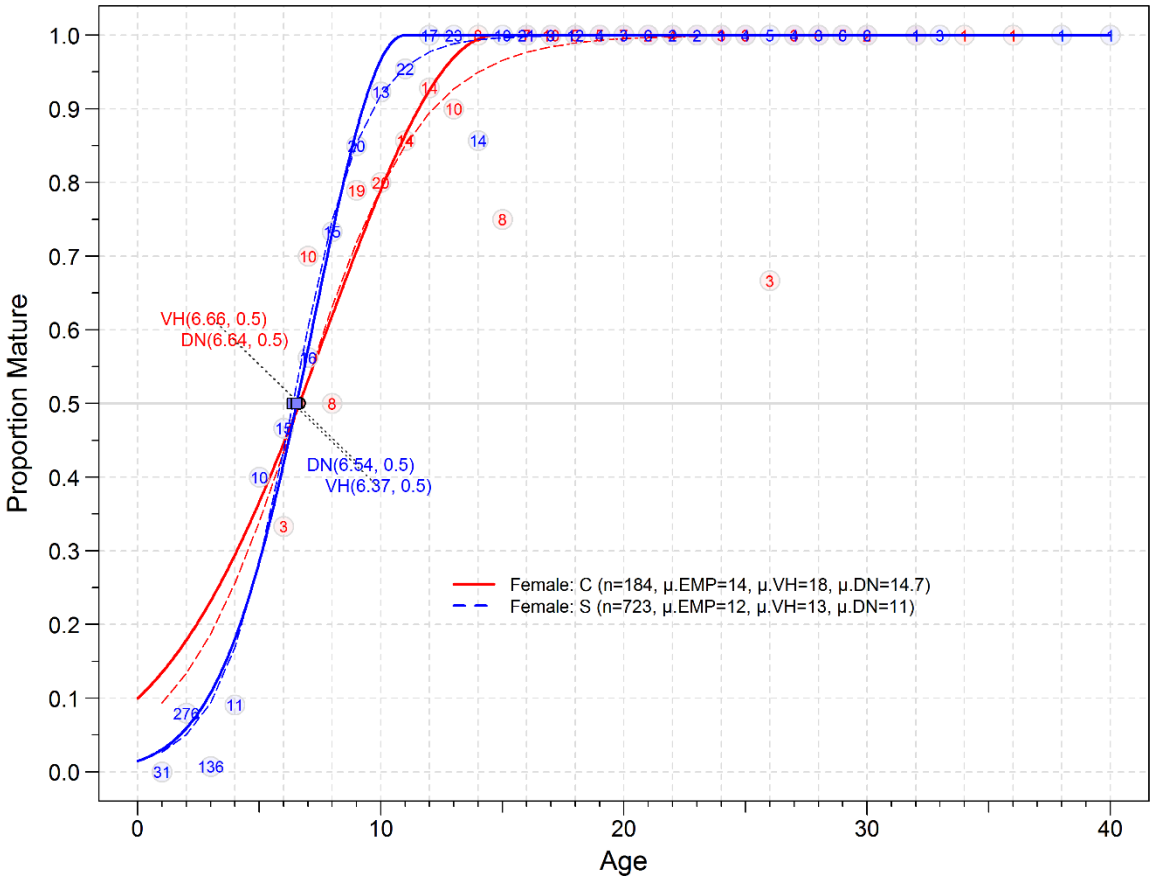

Figure D.9. Maturity ogives for BOR females. Solid line shows the double-normal (DN) curve fit; dashed line shows the logistic model fit (VH = Vivian Haist); numbers in circles denote number of female specimens used to calculate the input proportions-mature (EMP =empirical). Estimated ages at 50% maturity are indicated near the median line; ages at full maturity (μ.EMP, μ.VH, μ.DN) are displayed in the legend.

Table D.8. Proportion of survey (left) and commercial (right) BOR females mature by age (m_a, e.g., Eq.D.3) used in the catch-age model (last column of survey). Maturity stages 1 and 2 were assumed to be immature fish and all other staged fish (stages 3 to 7) were assumed to be mature. EMP = empirical, BL = binomial logit, VH =logistic used by Vivian Haist, DN = double normal (Eq.D.3), Mod = used in population model.

	Survey						Commercial					
Age	# Fish	EMP m_a	BL m_a	VH m_a	DN m_a	Mod m_a	# Fish	EMP m_a	BL m_a	VH m_a	DN m_a	Mod m_a
1	31	0	0.026	0.026	0.030	0	0	---	0.311	0.094	0.135	0
2	276	0.080	0.048	0.050	0.059	0	0	---	0.364	0.134	0.179	0
3	136	0.007	0.087	0.094	0.107	0	0	---	0.421	0.187	0.232	0
4	11	0.091	0.154	0.169	0.181	0	0	---	0.480	0.256	0.295	0
5	10	0.400	0.256	0.285	0.285	0.285	0	---	0.540	0.339	0.366	0.366
6	15	0.467	0.395	0.438	0.419	0.419	3	0.333	0.599	0.434	0.446	0.446
7	16	0.563	0.553	0.603	0.573	0.573	10	0.700	0.655	0.534	0.531	0.531
8	15	0.733	0.701	0.749	0.732	0.732	8	0.500	0.707	0.631	0.619	0.619
9	20	0.850	0.817	0.853	0.871	0.871	19	0.789	0.754	0.719	0.707	0.707
10	13	0.923	0.894	0.919	0.966	0.966	20	0.800	0.796	0.792	0.790	0.790
11	22	0.955	0.941	0.957	1	1	14	0.857	0.832	0.851	0.864	0.864
12	17	1	0.968	0.978	1	1	14	0.929	0.863	0.895	0.925	0.925
13	23	1	0.983	0.988	1	1	10	0.900	0.889	0.927	0.970	0.970
14	14	0.857	0.991	0.994	1	1	8	1	0.910	0.950	0.995	0.995

	Survey						Commercial					
Age	# Fish	EMP m_a	BL m_a	VH m_a	DN m_a	Mod m_a	# Fish	EMP m_a	BL m_a	VH m_a	DN m_a	Mod m_a
15	10	1	0.995	0.997	1	1	8	0.750	0.928	0.966	1	1
16	21	1	0.997	0.998	1	1	7	1	0.943	0.977	1	1
17	9	1	0.999	0.999	1	1	10	1	0.954	0.984	1	1
18	12	1	0.999	1.000	1	1	5	1	0.964	0.990	1	1
19	4	1	1.000	1.000	1	1	5	1	0.971	0.993	1	1
20	3	1	1.000	1.000	1	1	7	1	0.977	0.995	1	1
21	6	1	1.000	1.000	1	1	2	1	0.982	0.997	1	1
22	2	1	1.000	1.000	1	1	4	1	0.986	0.998	1	1
23	2	1	1.000	1.000	1	1	2	1	0.989	0.999	1	1
24	1	1	1.000	1.000	1	1	3	1	0.991	0.999	1	1
25	4	1	1.000	1.000	1	1	3	1	0.993	0.999	1	1
26	5	1	1.000	1.000	1	1	3	0.667	0.994	1.000	1	1
27	4	1	1.000	1.000	1	1	3	1	0.996	1.000	1	1
28	3	1	1.000	1.000	1	1	6	1	0.997	1.000	1	1
29	6	1	1.000	1.000	1	1	5	1	0.997	1.000	1	1
30	6	1	1.000	1.000	1	1	2	1	0.998	1.000	1	1
31	0	---	1.000	1.000	1	1	0	---	0.998	1.000	1	1
32	1	1	1.000	1.000	1	1	1	1	0.999	1.000	1	1
33	3	1	1.000	1.000	1	1	0	---	0.999	1.000	1	1
34	0	---	1.000	1.000	1	1	1	1	0.999	1.000	1	1
35	0	---	1.000	1.000	1	1	0	---	0.999	1.000	1	1
36	0	---	1.000	1.000	1	1	1	1	0.999	1.000	1	1
37	0	---	1.000	1.000	1	1	0	---	1.000	1.000	1	1
38	1	1	1.000	1.000	1	1	0	---	1.000	1.000	1	1
39	0	---	1.000	1.000	1	1	0	---	1.000	1.000	1	1
40	1	1	1.000	1.000	1	1	0	---	1.000	1.000	1	1

D.1.5. Natural Mortality

Natural mortality (*M*) estimates for Bocaccio in California waters include:

- 0.15 – fixed by MacCall (2008 and earlier assessments),
- 0.178 – estimated by He et al. (2015) using a lognormal prior $\mathcal{LN}$(0.128, 0.517),
- 0.18 – estimated by He and Field (2017) using a lognormal prior $\mathcal{LN}$(0.175, 0.438)

However, He and Field (2017) suggest that "*two demographic clusters exist centred around: (i) southern/central California and (ii) the west coast of BC, with low frequencies (particularly smaller fish) in the region between Cape Mendocino and the mouth of the Columbia River. The two clusters exhibit differences in growth, maturity and longevity; however, genetic evidence indicates a single Pacific west coast population*" (Matala et al. 2004, Field et al. 2010).

Previous assessments of Bocaccio in BC used a Bayesian Surplus Production (BSP) model with a lognormal prior on the intrinsic rate of increase *r* of $\mathcal{LN}$(0.117, 0.294). This prior was estimated assuming a plus group of 60 years and a lognormal random variable for female *M* $\mathcal{LN}$(0.075, 0.25) (Stanley et al. 2009).

In the DFO database GFBioSQL, the maximum BOR age is 70 years for one male specimen (69 cm in length) caught at 132 m depth in PMFC area 3C, specifically in a fishing locality called "Fingers" (major=3, minor=23, locality=6), on Apr 27, 2007. The mean age for BC BOR is 16.7 y (*n*=3,938), the median age is 13 y, and the 0.025. 0.975, and 0.99 quantiles are 2, 47, and 50 y, respectively.

The Hoenig (1983) estimator describes an exponential decay LN(*k*) = -*Z* t_L, where *Z* = natural mortality, t_L = longevity of a stock, and *k* = proportion of animals that are still alive at t_L. Quinn and Deriso (1999) popularised the estimator by re-arranging Hoenig's equation and setting *k*=0.01 (as originally suggested by Hoenig):

Eq. D.4 $$M = -\ln(0.01) / t_{\max}$$

Then et al. (2015) revisited various natural mortality estimators and recommended the use of an updated Hoenig estimator based on nonlinear least squares:

Eq. D.5 $$M_{\text{est}} = 4.899 t_{\max}^{-0.916}$$

where t_{max} = maximum age.

During the review process for Redstripe Rockfish (DFO 2022), one of the principal reviewers, Vladlena Gertseva (2018, Northwest Fisheries Science Center, NOAA, pers. comm.), noted that Then et al. (2015) did not consistently apply a log transformation. In real space, one might expect substantial heteroscedasticity in both the observation and process errors associated with the relationship of *M* to t_{max}. Re-evaluating the data used in Then et al. (2015) by fitting the one-parameter t_{max} model using a log-log transformation (such that the slope is forced to be -1 in the transformed space, as in Hamel 2015), Gertseva recalculated the point estimate for *M* as:

Eq. D.6 $$M_{\text{est}} = 5.4 / t_{\max}$$

In past assessment meetings, participants have been averse to adopting a maximum age that comes from a single, usually isolated individual, preferring instead to observe the tail distribution of ages (Figure D.10). For BOR, this suggests that age 55 y might be a more appropriate value for t_{max}, which means that *M* ranges from 0.08 to 0.12 (Table D.9). In this assessment, *M* is fixed to three values (0.07, 0.08, 0.09) for a variety of reasons discussed in the main document.

Table D.9. Estimates of BOR natural mortality using equations based on fish longevity. Three upper age values (t_{max}) are used to illustrated the variability in M base on maximum age.

Source	Equation	t_{max}= 50y	= 55y	= 60y
Hoenig (1983)	M = -LN(0.01)/tmax	0.092	0.084	0.077
Then et al. (2015)*	M = 4.899(tmax$^{-0.916}$)	0.136	0.125	0.115
Gertseva (pers.comm.)	M = 5.4/tmax	0.108	0.098	0.090

*Derived model without using log-log transformation, leading to biased estimates.

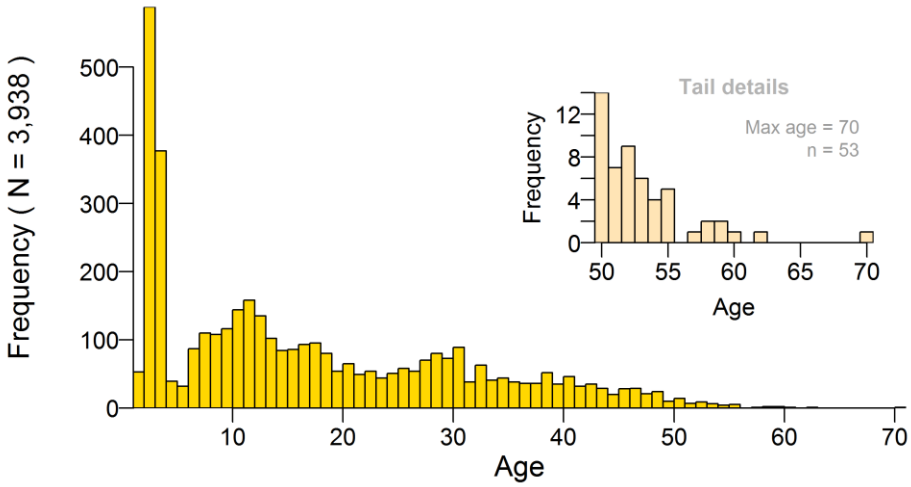

Figure D.10. Distribution of BOR female + male ages; inset shows details for ages >=50 y old, which is the 0.987 quantile of the complete age data set.

D.1.6. Generation Time

Generation time t_G is assumed to be the average age of adults (males and females) in the population, and takes the form:

Eq. D.7 $$t_G = k + \frac{1}{e^M - 1}$$

where k = age at 50% maturity,

M = instantaneous rate of natural mortality.

COSEWIC uses a rough approximation to generation time:

Eq. D.8 $$t_G = k + \frac{1}{M}$$

From Section D.1.4, k = 6.5 y. If we assume that M = 0.08, then the two formulae above yield estimates of generation time t_G = 18.5 y and 19 y, respectively. For simplicity, we adopt t_G = 20 y to be consistent with previous BOR assessments (e.g. Stanley et al. 2009).

D.2. WEIGHTED AGE PROPORTIONS

This section summarises a method for representing commercial and survey age structures in the stock assessment model for a given species (herein called 'target') through weighting observed age frequencies x_a or proportions x'_a by catch‖density in defined strata (h). (Throughout this section, the symbol '‖' is used to delimit parallel values for commercial and survey analyses, respectively, as the mechanics of the weighting procedure are similar for both. The symbol can be read 'or', e.g., catch or density.) For commercial samples, these strata comprise quarterly periods within a year, while for survey samples, the strata are defined by longitude, latitude, and depth boundaries unique to each survey series. A two-tiered weighting system is used as follows:

Within each stratum h, commercial age samples are identified by trip (usually one sample per trip) and the age frequencies per trip are weighted by the target catch weight (tonnes) of the tows that were sampled to yield one weighted age frequency per stratum (quarter). For each year, the quarterly age frequencies are then weighted by the quarterly fishery catch of the target. If a quarter has not been sampled, it does not get used in the weighting for the year. For example, if samples of the target were missing in Oct-Dec 2018, only the first three quarters of target catch would be used to prorate three quarterly age frequencies in 2018.

Annual survey ages are weighted similarly. Each sampled tow in a survey stratum is weighted by the tow's target catch density (t/km^2) to yield one weighted age frequency per stratum. As above, not all survey strata will have age samples and so weighted age frequencies by sampled stratum are weighted by the appropriate stratum area (km^2). For example, if only shallow strata are sampled for age, the deep strata areas are not used to prorate the shallow-strata age frequencies. As for commercial ages, the two-tiered weighting scheme yields one age frequency per survey year.

Ideally, sampling effort would be proportional to the amount of the target caught, but this is not usually the case. Personnel can control the sampling effort on surveys more than that aboard commercial vessels, but the relative catch among strata over the course of a year or survey cannot be known with certainty until the events have occurred. Therefore, the stratified weighting scheme outlined above and detailed below attempts to adjust for unequal sampling effort among strata.

For simplicity, the weighting of age frequencies x_a is used for illustration, unless otherwise specified. The weighting occurs at two levels: h (quarters for commercial ages, strata for survey ages) and i (years if commercial, stratum areas if survey). Notation is summarised in Table D.10.

Table D.10. Equations for weighting age frequencies or proportions; (c) = commercial, (s) = survey.

Symbol	Description
	Indices
a	age class (1 to A, where A is an accumulator age-class)
d	(c) trip ID as sample unit (usually one sample per trip) (s) sample ID as sample unit (usually one sample per survey tow)
h	(c) calendar year quarter (1 to 4), 91.5 days each (s) survey stratum (area-depth combination)
i	(c) calendar year (1977 to present) (s) single survey ID in survey series (e.g., 2003 QCS Synoptic)
	Data
x_{adhi}	observations-at-age a for sample unit d in quarter‖stratum h of year‖survey i
x'_{adhi}	proportion-at-age a for sample unit d in quarter‖stratum h of year‖survey i
C_{dhi}	(c) commercial catch (tonnes) of the target for sample unit d in quarter h of year i (s) density (t/km^2) of the target for sample unit d in stratum h of survey i
C'_{dhi}	C_{dhi} as a proportion of total catch‖density $C_{hi} = \sum_d C_{dhi}$
y_{ahi}	weighted age frequencies at age a in quarter‖stratum h of year‖survey i
K_{hi}	(c) total commercial catch (t) of the target in quarter h of year i (s) stratum area (km^2) of stratum h in survey i
K'_{hi}	K_{hi} as a proportion of total catch‖area $K_i = \sum_h K_{hi}$
p_{ai}	weighted frequencies at age a in year‖survey i
p'_{ai}	weighted proportions at age a in year‖survey i

For each quarter‖stratum h, sample unit frequencies x_{ad} are weighted by sample unit catch‖density of the target species. (For commercial ages, trip is used as the sample unit, though at times one trip may contain multiple samples. In these instances, multiple samples from a single trip will be merged into a single sample unit.) Within any quarter‖stratum h and year‖survey i there is a set of sample catches‖densities C_{dhi} that can be transformed into a set of proportions:

Eq. D.9 $$C'_{dhi} = C_{dhi} \Big/ \sum_d C_{dhi} \ .$$

The proportion C'_{dhi} is used to weight the age frequencies x_{adhi} summed over d, which yields weighted age frequencies by quarter‖stratum for each year‖survey:

Eq. D.10 $$y_{ahi} = \sum_{d} \left(C'_{dhi} x_{adhi} \right).$$

This transformation reduces the frequencies x from the originals, and so y_{ahi} is rescaled (multiplied) by the factor

Eq. D.11 $$\sum\nolimits_a x_{ahi} \Big/ \sum\nolimits_a y_{ahi}$$

to retain the original number of observations. (For proportions x' this is not needed.) Although this step is performed, it is strictly not necessary because at the end of the two-step weighting, the weighted frequencies are transformed to represent proportions-at-age.

At the second level of stratification by year‖survey i, the annual proportion of quarterly catch (t) for commercial ages or the survey proportion of stratum areas (km^2) for survey ages is calculated

Eq. D.12 $$K'_{hi} = K_{hi} \Big/ \sum\nolimits_h K_{hi}$$

to weight y_{ahi} and derive weighted age frequencies by year‖survey:

Eq. D.13 $$p_{ai} = \sum_{h} \left(K'_{hi} y_{ahi} \right).$$

Again, if this transformation is applied to frequencies (as opposed to proportions), it reduces them from the original, and so p_{ai} is rescaled (multiplied) by the factor

Eq. D.14 $$\sum\nolimits_a y_{ai} \Big/ \sum\nolimits_a p_{ai}$$

to retain the original number of observations.

Finally, the weighted frequencies are transformed to represent proportions-at-age:

Eq. D.15 $$p'_{ai} = p_{ai} \Big/ \sum\nolimits_a p_{ai}\,.$$

If initially we had used proportions x'_{adhi} instead of frequencies x_{adhi}, the final transformation would not be necessary; however, its application does not affect the outcome.

The choice of data input (frequencies x vs. proportions x') can sometimes matter: the numeric outcome can be very different, especially if the input samples comprise few observations. Theoretically, weighting frequencies emphasises our belief in individual observations at specific ages while weighting proportions emphasises our belief in sampled age distributions. Neither method yields inherently better results; however, if the original sampling methodology favoured sampling few fish from many tows rather than sampling many fish from few tows, then weighting frequencies probably makes more sense than weighting proportions. In this assessment, age frequencies x are weighted.

D.2.1. Commercial Ages

Sampled age frequencies from bottom and midwater trawl were combined after comparing cumulative age frequencies for each gear type by sex and capture year. There appear to be no consistent differences in the age frequencies between the two gear types for either sex (females: Figure D.11, males: Figure D.12), leading to the conclusion that a model would estimate similar selectivities for each capture method. Furthermore, there were insufficient AF samples for midwater trawl to reliably separate the two gear types into independent fisheries (Table D.11). Consequently, the model was run assuming a joint selectivity for the two fishing methods by combining the AFs and the catch data into a single trawl fishery.

The 2018 stock assessment of Redstripe Rockfish (Starr and Haigh, 2021a) did not separate sorted (by size or sex) and unsorted samples when introducing proportions-at-age into the model. This practice was also followed for the 2019 BOR stock assessment after exploratory runs using only sorted and only unsorted samples were examined. For BOR, there are only four years with sorted samples (two in 2002, three in 2004, one in 2005, and one in 2006). Usually there are more sorted samples and they occur earlier in the time series than do the unsorted samples. Consequently, dropping sorted samples loses information about early recruitment strength. Generally, using only unsorted samples is best left to analyses of mean weight over time (e.g., Section D.3.1), which is often used in delay-difference models.

Table D.11. Number of BOR age samples from commercial trips by gear type (BT= bottom trawl, MW=midwater trawl).

Year	BT	MW	Year	BT	MW	Year	BT	MW	Year	BT	MW
2001	55	-	2006	91	66	2010	50	50	2015	-	104
2002	96	-	2007	185	-	2011	80	-	2016	66	-
2004	282	122	2008	207	57	2013	48	-	2018	60	66
2005	101	-	2009	119	-	2014	32	50	-	-	-

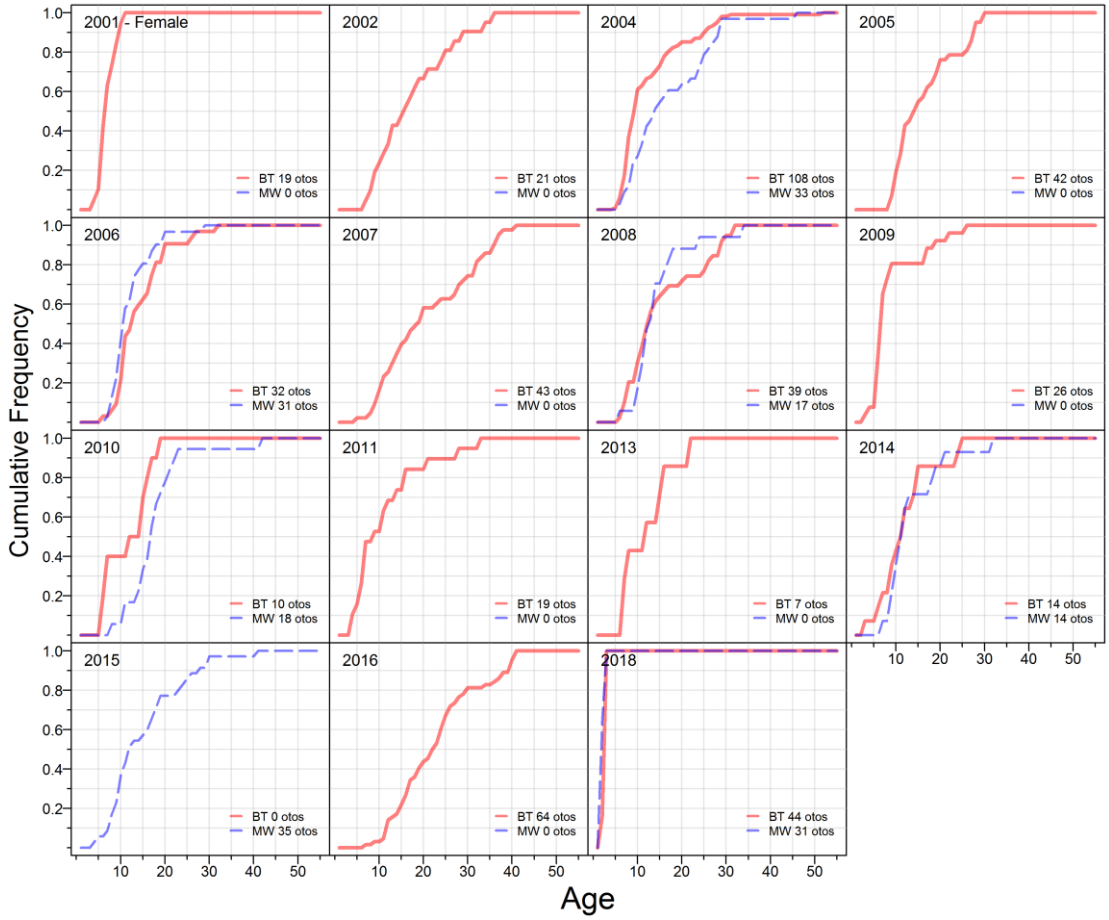

Figure D.11. Plots comparing the cumulative bottom trawl (red) and midwater trawl (blue) age frequencies by year for female BOR coastwide.

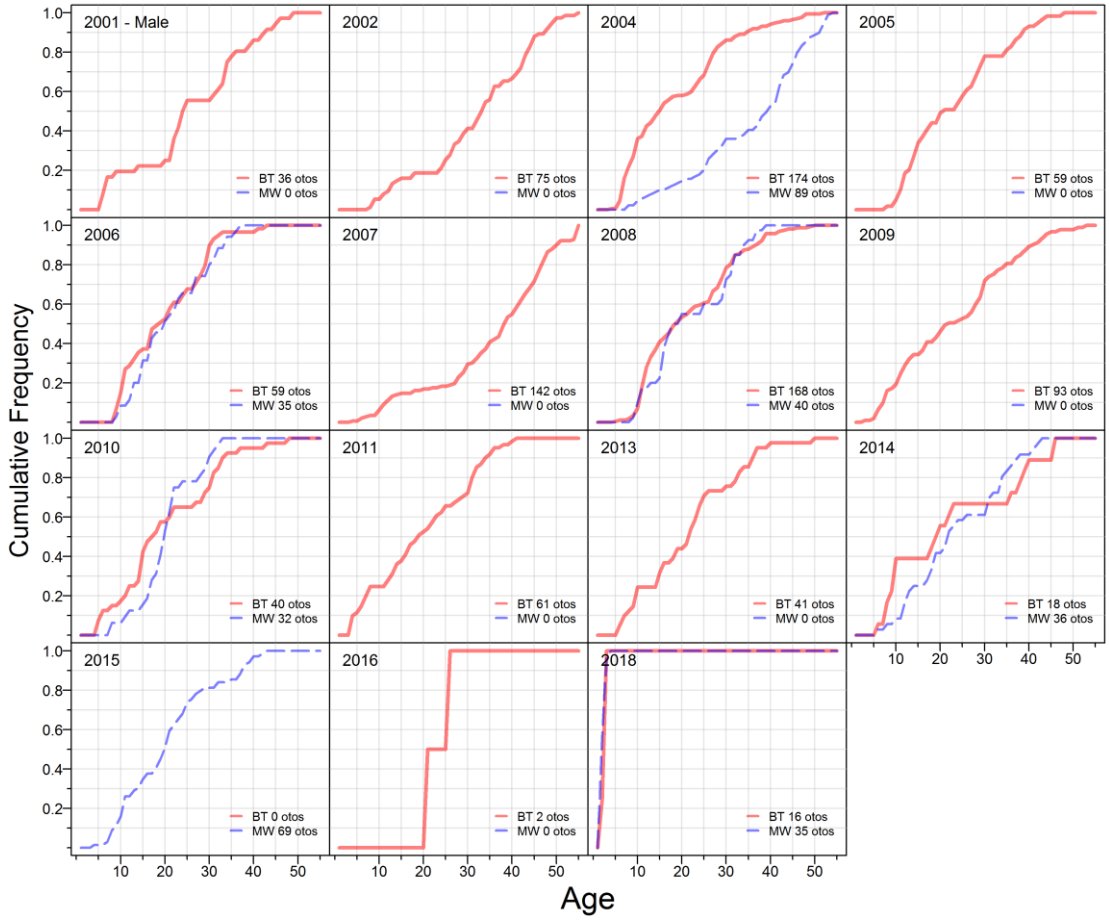

Figure D.12. Plots comparing the cumulative bottom trawl (red) and midwater trawl (blue) age frequencies by year for male BOR coastwide.

Table D.12. Commercial trip quarterly data from trawls used to weight BOR proportions-at-age: number of sampled trips, BOR catch (t) by sampled trip and by all trips.

Year	# Trips				Sampled trip catch (t)				All trip catch (t)			
	Q1	Q2	Q3	Q4	Q1	Q2	Q3	Q4	Q1	Q2	Q3	Q4
2001	1	-	-	-	0.39	-	-	-	45	82	79	62
2002	-	1	-	1	-	2.27	-	1.81	36	90	97	61
2004	1	4	3	1	0.45	6.07	5.17	0.20	23	39	55	34
2005	-	2	-	-	-	2.53	-	-	20	38	36	42
2006	2	-	1	-	0.42	-	1.36	-	25	33	26	29
2007	-	2	1	-	-	0.93	0.39	-	25	29	39	37
2008	3	-	-	1	0.83	-	-	0.26	24	21	38	25
2009	1	1	-	-	0.36	0.28	-	-	17	27	22	34
2010	2	-	-	-	0.70	-	-	-	27	23	18	23
2011	1	-	1	-	0.58	-	0.11	-	18	32	28	30
2013	-	1	-	-	-	0.32		-	19	13	18	20
2014	-	-	2	-	-	-	0.77	-	13	15	15	10
2015	2	1	-	1	0.98	0.49	-	0.29	12	10	13	10
2016		-	1	-	-	-	0.31	-	10	6	11	10
2018	1	-	-	1	2.04	-	-	0.05	26	15	30	21

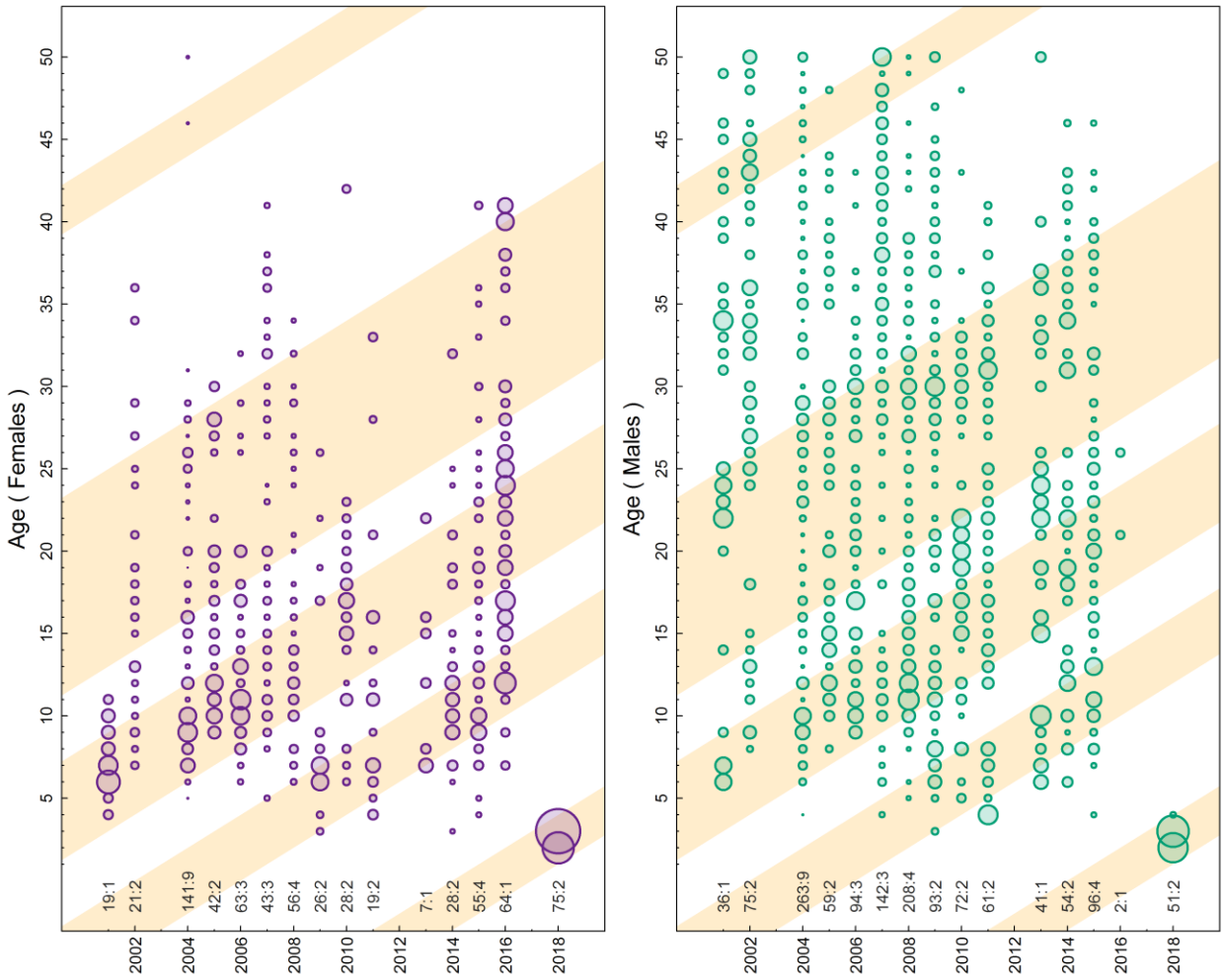

Figure D.13. Proportions-at-age for coastwide BOR caught by commercial trawl gear calculated as age frequencies weighted by trip catch within quarters and commercial catch within years. Diagonal shaded bands indicate cohorts that were born when the mean Pacific Decadal Oscillation was positive. Numbers displayed along the bottom axis indicate number of fish aged and number of samples (colon delimited) by year.

D.2.2. Research/Survey Ages

Age data for BOR from the surveys cover years from 2003 to 2019 (Table D.13). Three surveys show a large recruitment event, first evident in 2017 for the QCS and HS Synoptic surveys (Figure D.14 and Figure D.15, respectively).The WCVI survey (Figure D.16) also detected the signal in 2018 while the sparsely-sampled WCHG synoptic survey did not (Figure D.17). The HS synoptic survey indicates that the large 2017 proportion comprised 1-year old fish whereas the QCS synoptic 2017 and 2019 modes both occurred at 2 years. Either there were two good recruitment events or, more likely, observation error of (1,-1) implies that the QCS 2017 and 2019 modes occurred at 1 and 3 years.

As discussed above, the ageing lab agreed that their ageing of 1-3 year-old fish was highly uncertain, and based on empirical length distributions that suggested strongly a large cohort born in 2016, we adjusted the age-proportion data accordingly: QCS 2017 – ages 1-3 consolidated into age 1; QCS 2019 – ages 1-4 consolidated into age 3; WCVI 2018 – ages 2-5 consolidated into age 2; WCHG 2018 – ages 1-2 consolidated into age 2; and HS 2017 – ages

1-2 consolidated into age 1. Additionally, the WCVI 2016 data were removed because the age frequency based on only 17 otoliths did not represent anything coherent with the other synoptic survey age proportions.

Table D.13. Number of BOR age samples (s) collected from surveys and BOR density (d=kg/km^2) by survey stratum identifier (h); stratum area is shown in parentheses.

Survey Year	Survey Strata			
QCS Synoptic	h=18 (5012 km²)	h=19 (5300 km²)	h=20 (2640 km²)	h=21 (528 km²)
2003	-	s=1, d=0.033	-	-
2004	s=2, d=1.051	s=3, d=0.044	-	-
2005	s=3, d=0.45	s=5, d=0.023	s=5, d=0.051	-
2007	s=1, d=0.082	s=7, d=0.153	s=2, d=0.036	-
2009	s=1, d=0.366	s=2, d=0.029	s=5, d=0.03	-
2011	-	s=7, d=0.056	-	s=1, d=0.042
2013	s=1, d=0.006	s=1, d=2.011	-	-
2015	-	s=2, d=0.032	s=1, d=0.073	-
2017	s=9, d=0.007	s=28, d=0.013	s=2, d=0.049	s=1, d=0.033
2019	-	s=11, d=1.279	s=2, d=0.173	-
QCS Synoptic	h=22 (1740 km²)	h=23 (3928 km²)	h=24 (3664 km²)	h=25 (1236 km²)
2003	-	s=1, d=0.632	-	-
2004	s=1, d=0.048	s=5, d=0.043	s=3, d=0.072	s=1, d=0.056
2005	s=1, d=0.032	s=5, d=0.055	-	-
2007	s=1, d=0.069	s=2, d=0.032	s=2, d=0.025	-
2009	-	s=3, d=0.03	s=1, d=0.088	-
2011	-	s=2, d=0.029	-	-
2013	-	s=4, d=0.119	s=1, d=0.021	-
2015	-	s=1, d=0.036	s=2, d=0.032	-
2017	s=2, d=0.003	s=8, d=0.028	s=3, d=0.077	-
2019	-	s=7, d=0.314	-	-
HS Synoptic	h=72 (5948 km²)	h=73 (3048 km²)	h=74 (2456 km²)	h=75 (1856 km²)
2007	-	s=5, d=0.058	s=2, d=0.108	s=1, d=0.041
2009	-	-	s=6, d=0.051	-
2011	-	s=3, d=0.276	s=2, d=0.064	-
2013	-	s=1, d=0.083	s=1, d=0.037	-
2015	-	s=2, d=0.082	-	-
2017	s=5, d=0.002	s=2, d=0.04	s=2, d=0.01	-
WCVI Synoptic	h=65 (5716 km²)	h=66 (3768 km²)	h=67 (708 km²)	h=68 (572 km²)
2004	s=1, d=0.038	s=9, d=0.394	s=2, d=0.057	s=1, d=0.039
2006	s=5, d=0.048	s=14, d=0.337	s=9, d=0.07	-
2008	s=10, d=0.04	s=21, d=0.064	s=15, d=0.044	s=2, d=0.118
2010	s=4, d=0.057	s=10, d=0.083	s=1, d=0.069	s=1, d=0.061
2012	s=1, d=0.105	s=6, d=0.053	s=6, d=0.04	s=3, d=0.044
2014	s=4, d=0.023	s=2, d=0.065	s=6, d=0.067	-
2016	s=1, d=0.002	s=6, d=0.076	s=1, d=0.083	-
2018	s=4, d=0.113	s=15, d=0.401	s=10, d=0.289	-
WCHG Synoptic	h=126 (1266 km²)	h=151 (1076 km²)	h=152 (1004 km²)	-
2006	s=9, d=0.055	-	-	-
2007	-	s=9, d=0.056	-	-
2008	-	s=10, d=0.052	s=2, d=0.035	-
2010	-	s=8, d=0.054	s=1, d=0.029	-
2012	-	s=6, d=0.059	s=2, d=0.046	-
2014	-	s=4, d=0.054	s=1, d=0.058	-
2016	-	s=6, d=0.09	-	-
2018	-	s=8, d=0.08	s=1, d=0.039	-

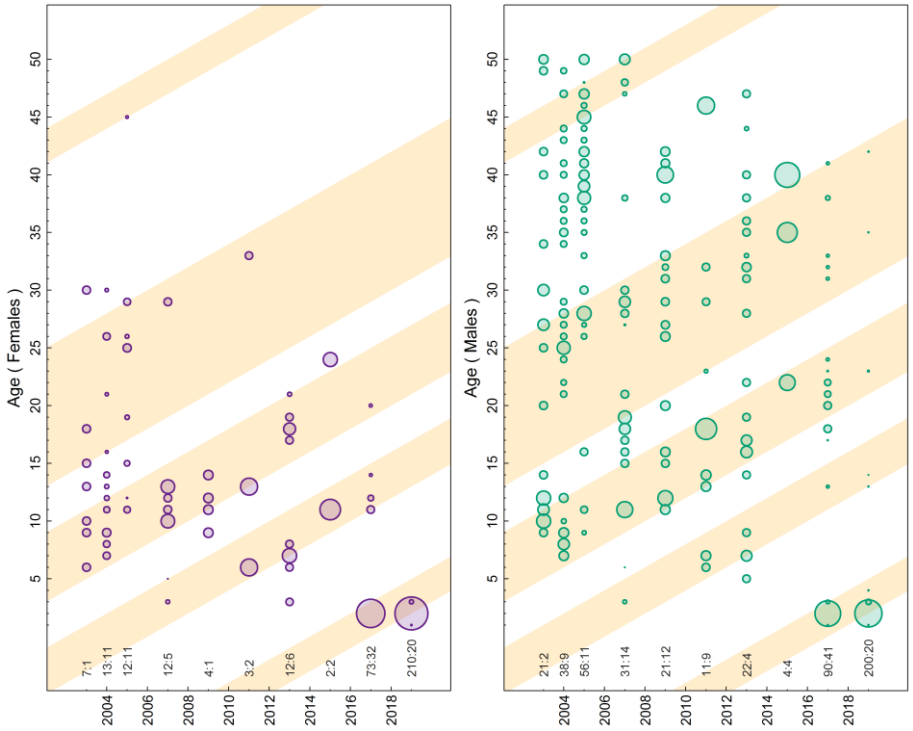

Figure D.14. QCS Synoptic survey: coastwide BOR proportions-at-age based on age frequencies weighted by mean fish density within strata and by total stratum area within survey (Table D.13). See Figure D.13 for details on diagonal shaded bands and displayed numbers.

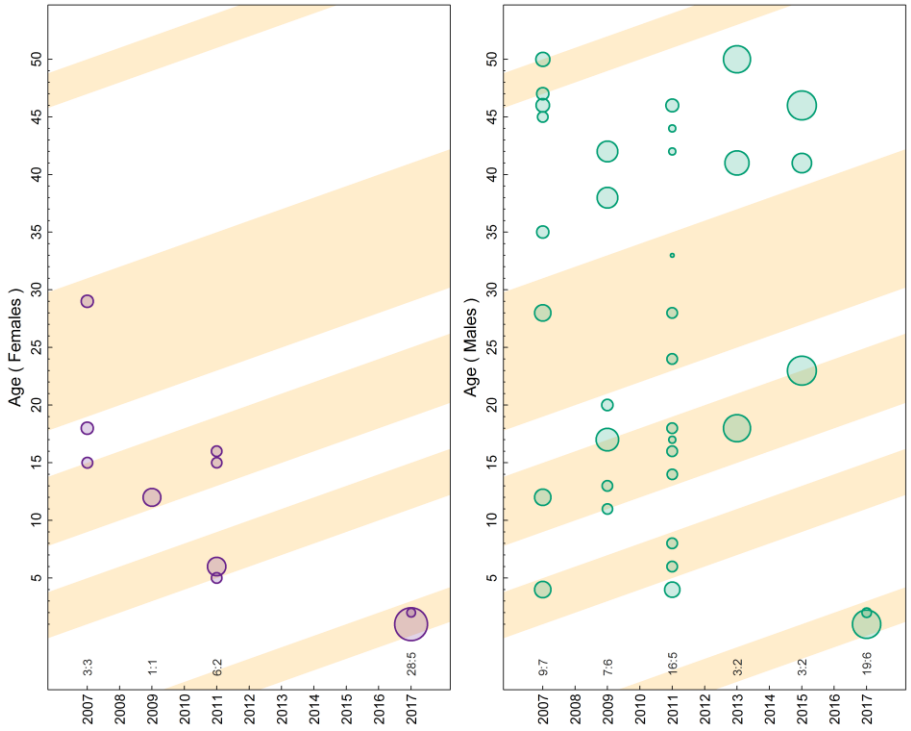

Figure D.15. HS Synoptic survey: coastwide BOR proportions-at-age based on age frequencies weighted by mean fish density within strata and by total stratum area within survey (Table D.13). See Figure D.13 for details on displayed numbers.

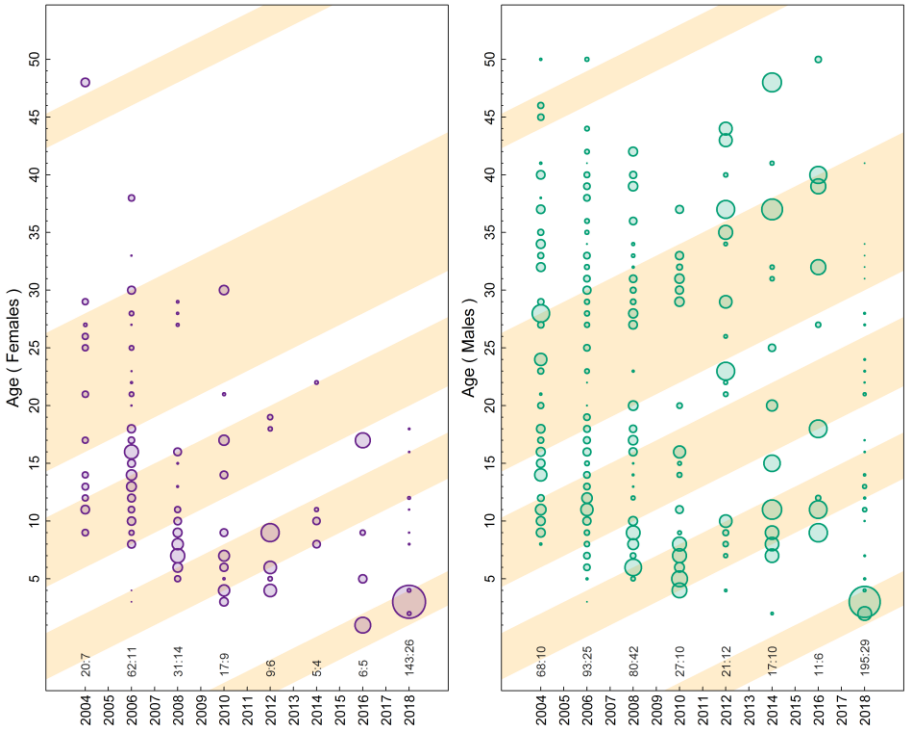

Figure D.16. WCVI Synoptic survey: coastwide BOR proportions-at-age based on age frequencies weighted by mean fish density within strata and by total stratum area within survey (Table D.13). See Figure D.13 for details on displayed numbers.

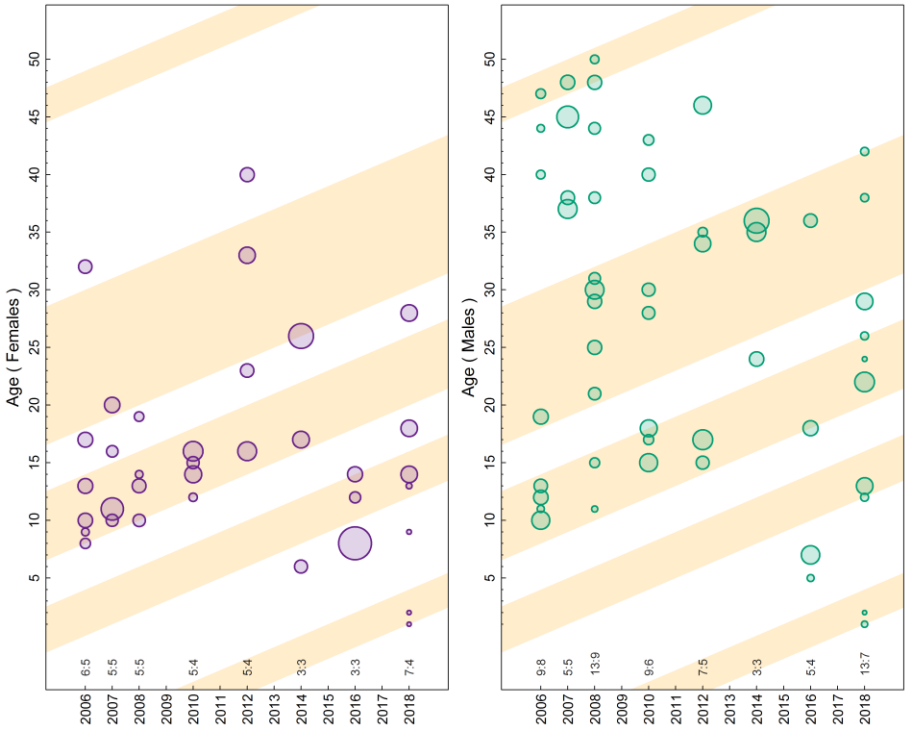

Figure D.17. WCHG Synoptic survey: coastwide BOR proportions-at-age based on age frequencies weighted by mean fish density within strata and by total stratum area within survey (Table D.13). See Figure D.13 for details on displayed numbers.

D.2.3. Ageing Error

Ageing error routinely arises as an issue in stock assessments. Figure D.18 suggests that BOR ages by the primary readers are often not reproduced consistently by secondary readers when performing spot-check analyses. The base population model for BOR, by necessity, uses an ageing error matrix. In past assessments, a matrix based on uniform distributions between minimum and maximum ages by all readers for each age (Figure D.19) have been tried; however, for BOR this matrix was not usable (model did not converge).

After many trials, one ageing error matrix was adopted that comprised: (a) narrow error for ages 1-4 from a normal distribution with quantiles 0.01 to 0.99 spanning three age classes along the diagonal (Figure D.20, left), and (b) wide error for ages 5-50 where the error was based on expanding CVs (increasing from 0.2 to 0.4 for ages 5 to 50) spanning seven age classes along the diagonal (Figure D.20, right). The narrow error structure was adopted for the young ages (1-4y) because we had adjusted the age proportions to match a presumed 2016 year class. The narrow ageing error matrix (Figure D.20, left) was used in its entirety as a sensitivity run to explore the effect of this assumption on the stock assessment results.

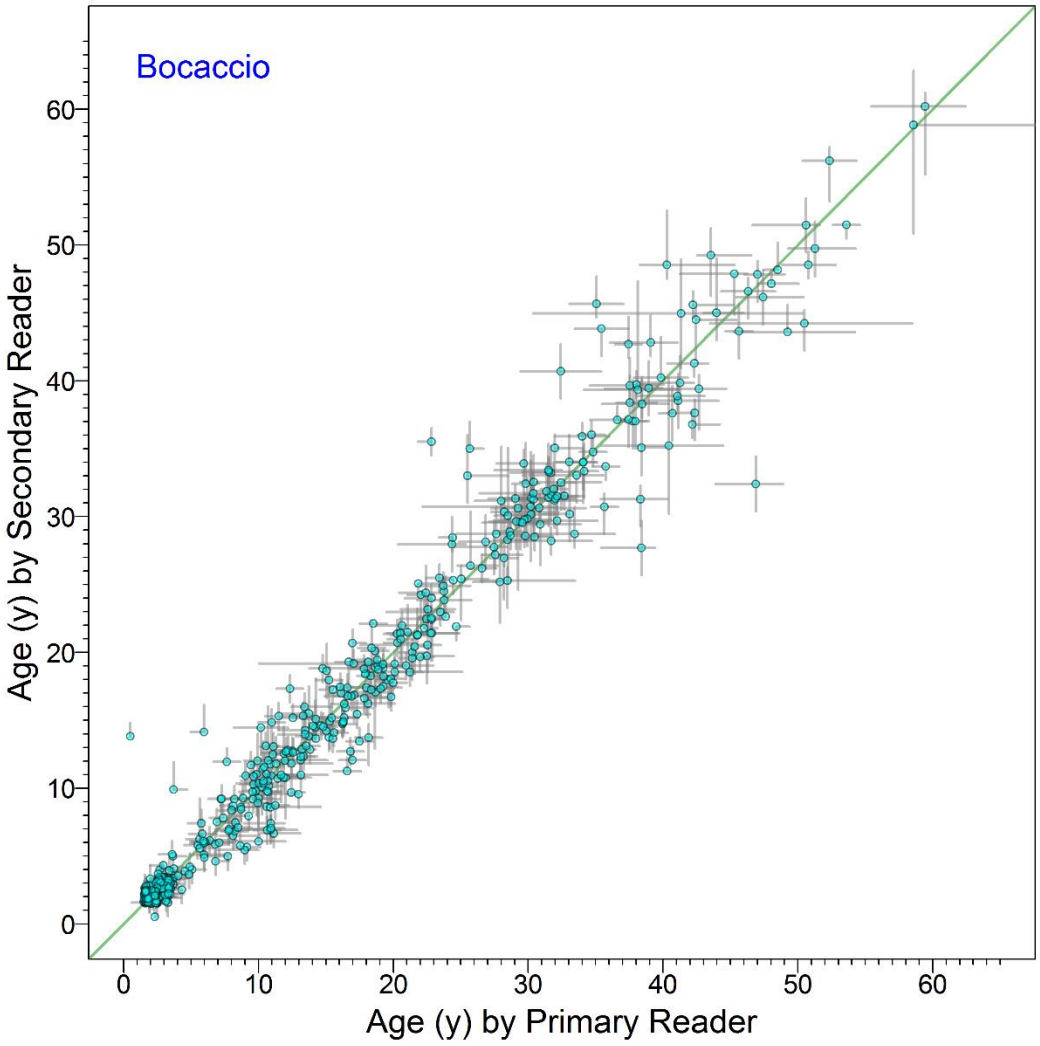

Figure D.18. Ageing error of BOR specified as the range between minimum and maximum age (grey bars) determined by primary and secondary readers for each accepted age (points). The data are jittered using a random uniform distribution between -0.5 and 0.5 y.

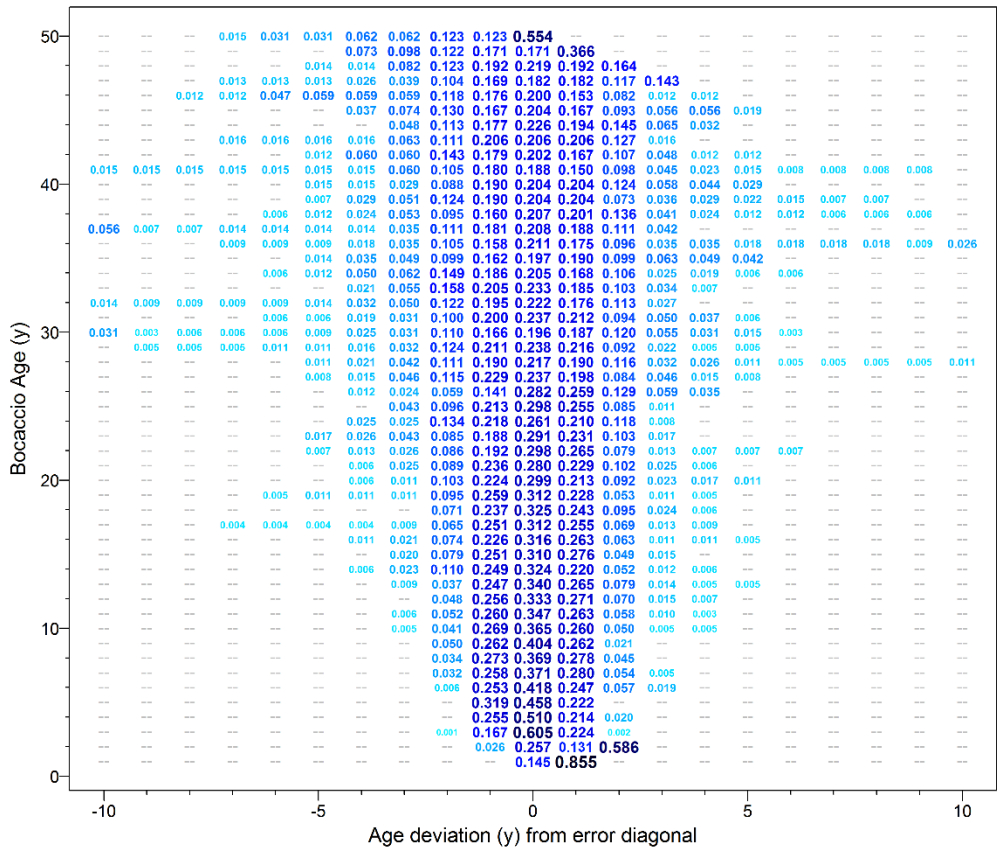

Figure D.19. Ageing error matrix calculated as cumulative probability assuming uniform distributions between minimum and maximum ages by all readers in Figure D.18, ultimately not used in the stock assessment.

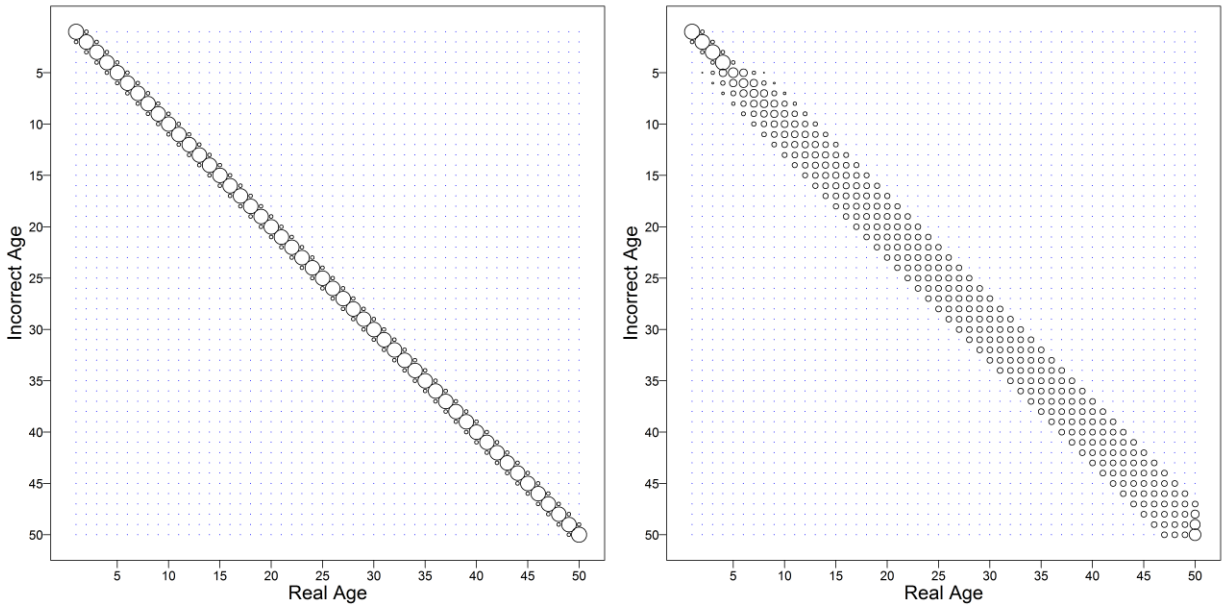

Figure D.20. Ageing error misclassification matrix (Hilborn et al. 2003) used for BOR by Awatea in this assessment. Left: 'narrow' error structure originally adopted but ultimately assigned to a sensitivity run. Right: 'wide' error structure used in the composite base case runs, including the central run.

D.2.4. Treatment of the 2016 cohort

Figure D.18 shows that there was ageing error even in the youngest ages, with misclassification occurring because of lack of experience among the agers with otoliths from such young fish in this species (Stephen Wischniowski 2019, DFO Sclerochronology Laboratory, pers. comm.). This led to problems when fitting the model to the age frequency data, with some runs putting the strong cohort into the 2015 year class rather than into 2016. Misalignment in the birth year would result in misleading projections, with the biomass increasing too soon. This was not an acceptable result, given that the main purpose of this stock assessment was to evaluate the impact of this large recruitment event.

The length frequency data associated with the large recruitment event were examined in detail by year, sex and data source (research survey or commercial). The length frequencies clearly show the recruitment of a single year class that dominates the available data, with a sharp increase in the number of observations (Table D.14) and with modal progression of lengths in each year (research: Figure 3; commercial: Figure D.22). Median length by sex and year corroborate the growth progression of the new recruitment, with the 2016 cohort showing up in the survey data as age 1 in 2017, lying between 23 and 29 cm for both males and females (Figure 3; Table D.15). The cohort grew to 31–39 cm as age 2s in both the commercial and research data and was between 39–47 cm by 2019 as age 3s (Figure 3; Figure D.22). These lengths are consistent with the length-at-age predictions made by the two growth models used in this stock assessment, with the possible exception of age one males (Table D.16).

Given this evidence that the observed strong recruitment of BOR can be assigned to a single cohort, we have chosen to assume that all juvenile BOR in the age composition data belong to the 2016 cohort by combining the observed frequencies for ages 2 to 4 into a single proportion that was placed in the appropriate age class depending on the year. This was done for both the commercial and survey data.

Table D.14. Number of BOR length frequency observations available by year and data source.

		Year			
Data source	Sex	2016	2017	2018	2019
WCVI synoptic survey	Male	11	-	231	-
	Female	6	-	186	-
	Total	17	-	417	-
QC Sound synoptic survey	Male	-	90	-	406
	Female	-	73	-	423
	Total	-	163	-	829
Hecate Strait synoptic survey	Male	-	19	-	32
	Female	-	29	-	26
	Total	-	48	-	58
All research data	Male	21	152	277	473
	Female	15	155	214	474
	Total	36	307	491	947
Commercial trawl fishery	Male	2	7	51	236
	Female	65	4	75	216
	Total	67	11	126	452

Table D.15. Median BOR length by year, sex and data source, beginning in 2016.

	Male		Female	
Year	Commercial	Research	Commercial	Research
2016	68.9	65.5	67.6	67.0
2017	69.5	26.5	69.3	26.0
2018	37.7	35.5	35.7	36.0
2019	42.4	42.0	42.5	43.5

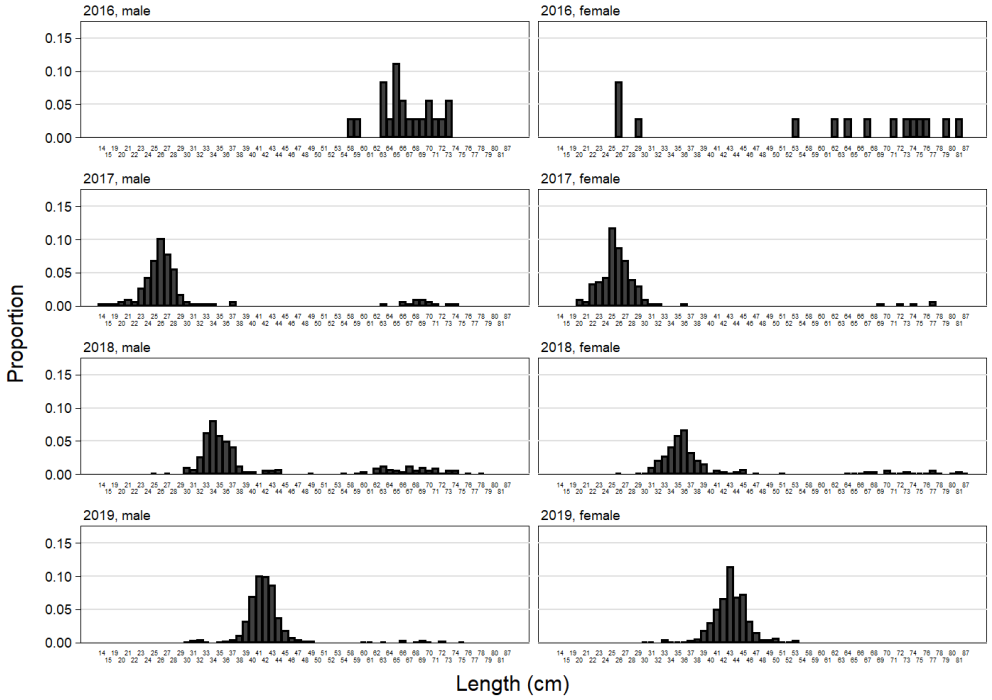

Figure D.21. Unweighted BOR length frequencies by year for all research surveys combined, beginning in 2016. The number of length observations in each year/sex cell can be found in Table D.14.

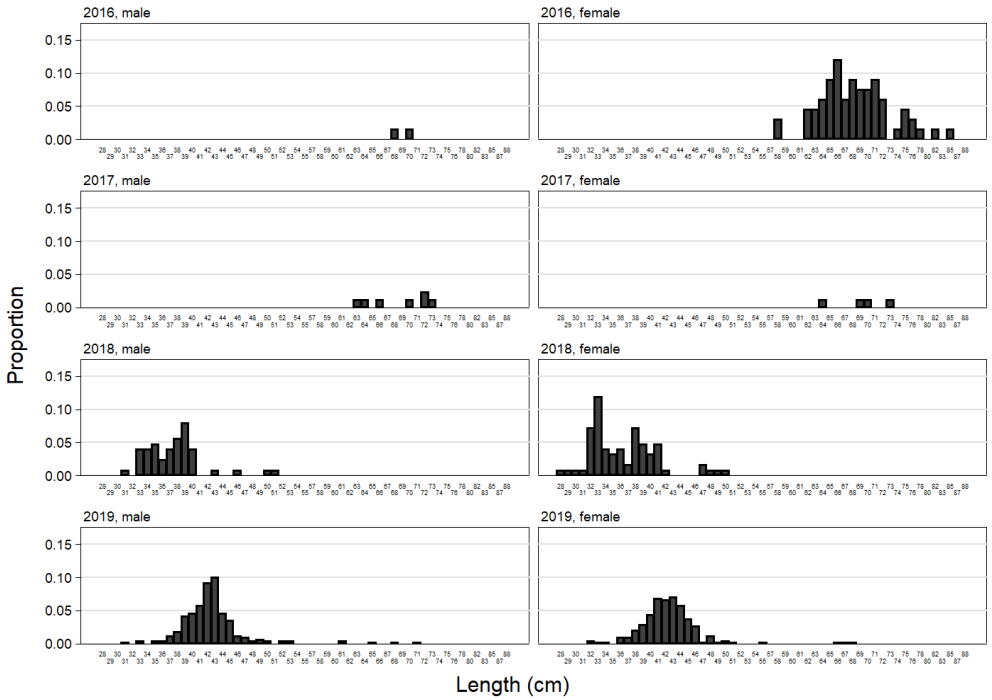

Figure D.22. Unweighted BOR length frequencies by year for all commercial observations, beginning in 2016. The number of length observations in each year/sex cell can be found in Table D.14.

Table D.16. Predicted mean length for first three ages using the growth models defined in the indicated tables.

	Model (Table D.5)		Model (Table D.4)	
Age	Male	Female	Male	Female
1	21.6	28.9	29.5	30.8
2	31.3	35.2	35.1	36.3
3	39.0	40.7	40.0	41.2

D.3. STOCK STRUCTURE ANALYSES

This stock assessment treats the BC population of BOR as a single coastwide stock. The rationale for this decision was based on analyses that showed no consistent differences when comparing data from two trial regional stock definitions:

- BCN – BC North comprising west coast Haida Gwaii (5ABCDE)
- BCS – BC South comprising west coast Vancouver Island (3CD)

Previous stock assessments of Redstripe Rockfish (RSR, Starr and Haigh 2021a) and Walleye Pollock (Starr and Haigh 2021b) each identified two stocks (one off WCHG, one further south). This separation may have been caused by the North Pacific Current bifurcation (Pickard and Emery 1982, Freeland 2006, Cummins and Freeland 2006, Batten and Freeland 2007) whereby free-swimming larvae from the two regions are kept apart. It was these observations which guided the above trial regional hypotheses; Section D.3.3 explores variation among three regions (5DE, 5ABC, 3CD).

D.3.1. Mean Weight in Commercial Fishery

Large differences in mean weight by region helped inform stock delineation decisions for Walleye Pollock (Starr and Haigh 2021b). Consequently, BOR mean weights were checked for persistent regional differences. Data used to estimate the mean weight by year were selected following the relevant guidelines in Table D.1. The initial BOR biological data contained 10,442 records which were filtered as follows:

• positive definite lengths	`len > 0`	`10,387` records
• all available years	`year = 1996:2019`	`7,054` records
• comm. trips incl. JV Hake	`ttype = c(1,4,5)`	`3,878` records
• random samples/total catch	`stype = c(1,2,6,7)`	`3,600` records
• trawl: bottom, midwater, unknown	`gear = c(1,6,8)`	`3,542` records
• sex: female, male	`sex = c(2,1)`	`2,752` records
• unsorted samples	`sort = "U"`	`1,382` records

In previous assessments, we use the GFBioSQL field called SPECIES_CATEGORY_CODE to delineate unsorted and sorted specimens ; however, for BOR this gave confusing results because occasionally samples were dominated by discards. For this reason we applied the algorithm used by Forrest et al. (2015) for Pacific Cod:

- `Unsorted (U):` `SPECIES_CATEGORY_CODE = 1 AND SAMPLE_SOURCE_CODE = 1 OR SPECIES_CATEGORY_CODE = 0 AND SAMPLE_SOURCE_CODE = 1`
- `Keepers (K):` `SPECIES_CATEGORY_CODE = 1 AND SAMPLE_SOURCE_CODE = 2 OR SPECIES_CATEGORY_CODE = 3 AND SAMPLE_SOURCE_CODE = 2 OR SPECIES_CATEGORY_CODE = 0 AND SAMPLE_SOURCE_CODE = 2`

- Discards (D): `SPECIES_CATEGORY_CODE = 1 AND SAMPLE_SOURCE_CODE = 3 OR SPECIES_CATEGORY_CODE = 4 AND SAMPLE_SOURCE_CODE = 3 OR SPECIES_CATEGORY_CODE = 0 AND SAMPLE_SOURCE_CODE = 3`

This process resulted in 1,382 BOR biological records from coastwide unsorted commercial samples. Weights were calculated from the measured lengths using the length-weight parameters specific for each regional stock hypothesis (Table D.2). The allometric parameters used were sex-specific (females, males).

Equations for the additive lognormal standardised regression model can be found in Appendix D of the RSR stock assessment (Starr and Haigh 2021a). The factors offered to the GLM were calendar year, sex, latitude, and fishing depth. The standardised and normalised mean weight trends by region resembled the coastwide trend and did not show any systematic regional differences (Figure D.23).

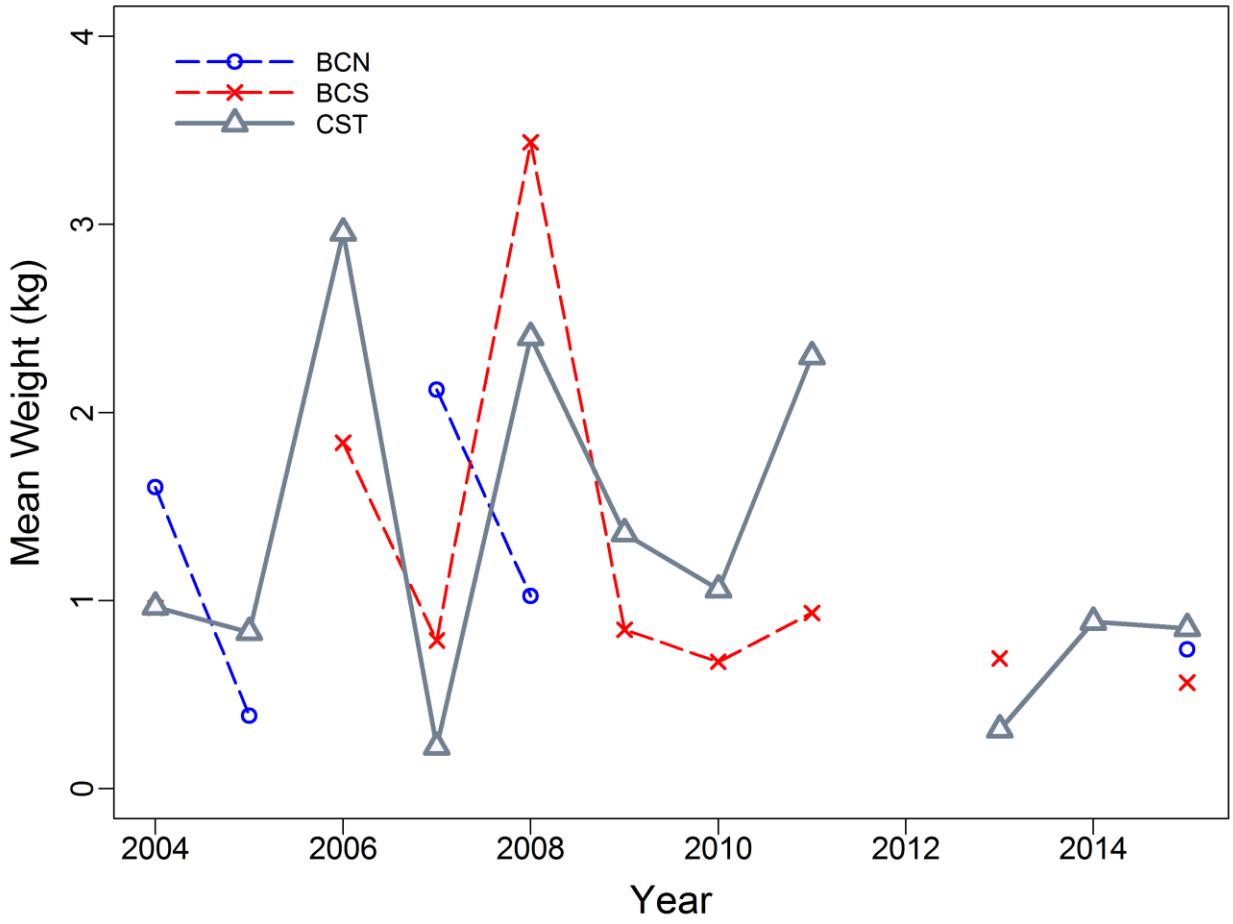

Figure D.23. Comparison of BOR mean weight series, after GLM-adjustment for various factors and normalisation, of the coastwide series (CST) with those of two subareas: BCN (5ABCDE) and BCS (3CD).

D.3.2. Fish Length Distributions

Simple comparisons of commercial length distributions across regions from the two trawl fisheries (bottom and midwater) show no evidence that length frequency distributions are markedly different between capture methods within each area (Figure D.24). This suggests that it is likely reasonable to combine data from bottom and midwater trawl gear.

When the two capture methods are combined across regions to increase the power of the comparison (Figure D.25), there is still no strong evidence of regional differences:

- length distributions largely overlap among areas;
- comparisons are reasonably consistent across years and sex.

These observations are similar to the equivalent observations from the above weight comparisons and do not support splitting BOR into component stocks.

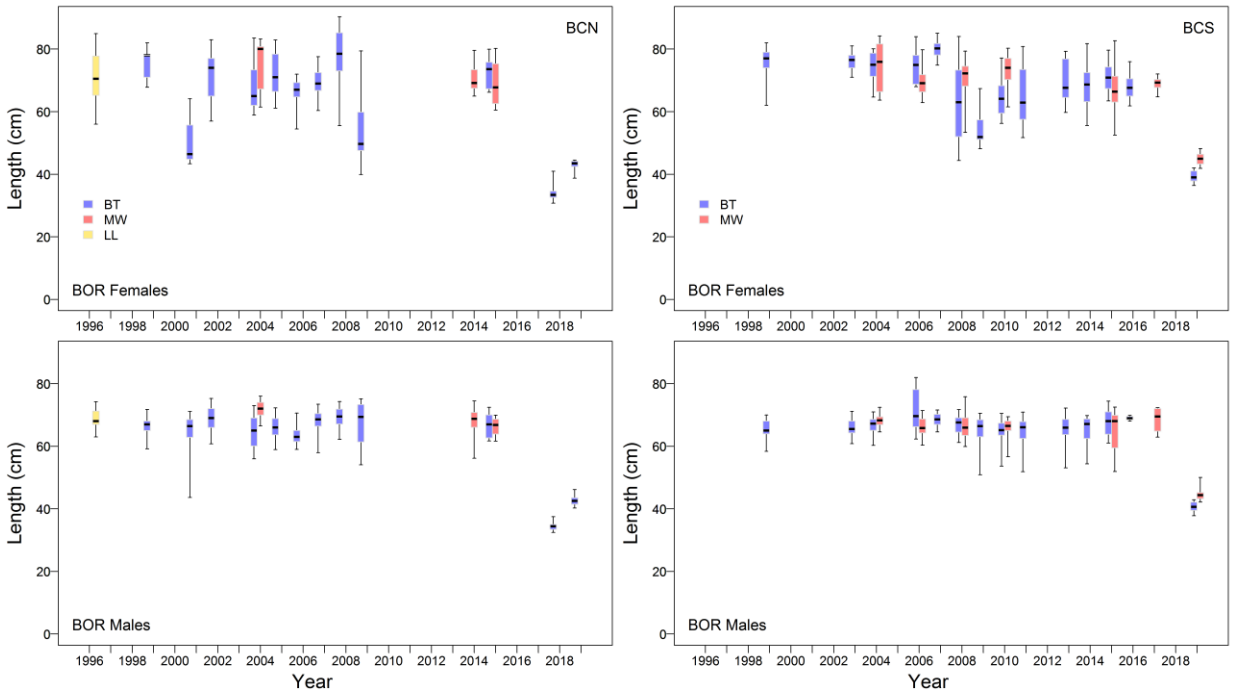

Figure D.24. Comparison of annual distributions of BOR length by sex between gear types (BT = bottom trawl, MW = midwater trawl, LL = longline) in two coastal regions: BCN (left) and BCS (right). Boxplot quantiles: 0.05, 0.25, 0.5, 0.75, 0.95.

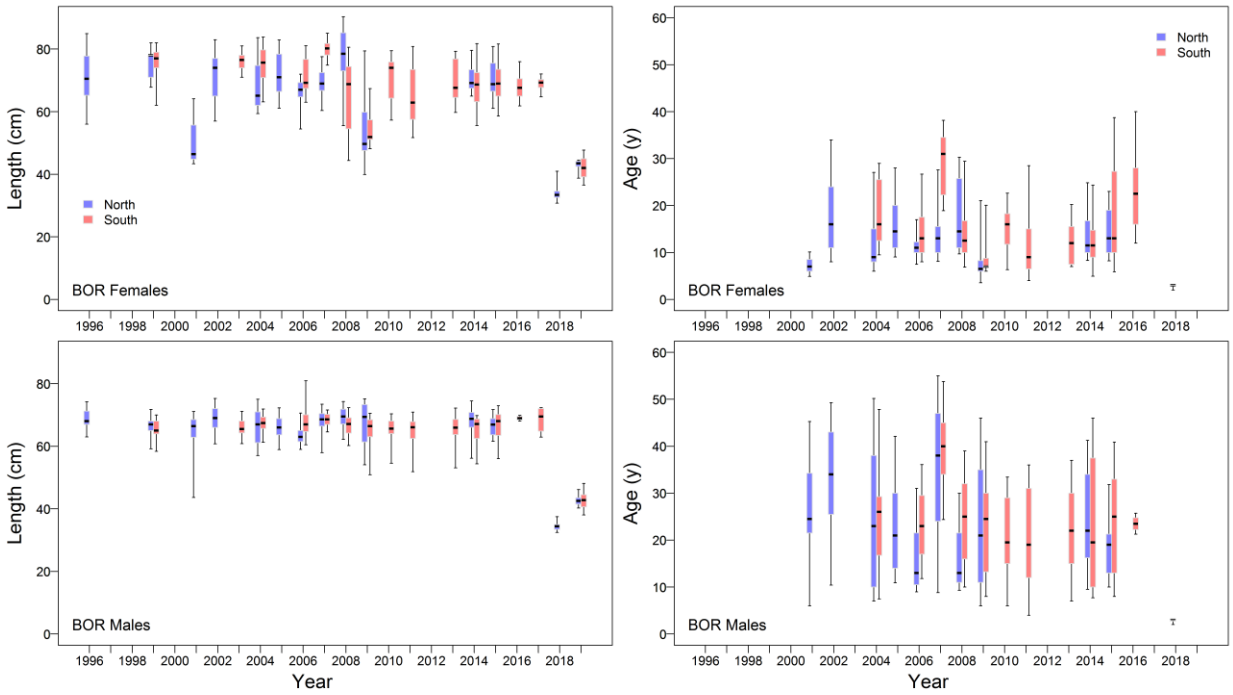

Figure D.25. Comparison of annual distributions of BOR length (left) and age (right) by sex between two coastal regions: BCN and BCS. Boxplot quantiles: 0.05, 0.25, 0.5, 0.75, 0.95.

The distribution of BOR lengths from a variety of surveys (Figure D.26) show similarities in mean length and highlight a large recruitment event of fish born in 2016:

- similar length frequencies until 2017 when age-1 fish appear in multiple surveys;
- a steady increase in size from 2017 to 2019, especially evident in the shrimp trawl surveys, the HS synoptic surveys, and the QCS synoptic surveys;
- a less-defined recruitment signal in the WCHG survey;
- no signal from the IPHC longline survey because large hooks catch only mature specimens (Brian Mose 2019, Groundfish Technical Advisory Committee, pers. comm.).

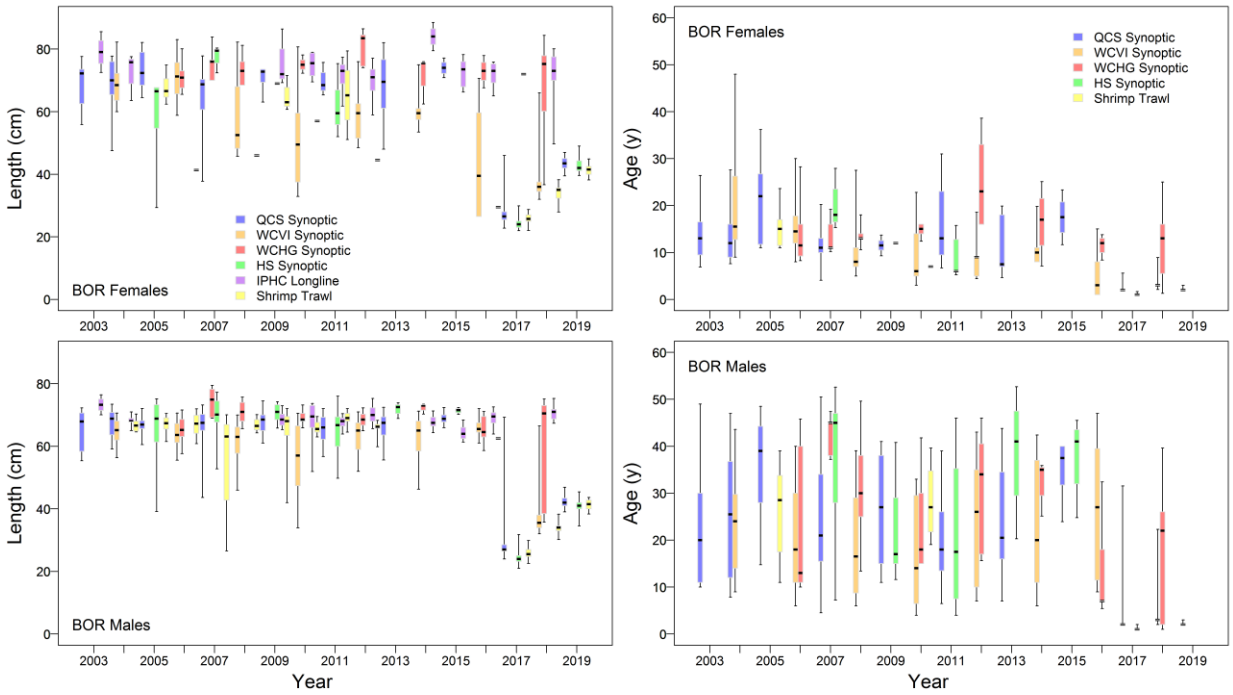

Figure D.26. Comparison of annual distributions of BOR length (left) and age (right) among six surveys (four synoptic trawl, one halibut longline, and one shrimp trawl). Boxplot quantiles: 0.05, 0.25, 0.5, 0.75, 0.95.

D.3.3. Comparison of Growth Models

A comparison of growth model fits between commercial and survey samples among the three regions outlined in Table D.4 suggests that, aside from the obvious difference between the sexes, there is a slight bias for fish to be larger going from south to north (Figure D.27). Using only survey data, which were more abundant and more likely to be sampled without bias, von Bertalanffy growth models were estimated using a Bayesian model (`rstan` package: Stan Development Team 2018). MCMC quantile distributions of the regional estimated parameters show a that males may be larger in the north (5DE) than further south, but female asymptotic length (L_∞) displayed more variability, with overlap among the regions (Figure D.28). The only outlier for the growth parameter (κ) was for 3CD females, which was fitted with a lower growth rate. The growth curves based on the median parameter estimates also suggest that area 5DE might host larger fish than in 5ABC and 3CD (Figure D.29); however, the uncertainty bounds on the parameter estimates, especially those for females, are too wide to justify separate stocks along the BC coast at this time.

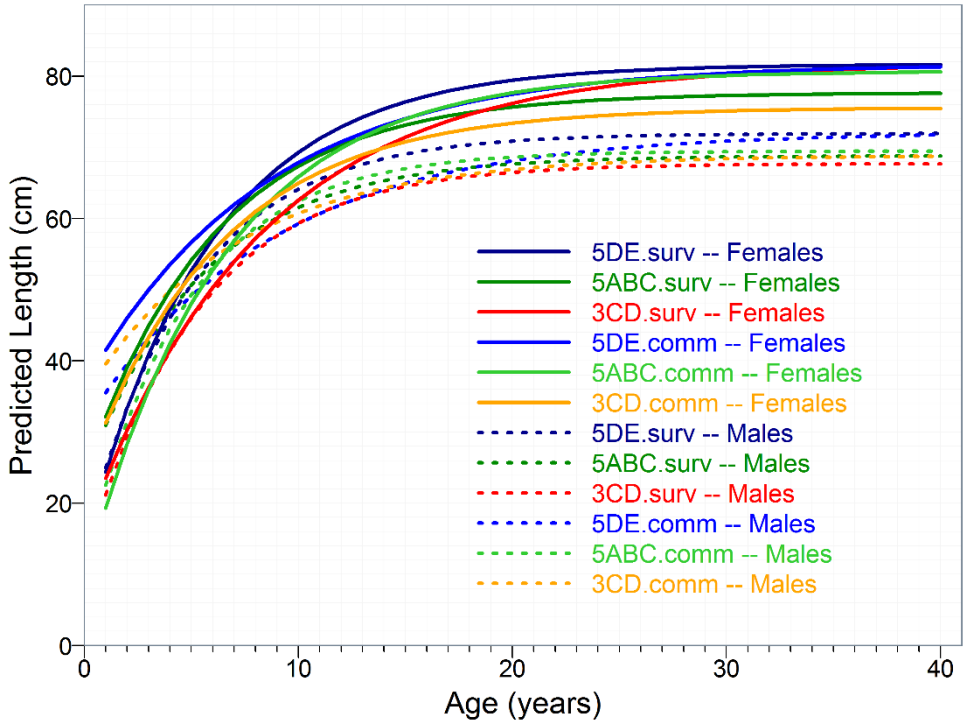

Figure D.27. Comparison of von Bertalanffy fits to BOR by sex and region using von Bertalanffy parameters from Table D.4.

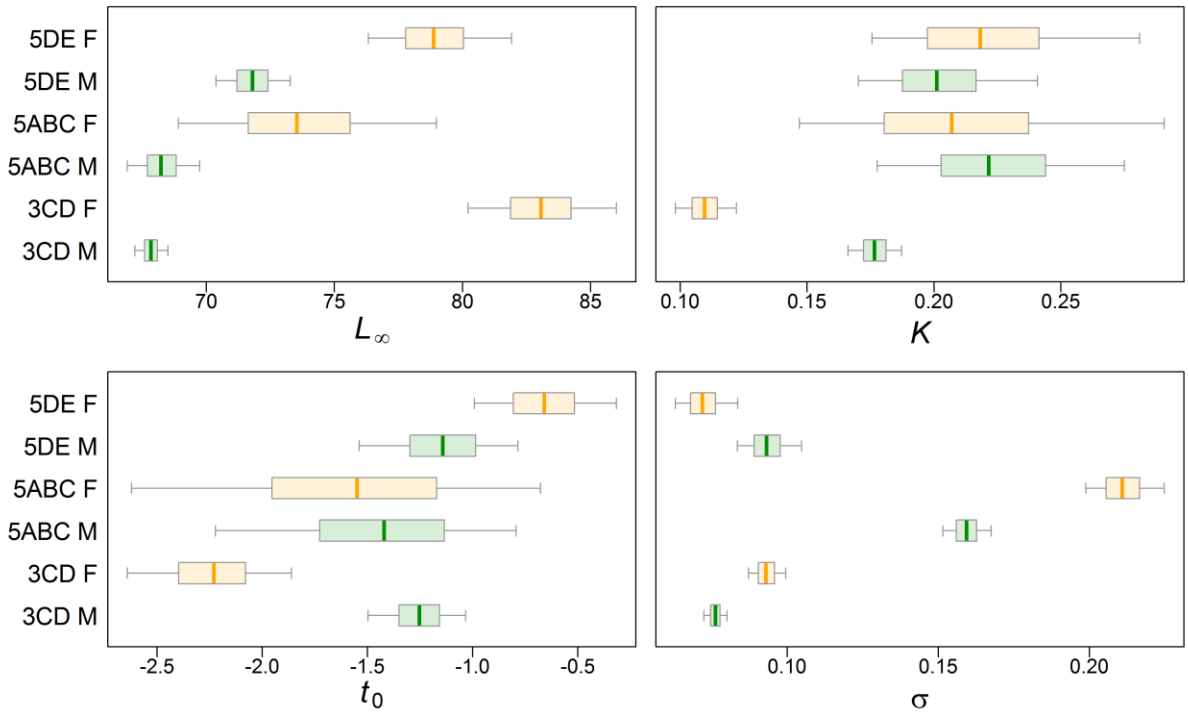

Figure D.28. MCMC samples (4 chains, 1000 each) for von Bertalanffy parameters using commercial fishery BOR length-age data by region. Boxplots (orange=females, green=males) show 0.05, 0.25, 0.5, 0.75, & 0.95 quantiles.

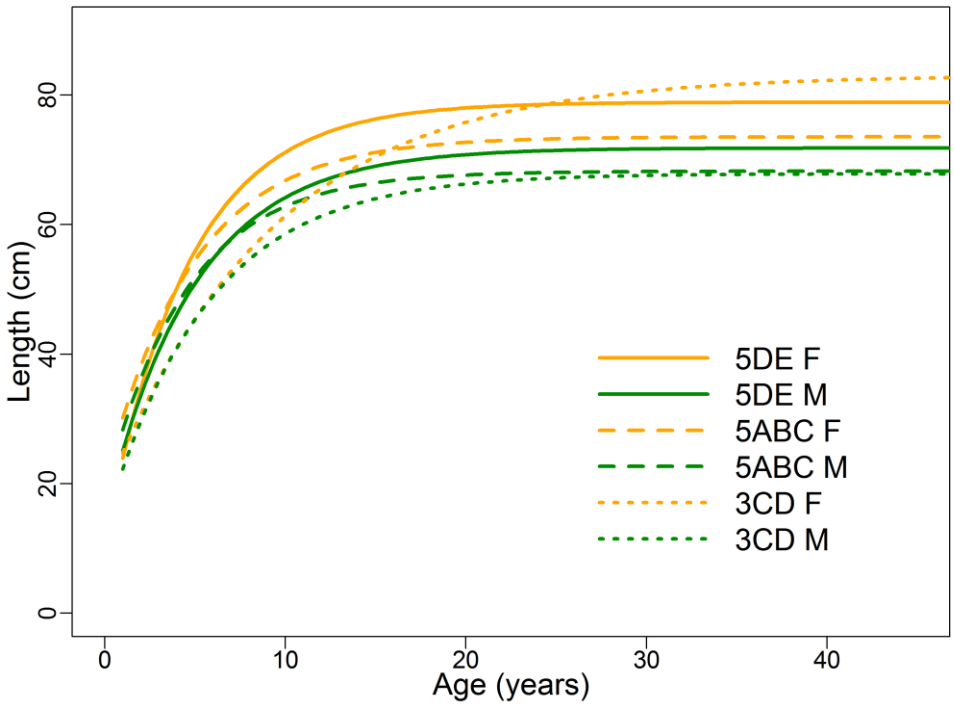

Figure D.29. von Bertalanffy fits using MPD parameter estimates from the rstan model fit to survey BOR length-age data by region. Line colour indicates sex (orange=female, green=male); line type indicates region (solid=5DE, dashed=5ABC, dotted=3CD).

D.4. REFERENCES – BIOLOGY

Batten, S.D. and Freeland, H.J. 2007. Plankton populations at the bifurcation of the North Pacific Current. Fisheries Oceanography 16(6): 536-546.

Cummins, P.F. and Freeland, H.J. 2007. Variability of the North Pacific Current and its bifurcation. Progress in Oceanography 75(2): 253-265.

DFO. 2022. Proceedings of the Pacific regional peer review of the Redstripe Rockfish (*Sebastes proriger*) stock assessment for British Columbia in 2018; June 13-14, 2018. DFO Can. Sci. Advis. Sec. Proceed. Ser. In press.

Forrest, R.E., Rutherford, K.L., Lacko, L., Kronlund, A.R., Starr, P.J. and McClelland, E.K. 2015. Assessment of Pacific Cod (*Gadus macrocephalus*) for Hecate Strait (5CD) and Queen Charlotte Sound (5AB) in 2013. DFO Can. Sci. Advis. Sec. Res. Doc. 2015/052. xii + 197 p.

Freeland, H.J. 2006. What proportion of the North Pacific Current finds its way into the Gulf of Alaska? Atmosphere-Ocean 44(4): 321-330.

Haist, V., Breen, P.A. and Starr, P.J. 2009. A multi-stock, length-based assessment model for New Zealand rock lobster (*Jasus edwardsii*). N.Z. J. Mar. Freshw. Res. 43: 355-371.

Hamel, O.S. 2015. A method for calculating a meta-analytical prior for the natural mortality rate using multiple life history correlates. ICES J. Mar. Sci. 72(1): 62-69.

Hicks, A.C. and Wetzel, C.R. 2015. The status of Widow Rockfish (*Sebastes entomelas*) along the U.S. west coast in 2015. Stock Assessment and Fishery Evaluation (SAFE) , NMFS, NOAA.

Hoenig, J.M. 1983. Empirical use of longevity data to estimate mortality rates. Fish. Bull. 82(1): 898-903.

MacLellan, S.E. 1997. How to age rockfish (*Sebastes*) using *S. alutus* as an example – the otolith burnt section technique. Can. Tech. Rep. Fish. Aquat. Sci. 2146: 39 p.

Pickard, G.L. and Emery, W.J. 1982. Descriptive Physical Oceanography, an Introduction. Pergamon Press, Oxford UK, 4th (SI) enlarged ed.

Quinn, T.J.I. and Deriso, R.B. 1999. Quantitative Fish Dynamics. Oxford University Press, New York, NY.

R Core Team. 2019. R: A Language and Environment for Statistical Computing. R Foundation for Statistical Computing, Vienna, Austria.

Stan Development Team. 2018. rstan: the R interface to Stan. R package version 2.18.2.

Stanley, R.D., Starr, P. and Olsen, N. 2009. Stock assessment for Canary rockfish (*Sebastes pinniger*) in British Columbia waters. DFO Can. Sci. Advis. Sec. Res. Doc. 2009/013. xxii + 198 p.

Starr, P.J. and Haigh, R. 2021a. Redstripe Rockfish (*Sebastes proriger*) stock assessment for British Columbia in 2018. DFO Can. Sci. Advis. Sec. Res. Doc. 2021/014. vii + 340 p.

Starr, P.J. and Haigh, R. 2021b. Walleye Pollock (*Theragra chalcogramma*) stock assessment for British Columbia in 2017. DFO Can. Sci. Advis. Sec. Res. Doc. 2021/004. vii + 265 p.

Then, A.Y., Hoenig, J.M., Hall, N.G. and Hewitt, D.A. 2015. Evaluating the predictive performance of empirical estimators of natural mortality rate using information on over 200 fish species. ICES J. Mar. Sci. 72(1): 82-92.

Westrheim, S. 1975. Reproduction, maturation, and identification of larvae of some *Sebastes* (Scorpaenidae) species in the northeast Pacific Ocean. J. Fish. Res. Bd. Can. 32: 2399-2411.

APPENDIX E. MODEL EQUATIONS

E.1. INTRODUCTION

The stock assessment of Bocaccio uses a sex-specific, age-structured model called 'Awatea' in a Bayesian framework to reconstruct a population trajectory and its uncertainty. The model can simultaneously estimate the steepness of the stock-recruitment function and separate mortalities for the sexes. This approach follows that used in BC stock assessments since 2010:

- 2019 – Widow Rockfish for the coast of BC (Starr and Haigh 2021*a*),
- 2018 – Redstripe Rockfish in PMFC areas 5DE and 3CD5ABC (Starr and Haigh 2021*b*),
- 2017 – Pacific Ocean Perch (POP) in Queen Charlotte Sound (Haigh et al. 2018*a*),
- 2014 – Yellowtail Rockfish for the coast of BC (DFO 2015),
- 2013 – Silvergray Rockfish along the Pacific coast of Canada (Starr et al. 2016),
- 2013 – Rock Sole in BC (Holt et al. 2016),
- 2012 – POP off the west coast of Vancouver Island (Edwards et al. 2014*b*),
- 2012 – POP off the west coast of Haida Gwaii (Edwards et al. 2014*a*),
- 2011 – Yellowmouth Rockfish along the Pacific coast of Canada (Edwards et al. 2012*a*),
- 2010 – POP in Queen Charlotte Sound (Edwards et al. 2012*b*).

The model structure is the same as that used previously, and, as for all the assessments above except 5ABC POP in 2010, this assessment used the weighting scheme of Francis (2011) described in Section E.6.2.

The Awatea model is a modified version of the Coleraine statistical catch-at-age software (Hilborn et al. 2003), and was originally created in 2006 and maintained by Allan Hicks (then at Univ. Washington, now at IPHC). There have been no changes to the code since 2012. Awatea is a platform for implementing the AD (Automatic Differentiation) Model Builder software (ADMB Project 2009), which provides (a) maximum posterior density estimates using a function minimiser and automatic differentiation, and (b) an approximation of the posterior distribution of the parameters using the Markov Chain Monte Carlo (MCMC) method, specifically using the Hastings-Metropolis algorithm (Gelman et al. 2004).

Running of Awatea is streamlined using custom R code (Haigh et al. 2018*b*), rather than through the original Microsoft Excel 97/2000 implementation (Hilborn et al. 2003). Figures and tables of output were automatically produced in R, an environment for statistical computing and graphics (R Core Team 2019), using code adapted from the R packages `scape` (Magnusson 2009) and `plotMCMC`, previously called `scapeMCMC` (Magnusson and Stewart 2020). The R function `Sweave` (Leisch 2002) automatically collates, via LaTeX, the large amount of figures and tables into a single '`.pdf`' file for each model run.

Below are details of the age-structured model, the Bayesian procedure, the reweighting scheme, the prior distributions, and the methods for calculating reference points and performing projections.

E.2. MODEL ASSUMPTIONS

The assumptions of the model are:

1. The assessed population of Bocaccio (BC) was treated as a single stock in combined PMFC areas 3CD+5ABCDE.

2. Annual catches were taken by two fisheries: trawl (bottom and midwater) and 'other' (halibut longline, sablefish trap, salmon troll, rockfish hook & line, and lingcod troll) known without error, and occurred in the middle of each year.
3. A time-invariant Beverton-Holt stock-recruitment relationship was assumed, with log-normal error structure.
4. Selectivity was different between surveys but the same between sexes, and remained invariant over time. Selectivity parameters were estimated when ageing data were available.
5. Natural mortality M was fixed at three values (0.07, 0.08, 0.09) for females and males, and held invariant over time.
6. Growth parameters were fixed and assumed to be invariant over time.
7. Maturity-at-age parameters for females were fixed and assumed to be invariant over time. Male maturity did not need to be considered, because it was assumed that there were always sufficient mature males.The mature male population is not tracked by this model, with spawning biomass expressed as mature females only.
8. Recruitment at age 1 was 50% females and 50% males.
9. Fish ages determined by surface ageing methods (before 1978) were too biased to use (Beamish 1979); however, this methodology was deemed suitable for very young rockfish (ages 1-3); however, no surface-read otoliths were used for BOR. Ages determined using the otolith break-and-burn methodology (MacLellan 1997) were aged without error.
10. Commercial samples of catch-at-age in a given year were assumed to be representative of the fishery if there were $\geq$2 samples in that year.
11. Relative abundance indices were assumed to be proportional to the vulnerable biomass at the mid point of the year, after half of the catch and half of the natural mortality had been accounted for.
12. The age composition samples were assumed to come from the middle of the year after half of the catch and half of the natural mortality had been accounted for.

E.3. MODEL NOTATION AND EQUATIONS

The notation for the model is given in Table E.1, the model equations in Tables E.2 and E.3, and description of prior distributions for estimated parameters in Table E.4. The model description is divided into the deterministic components, stochastic components and Bayesian priors. Full details of notation and equations are given after the tables.

The main structure is that the deterministic components in Table E.2 can iteratively calculate numbers of fish in each age class (and of each sex) through time. The only requirements are the commercial catch data, weight-at-age and maturity data, and known fixed values for all parameters.

Given that fixed values are not known for all parameters, many of them need to be estimated, and stochasticity needs to be added to recruitment. This is accomplished by the stochastic components given in Table E.3.

Incorporation of the prior distributions for estimated parameters gives the full Bayesian implementation, the goal of which is to minimise the objective function $f(\boldsymbol{\Theta})$ given by (E.23). This function is derived from the deterministic, stochastic and prior components of the model.

Table E.1. Notation for the Awatea catch-at-age model (continued overleaf).

Symbol	Description and units
	Indices (all subscripts)
a	age class, where $a = 1, 2, 3, ...A$, and $A \in \{50\}$ is the accumulator age class
t	model year, where $t = 1, 2, 3, ...T$, corresponds to actual years: 1935, ..., 2020, and $t = 0$ represents unfished equilibrium conditions
g	index for series (abundance|composition) data: 1 – QCS Synoptic trawl survey series 2 – WCVI Synoptic trawl survey series 3 – WCHG Synoptic trawl survey series 4 – HS Synoptic trawl survey series 5 – NMFS Triennial trawl survey series 6 – GIG Historical trawl survey series 7 – Trawl fishery|CPUE index 8 – Other fisheries index
s	sex, $1 =$ females, $2 =$ males
	Index ranges
A	accumulator age-class, $A \in \{50\}$
T	number of model years, $T = 86$
$\mathbf{T}_g$	sets of model years for survey abundance indices from series g, listed here for clarity as actual years (subtract 1934 to give model year t): $\mathbf{T}_1$ = {2003:2005, 2007, 2009, 2011, 2013, 2015, 2017, 2019} $\mathbf{T}_2$ = {2004, 2006, 2008, 2010, 2012, 2014, 2016, 2018} $\mathbf{T}_3$ = {2006:2008, 2010, 2012, 2014, 2016, 2018} $\mathbf{T}_4$ = {2005, 2007, 2009, 2011, 2013, 2015, 2017, 2019} $\mathbf{T}_5$ = {1980, 1983, 1989, 1992, 1995, 1998, 2001} $\mathbf{T}_6$ = {1967, 1969, 1971, 1973, 1976:1977, 1984} $\mathbf{T}_7$ = {1996, ..., 2012}
$\mathbf{U}_g$	sets of model years with proportion-at-age data for series g: $\mathbf{U}_1$ = {2003:2005, 2007, 2009, 2011, 2013, 2015, 2017, 2019} $\mathbf{U}_2$ = {2004, 2006, 2008, 2010, 2012, 2014, 2016, 2018} $\mathbf{U}_3$ = {2006:2008, 2010, 2012, 2014, 2016, 2018} $\mathbf{U}_4$ = {2007, 2009, 2011, 2013, 2015, 2017} $\mathbf{U}_7$ = {2002, 2004:2011, 2014:2015, 2018}
	Data and fixed parameters
p_{atgs}	observed weighted proportion of fish from series g in each year $t \in \mathbf{U}_g$ that are age-class a and sex s; so $\Sigma_{a=1}^{A}\Sigma_{s=1}^{2} p_{atgs} = 1$ for each $t \in \mathbf{U}_g$
n_{tg}	effective sample size that yields corresponding p_{atgs}
C_t	observed catch biomass (tonnes) in year $t = 1, 2, ..., T-1$
w_{as}	average weight (kg) of individual of age-class a of sex s from fixed parameters
m_a	proportion of age-class a females that are mature, fixed from data
I_{tg}	biomass estimates (tonnes) from surveys $g = 1, ..., 6$, for year $t \in \mathbf{T}_g$, tonnes
κ_{tg}	standard deviation of I_{tg}
σ_R	standard deviation parameter for recruitment process error, $\sigma_R = 0.9$

Symbol	Description and units
	Estimated parameters
$\boldsymbol{\Theta}$	set of estimated parameters
R_0	virgin recruitment of age-1 fish (numbers of fish, 1000s)
M_s	natural mortality rate for sex $s = 1, 2$ (M fixed for the BOR assessment)
h	steepness parameter for Beverton-Holt recruitment
q_g	catchability for survey series $g = 1, ..., 6$
μ_g	age of full selectivity for females for series $g = 1, ..., 4, 7$
Δ_g	shift in vulnerability for males for series $g = 1, ..., 4, 7$
v_{gL}	variance parameter for left limb of selectivity curve for series $g = 1, ..., 4, 7$
s_{ags}	selectivity for age-class a, series $g = 1, ..., 4, 7$, and sex s, calculated from the parameters μ_g, Δ_g and v_{gL}
α, β	alternative formulation of recruitment: $\alpha = (1-h)B_0/(4hR_0)$ and $\beta = (5h-1)/4hR_0$
$\widehat{x}$	estimated value of observed data x
	Derived states
N_{ats}	number of age-class a fish (1000s) of sex s at the start of year t
u_{ats}	proportion of age-class a and sex s fish in year t that are caught
u_t	exploitation ratio of total catch to vulnerable biomass in the middle of the year t
B_t	spawning biomass (tonnes mature females) at the start of year $t = 1, 2, 3, ..., T$
B_0	virgin spawning biomass (tonnes mature females) at the start of year 0
R_t	recruitment of age-1 fish (numbers of fish, 1000s) in year $t = 1, 2, ..., T-1$
V_t	vulnerable biomass (tonnes males + females) in the middle of year $t = 1, 2, 3, ..., T$
	Deviations and likelihood components
ϵ_t	Recruitment deviations arising from process error
$\log L_1(\boldsymbol{\Theta}\|\{\epsilon_t\})$	log-likelihood component related to recruitment residuals
$\log L_2(\boldsymbol{\Theta}\|\{\widehat{p}_{atgs}\})$	log-likelihood component related to estimated proportions-at-age
$\log L_3(\boldsymbol{\Theta}\|\{\widehat{I}_{tg}\})$	log-likelihood component related to estimated survey biomass indices
$\log L(\boldsymbol{\Theta})$	total log-likelihood
	Prior distributions and objective function
$\pi_j(\boldsymbol{\Theta})$	Prior distribution for parameter j
$\pi(\boldsymbol{\Theta})$	Joint prior distribution for all estimated parameters
$f(\boldsymbol{\Theta})$	Objective function to be minimised

Table E.2. Deterministic components. Using the catch, weight-at-age and maturity data, with fixed values for all parameters, the initial conditions are calculated from (E.4)-(E.6), and then state dynamics are iteratively calculated through time using the main equations (E.1)-(E.3), selectivity functions (E.7) and (E.8), and the derived states (E.9)-(E.13). Estimated observations for survey biomass indices and proportions-at-age can then be calculated using (E.14) and (E.15). In Table E.3, the estimated observations of these are compared to data.

Deterministic components

State dynamics ($2 \leq t \leq T,\ s = 1, 2$)

$$N_{1ts} = 0.5R_t \tag{E.1}$$

$$N_{ats} = e^{-M_s}(1 - u_{a-1,t-1,s})N_{a-1,t-1,s}\,; \quad 2 \leq a \leq A-1 \tag{E.2}$$

$$N_{Ats} = e^{-M_s}(1 - u_{A-1,t-1,s})N_{A-1,t-1,s} + e^{-M_s}(1 - u_{A,t-1,s})N_{A,t-1,s} \tag{E.3}$$

Initial conditions ($t = 1$)

$$N_{a1s} = 0.5R_0 e^{-M_s(a-1)}\,; \quad 1 \leq a \leq A-1,\ s = 1, 2 \tag{E.4}$$

$$N_{A1s} = 0.5R_0\,\frac{e^{-M_s(A-1)}}{1 - e^{-M_s}}\,; \quad s = 1, 2 \tag{E.5}$$

$$B_0 = B_1 = \sum_{a=1}^{A} w_{a1} m_a N_{a11} \tag{E.6}$$

Selectivities ($g = 1, ..., 8$)

$$s_{ag1} = \begin{cases} e^{-(a-\mu_g)^2/v_{gL}}, & a \leq \mu_g \\ 1, & a > \mu_g \end{cases} \tag{E.7}$$

$$s_{ag2} = \begin{cases} e^{-(a-\mu_g-\Delta_g)^2/v_{gL}}, & a \leq \mu_g + \Delta_g \\ 1, & a > \mu_g + \Delta_g \end{cases} \tag{E.8}$$

Derived states ($1 \leq t \leq T-1$)

$$B_t = \sum_{a=1}^{A} w_{a1} m_a N_{at1} \tag{E.9}$$

$$R_t = \frac{4hR_0 B_{t-1}}{(1-h)B_0 + (5h-1)B_{t-1}} \quad \left(\equiv \frac{B_{t-1}}{\alpha + \beta B_{t-1}}\right) \tag{E.10}$$

$$V_t = \sum_{s=1}^{2}\sum_{a=1}^{A} e^{-M_s/2}\, w_{as}\, s_{a7,8s}\, N_{ats} \tag{E.11}$$

$$u_t = \frac{C_t}{V_t} \tag{E.12}$$

$$u_{ats} = s_{a7,8s}\, u_t\,; \quad 1 \leq a \leq A,\ s = 1, 2 \tag{E.13}$$

Estimated observations

$$\widehat{I}_{tg} = q_g \sum_{s=1}^{2}\sum_{a=1}^{A} e^{-M_s/2}(1 - u_{ats}/2) w_{as} s_{ags} N_{ats}\,; \quad t \in \mathbf{T}_g,\ g = 1, ..., 7 \tag{E.14}$$

$$\widehat{p}_{atgs} = \frac{e^{-M_s/2}(1 - u_{ats}/2) s_{ags} N_{ats}}{\sum_{s=1}^{2}\sum_{a=1}^{A} e^{-M_s/2}(1 - u_{ats}/2) s_{ags} N_{ats}};\ {\scriptstyle 1\leq a\leq A,\ t\in\mathbf{U}_g,\ g=1,...,4,7,\ s=1,2} \tag{E.15}$$

Table E.3. Stochastic components. Calculation of likelihood function $L(\boldsymbol{\Theta})$ for stochastic components of the model in Table E.2, and resulting objective function $f(\boldsymbol{\Theta})$ to be minimised.

Stochastic components

Estimated parameters

$$\boldsymbol{\Theta} = \{R_0; M_{1,2}; h; q_{1,\ldots,7}; \mu_{1,\ldots,4,7}; \Delta_{1,\ldots,4,7}; v_{1,\ldots,4,7L}\} \tag{E.16}$$

Recruitment deviations

$$\epsilon_t = \log R_t - \log B_{t-1} + \log(\alpha + \beta B_{t-1}) + \sigma_R^2/2\,; \;\; 1 \leq t \leq T-1 \tag{E.17}$$

Log-likelihood functions

$$\log L_1(\boldsymbol{\Theta}|\{\epsilon_t\}) = -\frac{T}{2}\log 2\pi - T\log\sigma_R - \frac{1}{2\sigma_R^2}\sum_{t=1}^{T-1}\epsilon_t^2 \tag{E.18}$$

$$\begin{aligned}\log L_2(\boldsymbol{\Theta}|\{\widehat{p}_{atgs}\}) = &-\frac{1}{2}\sum_{g=1,\ldots,4,7}\sum_{a=1}^{A}\sum_{t\in\mathbf{U}_g}\sum_{s=1}^{2}\log\left[p_{atgs}(1-p_{atgs}) + \frac{1}{10A}\right] \\ &+ \sum_{g=1,\ldots,4,7}\sum_{a=1}^{A}\sum_{t\in\mathbf{U}_g}\sum_{s=1}^{2}\log\left[\exp\left\{\frac{-(p_{atgs}-\widehat{p}_{atgs})^2\, n_{tg}}{2\left(p_{atgs}(1-p_{atgs}) + \frac{1}{10A}\right)}\right\} + \frac{1}{100}\right]\end{aligned} \tag{E.19}$$

$$\log L_3(\boldsymbol{\Theta}|\{\widehat{I}_{tg}\}) = \sum_{g=1,\ldots,4,7}\sum_{t\in\mathbf{T}_g}\left[-\frac{1}{2}\log 2\pi - \log\kappa_{tg} - \frac{(\log I_{tg} - \log\widehat{I}_{tg})^2}{2\kappa_{tg}^2}\right] \tag{E.20}$$

$$\log L(\boldsymbol{\Theta}) = \sum_{i=1}^{3}\log L_i(\boldsymbol{\Theta}|\cdot) \tag{E.21}$$

Joint prior distribution and objective function

$$\log(\pi(\boldsymbol{\Theta})) = \sum_j \log(\pi_j(\boldsymbol{\Theta})) \tag{E.22}$$

$$f(\boldsymbol{\Theta}) = -\log L(\boldsymbol{\Theta}) - \log(\pi(\boldsymbol{\Theta})) \tag{E.23}$$

Table E.4. Details for estimation of parameters, including prior distributions with corresponding means and standard deviations, bounds between which parameters are constrained, and initial values to start the minimisation procedure for the MPD (mode of the posterior density) calculations. For uniform prior distributions, the bounds completely parameterise the prior. The resulting non-uniform prior probability density functions are the $\pi_j(\mathbf{\Theta})$ functions that contribute to the joint prior distribution in (E.22).

Parameter	Phase	Prior distribution	Mean, SD	Bounds	Initial value
R_0	1	uniform	—	[1, 10e7]	10e4
M_1, M_2	-	fixed	—	—	{0.07,0.08,0.09}
A	-	fixed	—	—	50
h	5	beta	4.574, 2.212	[0.2, 0.999]	0.674
$\log \epsilon_t$	2	normal	0, 0.9	[-15, 15]	0
$\log q_{1,...,4}$	1	uniform	0, 0.6	[-12, 5]	-5
$\log q_7$	1	uniform	0, 0.1	[-15, 15]	-1.609
$\mu_{1,..,4}$	3	normal	12, 3	[5, 40]	12
$\mu_{5,6}$	-	fixed	12, 3	[5, 40]	12
μ_7	3	normal	12, 3	[5, 30]	12
μ_8	-	fixed	12, 3	[5, 30]	12
$\log v_{1,2,3,4,7}$	4	normal	3.6, 0.9	[-15, 15]	3.6
$\log v_{5,6,8}$	-	fixed	3.6, 0.9	[-15, 15]	3.6
$\Delta_{1,2,3,4,7}$	4	normal	1, 0.3	[-8. 10]	1
$\Delta_{5,6,8}$	-	fixed	1, 0.3	[-8, 10]	1

E.4. DESCRIPTION OF DETERMINISTIC COMPONENTS

Notation (Table E.1) and set up of the deterministic components (Table E.2) are now described.

E.4.1. Age classes

Index (subscript) a represents age classes, going from 1 to the accumulator age class A of 50. Age class $a = 5$, for example, represents fish aged 4-5 years (which is the usual, though not universal, convention, Caswell 2001), and so an age-class 1 fish was born the previous year. The variable N_{ats} is the number of age-class a fish of sex s at the *start* of year t, so the model is run to year T which corresponds to 2020.

E.4.2. Years

Index t represents model years, going from 1 to $T = 86$, and $t = 0$ represents unfished equilibrium conditions. The actual year corresponding to $t = 1$ is 1935, and so model year $T = 86$ corresponds to 2020. The interpretation of year depends on the model's derived state or data input:

- beginning of year: N_{ats}, B_t, R_t
- middle of year: C_t, V_t, u_t, I_{tg}, p_{atgs}

E.4.3. Survey data

Data from $1, ..., 6$ series were used, as described in detail in Appendix B. Along the coast, g = 1 denotes the Queen Charlotte Sound (QCS) Synoptic series, g = 2 denotes the West Coast Vancouver Island (WCVI) Synoptic series, g = 3 denotes the West Coast Haida Gwaii (WCHG) Synoptic series, g = 4 denotes the Hecate Strait (HS) Synoptic series, g = 5 denotes the NMFS Triennial series, g = 6 denotes the Goose Island Gully (GIG) Historical series. The years for which data were available for each survey are given in Table E.1; $\mathbf{T}_g$ corresponds to years for the survey biomass estimates I_{tg} (and corresponding standard deviations κ_{tg}), and $\mathbf{U}_g$ corresponds to years for proportion-at-age data p_{atgs} (with effective sample sizes n_{tg}). Note that sample size refers to the number of samples, where each sample comprises multiple specimens, typically $\sim$30-350 fish.

E.4.4. Commercial data

As described in Appendix A, the commercial catch was reconstructed back to 1918 for five fisheries. In this assessment, two fisheries are used – trawl and non-trawl (halibut longline + sablefish trap|logline + dogfish|lingcod troll + hook-and-line rockfish). Given the negligible catches in the early years, the model was started in 1935, and catches prior to 1935 were not considered. The time series for catches is denoted C_t. The set $\mathbf{U}_{1,...,4,7}$ (Table E.1) gives the years of available ageing data from the commercial fishery. The proportions-at-age values are given by p_{atgs} with effective sample size n_{tg}, where $g = 7, 8$ (to correspond to the commercial data). These proportions are the weighted proportions calculated using the stratified weighting scheme described in Appendix D, that adjusts for unequal sampling effort across temporal and spatial strata.

E.4.5. Sex

A two-sex model was used, with subscript $s = 1$ for females and $s = 2$ for males (note that these subscripts are the reverse of the codes used in the GFBioSQL database). Ageing data were partitioned by sex, as were the weights-at-age inputs. Selectivities and natural mortality were estimated by sex.

E.4.6. Weights-at-age

The weights-at-age w_{as} were assumed fixed over time and were based on sex-specific allometric (length-weight) and growth (age-length) model parameters derived from the biological data; see Appendix D for details.

E.4.7. Maturity of females

The proportion of age-class a females that are mature is m_a, and was assumed fix over time; see Appendix D for details.

E.4.8. State dynamics

The crux of the model is the set of dynamical equations (E.1)-(E.3) for the estimated number N_{ats} of age-class a fish of sex s at the start of year t. Equation (E.1) states that half of new recruits are males and half are females. Equation (E.2) calculates the numbers of fish in each age class (and of each sex) that survive to the following year, where u_{ats} represents the proportion caught by the

commercial fishery, and e^{-M_s} accounts for natural mortality. Equation (E.3) is for the accumulator age class A, whereby survivors from this class remain in this class the following year.

Natural mortality M_s was estimated separately for males and females. It enters the equations in the form e^{-M_s} as the proportion of unfished individuals that survive the year.

E.4.9. Initial conditions

An unfished equilibrium situation at the beginning of the reconstruction was assumed because there was no evidence of significant removals prior to 1935. The initial conditions (E.4) and (E.5) were obtained by setting $R_t = R_0$ (virgin recruitment), $N_{ats} = N_{a1s}$ (equilibrium condition) and $u_{ats} = 0$ (no fishing) into (E.1)-(E.3). The virgin spawning biomass B_0 was then obtained from (E.9).

E.4.10. Selectivities

Separate selectivities were modelled for the commercial fishery and for each survey series (except WCVI Triennial and GIG Historical). In this stock assessment (2019 Bocaccio), the selectivity priors, including initial values, were approximated to resemble the estimated maturity function. It differed slightly from the estimated maturity function by accepting the observed age of maximum vulnerability at age 12 rather the estimated age 11. Specifically, the BOR selectivity priors were: age at full selectivity = 12, left-hand variance = 3.6, and male selectivity shift parameter = 1.

These priors were used for all six surveys and the two commercial fisheries. Selectivity parameters were estimated for the 4 surveys (WCVI synoptic, QCS synoptic, WCHG synoptic, HS synoptic) and the commercial trawl fishery, all of which had associated age frequency data. Selectivity was fixed at the prior values for the two surveys and the combined non-trawl fisheries, all of which had no associated age frequency data.

A half-Gaussian formulation was used, as given in (E.7) and (E.8), to give selectivities s_{ags}. (Note that the subscript $\cdot_s$ always represents the index for sex, whereas $s_{\ldots}$ always represents selectivity). This results in an increasing selectivity up to the age of full selection (μ_g for females). Given there was no evidence to suggest a dome-shaped function, it was assumed that fish older than μ_g remained fully selected. The rate of ascent of the left limb is controlled by the parameter v_{gL} for females. For males, the same function is used except that the age of full selection is shifted by an amount Δ_g, see (E.8). In this assessment, the prior mean for the male selectivity shift parameter Δ_g was set to 1 for all surveys and the commercial fishery because males tended to be older than females in most age frequency samples.

E.4.11. Derived states

The spawning biomass (biomass of mature females, in tonnes) B_t at the start of year t is calculated in (E.9) by multiplying the numbers of females N_{at1} by the proportion that are mature (m_a), and converting to biomass by multiplying by the weights-at-age w_{a1}.

Equation (E.13) calculates, for year t, the proportion u_{ats} of age-class a and sex s fish that are caught. This requires the commercial selectivities $s_{a7,8s}$ and the ratio u_t, which equation (E.12) shows is the ratio of total catch (assumed taken all at once mid-year) to vulnerable biomass in the middle of the year, V_t, given by equation (E.11). Therefore, (E.12) calculates the proportion of the vulnerable biomass that is caught, and (E.13) partitions this out by sex and age.

E.4.12. Stock-recruitment function

A Beverton-Holt recruitment function is used, parameterised in terms of steepness, h, which is the proportion of the long-term unfished recruitment obtained when the stock abundance is reduced to 20% of the virgin level (Mace and Doonan 1988; Michielsens and McAllister 2004). This was done so that a prior for h could be taken from Forrest et al. (2010). The formulation shown in (E.10) comes from substituting $\alpha = (1-h)B_0/(4hR_0)$ and $\beta = (5h-1)/4hR_0$ into the Beverton-Holt equation $R_t = B_{t-1}/(\alpha + \beta B_{t-1})$, where α and β are from the standard formulation given in the Coleraine manual (Hilborn et al. 2003; see also Michielsens and McAllister 2004), R_0 is the virgin recruitment, R_t is the recruitment in year t, B_t is the spawning biomass at the start of year t, and B_0 is the virgin spawning biomass.

E.4.13. Estimates of observed data

The model estimates of the survey biomass indices I_{tg} are denoted $\widehat{I}_{tg}$ and are calculated in (E.14). The estimated numbers N_{ats} are multiplied by the natural mortality term $e^{-M_s/2}$ (that accounts for half of the annual natural mortality), the term $1 - u_{ats}/2$ (that accounts for half of the commercial catch), weights-at-age w_{as} (to convert to biomass), and selectivity s_{ags}. The sum (over ages and sexes) is then multiplied by the catchability parameter q_g to give the model biomass estimate $\widehat{I}_{tg}$. A coefficient of 0.001 in (E.14) is not needed to convert kg into tonnes, because N_{ats} is in 1000s of fish (true also for (E.6) and (E.9)).

The estimated proportions-at-age $\widehat{p}_{atgs}$ are calculated in (E.15). For a particular year and gear type, the product $e^{-M_s/2}(1-u_{ats}/2)s_{ags}N_{ats}$ gives the relative expected numbers of fish caught for each combination of age and sex. Division by $\sum_{s=1}^{2}\sum_{a=1}^{A} e^{-M_s/2}(1-u_{ats}/2)s_{ags}N_{ats}$ converts these to estimated proportions for each age-sex combination, such that $\sum_{s=1}^{2}\sum_{a=1}^{A}\widehat{p}_{atgs} = 1$.

E.5. DESCRIPTION OF STOCHASTIC COMPONENTS

E.5.1. Parameters

The set $\boldsymbol{\Theta}$ gives the parameters that are estimated. The estimation procedure is described in the Bayesian Computations section below.

E.5.2. Recruitment deviations

For recruitment, a log-normal process error is assumed, such that the stochastic version of the deterministic stock-recruitment function (E.10) is

$$R_t = \frac{B_{t-1}}{\alpha + \beta B_{t-1}} e^{\epsilon_t - \sigma_R^2/2} \tag{E.24}$$

where $\epsilon_t \sim \text{Normal}(0, \sigma_R^2)$, and the bias-correction term $-\sigma_R^2/2$ term in (E.24) ensures that the mean of the recruitment deviations equals 0. This then gives the recruitment deviation equation (E.17) and log-likelihood function (E.18). In this assessment, the value of σ_R was fixed at 0.9 based on trials with $\sigma_R \in \{0.6, 0.9, 1.2\}$. Previous assessments have used σ_R = 0.6 following an assessment of Silvergray Rockfish (Starr et al. 2016) in which the authors stated that the value was typical for marine 'redfish' (Mertz and Myers 1996). An Awatea model of Rock Sole used σ_R = 0.6 (Holt et al. 2016), citing that it was a commonly used default for finfish assessments

(Beddington and Cooke 1983). In other rockfish assessments, authors have adopted σ_R = 0.9 based on an empirical model fit consistent with the age composition data for 5ABC POP (Edwards et al. 2012*b*). A study by Thorson et al. (2014) examined 154 fish populations and estimated σ_R = 0.74 (SD=0.35) across seven taxonomic orders; the marginal value for Scorpaeniformes was σ_R=0.78 (SD=0.32) but was only based on 7 stocks.

E.5.3. Log-likelihood functions

The log-likelihood function (E.19) arises from comparing the estimated proportions-at-age with the data. It is the Coleraine (Hilborn et al. 2003) modification of the Fournier et al. (1990, 1998) robust likelihood equation. The Coleraine formulation replaces the expected proportions $\widehat{p}_{atgs}$ from the Fournier et al. (1990, 1998) formulation with the observed proportions p_{atgs}, except in the $(p_{atgs} - \widehat{p}_{atgs})^2$ term (Bull et al. 2005).

The $1/(10A)$ term in (E.19) reduces the weight of proportions that are close to or equal zero. The $1/100$ term reduces the weight of large residuals $(p_{atgs} - \widehat{p}_{atgs})$. The net effect (Stanley et al. 2009) is that residuals larger than three standard deviations from the fitted proportion are treated roughly as $3(p_{atgs}(1 - p_{atgs}))^{1/2}$.

Lognormal error is assumed for the survey indices, resulting in the log-likelihood equation (E.20). The total log-likelihood $\log L(\mathbf{\Theta})$ is then the sum of the likelihood components – see (E.21).

E.6. BAYESIAN COMPUTATIONS

Estimation of parameters compares the estimated (model-based) observations of survey biomass indices and proportions-at-age with the data, and minimises the recruitment deviations. This is done by minimising the objective function $f(\mathbf{\Theta})$, which equation (E.23) shows is the negative of the sum of the total log-likelihood function and the logarithm of the joint prior distribution, given by (E.22).

The procedure for the Bayesian computations is as follows:

1. minimise the objective function $f(\mathbf{\Theta})$ to give estimates of the mode of the posterior density (MPD) for each parameter:
   - this is done in phases,
   - a reweighting procedure is performed;
2. generate samples from the joint posterior distributions of the parameters using Monte Carlo Markov Chain (MCMC) procedure, starting the chains from the MPD estimates.

E.6.1. Phases

The MPD estimates were obtained by minimising the objective function $f(\mathbf{\Theta})$, from the stochastic (non-Bayesian version) of the model. The resulting estimates were then used to initiate the chains for the MCMC procedure for the full Bayesian model.

Simultaneously estimating all the estimable parameters for complex nonlinear models is ill advised, and so ADMB allows some of the estimable parameters to be kept fixed during the initial part of the optimisation process ADMB Project (2009). Some parameters are estimated in phase 1, then some further ones in phase 2, and so on. The order used here was:

phase 1: virgin recruitment R_0 and survey catchabilities $q_{1,...,6}$;
phase 2: recruitment deviations ϵ_t (held at 0 in phase 1);
phase 3: age of full selectivity for females $\mu_{1,...,4,7}$;
phase 4: natural mortality $M_{1,2}$ and selectivity parameters Δ_g, v_{gL} for $g = 1, ..., 4, 7$;
phase 5: steepness h.

E.6.2. Reweighting

Given that sample sizes are not comparable between different types of data, a procedure that adjusts the relative weights between data sources (abundance vs. composition) is required. The QCS POP assessment (Edwards et al. 2012*b*) used an iterative reweighting scheme based on adjusting the standard deviation of normal (Pearson) residuals (SDNRs) of data sets until these standard deviations were approximately 1 (which is the predicted standard deviation of a normal distribution with μ=0). This procedure did not perform well for the Yellowmouth Rockfish assessment (Edwards et al. 2012*a*), leading to spurious cohorts; therefore, the Yellowmouth assessment used the reweighting scheme proposed by Francis (2011). Rockfish stock assessments using the Awatea model since 2011, including this one, have adopted the Francis (2011) reweighting approach – adding series-specific process error to abundance index CVs on the first reweight, and iteratively reweighting age frequency (composition data) sample size by mean age on the first and subsequent reweights (see Section E.6.2.). For the Bocaccio data set, one reweight using mean age was performed for all presented model runs.

For abundance data such as survey indices, Francis (2011) recommends reweighting observed coefficients of variation, c_0, by first adding process error $c_\mathrm{p} \sim$= 0.2 to give a reweighted coefficient of variation

$$c_1 = \sqrt{c_0^2 + c_\mathrm{p}^2}\,. \tag{E.25}$$

For each model run, the abundance index CVs were adjusted on the first reweight only using the process error c_p = 0.25, 0.25, 0.25, 0.25, 0.25, 0.25, and 0.1514 along the Coast (g=1,...7). This last value was the CV of the residuals to the CPUE indices after a smoothing function was passed through the CPUE series, giving an approximation of the eventual fit to the indices (see Section E.6.2.1.).

Francis (2011) maintains that correlation effects are usually strong in age-composition data. Each age-composition data set has a sample size n_{tg} ($g = 1, ..., 4, 7$, $t \in \mathbf{U}_g$), which is typically in the range 3-20, each sample comprising $\sim$30-350 specimen ages. Equation (T3.4) of Francis (2011) is used to iteratively reweight the sample size as

$$n_{tg}^{(r)} = W_g^{(r)} n_{tg}^{(r-1)} \tag{E.26}$$

where $r = 1, 2, 3$ represents the reweighting iteration, $n_{tg}^{(r)}$ is the effective sample size for reweighting r, $W_g^{(r)}$ is the weight applied to obtain reweighting r, and $n_{tg}^{(0)} = n_{tg}$. So a single weight $W_g^{(r)}$ is calculated for each series $g = 1, ..., 4, 7$ for reweighting r. (See Table E.5 for the Francis weights used in the assessment, where $r = 1$ for the first reweight).

The Francis (2011) weight $W_g^{(r)}$ given to each data set takes into account deviations from the mean age for each year, rather than using deviations from each proportion-at-age value (e.g.,

Edwards et al. 2012*b*). The weight is given by equation (TA1.8) of Francis (2011):

$$W_g^{(r)} = \left\{ \text{Var}_t \left[\frac{\overline{O}_{tg} - \overline{E}_{tg}}{\sqrt{\theta_{tg}/n_{tg}^{(r-1)}}} \right] \right\}^{-1} \tag{E.27}$$

where the observed mean age, the expected mean age and the variance of the expected age distribution are, respectively,

$$\overline{O}_{tg} = \sum_{a=1}^{A} \sum_{s=1}^{2} a p_{atgs} \tag{E.28}$$

$$\overline{E}_{tg} = \sum_{a=1}^{A} \sum_{s=1}^{2} a \widehat{p}_{atgs} \tag{E.29}$$

$$\theta_{tg} = \sum_{a=1}^{A} \sum_{s=1}^{2} a^2 \widehat{p}_{atgs} - \overline{E}_{tg}^2 \tag{E.30}$$

and Var_t is the usual finite-sample variance function applied over the index t.

The reweighting of abundance CVs (once) and age frequencies over r reweights affects the model fit to the abundance index series $\widehat{I}_{tg}$ after each reweight. These predicted indices at reweight r are used to calculate normalised residuals for each survey index:

$$\delta_{tg}^{(r)} = \frac{\log I_{tg}^{(r-1)} - \log \widehat{I}_{tg}^{(r)} + 0.5 \log(1 + c_{tg}^2)^2}{\sqrt{\log(1 + c_{tg}^2)}}, \tag{E.31}$$

where $I_{tg}^{(r-1)}$ = the observed survey indices from the previous reweight r, and the standard deviation of normalised residuals (SDNR) for each survey g is simply:

$$\sigma_{\delta_g}^{(r)} = \sqrt{\frac{\sum_t (\delta_{tg}^{(r)} - \overline{\delta}_{tg}^{(r)})^2}{\eta_g - 1}} \tag{E.32}$$

where η_g = number of indices (years t) for index series g.

The reweighted dataset chosen for MCMC analysis is typically the one where the sum of the absolute deviation from unity of the SDNRs for the 7 abundance index series was the lowest (E.33); however, the first reweight was chosen for all model runs in this assessment, including the sensitivity runs.

$$r' = \min_{r \in 1:3} \sum_{g=1,\ldots,7} |1 - \sigma_{\delta_g}^{(r)}|. \tag{E.33}$$

Table E.5. The Francis (2011) weight $W_g^{(1)}$ given to each composition data using deviations from the mean age for each year.

Run	Trawl W_7	QCS W_1	WCVI W_2	WCHG W_3	HS W_4
B01 (R01)	2.99669	0.27297	0.42620	0.09072	0.83485
B02 (R02)	2.98866	0.26379	0.42850	0.08546	0.84108
B03 (R03)	2.97701	0.25374	0.42987	0.08028	0.84649
S01 (R05)	0.96021	0.11777	0.10762	0.20558	0.44341
S02 (R07)	3.13549	0.36904	0.45819	0.18020	0.78627
S03 (R08)	2.92067	0.21345	0.41322	0.06156	0.83500
S04 (R09)	3.78751	0.30188	0.44684	0.10216	0.84301
S05 (R10)	2.91156	0.26146	0.41784	0.08658	0.83618
S06 (R11)	3.00774	0.25882	0.42640	0.08302	0.84031
S07 (R12)	2.96484	0.26722	0.43064	0.08745	0.84165
S08 (R13)	3.06098	0.29190	0.43042	0.09818	0.83003
S09 (R14)	2.98734	0.26319	0.42858	0.08523	0.84109

E.6.2.1. Process error for commercial CPUE

A procedure was developed for estimating process error c_{p} to add to the commercial CPUE using a spline-smoother analysis. Francis (2011) (citing Clark and Hare 2006) recommends using a smoothing function to determine the appropriate level of process error to add to CPUE data, with the goal of finding a balance between rigorously fitting the indices while not removing the majority of the signal in the data. An arbitrary sequence of length 50, comprising degrees of freedom (DF, ν_i), where $i = 2, ..., N$ and N = number of CPUE values U_t from $t = 1996, ..., 2012$, was used to fit the CPUE data with a spline smoother. At $i = N$, the spline curve fit the data perfectly and the residual sum of squares (RSS, ρ_N) was 0. Using spline fits across a range of trial DF ν_i, values of RSS ρ_i formed a logistic-type curve with an inflection point at $i = k$ (Figure E.1). The difference between point estimates of ρ_i (proxy for the slope δ_i) yielded a concave curve with a minimum δ_i, which occurred close to the inflection point k. At the inflection point k, ν_k=3.5306 that corresponded to ρ_k=0.6820, which was converted to a c_{p} of 0.1514 using:

$$c_{\mathrm{p}} = \sqrt{\frac{\rho_k}{N-2}} \quad \left[\frac{1}{N}\sum_{t=1996}^{2012} U_t\right]^{-1}. \tag{E.34}$$

E.6.3. Prior distributions

Descriptions of the prior distributions for the estimated parameters (without including recruitment deviations) are given in Table E.4. The resulting probability density functions give the $\pi_j(\boldsymbol{\Theta})$, whose logarithms are then summed in (E.22) to give the joint prior distribution $\pi(\boldsymbol{\Theta})$. Since uniform priors are, by definition, constant across their bounded range (and zero outside), their contributions to the objective function can be ignored. Thus, in the calculation (E.22) of the joint prior distribution $\pi(\boldsymbol{\Theta})$, only those priors that are not uniform need to be considered in the summation.

A uniform prior over a large range was used for R_0. Normal priors for female and male natural mortality, M_1 and M_2 respectively, were explored using various natural mortality estimators (Hoenig 1983; Then et al. 2015; Hamel 2015) at observed ages $A_{\max} \in \{50, 55, 60\}$y

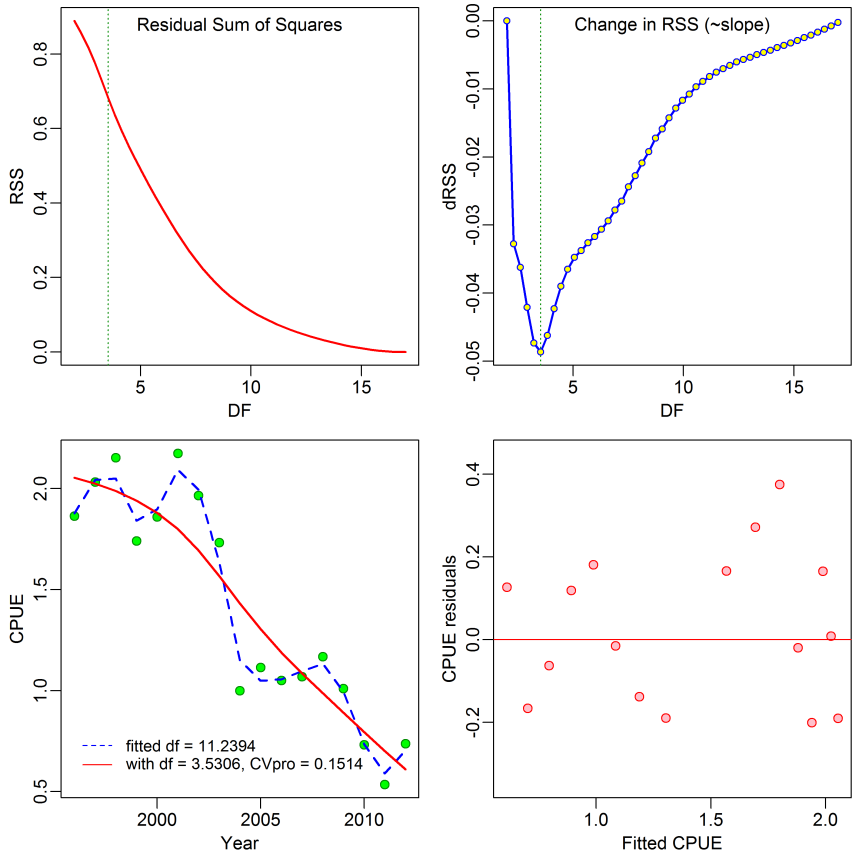

Figure E.1. Estimating process error to add to commercial CPUE data: top left – residual sum of squares (RSS) from spline-smoother at various degrees of freedom; top right – slope of RSS (∼ first derivative), vertical dotted line at DF where slope is at a minimum; bottom left – CPUE index data with spline-fittted DF (dashed blue curve) and DF=3.5306 (solid red curve); bottom right – standardised residual fit.

(Appendix D). Excluding the estimates from the equation by Then et al. (2015) (see Appendix D for rationale), M appears to range from 0.075 to 0.10 for Bocaccio. Model fitting to fixed values other than M=0.08 did not minimise well given this data set.

For steepness, h, the same prior was used as for the QCS POP assessment (Edwards et al. 2012*b*) – a beta distribution with values fitted to the posterior distribution for rockfish calculated by Forrest et al. (2010). The mean of the beta distribution (Cooper and Weekes 1983) in terms of its two shape parameters (a=4.574 and b=2.212 in this assessment) is equal to $a/(a+b)$ = 0.674, and the standard deviation is $\mathrm{sqrt}(ab/[(a+b+1)(a+b)^2])$ = 0.168. Uniform priors on a logarithmic scale were used for the catchability parameters q_g. Selectivity is discussed more fully in Section E.4.10. Selectivity priors (means and standard deviations) were based on observed proportions mature by age in the survey data.

E.6.4. MCMC properties

The MCMC procedure started the search from the MPD values and performed 6 million iterations, sampling every 5000$^{\mathrm{th}}$ for 1200 samples, 1000 of which were used after removing the first 200 for a burn-in period.

E.7. REFERENCES POINTS, PROJECTIONS AND ADVICE TO MANAGERS

Advice to managers is given with respect to a suite of reference points. The first set is based on MSY (maximum sustainable yield) and includes the provisional reference points of the DFO Precautionary Approach (DFO 2006), namely $0.4B_{\mathrm{MSY}}$ and $0.8B_{\mathrm{MSY}}$ (and also provided are B_{MSY} and u_{MSY}, which denote the estimated equilibrium spawning biomass and harvest rate at MSY, respectively). A second set of reference points, the current spawning biomass B_{2020} and harvest rate u_{2019}, is used to show the probability of increasing from the current female spawning biomass or decreasing from the current harvest rate. A third set of reference points, $0.2B_0$ and $0.4B_0$, is based on the estimated unfished equilibrium spawning biomass B_0. See main text for further discussion.

To estimate B_{MSY}, the model was projected forward across a range (0 to 0.401 incremented by 0.001) of constant harvest rates (u_t), for a maximum of 15,000 years until equilibrium was reached (with a tolerance of 0.01 t). The MSY is the largest of the equilibrium yields, and the associated exploitation rate is then u_{MSY} and the associated spawning biomass is B_{MSY}. This calculation was done for each of the 1000 MCMC samples, resulting in marginal posterior distributions for MSY, u_{MSY} and B_{MSY}.

The probability $\mathrm{P}(B_{2020} > 0.4B_{\mathrm{MSY}})$ is then calculated as the proportion of the 1000 MCMC samples for which $B_{2020} > 0.4B_{\mathrm{MSY}}$ (and similarly for the other biomass-based reference points). For harvest rates, the probability $\mathrm{P}(u_{2019} < u_{\mathrm{MSY}})$ is calculated so that both B- and u-based stock status indicators (and projections when $t = 2020, ..., 2030$) state the probability of being in a 'good' place.

Projections were made for 10 years starting with the biomass and age structure calculated for the start of 2020. A range of constant catch strategies were used, from 0 to 600 t at 50 t increments (the average catch from 2015 to 2019 was 69 t along the BC Coast). For each strategy, projections were performed for each of the 1000 MCMC samples (resulting in posterior distributions of future spawning biomass). Recruitments were randomly calculated using (E.24) (i.e. based on lognormal recruitment deviations from the estimated stock-recruitment curve), using randomly generated values of $\epsilon_t \sim \mathrm{Normal}(0, \sigma_R^2)$. For each of the 1000 MCMC samples a time series of $\{\epsilon_t\}$ was generated. For each MCMC sample, the same time series of $\{\epsilon_t\}$ was used for each catch strategy (so that, for a given MCMC sample, all catch strategies experience the same recruitment stochasticity).

E.8. REFERENCES – MODEL RESULTS

ADMB Project. 2009. AD Model Builder: Automatic Differentiation Model Builder. Developed by David Fournier and freely available from admb-project.org.

Beamish, R.J. 1979. New information on the longevity of Pacific ocean perch (*Sebastes alutus*). Can. J. Fish. Aquat. Sci. 36(11). 1395–1400.

Beddington, J.R. and Cooke, J.G. 1983. The potential yield of fish stocks. FAO Fish. Tech. Paper 242. v + 47 p.

Bull, B., Francis, R.I.C.C., Dunn, A., McKenzie, A., Gilbert, D.J. and Smith, M.H. 2005. CASAL (C++ algorithmic stock assessment laboratory), user manual v2.07-2005/08/21. NIWA Tech. Rep. 127. 274 p.

Caswell, H. 2001. Matrix Population Models: Construction, Analysis and Interpretation. Sinauer Associates, Massachusetts.

Clark, W.G. and Hare, S.R. 2006. Assessment and management of Pacific halibut: data, methods, and policy. Sci. Rep. 83, International Pacific Halibut Commission, Seattle, WA.

Cooper, R.A. and Weekes, A.J. 1983. Data, Models and Statistical Analysis. Barnes & Noble Books, Totowa NJ. Printed in Great Britain.

DFO. 2006. A harvest strategy compliant with the precautionary approach. DFO Can. Sci. Advis. Sec. Sci. Advis. Rep. 2006/023. 7 p.

DFO. 2015. Yellowtail Rockfish (*Sebastes flavidus*) stock assessment for the coast of British Columbia, Canada. DFO Can. Sci. Advis. Sec. Sci. Advis. Rep. 2015/010. 14 p.

Edwards, A.M., Haigh, R. and Starr, P.J. 2014*a*. Pacific Ocean Perch (*Sebastes alutus*) stock assessment for the north and west coasts of Haida Gwaii, British Columbia. DFO Can. Sci. Advis. Sec. Res. Doc. 2013/092. vi + 126 p.

Edwards, A.M., Haigh, R. and Starr, P.J. 2014*b*. Pacific Ocean Perch (*Sebastes alutus*) stock assessment for the west coast of Vancouver Island, British Columbia. DFO Can. Sci. Advis. Sec. Res. Doc. 2013/093. vi + 135 p.

Edwards, A.M., Haigh, R. and Starr, P.J. 2012*a*. Stock assessment and recovery potential assessment for Yellowmouth Rockfish (*Sebastes reedi*) along the Pacific coast of Canada. DFO Can. Sci. Advis. Sec. Res. Doc. 2012/095. iv + 188 p.

Edwards, A.M., Starr, P.J. and Haigh, R. 2012*b*. Stock assessment for Pacific ocean perch (*Sebastes alutus*) in Queen Charlotte Sound, British Columbia. DFO Can. Sci. Advis. Sec. Res. Doc. 2011/111. viii + 172 p.

Forrest, R.E., McAllister, M.K., Dorn, M.W., Martell, S.J.D. and Stanley, R.D. 2010. Hierarchical Bayesian estimation of recruitment parameters and reference points for Pacific rockfishes (*Sebastes* spp.) under alternative assumptions about the stock-recruit function. Can. J. Fish. Aquat. Sci. 67. 1611–1634.

Fournier, D.A., Hampton, J. and Sibert, J.R. 1998. MULTIFAN-CL: a length-based, age-structured model for fisheries stock assessment, with application to South Pacific albacore, *Thunnus alalunga*. Can. J. Fish. Aquat. Sci. 55(9). 2105–2116.

Fournier, D.A., Sibert, J.R., Majkowski, J. and Hampton, J. 1990. MULTIFAN a likelihood-based method for estimating growth parameters and age composition from multiple length frequency data sets illustrated using data for southern bluefin tuna (*Thunnus maccoyii*). Can. J. Fish. Aquat. Sci. 47(2). 301–317.

Francis, R.I.C.C. 2011. Data weighting in statistical fisheries stock assessment models. Can. J. Fish. Aquat. Sci. 68(6). 1124–1138.

Gelman, A., Carlin, J.B., Stern, H.S. and Rubin, D.B. 2004. Bayesian Data Analysis, 2nd edition. Chapman and Hall/CRC, New York.

Haigh, R., Starr, P.J., Edwards, A.M., King, J.R. and Lecomte, J.B. 2018*a*. Stock assessment for Pacific Ocean Perch (*Sebastes alutus*) in Queen Charlotte Sound, British Columbia in 2017. DFO Can. Sci. Advis. Sec. Res. Doc. 2018/038. v + 227 p.

Haigh, R., Edwards, A.M. and Starr, P.J. 2018*b*. PBSawatea: Tools for Running Awatea and Visualizing the Results. R package version 1.4.2.

Hamel, O.S. 2015. A method for calculating a meta-analytical prior for the natural mortality rate using multiple life history correlates. ICES J. Mar. Sci. 72(1). 62–69.

Hilborn, R., Maunder, M., Parma, A., Ernst, B., Payne, J. and Starr, P. 2003. Coleraine: A generalized age-structured stock assessment model. User's manual version 2.0. University of Washington Report SAFS-UW-0116. Tech. rep., University of Washington.

Hoenig, J.M. 1983. Empirical use of longevity data to estimate mortality rates. Fish. Bull. 82(1). 898–903.

Holt, K.R., Starr, P.J., Haigh, R. and Krishka, B. 2016. Stock assessment and harvest advice for Rock Sole (*Lepidopsetta* spp.) in British Columbia. DFO Can. Sci. Advis. Sec. Res. Doc. 2016/009. ix + 256 p.

Leisch, F. 2002. Sweave: dynamic generation of statistical reports using literate data analysis. In W. Härdle and B. Rönz, eds., Compstat 2002 - Proceedings in Computational Statistics, p. 575–580. Physica Verlag, Heidelberg.

Mace, P.M. and Doonan, I.J. 1988. A generalized bioeconomic simulation for fish population dynamics. NZ Fish. Assess. Res. Doc. 88/4. 51 p.

MacLellan, S.E. 1997. How to age rockfish (*Sebastes*) using *S. alutus* as an example – the otolith burnt section technique. Can. Tech. Rep. Fish. Aquat. Sci. 2146. 39 p.

Magnusson, A. 2009. Scape – statistical catch-at-age plotting environment. R package .

Magnusson, A. and Stewart, I. 2020. plotMCMC: MCMC diagnostic plots. R package version 2.0.1.

Mertz, G. and Myers, R. 1996. Influence of fecundity on recruitment variability of marine fish. Can. J. Fish. Aquat. Sci. 53(7). 1618–1625.

Michielsens, C.G.J. and McAllister, M.K. 2004. A Bayesian hierarchical analysis of stock-recruit data: quantifying structural and parameter uncertainties. Can. J. Fish. Aquat. Sci. 61(6). 1032–1047.

R Core Team. 2019. R: A Language and Environment for Statistical Computing. R Foundation for Statistical Computing, Vienna, Austria.

Stanley, R.D., Starr, P. and Olsen, N. 2009. Stock assessment for Canary Rockfish (*Sebastes pinniger*) in British Columbia waters. DFO Can. Sci. Advis. Sec. Res. Doc. 2009/013. xxii + 198 p.

Starr, P.J. and Haigh, R. 2021*a*. Widow Rockfish (*Sebastes entomelas*) stock assessment for British Columbia in 2019. DFO Can. Sci. Advis. Sec. Res. Doc. 2021/039. vi + 238 p.

Starr, P.J. and Haigh, R. 2021*b*. Redstripe Rockfish (*Sebastes proriger*) stock assessment for British Columbia in 2018. DFO Can. Sci. Advis. Sec. Res. Doc. 2021/014. vii + 340 p.

Starr, P.J., Haigh, R. and Grandin, C. 2016. Stock assessment for Silvergray Rockfish (*Sebastes brevispinis*) along the Pacific coast of Canada. DFO Can. Sci. Advis. Sec. Res. Doc. 2016/042. vi + 170 p.

Then, A.Y., Hoenig, J.M., Hall, N.G. and Hewitt, D.A. 2015. Evaluating the predictive performance of empirical estimators of natural mortality rate using information on over 200 fish species. ICES J. Mar. Sci. 72(1). 82–92.

Thorson, J.T., Jensen, O.P. and Zipkin, E.F. 2014. How variable is recruitment for exploited marine fishes? A hierarchical model for testing life history theory. Can. J. Fish. Aquat. Sci. 71(7). 973–983.

APPENDIX F. MODEL RESULTS

F.1. INTRODUCTION

This Appendix describes results for one coastwide stock of Bocaccio (BOR) using:

- mode of the posterior distribution (MPD) calculations to compare model estimates to observations,
- Markov chain Monte Carlo (MCMC) simulations to derive posterior distributions for the estimated parameters for a composite base case,
- MCMC diagnostics for the component runs of the composite base case, and
- a range of sensitivity model runs, including MCMC diagnostics.

The final advice consists of a composite base case which provides the primary guidance. A range of sensitivity runs are presented to show the effect of some of the main modelling assumptions. Estimates of major quantities and advice to management (decision tables) are presented here and in the main text.

F.2. BC COAST STOCK

F.2.1. BASE CASE

The base case for Bocaccio was selected from combined model runs 1-3. Important decisions made during the assessment of BOR included:

- fixed natural mortality M to three levels: 0.07, 0.08, and 0.09 for a total of three reference models, using 50 as the pooled age A;
- used six survey abundance index series (QCS Synoptic, WCVI Synoptic, WCHG Synoptic, HS Synoptic, NMFS Triennial, and GIG Historical), the first four with age frequency (AF) data;
- used one commercial fishery abundance index series (bottom trawl CPUE index), truncated after 2012;
- assumed two fisheries (1=commercial bottom + midwater trawl; 2=halibut longline, sablefish trap, lingcod longline, inshore longline, salmon troll), each with pooled catches and AF data only for the trawl fishery);
- assumed two sexes (females, males);
- used fairly arbitrary selectivity priors loosely based on the fitted maturity function; the prior assumed an age shift of plus one year for males relative to females;
- applied abundance reweighting: added CV process error to index CVs, c_{p}=0.25 for surveys and c_{p}=0.1514 for commercial CPUE series (see Appendix E);
- applied composition reweighting: adjusted AF effective sample sizes using the mean-age method of Francis (2011);
- fixed standard deviation of recruitment residuals (σ_R) to 0.9;
- excluded the 1995 survey index from the GIG Historical series (design incompatible);
- excluded water hauls from the WCVI Triennial series;
- excluded the 2016 WCVI synoptic survey age frequency data (caused instability in the minimisations and MCMC simulations);
- used the ‘wide’ ageing error matrix described in Appendix D, Section D.2.3 and plotted in Figure D.20 (right).

Three fixed M values produced three separate model runs, with the respective posterior distributions pooled as a base case for advice to managers. The central run of the composite base case (Run02: M=0.08, A=50) was used as an example reference case against which 9 sensitivity runs were compared.

All model runs were reweighted one time for (i) abundance, by adding process error $c_{\mathrm{p}} \in$ { 0.25, 0.25, 0.25, 0.25, 0.25, 0.25, and 0.1514 } to the index CVs for the QCS Synoptic, WCVI Synoptic, WCHG Synoptic, HS Synoptic, NMFS Triennial, GIG Historical, and commercial trawl CPUE, respectively, and (ii) composition using the procedure of Francis (2011) for age frequencies.

F.2.1.1. Central Run MPD

The procedure followed in this assessment was to first determine the best MPD fit to the data by minimising the negative log likelihood. Because the BOR composite base case involved three models, only the central run (M=0.08, wide ageing error matrix) was used as an example (Tables F.1 and F.2). These MPD runs became the starting points for the MCMC simulations. The following plot references apply to the central run.

- Figure F.1 – survey index fits across all survey years;
- Figures F.2 to F.7 – individual survey fits and residuals;
- Figure F.8 – bottom trawl CPUE fit and its residuals;
- Figures F.9-F.11 model fits to the female and male age frequency data for the commercial trawl fishery and combined-sex residuals;
- Figure F.12 and F.13 – model fits and residuals to the age data for the Queen Charlotte Sound (QCS) synoptic survey;
- Figure F.14 and F.15 – model fits and residuals to the age data for the West Coast Vancouver Island (WCVI) synoptic survey;
- Figure F.16 and F.17 – model fits and residuals to the age data for the West Coast Haida Gwaii (WCHG) synoptic survey;
- Figure F.18 and F.19 – model fits and residuals to the age data for the Hecate Strait (HS) synoptic survey;
- Figure F.20 – model estimates of mean age compared to the observed mean ages;
- Figure F.21 – the stock-recruitment relationship and recruitment time series;
- Figure F.22 – the recruitment deviations and auto-correlation of these deviations;
- Figure F.23 – estimated gear selectivities, together with the ogive for female maturity;
- Figure F.24 – exploitation rates and catches by gear type over time.

The model fits to the abundance indices were generally satisfactory (Figures F.1 to F.7), although there were some very large residuals. In general, the survey indices were low (given the apparent low BOR biomass) and had little contrast, which meant that the model had little difficulty in fitting the data points. Two notable exceptions to this generalisation was the lack of fit to the very large 1980 Triennial survey index and the failure to match the large uptick in the 2019 QCS synoptic index (Figure F.2). The overall downward trend to the biomass also allowed for a reasonable fit to the CPUE series (Figure F.8).

Fits to the commercial age frequency data showed trends in the residuals, with long runs of negative residuals in the fits to the survey AF data. In particular, the model struggled to match the strong 2016 age frequencies which clearly dominated in the years that cohort was present. Most of the Pearson residuals generally lay between -1 and +1 although there were some residuals around -2 associated with the 2016 cohort (e.g., Figures F.13 and F.15). However, model

estimates of mean age tended to match the observed mean ages in nearly every year and for all five age frequency data sets (commercial trawl and the four synoptic surveys; Figure F.20). We tended to accept model runs where the correspondence of the model mean age matched the observed mean age (as in Figure F.20) because we discovered that the models which failed to minimise tended to completely miss these observations, with the model mean age estimates consistently above or below the observations by a wide margin.

Unlike other recent rockfish stock assessments, recruitment estimates has been consistently low at all biomass levels. This is because all the ageing data were relatively recent (since 2003) and, because recent biomass levels have been low, model estimates of recruitment are also low, regardless of the underlying level of biomass, resulting in an unusual stock-recruitment relationship (Figure F.21). This behaviour also causes significant auto-correlation in the recruitment deviations at every lag out to about age 10 (Figure F.22). The recruitment for these pre-2016 year classes will also be affected by the size of 2016 cohort and the requirement imposed in the model for the entire recruitment series to have a mean of zero in log space.

The MPD estimates for the commercial selectivity function differ little from the prior and neatly overlay the female maturity ogive (see Figure F.23). This is not the case for some of the survey selectivities, with the QCS survey having a broader left-hand variance term while showing little change in the age at maximum selectivity. On the other hand, the WCVI survey shows a two-year leftward shift in the maximum selectivity age, but which is balanced by little change in the left side variance parameter.

Table F.1. CR.02.01: Priors and MPD estimates for estimated parameters. Prior information – distributions: 0 = uniform, 1 = normal, 2 = lognormal, 5 = beta

Phase	Range	Type	(Mean,SD)	Initial	MPD
R_0 **(recruitment in virgin condition)**					
1	(1,1e+07)	0	(0,0)	10000	1862.7
M_s **(natural mortality by sex** s**, where** $s = 1\ [\mathrm{female}], 2\ [\mathrm{male}]$**)**					
-4	(0.01,0.2)	1	(0.08,0.02)	0.08	0.08
-4	(0.01,0.2)	1	(0.08,0.02)	0.08	0.08
-5	(0.01,0.2)	1	(0.12,0.03)	0.12	0.12
h **(steepness of spawner-recruit curve)**					
5	(0.2,0.999)	5	(4.574,2.212)	0.674	0.656913
ϵ_t **(recruitment deviations)**					
2	(-15,15)	1	(0,0.9)	0	Fig F.22
ω **(initial recruitment)**					
-1	(0,2)	0	(1,0.1)	1	1

Table F.2. CR.02.01: Priors and MPD estimates for index g (survey and commercial).

Index g	Phase	Range	Type	(Mean,SD)	Initial	MPD	exp (MPD)
CPUE catchability mode ($\log q_g$ **where** $g = 7, ...7$**)**							
7	1	(-15,15)	0	(0,0.1)	-1.60944	-8.012	0.00033146
Survey catchability mode ($\log q_g$**, where** $g = 1, ..., 6$**)**							
1	1	(-12,5)	0	(0,0.6)	-5	-3.2959	0.037036
2	1	(-12,5)	0	(0,0.6)	-5	-3.1917	0.041101
3	1	(-12,5)	0	(0,0.6)	-5	-5.5622	0.0038404
4	1	(-12,5)	0	(0,0.6)	-5	-4.7359	0.0087743
5	1	(-12,5)	0	(0,0.6)	-5	-2.8277	0.059148
6	1	(-12,5)	0	(0,0.6)	-5	-3.7963	0.022453
Commercial selectivity (μ_g**, where** $g = 7, 8$**)**							
7	3	(5,30)	1	(12,3)	12	11.244	
8	-3	(5,30)	1	(12,3)	12	12	
Survey selectivity (μ_g**, where** $g = 1, ..., 6$**)**							
1	3	(5,40)	1	(12,3)	12	12.315	
2	3	(5,40)	1	(12,3)	12	10.069	
3	3	(5,40)	1	(12,3)	12	12.543	
4	3	(5,40)	1	(12,3)	12	14.189	
5	-3	(5,40)	1	(12,3)	12	12	
6	-3	(5,40)	1	(12,3)	12	12	
Variance (left) of commercial selectivity curve ($\log v_{gL}$**, where** $g = 7, 8$**)**							
7	4	(-15,15)	1	(3.6,0.9)	3.6	3.5448	
8	-4	(-15,15)	1	(3.6,0.9)	3.6	3.6	
Variance (left) of survey selectivity curve ($\log v_{gL}$**, where** $g = 1, ..., 6$**)**							
1	4	(-15,15)	1	(3.6,0.9)	3.6	4.5744	
2	4	(-15,15)	1	(3.6,0.9)	3.6	3.7777	
3	4	(-15,15)	1	(3.6,0.9)	3.6	3.1864	
4	4	(-15,15)	1	(3.6,0.9)	3.6	4.4214	
5	-4	(-15,15)	1	(3.6,0.9)	3.6	3.6	
6	-4	(-15,15)	1	(3.6,0.9)	3.6	3.6	
Shift in commercial selectivity for males (Δ_g**, where** $g = 7, 8$**)**							
7	4	(-8,10)	1	(1,0.3)	1	1.0325	
8	-4	(-8,10)	1	(1,0.3)	1	1	
Shift in survey selectivity for males (Δ_g**, where** $g = 1, ..., 6$**)**							
1	4	(-8,10)	1	(1,0.3)	1	0.98501	
2	4	(-8,10)	1	(1,0.3)	1	0.85213	
3	4	(-8,10)	1	(1,0.3)	1	0.97016	
4	4	(-8,10)	1	(1,0.3)	1	0.97457	
5	-4	(-8,10)	1	(1,0.3)	1	1	
6	-4	(-8,10)	1	(1,0.3)	1	1	

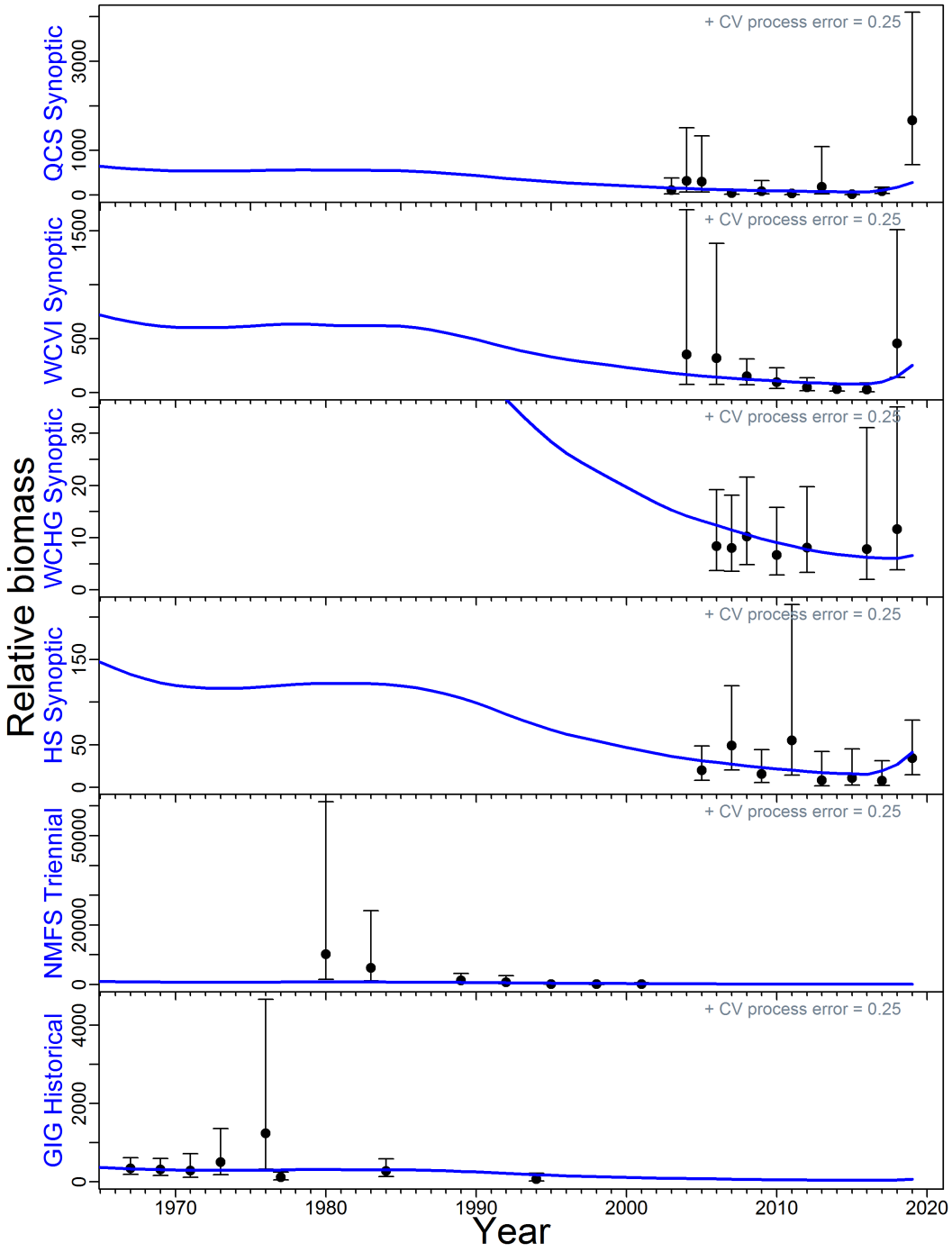

Figure F.1. CR.02.01: Survey index values (points) with 95% confidence intervals (bars) and MPD model fits (curves) for the fishery-independent survey series.

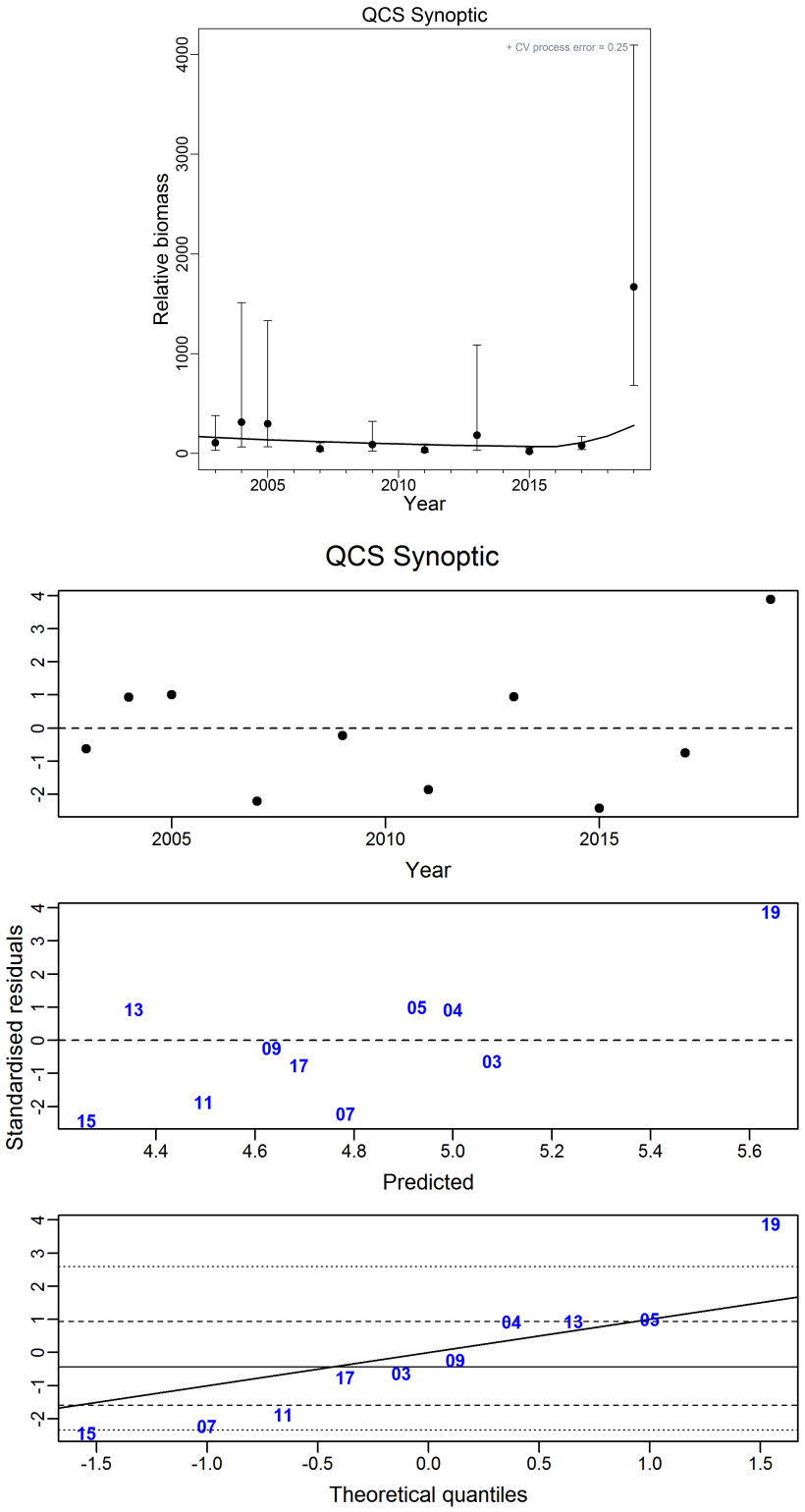

Figure F.2. CR.02.01: Fit (top) and residuals of fits (bottom) of model to QCS Synoptic survey series (MPD values). Vertical axes are standardised residuals. The three plots show, respectively, residuals by year of index, residuals relative to predicted index, and normal quantile-quantile plot for residuals (horizontal lines give 5, 25, 50, 75 and 95 percentiles).

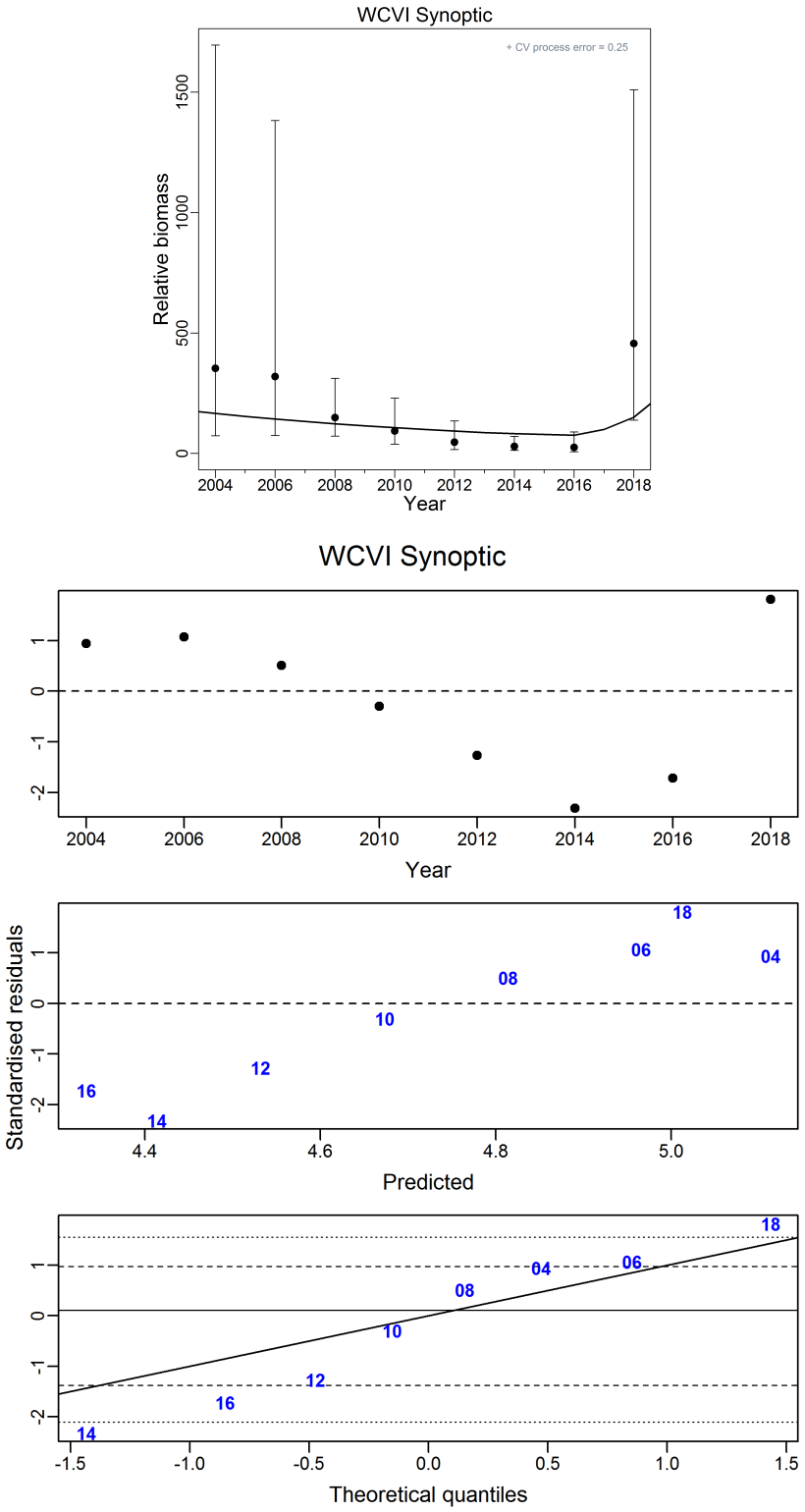

Figure F.3. CR.02.01: Fit (top) and residuals of fits (bottom) of model to WCVI Synoptic survey series (MPD values). Vertical axes are standardised residuals. The three plots show, respectively, residuals by year of index, residuals relative to predicted index, and normal quantile-quantile plot for residuals (horizontal lines give 5, 25, 50, 75 and 95 percentiles).

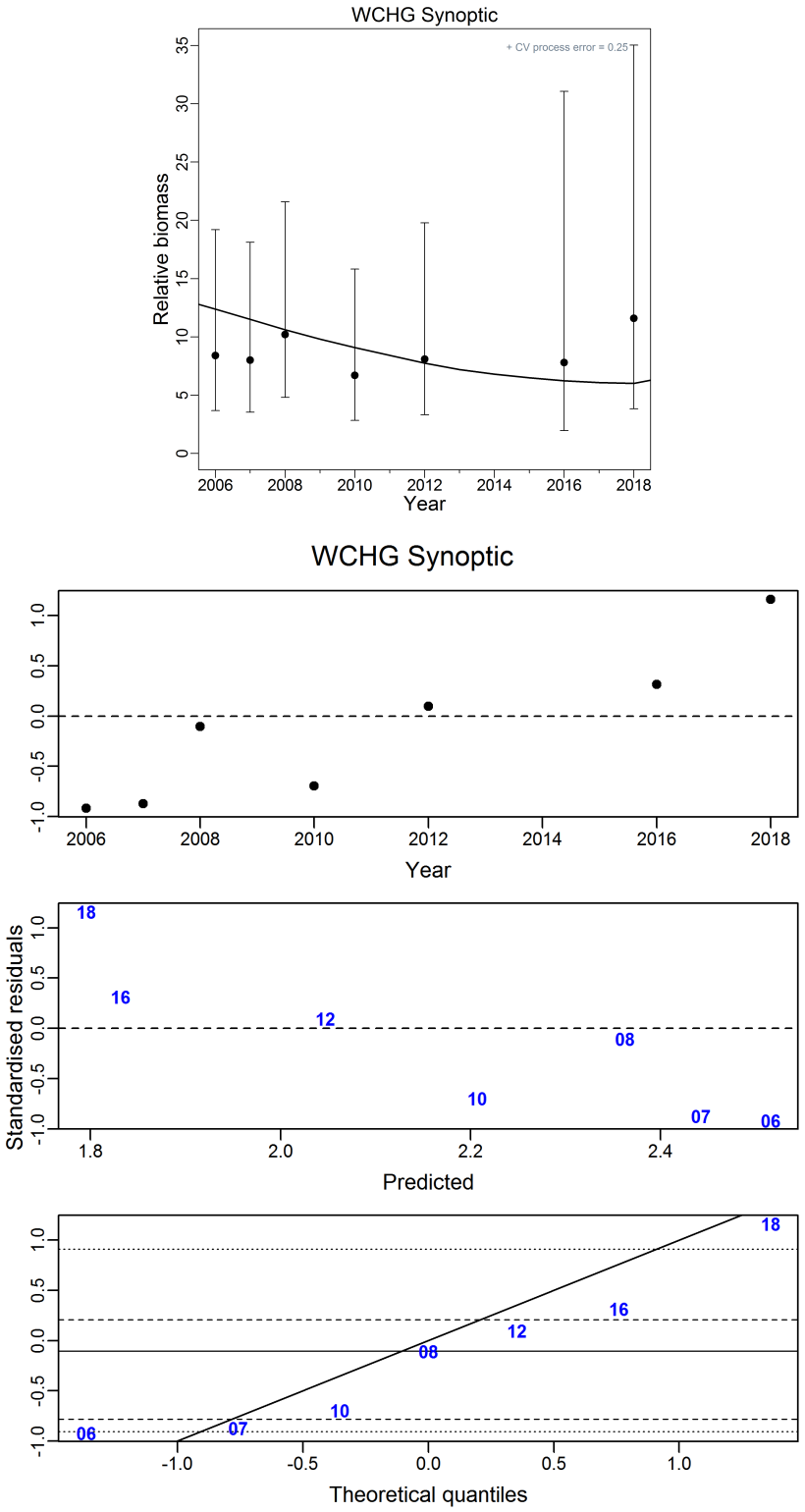

Figure F.4. CR.02.01: Fit (top) and residuals of fits (bottom) of model to WCHG Synoptic survey series (MPD values). Vertical axes are standardised residuals. The three plots show, respectively, residuals by year of index, residuals relative to predicted index, and normal quantile-quantile plot for residuals (horizontal lines give 5, 25, 50, 75 and 95 percentiles).

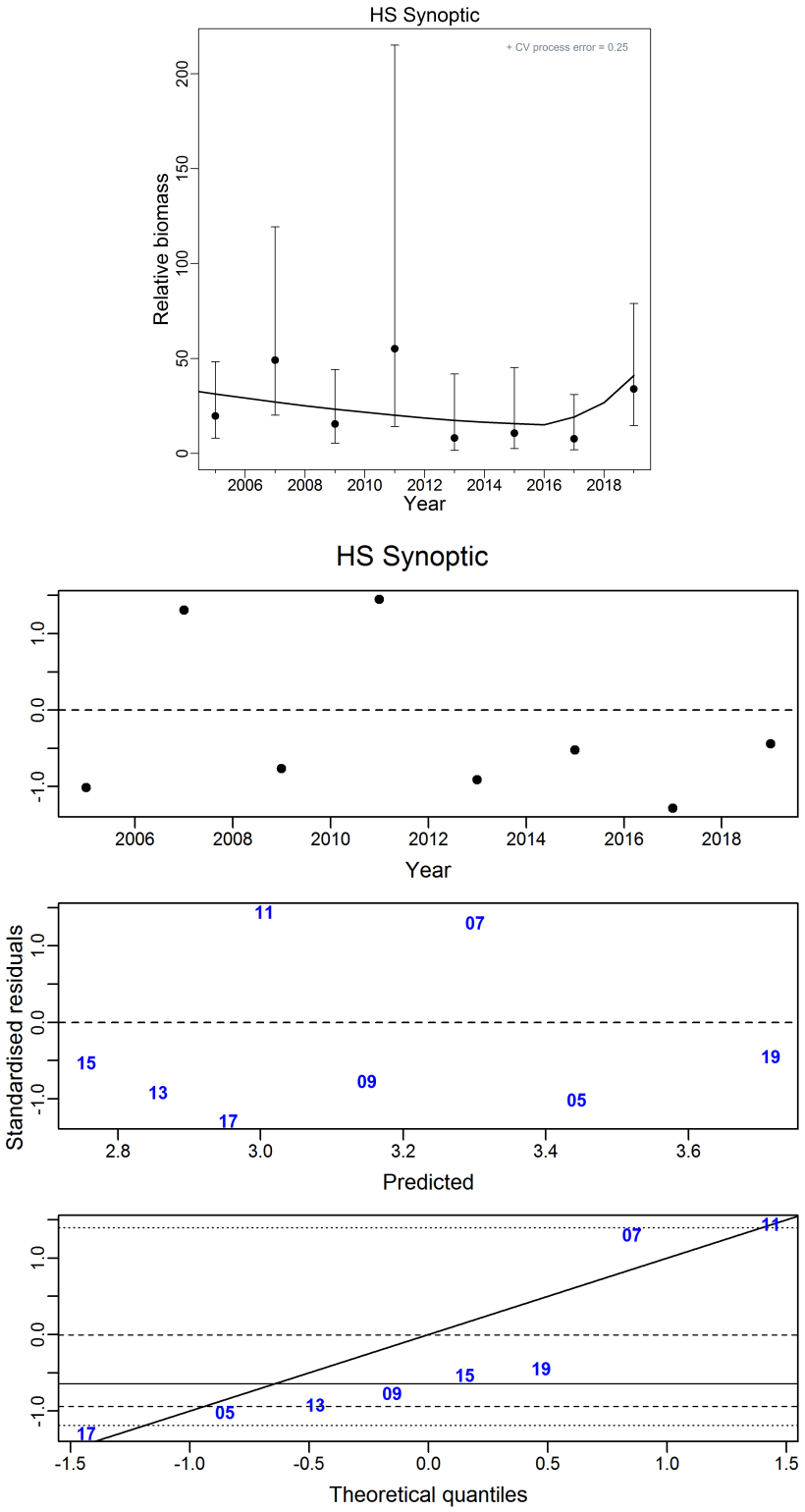

Figure F.5. CR.02.01: Fit (top) and residuals of fits (bottom) of model to HS Synoptic survey series (MPD values). Vertical axes are standardised residuals. The three plots show, respectively, residuals by year of index, residuals relative to predicted index, and normal quantile-quantile plot for residuals (horizontal lines give 5, 25, 50, 75 and 95 percentiles).

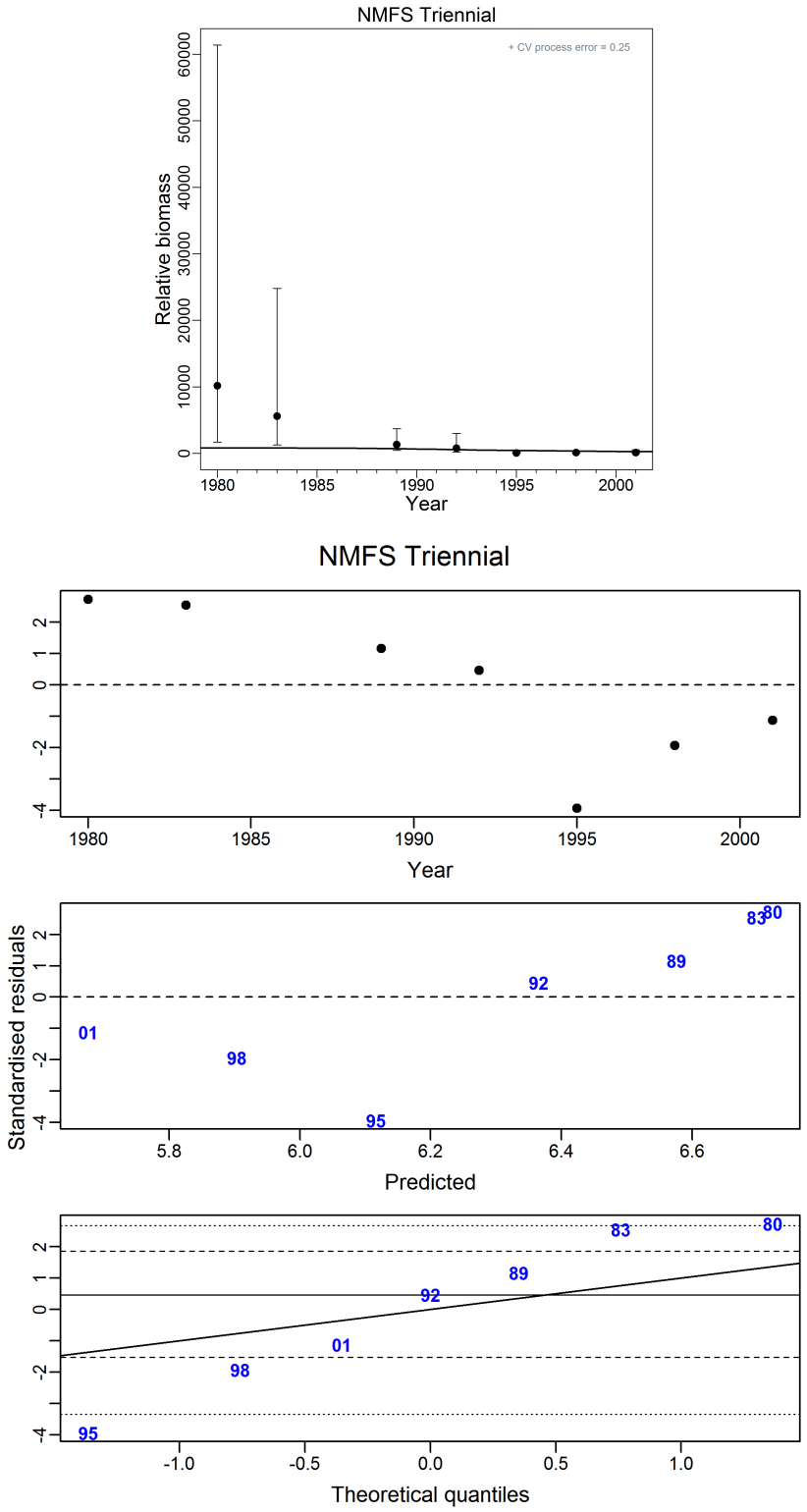

Figure F.6. CR.02.01: Fit (top) and residuals of fits (bottom) of model to NMFS Triennial survey series (MPD values). Vertical axes are standardised residuals. The three plots show, respectively, residuals by year of index, residuals relative to predicted index, and normal quantile-quantile plot for residuals (horizontal lines give 5, 25, 50, 75 and 95 percentiles).

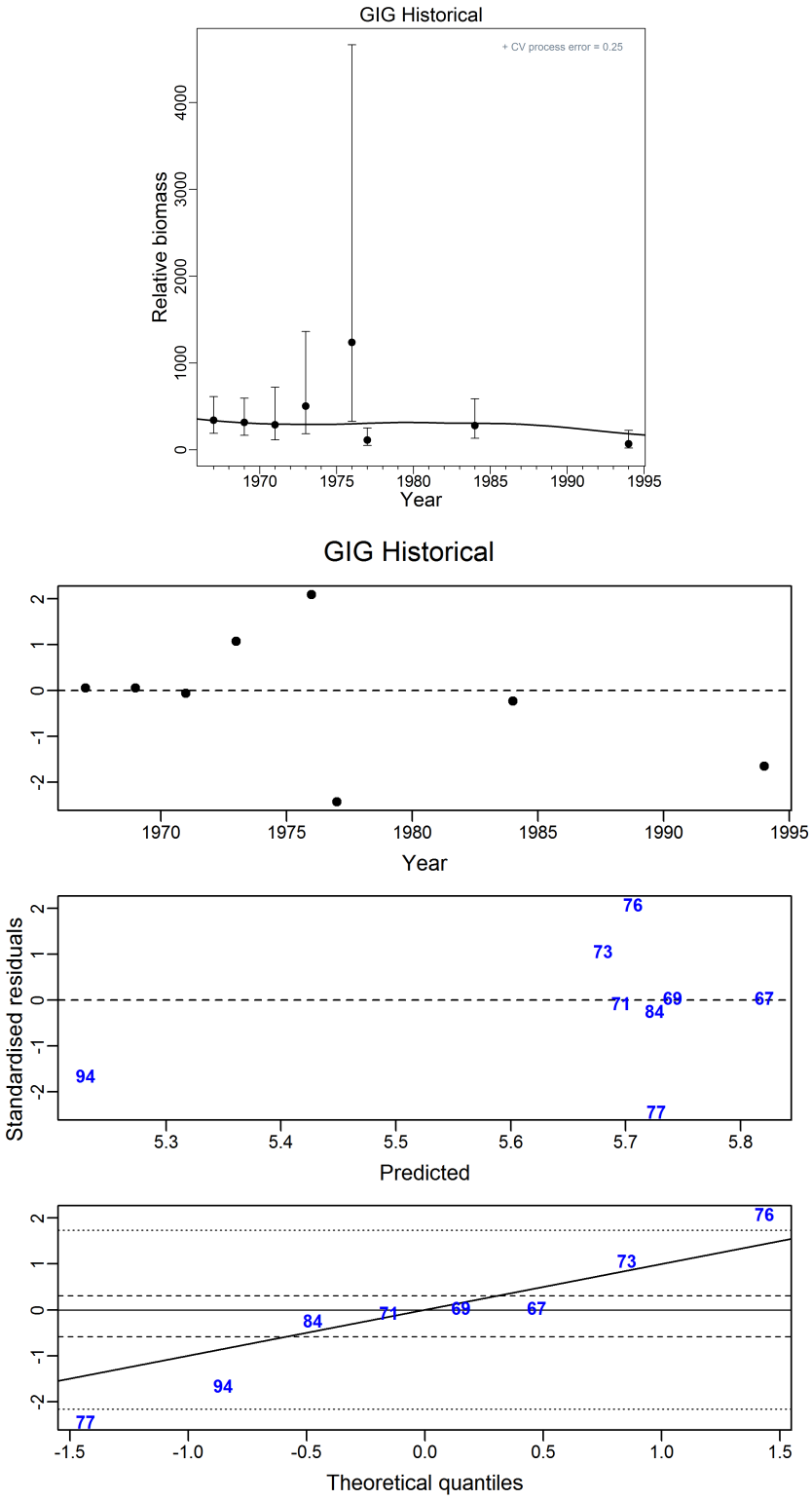

Figure F.7. CR.02.01: Fit (top) and residuals of fits (bottom) of model to GIG Historical survey series (MPD values). Vertical axes are standardised residuals. The three plots show, respectively, residuals by year of index, residuals relative to predicted index, and normal quantile-quantile plot for residuals (horizontal lines give 5, 25, 50, 75 and 95 percentiles).

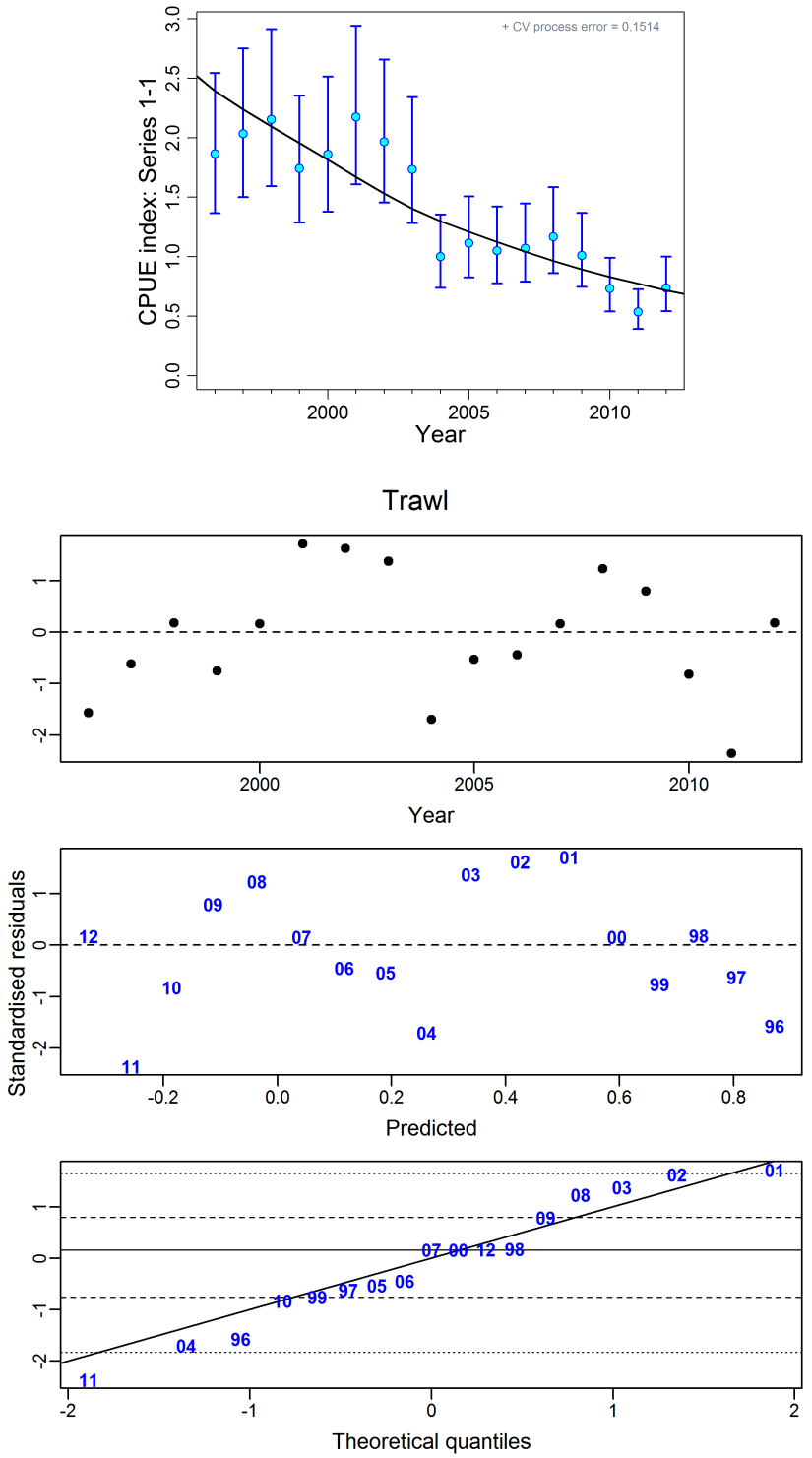

Figure F.8. CR.02.01: Fit (top) and residuals of fits (bottom) of model to Bottom Trawl CPUE series (MPD values). Vertical axes are standardised residuals. The three plots show, respectively, residuals by year of index, residuals relative to predicted index, and normal quantile-quantile plot for residuals (horizontal lines give 5, 25, 50, 75 and 95 percentiles).

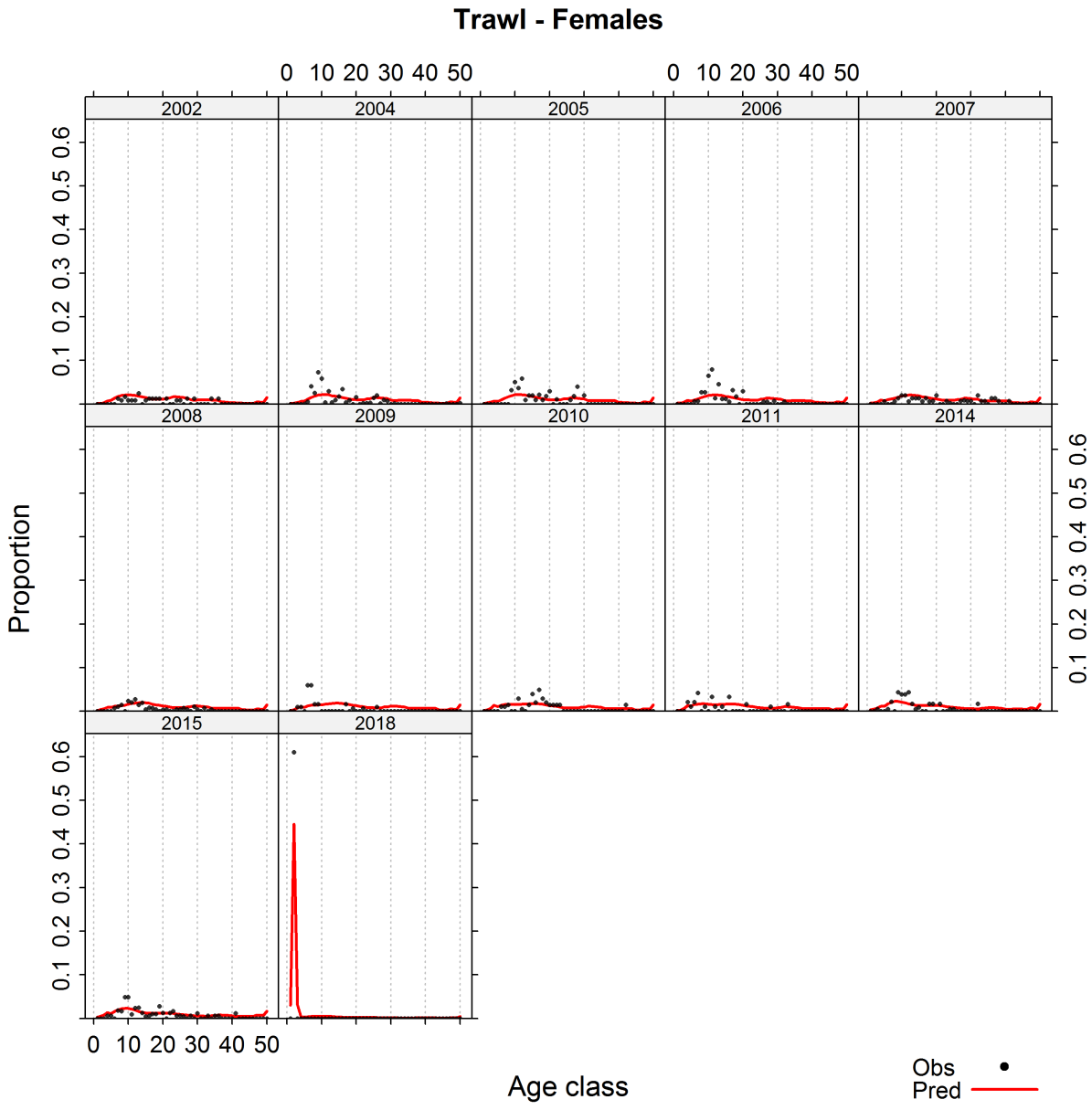

Figure F.9. CR.02.01: Observed and predicted commercial (trawl) proportions-at-age for females. Note that years are not necessarily consecutive.

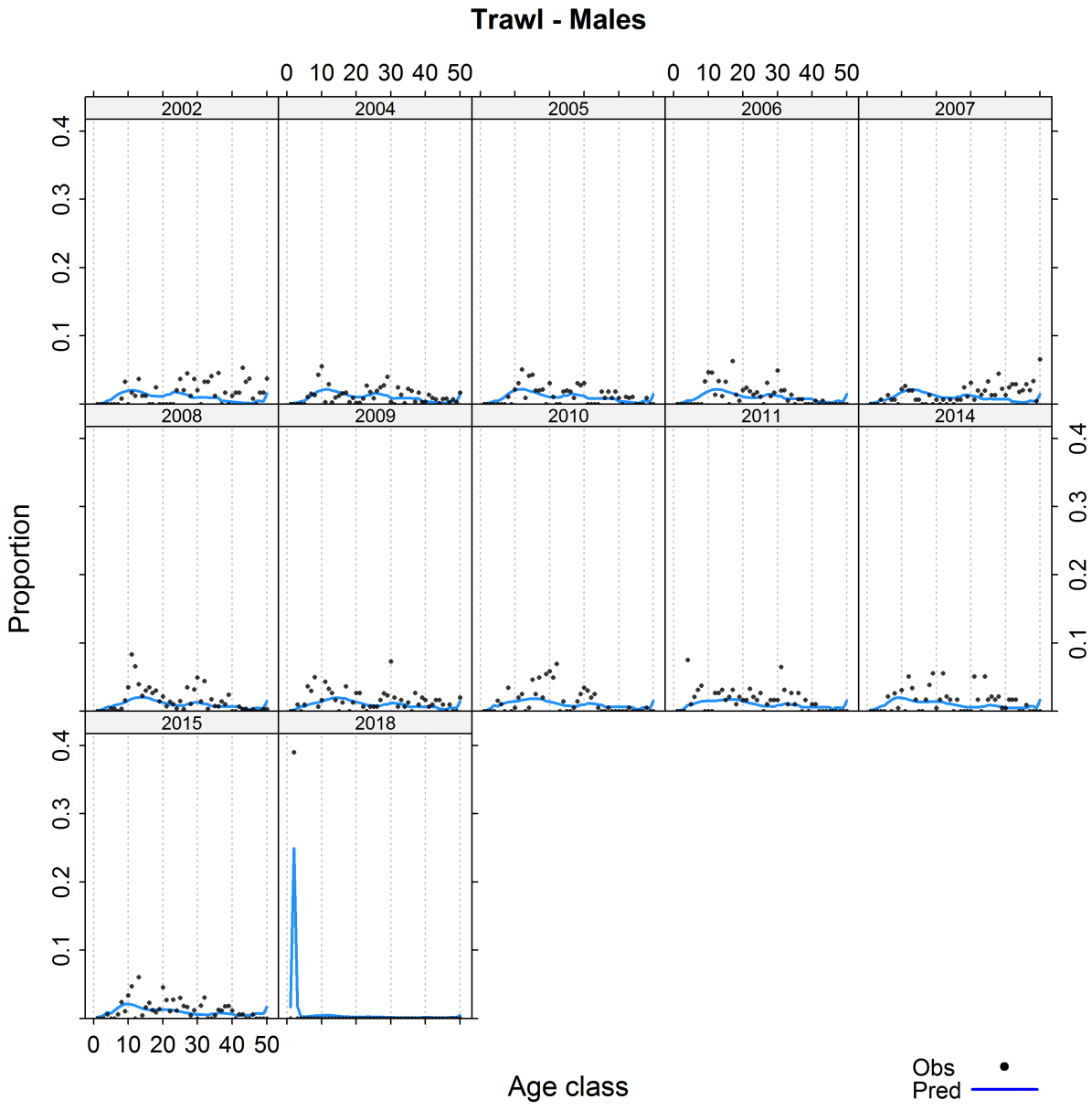

Figure F.10. CR.02.01: Observed and predicted commercial (trawl) proportions-at-age for males. Note that years are not necessarily consecutive.

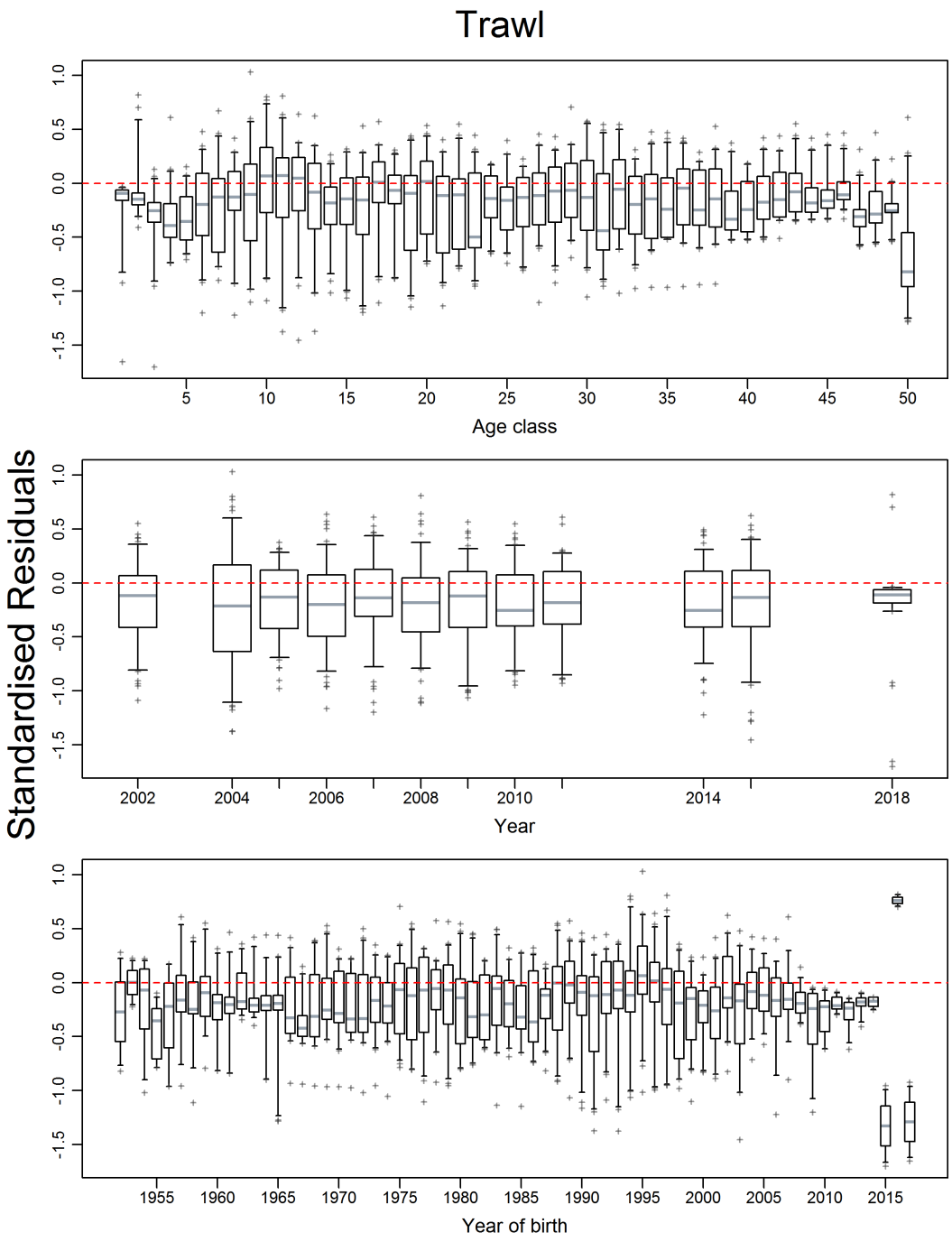

Figure F.11. CR.02.01: Residuals (1176 in total) of model fits to commercial proportion-at-age data (MPD values) for Trawl events. Vertical axes are standardised residuals. Boxplots show, respectively, residuals by age class, by year of data, and by year of birth (following a cohort through time). Boxes give quantile ranges (0.25-0.75) with horizontal lines at medians, vertical whiskers extend to the the 0.05 and 0.95 quantiles, and outliers appear as plus signs.

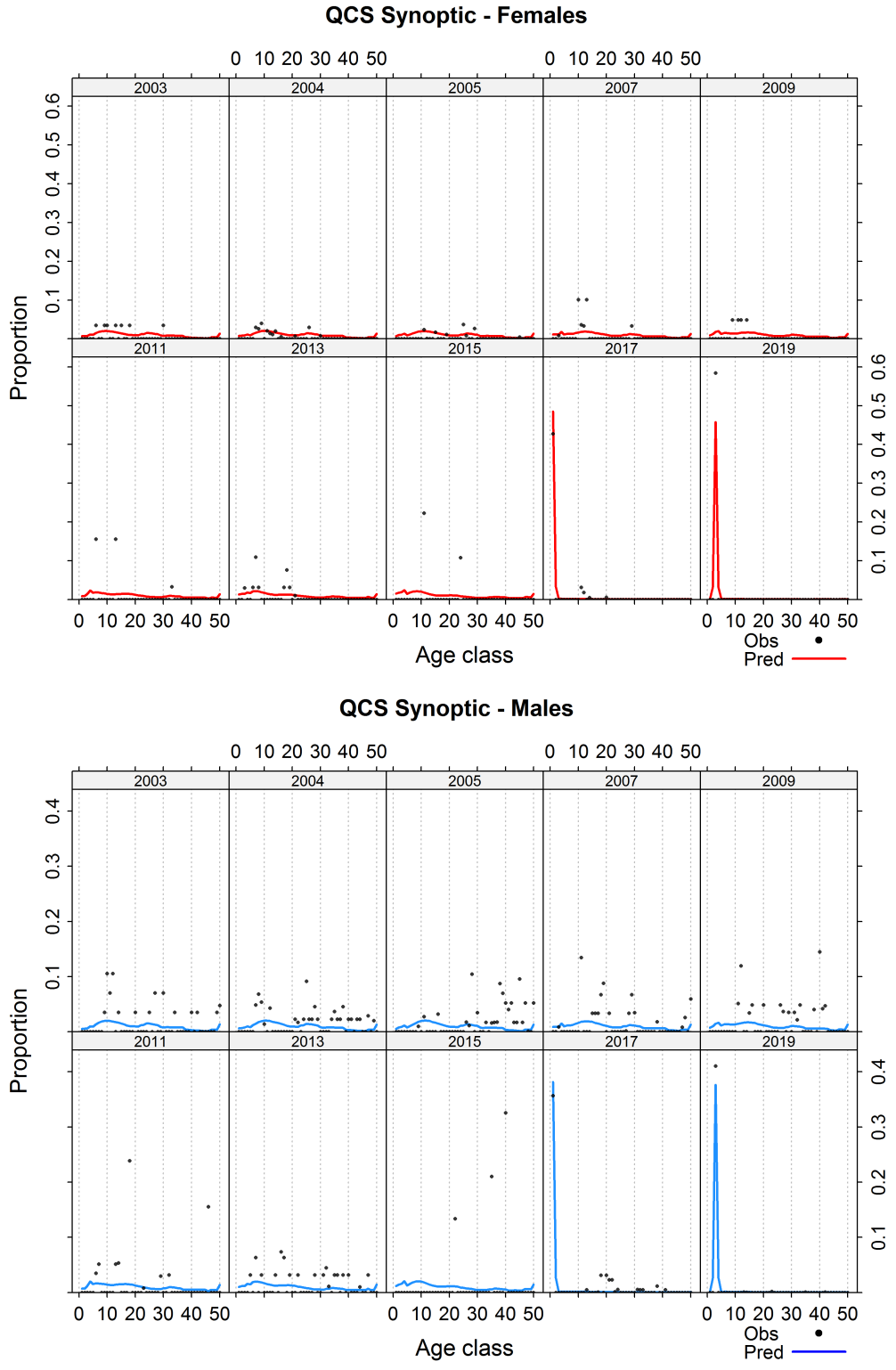

Figure F.12. CR.02.01: Observed and predicted proportions-at-age for QCS Synoptic survey.

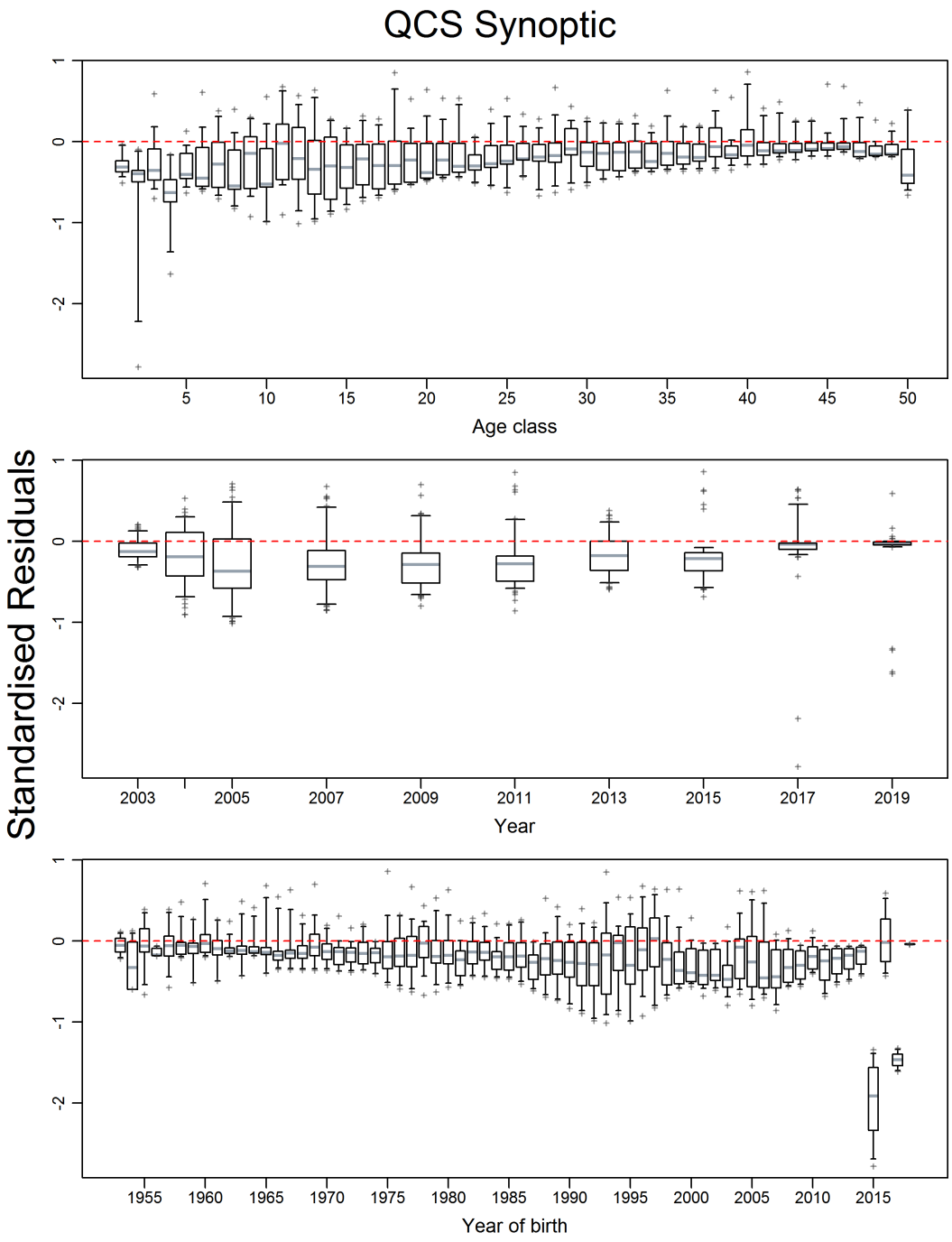

Figure F.13. CR.02.01: Residuals of model fits to proportion-at-age data (MPD values) from the QCS Synoptic survey series. Details as for Figure F.11, for a total of 980 residuals.

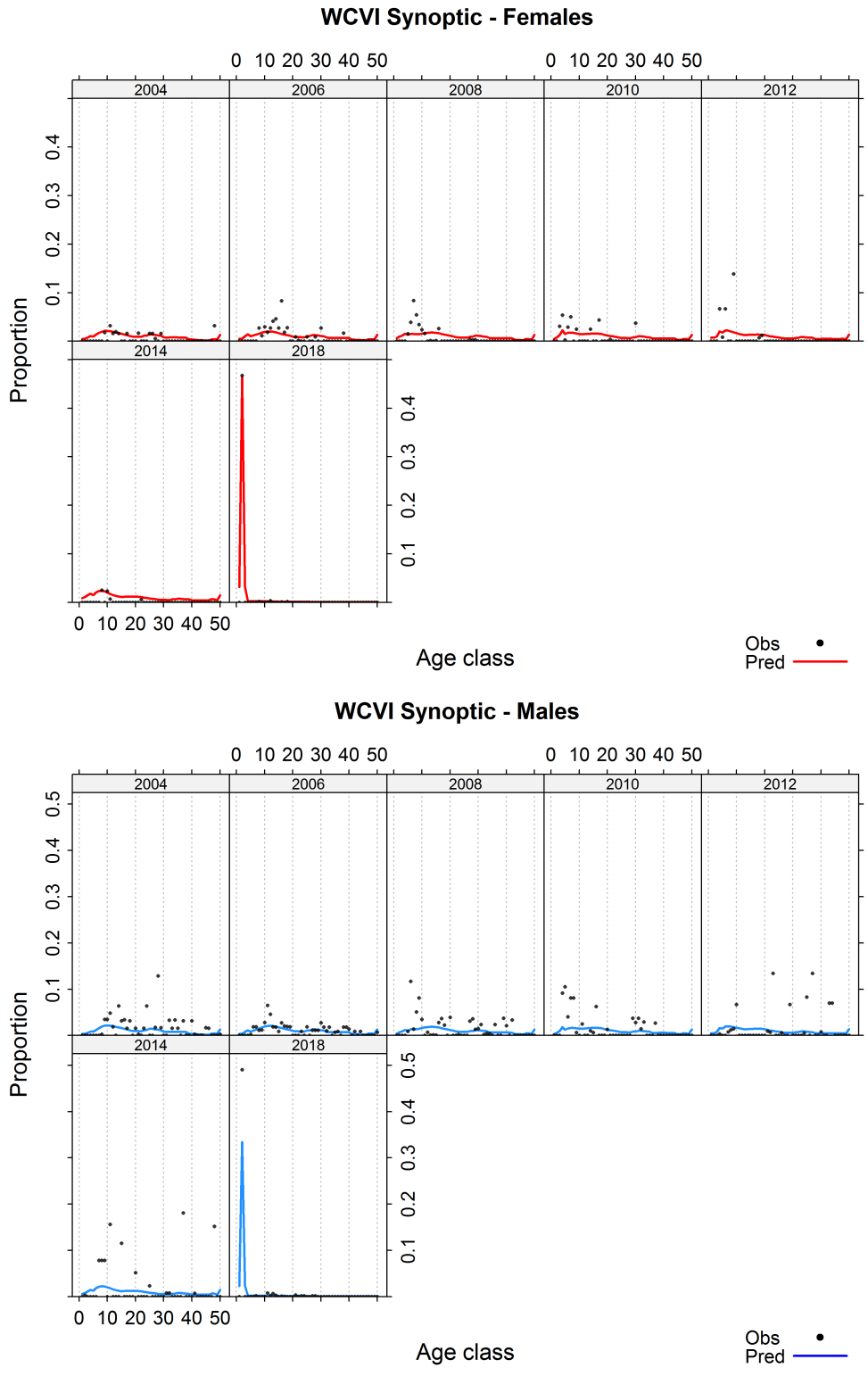

Figure F.14. CR.02.01: Observed and predicted proportions-at-age for WCVI Synoptic survey.

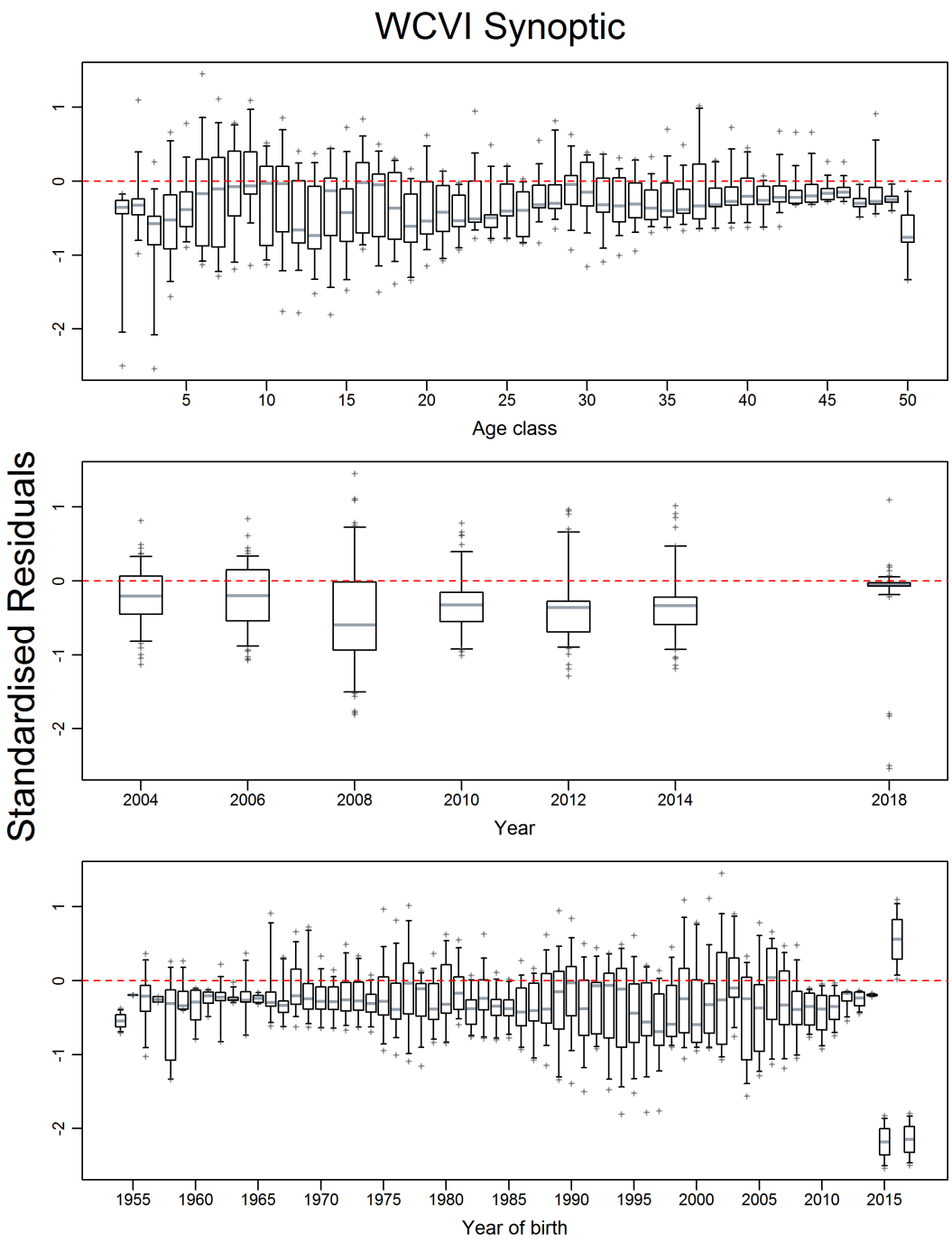

Figure F.15. CR.02.01: Residuals of model fits to proportion-at-age data (MPD values) from the WCVI Synoptic survey series. Details as for Figure F.11, for a total of 686 residuals.

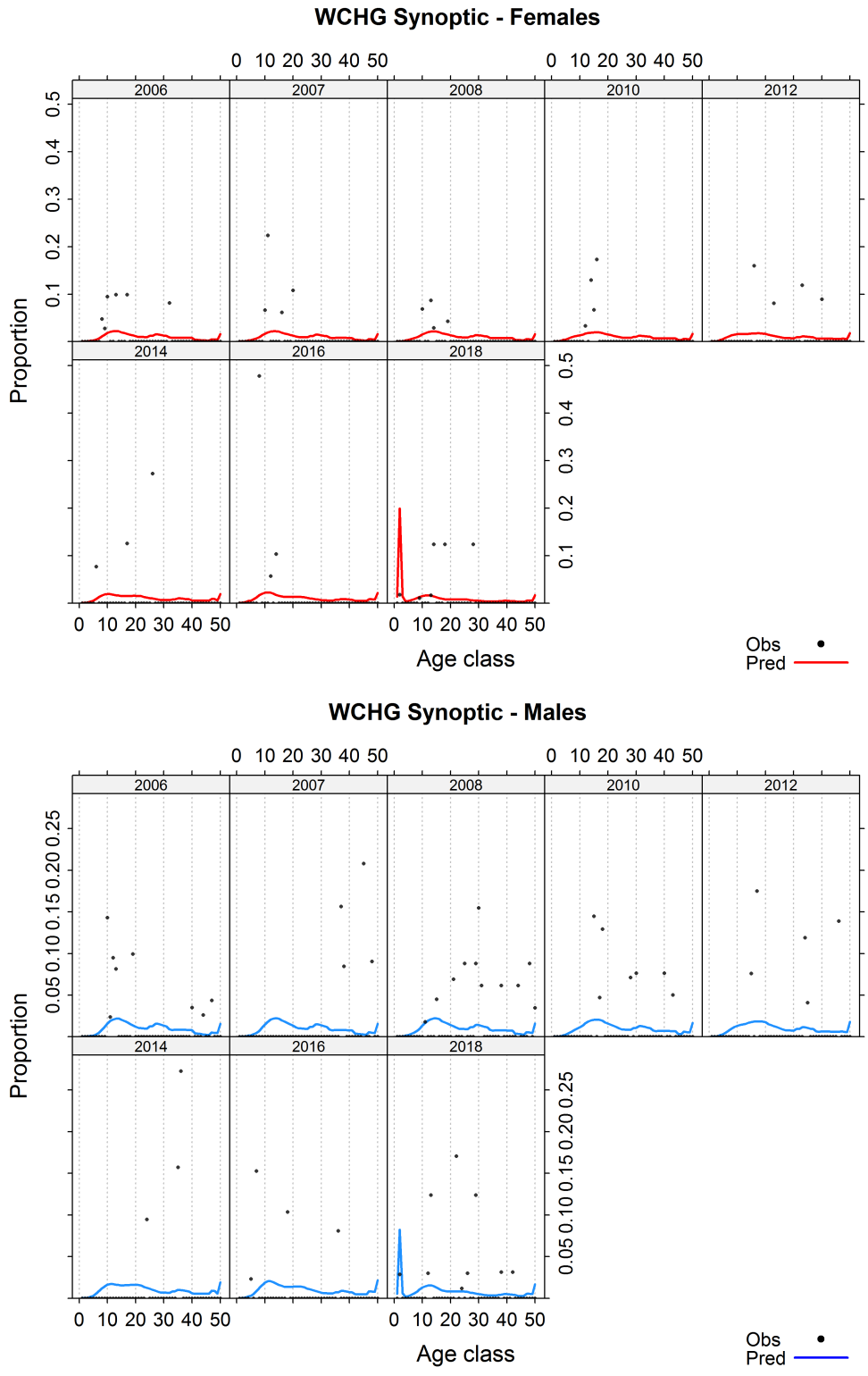

Figure F.16. CR.02.01: Observed and predicted proportions-at-age for WCHG Synoptic survey.

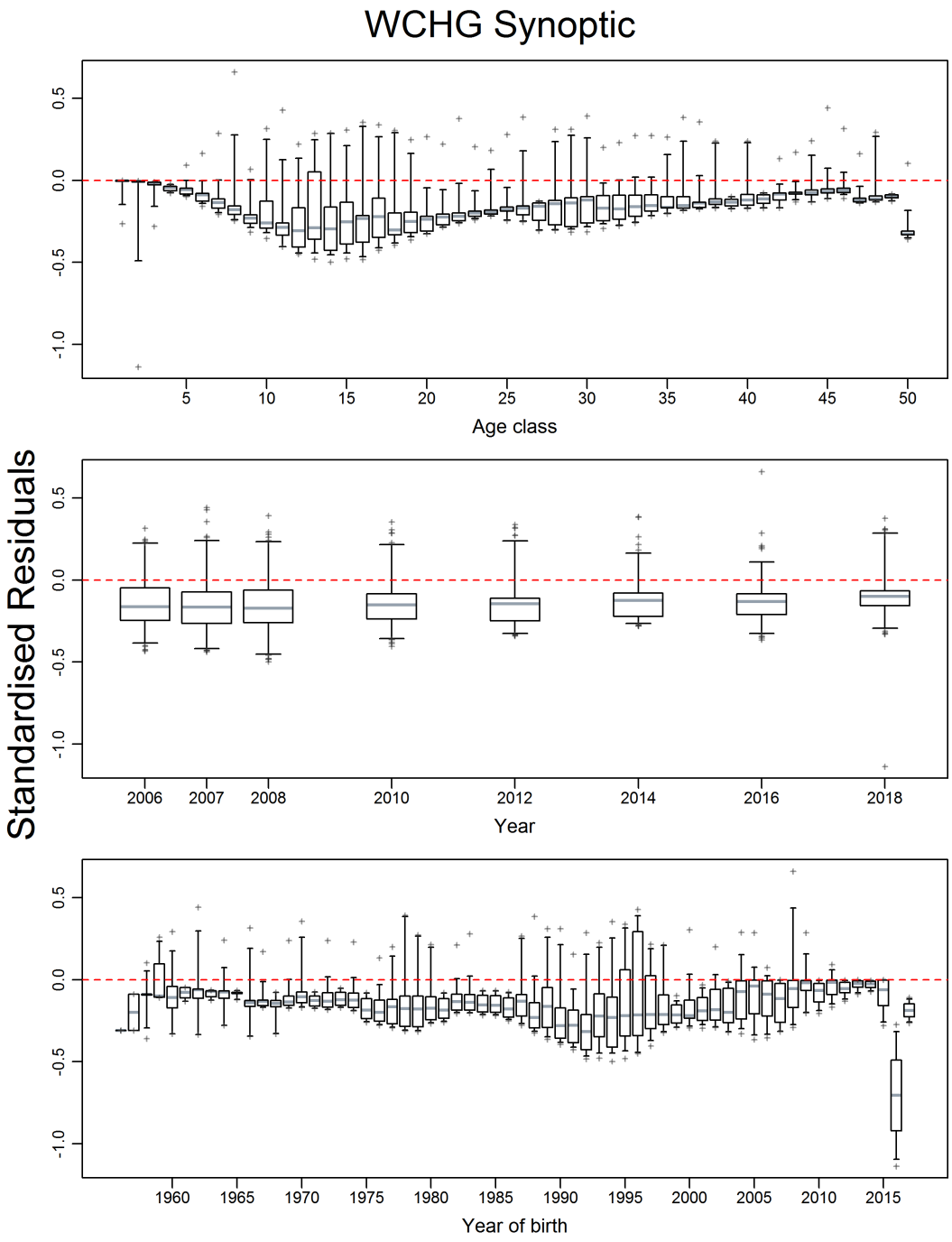

Figure F.17. CR.02.01: Residuals of model fits to proportion-at-age data (MPD values) from the WCHG Synoptic survey series. Details as for Figure F.11, for a total of 784 residuals.

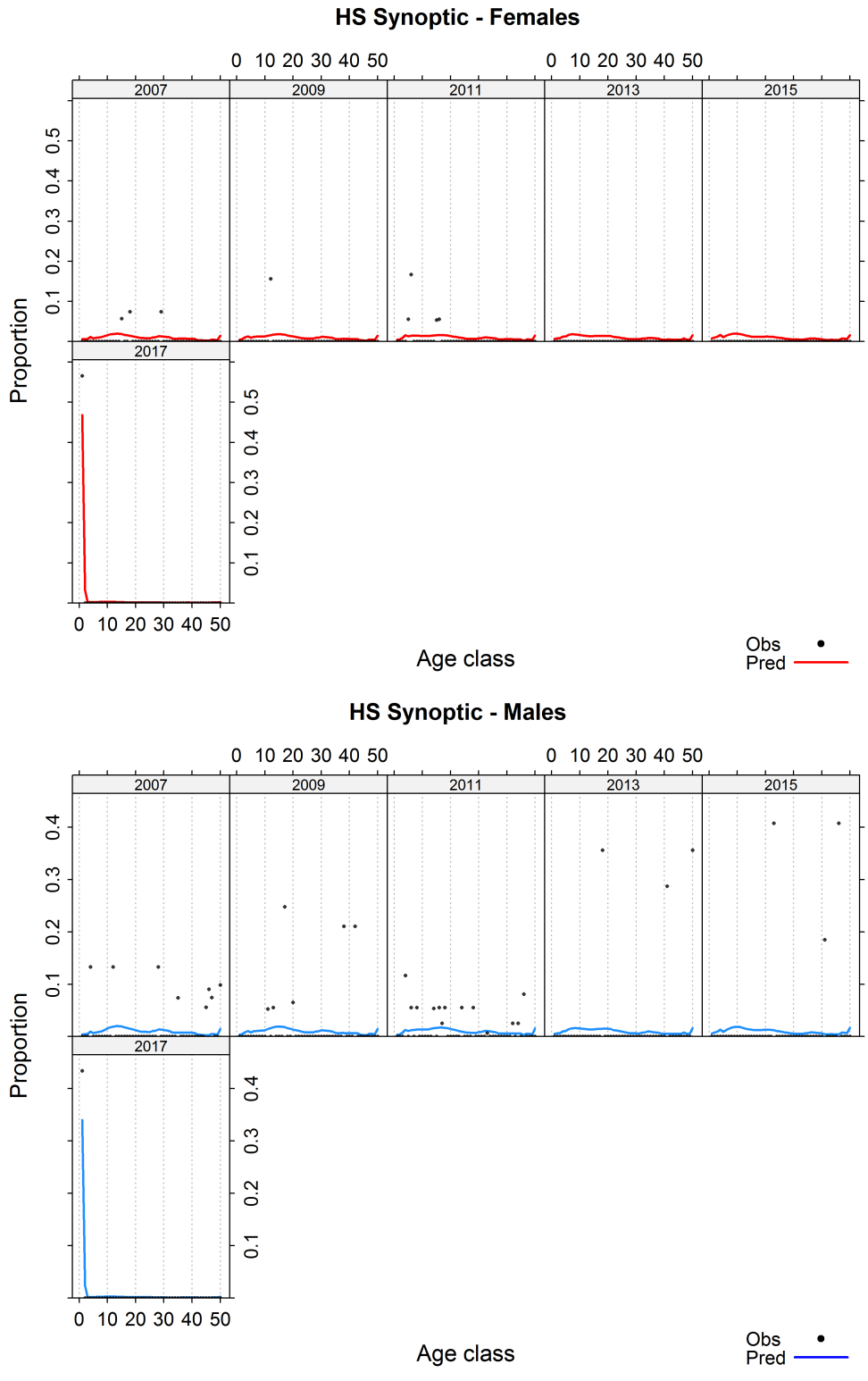

Figure F.18. CR.02.01: Observed and predicted proportions-at-age for HS Synoptic survey.

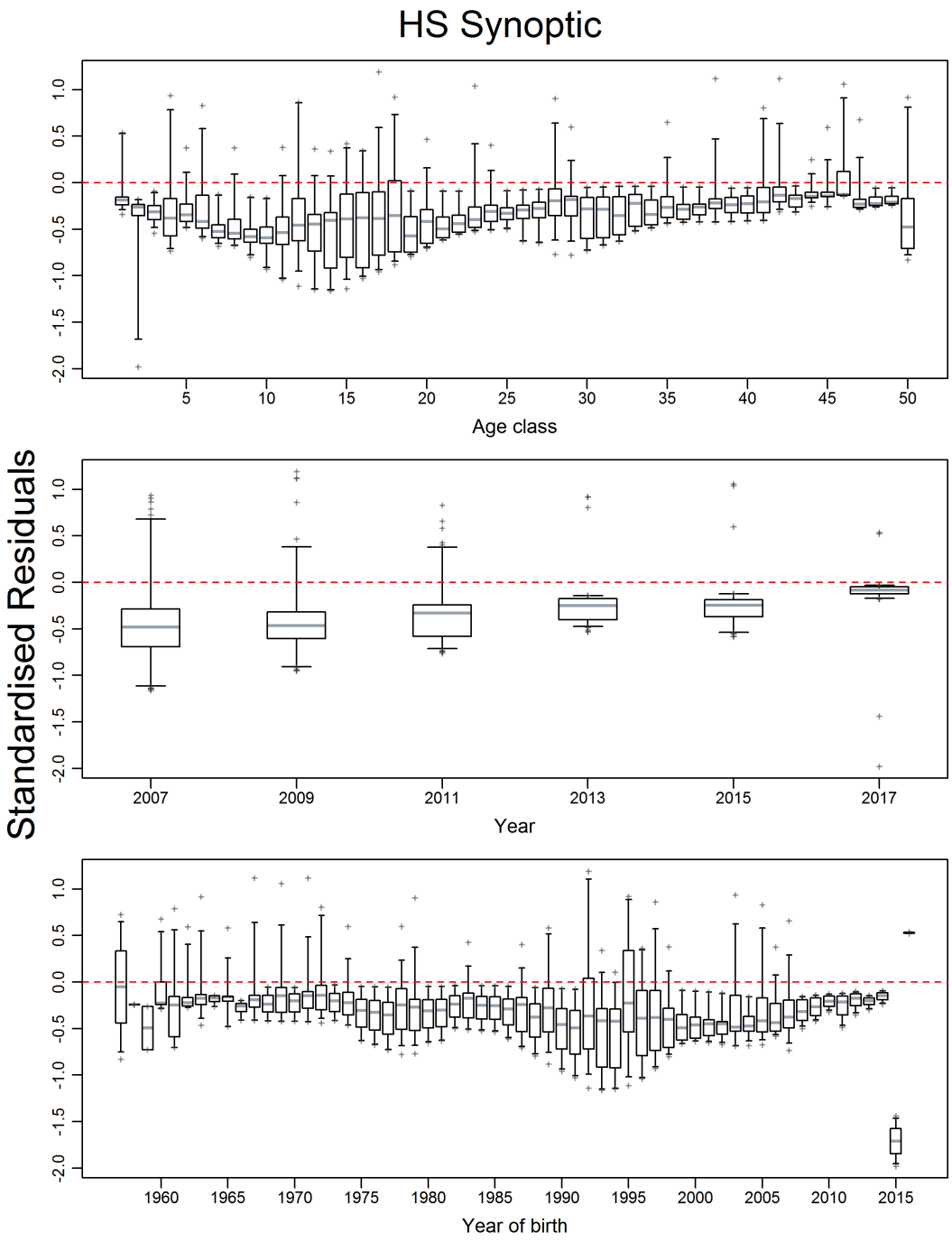

Figure F.19. CR.02.01: Residuals of model fits to proportion-at-age data (MPD values) from the HS Synoptic survey series. Details as for Figure F.11, for a total of 588 residuals.

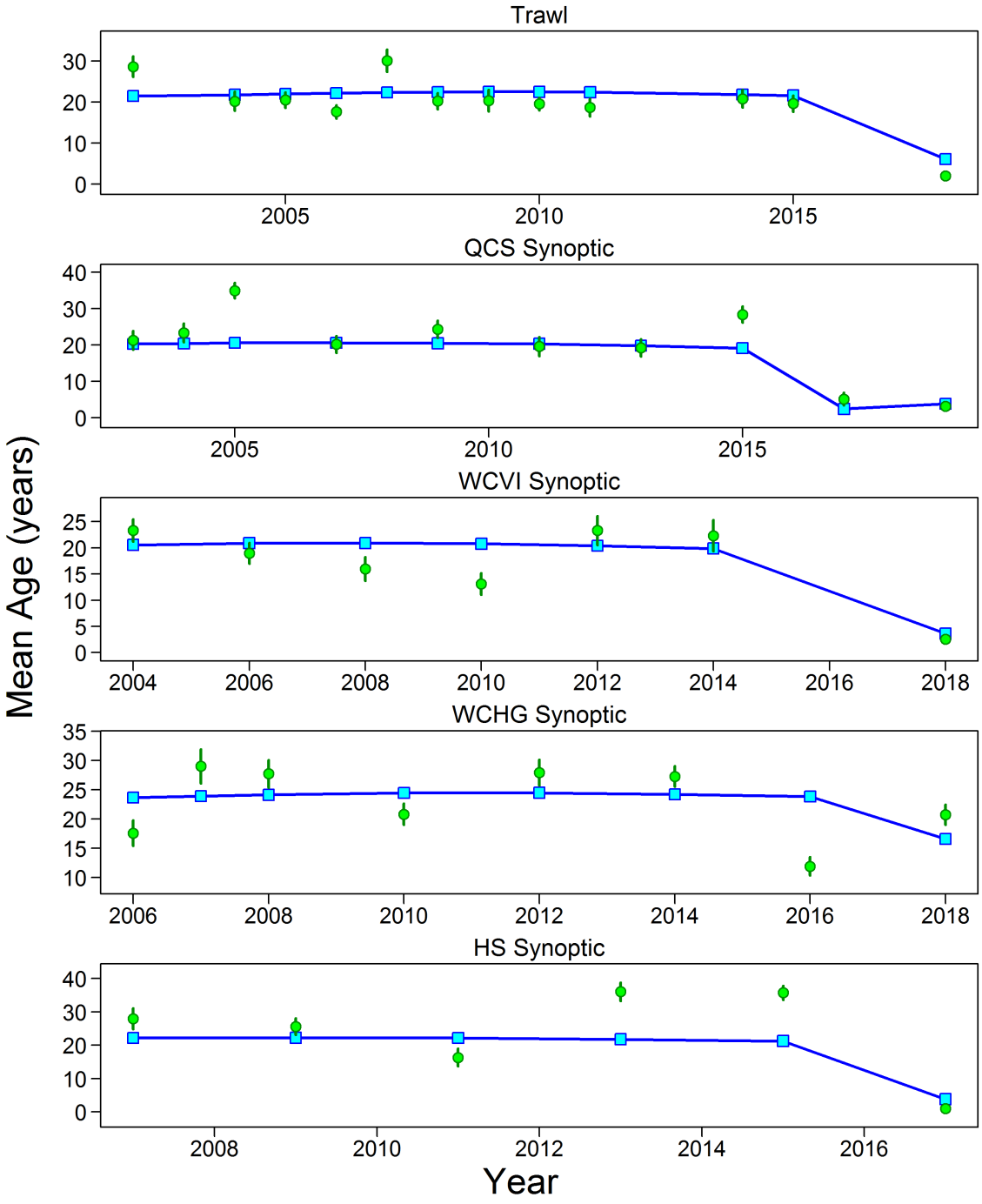

Figure F.20. CR.02.01: Mean ages each year for the data (solid circles) with 95% confidence intervals and model estimates (joined open squares) for the commercial and survey age data.

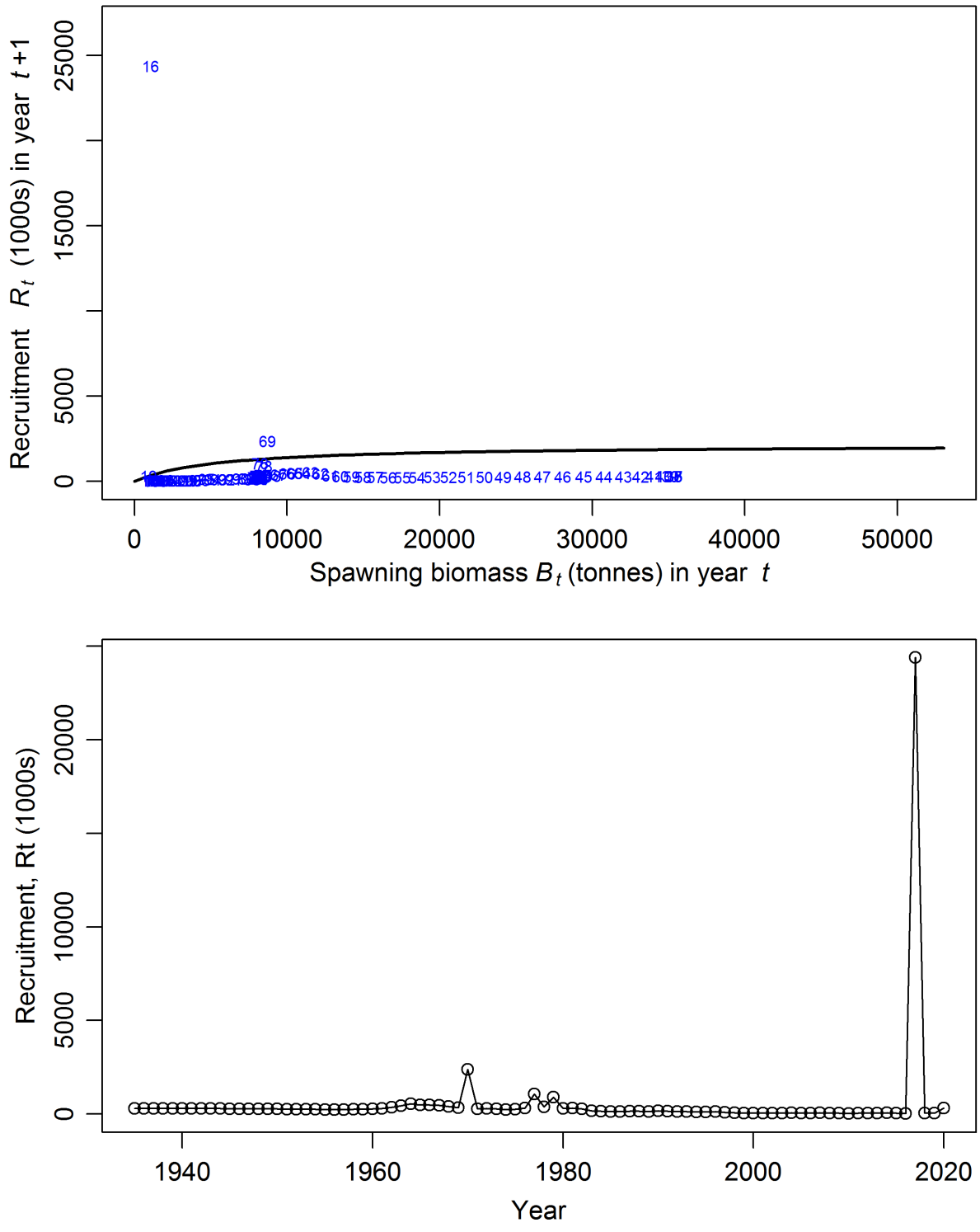

Figure F.21. CR.02.01: Top: deterministic stock-recruit relationship (black curve) and observed values (labelled by year of spawning) using MPD values. Bottom: recruitment (MPD values of age-1 individuals in year t) over time, in 1,000s of age-1 individuals, with a mean of 536.72.

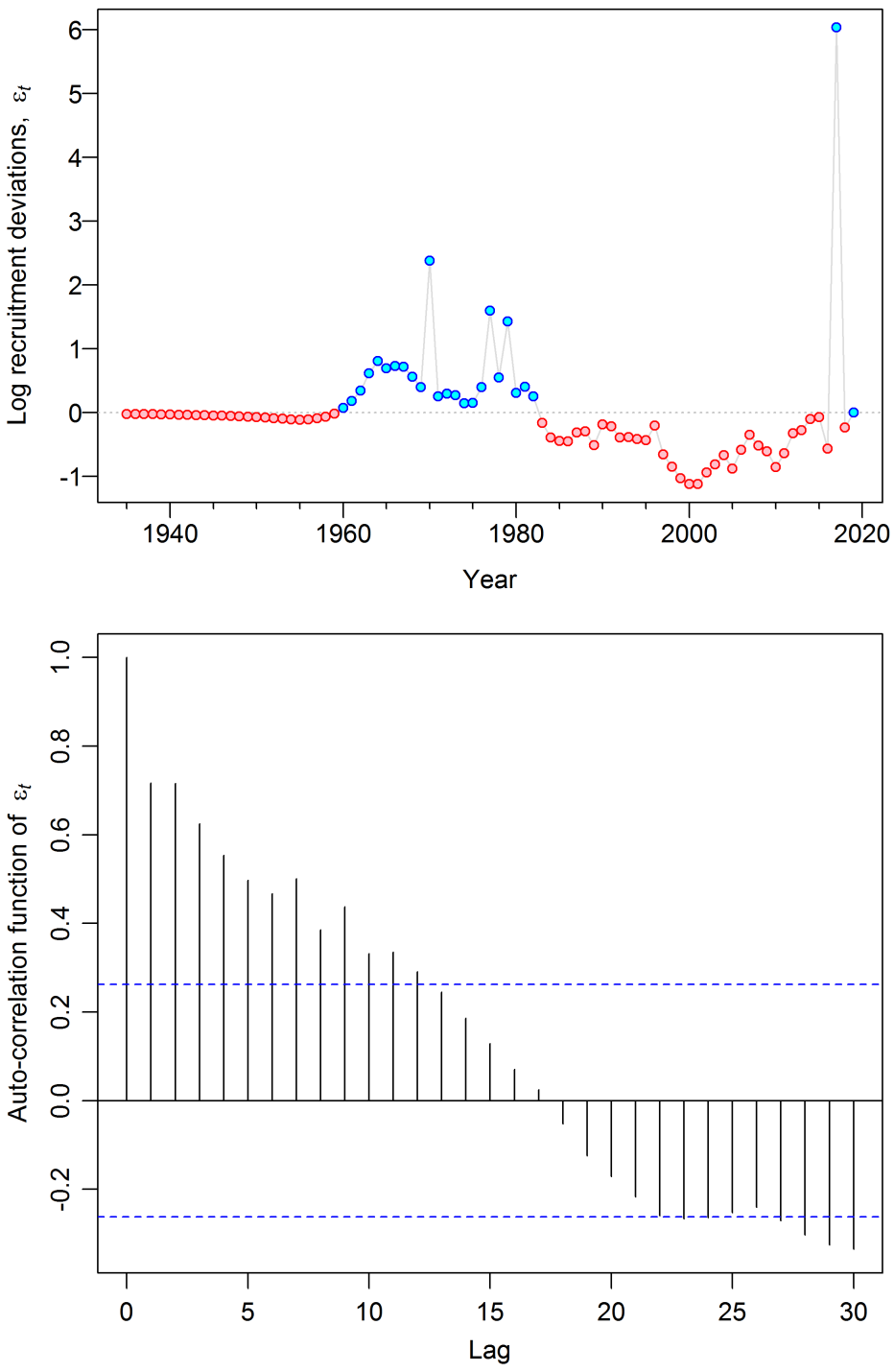

Figure F.22. CR.02.01: Top: log of the annual recruitment deviations, ϵ_t, where bias-corrected multiplicative deviation is $e^{\epsilon_t - \sigma_R^2/2}$ where $\epsilon_t \sim$ Normal$(0, \sigma_R^2)$. Bottom: auto-correlation function of the logged recruitment deviations (ϵ_t), for years 1958-2013. The start of this range is calculated as the first year of commercial age data (2002) minus the accumulator age class (A =50) plus the age for which commercial selectivity for females is 0.5 (namely 6); if the result is earlier than the model start year (1935), then the model start year is used. The end of the range is the final year that recruitments are calculated (2019) minus the age for which commercial selectivity for females is 0.5 (namely 6).

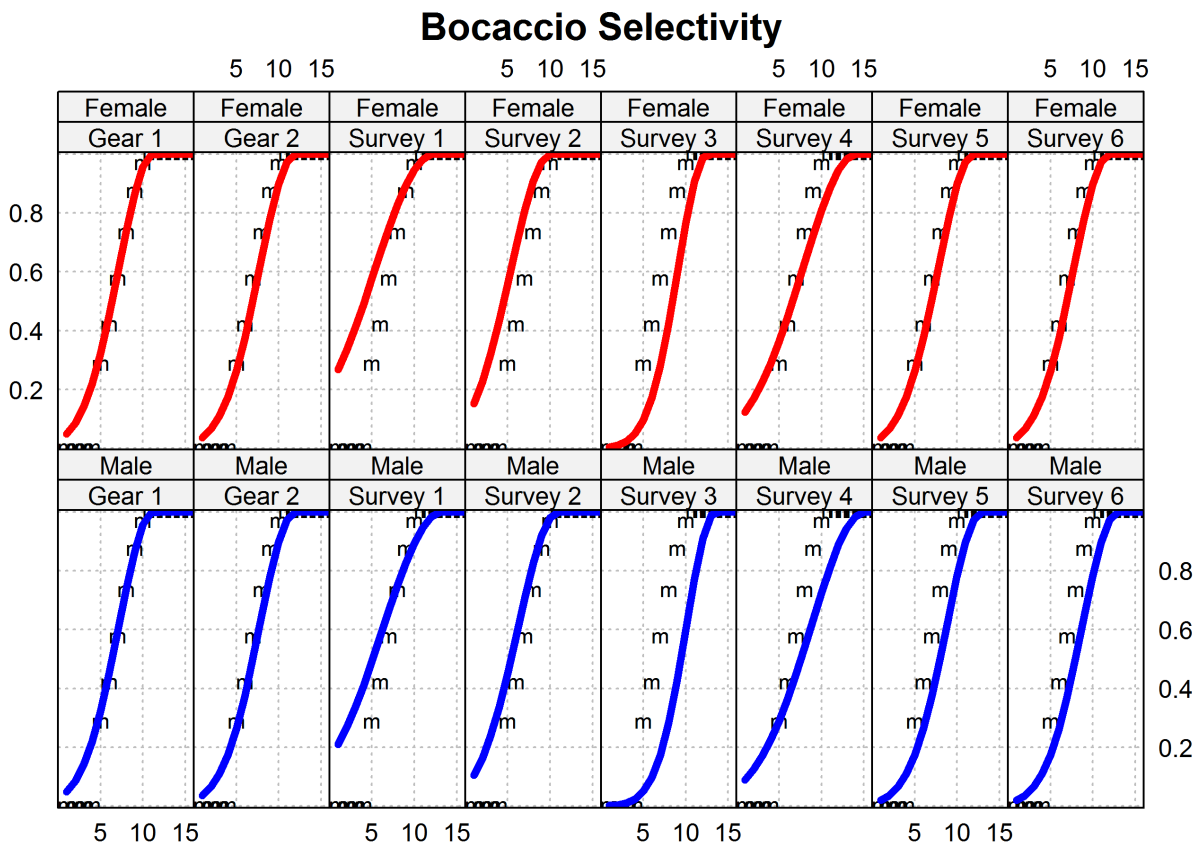

Figure F.23. CR.02.01: Selectivities for commercial catch (Gear 1: Trawl, Gear 2: Other) and surveys (all MPD values), with maturity ogive for females indicated by 'm'.

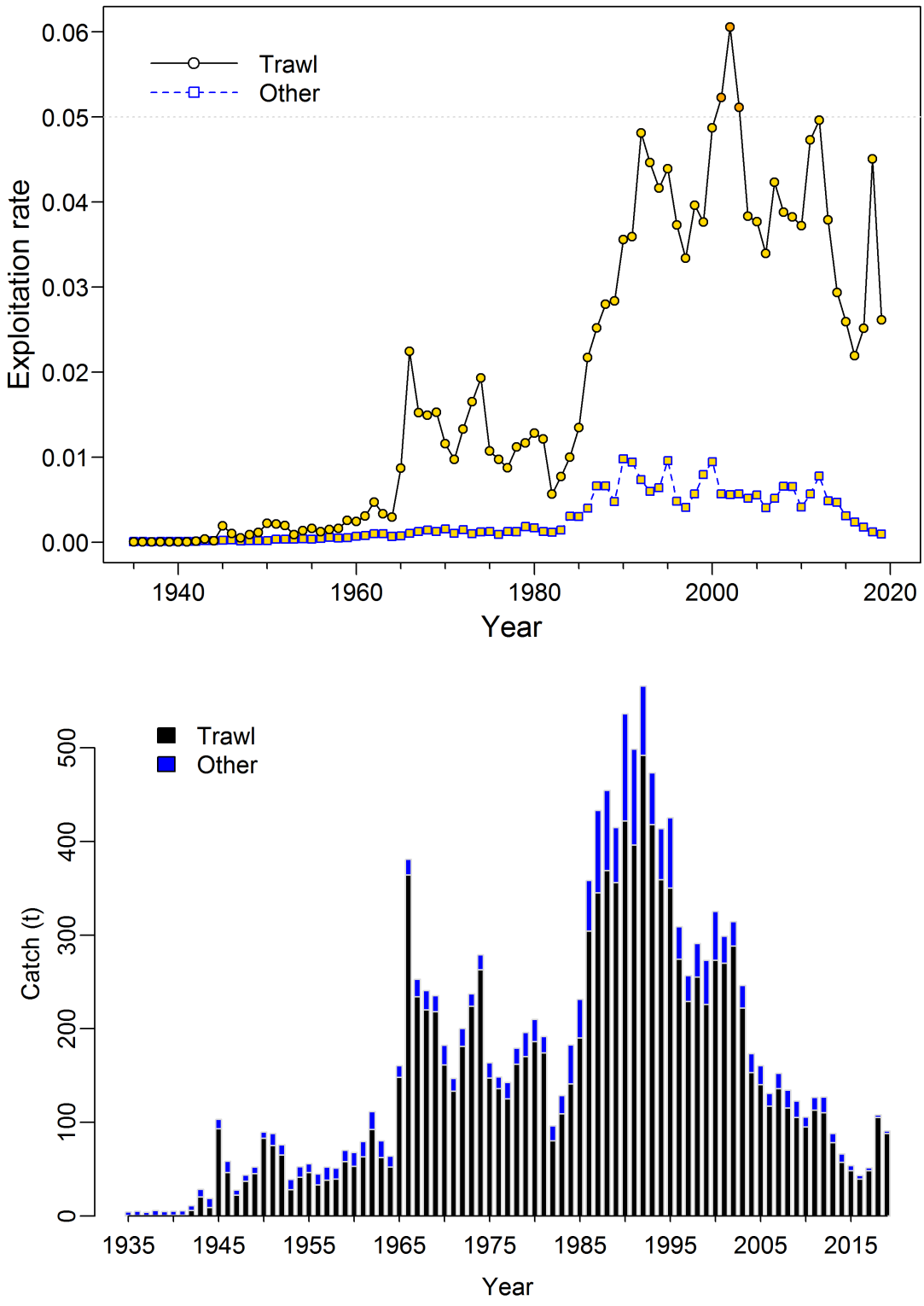

Figure F.24. CR.02.01: Top: exploitation rate (MPD) over time. Bottom: catch (t) by gear type.

F.2.1.2. Central Run MCMC

The MCMC procedure performed 6 million iterations, sampling every 5,000$^{\text{th}}$ to give 1200 MCMC samples. The first 200 samples were discarded and 1000 samples were used for the MCMC analysis.

The MCMC plots show:

- Figure F.25 – traces for 1000 samples of the primary estimated parameters;
- Figure F.26 – split-chain diagnostic plots for the primary estimated parameters;
- Figure F.27 – auto-correlation diagnostic plots for the primary estimated parameters;
- Figure F.28 – marginal posterior densities for the primary parameters compared to their respective prior density functions.

MCMC traces showed acceptable convergence properties (no trend with increasing sample number) for the estimated parameters (Figure F.25), as did diagnostic analyses that split the posterior samples into three equal consecutive segments (Figure F.26) and checked for parameter autocorrelation out to 60 lags (Figure F.27). Most of the parameters (e.g., R_0, h, μ_7) did not move very much from the initial MPD estimate to a median value that differed from the MPD (Figure F.28).

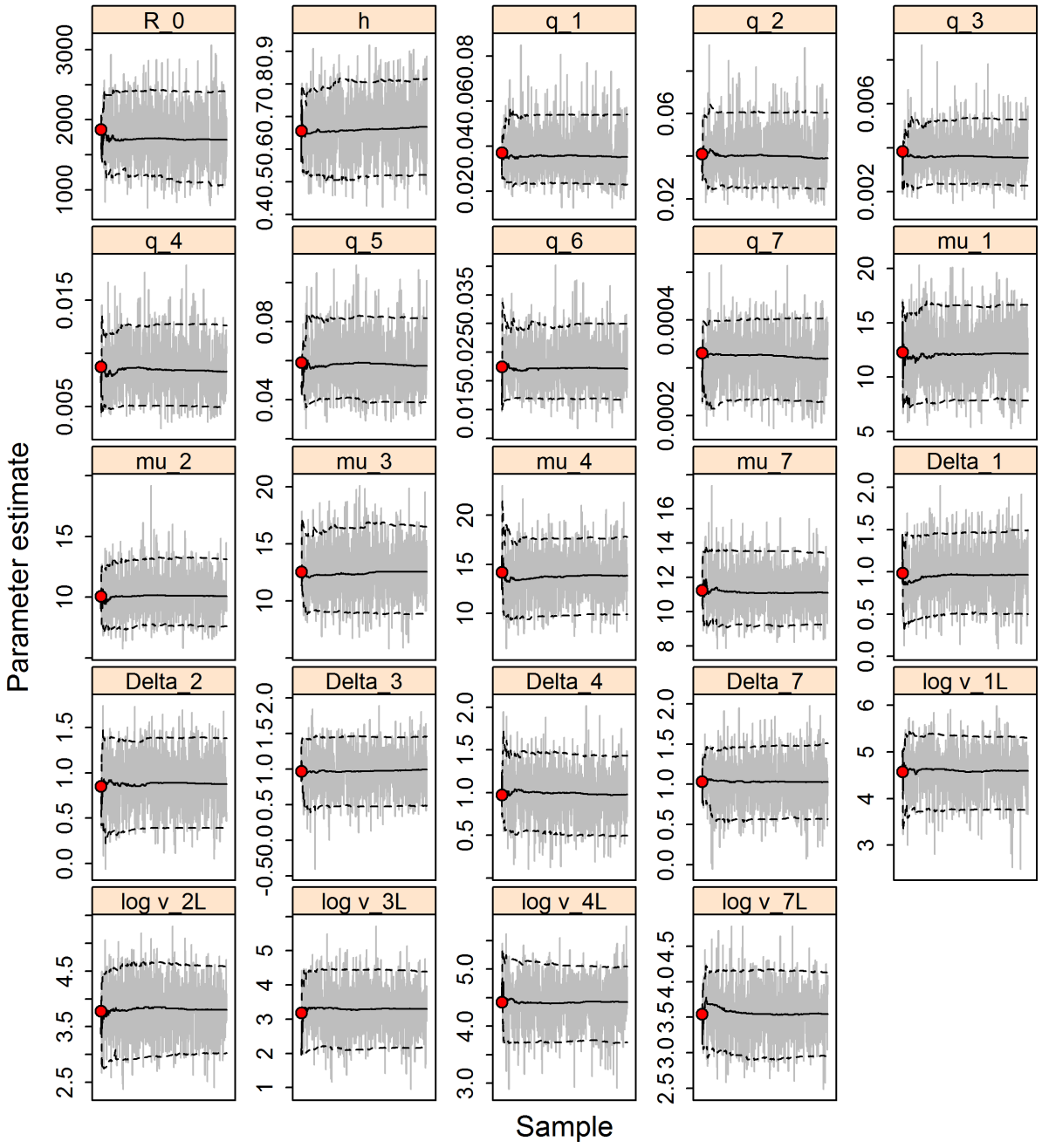

Figure F.25. CR.02.01: MCMC traces for the estimated parameters. Grey lines show the 1000 samples for each parameter, solid lines show the cumulative median (up to that sample), and dashed lines show the cumulative 0.05 and 0.95 quantiles. Red circles are the MPD estimates. For parameters other than M (if estimated), subscripts ≤ 6 correspond to fishery-independent surveys, and subscripts ≥ 7 denote the commercial fishery. Parameter notation is described in Appendix E.

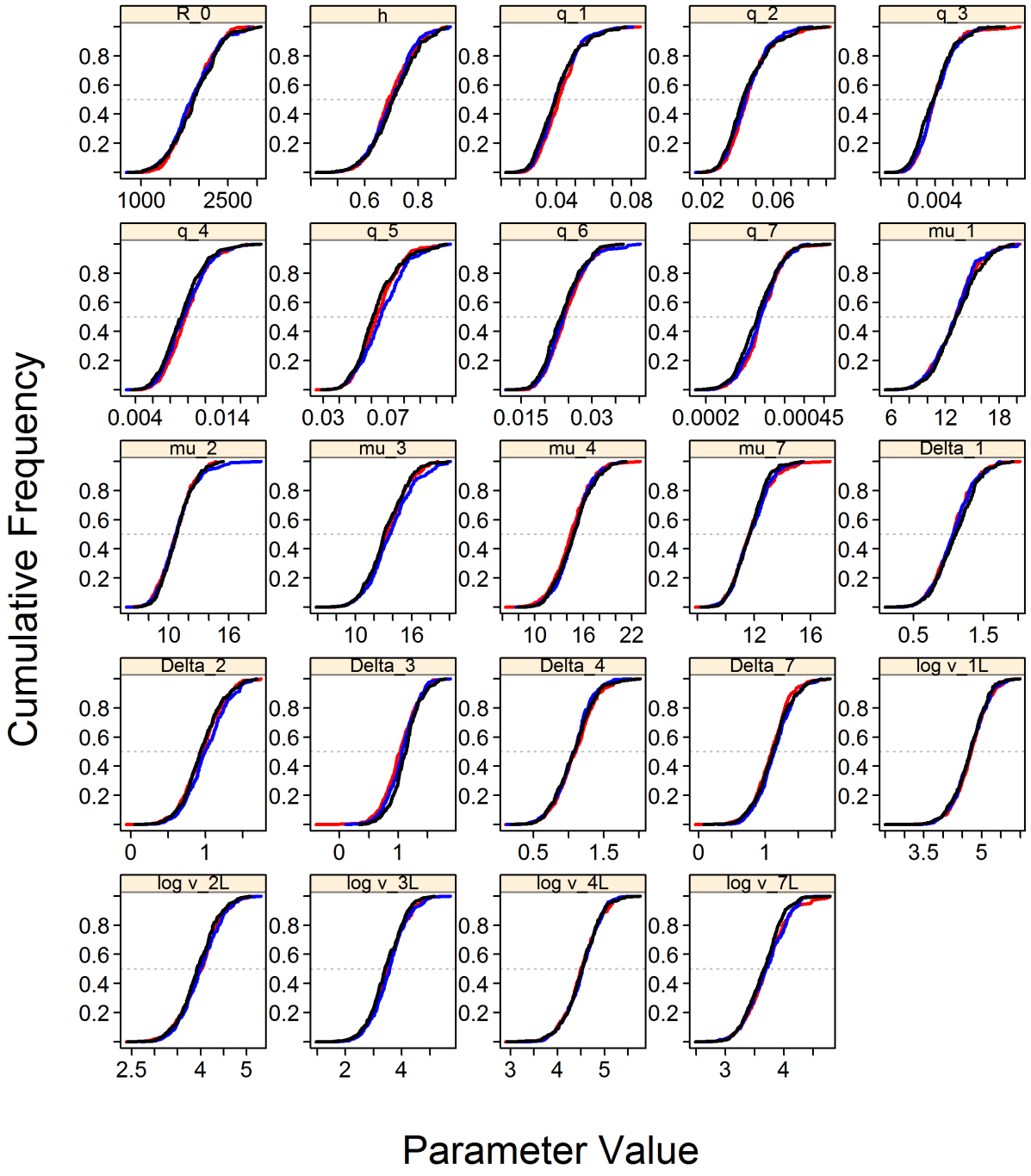

Figure F.26. CR.02.01: Diagnostic plot obtained by dividing the MCMC chain of 1000 MCMC samples into three segments, and overplotting the cumulative distributions of the first segment (red), second segment (blue) and final segment (black).

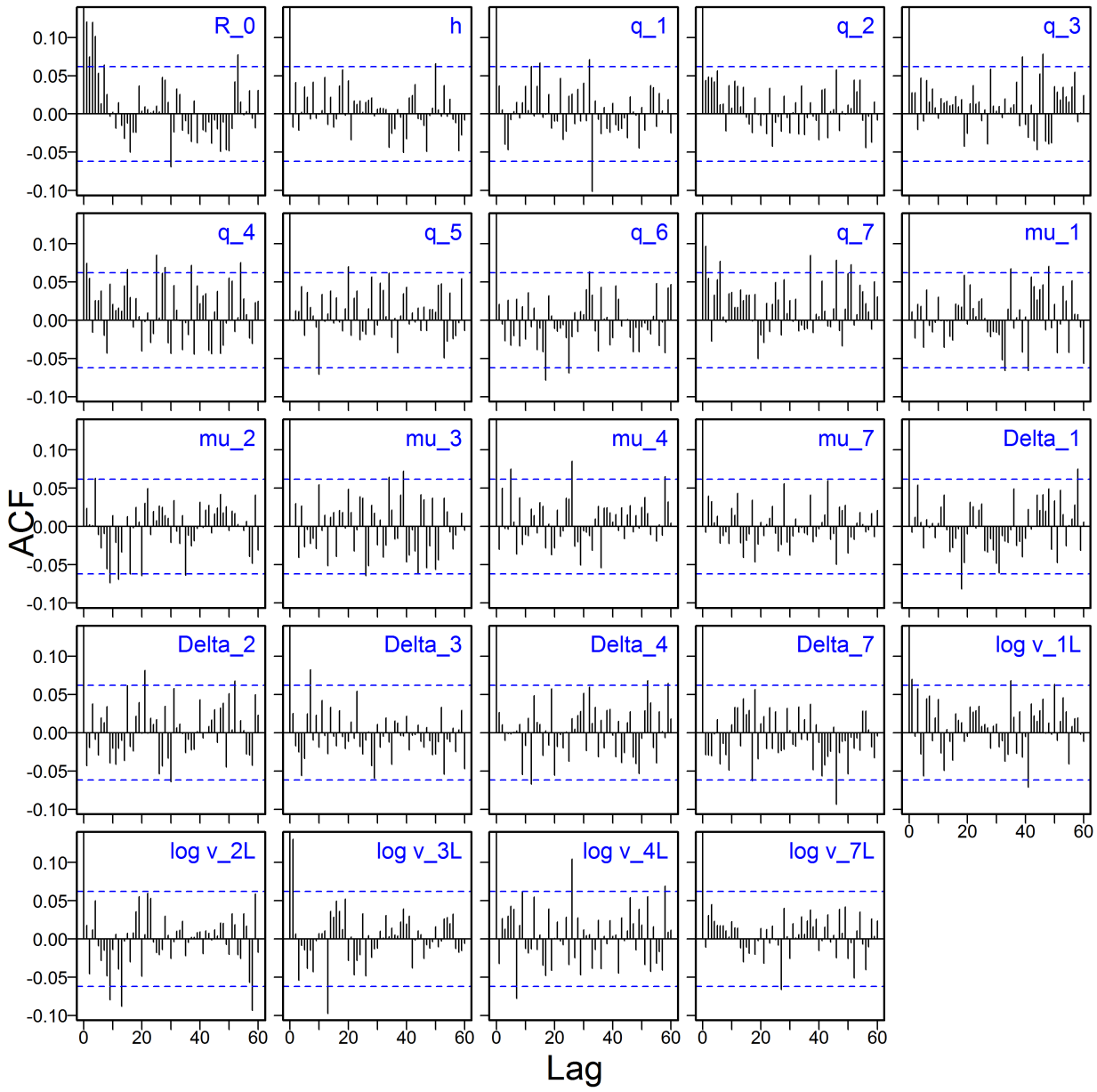

Figure F.27. CR.02.01: Autocorrelation plots for the estimated parameters from the MCMC output. Horizontal dashed blue lines delimit the 95% confidence interval for each parameter's set of lagged correlations.

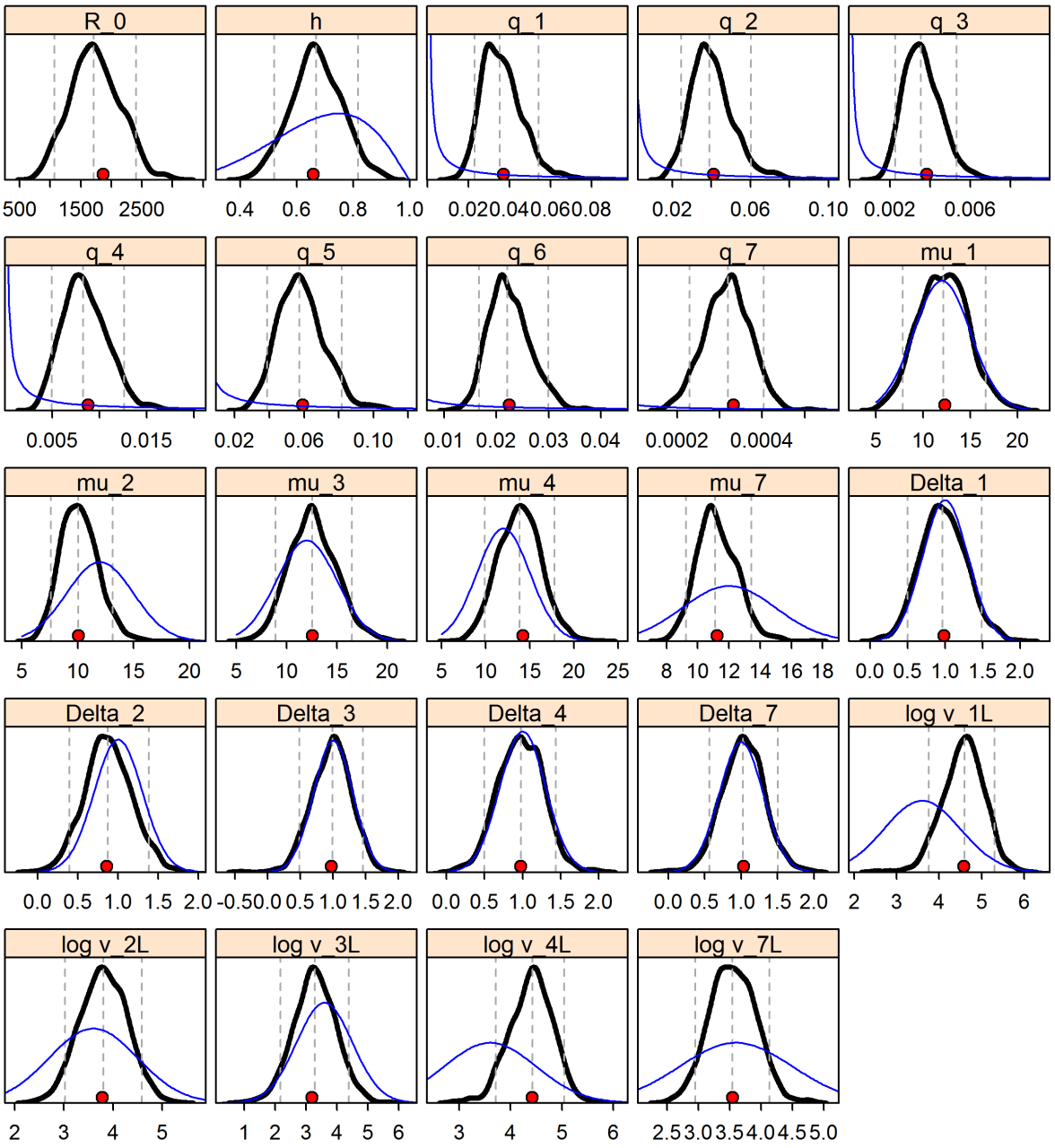

Figure F.28. CR.02.01: Marginal posterior densities (thick black curves) and prior density functions (thin blue curves) for the estimated parameters. Vertical lines represent the 0.05, 0.5, and 0.95 quantiles, and red filled circles are the MPD estimates. For R_0 the prior is a uniform distribution on the range [1, 10000000]. The priors for q_g are uniform on a log-scale, and so the probability density function is $1/(x(b-a))$ on a linear scale (where a and b are the bounds on the log scale).

F.2.1.3. Composite Base Case

The composite base case comprised three runs which spanned one major axis of uncertainty (M) for this stock assessment:

- **B1** (Run01) – fixed $M_{1,2} = 0.07$ and set $A = 50$;
- **B2** (Run02) – fixed $M_{1,2} = 0.08$ and set $A = 50$;
- **B3** (Run03) – fixed $M_{1,2} = 0.09$ and set $A = 50$.

For each run, 1000 MCMC samples were pooled to provide an average stock trajectory for population status and advice to managers. Estimating M was not possible given the uninformative nature of the data, with MPD estimates not shifting from the prior means. MCMC runs that estimated M exhibited unstable behaviour with no credible convergence.

Composite base case median parameter estimates appear in Table F.3, and derived quantities at equilibrium and associated with maximum sustainable yield (MSY) appear in Table F.4. The differences among the component base runs are summarised by various figures:

- Figure F.29 – MCMC traces of R_0 for the 3 component base runs;
- Figure F.30 – three chain segments of R_0 MCMC chains;
- Figure F.31 – autocorrelation plots for R_0 MCMC output;
- Figure F.32 – quantile plots of parameter estimates from 3 component base runs;
- Figure F.33 – quantile plots of selected derived quantities from 3 component base runs.

Various model trajectories and final stock status for the composite base case appear in the figures:

- Figure F.34 – estimates of spawning biomass B_t (tonnes) from pooled model posteriors;
- Figure F.35 – estimates of vulnerable biomass V_t (tonnes) from pooled model posteriors;
- Figure F.36 – estimates of exploitation rate u_t from pooled model posteriors;
- Figure F.37 – estimates of reconstructed (1935-2020) and projected (2021-2080) recruitment R_t (1000s age-1 fish) from pooled model posteriors;
- Figure F.38 – phase plot through time of median B_t/B_{MSY} and u_{t-1}/u_{MSY} relative to DFO's Precautionary Approach (PA) provisional reference points;
- Figure F.39 – BOR stock status at beginning of 2020.

Uncertainty in M was thought to be the most important component of uncertainty in this stock assessment, particularly when it was not possible to estimate this parameter. We explored additional sources of uncertainty through sensitivity runs.

For each component base run, 1000 MCMC samples were generated then pooled to provide an average stock trajectory for population status and advice to managers. Estimating M was not possible given the uninformative nature of the data, showing difficulty with finding a true minimum in the data and with the MCMC runs that estimated M exhibiting unstable behaviour without converging.

The three component runs outlined above converged without serious pathologies in the MCMC diagnostics (similar diagnostic results to those outlined for the central run). Figures F.29 to F.31 show diagnostics for the R_0 parameter in each of the three component runs, and Figure F.32 shows the distribution of all the estimated parameters. In most cases, the component runs had parameter estimates with very similar distributions. The R_0, h and q parameters varied with M, with R_0 increasing and h and q estimates decreasing with increasing M. The selectivity patterns differed little among the three M estimates (Figure F.32).

The composite base case, comprising three pooled MCMC runs, was used to calculate a set of parameter estimates (Table F.3) and derived quantities at equilibrium and those associated with MSY (Table F.4). The composite base case population trajectory from 1935 to 2020 and projected biomass to 2080 (Figure F.34), assuming a constant catch policy of 200 t/y (or a harvest rate policy of u=0.04), indicates that the median stock biomass will rebuild to above the USR in less than five years.

A phase plot of the time-evolution of spawning biomass and exploitation rate in the two modelled fisheries in MSY space (Figure F.38) suggests that the stock has been overfished since the 1990s, with a current position at $B_{2020}/B_{\mathrm{MSY}}$ = 0.096 (0.042, 0.234), $u_{2019(\mathrm{trawl})}/u_{\mathrm{MSY}}$ = 0.291 (0.116, 0.664), and $u_{2019(\mathrm{other})}/u_{\mathrm{MSY}}$ = 0.011 (0.004, 0.026).

Table F.3. The 0.05, 0.5, and 0.95 quantiles for pooled model parameters (defined in Appendix E) from MCMC estimation of 3 base model runs.

	5%	50%	95%
R_0	703	1,713	4,633
h	0.503	0.671	0.846
q_1	0.0190	0.0355	0.0578
q_2	0.0211	0.0394	0.0647
q_3	0.00195	0.00356	0.00566
q_4	0.00438	0.00826	0.0136
q_5	0.0340	0.0573	0.0910
q_6	0.0130	0.0221	0.0342
q_7	0.000196	0.000321	0.000445
μ_1	7.83	12.0	16.7
μ_2	7.60	10.0	13.1
μ_3	8.74	12.5	16.3
μ_4	9.69	13.8	17.9
μ_7	9.24	11.1	13.4
Δ_1	0.499	0.983	1.46
Δ_2	0.393	0.863	1.35
Δ_3	0.473	0.976	1.46
Δ_4	0.509	0.979	1.45
Δ_7	0.576	1.04	1.51
$\log v_{1L}$	3.72	4.59	5.35
$\log v_{2L}$	3.01	3.80	4.58
$\log v_{3L}$	2.18	3.30	4.49
$\log v_{4L}$	3.67	4.41	5.07
$\log v_{7L}$	2.97	3.55	4.14

Table F.4. The 0.05, 0.5, and 0.95 quantiles of MCMC-derived quantities from 3000 samples pooled from 3 MCMC posteriors. Definitions are: B_0 – unfished equilibrium spawning biomass (mature females), V_0 – unfished equilibrium vulnerable biomass (males and females), B_{2020} – spawning biomass at the start of 2020, V_{2020} – vulnerable biomass in the middle of 2020, u_{2019} – exploitation rate (ratio of total catch to vulnerable biomass) in the middle of 2019, $u_{\max}$ – maximum exploitation rate (calculated for each sample as the maximum exploitation rate from 1935-2019), B_{MSY} – equilibrium spawning biomass at MSY (maximum sustainable yield), u_{MSY} – equilibrium exploitation rate at MSY, V_{MSY} – equilibrium vulnerable biomass at MSY. All biomass values (and MSY) are in tonnes. For reference, the average catch over the last 5 years (2015-2019) was 69 t.

	5%	50%	95%
B_0	16,460	32,289	71,710
V_0 (trawl)	27,930	55,089	123,319
V_0 (other)	27,286	53,564	119,116
B_{2020}	552	899	1,655
V_{2020} (trawl)	3,046	5,703	12,273
V_{2020} (other)	2,582	4,709	9,812
B_{2020}/B_0	0.0132	0.0278	0.0578
V_{2020}/V_0 (trawl)	0.0496	0.104	0.213
V_{2020}/V_0 (other)	0.0426	0.0875	0.175
u_{2019} (trawl)	0.0121	0.0250	0.0441
u_{2019} (other)	0.000467	0.000930	0.00161
$u_{\max}$ (trawl)	0.0369	0.0588	0.0792
$u_{\max}$ (other)	0.00654	0.00968	0.0124
MSY	703	1,461	3,623
B_{MSY}	4,134	9,462	22,469
$0.4B_{2020}$	1,653	3,785	8,988
$0.8B_{2020}$	3,307	7,570	17,976
$B_{2020}/B_{\mathrm{MSY}}$	0.0417	0.0963	0.234
B_{MSY}/B_0	0.225	0.291	0.353
V_{MSY}	7,858	17,554	41,876
V_{MSY}/V_0 (trawl)	0.252	0.319	0.378
V_{MSY}/V_0 (other)	0.253	0.328	0.396
u_{MSY}	0.0540	0.0850	0.133
$u_{2019}/u_{\mathrm{MSY}}$ (trawl)	0.116	0.291	0.664
$u_{2019}/u_{\mathrm{MSY}}$ (other)	0.00421	0.0109	0.0258

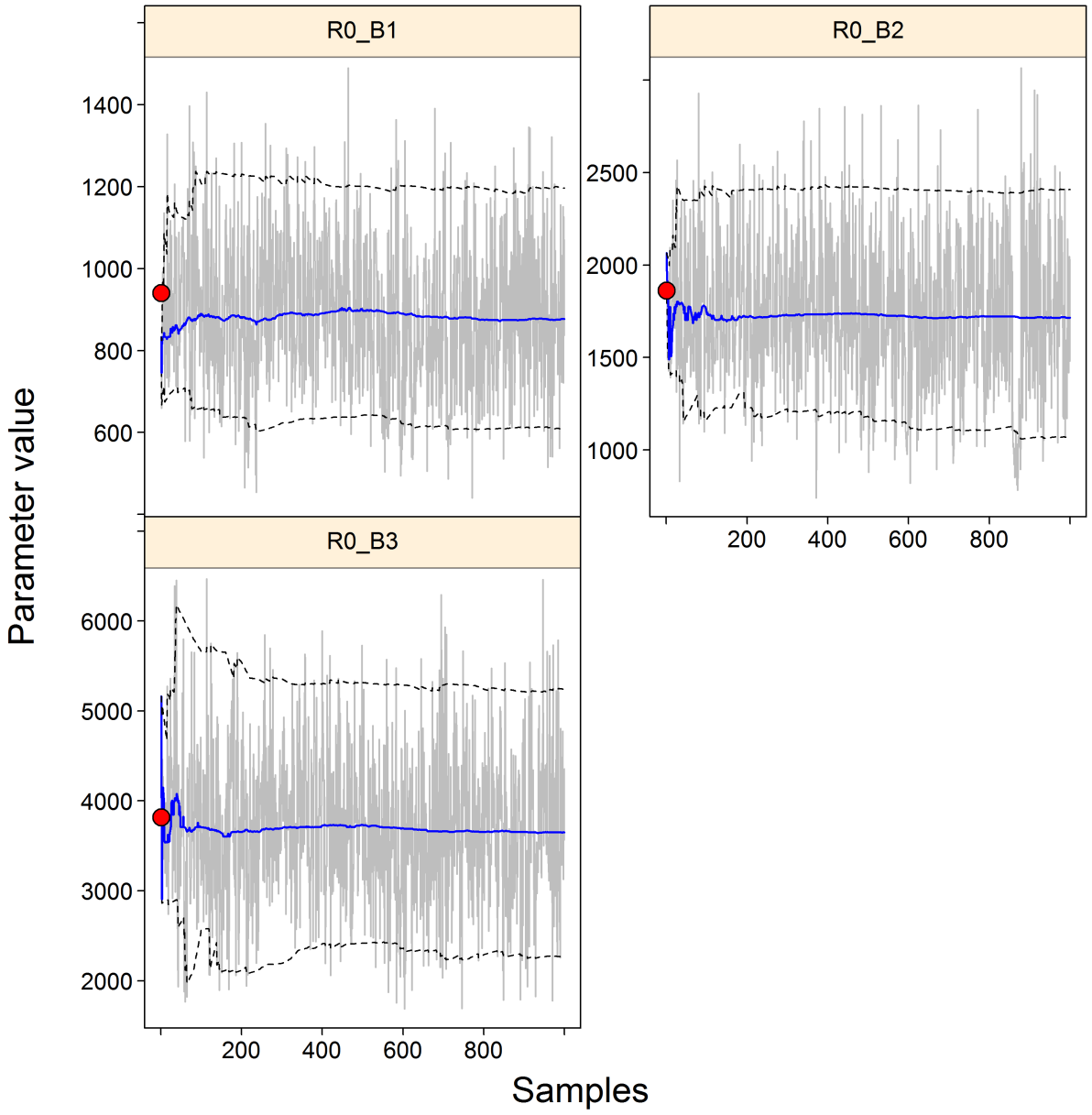

Figure F.29. Component base: MCMC traces of R_0 for the 3 component base runs. Grey lines show the 1000 samples for the R_0 parameter, solid lines show the cumulative median (up to that sample), and dashed lines show the cumulative 0.05 and 0.95 quantiles. Red circles are the MPD estimates.

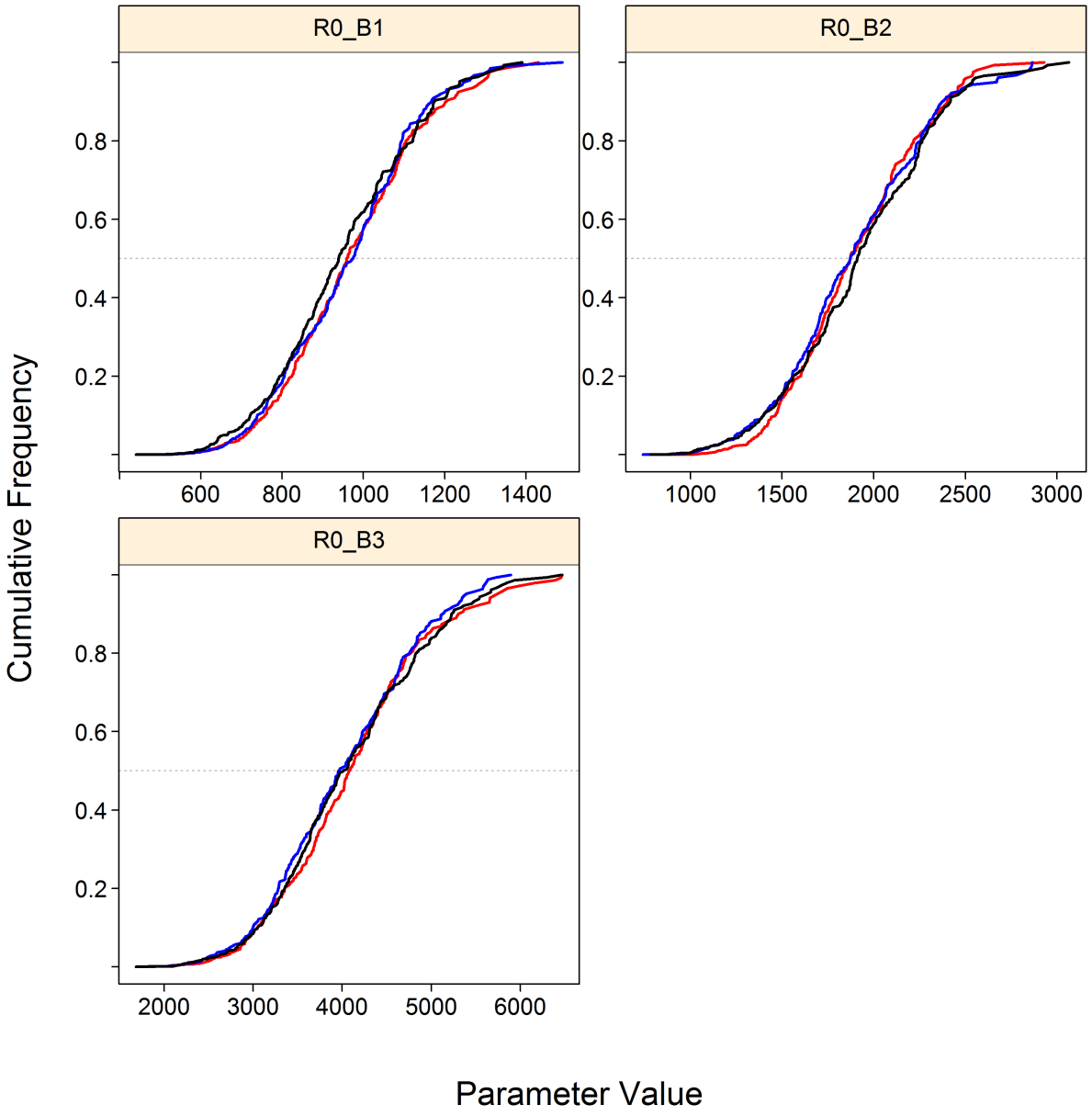

Figure F.30. Component base: diagnostic plots obtained by dividing the R_0 MCMC chains of 1000 MCMC samples into three segments, and overplotting the cumulative distributions of the first segment (red), second segment (blue) and final segment (black).

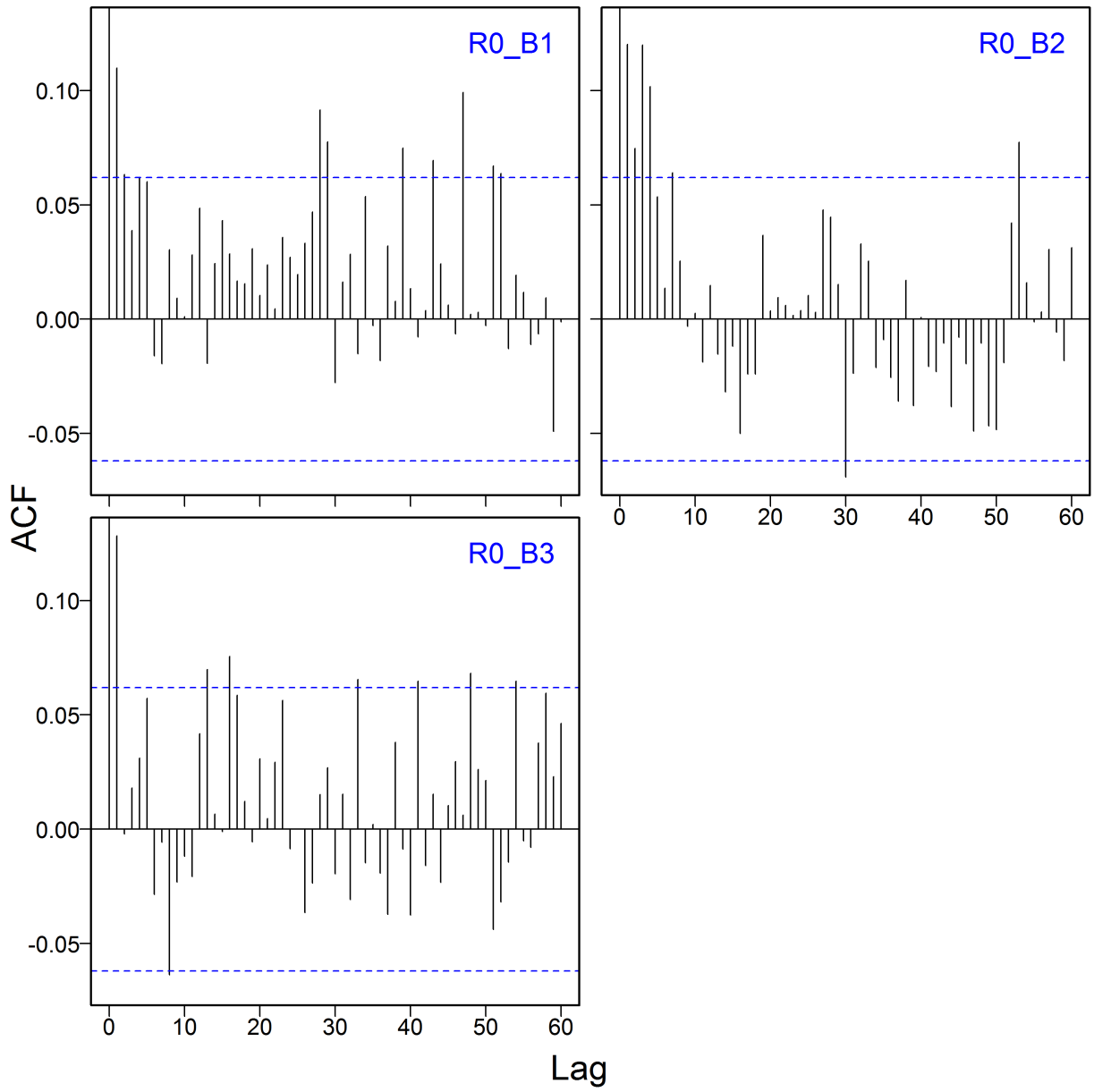

Figure F.31. Component base: autocorrelation plots for the component base R_0 parameters from the MCMC output. Horizontal dashed blue lines delimit the 95% confidence interval for each parameter's set of lagged correlations.

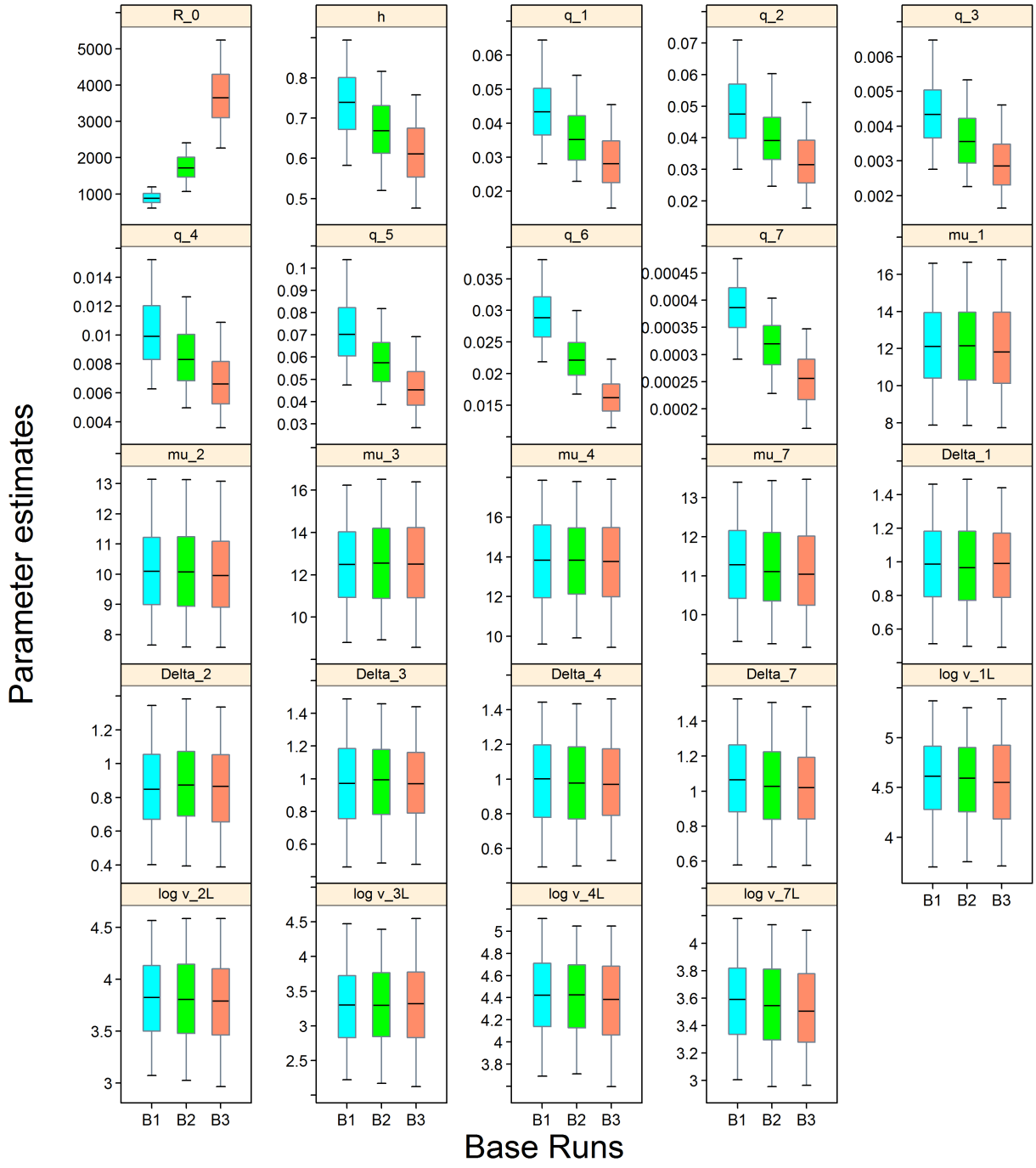

Figure F.32. Component base: quantile plots of the parameter estimates from 3 component runs of the base case, where blue boxes denote M=0.07, green boxes denote M=0.08, red boxes denote M=0.09. The boxplots delimit the 0.05, 0.25, 0.5, 0.75, and 0.95 quantiles.

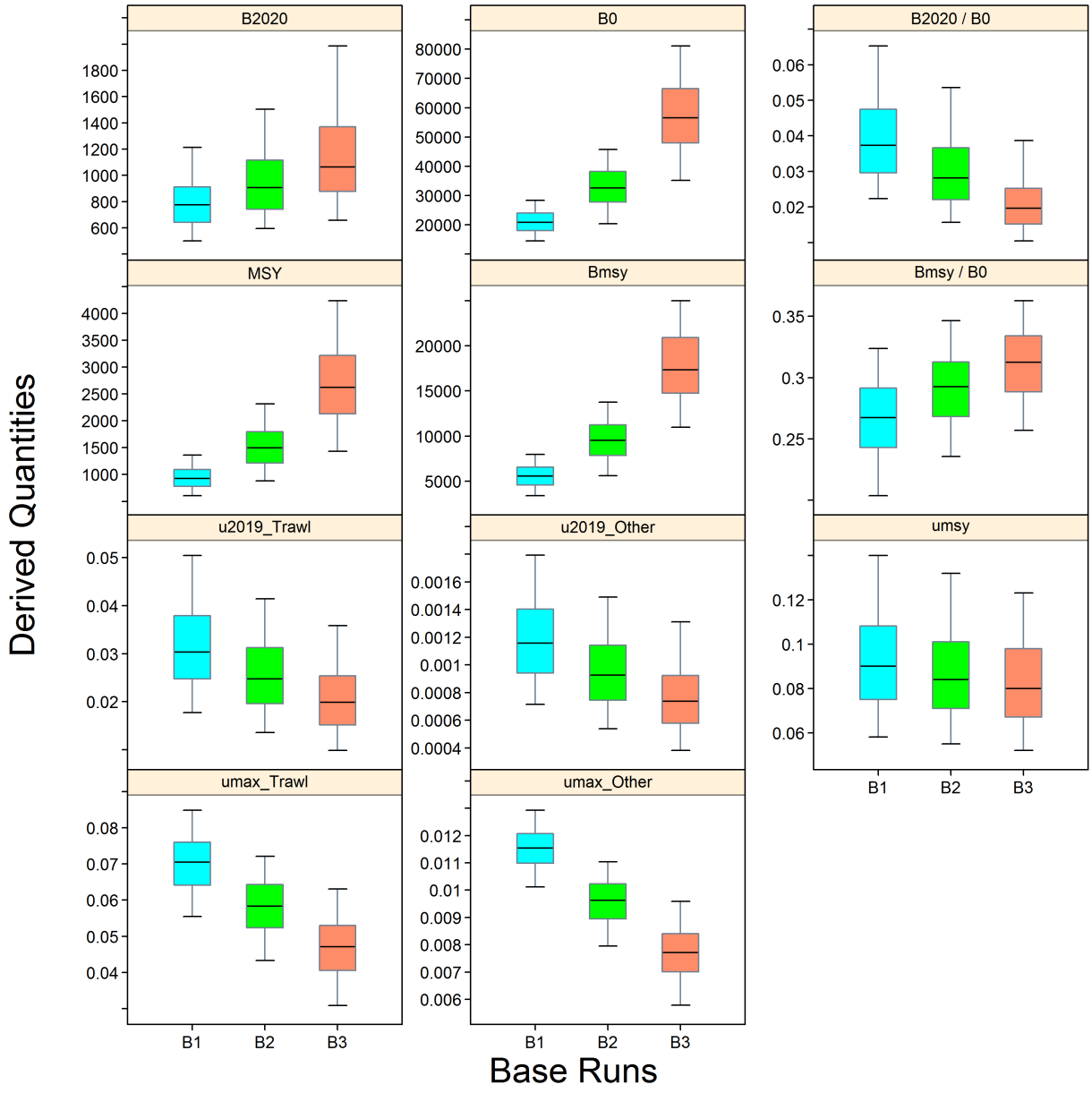

Figure F.33. Component base: quantile plots of selected derived quantities (B_{2020}, B_0, B_{2020}/B_0, MSY, B_{MSY}, B_{MSY}/B_0, u_{2019}, u_{MSY}, $u_{\max}$) from 3 component runs of the base case, where blue boxes denote M=0.07, green boxes denote M=0.08, red boxes denote M=0.09. The boxplots delimit the 0.05, 0.25, 0.5, 0.75, and 0.95 quantiles.

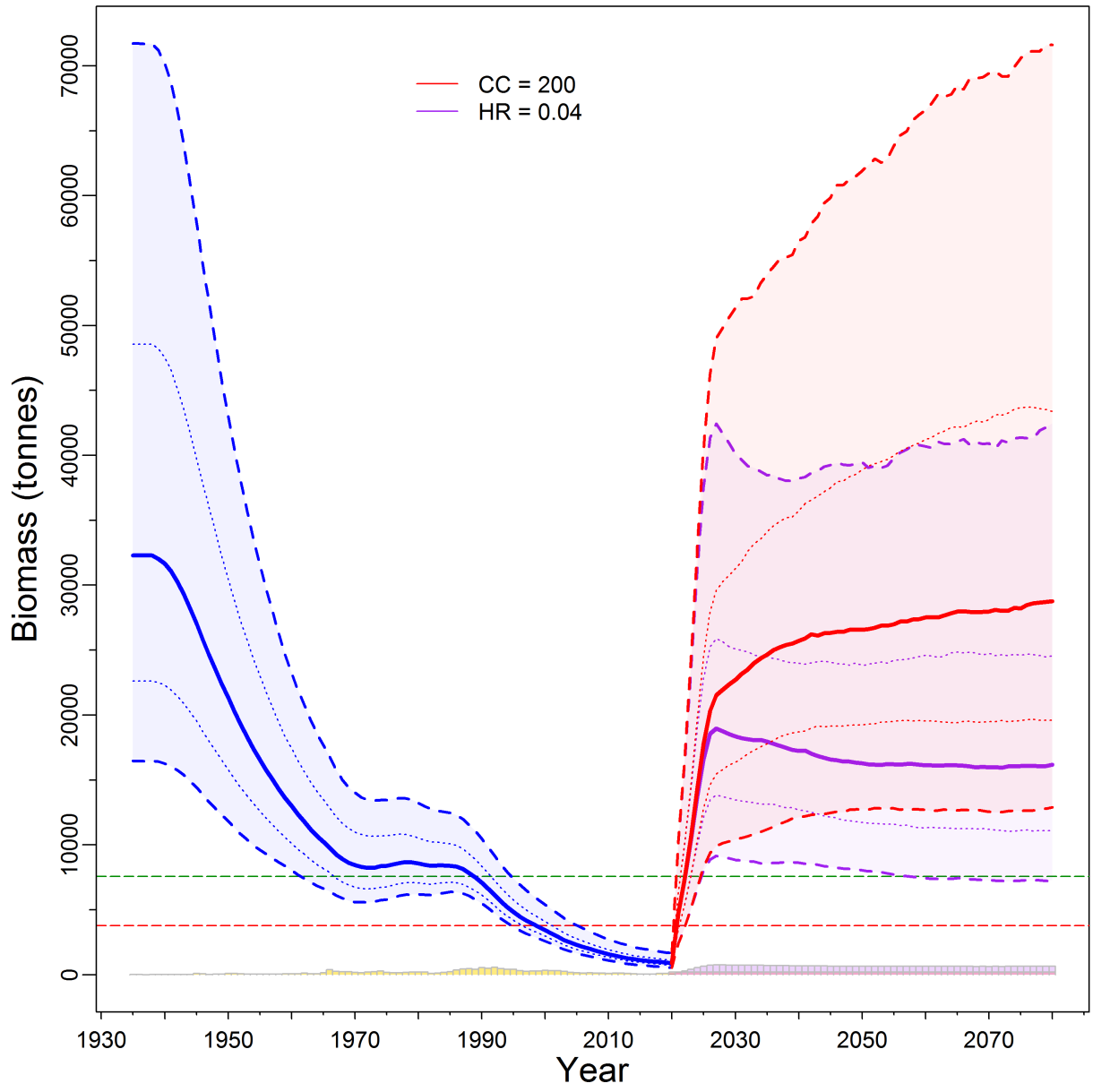

Figure F.34. Composite base: estimates of spawning biomass B_t (tonnes) from pooled model posteriors. The median biomass trajectory appears as a solid curve surrounded by a 90% credibility envelope (quantiles: 0.05-0.95) in light blue and delimited by dashed lines for years t=1935:2020; projected biomass appears in light red for years t=2021:2080. Also delimited is the 50% credibility interval (quantiles: 0.25-0.75) delimited by dotted lines. The horizontal dashed lines show the median LRP and USR. Catches are represented as bars along the bottom axis and assumed catch policies appear in the legend, where CC = t/y and HR = harvest rate.

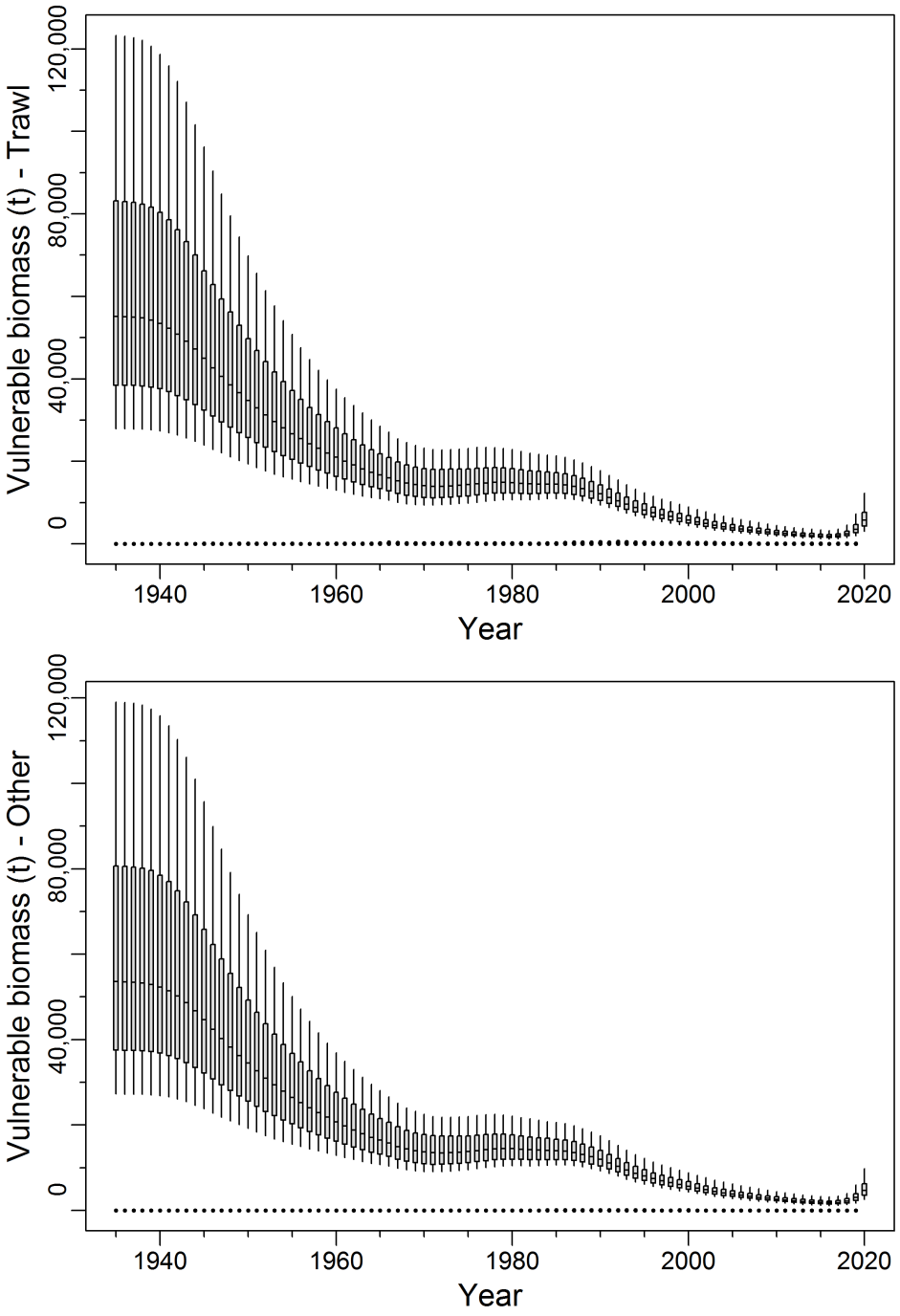

Figure F.35. Composite base: estimated vulnerable biomass trajectory for two fisheries (boxplots) and commercial catch history (vertical bars), in tonnes. Boxplots show the 0.05, 0.25, 0.5, 0.75, and 0.95 quantiles from the MCMC results.

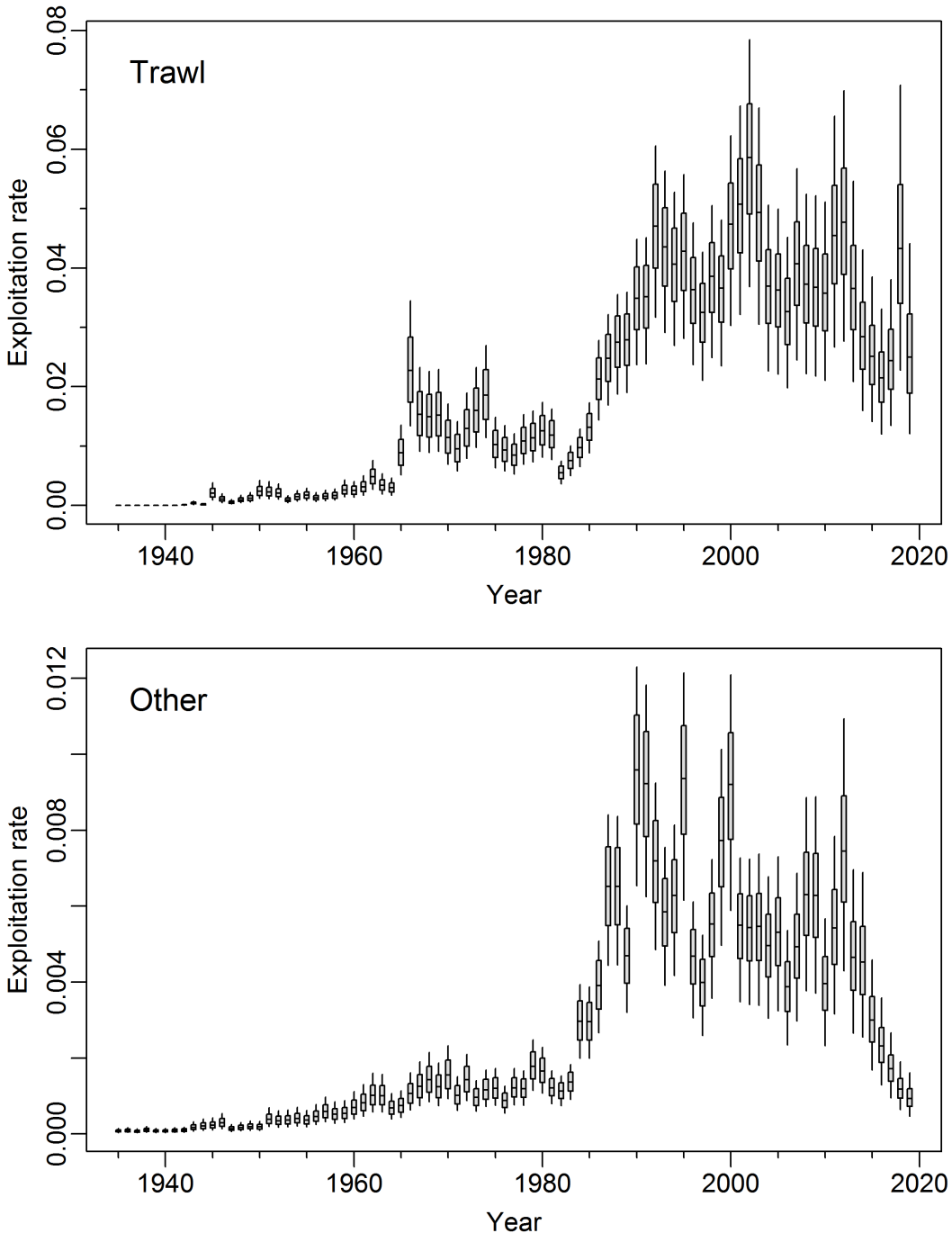

Figure F.36. Composite base: marginal posterior distribution of exploitation rate trajectory for two fisheries. Boxplots show the 0.05, 0.25, 0.5, 0.75, and 0.95 quantiles from the MCMC results.

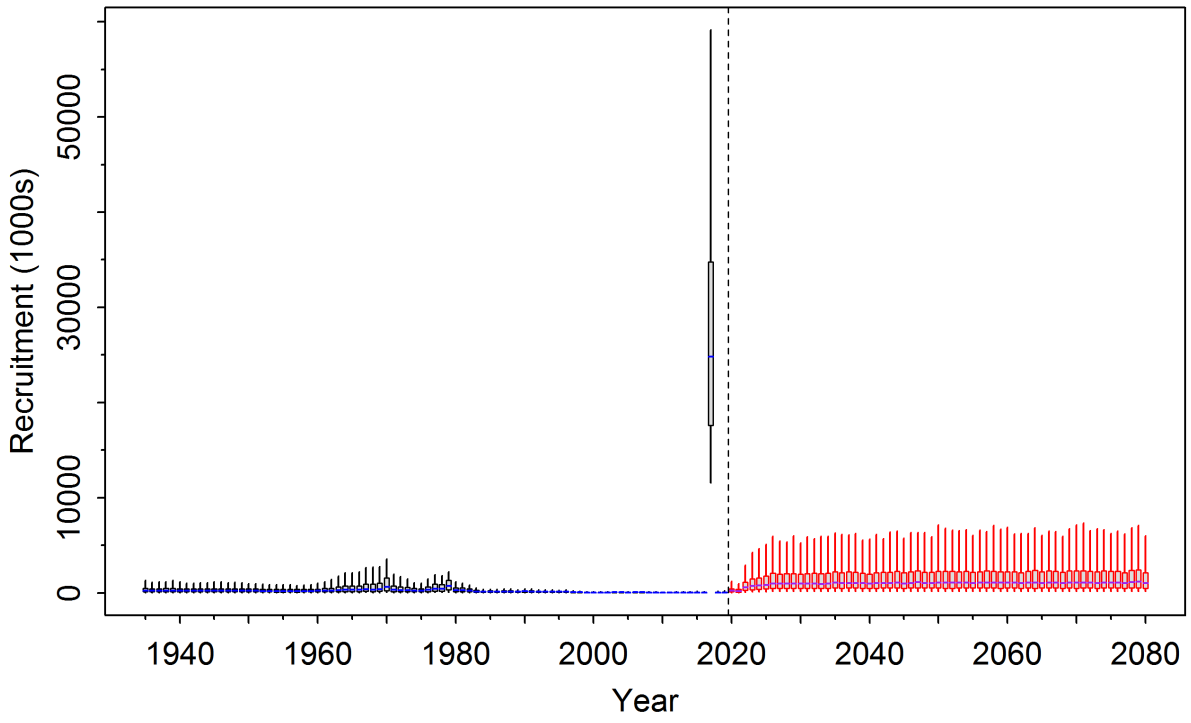

Figure F.37. Composite base: marginal posterior distribution of recruitment trajectory (reconstructed: 1935-2020, projected: 2021-2080) in 1,000s of age-1 fish.

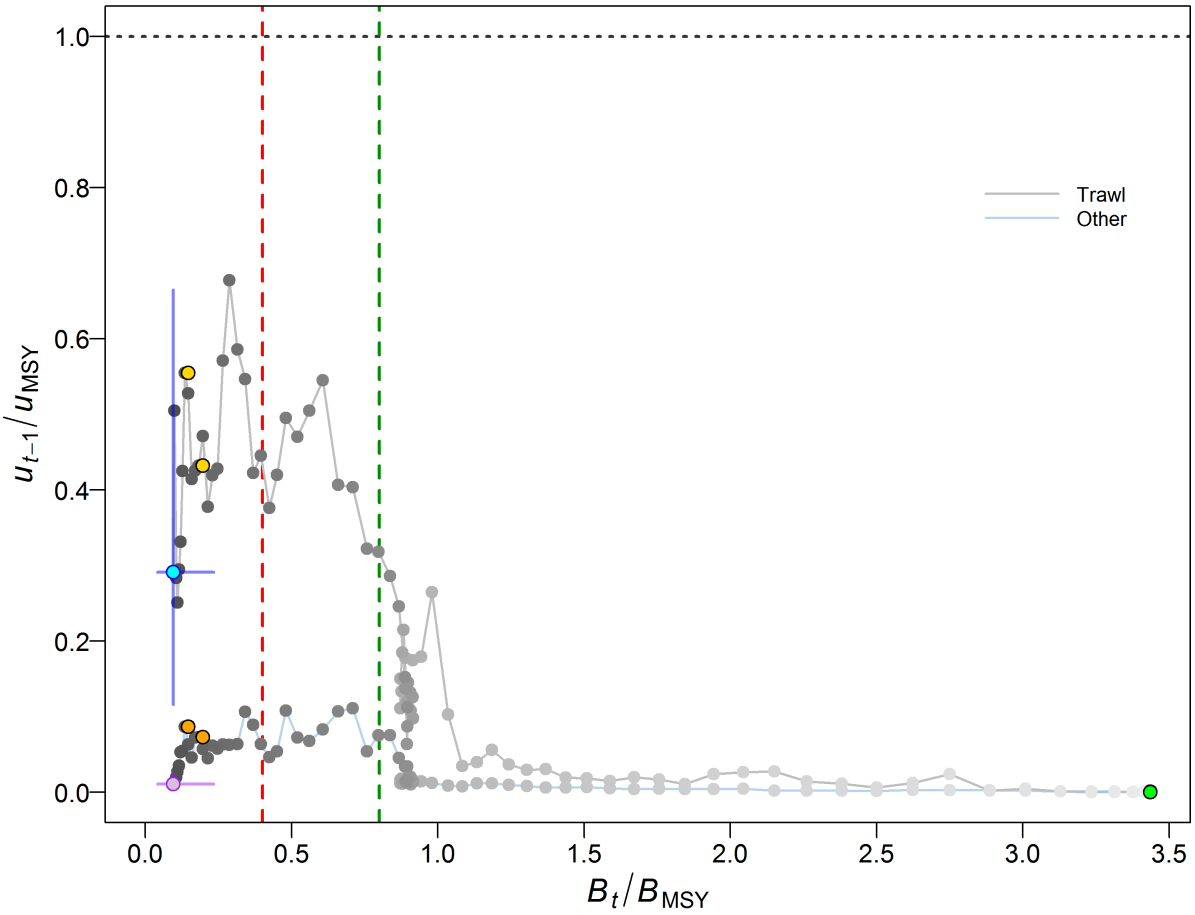

Figure F.38. Composite base: phase plot through time of the medians of the ratios B_t/B_{MSY} (the spawning biomass in year t relative to B_{MSY}) and u_{t-1}/u_{MSY} (the exploitation rate in year $t-1$ relative to u_{MSY}) for two fisheries (trawl/other). The filled green circle is the starting year (1936). Years then proceed along lines gradually darkening from light grey/blue, with the final year (2020) as a filled cyan/purple circle, and the blue/purple cross lines represent the 0.05 and 0.95 quantiles of the posterior distributions for the final year. Previous assessment years (2008, 2012) are indicated by gold/orange circles. Red and green vertical dashed lines indicate the PA provisional limit and upper stock reference points (0.4, 0.8 B_{MSY}), and the horizontal grey dotted line indicates u at MSY.

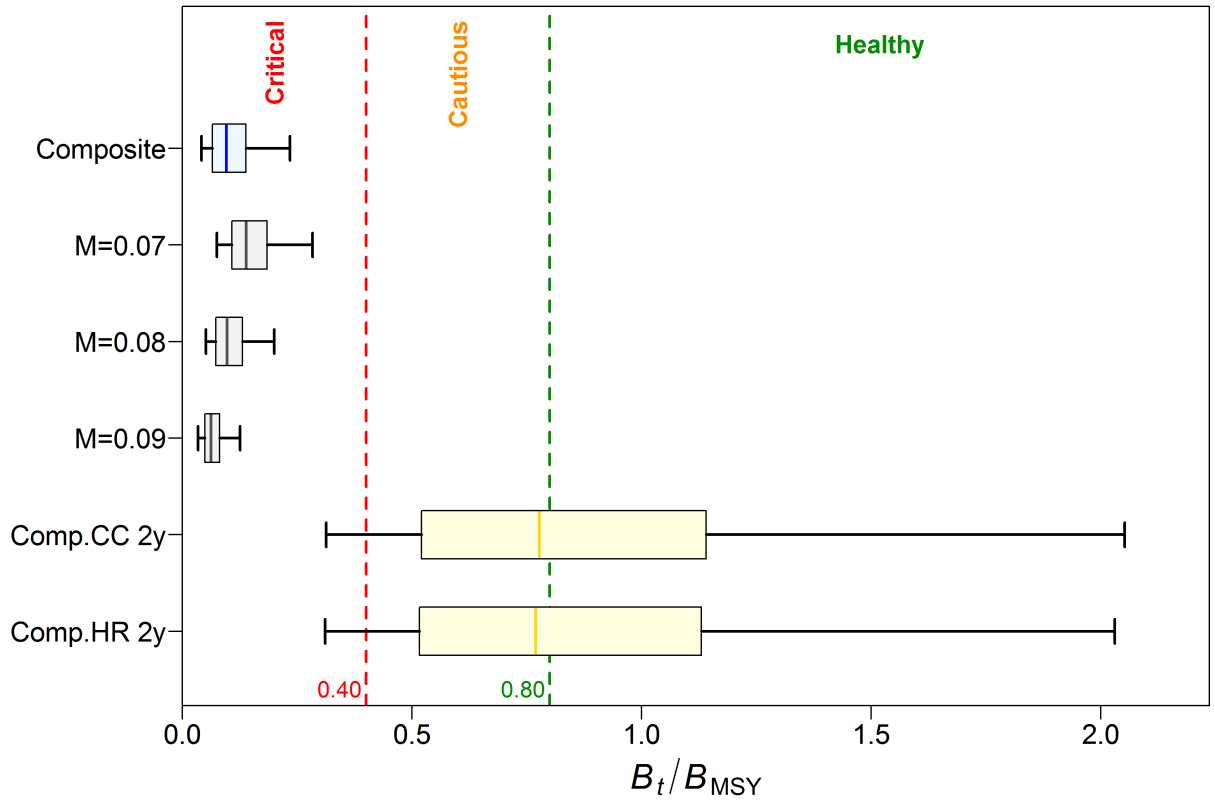

Figure F.39. Composite base: status at beginning of 2020 of the Bocaccio (2F) stock relative to the PA provisional reference points of 0.4B_{MSY} and 0.8B_{MSY} for a base case comprising 3 model runs. The top quantile plot shows the composite distribution and below are the 3 contributing runs. Also shown are projected stock status for the composite base case at the beginning of 2022 after fishing at a constant catch = 200 t/year or a constant exploitation rate of 0.04/year. Year 2022 is the second year that the 2016 cohort is assumed to contribute to the spawning population. Quantile plots show the 0.05, 0.25, 0.5, 0.75, and 0.95 quantiles from the MCMC posteriors.

F.2.1.4. Decision Tables

F.2.1.4.1. GMU – Guidance for setting TACs

Decision tables for the composite base case provide advice to managers as probabilities that current and projected biomass B_t ($t = 2020, ..., 2030$) will exceed biomass-based reference points (or that projected exploitation rate u_t will fall below harvest-based reference points) under constant catch (CC) and harvest rate (HR) policies. Specifically:

- Tables F.5 & F.6 – probability of B_t exceeding the LRP, P$(B_t > 0.4B_{\mathrm{MSY}})$, under CC and HR policies;
- Tables F.7 & F.8 – probability of B_t exceeding the USR, P$(B_t > 0.8B_{\mathrm{MSY}})$, under CC and HR policies;
- Tables F.9 & F.10 – probability of B_t exceeding biomass at MSY, P$(B_t > B_{\mathrm{MSY}})$, under CC and HR policies;
- Tables F.11 & F.12 – probability of u_t falling below harvest rate at MSY, P$(u_t < u_{\mathrm{MSY}})$, under CC and HR policies;
- Tables F.13 & F.14 – probability of B_t exceeding current-year biomass, P$(B_t > B_{2020})$, under CC and HR policies;
- Tables F.15 & F.16 – probability of u_t falling below current-year harvest rate, P$(u_t < u_{2019})$, under CC and HR policies;
- Tables F.17 & F.18 – probability of B_t exceeding a non-DFO 'soft limit', P$(B_t > 0.2B_0)$, under CC and HR policies;
- Tables F.19 & F.20 – probability of B_t exceeding a non-DFO 'target' biomass, P$(B_t > 0.4B_0)$, under CC and HR policies.

MSY-based reference points estimated within a stock assessment model can be highly sensitive to model assumptions about natural mortality and stock recruitment dynamics (Forrest et al. 2018). As a result, other jurisdictions use reference points that are expressed in terms of B_0 rather than B_{MSY} (e.g., N.Z. Min. Fish. 2011), because B_{MSY} is often poorly estimated as it depends on estimated parameters and a consistent fishery (although B_0 shares several of these same problems). Therefore, the reference points of $0.2B_0$ and $0.4B_0$ are also presented here. These are default values used in New Zealand respectively as a 'soft limit', below which management action needs to be taken, and a 'target' biomass for low productivity stocks, a mean around which the biomass is expected to vary. The 'soft limit' is equivalent to the upper stock reference (USR, $0.8B_{\mathrm{MSY}}$) in the provisional DFO Sustainable Fisheries Framework while a 'target' biomass is not specified by the provisional DFO SFF. Additionally, results are provided comparing projected biomass to B_{MSY} and to current spawning biomass B_{2020}, and comparing projected harvest rate to current harvest rate u_{2019}.

Table F.5. Decision table (BC Coast) concerning the limit reference point $0.4B_{\mathrm{MSY}}$ for 1-10-year projections for a range of **constant catch** *strategies (in tonnes). Values are P$(B_t > 0.4B_{\mathrm{MSY}})$, i.e. the probability of the spawning biomass (mature females) at the start of year t being greater than the limit reference point. The probabilities are the proportion (to two decimal places) of the 3000 MCMC samples for which $B_t > 0.4B_{\mathrm{MSY}}$. For reference, the average catch over the last 5 years (2015-2019) was 69 t.*

CC	2020	2021	2022	2023	2024	2025	2026	2027	2028	2029	2030
0	<0.01	0.66	0.88	0.97	0.99	>0.99	>0.99	>0.99	>0.99	>0.99	>0.99
50	<0.01	0.66	0.88	0.97	0.99	>0.99	>0.99	>0.99	>0.99	>0.99	>0.99
100	<0.01	0.66	0.88	0.97	0.99	>0.99	>0.99	>0.99	>0.99	>0.99	>0.99
150	<0.01	0.66	0.88	0.97	0.99	>0.99	>0.99	>0.99	>0.99	>0.99	>0.99
200	<0.01	0.65	0.87	0.97	0.99	>0.99	>0.99	>0.99	>0.99	>0.99	>0.99
250	<0.01	0.65	0.87	0.97	0.99	>0.99	>0.99	>0.99	>0.99	>0.99	>0.99
300	<0.01	0.65	0.87	0.96	0.99	>0.99	>0.99	>0.99	>0.99	>0.99	>0.99
350	<0.01	0.65	0.86	0.96	0.99	>0.99	>0.99	>0.99	>0.99	>0.99	>0.99
400	<0.01	0.64	0.86	0.96	0.99	>0.99	>0.99	>0.99	>0.99	>0.99	>0.99
450	<0.01	0.64	0.86	0.96	0.99	0.99	>0.99	>0.99	>0.99	>0.99	>0.99
500	<0.01	0.64	0.86	0.96	0.99	0.99	>0.99	>0.99	>0.99	>0.99	>0.99
550	<0.01	0.64	0.85	0.96	0.98	0.99	>0.99	>0.99	>0.99	>0.99	>0.99
600	<0.01	0.64	0.85	0.95	0.98	0.99	0.99	>0.99	>0.99	0.99	0.99

Table F.6. Decision table (BC Coast) concerning the limit reference point $0.4B_{\mathrm{MSY}}$ for 1-10-year projections for a range of **harvest rate** *strategies. Values are P$(B_t > 0.4B_{\mathrm{MSY}})$, i.e. the probability of the spawning biomass (mature females) at the start of year t being greater than the limit reference point. The probabilities are the proportion (to two decimal places) of the 3000 MCMC samples for which $B_t > 0.4B_{\mathrm{MSY}}$. For reference, the average harvest rate over the last 5 years (2015-2019) was 0.026.*

HR	2020	2021	2022	2023	2024	2025	2026	2027	2028	2029	2030
0	<0.01	0.66	0.88	0.97	0.99	>0.99	>0.99	>0.99	>0.99	>0.99	>0.99
0.01	<0.01	0.66	0.88	0.97	0.99	>0.99	>0.99	>0.99	>0.99	>0.99	>0.99
0.02	<0.01	0.66	0.88	0.97	0.99	>0.99	>0.99	>0.99	>0.99	>0.99	>0.99
0.03	<0.01	0.66	0.87	0.97	0.99	>0.99	>0.99	>0.99	>0.99	>0.99	>0.99
0.04	<0.01	0.65	0.87	0.96	0.99	>0.99	>0.99	>0.99	>0.99	>0.99	>0.99
0.05	<0.01	0.65	0.87	0.96	0.99	>0.99	>0.99	>0.99	>0.99	>0.99	>0.99
0.06	<0.01	0.65	0.86	0.96	0.99	>0.99	>0.99	>0.99	>0.99	>0.99	0.99
0.07	<0.01	0.65	0.86	0.96	0.99	0.99	>0.99	>0.99	>0.99	0.99	0.99
0.08	<0.01	0.64	0.86	0.96	0.98	0.99	>0.99	>0.99	0.99	0.99	0.99
0.09	<0.01	0.64	0.85	0.96	0.98	0.99	0.99	0.99	0.99	0.99	0.98
0.1	<0.01	0.64	0.85	0.95	0.98	0.99	0.99	0.99	0.99	0.98	0.98
0.11	<0.01	0.64	0.85	0.95	0.98	0.99	0.99	0.99	0.98	0.97	0.97
0.12	<0.01	0.63	0.84	0.95	0.98	0.99	0.99	0.98	0.98	0.97	0.96

Table F.7. Decision table (BC Coast) concerning the upper stock reference point $0.8B_{\mathrm{MSY}}$ for 1-10-year projections for a range of **constant catch** *strategies (in tonnes), such that values are P$(B_t > 0.8B_{\mathrm{MSY}})$. For reference, the average catch over the last 5 years (2015-2019) was 69 t.*

CC	2020	2021	2022	2023	2024	2025	2026	2027	2028	2029	2030
0	0	0.21	0.50	0.73	0.87	0.94	0.96	0.97	0.97	0.97	0.98
50	0	0.20	0.49	0.73	0.87	0.93	0.96	0.97	0.97	0.97	0.97
100	0	0.20	0.49	0.73	0.86	0.93	0.96	0.97	0.97	0.97	0.97
150	0	0.20	0.48	0.72	0.85	0.93	0.96	0.96	0.96	0.97	0.97
200	0	0.20	0.48	0.72	0.85	0.92	0.95	0.96	0.96	0.96	0.97
250	0	0.20	0.48	0.72	0.85	0.92	0.95	0.96	0.96	0.96	0.96
300	0	0.20	0.48	0.71	0.85	0.92	0.94	0.95	0.96	0.96	0.96
350	0	0.20	0.47	0.71	0.84	0.91	0.94	0.95	0.95	0.96	0.96
400	0	0.19	0.47	0.70	0.84	0.91	0.94	0.95	0.95	0.95	0.95
450	0	0.19	0.46	0.70	0.83	0.90	0.93	0.94	0.94	0.95	0.95
500	0	0.19	0.46	0.70	0.83	0.90	0.93	0.94	0.94	0.94	0.94
550	0	0.19	0.46	0.69	0.82	0.89	0.93	0.93	0.93	0.93	0.94
600	0	0.19	0.45	0.68	0.82	0.89	0.92	0.93	0.93	0.93	0.93

Table F.8. Decision table (BC Coast) concerning the upper stock reference point $0.8B_{\mathrm{MSY}}$ for 1-10-year projections for a range of **harvest rate** *strategies, such that values are P$(B_t > 0.8B_{\mathrm{MSY}})$. For reference, the average harvest rate over the last 5 years (2015-2019) was 0.026.*

HR	2020	2021	2022	2023	2024	2025	2026	2027	2028	2029	2030
0	0	0.21	0.50	0.73	0.87	0.94	0.96	0.97	0.97	0.97	0.98
0.01	0	0.20	0.49	0.73	0.86	0.93	0.96	0.96	0.96	0.97	0.97
0.02	0	0.20	0.49	0.72	0.85	0.92	0.95	0.96	0.96	0.96	0.96
0.03	0	0.20	0.48	0.72	0.85	0.92	0.94	0.95	0.95	0.95	0.95
0.04	0	0.20	0.48	0.71	0.84	0.91	0.93	0.94	0.94	0.94	0.93
0.05	0	0.20	0.47	0.70	0.83	0.90	0.92	0.93	0.92	0.92	0.92
0.06	0	0.19	0.47	0.70	0.83	0.89	0.92	0.92	0.91	0.90	0.89
0.07	0	0.19	0.46	0.69	0.82	0.88	0.91	0.91	0.89	0.88	0.87
0.08	0	0.19	0.46	0.68	0.81	0.87	0.89	0.89	0.87	0.85	0.85
0.09	0	0.19	0.45	0.67	0.80	0.86	0.88	0.87	0.85	0.83	0.81
0.1	0	0.19	0.45	0.66	0.79	0.85	0.86	0.85	0.83	0.80	0.78
0.11	0	0.18	0.44	0.65	0.78	0.83	0.85	0.84	0.80	0.77	0.75
0.12	0	0.18	0.43	0.65	0.77	0.82	0.84	0.81	0.77	0.74	0.71

Table F.9. Decision table (BC Coast) concerning the reference point B_{MSY} for 1-10-year projections-year projections for a range of **constant catch** *strategies (in tonnes), such that values are P$(B_t > B_{\mathrm{MSY}})$. For reference, the average catch over the last 5 years (2015-2019) was 69 t.*

CC	2020	2021	2022	2023	2024	2025	2026	2027	2028	2029	2030
0	0	0.12	0.34	0.60	0.77	0.86	0.91	0.93	0.93	0.94	0.94
50	0	0.12	0.34	0.59	0.76	0.86	0.91	0.92	0.93	0.94	0.94
100	0	0.12	0.34	0.59	0.76	0.85	0.90	0.92	0.92	0.93	0.94
150	0	0.12	0.33	0.59	0.75	0.85	0.90	0.92	0.92	0.93	0.93
200	0	0.11	0.33	0.58	0.75	0.85	0.89	0.91	0.92	0.92	0.92
250	0	0.11	0.32	0.57	0.75	0.84	0.89	0.91	0.91	0.92	0.92
300	0	0.11	0.32	0.57	0.74	0.84	0.88	0.90	0.90	0.91	0.91
350	0	0.11	0.32	0.57	0.74	0.83	0.88	0.89	0.90	0.90	0.91
400	0	0.11	0.32	0.56	0.73	0.83	0.87	0.89	0.89	0.90	0.90
450	0	0.11	0.31	0.56	0.73	0.82	0.86	0.88	0.89	0.89	0.90
500	0	0.11	0.31	0.55	0.72	0.82	0.86	0.88	0.88	0.88	0.89
550	0	0.11	0.31	0.55	0.72	0.81	0.85	0.87	0.87	0.87	0.88
600	0	0.11	0.31	0.54	0.71	0.80	0.84	0.86	0.86	0.86	0.87

Table F.10. Decision table (BC Coast) concerning the reference point B_{MSY} for 1-10-year projections-year projections for a range of **harvest rate** *strategies, such that values are P$(B_t > B_{\mathrm{MSY}})$. For reference, the average harvest rate over the last 5 years (2015-2019) was 0.026.*

HR	2020	2021	2022	2023	2024	2025	2026	2027	2028	2029	2030
0	0	0.12	0.34	0.60	0.77	0.86	0.91	0.93	0.93	0.94	0.94
0.01	0	0.12	0.34	0.59	0.76	0.85	0.90	0.92	0.92	0.93	0.93
0.02	0	0.12	0.33	0.58	0.75	0.84	0.89	0.90	0.90	0.91	0.91
0.03	0	0.11	0.32	0.58	0.74	0.83	0.87	0.89	0.89	0.88	0.89
0.04	0	0.11	0.32	0.56	0.73	0.82	0.86	0.87	0.86	0.86	0.86
0.05	0	0.11	0.32	0.56	0.72	0.81	0.85	0.85	0.84	0.84	0.84
0.06	0	0.11	0.31	0.55	0.72	0.80	0.83	0.83	0.83	0.81	0.80
0.07	0	0.11	0.31	0.54	0.71	0.78	0.82	0.82	0.80	0.78	0.77
0.08	0	0.11	0.30	0.53	0.70	0.77	0.80	0.80	0.77	0.76	0.74
0.09	0	0.11	0.30	0.53	0.69	0.76	0.78	0.77	0.75	0.73	0.70
0.1	0	0.11	0.30	0.52	0.67	0.74	0.76	0.75	0.73	0.69	0.67
0.11	0	0.11	0.29	0.51	0.66	0.73	0.75	0.73	0.70	0.66	0.63
0.12	0	0.11	0.29	0.50	0.65	0.72	0.73	0.71	0.66	0.62	0.58

Table F.11. Decision table (BC Coast) comparing the projected exploitation rate to that at MSY for a range of **constant catch** *strategies, such that values are P$(u_t < u_{\mathrm{MSY}})$, i.e. the probability of the exploitation rate in the middle of year t being less than that at MSY. For reference, the average catch over the last 5 years (2015-2019) was 69 t.*

CC	2020	2021	2022	2023	2024	2025	2026	2027	2028	2029	2030
0	1	1	1	1	1	1	1	1	1	1	1
50	1	1	1	1	1	1	1	1	1	1	1
100	>0.99	>0.99	1	1	1	1	1	1	1	1	1
150	0.98	>0.99	>0.99	1	1	1	1	1	1	1	1
200	0.95	0.99	>0.99	>0.99	>0.99	1	1	1	1	1	1
250	0.89	0.97	0.99	>0.99	>0.99	>0.99	1	1	1	1	1
300	0.81	0.94	0.99	0.99	>0.99	>0.99	>0.99	>0.99	>0.99	>0.99	>0.99
350	0.72	0.91	0.97	0.99	>0.99	>0.99	>0.99	>0.99	>0.99	>0.99	>0.99
400	0.63	0.86	0.96	0.99	0.99	>0.99	>0.99	>0.99	>0.99	>0.99	>0.99
450	0.56	0.82	0.93	0.97	0.99	0.99	0.99	>0.99	>0.99	0.99	0.99
500	0.49	0.76	0.91	0.96	0.98	0.99	0.99	0.99	0.99	0.99	0.99
550	0.42	0.71	0.88	0.95	0.97	0.98	0.99	0.99	0.99	0.99	0.99
600	0.36	0.65	0.85	0.93	0.96	0.98	0.98	0.98	0.98	0.98	0.98

Table F.12. Decision table (BC Coast) comparing the projected exploitation rate to that at MSY for a range of **harvest rate** *strategies, such that values are P$(u_t < u_{\mathrm{MSY}})$, i.e. the probability of the exploitation rate in the middle of year t being less than that at MSY. For reference, the average harvest rate over the last 5 years (2015-2019) was 0.026.*

HR	2020	2021	2022	2023	2024	2025	2026	2027	2028	2029	2030
0	1	1	1	1	1	1	1	1	1	1	1
0.01	1	1	1	1	1	1	1	1	1	1	1
0.02	1	1	1	1	1	1	1	1	1	1	1
0.03	>0.99	>0.99	>0.99	>0.99	>0.99	>0.99	>0.99	>0.99	>0.99	>0.99	>0.99
0.04	>0.99	>0.99	>0.99	>0.99	>0.99	>0.99	>0.99	0.99	>0.99	>0.99	>0.99
0.05	0.97	0.97	0.97	0.97	0.97	0.97	0.97	0.97	0.97	0.97	0.97
0.06	0.90	0.90	0.90	0.90	0.90	0.90	0.90	0.90	0.90	0.90	0.90
0.07	0.77	0.77	0.77	0.77	0.77	0.77	0.77	0.77	0.77	0.77	0.77
0.08	0.58	0.58	0.58	0.58	0.58	0.58	0.58	0.58	0.58	0.58	0.58
0.09	0.41	0.41	0.41	0.41	0.41	0.41	0.41	0.42	0.41	0.41	0.41
0.1	0.28	0.28	0.28	0.28	0.28	0.28	0.28	0.28	0.28	0.28	0.28
0.11	0.17	0.17	0.17	0.17	0.17	0.17	0.17	0.17	0.17	0.17	0.17
0.12	0.10	0.10	0.10	0.10	0.10	0.10	0.10	0.10	0.10	0.10	0.10

Table F.13. Decision table (BC Coast) comparing the projected biomass to current biomass for a range of **constant catch** *strategies, given by probabilities P*$(B_t > B_{2020})$*. For reference, the average catch over the last 5 years (2015-2019) was 69 t.*

CC	2020	2021	2022	2023	2024	2025	2026	2027	2028	2029	2030
0	0	1	1	1	1	1	1	1	1	1	1
50	0	1	1	1	1	1	1	1	1	1	1
100	0	1	1	1	1	1	1	1	1	1	1
150	0	1	1	1	1	1	1	1	1	1	1
200	0	1	1	1	1	1	1	1	1	1	1
250	0	1	1	1	1	1	1	1	1	1	1
300	0	1	1	1	1	1	1	1	1	1	1
350	0	1	1	1	1	1	1	1	1	1	1
400	0	1	1	1	1	1	1	1	1	1	1
450	0	1	1	1	1	1	1	1	1	1	1
500	0	1	1	1	1	1	1	1	1	1	1
550	0	1	1	1	1	1	1	1	1	1	1
600	0	1	1	1	1	1	1	1	1	1	1

Table F.14. Decision table (BC Coast) comparing the projected biomass to current biomass for a range of **harvest rate** *strategies, given by probabilities P*$(B_t > B_{2020})$*. For reference, the average harvest rate over the last 5 years (2015-2019) was 0.026.*

HR	2020	2021	2022	2023	2024	2025	2026	2027	2028	2029	2030
0	0	1	1	1	1	1	1	1	1	1	1
0.01	0	1	1	1	1	1	1	1	1	1	1
0.02	0	1	1	1	1	1	1	1	1	1	1
0.03	0	1	1	1	1	1	1	1	1	1	1
0.04	0	1	1	1	1	1	1	1	1	1	1
0.05	0	1	1	1	1	1	1	1	1	1	1
0.06	0	1	1	1	1	1	1	1	1	1	1
0.07	0	1	1	1	1	1	1	1	1	1	1
0.08	0	1	1	1	1	1	1	1	1	1	1
0.09	0	1	1	1	1	1	1	1	1	1	1
0.1	0	1	1	1	1	1	1	1	1	1	1
0.11	0	1	1	1	1	1	1	1	1	1	1
0.12	0	1	1	1	1	1	1	1	1	1	1

Table F.15. Decision table (BC Coast) comparing the projected exploitation rate to that in 2019 for a range of **constant catch** *strategies, such that values are P$(u_t < u_{2019})$. For reference, the average catch over the last 5 years (2015-2019) was 69 t.*

CC	2020	2021	2022	2023	2024	2025	2026	2027	2028	2029	2030
0	1	1	1	1	1	1	1	1	1	1	1
50	1	1	1	1	1	1	1	1	1	1	1
100	1	1	1	1	1	1	1	1	1	1	1
150	0.09	>0.99	1	1	1	1	1	1	1	1	1
200	0	0.68	>0.99	1	1	1	1	1	1	1	1
250	0	0.16	0.92	>0.99	1	1	1	1	1	1	1
300	0	0.02	0.65	0.97	>0.99	>0.99	1	1	1	1	1
350	0	<0.01	0.37	0.86	0.98	>0.99	>0.99	>0.99	>0.99	>0.99	>0.99
400	0	<0.01	0.16	0.69	0.93	0.98	0.99	>0.99	>0.99	0.99	0.99
450	0	0	0.07	0.52	0.83	0.95	0.98	0.98	0.99	0.99	0.99
500	0	0	0.03	0.35	0.71	0.88	0.94	0.96	0.97	0.97	0.96
550	0	0	0.01	0.22	0.58	0.79	0.89	0.92	0.93	0.93	0.92
600	0	0	<0.01	0.14	0.46	0.68	0.80	0.85	0.87	0.87	0.87

Table F.16. Decision table (BC Coast) comparing the projected exploitation rate to that in 2019 for a range of **harvest rate** *strategies, such that values are P$(u_t < u_{2019})$. For reference, the average harvest rate over the last 5 years (2015-2019) was 0.026.*

HR	2020	2021	2022	2023	2024	2025	2026	2027	2028	2029	2030
0	1	1	1	1	1	1	1	1	1	1	1
0.01	0.97	0.97	0.97	0.97	0.97	0.97	0.97	0.97	0.97	0.97	0.97
0.02	0.67	0.67	0.67	0.67	0.67	0.67	0.67	0.67	0.67	0.67	0.67
0.03	0.27	0.27	0.27	0.27	0.27	0.27	0.27	0.27	0.27	0.27	0.27
0.04	0.07	0.07	0.07	0.07	0.07	0.07	0.07	0.07	0.07	0.07	0.07
0.05	0.01	0.01	0.01	0.01	0.01	0.01	0.01	0.01	0.01	0.01	0.01
0.06	<0.01	<0.01	<0.01	<0.01	<0.01	<0.01	<0.01	<0.01	<0.01	<0.01	<0.01
0.07	0	0	0	0	0	0	0	0	0	0	0
0.08	0	0	0	0	0	0	0	0	0	0	0
0.09	0	0	0	0	0	0	0	0	0	0	0
0.1	0	0	0	0	0	0	0	0	0	0	0
0.11	0	0	0	0	0	0	0	0	0	0	0
0.12	0	0	0	0	0	0	0	0	0	0	0

Table F.17. Decision table for the alternative limit reference point $0.2B_0$ for 1-10 year projections for a range of **constant catch** *strategies, such that values are P$(B_t > 0.2B_0)$. For reference, the average catch over the last 5 years (2015-2019) was 69 t.*

CC	2020	2021	2022	2023	2024	2025	2026	2027	2028	2029	2030
0	0	0.24	0.62	0.86	0.96	0.99	0.99	>0.99	>0.99	>0.99	>0.99
50	0	0.24	0.62	0.85	0.96	0.99	0.99	>0.99	>0.99	>0.99	>0.99
100	0	0.24	0.61	0.85	0.95	0.98	0.99	>0.99	>0.99	>0.99	>0.99
150	0	0.24	0.61	0.85	0.95	0.98	0.99	0.99	0.99	0.99	>0.99
200	0	0.24	0.60	0.84	0.95	0.98	0.99	0.99	0.99	0.99	0.99
250	0	0.23	0.59	0.84	0.95	0.98	0.99	0.99	0.99	0.99	0.99
300	0	0.23	0.59	0.84	0.95	0.98	0.99	0.99	0.99	0.99	0.99
350	0	0.23	0.59	0.83	0.94	0.98	0.99	0.99	0.99	0.99	0.99
400	0	0.22	0.58	0.82	0.94	0.97	0.98	0.99	0.99	0.99	0.99
450	0	0.22	0.58	0.82	0.94	0.97	0.98	0.99	0.99	0.99	0.99
500	0	0.22	0.57	0.82	0.93	0.97	0.98	0.98	0.98	0.98	0.98
550	0	0.22	0.57	0.81	0.93	0.97	0.98	0.98	0.98	0.98	0.98
600	0	0.22	0.56	0.81	0.92	0.96	0.98	0.98	0.98	0.98	0.98

Table F.18. Decision table for the alternative limit reference point $0.2B_0$ for 1-10 year projections for a range of **harvest rate** *strategies, such that values are P$(B_t > 0.2B_0)$. For reference, the average harvest rate over the last 5 years (2015-2019) was 0.026.*

HR	2020	2021	2022	2023	2024	2025	2026	2027	2028	2029	2030
0	0	0.24	0.62	0.86	0.96	0.99	0.99	>0.99	>0.99	>0.99	>0.99
0.01	0	0.24	0.62	0.85	0.95	0.98	0.99	>0.99	>0.99	>0.99	>0.99
0.02	0	0.24	0.61	0.85	0.95	0.98	0.99	0.99	0.99	0.99	0.99
0.03	0	0.24	0.60	0.84	0.95	0.98	0.99	0.99	0.99	0.99	0.99
0.04	0	0.23	0.60	0.84	0.94	0.97	0.99	0.99	0.99	0.98	0.98
0.05	0	0.23	0.59	0.83	0.94	0.97	0.98	0.98	0.98	0.98	0.97
0.06	0	0.23	0.58	0.82	0.93	0.97	0.98	0.98	0.97	0.97	0.97
0.07	0	0.23	0.58	0.82	0.93	0.96	0.97	0.97	0.96	0.96	0.96
0.08	0	0.22	0.57	0.81	0.92	0.96	0.97	0.96	0.96	0.95	0.94
0.09	0	0.22	0.56	0.80	0.91	0.95	0.96	0.96	0.95	0.93	0.92
0.1	0	0.22	0.56	0.79	0.91	0.95	0.96	0.95	0.93	0.91	0.90
0.11	0	0.21	0.55	0.78	0.90	0.94	0.95	0.93	0.92	0.89	0.87
0.12	0	0.21	0.55	0.78	0.89	0.93	0.94	0.92	0.89	0.86	0.84

Table F.19. Decision table for the alternative upper stock reference point $0.4B_0$ for 1-10 year projections for a range of **constant catch** *strategies, such that values are P$(B_t > 0.4B_0)$. For reference, the average catch over the last 5 years (2015-2019) was 69 t.*

CC	2020	2021	2022	2023	2024	2025	2026	2027	2028	2029	2030
0	0	0.01	0.11	0.35	0.61	0.75	0.83	0.86	0.87	0.88	0.89
50	0	0.01	0.11	0.35	0.60	0.75	0.82	0.85	0.86	0.87	0.88
100	0	0.01	0.11	0.35	0.59	0.74	0.82	0.85	0.86	0.87	0.88
150	0	0.01	0.11	0.34	0.58	0.74	0.81	0.84	0.85	0.86	0.87
200	0	0.01	0.11	0.34	0.58	0.73	0.80	0.83	0.84	0.85	0.86
250	0	0.01	0.11	0.33	0.57	0.72	0.80	0.82	0.83	0.84	0.85
300	0	0.01	0.10	0.33	0.56	0.72	0.79	0.82	0.82	0.83	0.84
350	0	0.01	0.10	0.32	0.56	0.71	0.78	0.81	0.81	0.82	0.83
400	0	0.01	0.10	0.32	0.55	0.70	0.77	0.79	0.80	0.81	0.82
450	0	0.01	0.10	0.32	0.54	0.69	0.76	0.79	0.79	0.80	0.81
500	0	0.01	0.10	0.31	0.54	0.68	0.76	0.78	0.79	0.79	0.80
550	0	0.01	0.09	0.31	0.53	0.68	0.75	0.77	0.78	0.79	0.79
600	0	0.01	0.09	0.30	0.52	0.67	0.74	0.77	0.77	0.78	0.78

Table F.20. Decision table for the alternative upper stock reference point $0.4B_0$ for 1-10 year projections for a range of **harvest rate** *strategies, such that values are P$(B_t > 0.4B_0)$. For reference, the average harvest rate over the last 5 years (2015-2019) was 0.026.*

HR	2020	2021	2022	2023	2024	2025	2026	2027	2028	2029	2030
0	0	0.01	0.11	0.35	0.61	0.75	0.83	0.86	0.87	0.88	0.89
0.01	0	0.01	0.11	0.35	0.59	0.74	0.81	0.84	0.85	0.85	0.87
0.02	0	0.01	0.11	0.34	0.58	0.73	0.79	0.81	0.82	0.82	0.83
0.03	0	0.01	0.11	0.33	0.56	0.71	0.77	0.79	0.79	0.79	0.79
0.04	0	0.01	0.10	0.32	0.55	0.69	0.75	0.77	0.76	0.76	0.75
0.05	0	0.01	0.10	0.31	0.54	0.67	0.74	0.74	0.73	0.72	0.72
0.06	0	0.01	0.10	0.30	0.52	0.65	0.71	0.72	0.70	0.68	0.67
0.07	0	0.01	0.09	0.29	0.50	0.63	0.69	0.69	0.66	0.64	0.62
0.08	0	0.01	0.09	0.28	0.49	0.61	0.66	0.66	0.62	0.59	0.56
0.09	0	0.01	0.09	0.27	0.47	0.60	0.64	0.62	0.58	0.54	0.51
0.1	0	<0.01	0.08	0.27	0.46	0.57	0.61	0.59	0.54	0.49	0.45
0.11	0	<0.01	0.08	0.26	0.44	0.55	0.58	0.56	0.50	0.44	0.40
0.12	0	<0.01	0.08	0.25	0.43	0.53	0.56	0.52	0.45	0.39	0.33

F.2.1.4.2. GMU – Guidance for rebuilding

Table F.21. Decision table for the limit reference point $0.4B_{\mathrm{MSY}}$ for selected projection years over 3 generations (60 years) and for a range of **constant catch** *strategies, such that values are P$(B_t > 0.4B_{\mathrm{MSY}})$. For reference, the average catch over the last 5 years (2015-2019) was 69 t.*

CC	2020	2025	2030	2035	2040	2045	2050	2055	2060	2070	2080
0	<0.01	>0.99	>0.99	1	1	1	1	1	1	1	1
50	<0.01	>0.99	>0.99	1	1	1	1	1	1	1	1
100	<0.01	>0.99	>0.99	>0.99	1	1	1	1	1	1	1
150	<0.01	>0.99	>0.99	>0.99	>0.99	>0.99	1	1	1	1	1
200	<0.01	>0.99	>0.99	>0.99	>0.99	>0.99	>0.99	>0.99	1	1	1
250	<0.01	>0.99	>0.99	>0.99	>0.99	>0.99	>0.99	>0.99	1	1	1
300	<0.01	>0.99	>0.99	>0.99	>0.99	>0.99	>0.99	>0.99	>0.99	>0.99	>0.99
350	<0.01	>0.99	>0.99	>0.99	>0.99	>0.99	>0.99	>0.99	>0.99	>0.99	>0.99
400	<0.01	>0.99	>0.99	>0.99	>0.99	>0.99	>0.99	>0.99	>0.99	>0.99	>0.99
450	<0.01	0.99	>0.99	>0.99	>0.99	>0.99	>0.99	>0.99	>0.99	>0.99	>0.99
500	<0.01	0.99	>0.99	>0.99	>0.99	>0.99	>0.99	>0.99	>0.99	0.99	0.99
550	<0.01	0.99	>0.99	>0.99	0.99	0.99	0.99	0.99	0.99	0.99	0.99
600	<0.01	0.99	0.99	0.99	0.99	0.99	0.99	0.99	0.99	0.99	0.99

Table F.22. Decision table for the limit reference point $0.4B_{\mathrm{MSY}}$ for selected projection years over 3 generations (60 years) and for a range of **harvest rate** *strategies, such that values are P$(B_t > 0.4B_{\mathrm{MSY}})$. For reference, the average harvest rate over the last 5 years (2015-2019) was 0.026.*

HR	2020	2025	2030	2035	2040	2045	2050	2055	2060	2070	2080
0	<0.01	>0.99	>0.99	1	1	1	1	1	1	1	1
0.01	<0.01	>0.99	>0.99	>0.99	>0.99	>0.99	1	1	1	1	1
0.02	<0.01	>0.99	>0.99	>0.99	>0.99	>0.99	>0.99	>0.99	1	1	>0.99
0.03	<0.01	>0.99	>0.99	>0.99	>0.99	>0.99	>0.99	>0.99	>0.99	>0.99	>0.99
0.04	<0.01	>0.99	>0.99	>0.99	>0.99	>0.99	>0.99	>0.99	>0.99	>0.99	>0.99
0.05	<0.01	>0.99	>0.99	>0.99	>0.99	>0.99	>0.99	>0.99	>0.99	>0.99	>0.99
0.06	<0.01	>0.99	0.99	0.99	>0.99	0.99	>0.99	0.99	0.99	0.99	0.99
0.07	<0.01	0.99	0.99	0.99	0.99	0.99	0.99	0.99	0.99	0.98	0.98
0.08	<0.01	0.99	0.99	0.98	0.98	0.98	0.98	0.97	0.97	0.96	0.97
0.09	<0.01	0.99	0.98	0.98	0.97	0.97	0.96	0.95	0.95	0.94	0.94
0.1	<0.01	0.99	0.98	0.97	0.95	0.94	0.93	0.92	0.92	0.90	0.89
0.11	<0.01	0.99	0.97	0.95	0.93	0.91	0.90	0.88	0.87	0.85	0.84
0.12	<0.01	0.99	0.96	0.93	0.91	0.88	0.85	0.83	0.81	0.78	0.76

Table F.23. Decision table for the upper stock reference $0.8B_{\mathrm{MSY}}$ for selected projection years over 3 generations (60 years) and for a range of **constant catch** *strategies, such that values are $P(B_t > 0.8B_{\mathrm{MSY}})$. For reference, the average catch over the last 5 years (2015-2019) was 69 t.*

CC	2020	2025	2030	2035	2040	2045	2050	2055	2060	2070	2080
0	0	0.94	0.98	0.99	>0.99	>0.99	>0.99	>0.99	>0.99	1	>0.99
50	0	0.93	0.97	0.99	>0.99	>0.99	>0.99	>0.99	>0.99	>0.99	>0.99
100	0	0.93	0.97	0.99	>0.99	>0.99	>0.99	>0.99	>0.99	>0.99	>0.99
150	0	0.93	0.97	0.99	0.99	>0.99	>0.99	>0.99	>0.99	>0.99	>0.99
200	0	0.92	0.97	0.98	0.99	0.99	>0.99	>0.99	>0.99	>0.99	>0.99
250	0	0.92	0.96	0.98	0.99	0.99	>0.99	>0.99	>0.99	>0.99	>0.99
300	0	0.92	0.96	0.98	0.99	0.99	0.99	>0.99	>0.99	>0.99	>0.99
350	0	0.91	0.96	0.97	0.98	0.99	0.99	0.99	>0.99	>0.99	>0.99
400	0	0.91	0.95	0.97	0.98	0.99	0.99	0.99	0.99	0.99	0.99
450	0	0.90	0.95	0.96	0.98	0.98	0.99	0.99	0.99	0.99	0.99
500	0	0.90	0.94	0.96	0.97	0.98	0.98	0.98	0.98	0.98	0.99
550	0	0.89	0.94	0.95	0.96	0.97	0.98	0.98	0.98	0.98	0.98
600	0	0.89	0.93	0.94	0.95	0.96	0.97	0.97	0.97	0.98	0.98

Table F.24. Decision table for the upper stock reference $0.8B_{\mathrm{MSY}}$ for selected projection years over 3 generations (60 years) and for a range of **harvest rate** *strategies, such that values are $P(B_t > 0.8B_{\mathrm{MSY}})$. For reference, the average harvest rate over the last 5 years (2015-2019) was 0.026.*

HR	2020	2025	2030	2035	2040	2045	2050	2055	2060	2070	2080
0	0	0.94	0.98	0.99	>0.99	>0.99	>0.99	>0.99	>0.99	1	>0.99
0.01	0	0.93	0.97	0.98	0.99	>0.99	>0.99	>0.99	>0.99	>0.99	>0.99
0.02	0	0.92	0.96	0.97	0.98	0.99	0.99	>0.99	>0.99	>0.99	>0.99
0.03	0	0.92	0.95	0.96	0.97	0.98	0.99	0.99	0.99	0.99	>0.99
0.04	0	0.91	0.93	0.94	0.96	0.96	0.97	0.97	0.97	0.98	0.98
0.05	0	0.90	0.92	0.92	0.93	0.94	0.94	0.94	0.95	0.95	0.95
0.06	0	0.89	0.89	0.90	0.90	0.90	0.90	0.90	0.90	0.90	0.90
0.07	0	0.88	0.87	0.86	0.86	0.85	0.84	0.83	0.83	0.83	0.83
0.08	0	0.87	0.85	0.82	0.81	0.79	0.77	0.75	0.74	0.73	0.71
0.09	0	0.86	0.81	0.77	0.74	0.71	0.68	0.65	0.64	0.62	0.59
0.1	0	0.85	0.78	0.73	0.67	0.62	0.57	0.54	0.52	0.50	0.48
0.11	0	0.83	0.75	0.68	0.59	0.53	0.47	0.44	0.42	0.39	0.36
0.12	0	0.82	0.71	0.61	0.52	0.43	0.37	0.35	0.32	0.29	0.28

Table F.25. Decision table for biomass at maximum sustainable yield B_{MSY} for selected projection years over 3 generations (60 years) and for a range of **constant catch** *strategies, such that values are P$(B_t > B_{\mathrm{MSY}})$. For reference, the average catch over the last 5 years (2015-2019) was 69 t.*

CC	2020	2025	2030	2035	2040	2045	2050	2055	2060	2070	2080
0	0	0.86	0.94	0.97	0.99	0.99	>0.99	>0.99	>0.99	>0.99	>0.99
50	0	0.86	0.94	0.97	0.98	0.99	>0.99	>0.99	>0.99	>0.99	>0.99
100	0	0.85	0.94	0.96	0.98	0.99	>0.99	>0.99	>0.99	>0.99	>0.99
150	0	0.85	0.93	0.96	0.98	0.99	0.99	>0.99	>0.99	>0.99	>0.99
200	0	0.85	0.92	0.95	0.97	0.98	0.99	0.99	>0.99	>0.99	>0.99
250	0	0.84	0.92	0.95	0.97	0.98	0.99	0.99	0.99	0.99	>0.99
300	0	0.84	0.91	0.94	0.96	0.98	0.98	0.99	0.99	0.99	>0.99
350	0	0.83	0.91	0.94	0.96	0.97	0.98	0.98	0.99	0.99	0.99
400	0	0.83	0.90	0.93	0.95	0.96	0.97	0.98	0.98	0.98	0.99
450	0	0.82	0.90	0.92	0.95	0.96	0.97	0.97	0.98	0.98	0.98
500	0	0.82	0.89	0.92	0.94	0.95	0.96	0.97	0.97	0.98	0.98
550	0	0.81	0.88	0.91	0.93	0.94	0.95	0.96	0.97	0.97	0.98
600	0	0.80	0.87	0.90	0.92	0.94	0.95	0.95	0.96	0.96	0.97

Table F.26. Decision table for biomass at maximum sustainable yield B_{MSY} for selected projection years over 3 generations (60 years) and for a range of **harvest rate** *strategies, such that values are P$(B_t > B_{\mathrm{MSY}})$. For reference, the average harvest rate over the last 5 years (2015-2019) was 0.026.*

HR	2020	2025	2030	2035	2040	2045	2050	2055	2060	2070	2080
0	0	0.86	0.94	0.97	0.99	0.99	>0.99	>0.99	>0.99	>0.99	>0.99
0.01	0	0.85	0.93	0.95	0.98	0.98	0.99	>0.99	>0.99	>0.99	>0.99
0.02	0	0.84	0.91	0.94	0.96	0.97	0.98	0.98	0.99	0.99	>0.99
0.03	0	0.83	0.89	0.91	0.93	0.95	0.96	0.96	0.97	0.97	0.98
0.04	0	0.82	0.86	0.88	0.90	0.91	0.92	0.93	0.93	0.94	0.95
0.05	0	0.81	0.84	0.85	0.86	0.86	0.87	0.87	0.88	0.87	0.89
0.06	0	0.80	0.80	0.80	0.80	0.80	0.79	0.79	0.79	0.79	0.78
0.07	0	0.78	0.77	0.75	0.74	0.72	0.70	0.68	0.68	0.66	0.64
0.08	0	0.77	0.74	0.71	0.65	0.62	0.59	0.57	0.55	0.53	0.52
0.09	0	0.76	0.70	0.64	0.58	0.53	0.47	0.45	0.43	0.40	0.38
0.1	0	0.74	0.67	0.57	0.50	0.42	0.36	0.34	0.32	0.29	0.28
0.11	0	0.73	0.63	0.51	0.41	0.32	0.28	0.25	0.23	0.21	0.21
0.12	0	0.72	0.58	0.44	0.33	0.25	0.20	0.18	0.17	0.15	0.15

Table F.27. Decision table for harvest rate at maximum sustainable yield u_{MSY} for selected projection years over 3 generations (60 years) and for a range of **constant catch** *strategies, such that values are P$(u_t < u_{\mathrm{MSY}})$. For reference, the average catch over the last 5 years (2015-2019) was 69 t.*

CC	2020	2025	2030	2035	2040	2045	2050	2055	2060	2070	2080
0	1	1	1	1	1	1	1	1	1	1	1
50	1	1	1	1	1	1	1	1	1	1	1
100	>0.99	1	1	1	1	1	1	1	1	1	1
150	0.98	1	1	1	1	1	1	1	1	1	1
200	0.95	1	1	1	1	1	1	1	1	1	1
250	0.89	>0.99	1	1	1	1	>0.99	1	1	>0.99	1
300	0.81	>0.99	>0.99	>0.99	>0.99	>0.99	>0.99	>0.99	>0.99	>0.99	>0.99
350	0.72	>0.99	>0.99	>0.99	>0.99	>0.99	>0.99	>0.99	>0.99	>0.99	>0.99
400	0.63	>0.99	>0.99	>0.99	>0.99	>0.99	>0.99	>0.99	>0.99	>0.99	>0.99
450	0.56	0.99	0.99	0.99	0.99	0.99	0.99	0.99	0.99	0.99	0.99
500	0.49	0.99	0.99	0.99	0.99	0.99	0.99	0.99	0.99	0.99	0.99
550	0.42	0.98	0.99	0.99	0.99	0.99	0.99	0.98	0.98	0.98	0.98
600	0.36	0.98	0.98	0.98	0.98	0.98	0.98	0.98	0.98	0.98	0.98

Table F.28. Decision table for harvest rate at maximum sustainable yield u_{MSY} for selected projection years over 3 generations (60 years) and for a range of **harvest rate** *strategies, such that values are P$(u_t < u_{\mathrm{MSY}})$. For reference, the average harvest rate over the last 5 years (2015-2019) was 0.026.*

HR	2020	2025	2030	2035	2040	2045	2050	2055	2060	2070	2080
0	1	1	1	1	1	1	1	1	1	1	1
0.01	1	1	1	1	1	1	1	1	1	1	1
0.02	1	1	1	1	1	1	1	1	1	1	1
0.03	>0.99	>0.99	>0.99	>0.99	>0.99	>0.99	>0.99	>0.99	>0.99	>0.99	>0.99
0.04	>0.99	>0.99	>0.99	>0.99	>0.99	>0.99	>0.99	>0.99	>0.99	>0.99	>0.99
0.05	0.97	0.97	0.97	0.97	0.97	0.97	0.97	0.97	0.97	0.97	0.97
0.06	0.90	0.90	0.90	0.90	0.90	0.90	0.90	0.90	0.90	0.90	0.90
0.07	0.77	0.77	0.77	0.77	0.77	0.77	0.77	0.77	0.77	0.78	0.77
0.08	0.58	0.58	0.58	0.58	0.58	0.58	0.58	0.58	0.58	0.58	0.58
0.09	0.41	0.41	0.41	0.41	0.41	0.42	0.41	0.41	0.41	0.41	0.41
0.1	0.28	0.28	0.28	0.28	0.28	0.28	0.28	0.28	0.28	0.28	0.28
0.11	0.17	0.17	0.17	0.17	0.17	0.17	0.17	0.17	0.17	0.17	0.17
0.12	0.10	0.10	0.10	0.10	0.10	0.10	0.10	0.10	0.10	0.10	0.10

Table F.29. Decision table for comparing projected biomass to current biomass B_{2020} for selected projection years over 3 generations (60 years) and for a range of **constant catch** *strategies, such that values are P($B_t > B_{2020}$). For reference, the average catch over the last 5 years (2015-2019) was 69 t.*

CC	2020	2025	2030	2035	2040	2045	2050	2055	2060	2070	2080
0	0	1	1	1	1	1	1	1	1	1	1
50	0	1	1	1	1	1	1	1	1	1	1
100	0	1	1	1	1	1	1	1	1	1	1
150	0	1	1	1	1	1	1	1	1	1	1
200	0	1	1	1	1	1	1	1	1	1	1
250	0	1	1	1	1	1	1	1	1	1	1
300	0	1	1	1	1	1	1	1	1	1	1
350	0	1	1	1	1	1	1	1	1	1	>0.99
400	0	1	1	1	1	1	1	1	>0.99	>0.99	>0.99
450	0	1	1	1	1	1	>0.99	>0.99	>0.99	>0.99	>0.99
500	0	1	1	1	1	>0.99	>0.99	>0.99	>0.99	>0.99	>0.99
550	0	1	1	1	1	>0.99	>0.99	>0.99	>0.99	0.99	0.99
600	0	1	1	1	>0.99	>0.99	>0.99	>0.99	>0.99	0.99	0.99

Table F.30. Decision table for comparing projected biomass to current biomass B_{2020} for selected projection years over 3 generations (60 years) and for a range of **harvest rate** *strategies, such that values are P($B_t > B_{2020}$). For reference, the average harvest rate over the last 5 years (2015-2019) was 0.026.*

HR	2020	2025	2030	2035	2040	2045	2050	2055	2060	2070	2080
0	0	1	1	1	1	1	1	1	1	1	1
0.01	0	1	1	1	1	1	1	1	1	1	1
0.02	0	1	1	1	1	1	1	1	1	1	1
0.03	0	1	1	1	1	1	1	1	1	1	1
0.04	0	1	1	1	1	1	1	1	1	1	1
0.05	0	1	1	1	1	1	1	1	1	1	1
0.06	0	1	1	1	1	1	1	1	1	1	1
0.07	0	1	1	1	1	1	1	1	1	1	1
0.08	0	1	1	1	1	1	1	1	1	1	1
0.09	0	1	1	1	1	1	1	1	1	1	>0.99
0.1	0	1	1	1	1	1	1	1	1	>0.99	>0.99
0.11	0	1	1	1	1	1	1	1	>0.99	>0.99	>0.99
0.12	0	1	1	1	1	1	1	>0.99	>0.99	0.99	0.99

Table F.31. Decision table for comparing projected harvest rate to current harvest rate u_{2019} for selected projection years over 3 generations (60 years) and for a range of **constant catch** *strategies, such that values are P$(u_t < u_{2019})$. For reference, the average catch over the last 5 years (2015-2019) was 69 t.*

CC	2020	2025	2030	2035	2040	2045	2050	2055	2060	2070	2080
0	1	1	1	1	1	1	1	1	1	1	1
50	1	1	1	1	1	1	1	1	1	1	1
100	1	1	1	1	1	1	1	1	1	1	1
150	0.09	1	1	1	1	1	1	1	1	1	1
200	0	1	1	1	1	1	1	1	1	1	1
250	0	1	1	1	1	1	1	1	1	1	1
300	0	>0.99	1	1	>0.99	>0.99	>0.99	>0.99	>0.99	>0.99	>0.99
350	0	>0.99	>0.99	>0.99	>0.99	>0.99	>0.99	0.99	0.99	0.99	0.99
400	0	0.98	0.99	0.99	0.99	0.99	0.99	0.99	0.98	0.97	0.97
450	0	0.95	0.99	0.98	0.98	0.98	0.97	0.96	0.96	0.95	0.94
500	0	0.88	0.96	0.96	0.95	0.94	0.93	0.92	0.92	0.90	0.89
550	0	0.79	0.92	0.91	0.90	0.90	0.89	0.87	0.85	0.84	0.84
600	0	0.68	0.87	0.85	0.84	0.84	0.82	0.80	0.80	0.79	0.77

Table F.32. Decision table for comparing projected harvest rate to current harvest rate u_{2019} for selected projection years over 3 generations (60 years) and for a range of **harvest rate** *strategies, such that values are P$(u_t < u_{2019})$. For reference, the average harvest rate over the last 5 years (2015-2019) was 0.026.*

HR	2020	2025	2030	2035	2040	2045	2050	2055	2060	2070	2080
0	1	1	1	1	1	1	1	1	1	1	1
0.01	0.97	0.97	0.97	0.97	0.97	0.97	0.97	0.97	0.97	0.97	0.97
0.02	0.67	0.67	0.67	0.67	0.67	0.67	0.67	0.67	0.67	0.67	0.67
0.03	0.27	0.27	0.27	0.27	0.27	0.27	0.27	0.27	0.27	0.27	0.27
0.04	0.07	0.07	0.07	0.07	0.07	0.07	0.07	0.07	0.07	0.07	0.07
0.05	0.01	0.01	0.01	0.01	0.01	0.01	0.01	0.01	0.01	0.01	0.01
0.06	<0.01	<0.01	<0.01	<0.01	<0.01	<0.01	<0.01	<0.01	<0.01	<0.01	<0.01
0.07	0	0	0	0	0	0	0	0	0	0	0
0.08	0	0	0	0	0	0	0	0	0	0	0
0.09	0	0	0	0	0	0	0	0	0	0	0
0.1	0	0	0	0	0	0	0	0	0	0	0
0.11	0	0	0	0	0	0	0	0	0	0	0
0.12	0	0	0	0	0	0	0	0	0	0	0

Table F.33. Decision table for alternative limit reference point $0.2B_0$ for selected projection years over 3 generations (60 years) and for a range of **constant catch** *strategies, such that values are P$(B_t > 0.2B_0)$. For reference, the average catch over the last 5 years (2015-2019) was 69 t.*

CC	2020	2025	2030	2035	2040	2045	2050	2055	2060	2070	2080
0	0	0.99	>0.99	>0.99	>0.99	>0.99	>0.99	>0.99	1	1	1
50	0	0.99	>0.99	>0.99	>0.99	>0.99	>0.99	>0.99	1	1	1
100	0	0.98	>0.99	>0.99	>0.99	>0.99	>0.99	>0.99	1	1	1
150	0	0.98	>0.99	>0.99	>0.99	>0.99	>0.99	>0.99	1	1	1
200	0	0.98	0.99	>0.99	>0.99	>0.99	>0.99	>0.99	>0.99	1	1
250	0	0.98	0.99	>0.99	>0.99	>0.99	>0.99	>0.99	>0.99	>0.99	>0.99
300	0	0.98	0.99	>0.99	>0.99	>0.99	>0.99	>0.99	>0.99	>0.99	>0.99
350	0	0.98	0.99	0.99	>0.99	>0.99	>0.99	>0.99	>0.99	>0.99	>0.99
400	0	0.97	0.99	0.99	>0.99	>0.99	>0.99	>0.99	>0.99	>0.99	>0.99
450	0	0.97	0.99	0.99	0.99	0.99	>0.99	>0.99	0.99	0.99	0.99
500	0	0.97	0.98	0.99	0.99	0.99	0.99	0.99	0.99	0.99	0.99
550	0	0.97	0.98	0.99	0.99	0.99	0.99	0.99	0.99	0.99	0.99
600	0	0.96	0.98	0.98	0.99	0.99	0.99	0.98	0.98	0.98	0.98

Table F.34. Decision table for alternative limit reference point $0.2B_0$ for selected projection years over 3 generations (60 years) and for a range of **harvest rate** *strategies, such that values are P$(B_t > 0.2B_0)$. For reference, the average harvest rate over the last 5 years (2015-2019) was 0.026.*

HR	2020	2025	2030	2035	2040	2045	2050	2055	2060	2070	2080
0	0	0.99	>0.99	>0.99	>0.99	>0.99	>0.99	>0.99	1	1	1
0.01	0	0.98	>0.99	>0.99	>0.99	>0.99	>0.99	>0.99	1	1	1
0.02	0	0.98	0.99	>0.99	>0.99	>0.99	>0.99	>0.99	>0.99	>0.99	>0.99
0.03	0	0.98	0.99	0.99	>0.99	>0.99	>0.99	>0.99	>0.99	>0.99	>0.99
0.04	0	0.97	0.98	0.99	0.99	0.99	>0.99	>0.99	>0.99	>0.99	>0.99
0.05	0	0.97	0.97	0.98	0.98	0.99	0.99	0.99	0.99	0.99	0.99
0.06	0	0.97	0.97	0.97	0.97	0.97	0.97	0.97	0.97	0.97	0.97
0.07	0	0.96	0.96	0.95	0.95	0.94	0.94	0.94	0.93	0.93	0.93
0.08	0	0.96	0.94	0.92	0.92	0.91	0.89	0.88	0.87	0.85	0.85
0.09	0	0.95	0.92	0.90	0.88	0.85	0.82	0.79	0.78	0.76	0.74
0.1	0	0.95	0.90	0.86	0.82	0.77	0.72	0.69	0.67	0.63	0.60
0.11	0	0.94	0.87	0.81	0.74	0.67	0.60	0.57	0.53	0.49	0.47
0.12	0	0.93	0.84	0.75	0.65	0.57	0.49	0.44	0.40	0.37	0.36

Table F.35. Decision table for alternative upper stock reference $0.4B_0$ for selected projection years over 3 generations (60 years) and for a range of **constant catch** *strategies, such that values are P$(B_t > 0.4B_0)$. For reference, the average catch over the last 5 years (2015-2019) was 69 t.*

CC	2020	2025	2030	2035	2040	2045	2050	2055	2060	2070	2080
0	0	0.75	0.89	0.94	0.97	0.99	>0.99	>0.99	>0.99	>0.99	>0.99
50	0	0.75	0.88	0.94	0.97	0.98	0.99	>0.99	>0.99	>0.99	>0.99
100	0	0.74	0.88	0.93	0.96	0.98	0.99	0.99	>0.99	>0.99	>0.99
150	0	0.74	0.87	0.92	0.96	0.98	0.99	0.99	>0.99	>0.99	>0.99
200	0	0.73	0.86	0.91	0.95	0.97	0.98	0.99	0.99	>0.99	>0.99
250	0	0.72	0.85	0.91	0.94	0.96	0.98	0.98	0.99	0.99	>0.99
300	0	0.72	0.84	0.90	0.94	0.96	0.97	0.98	0.98	0.99	0.99
350	0	0.71	0.83	0.89	0.93	0.95	0.96	0.97	0.98	0.98	0.99
400	0	0.70	0.82	0.88	0.92	0.94	0.96	0.96	0.97	0.98	0.98
450	0	0.69	0.81	0.87	0.91	0.93	0.95	0.95	0.96	0.97	0.98
500	0	0.68	0.80	0.86	0.89	0.92	0.94	0.95	0.95	0.96	0.97
550	0	0.68	0.79	0.84	0.88	0.91	0.92	0.93	0.94	0.94	0.95
600	0	0.67	0.78	0.83	0.87	0.90	0.90	0.91	0.92	0.92	0.93

Table F.36. Decision table for alternative upper stock reference $0.4B_0$ for selected projection years over 3 generations (60 years) and for a range of **harvest rate** *strategies, such that values are P$(B_t > 0.4B_0)$. For reference, the average harvest rate over the last 5 years (2015-2019) was 0.026.*

HR	2020	2025	2030	2035	2040	2045	2050	2055	2060	2070	2080
0	0	0.75	0.89	0.94	0.97	0.99	>0.99	>0.99	>0.99	>0.99	>0.99
0.01	0	0.74	0.87	0.91	0.95	0.97	0.98	0.99	0.99	>0.99	>0.99
0.02	0	0.73	0.83	0.88	0.92	0.94	0.95	0.96	0.97	0.98	0.99
0.03	0	0.71	0.79	0.83	0.87	0.89	0.90	0.91	0.92	0.93	0.94
0.04	0	0.69	0.75	0.78	0.79	0.80	0.81	0.81	0.82	0.81	0.81
0.05	0	0.67	0.72	0.71	0.70	0.68	0.67	0.66	0.65	0.63	0.61
0.06	0	0.65	0.67	0.64	0.59	0.55	0.50	0.48	0.44	0.42	0.42
0.07	0	0.63	0.62	0.54	0.48	0.40	0.33	0.30	0.29	0.27	0.26
0.08	0	0.61	0.56	0.46	0.35	0.26	0.20	0.18	0.18	0.16	0.16
0.09	0	0.60	0.51	0.38	0.25	0.16	0.11	0.10	0.10	0.09	0.09
0.1	0	0.57	0.45	0.28	0.15	0.10	0.06	0.06	0.06	0.05	0.05
0.11	0	0.55	0.40	0.21	0.10	0.06	0.04	0.03	0.03	0.02	0.03
0.12	0	0.53	0.33	0.15	0.06	0.03	0.02	0.02	0.02	0.01	0.02

F.2.1.4.3. COSEWIC – Reference criteria

Table F.37. Decision table for probabilities of satisfying the A2 criterion of $\leq 50\%$ decline over 3 generations (60 years) for 10-year projections and for a range of **constant catch** *strategies. For reference, the average catch over the last 5 years (2015-2019) was 69 t.*

CC	2020	2021	2022	2023	2024	2025	2026	2027	2028	2029	2030
0	0	0.26	0.71	0.94	0.99	>0.99	>0.99	>0.99	>0.99	1	1
50	0	0.25	0.71	0.94	0.99	>0.99	>0.99	>0.99	>0.99	>0.99	>0.99
100	0	0.25	0.70	0.94	0.99	>0.99	>0.99	>0.99	>0.99	>0.99	>0.99
150	0	0.25	0.69	0.93	0.99	>0.99	>0.99	>0.99	>0.99	>0.99	>0.99
200	0	0.25	0.69	0.93	0.99	>0.99	>0.99	>0.99	>0.99	>0.99	>0.99
250	0	0.24	0.68	0.93	0.98	>0.99	>0.99	>0.99	>0.99	>0.99	>0.99
300	0	0.24	0.68	0.92	0.98	>0.99	>0.99	>0.99	>0.99	>0.99	>0.99
350	0	0.24	0.67	0.92	0.98	>0.99	>0.99	>0.99	>0.99	>0.99	>0.99
400	0	0.24	0.67	0.91	0.98	0.99	>0.99	>0.99	>0.99	>0.99	>0.99
450	0	0.24	0.66	0.91	0.98	0.99	>0.99	>0.99	>0.99	>0.99	>0.99
500	0	0.23	0.65	0.90	0.98	0.99	>0.99	>0.99	>0.99	>0.99	>0.99
550	0	0.23	0.65	0.90	0.97	0.99	>0.99	>0.99	>0.99	>0.99	>0.99
600	0	0.23	0.64	0.90	0.97	0.99	0.99	>0.99	>0.99	>0.99	>0.99

Table F.38. Decision table for probabilities of satisfying the A2 criterion of $\leq 50\%$ decline over 3 generations (60 years) for 10-year projections and for a range of **harvest rate** *strategies. For reference, the average harvest rate over the last 5 years (2015-2019) was 0.026.*

HR	2020	2021	2022	2023	2024	2025	2026	2027	2028	2029	2030
0	0	0.26	0.71	0.94	0.99	>0.99	>0.99	>0.99	>0.99	1	1
0.01	0	0.25	0.71	0.94	0.99	>0.99	>0.99	>0.99	>0.99	>0.99	>0.99
0.02	0	0.25	0.70	0.94	0.99	>0.99	>0.99	>0.99	>0.99	>0.99	>0.99
0.03	0	0.25	0.69	0.93	0.99	>0.99	>0.99	>0.99	>0.99	>0.99	>0.99
0.04	0	0.24	0.68	0.93	0.99	>0.99	>0.99	>0.99	>0.99	>0.99	>0.99
0.05	0	0.24	0.67	0.92	0.98	>0.99	>0.99	>0.99	>0.99	>0.99	>0.99
0.06	0	0.24	0.67	0.91	0.98	>0.99	>0.99	>0.99	>0.99	>0.99	>0.99
0.07	0	0.24	0.66	0.91	0.98	0.99	>0.99	>0.99	>0.99	>0.99	>0.99
0.08	0	0.23	0.66	0.91	0.98	0.99	>0.99	>0.99	>0.99	>0.99	>0.99
0.09	0	0.23	0.65	0.90	0.97	0.99	0.99	>0.99	0.99	0.99	0.99
0.1	0	0.23	0.65	0.90	0.97	0.99	0.99	0.99	0.99	0.99	0.99
0.11	0	0.23	0.64	0.89	0.97	0.99	0.99	0.99	0.99	0.99	0.99
0.12	0	0.22	0.63	0.88	0.96	0.98	0.99	0.99	0.99	0.98	0.98

Table F.39. Decision table for probabilities of satisfying the A2 criterion of $\leq 30\%$ decline over 3 generations (60 years) for 10-year projections and for a range of **constant catch** *strategies. For reference, the average catch over the last 5 years (2015-2019) was 69 t.*

CC	2020	2021	2022	2023	2024	2025	2026	2027	2028	2029	2030
0	0	0.06	0.40	0.78	0.94	0.99	>0.99	>0.99	>0.99	>0.99	>0.99
50	0	0.06	0.39	0.78	0.94	0.98	0.99	>0.99	>0.99	>0.99	>0.99
100	0	0.06	0.39	0.77	0.94	0.98	0.99	>0.99	>0.99	>0.99	>0.99
150	0	0.06	0.39	0.77	0.93	0.98	0.99	>0.99	>0.99	>0.99	>0.99
200	0	0.06	0.38	0.76	0.93	0.98	0.99	0.99	>0.99	>0.99	>0.99
250	0	0.06	0.38	0.75	0.92	0.98	0.99	0.99	0.99	>0.99	>0.99
300	0	0.06	0.38	0.75	0.92	0.97	0.99	0.99	0.99	>0.99	>0.99
350	0	0.06	0.37	0.74	0.91	0.97	0.98	0.99	0.99	0.99	>0.99
400	0	0.06	0.37	0.73	0.91	0.97	0.98	0.99	0.99	0.99	0.99
450	0	0.06	0.36	0.72	0.90	0.96	0.98	0.99	0.99	0.99	0.99
500	0	0.06	0.36	0.71	0.90	0.96	0.98	0.98	0.99	0.99	0.99
550	0	0.06	0.36	0.71	0.89	0.96	0.98	0.98	0.98	0.99	0.99
600	0	0.06	0.35	0.70	0.89	0.95	0.97	0.98	0.98	0.98	0.98

Table F.40. Decision table for probabilities of satisfying the A2 criterion of $\leq 30\%$ decline over 3 generations (60 years) for 10-year projections and for a range of **harvest rate** *strategies. For reference, the average harvest rate over the last 5 years (2015-2019) was 0.026.*

HR	2020	2021	2022	2023	2024	2025	2026	2027	2028	2029	2030
0	0	0.06	0.40	0.78	0.94	0.99	>0.99	>0.99	>0.99	>0.99	>0.99
0.01	0	0.06	0.39	0.78	0.94	0.98	0.99	>0.99	>0.99	>0.99	>0.99
0.02	0	0.06	0.39	0.77	0.93	0.98	0.99	>0.99	>0.99	>0.99	>0.99
0.03	0	0.06	0.38	0.76	0.92	0.98	0.99	0.99	0.99	>0.99	>0.99
0.04	0	0.06	0.38	0.74	0.92	0.97	0.99	0.99	0.99	0.99	0.99
0.05	0	0.06	0.37	0.73	0.91	0.97	0.98	0.99	0.99	0.99	0.99
0.06	0	0.06	0.36	0.72	0.90	0.96	0.98	0.99	0.99	0.99	0.99
0.07	0	0.06	0.36	0.71	0.90	0.96	0.98	0.98	0.98	0.98	0.98
0.08	0	0.05	0.35	0.70	0.89	0.95	0.97	0.98	0.98	0.98	0.98
0.09	0	0.05	0.34	0.69	0.88	0.94	0.97	0.97	0.97	0.97	0.97
0.1	0	0.05	0.34	0.68	0.87	0.94	0.96	0.96	0.96	0.95	0.95
0.11	0	0.05	0.33	0.67	0.86	0.93	0.95	0.95	0.95	0.94	0.93
0.12	0	0.05	0.33	0.66	0.85	0.92	0.94	0.94	0.93	0.92	0.91

Table F.41. Decision table for reference criterion $0.5B_0$ for 10-year projections and for a range of **constant catch** *strategies, such that values are P$(B_t > 0.5B_0)$. For reference, the average catch over the last 5 years (2015-2019) was 69 t.*

CC	2020	2021	2022	2023	2024	2025	2026	2027	2028	2029	2030
0	0	0	0.04	0.19	0.43	0.60	0.70	0.74	0.75	0.77	0.78
50	0	0	0.04	0.19	0.42	0.59	0.69	0.73	0.74	0.76	0.77
100	0	0	0.04	0.18	0.41	0.58	0.68	0.72	0.73	0.75	0.76
150	0	0	0.04	0.18	0.41	0.57	0.68	0.72	0.73	0.74	0.75
200	0	0	0.04	0.18	0.40	0.57	0.67	0.71	0.72	0.73	0.74
250	0	0	0.04	0.18	0.39	0.56	0.66	0.70	0.71	0.72	0.73
300	0	0	0.04	0.17	0.39	0.55	0.65	0.69	0.70	0.71	0.72
350	0	0	0.04	0.17	0.38	0.54	0.64	0.68	0.69	0.70	0.71
400	0	0	0.04	0.17	0.37	0.54	0.63	0.66	0.68	0.69	0.70
450	0	0	0.04	0.16	0.37	0.52	0.62	0.66	0.67	0.68	0.69
500	0	0	0.03	0.16	0.36	0.52	0.61	0.64	0.65	0.66	0.67
550	0	0	0.03	0.16	0.35	0.51	0.60	0.63	0.64	0.65	0.66
600	0	0	0.03	0.16	0.35	0.50	0.59	0.62	0.63	0.63	0.64

Table F.42. Decision table for reference criterion $0.5B_0$ for 10-year projections and for a range of **harvest rate** *strategies, such that values are P$(B_t > 0.5B_0)$. For reference, the average harvest rate over the last 5 years (2015-2019) was 0.026.*

HR	2020	2021	2022	2023	2024	2025	2026	2027	2028	2029	2030
0	0	0	0.04	0.19	0.43	0.60	0.70	0.74	0.75	0.77	0.78
0.01	0	0	0.04	0.18	0.41	0.58	0.68	0.71	0.72	0.73	0.74
0.02	0	0	0.04	0.18	0.39	0.56	0.65	0.68	0.69	0.69	0.70
0.03	0	0	0.04	0.17	0.38	0.54	0.63	0.65	0.66	0.65	0.65
0.04	0	0	0.04	0.16	0.36	0.52	0.60	0.62	0.61	0.61	0.60
0.05	0	0	0.04	0.16	0.35	0.49	0.57	0.59	0.57	0.56	0.55
0.06	0	0	0.03	0.16	0.33	0.48	0.55	0.55	0.53	0.51	0.49
0.07	0	0	0.03	0.15	0.32	0.46	0.52	0.52	0.49	0.46	0.43
0.08	0	0	0.03	0.15	0.31	0.44	0.49	0.49	0.45	0.41	0.38
0.09	0	0	0.03	0.14	0.29	0.41	0.47	0.45	0.40	0.36	0.32
0.1	0	0	0.03	0.14	0.28	0.39	0.43	0.41	0.36	0.31	0.27
0.11	0	0	0.03	0.13	0.27	0.37	0.40	0.37	0.32	0.27	0.23
0.12	0	0	0.03	0.13	0.26	0.35	0.38	0.34	0.28	0.23	0.18

Table F.43. Decision table for reference criterion $0.7B_0$ for 10-year projections and for a range of **constant catch** *strategies, such that values are P$(B_t > 0.7B_0)$. For reference, the average catch over the last 5 years (2015-2019) was 69 t.*

CC	2020	2021	2022	2023	2024	2025	2026	2027	2028	2029	2030
0	0	0	<0.01	0.05	0.18	0.33	0.44	0.49	0.51	0.53	0.55
50	0	0	<0.01	0.05	0.17	0.32	0.43	0.48	0.50	0.52	0.53
100	0	0	<0.01	0.05	0.17	0.31	0.42	0.47	0.49	0.50	0.52
150	0	0	<0.01	0.05	0.16	0.31	0.41	0.46	0.48	0.50	0.51
200	0	0	<0.01	0.05	0.16	0.30	0.41	0.45	0.47	0.48	0.50
250	0	0	<0.01	0.05	0.16	0.30	0.40	0.45	0.46	0.47	0.49
300	0	0	<0.01	0.05	0.15	0.29	0.39	0.43	0.45	0.46	0.47
350	0	0	<0.01	0.04	0.15	0.28	0.38	0.43	0.44	0.45	0.46
400	0	0	<0.01	0.04	0.15	0.27	0.37	0.41	0.43	0.44	0.45
450	0	0	<0.01	0.04	0.15	0.27	0.36	0.40	0.42	0.43	0.44
500	0	0	<0.01	0.04	0.14	0.26	0.36	0.40	0.41	0.42	0.43
550	0	0	<0.01	0.04	0.14	0.25	0.35	0.39	0.40	0.41	0.42
600	0	0	<0.01	0.04	0.14	0.25	0.34	0.38	0.39	0.39	0.40

Table F.44. Decision table for reference criterion $0.7B_0$ for 10-year projections and for a range of **harvest rate** *strategies, such that values are P$(B_t > 0.7B_0)$. For reference, the average harvest rate over the last 5 years (2015-2019) was 0.026.*

HR	2020	2021	2022	2023	2024	2025	2026	2027	2028	2029	2030
0	0	0	<0.01	0.05	0.18	0.33	0.44	0.49	0.51	0.53	0.55
0.01	0	0	<0.01	0.05	0.16	0.31	0.41	0.46	0.47	0.48	0.49
0.02	0	0	<0.01	0.05	0.16	0.29	0.38	0.42	0.43	0.43	0.44
0.03	0	0	<0.01	0.05	0.15	0.27	0.36	0.38	0.39	0.38	0.38
0.04	0	0	<0.01	0.04	0.14	0.25	0.33	0.35	0.34	0.33	0.32
0.05	0	0	<0.01	0.04	0.14	0.24	0.31	0.32	0.31	0.29	0.27
0.06	0	0	<0.01	0.04	0.13	0.22	0.28	0.29	0.27	0.25	0.23
0.07	0	0	<0.01	0.04	0.12	0.20	0.26	0.26	0.23	0.20	0.18
0.08	0	0	<0.01	0.04	0.11	0.19	0.24	0.23	0.20	0.17	0.14
0.09	0	0	<0.01	0.03	0.11	0.17	0.21	0.20	0.17	0.14	0.12
0.1	0	0	<0.01	0.03	0.10	0.16	0.19	0.18	0.15	0.12	0.09
0.11	0	0	<0.01	0.03	0.09	0.15	0.17	0.16	0.12	0.09	0.07
0.12	0	0	<0.01	0.03	0.08	0.14	0.15	0.14	0.10	0.07	0.05

Table F.45. Decision table for probabilities of satisfying the A2 criterion of $\leq 50\%$ decline over 3 generations (60 years) for selected projection years and for a range of **constant catch** *strategies. For reference, the average catch over the last 5 years (2015-2019) was 69 t.*

CC	2020	2025	2030	2035	2040	2045	2050	2055	2060	2070	2080
0	0	>0.99	1	1	1	1	1	1	1	1	1
50	0	>0.99	>0.99	1	1	1	1	1	1	1	1
100	0	>0.99	>0.99	1	1	1	1	1	1	1	1
150	0	>0.99	>0.99	1	1	1	1	1	1	1	1
200	0	>0.99	>0.99	1	1	1	1	1	1	1	1
250	0	>0.99	>0.99	>0.99	1	1	1	1	1	1	1
300	0	>0.99	>0.99	>0.99	>0.99	>0.99	>0.99	1	1	1	1
350	0	>0.99	>0.99	>0.99	>0.99	>0.99	>0.99	>0.99	1	1	>0.99
400	0	0.99	>0.99	>0.99	>0.99	>0.99	>0.99	>0.99	>0.99	>0.99	>0.99
450	0	0.99	>0.99	>0.99	>0.99	>0.99	>0.99	>0.99	>0.99	>0.99	>0.99
500	0	0.99	>0.99	>0.99	>0.99	>0.99	>0.99	>0.99	>0.99	>0.99	>0.99
550	0	0.99	>0.99	>0.99	>0.99	>0.99	0.99	>0.99	>0.99	0.99	0.99
600	0	0.99	>0.99	0.99	0.99	0.99	0.99	0.99	0.99	0.99	0.99

Table F.46. Decision table for probabilities of satisfying the A2 criterion of $\leq 50\%$ decline over3 generations (60 years) for selected projection years and for a range of **harvest rate** *strategies. For reference, the average harvest rate over the last 5 years (2015-2019) was 0.026.*

HR	2020	2025	2030	2035	2040	2045	2050	2055	2060	2070	2080
0	0	>0.99	1	1	1	1	1	1	1	1	1
0.01	0	>0.99	>0.99	1	1	1	1	1	1	1	1
0.02	0	>0.99	>0.99	1	1	1	1	1	1	1	1
0.03	0	>0.99	>0.99	1	1	1	1	1	1	1	1
0.04	0	>0.99	>0.99	>0.99	>0.99	>0.99	1	1	1	1	1
0.05	0	>0.99	>0.99	>0.99	>0.99	>0.99	>0.99	1	1	1	1
0.06	0	>0.99	>0.99	>0.99	>0.99	>0.99	>0.99	1	1	1	1
0.07	0	0.99	>0.99	>0.99	>0.99	0.99	>0.99	>0.99	1	1	1
0.08	0	0.99	>0.99	0.99	0.99	0.99	0.99	>0.99	>0.99	1	1
0.09	0	0.99	0.99	0.99	0.98	0.97	0.98	0.99	>0.99	1	1
0.1	0	0.99	0.99	0.98	0.97	0.95	0.96	0.99	0.99	>0.99	1
0.11	0	0.99	0.99	0.97	0.94	0.91	0.93	0.98	0.99	>0.99	>0.99
0.12	0	0.98	0.98	0.95	0.90	0.86	0.88	0.96	0.98	0.99	>0.99

Table F.47. Decision table for probabilities of satisfying the A2 criterion of $\leq 30\%$ decline over 3 generations (60 years) for selected projection years and for a range of **constant catch** *strategies. For reference, the average catch over the last 5 years (2015-2019) was 69 t.*

CC	2020	2025	2030	2035	2040	2045	2050	2055	2060	2070	2080
0	0	0.99	>0.99	>0.99	1	1	1	1	1	1	1
50	0	0.98	>0.99	>0.99	1	1	1	1	1	1	1
100	0	0.98	>0.99	>0.99	>0.99	1	1	1	1	1	1
150	0	0.98	>0.99	>0.99	>0.99	>0.99	1	1	1	1	1
200	0	0.98	>0.99	>0.99	>0.99	>0.99	1	1	1	1	1
250	0	0.98	>0.99	>0.99	>0.99	>0.99	>0.99	1	1	1	1
300	0	0.97	>0.99	>0.99	>0.99	>0.99	>0.99	>0.99	1	1	1
350	0	0.97	>0.99	>0.99	>0.99	>0.99	>0.99	>0.99	>0.99	>0.99	>0.99
400	0	0.97	0.99	>0.99	>0.99	>0.99	>0.99	>0.99	>0.99	>0.99	>0.99
450	0	0.96	0.99	0.99	0.99	0.99	>0.99	>0.99	>0.99	>0.99	>0.99
500	0	0.96	0.99	0.99	0.99	0.99	0.99	>0.99	>0.99	>0.99	>0.99
550	0	0.96	0.99	0.99	0.99	0.99	0.99	0.99	>0.99	0.99	0.99
600	0	0.95	0.98	0.99	0.99	0.99	0.99	0.99	0.99	0.99	0.99

Table F.48. Decision table for probabilities of satisfying the A2 criterion of $\leq 30\%$ decline over 3 generations (60 years) for selected projection years and for a range of **harvest rate** *strategies. For reference, the average harvest rate over the last 5 years (2015-2019) was 0.026.*

HR	2020	2025	2030	2035	2040	2045	2050	2055	2060	2070	2080
0	0	0.99	>0.99	>0.99	1	1	1	1	1	1	1
0.01	0	0.98	>0.99	>0.99	1	1	1	1	1	1	1
0.02	0	0.98	>0.99	>0.99	>0.99	>0.99	1	1	1	1	1
0.03	0	0.98	>0.99	>0.99	>0.99	>0.99	>0.99	1	1	1	1
0.04	0	0.97	0.99	>0.99	>0.99	>0.99	>0.99	1	1	1	1
0.05	0	0.97	0.99	0.99	0.99	0.99	>0.99	>0.99	1	1	1
0.06	0	0.96	0.99	0.99	0.99	0.98	0.99	>0.99	1	1	1
0.07	0	0.96	0.98	0.98	0.97	0.96	0.97	>0.99	>0.99	1	1
0.08	0	0.95	0.98	0.96	0.94	0.93	0.95	0.99	>0.99	>0.99	1
0.09	0	0.94	0.97	0.94	0.91	0.87	0.91	0.98	0.99	>0.99	1
0.1	0	0.94	0.95	0.91	0.85	0.79	0.84	0.95	0.98	>0.99	>0.99
0.11	0	0.93	0.93	0.87	0.79	0.70	0.76	0.92	0.97	0.99	>0.99
0.12	0	0.92	0.91	0.83	0.70	0.60	0.68	0.87	0.94	0.99	>0.99

Table F.49. Decision table for reference criterion $0.5B_0$ for selected projection years over 3 generations (60 years) and for a range of **constant catch** *strategies, such that valuTabes are P$(B_t > 0.5B_0)$. For reference, the average catch over the last 5 years (2015-2019) was 69 t.*

CC	2020	2025	2030	2035	2040	2045	2050	2055	2060	2070	2080
0	0	0.60	0.78	0.86	0.92	0.95	0.97	0.98	0.99	>0.99	>0.99
50	0	0.59	0.77	0.85	0.91	0.95	0.97	0.98	0.99	0.99	>0.99
100	0	0.58	0.76	0.84	0.90	0.94	0.96	0.97	0.98	0.99	0.99
150	0	0.57	0.75	0.83	0.89	0.93	0.95	0.97	0.98	0.99	0.99
200	0	0.57	0.74	0.81	0.88	0.92	0.94	0.96	0.97	0.98	0.99
250	0	0.56	0.73	0.80	0.87	0.91	0.93	0.95	0.96	0.97	0.98
300	0	0.55	0.72	0.79	0.86	0.90	0.92	0.94	0.95	0.96	0.98
350	0	0.54	0.71	0.78	0.84	0.88	0.91	0.93	0.94	0.96	0.97
400	0	0.54	0.70	0.76	0.82	0.86	0.89	0.91	0.92	0.94	0.96
450	0	0.52	0.69	0.74	0.81	0.84	0.87	0.89	0.91	0.92	0.94
500	0	0.52	0.67	0.73	0.79	0.82	0.85	0.87	0.89	0.90	0.91
550	0	0.51	0.66	0.71	0.77	0.80	0.83	0.85	0.86	0.88	0.88
600	0	0.50	0.64	0.70	0.75	0.78	0.81	0.82	0.84	0.85	0.85

Table F.50. Decision table for reference criterion $0.5B_0$ for selected projection years over 3 generations (60 years) and for a range of **harvest rate** *strategies, such that values are P$(B_t > 0.5B_0)$. For reference, the average harvest rate over the last 5 years (2015-2019) was 0.026.*

HR	2020	2025	2030	2035	2040	2045	2050	2055	2060	2070	2080
0	0	0.60	0.78	0.86	0.92	0.95	0.97	0.98	0.99	>0.99	>0.99
0.01	0	0.58	0.74	0.81	0.87	0.91	0.93	0.95	0.96	0.98	0.99
0.02	0	0.56	0.70	0.75	0.79	0.83	0.85	0.88	0.89	0.90	0.92
0.03	0	0.54	0.65	0.68	0.70	0.72	0.73	0.73	0.75	0.74	0.74
0.04	0	0.52	0.60	0.60	0.59	0.57	0.55	0.54	0.52	0.51	0.50
0.05	0	0.49	0.55	0.51	0.47	0.42	0.36	0.33	0.32	0.31	0.30
0.06	0	0.48	0.49	0.42	0.34	0.27	0.21	0.18	0.18	0.17	0.17
0.07	0	0.46	0.43	0.33	0.22	0.15	0.11	0.09	0.10	0.09	0.09
0.08	0	0.44	0.38	0.25	0.14	0.08	0.06	0.05	0.05	0.04	0.04
0.09	0	0.41	0.32	0.17	0.08	0.04	0.03	0.03	0.03	0.02	0.02
0.1	0	0.39	0.27	0.12	0.04	0.02	0.02	0.02	0.02	0.01	0.01
0.11	0	0.37	0.23	0.08	0.02	0.01	0.01	0.01	0.01	<0.01	0.01
0.12	0	0.35	0.18	0.05	0.01	0.01	0.01	0.01	0.01	<0.01	<0.01

Table F.51. Decision table for reference criterion $0.7B_0$ for selected projection years over 3 generations (60 years) and for a range of **constant catch** *strategies, such that values are P$(B_t > 0.7B_0)$. For reference, the average catch over the last 5 years (2015-2019) was 69 t.*

CC	2020	2025	2030	2035	2040	2045	2050	2055	2060	2070	2080
0	0	0.33	0.55	0.64	0.71	0.77	0.82	0.86	0.89	0.92	0.94
50	0	0.32	0.53	0.62	0.69	0.75	0.80	0.84	0.87	0.90	0.93
100	0	0.31	0.52	0.60	0.67	0.74	0.78	0.81	0.85	0.88	0.91
150	0	0.31	0.51	0.58	0.65	0.71	0.76	0.79	0.83	0.86	0.89
200	0	0.30	0.50	0.57	0.63	0.69	0.73	0.76	0.80	0.83	0.86
250	0	0.30	0.49	0.55	0.61	0.66	0.71	0.74	0.76	0.80	0.82
300	0	0.29	0.47	0.54	0.59	0.64	0.67	0.71	0.74	0.77	0.78
350	0	0.28	0.46	0.52	0.57	0.61	0.65	0.67	0.71	0.73	0.74
400	0	0.27	0.45	0.51	0.55	0.59	0.61	0.64	0.67	0.70	0.70
450	0	0.27	0.44	0.49	0.53	0.55	0.58	0.61	0.63	0.65	0.65
500	0	0.26	0.43	0.47	0.51	0.53	0.55	0.57	0.59	0.61	0.61
550	0	0.25	0.42	0.46	0.49	0.50	0.52	0.54	0.55	0.58	0.57
600	0	0.25	0.40	0.44	0.46	0.48	0.49	0.51	0.51	0.53	0.53

Table F.52. Decision table for reference criterion $0.7B_0$ for selected projection years over 3 generations (60 years) and for a range of **harvest rate** *strategies, such that values are P$(B_t > 0.7B_0)$. For reference, the average harvest rate over the last 5 years (2015-2019) was 0.026.*

HR	2020	2025	2030	2035	2040	2045	2050	2055	2060	2070	2080
0	0	0.33	0.55	0.64	0.71	0.77	0.82	0.86	0.89	0.92	0.94
0.01	0	0.31	0.49	0.55	0.60	0.63	0.66	0.69	0.71	0.74	0.74
0.02	0	0.29	0.44	0.46	0.47	0.47	0.46	0.45	0.45	0.45	0.46
0.03	0	0.27	0.38	0.36	0.34	0.30	0.26	0.23	0.23	0.23	0.23
0.04	0	0.25	0.32	0.28	0.21	0.16	0.12	0.10	0.11	0.10	0.11
0.05	0	0.24	0.27	0.20	0.12	0.08	0.06	0.05	0.05	0.04	0.04
0.06	0	0.22	0.23	0.14	0.07	0.04	0.02	0.02	0.02	0.01	0.02
0.07	0	0.20	0.18	0.09	0.03	0.02	0.01	0.01	0.01	<0.01	0.01
0.08	0	0.19	0.14	0.06	0.01	0.01	0.01	0.01	0.01	<0.01	0.01
0.09	0	0.17	0.12	0.03	0.01	0.01	<0.01	<0.01	<0.01	<0.01	<0.01
0.1	0	0.16	0.09	0.01	<0.01	<0.01	<0.01	<0.01	<0.01	0	<0.01
0.11	0	0.15	0.07	0.01	<0.01	<0.01	<0.01	<0.01	<0.01	0	<0.01
0.12	0	0.14	0.05	<0.01	<0.01	<0.01	<0.01	<0.01	0	0	<0.01

F.2.1.4.4. Time to reach targets

Table F.53. Estimated time (years) for projected biomass B_t to exceed reference points and criteria with a probability of 50%, for for a range of **constant catch** *strategies. An estimated time of 0 means that the condition is satisfied and remains so over the 60-year projection; an estimated time of 60 means that the condition never becomes satisfied over the 3-generation projection. A further condition is that the probability of satisfying the condition must increase for two consecutive years. Columns respectively correspond to the provisional DFO reference points: LRP = $0.4B_{\mathrm{MSY}}$, USR = $0.8B_{\mathrm{MSY}}$; alternative reference points: B_{MSY}, B_{2020}, $0.2B_0$, $0.4B_0$; and COSEWIC reference criteria: $0.5B_{t\text{-}3\mathrm{G}}$ = $\leq 50\%$ decline over 3 generations (G), $0.7B_{t\text{-}3\mathrm{G}}$ = $\leq 30\%$ decline over 3G, $0.5B_0$, $0.7B_0$.*

	LRP	USR	B_{MSY}	B_{2020}	$0.2B_0$	$0.4B_0$	$0.5B_{t\text{-}3\mathrm{G}}$	$0.7B_{t\text{-}3\mathrm{G}}$	$0.5B_0$	$0.7B_0$
0	1	3	3	0	2	4	2	3	5	8
50	1	3	3	0	2	4	2	3	5	9
100	1	3	3	0	2	4	2	3	5	9
150	1	3	3	0	2	4	2	3	5	10
200	1	3	3	0	2	4	2	3	5	11
250	1	3	3	0	2	4	2	3	5	11
300	1	3	3	0	2	4	2	3	5	12
350	1	3	3	0	2	4	2	3	5	13
400	1	3	3	0	2	4	2	3	5	15
450	1	3	3	0	2	4	2	3	5	16
500	1	3	3	0	2	4	2	3	5	20
550	1	3	3	0	2	4	2	3	5	24
600	1	3	3	0	2	4	2	3	5	34

Table F.54. Estimated time (years) for projected biomass B_t to exceed reference points and criteria with a probability of 50%, for for a range of **harvest rate** *strategies. See caption in Table F.53 for further details*

	LRP	USR	B_{MSY}	B_{2020}	$0.2B_0$	$0.4B_0$	$0.5B_{t\text{-}3\mathrm{G}}$	$0.7B_{t\text{-}3\mathrm{G}}$	$0.5B_0$	$0.7B_0$
0	1	3	3	0	2	4	2	3	5	8
0.01	1	3	3	0	2	4	2	3	5	11
0.02	1	3	3	0	2	4	2	3	5	60
0.03	1	3	3	0	2	4	2	3	5	60
0.04	1	3	3	0	2	4	2	3	5	60
0.05	1	3	3	0	2	4	2	3	6	60
0.06	1	3	3	0	2	4	2	3	6	60
0.07	1	3	3	0	2	4	2	3	6	60
0.08	1	3	3	0	2	5	2	3	60	60
0.09	1	3	3	0	2	5	2	3	60	60
0.1	1	3	3	0	2	5	2	3	60	60
0.11	1	3	3	0	2	5	2	3	60	60
0.12	1	3	3	0	2	5	2	3	60	60

Table F.55. Estimated time (years) for projected biomass B_t to exceed reference points and criteria with a probability of 65%, for for a range of **constant catch** *strategies. See caption in Table F.53 for further details.*

	LRP	USR	B_{MSY}	B_{2020}	$0.2B_0$	$0.4B_0$	$0.5B_{t\text{-}3\mathrm{G}}$	$0.7B_{t\text{-}3\mathrm{G}}$	$0.5B_0$	$0.7B_0$
0	1	3	4	0	3	5	2	3	6	16
50	1	3	4	0	3	5	2	3	6	17
100	1	3	4	0	3	5	2	3	6	19
150	1	3	4	0	3	5	2	3	6	20
200	1	3	4	0	3	5	2	3	6	22
250	1	3	4	0	3	5	2	3	6	24
300	2	3	4	0	3	5	2	3	7	27
350	2	3	4	0	3	5	2	3	7	31
400	2	3	4	0	3	5	2	3	7	37
450	2	3	4	0	3	5	2	3	7	48
500	2	3	4	0	3	5	2	3	8	60
550	2	3	4	0	3	5	3	3	10	60
600	2	3	4	0	3	5	3	3	11	60

Table F.56. Estimated time (years) for projected biomass B_t to exceed reference points and criteria with a probability of 65%, for for a range of **harvest rate** *strategies. See caption in Table F.53 for further details.*

	LRP	USR	B_{MSY}	B_{2020}	$0.2B_0$	$0.4B_0$	$0.5B_{t\text{-}3\mathrm{G}}$	$0.7B_{t\text{-}3\mathrm{G}}$	$0.5B_0$	$0.7B_0$
0	1	3	4	0	3	5	2	3	6	16
0.01	1	3	4	0	3	5	2	3	6	28
0.02	1	3	4	0	3	5	2	3	6	60
0.03	1	3	4	0	3	5	2	3	7	60
0.04	1	3	4	0	3	5	2	3	60	60
0.05	1	3	4	0	3	5	2	3	60	60
0.06	2	3	4	0	3	5	2	3	60	60
0.07	2	3	4	0	3	6	2	3	60	60
0.08	2	3	4	0	3	6	2	3	60	60
0.09	2	3	4	0	3	60	2	3	60	60
0.1	2	3	4	0	3	60	3	3	60	60
0.11	2	3	4	0	3	60	3	3	60	60
0.12	2	4	5	0	3	60	3	3	60	60

Table F.57. Estimated time (years) for projected biomass B_t to exceed reference points and criteria with a probability of 80%, for for a range of **constant catch** *strategies. See caption in Table F.53 for further details.*

	LRP	USR	B_{MSY}	B_{2020}	$0.2B_0$	$0.4B_0$	$0.5B_{t\text{-}3\mathrm{G}}$	$0.7B_{t\text{-}3\mathrm{G}}$	$0.5B_0$	$0.7B_0$
0	2	4	5	0	3	6	3	4	12	28
50	2	4	5	0	3	6	3	4	12	31
100	2	4	5	0	3	6	3	4	13	33
150	2	4	5	0	3	6	3	4	14	37
200	2	4	5	0	3	6	3	4	14	40
250	2	4	5	0	3	7	3	4	15	51
300	2	4	5	0	3	7	3	4	16	60
350	2	4	5	0	3	7	3	4	17	60
400	2	4	5	0	3	8	3	4	18	60
450	2	4	5	0	3	10	3	4	20	60
500	2	4	5	0	3	11	3	4	22	60
550	2	4	5	0	3	12	3	4	25	60
600	2	4	5	0	3	13	3	4	29	60

Table F.58. Estimated time (years) for projected biomass B_t to exceed reference points and criteria with a probability of 80%, for for a range of **harvest rate** *strategies. See caption in Table F.53 for further details.*

	LRP	USR	B_{MSY}	B_{2020}	$0.2B_0$	$0.4B_0$	$0.5B_{t\text{-}3\mathrm{G}}$	$0.7B_{t\text{-}3\mathrm{G}}$	$0.5B_0$	$0.7B_0$
0	2	4	5	0	3	6	3	4	12	28
0.01	2	4	5	0	3	6	3	4	15	60
0.02	2	4	5	0	3	7	3	4	21	60
0.03	2	4	5	0	3	11	3	4	60	60
0.04	2	4	5	0	3	22	3	4	60	60
0.05	2	4	5	0	3	60	3	4	60	60
0.06	2	4	6	0	3	60	3	4	60	60
0.07	2	4	6	0	3	60	3	4	60	60
0.08	2	4	6	0	3	60	3	4	60	60
0.09	2	4	60	0	4	60	3	4	60	60
0.1	2	5	60	0	4	60	3	4	60	60
0.11	2	5	60	0	4	60	3	4	60	60
0.12	2	5	60	0	4	60	3	4	60	60

Table F.59. Estimated time (years) for projected biomass B_t to exceed reference points and criteria with a probability of 95%, for for a range of **constant catch** *strategies. See caption in Table F.53 for further details.*

	LRP	USR	B_{MSY}	B_{2020}	$0.2B_0$	$0.4B_0$	$0.5B_{t\text{-}3\mathrm{G}}$	$0.7B_{t\text{-}3\mathrm{G}}$	$0.5B_0$	$0.7B_0$
0	3	6	12	0	4	16	4	5	25	60
50	3	6	12	0	4	17	4	5	27	60
100	3	6	13	0	4	18	4	5	28	60
150	3	6	14	0	4	19	4	5	31	60
200	3	6	15	0	4	21	4	5	32	60
250	3	7	16	0	5	22	4	5	36	60
300	3	7	17	0	5	24	4	5	40	60
350	3	7	18	0	5	26	4	5	46	60
400	3	9	20	0	5	29	4	5	56	60
450	3	11	22	0	5	32	4	5	60	60
500	3	13	25	0	5	38	4	5	60	60
550	3	15	29	0	5	56	4	5	60	60
600	3	17	33	0	5	60	4	5	60	60

Table F.60. Estimated time (years) for projected biomass B_t to exceed reference points and criteria with a probability of 95%, for for a range of **harvest rate** *strategies. See caption in Table F.53 for further details.*

	LRP	USR	B_{MSY}	B_{2020}	$0.2B_0$	$0.4B_0$	$0.5B_{t\text{-}3\mathrm{G}}$	$0.7B_{t\text{-}3\mathrm{G}}$	$0.5B_0$	$0.7B_0$
0	3	6	12	0	4	16	4	5	25	60
0.01	3	6	15	0	4	21	4	5	35	60
0.02	3	6	19	0	4	30	4	5	60	60
0.03	3	12	28	0	5	60	4	5	60	60
0.04	3	18	60	0	5	60	4	5	60	60
0.05	3	49	60	0	5	60	4	5	60	60
0.06	3	60	60	0	5	60	4	5	60	60
0.07	3	60	60	0	5	60	4	5	60	60
0.08	3	60	60	0	5	60	4	5	60	60
0.09	3	60	60	0	5	60	4	6	60	60
0.1	3	60	60	0	6	60	4	6	60	60
0.11	4	60	60	0	60	60	4	6	60	60
0.12	4	60	60	0	60	60	4	41	60	60

F.2.2. SENSITIVITY RUNS

Nine sensitivity analyses were run (with full MCMC simulations) relative to the central run (Run02: M=0.08) to test the sensitivity of the outputs to alternative model assumptions:

- **S01** (Run05) – used constrained 'narrow' ageing error matrix (Figure D.20, left);
- **S02** (Run07) – decreased σ_R from 0.9 to 0.6;
- **S03** (Run08) – increased σ_R from 0.9 to 1.2;
- **S04** (Run09) – removed the CPUE index series;
- **S05** (Run10) – removed the NMFS Triennial and GIG Historical index series;
- **S06** (Run11) – reduced commercial catch by one third in years spanning foreign fleet activity and possible misreporting by domestic fleet (1965-1995);
- **S07** (Run12) – increased commercial catch by 50% in years spanning foreign fleet activity and possible misreporting by domestic fleet (1965-1995);
- **S08** (Run13) – used MLE von Bertalanffy growth model estimated with no ageing error;
- **S09** (Run14) – used full maturity ogive, allowing estimated maturities for ages 1 to 4.

Each sensitivity was reweighted only once using the procedure of Francis (2011) for age frequencies. The abundance index CVs were adjusted on the first reweight only using the same process error adopted in the base case: c_{p} = 0.25, 0.25, 0.25, 0.25, 0.25, 0.25, and 0.1514. The MPD (mode of the posterior distribution) 'best fit' was used as the starting point for a Bayesian search across the joint posterior distributions of the parameters using the Monte Carlo Markov Chain (MCMC) procedure. All sensitivity runs, except for S04 and S05, were judged to have converged after 6 million iterations, sampling every 5,000$^{\mathrm{th}}$ to give 1200 draws. The first 200 samples were discarded and 1000 samples were used for the MCMC analysis.

The differences among the sensitivity runs (including the central run) are summarised in tables of median parameter estimates (Table F.61) and median MSY-based quantities (Table F.62). Sensitivity plots appear in:

- Figure F.40 – trace plots for chains of R_0 MCMC samples;
- Figure F.41 – diagnostic split-chain plots for R_0 MCMC samples;
- Figure F.42 – diagnostic autocorrelation plots for R_0 MCMC sample;
- Figure F.43 – trajectories of median B_t/B_0;
- Figure F.44 – trajectories of $\log_{10}$ median recruitment R_t (one-year old fish);
- Figure F.45 – trajectories of median exploitation rate u_t;
- Figure F.46 – quantile plots of selected parameters for the sensitivity runs;
- Figure F.47 – quantile plots of selected derived quantities for the sensitivity runs;
- Figure F.48 – stock status plots of $B_{2020}/B_{\mathrm{MSY}}$.

The trajectories of the B_t medians relative to B_0 (Figure F.43) indicate that dropping the GIG Historical and the WCVI Triennial surveys (S05) resulted in the most optimistic scenario, while the most pessimistic run was the increased pre-1996 catches (foreign and pre-observer domestic) (S12). All of these sensitivity runs (apart from S05), tended to closely reflect the central run, particularly at the end of the reconstruction period where all models estimated similar low spawning biomass levels at the beginning of 2020. The overall conclusion is that, other than being sensitive to values of M, the model outcome is largely driven by the data because the only substantive changes in advice resulted when data series were omitted or changed. It is interesting to note that this model, unlike other recent rockfish models, needs the stabilising influence of the CPUE series and the early trawl survey data, because the runs which omitted

these data were not credible. This may be due to the lack of contrast in the research survey biomass indices and the consequent poor recruitment which result in a monotonic declining trend which is known to be hard to fit in this type of model.

The diagnostic plots (Figures F.40 to F.42) suggest that six of the nine sensitivities exhibited good MCMC behaviour, one was marginal but provisionally acceptable, one had poor diagnostics and one was so poor it needed to be rejected:

- Good – no trend in traces, split-chains align, no autocorrelation
  - S02 (σ_R=0.6)
  - S06 (-33% pre-1996 commercial catch)
  - S07 (+50% pre-1996 commercial catch)
  - S08 (use MLE non-linear von Bertalanffy model)
  - S09 (use full maturation ogive, including maturity estimates for ages 1-4)
- Marginal – trace trend temporarily interrupted, split-chains somewhat frayed, some autocorrelation
  - S01 (narrow ageing error matrix)
- Poor – trace trend fluctuates substantially or shows a persistent increase/decrease, split-chains differ from each other, substantial autocorrelation
  - S05 (drop WCVI Triennial and GIG Historical surveys)
- Unacceptable – trace trend shows a persistent increase that has not levelled, split-chains differ markedly from each other, substantial autocorrelation
  - S04 (drop CPUE series)

The run that dropped CPUE (S04) clearly did not converge, climbing in one long correlated trend (see Figure F.40). The model needs the stability introduced by this series, because the biomass trajectory is a 'one-way trip', a configuration that is notoriously difficult to estimate reliably (Hilborn and Walters 1992). Consequently, the results from this run have not been reported. Similarly, the run which dropped the two early surveys (S05) also showed convergence difficulties, although not as extreme as for sensitivity run S04. These results are reported, showing a model run which does not decline as rapidly as the central run and has a median estimate of B_{2020}/B_0 of 0.093, which is notably higher than for the remaining sensitivity runs (Figure F.43).

The 'narrow' ageing error run was meant to show the sensitivity of the stock assessment to this ageing error assumption. Although the relative trajectory for this run departs from the central run between 1960 and 1980, the two runs converge after 1980 and end up in the same place (Figure F.43), indicating that the model predictions are robust to the ageing error assumptions tested. Similarly, decreasing σ_R to 0.6 increased the model predictions for B_t/B_0 slightly relative to the central run (median B_{2020}/B_0 is estimated at 0.033 instead of 0.021) while there was virtually no difference compared to the central run when σ_R was increased to 1.2.

Changing the catch histories predictably affected the model predictions, with run S06 (decrease by 33%) slightly improving B_t/B_0 relative to the central run while the opposite occurred when the catch was increased by 50% (run S07). It is not known how accurate is the catch history used in the component base runs and the other sensitivity runs, but what is presented is the best that can be done at present with the available information.

Sensitivity run S08 uses the MLE von-Bertalanffy growth model which makes virtually identical model predictions compared to the central run. This is a good result, indicating that this stock

assessment is not sensitive to the alternative growth model estimated in a more traditional manner. Finally, sensitivity run S09 shows that the assumption that young (<age 5) BOR make no contribution to the spawning population has an important effect on the current estimates of stock status, given that the 2016 cohort has only reached age 4 by 2020. While we are not prepared to alter this assumption (for reasons given in Appendix D, Section D.1.4), we note that the 2020 estimates of stock status for all runs except S09 represent the status of the BOR population prior to the recruitment of the 2016 cohort.

Table F.61. Median values of MCMC samples for the primary estimated parameters, comparing the central run to 8 sensitivity runs (1000 samples each). C =Central, R = Run, S = Sensitivity. Numeric subscripts other than those for R_0 and M indicate the following gear types g: 1 = QCS Synoptic, 2 = WCVI Synoptic, 3 = WCHG Synoptic, 4 = HS Synoptic, 5 = NMFS Triennial, 6 = GIG Historical, and 7 = commercial trawl CPUE. Sensitivity runs: S01 = AE narrow, S02 = sigmaR=0.6, S03 = sigmaR=1.2, S05 = no GIG NMFS, S06 = decrease catch, S07 = increase catch, S08 = original vonB, S09 = fit early mats

	C(R02)	S01(R05)	S02(R07)	S03(R08)	S05(R10)	S06(R11)	S07(R12)	S08(R13)	S09(R14)
R_0	1,716	1,459	1,627	1,674	1,988	1,391	2,240	1,688	1,759
h	0.669	0.628	0.427	0.781	0.771	0.709	0.633	0.650	0.667
q_1	0.0352	0.0367	0.0359	0.0361	0.0124	0.0345	0.0362	0.0357	0.0353
q_2	0.0391	0.0420	0.0345	0.0433	0.0134	0.0388	0.0398	0.0398	0.0392
q_3	0.00355	0.00372	0.00308	0.00391	0.00122	0.00353	0.00359	0.00352	0.00354
q_4	0.00830	0.00892	0.00734	0.00900	0.00276	0.00814	0.00820	0.00835	0.00836
q_5	0.0574	0.0625	0.0537	0.0605	—	0.0600	0.0538	0.0581	0.0571
q_6	0.0221	0.0231	0.0197	0.0239	—	0.0253	0.0182	0.0222	0.0220
q_7	0.000320	0.000345	0.000282	0.000345	0.000130	0.000317	0.000320	0.000321	0.000319
μ_1	12.2	10.1	13.4	11.4	11.7	12.2	11.9	12.3	12.0
μ_2	10.1	10.2	10.1	9.94	9.88	10.0	9.99	10.1	9.94
μ_3	12.5	12.3	12.5	12.5	12.3	12.6	12.4	12.4	12.4
μ_4	13.8	12.9	13.4	13.6	13.2	13.8	13.5	13.7	13.7
μ_7	11.1	11.1	11.5	11.0	11.1	11.2	11.2	11.2	11.1
Δ_1	0.966	0.982	0.982	0.967	0.984	0.984	0.966	0.975	0.969
Δ_2	0.873	0.977	0.879	0.885	0.877	0.842	0.869	0.871	0.874
Δ_3	0.993	1.03	0.974	0.983	0.955	0.993	0.976	0.979	0.962
Δ_4	0.977	0.981	0.988	0.964	0.970	0.990	0.977	0.976	0.983
Δ_7	1.03	1.00	1.06	1.03	1.01	1.02	1.06	1.04	1.04
$\log v_{1L}$	4.59	4.63	4.84	4.47	4.55	4.59	4.57	4.52	4.57
$\log v_{2L}$	3.80	4.20	3.87	3.82	3.76	3.80	3.84	3.83	3.79
$\log v_{3L}$	3.29	3.75	3.49	3.38	3.26	3.28	3.26	3.27	3.28
$\log v_{4L}$	4.42	4.36	4.64	4.28	4.40	4.38	4.39	4.39	4.39
$\log v_{7L}$	3.55	3.70	3.76	3.47	3.58	3.52	3.57	3.56	3.54

Table F.62. Medians of MCMC-derived quantities from the central run and 8 sensitivity runs (1000 samples each) from their respective MCMC posteriors. Definitions are: B_0 – unfished equilibrium spawning biomass (mature females), V_0 – unfished equilibrium vulnerable biomass (males and females), B_{2020} – spawning biomass at the start of 2020, V_{2020} – vulnerable biomass in the middle of 2020, u_{2019} – exploitation rate (ratio of total catch to vulnerable biomass) in the middle of 2019, $u_{\max}$ – maximum exploitation rate (calculated for each sample as the maximum exploitation rate from 1935 - 2019), B_{MSY} – equilibrium spawning biomass at MSY (maximum sustainable yield), u_{MSY} – equilibrium exploitation rate at MSY, V_{MSY} – equilibrium vulnerable biomass at MSY. All biomass values (and MSY) are in tonnes. Sensitivity runs: S01 = AE narrow, S02 = sigmaR=0.6, S03 = sigmaR=1.2, S05 = no GIG NMFS, S06 = decrease catch, S07 = increase catch, S08 = original vonB, S09 = fit early mats

	C(R02)	S01(R05)	S02(R07)	S03(R08)	S05(R10)	S06(R11)	S07(R12)	S08(R13)	S09(R14)
B_0	32,289	27,674	30,878	31,767	37,733	26,408	42,484	32,728	33,583
V_0 (Trawl)	55,089	47,601	52,910	54,189	64,398	44,895	72,654	53,874	56,779
V_0 (Other)	53,564	45,939	51,260	52,737	62,640	43,836	70,524	52,844	55,360
B_{2020}	899	843	1,073	762	3,268	918	882	914	3,004
V_{2020} (Trawl)	5,703	5,406	4,169	6,616	17,661	6,049	5,543	5,282	5,714
V_{2020} (Other)	4,709	3,744	3,243	5,608	14,069	5,025	4,434	4,304	4,793
B_{2020}/B_0	0.0278	0.0308	0.0354	0.0243	0.0928	0.0355	0.0207	0.0288	0.0884
V_{2020}/V_0 (Trawl)	0.104	0.118	0.0789	0.125	0.296	0.136	0.0771	0.0998	0.101
V_{2020}/V_0 (Other)	0.0875	0.0833	0.0634	0.110	0.248	0.117	0.0624	0.0842	0.0856
u_{2019} (Trawl)	0.0250	0.0255	0.0283	0.0237	0.00775	0.0239	0.0253	0.0255	0.0251
u_{2019} (Other)	0.000930	0.00111	0.00111	0.000854	0.000300	0.000883	0.000968	0.000955	0.000920
$u_{\max}$ (Trawl)	0.0588	0.0628	0.0528	0.0628	0.0256	0.0582	0.0647	0.0589	0.0583
$u_{\max}$ (Other)	0.00968	0.0107	0.00926	0.00997	0.00540	0.00912	0.0137	0.00978	0.00961
MSY	1,461	1,160	829	1,714	1,946	1,296	1,820	1,329	1,544
B_{MSY}	9,462	8,474	11,842	7,959	9,908	7,375	12,955	9,924	9,877
$0.4B_{2020}$	3,785	3,390	4,737	3,184	3,963	2,950	5,182	3,970	3,951
$0.8B_{2020}$	7,570	6,779	9,474	6,367	7,926	5,900	10,364	7,939	7,902
$B_{2020}/B_{\mathrm{MSY}}$	0.0963	0.0994	0.0922	0.0973	0.374	0.126	0.0680	0.0941	0.300
B_{MSY}/B_0	0.291	0.308	0.382	0.250	0.255	0.278	0.306	0.304	0.293
V_{MSY}	17,554	16,156	21,276	15,121	19,001	13,787	24,129	17,562	18,183
V_{MSY}/V_0 (Trawl)	0.319	0.339	0.402	0.282	0.288	0.308	0.334	0.328	0.319
V_{MSY}/V_0 (Other)	0.328	0.353	0.417	0.289	0.298	0.317	0.345	0.336	0.327
u_{MSY}	0.0850	0.0720	0.0390	0.113	0.108	0.0930	0.0760	0.0760	0.0850
$u_{2019}/u_{\mathrm{MSY}}$ (Trawl)	0.291	0.349	0.733	0.207	0.0679	0.255	0.333	0.338	0.287
$u_{2019}/u_{\mathrm{MSY}}$ (Other)	0.0109	0.0153	0.0284	0.00749	0.00267	0.00947	0.0128	0.0127	0.0107

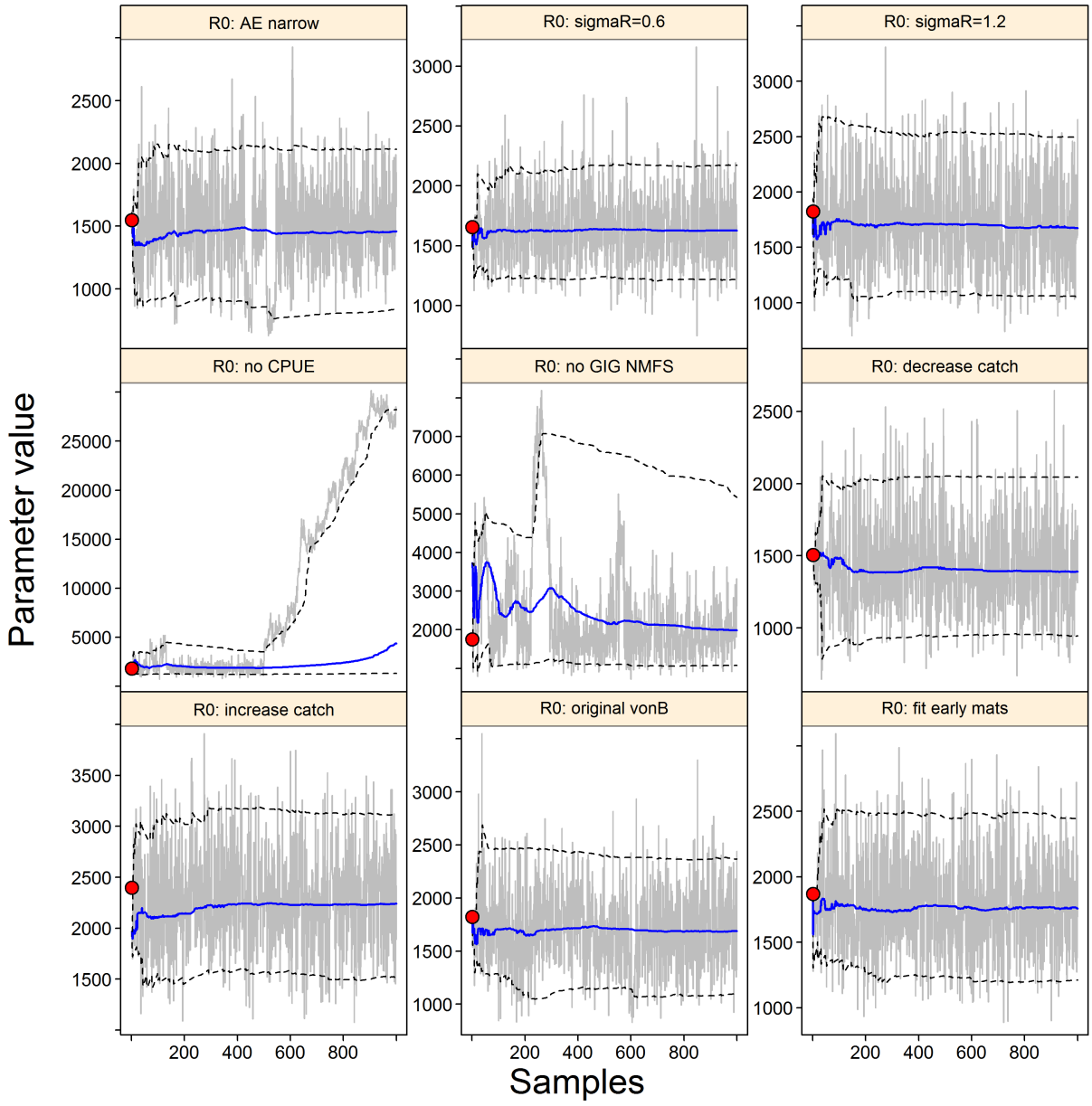

Figure F.40. Sensitivity R_0: MCMC traces for the estimated parameters. Grey lines show the 1000 samples for each parameter, solid blue lines show the cumulative median (up to that sample), and dashed lines show the cumulative 0.05 and 0.95 quantiles. Red circles are the MPD estimates.

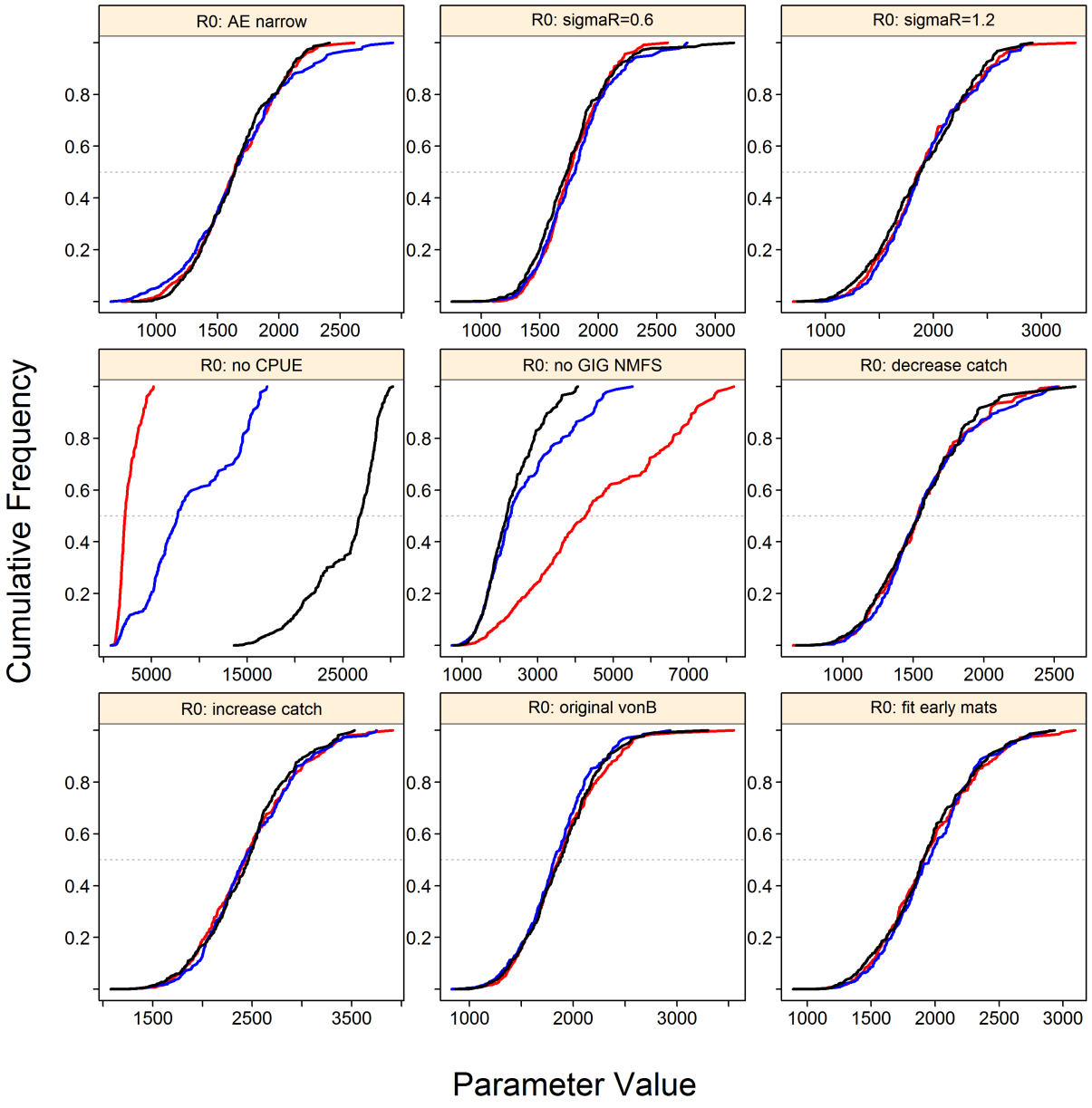

Figure F.41. Sensitivity R_0: diagnostic plot obtained by dividing the MCMC chain of 1000 MCMC samples into three segments, and overplotting the cumulative distributions of the first segment (red), second segment (blue) and final segment (black).

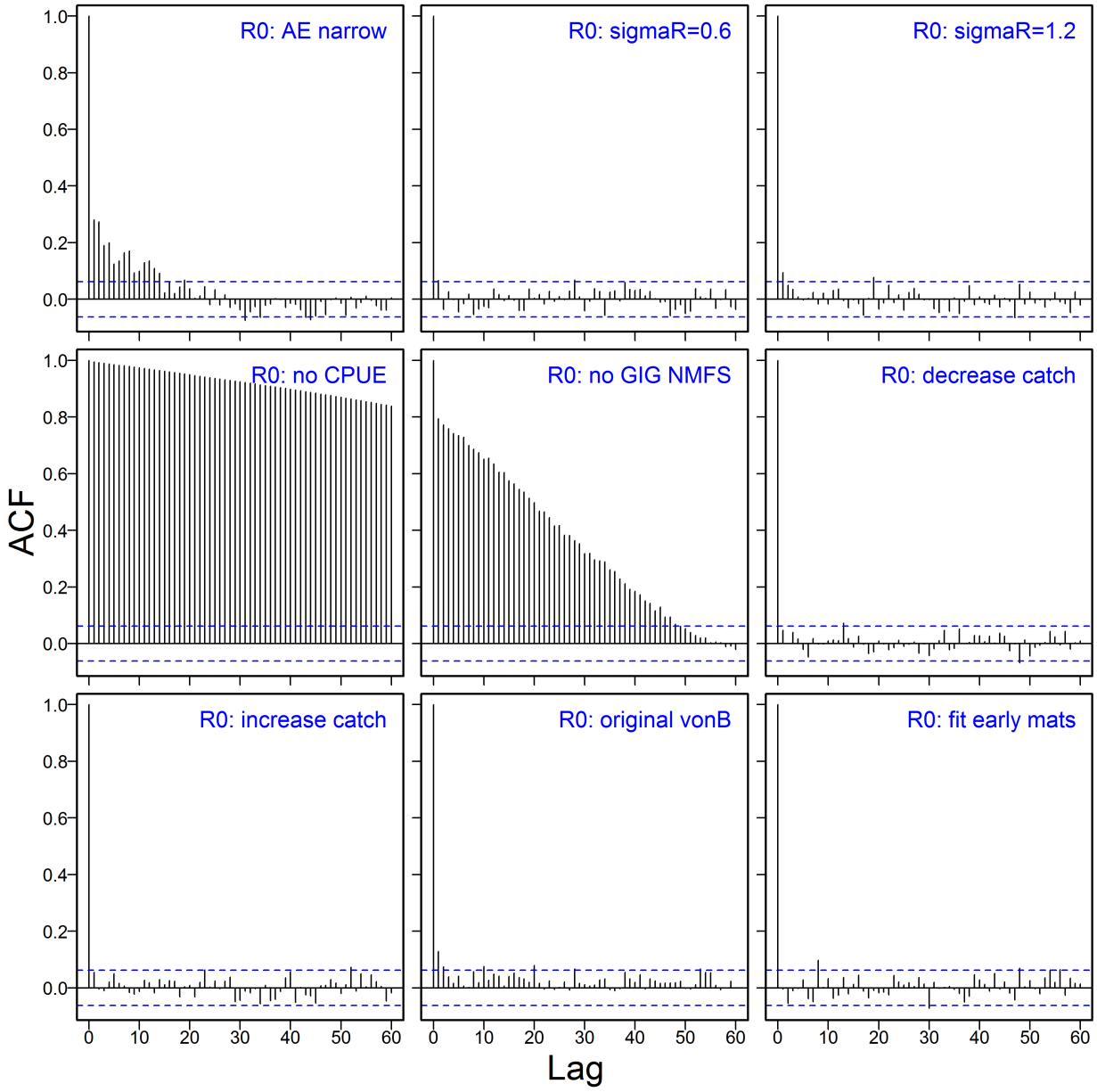

Figure F.42. Sensitivity R_0: autocorrelation plots for the estimated parameters from the MCMC output. Horizontal dashed blue lines delimit the 95% confidence interval for each parameter's set of lagged correlations.

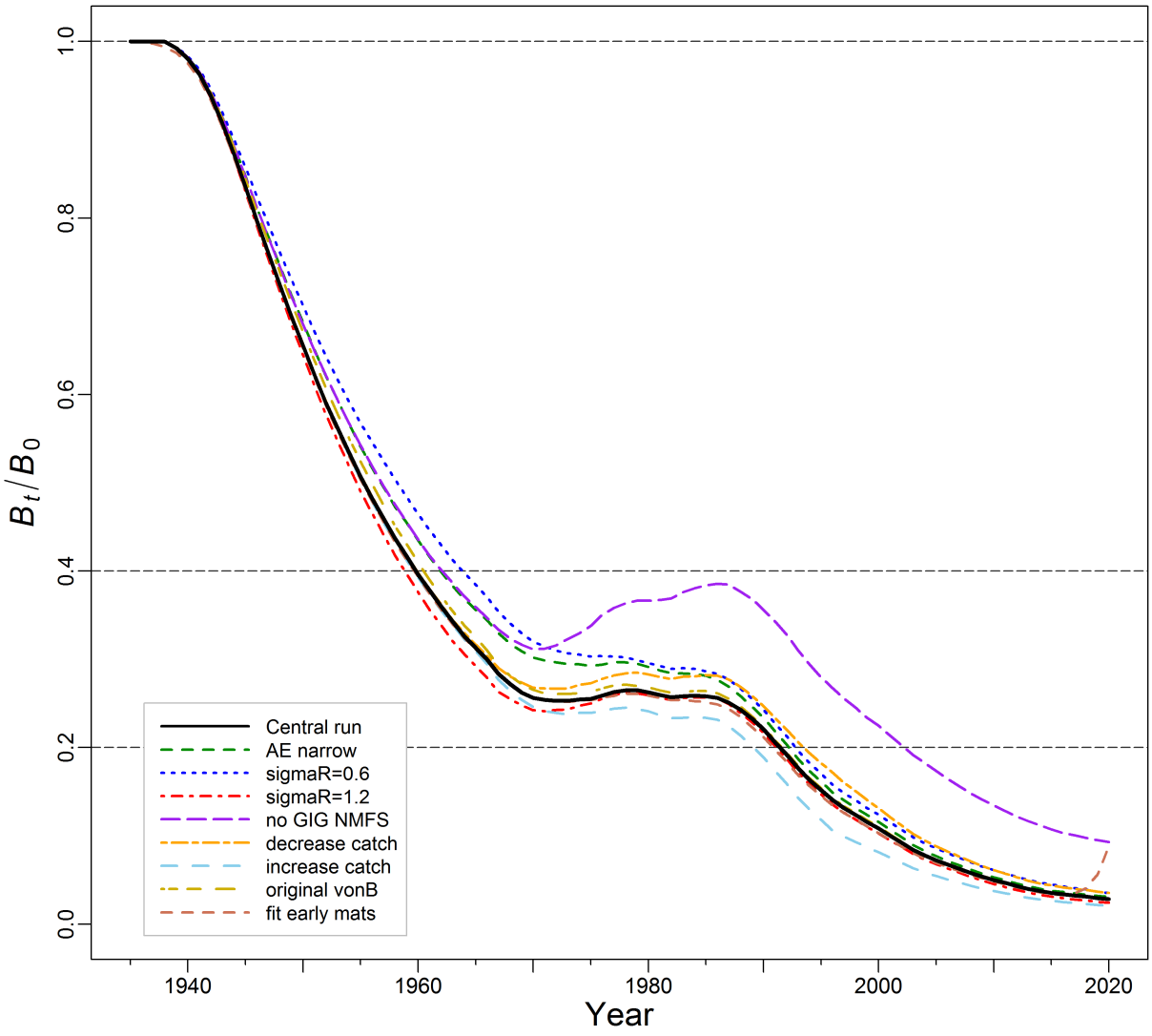

Figure F.43. Sensitivity: model trajectories of median spawning biomass as a proportion of unfished equilibrium biomass (B_t/B_0) for the central run of the composite base case and 8 sensitivity runs (see legend lower left). Horizontal dashed lines show alternative reference points used by other jurisdictions: 0.2B_0 (~DFO's USR), 0.4B_0 (often a target level above B_{MSY}), and B_0 (equilibrium spawning biomass).

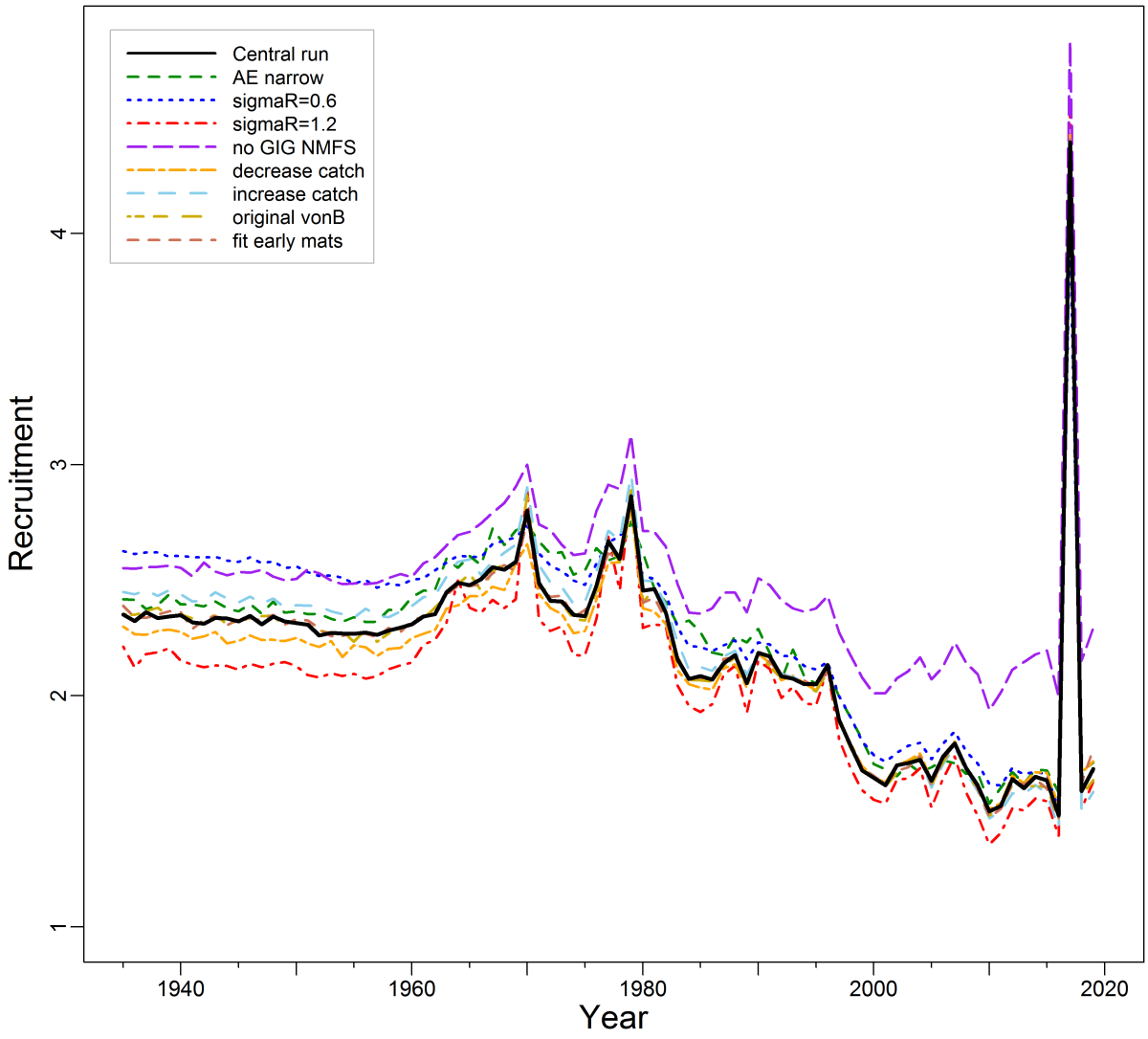

Figure F.44. Sensitivity: model trajectories of $\log_{10}$ median recruitment of one-year old fish (R_t, 1000s) for the central run of the composite base case and 8 sensitivity runs (see legend upper right).

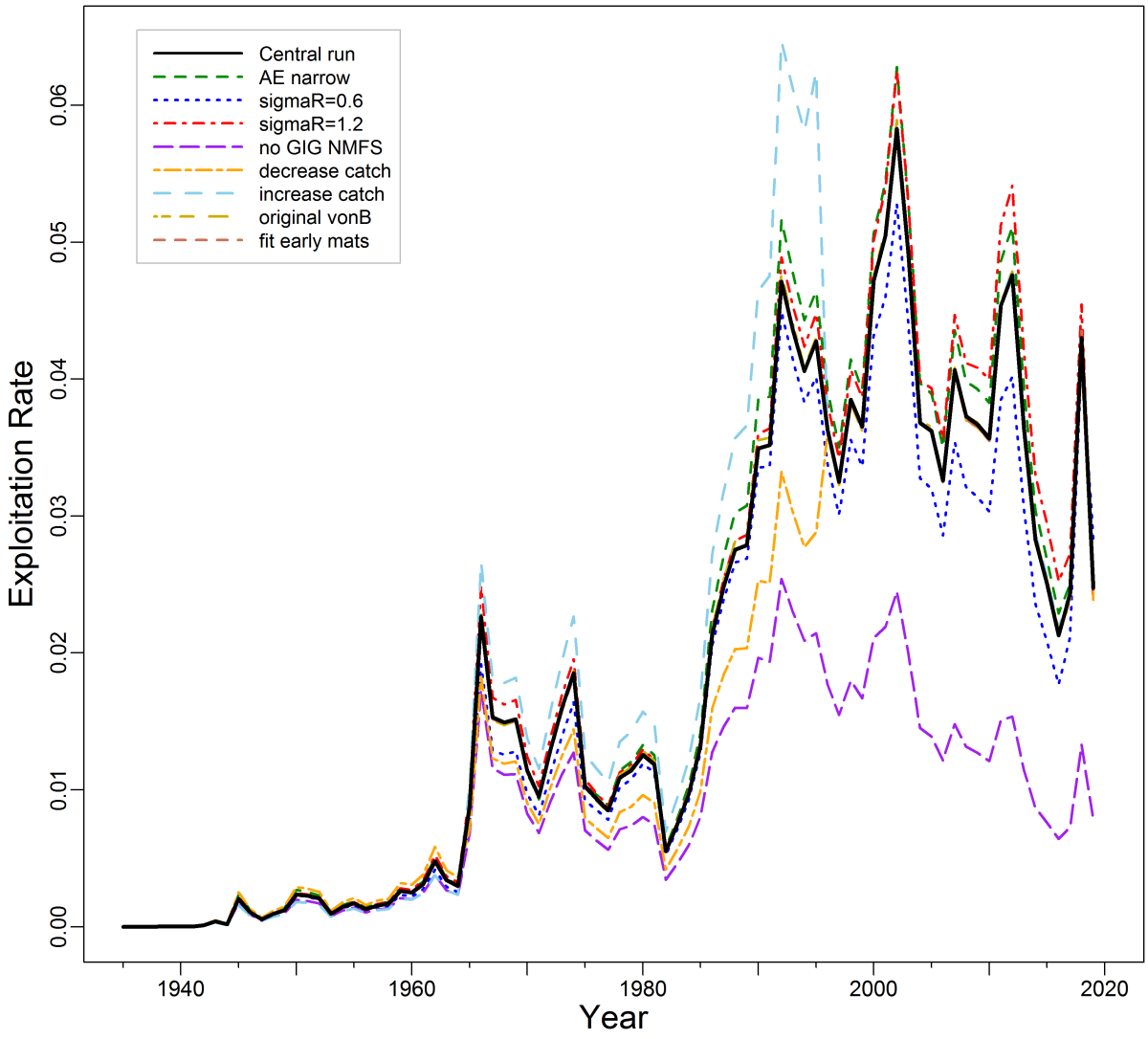

Figure F.45. Sensitivity: model trajectories of median exploitation rate of vulnerable biomass (u_t) for the central run of the composite base case and 8 sensitivity runs (see legend upper left).

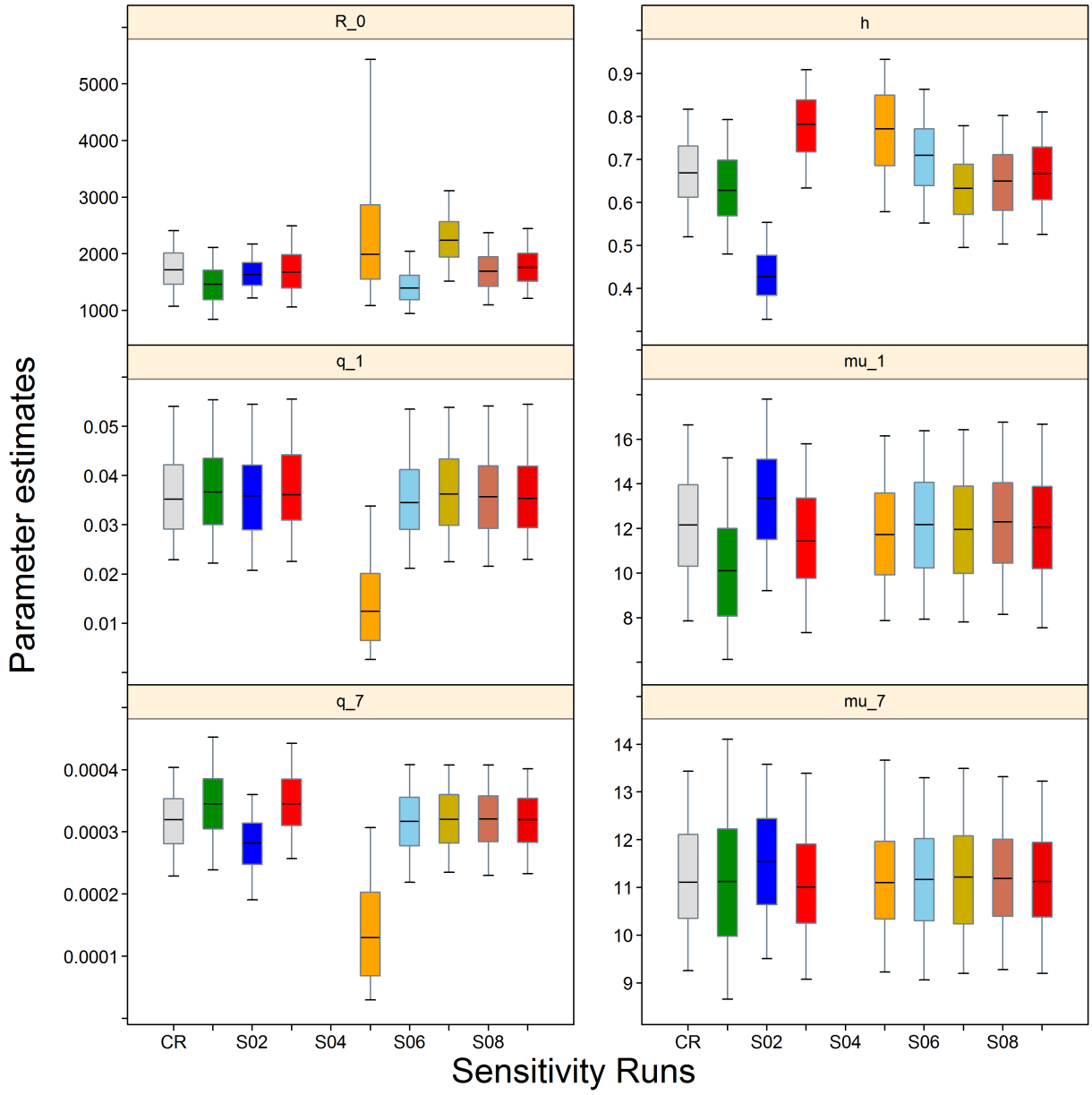

Figure F.46. Sensitivity: quantile plots of selected parameter estimates (R_0, h, q_g, μ_g) comparing the central run with 8 sensitivity runs. Subscripts: g=2 corresponds to the QCS synoptic survey, g=6 corresponds to the commercial trawl fishery. See text on sensitivity numbers. The boxplots delimit the 0.05, 0.25, 0.5, 0.75, and 0.95 quantiles; outliers are excluded.

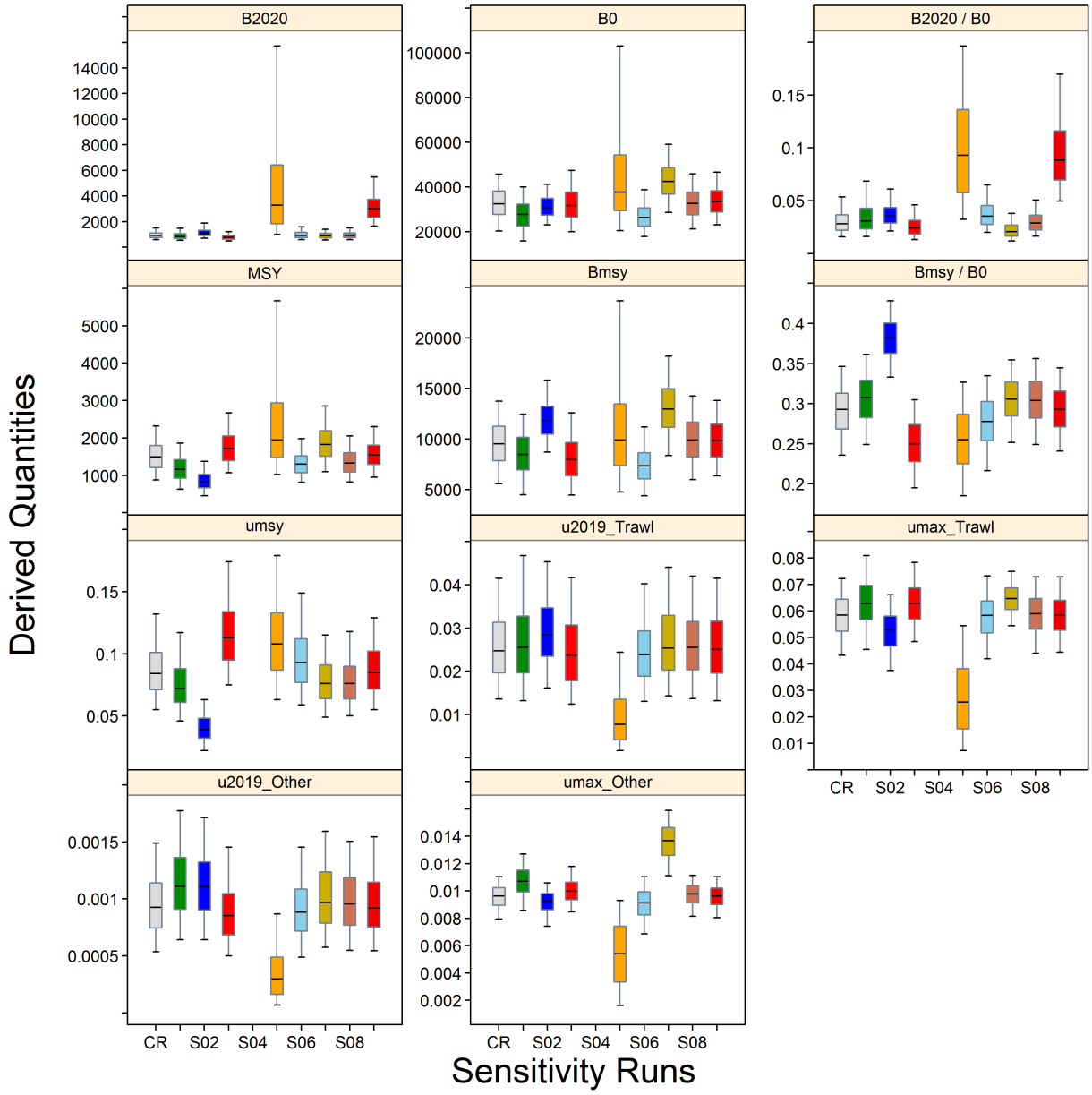

Figure F.47. Sensitivity: quantile plots of selected derived quantities (B_{2020}, B_0, B_{2020}/B_0, MSY, B_{MSY}, B_{MSY}/B_0, u_{2019}, u_{MSY}, $u_{\max}$) comparing the central run with 8 sensitivity runs. See text on sensitivity numbers. The boxplots delimit the 0.05, 0.25, 0.5, 0.75, and 0.95 quantiles; outliers are excluded.

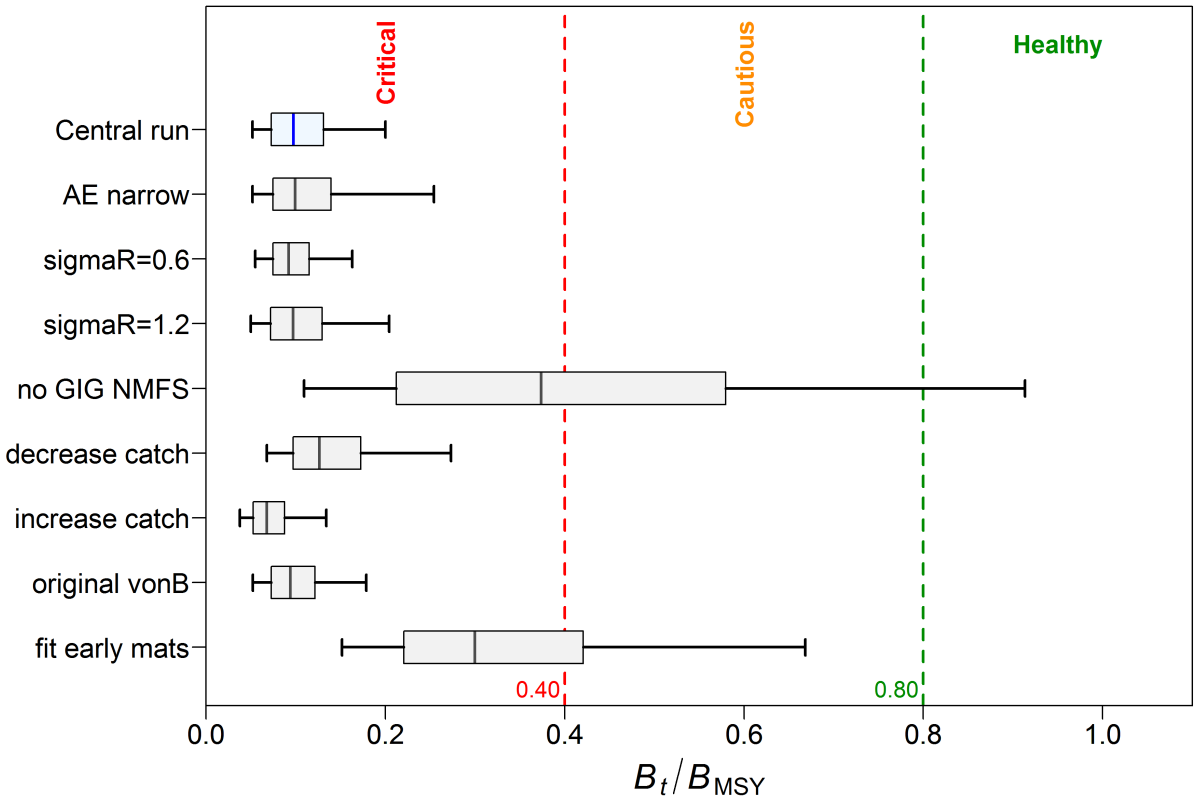

Figure F.48. Sensitivity: status at beginning of 2020 of the Bocaccio (2F) stock relative to the DFO PA provisional reference points of $0.4B_{\mathrm{MSY}}$ and $0.8B_{\mathrm{MSY}}$ for the central run of the composite base case (Run02) and 8 sensitivity runs: S1 = (Run05) use a narrow ageing error matrix; S2 = (Run07) decrease σ_R from 0.9 to 0.6; S3 = (Run08) increase σ_R from 0.9 to 1.2; S5 = (Run10) remove the NMFS Triennial and GIG Historical index series; S6 = (Run11) reduce commercial catch by one third in years 1965-95; S7 = (Run12) increase commercial catch by 50% in years 1965-95; S8 = (Run13) use growth parameters from original von Bertalanffy fits; S9 = (Run14) include maturity fits to early ages (1-4y). Boxplots show the 0.05, 0.25, 0.5, 0.75, and 0.95 quantiles from the MCMC posterior.

F.2.3. PROJECTION SENSITIVITY

Uncertainty in the strength of the 2016 cohort was explored through a projection sensitivity run which used only the lowest 5th percentile of the 2016 recruitment posterior distribution (Figure F.49) to estimate future stock status (Figure F.50). These projections extended the time required to rebuild biomass above the LRP and the USR by only two years (Tables F.63 and F.64).

While occasional large recruitment events can be considered to be typical among species of *Sebastes*, such events tend to occur every 10 to 25 years in other species of this genus that have been assessed. Bocaccio appears to be an outlier species, with only one large cohort observed in over 60 years of potential data. While the existence of the large 2016 cohort is welcome information that is predicted to lead to recovery, it is noted that the southern California population of Bocaccio has had several good recent recruitments that have led to recovery in that population.

Table F.63. Decision table for 150 low-recruitment subsamples concerning the limit reference point $0.4B_{\mathrm{MSY}}$ for 1-10-year projections for a range of **constant catch** *strategies (in tonnes). Values are P$(B_t > 0.4B_{\mathrm{MSY}})$, i.e. the probability of the spawning biomass (mature females) at the start of year t being greater than the limit reference point. The probabilities are the proportion (to two decimal places) of the 150 MCMC samples for which $B_t > 0.4B_{\mathrm{MSY}}$. For reference, the average catch over the last 5 years (2015-2019) was 69 t.*

CC	2020	2021	2022	2023	2024	2025	2026	2027	2028	2029	2030
0	0	0.25	0.71	0.90	0.96	0.98	0.99	0.99	0.99	0.99	0.99
50	0	0.25	0.71	0.90	0.96	0.98	0.99	0.99	0.99	0.99	0.99
100	0	0.25	0.69	0.89	0.96	0.98	0.99	0.99	0.99	0.99	0.99
150	0	0.24	0.68	0.88	0.95	0.98	0.99	0.99	0.99	0.99	0.99
200	0	0.24	0.67	0.88	0.94	0.97	0.98	0.99	0.99	0.99	0.99
250	0	0.23	0.66	0.87	0.94	0.97	0.98	0.98	0.98	0.98	0.99
300	0	0.22	0.65	0.86	0.93	0.96	0.98	0.98	0.98	0.98	0.98
350	0	0.21	0.63	0.85	0.93	0.96	0.97	0.98	0.98	0.97	0.97
400	0	0.21	0.61	0.85	0.93	0.95	0.97	0.97	0.97	0.95	0.95
450	0	0.21	0.61	0.83	0.92	0.94	0.96	0.96	0.95	0.95	0.95
500	0	0.19	0.59	0.83	0.92	0.94	0.95	0.95	0.95	0.95	0.95
550	0	0.19	0.59	0.81	0.91	0.94	0.94	0.95	0.95	0.94	0.93
600	0	0.18	0.57	0.81	0.91	0.93	0.94	0.94	0.94	0.93	0.93

Table F.64. Decision table for 150 low-recruitment subsamples concerning the upper stock reference point $0.8B_{\mathrm{MSY}}$ for 1-10-year projections for a range of **constant catch** *strategies (in tonnes), such that values are P$(B_t > 0.8B_{\mathrm{MSY}})$. For reference, the average catch over the last 5 years (2015-2019) was 69 t.*

CC	2020	2021	2022	2023	2024	2025	2026	2027	2028	2029	2030
0	0	0	0.05	0.33	0.67	0.81	0.88	0.89	0.90	0.91	0.92
50	0	0	0.05	0.31	0.65	0.80	0.87	0.89	0.89	0.89	0.90
100	0	0	0.04	0.31	0.64	0.79	0.85	0.88	0.88	0.89	0.90
150	0	0	0.03	0.29	0.61	0.77	0.85	0.86	0.87	0.88	0.89
200	0	0	0.03	0.29	0.61	0.75	0.83	0.85	0.85	0.87	0.88
250	0	0	0.03	0.27	0.60	0.73	0.80	0.85	0.85	0.85	0.86
300	0	0	0.03	0.25	0.58	0.73	0.79	0.81	0.84	0.85	0.85
350	0	0	0.03	0.23	0.56	0.70	0.78	0.79	0.80	0.82	0.82
400	0	0	0.03	0.23	0.53	0.69	0.76	0.77	0.77	0.79	0.79
450	0	0	0.03	0.23	0.50	0.65	0.75	0.77	0.76	0.77	0.77
500	0	0	0.03	0.22	0.47	0.64	0.73	0.75	0.74	0.73	0.75
550	0	0	0.03	0.21	0.44	0.61	0.69	0.72	0.70	0.69	0.69
600	0	0	0.03	0.17	0.41	0.61	0.66	0.68	0.67	0.67	0.66

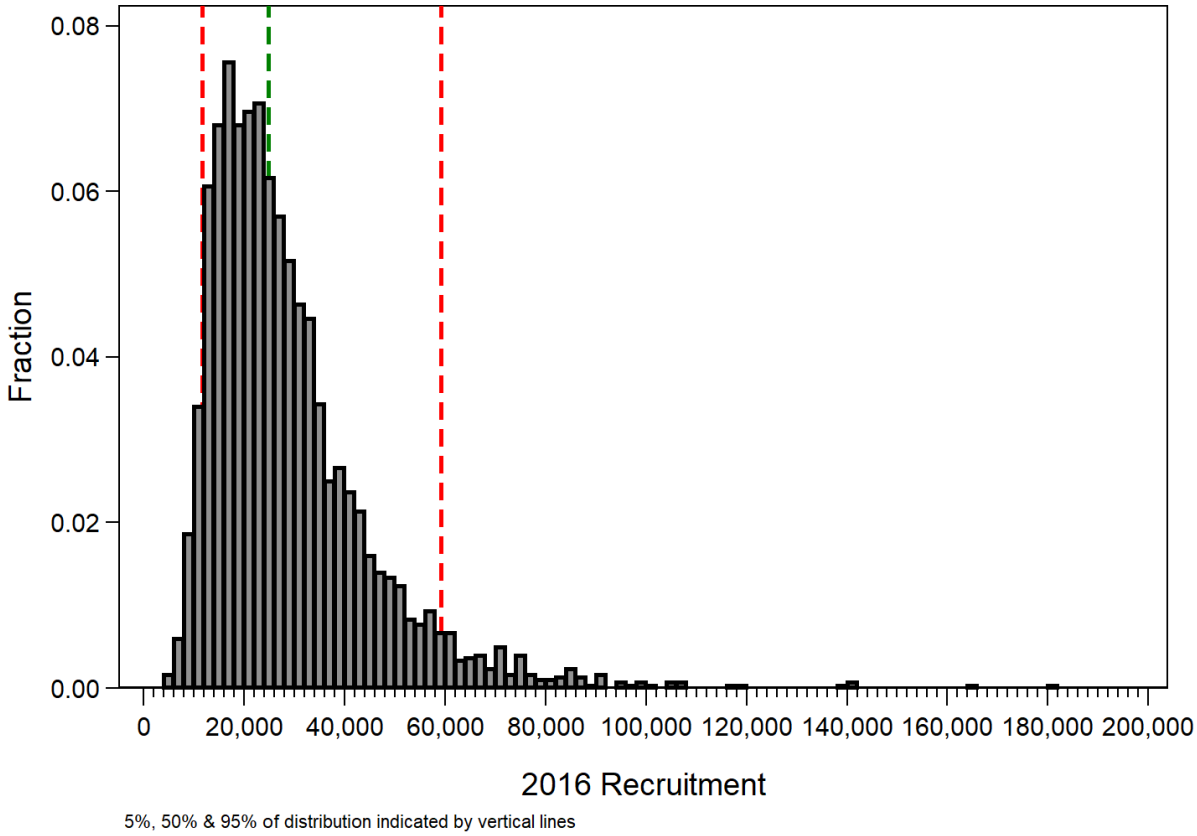

Figure F.49. Projection sensitivity: frequency distribution of 3000 MCMC samples of the estimated 2016 cohort, represented as R_{2017}, showing the 0.05, 0.5, and 0.95 quantile limits. Samples lower than the 0.05 quantile limit were used to rebuild the population trajectory and projections in Figure F.50 and to reconstruct the decision tables (Tables F.63 and F.64).

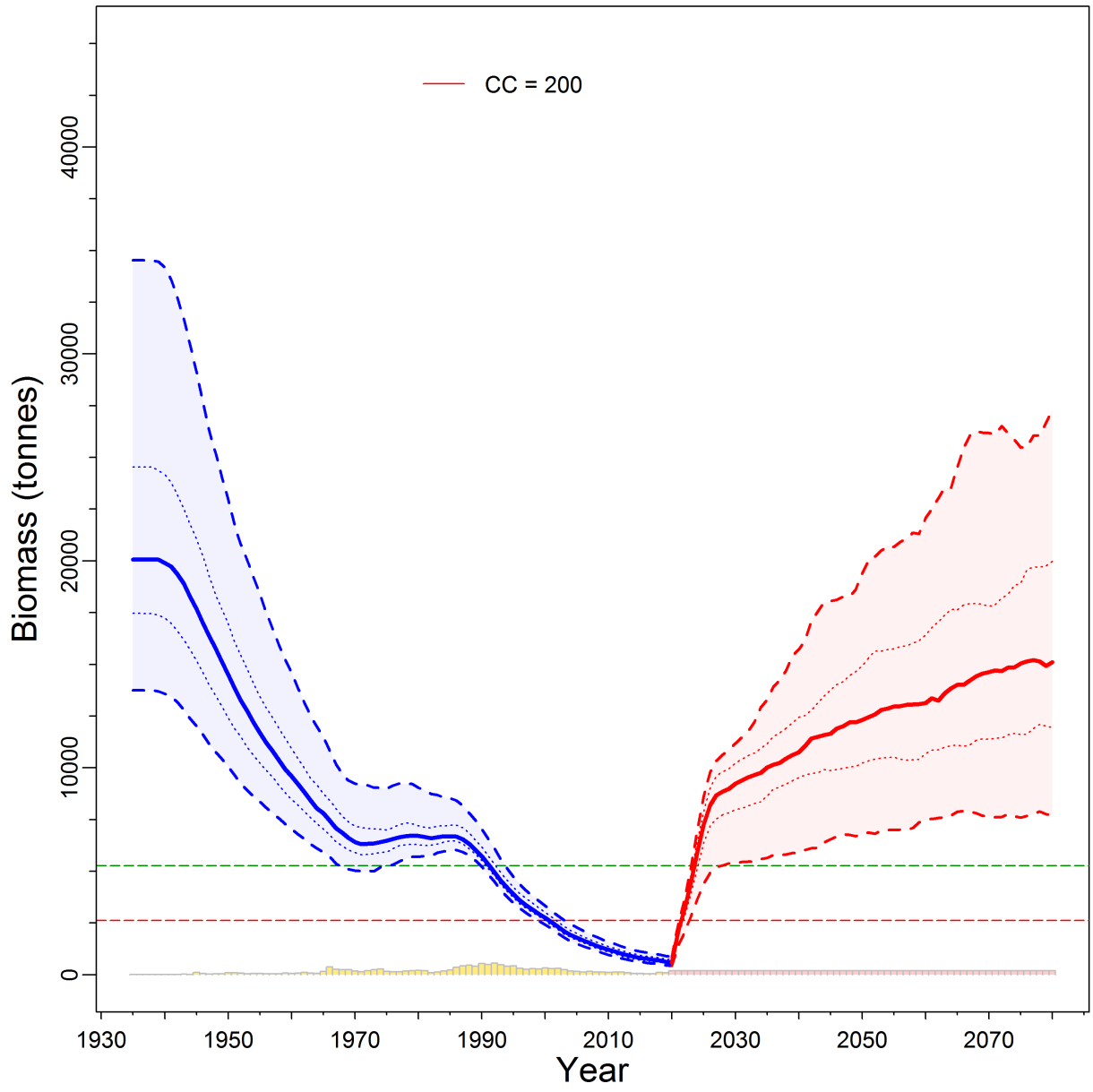

Figure F.50. Projection sensitivity: estimates of spawning biomass B_t (tonnes) using 150 low-recruitment subsamples from the pooled model posteriors. The median biomass trajectory appears as a solid curve surrounded by a 90% credibility envelope (quantiles: 0.05-0.95) in light blue and delimited by dashed lines for years t=1935:2020; projected biomass appears in light red for years t=2021:2080. Also delimited is the 50% credibility interval (quantiles: 0.25-0.75) delimited by dotted lines. The horizontal dashed lines show the median LRP and USR. Catches are represented as bars along the bottom axis and assumed catch policies appear in the legend, where CC = t/y.

F.3. REFERENCES – MODEL RESULTS

Forrest, R.E., Holt, K.R. and Kronlund, A.R. 2018. Performance of alternative harvest control rules for two Pacific groundfish stocks with uncertain natural mortality: bias, robustness and trade-offs. Fish. Res. 206. 259–286.

Francis, R.I.C.C. 2011. Data weighting in statistical fisheries stock assessment models. Can. J. Fish. Aquat. Sci. 68(6). 1124–1138.

Hilborn, R. and Walters, C.J. 1992. Quantitative Fisheries Stock Assessment: Choice, Dynamics and Uncertainty. Chapman and Hall, New York NY.

N.Z. Min. Fish. 2011. Operational Guidelines for New Zealand's Harvest Strategy Standard. Ministry of Fisheries, New Zealand.

APPENDIX G. ECOSYSTEM INFORMATION

Preface: This appendix describes ecosystem information relevant to Bocaccio (BOR) along the British Columbia (BC) coast. This information is not used for the purposes of stock assessment but provides information that might be useful to other agencies and the interpretation of BOR spatial and biological information.

G.1. SPATIAL DISTRIBUTION

Data for spatial analyses of BOR were extracted from the SQL DFO databases 'PacHarvest' and 'GFFOS' on Oct 22, 2019. Some of the analyses below are designed to facilitate the reporting of findings to COSEWIC (Committee on the Status of Endangered Wildlife in Canada), regardless of its assessed status.

Bocaccio is ubiquitous along the BC coast. Broadly, its 'extent of occurrence' (EO) covers 118,967 km^2 (on water and excluding seamounts data) using historical fishing events (1982-2019) to determine a convex hull envelope (Figure G.1). Of the bottom trawl tows capturing BOR, 99% of the tows have starting depths between 62 m and 379 m (Figure G.2). Using the bottom-tow depth range as a proxy for suitable BOR benthic habitat, a refined estimate of EO is 70,075 km^2 in BC's Exclusive Economic Zone (Figure G.3). To estimate the 'area of occupancy' (AO), the catch of BOR was located within a grid comprising 4 km^2 cells (2km × 2km), and the cells occupied by BOR were summed to estimate an AO of 15,416 km^2 along the BC coast spanning 1996 to 2019 (Figure G.4). Figure G.5 and Figure G.6 provide alternative visualisations of relative abundance by fishing locality.

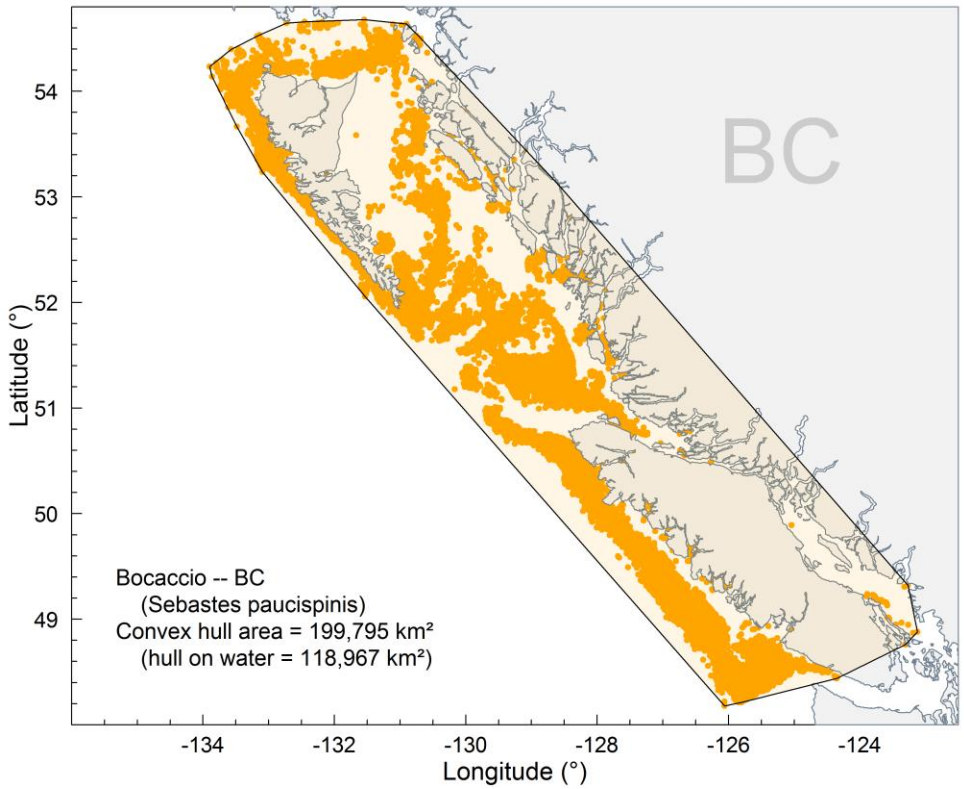

Figure G.1. Extent of Occurrence as a convex hull surrounding fishing events that caught BOR along the BC coast; the shading within the hull on water covers 118,967 km^2.

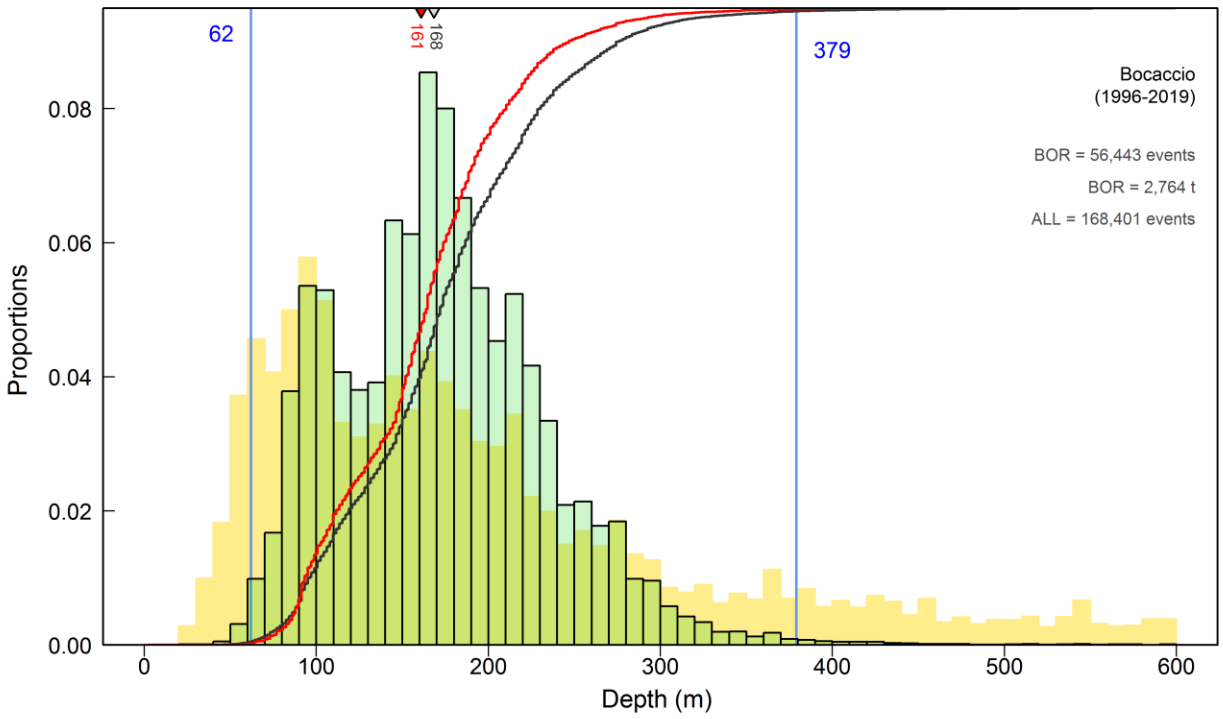

Figure G.2. BC Offshore – Depth frequency of bottom trawl tows (green histogram) that captured BOR from commercial logs (1996-2019 in PacHarvest and GFFOS) in areas outside the Strait of Georgia. The vertical solid lines denote the 0.005 and 0.995 quantiles. The black curve shows the cumulative frequency of tows that encounter BOR while the red curve shows the cumulative catch of BOR at depth (scaled from 0 to 1). The median depths of BOR encounters (inverted grey triangle) and of cumulative catch (inverted red triangle) are indicated along the upper axis. The yellow histogram in the background reports the relative trawl effort on all species offshore down to 600 m.

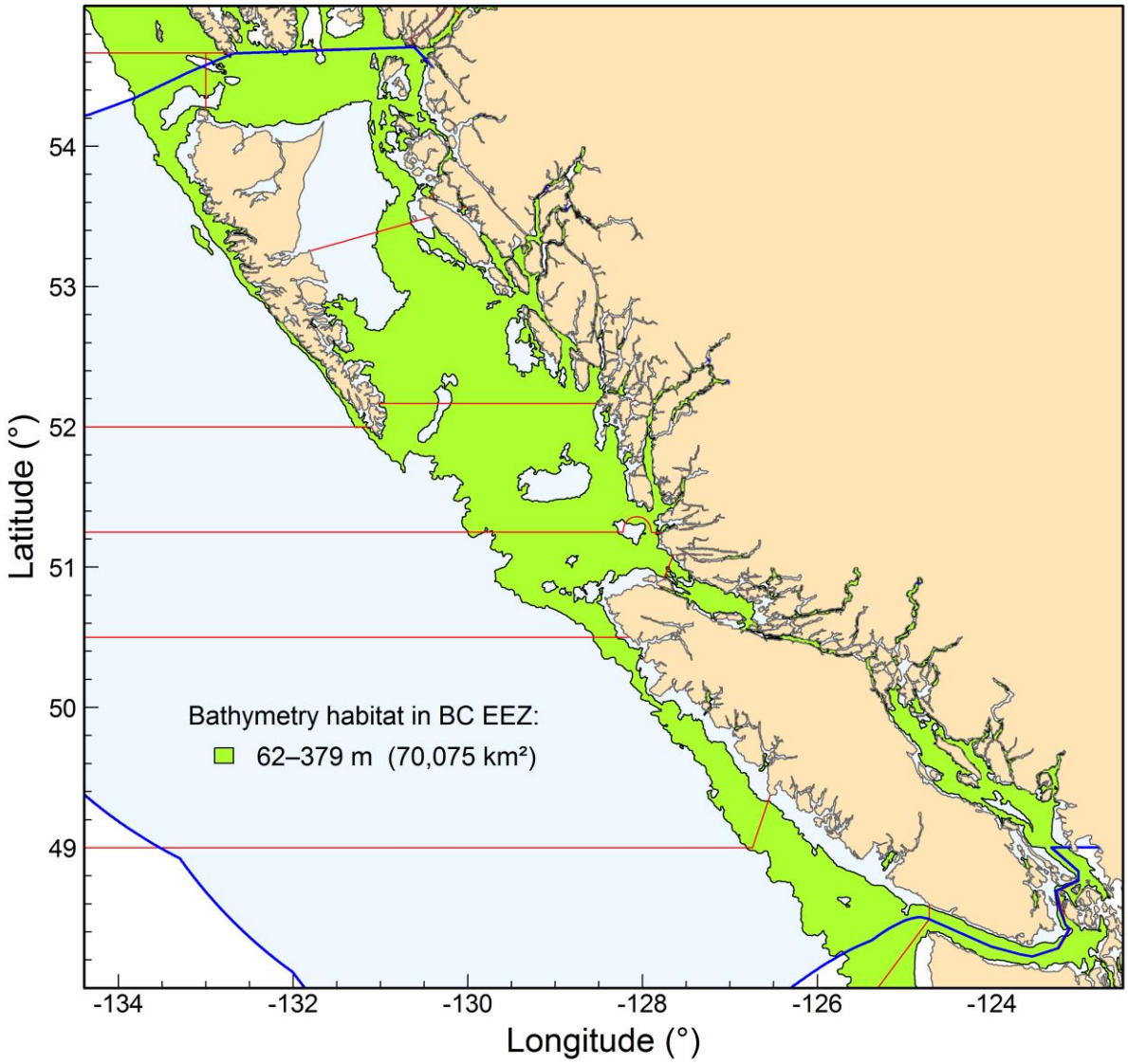

Figure G.3. Highlighted bathymetry (green) between 62 and 379 m serves as a proxy for benthic habitat for BOR along the BC coast. The green highlighted region within Canada's exclusive economic zone (EEZ, blue highlighted area) covers 70,075 km². The boundaries in red delimit PMFC areas.

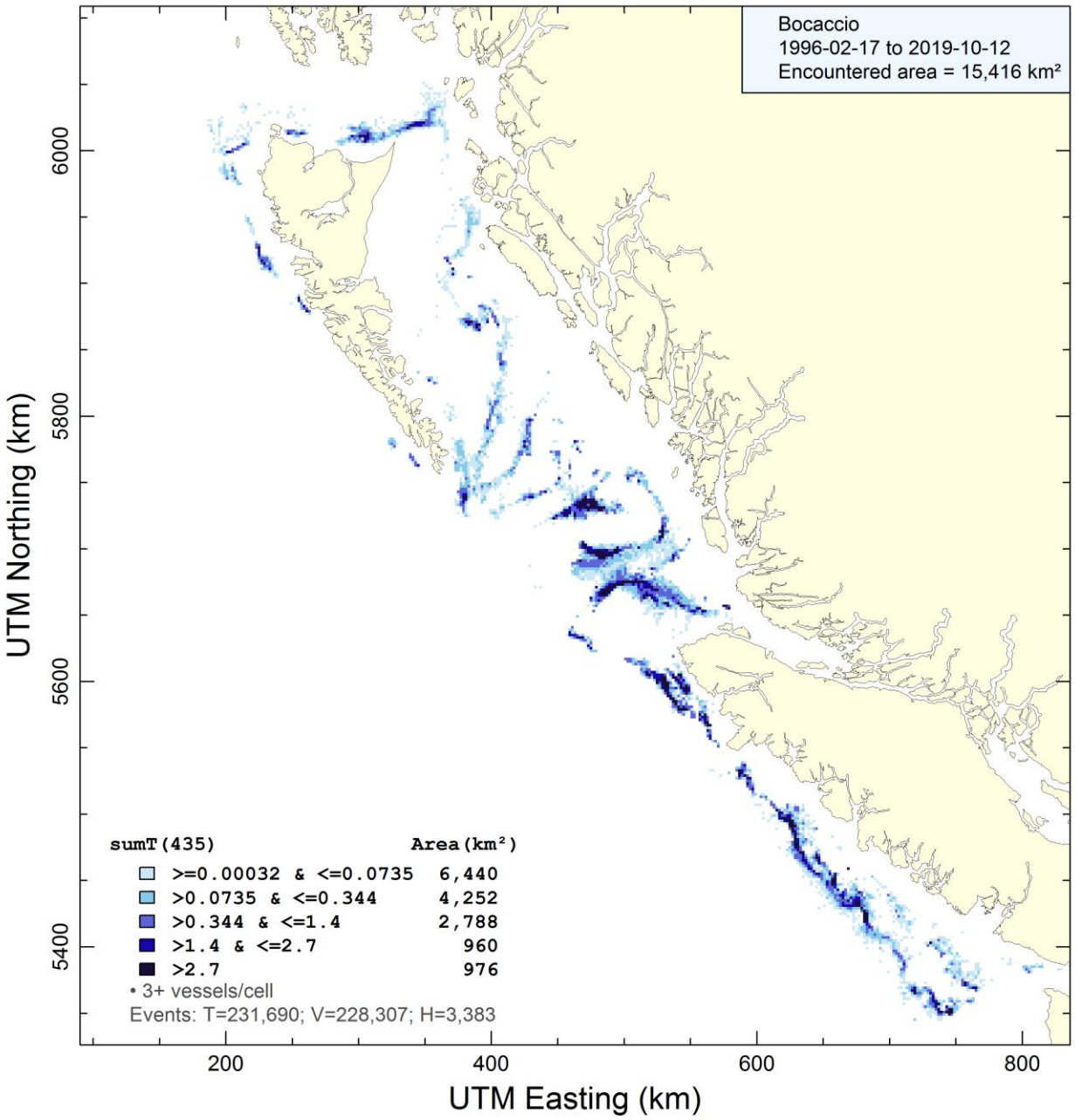

Figure G.4. Area of Occupancy (AO) determined by bottom trawl capture of BOR in grid cells 2km × 2km. Cells with fewer than three fishing vessels are excluded. The estimated AO is 15,416 km² along the BC coast.

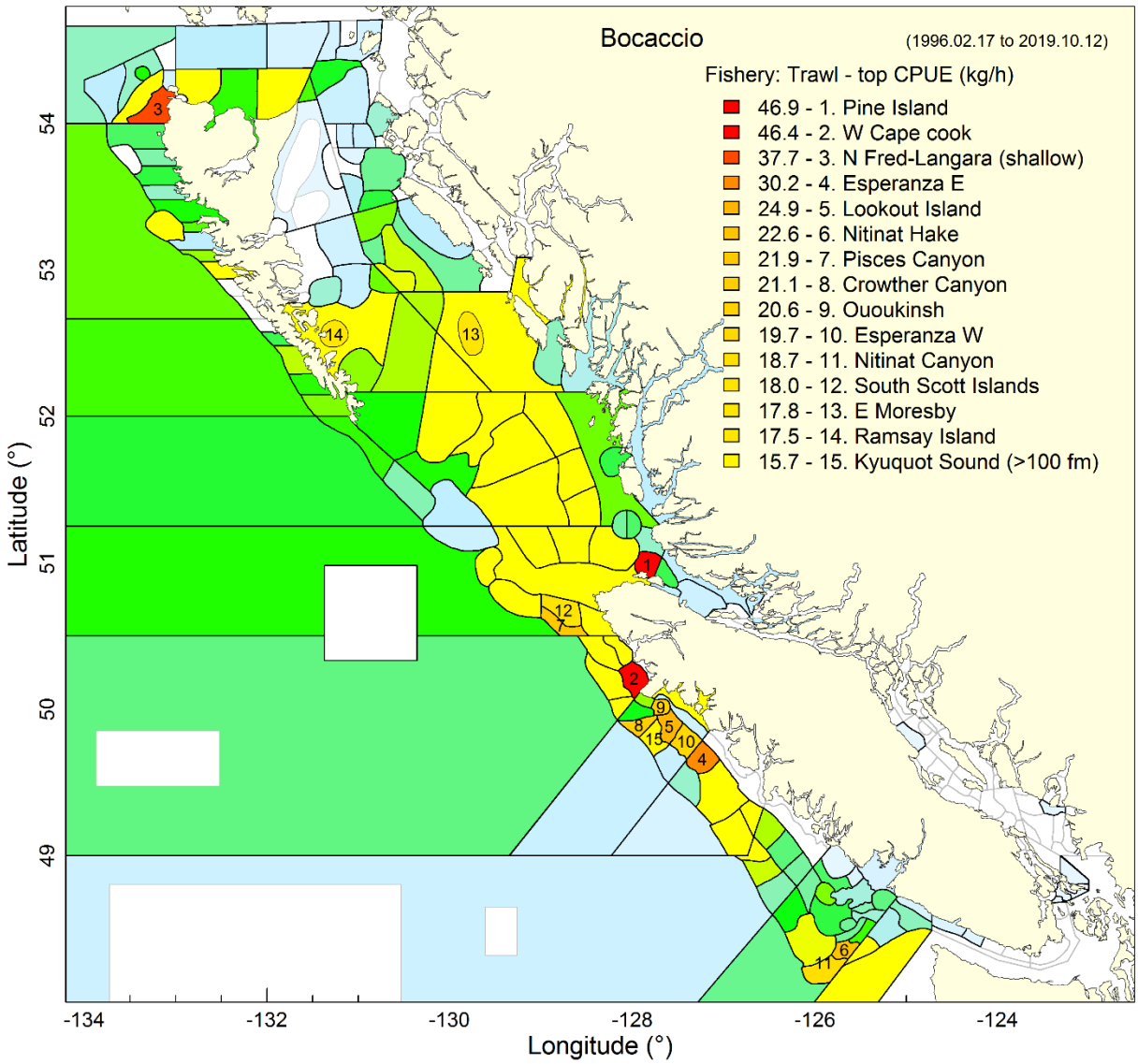

Figure G.5. Top 15 fishing localities by mean CPUE (kg/h) where BOR was caught by the trawl fleet. All shaded localities indicate areas where BOR was encountered from 1996 to 2019, ranging from relatively low numbers in cool blue, through the spectrum, to relatively high catch rates in red.

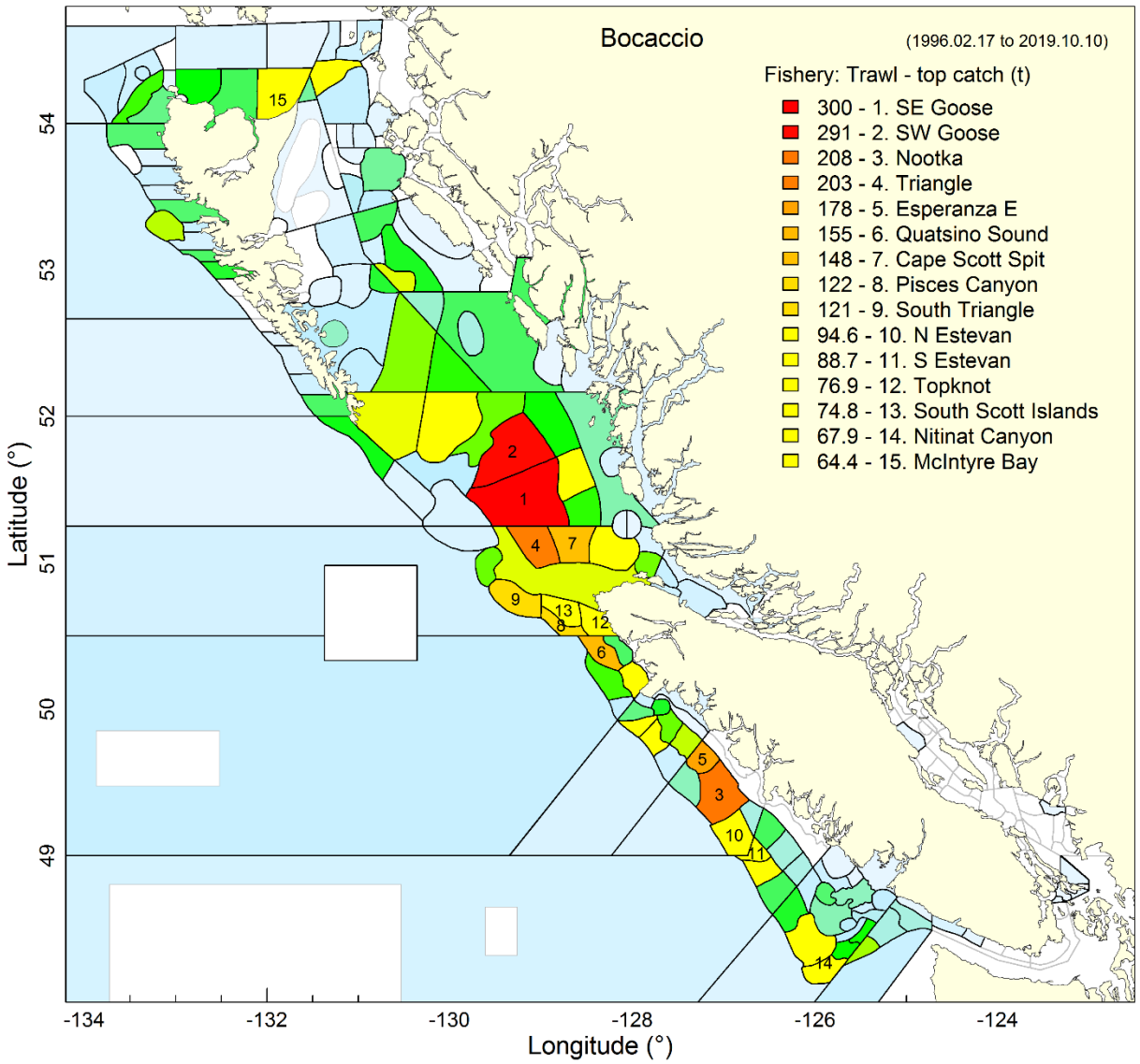

Figure G.6. Top 15 fishing localities by total catch (tonnes) where BOR was caught by the trawl fleet. All shaded localities indicate areas where BOR was encountered from 1996 to 2019, ranging from relatively low numbers in cool blue, through the spectrum, to relatively high catches in red.

G.2. CONCURRENT SPECIES

Species caught concurrently in coastwide bottom trawl tows that capture at least one BOR specimen are dominated by species other than BOR, which only accounts for <1% of total catch by weight and does not make it into the top 25 species (Table G.17, Figure G.7). The six predominant species comprise Arrowtooth Flounder (21%), Pacific Ocean Perch (17%), Yellowtail Rockfish (8%), Dover Sole (5%), Yellowmouth Rockfish (5%), and Silvergray Rockfish (5%). Choosing the rockfish that occur in Table G.17, Figure G.8 presents a cluster analysis on commercial catch data to show how Bocaccio is associated with these rockfish species. Generally, BOR co-occurs with shelf species in the first four groups, and has the strongest association with Redstripe and Redbanded Rockfish in group 1.

*Table G.17. BC Offshore – Top 25 species by catch weight (sum of landed + discarded from 1996 to 2019) that co-occur in BOR **bottom** trawl tows along the BC coast (Figure G.7). Rockfish species of interest to COSEWIC appear in red font, target species (which occurs in every tow) appears in blue font.*

Code	Species	Latin Name	Catch (t)	Catch (%)
602	Arrowtooth Flounder	*Atheresthes stomias*	135,717	20.87
396	Pacific Ocean Perch	*Sebastes alutus*	110,882	17.05
418	Yellowtail Rockfish	*Sebastes flavidus*	51,636	7.94
626	Dover Sole	*Microstomus pacificus*	31,203	4.80
440	Yellowmouth Rockfish	*Sebastes reedi*	30,853	4.74
405	Silvergray Rockfish	*Sebastes brevispinis*	30,565	4.70
467	Lingcod	*Ophiodon elongatus*	28,770	4.42
222	Pacific Cod	*Gadus macrocephalus*	23,368	3.59
44	Spiny Dogfish	*Squalus acanthias*	19,414	2.99
628	English Sole	*Parophrys vetulus*	16,350	2.51
439	Redstripe Rockfish	*Sebastes proriger*	16,225	2.49
437	Canary Rockfish	*Sebastes pinniger*	15,933	2.45
56	Big Skate	*Raja binoculata*	15,833	2.43
66	Spotted Ratfish	*Hydrolagus colliei*	12,311	1.89
610	Rex Sole	*Errex zachirus*	11,711	1.80
621	Rock Sole	*Lepidopsetta bilineatus*	11,496	1.77
607	Petrale Sole	*Eopsetta jordani*	11,051	1.70
614	Pacific Halibut	*Hippoglossus stenolepis*	9,294	1.43
394	Rougheye Rockfish	*Sebastes aleutianus*	7,882	1.21
450	Sharpchin Rockfish	*Sebastes zacentrus*	7,500	1.15
225	Pacific Hake	*Merluccius productus*	6,427	0.99
455	Sablefish	*Anoplopoma fimbria*	6,066	0.93
417	Widow Rockfish	*Sebastes entomelas*	5,733	0.88
228	Walleye Pollock	*Theragra chalcogramma*	4,978	0.77
401	Redbanded Rockfish	*Sebastes babcocki*	4,840	0.74

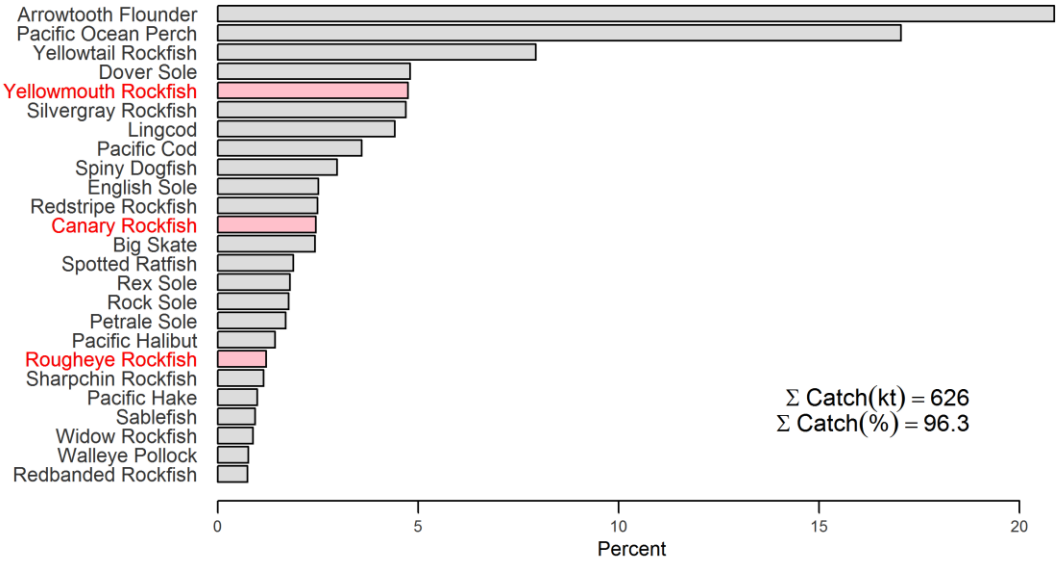

*Figure G.7. BC Offshore – Distribution of catch weights summed over the period February 1996 to October 2019 for important finfish species in **bottom** trawl tows that caught at least one BOR coastwide. Tows were selected over a depth range between 62 and 379 m (the 0.005 and 0.995 quantile range, see Figure G.2). Relative concurrence is expressed as a percentage by species relative to the total catch weight summed over all finfish species in the specified period. Bocaccio does not make it into the top 25 species; other species of interest to COSEWIC are indicated in red.*

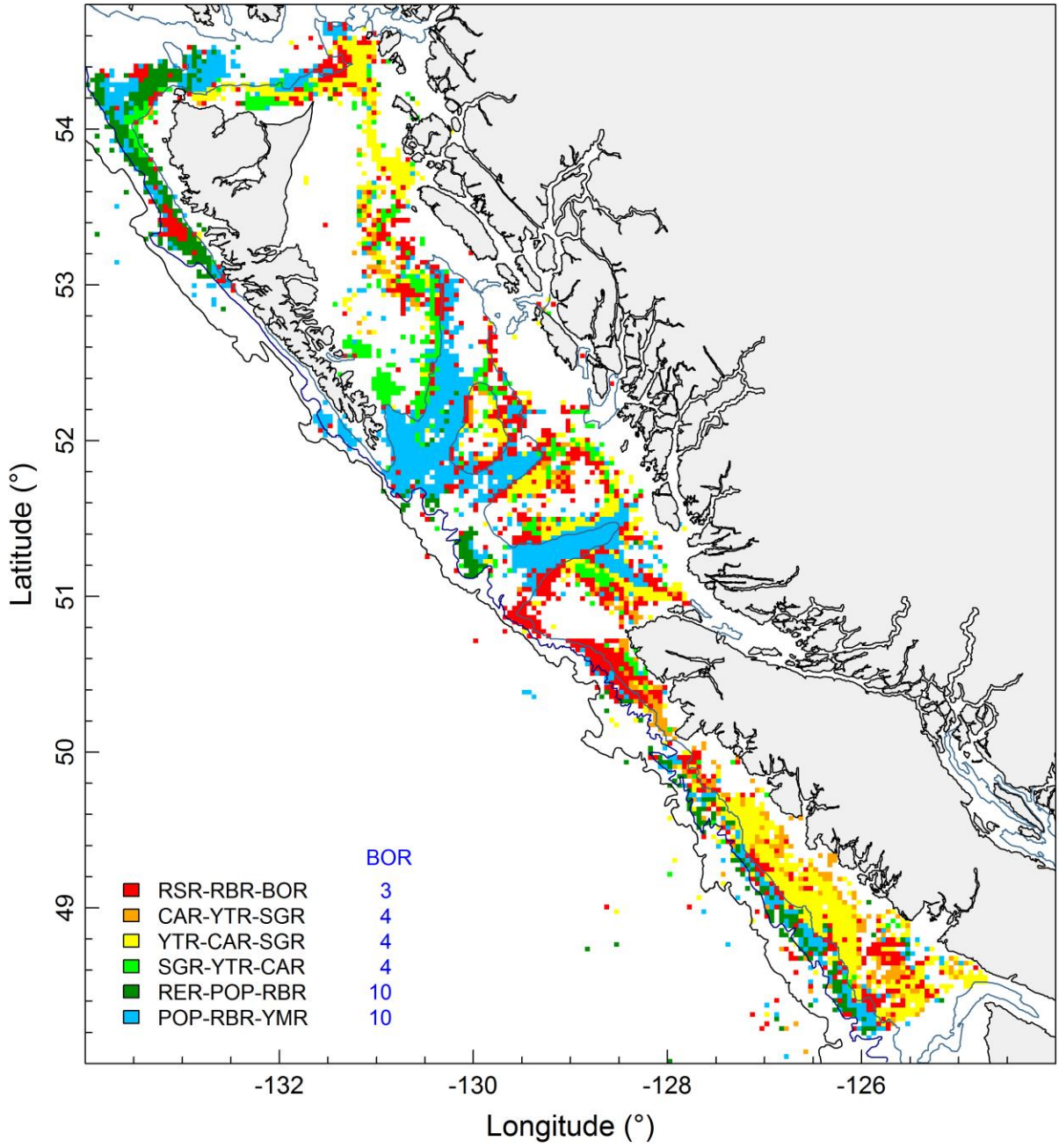

Figure G.8. Groups of rockfish in bottom trawl tows (1996-2019) identified by clara (clustering large applications) in R's package cluster (Maechler et al. 2018). Isobaths trace the 200, 1000, and 1800 m depth contours. The legend identifies six clusters represented by the top three species comprising the medoids; the clusters are ordered by the contribution of Bocaccio (BOR) to each medoid. Species codes: CAR = Canary Rockfish, POP =Pacific Ocean Perch, RBR = Redbanded Rockfish, RER =Rougheye Rockfish, RSR = Redstripe Rockfish, SGR Silvergray Rockfish, YMR = Yellowmouth Rockfish, and YTR =Yellowtail Rockfish.

G.3. TROPHIC INTERACTIONS

The diet of larval Bocaccio includes larval euphausiids, diatoms, dinoflagellates, tintinnids, cladocerans, and calanoid copepods (Sumida and Moser 1984).

Bocaccio becomes piscivorous from an early age (before age 1), eating the young of other fish species such as inshore rockfish (Phillips 1964). In California, young BOR have been observed actively pursuing young Kelp Rockfish (*S. atrovirens*), and predation by BOR has a significant impact on recruitment success of young rockfish species in kelp canopies (Nelson 2001). When the adults move to deeper waters, they feed on smaller rockfish (*Sebastes* spp.), Sablefish (*Anoplopoma fimbria*), anchovies, lanternfish, and squids such as *Loligo opalescens* (Phillips 1964).

A cursory look at the BOR specimens collected in Appendix D from GFBioSQL (accessed 2019-10-03) yields very little information on stomach contents: Pacific Herring (*Clupea pallasi*) from one BOR stomach.

There are few reports of predators on *S. entomelas*. Love et al. (2002) mentions that young BOR are eaten by Chinook Salmon (*Oncorhynchus tshawytscha*) and Harbour Seals (*Phoca vitulina*).

G.4. ENVIRONMENTAL EFFECTS

Zabel et al. (2011) developed an environmental model for Bocaccio demonstrating that juvenile survival (recruitment success) could be explained by an interaction between density dependence and climate, specifically, combinations of monthly indices of the Northern Oscillation Index (NOI) and sequential life stages. For example, juvenile survival was correlated with NOI in June and November, months that experience higher offshore currents in California, which can affect mating, rearing, dispersal, and settling. Additionally, when conditions were cooler, and consequently more productive, density-dependent mortality was reduced.

A more recent study by Schroeder et al. (2019) demonstrated that the advection of source water characterised by cool temperatures, low salinity, and high oxygen levels into adult rockfish habitat at depth provided a more robust indicator than ocean conditions at the surface. During a large marine heatwave (LMH) in the northeast Pacific Ocean from 2014 to 2016, compounded by an El Niño in 2015-16, sea surface conditions were not amenable to ecosystem productivity. Contrary to expectations, rockfish recruitment during the LMH was higher than normal, which the authors suggested was due, in part, to the advection of oxygen-rich water to females at depth during gestation, when metabolic demands increase.

The effect of marine protected areas (MPAs) remains inconclusive in BC (Haggarty et al. 2016); however, Thompson et al. (2017) found that large MPAs off California hosted higher rates of increasing larval rockfish abundance than in areas outside MPAs. The latter concluded that MPAs facilitate the recovery of rockfish species.

G.5. ADVICE FOR MANAGERS

There is potential for environmental series to be incorporated into stock assessment models. However, a previous attempt to link recruitment estimates for 5ABC Pacific Ocean Perch with a number of environmental indicators (Haigh et al. 2018) proved inconclusive. Similarly, early analyses that used sea level indicators to predict Pacific Cod recruitment have since broken down (Forrest et al. 2018). This type of oceanographic information falls outside the usual data sources in the stock assessment group, but collaboration with other DFO personnel or external colleagues may result in potentially useful hypotheses that could be incorporated into the stock assessment.

G.6. REFERENCES – ECOSYSTEM

Forrest, R.E., Anderson, S.C., Grandin, C.J., and Starr, P.J. 2020. Assessment of Pacific Cod (*Gadus macrocephalus*) for Hecate Strait and Queen Charlotte Sound (Area 5ABCD), and West Coast Vancouver Island (Area 3CD) in 2018. DFO Can. Sci. Advis. Sec. Res. Doc. 2020/070. v + 215 p.

Haggarty, D.R., Shurin, J.B. and Yamanaka, K.L. 2016. Assessing population recovery inside British Columbia's rockfish conservation areas with a remotely operated vehicle. Fish. Res. 183: 165-179.

Haigh, R., Starr, P.J., Edwards, A.M., King, J.R. and Lecomte, J.B. 2018. Stock assessment for Pacific Ocean Perch (*Sebastes alutus*) in Queen Charlotte Sound, British Columbia in 2017. DFO Can. Sci. Advis. Sec. Res. Doc. 2018/038. v + 227 p.

Love, M.S., Yoklavich, M. and Thorsteinson, L. 2002. The Rockfishes of the Northeast Pacific. University of California Press, Berkeley and Los Angeles, California.

Maechler, M., Rousseeuw, P., Struyf, A., Hubert, M. and Hornik, K. 2018. cluster: Cluster Analysis Basics and Extensions. R package version 2.0.7-1.

Nelson, P.A. 2001. Behavioral ecology of young-of-the-year kelp rockfish, *Sebastes atrovirens* Jordan and Gilbert (Pisces: Scorpaenidae). J. Exper. Mar. Biol. Ecol. 256: 33-50.

Phillips, J.B. 1964. Life history studies on ten species of rockfish (genus *Sebastodes*). Fish Bull. 1-70.

Schroeder, I.D., Santora, J.A., Bograd, S.J., Hazen, E.L., Sakuma, K.M., Moore, A.M., Edwards, C.A., Wells, B.K. and Field, J.C. 2019. Source water variability as a driver of rockfish recruitment in the California Current Ecosystem: implications for climate change and fisheries management. Can. J. Fish. Aquat. Sci. 76(6): 950-960.

Sumida, B.Y. and Moser, H.G. 1984. Food and feeding of Bocaccio (*Sebastes paucispinis*) and comparison with Pacific Hake (*Merluccius productus*) larvae in the California Current. CalCOFI Rep. XXV: 112-118.

Thompson, A.R., Chen, D.C., Guo, L.W., Hyde, J.R. and Watson, W. 2017. Larval abundances of rockfishes that were historically targeted by fishing increased over 16 years in association with a large marine protected area. R. Soc. Open Sci. 4: 170639.

Zabel, R.W., Levin, P.S., Tolimieri, N. and Mantua, N.J. 2011. Interactions between climate and population density in the episodic recruitment of bocaccio, *Sebastes paucispinis*, a Pacific rockfish. Fish. Oceanogr. 20(4): 294-304.